RECENT ADVANCES IN BASIC AND TRANSLATIONAL OSTEOIMMUNOLOGY

EDITED BY: Rupesh K. Srivastava, Naibedya Chattopadhyay, Katharina Schmidt-Bleek, Pradyumna Kumar Mishra and Massimo De Martinis

PUBLISHED IN: Frontiers in Immunology and Frontiers in Endocrinology

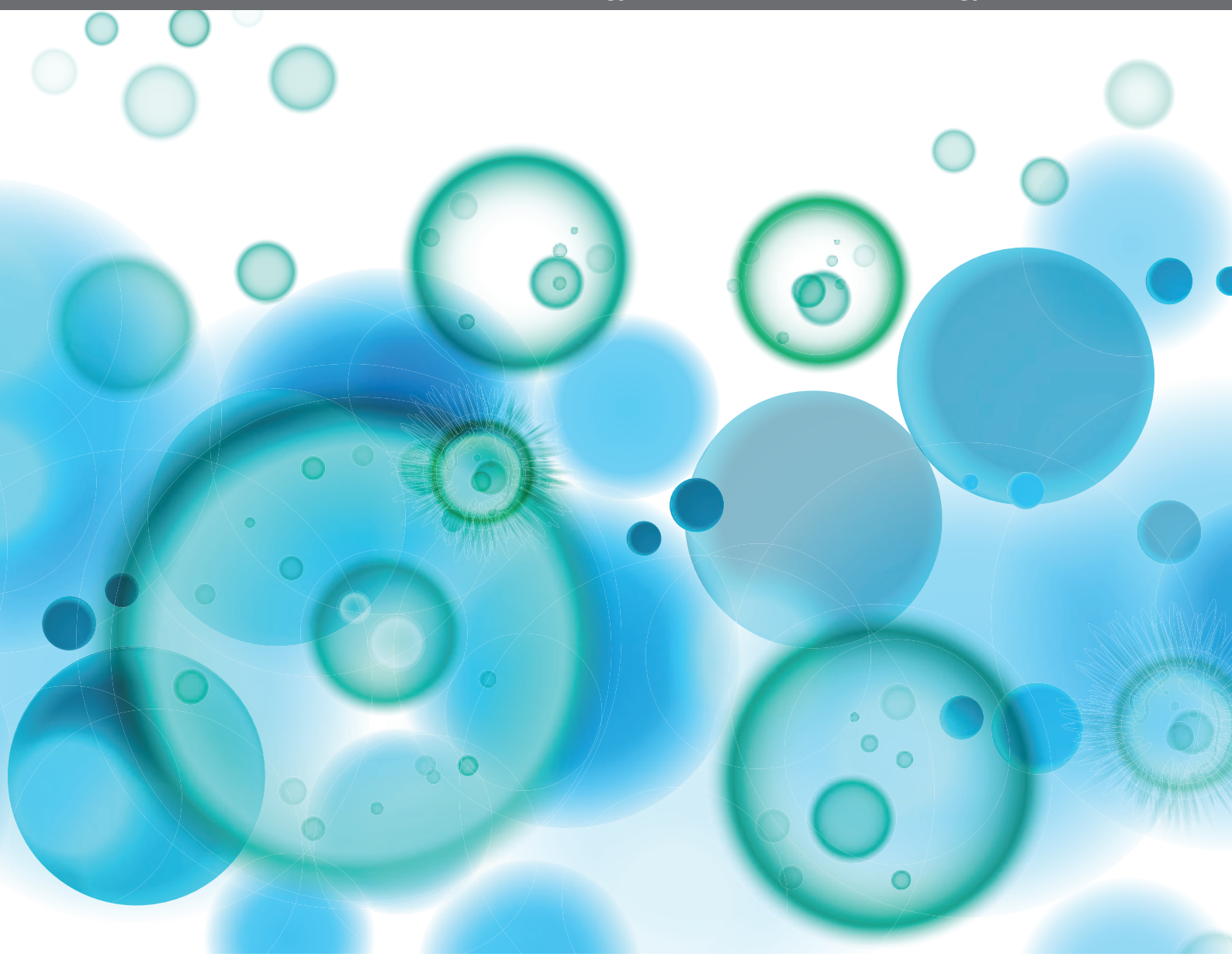

frontiers Research Topics

ISSN 1664-8714
ISBN 978-2-88974-014-7
DOI 10.3389/978-2-88974-014-7

About Frontiers

Frontiers is more than just an open-access publisher of scholarly articles: it is a pioneering approach to the world of academia, radically improving the way scholarly research is managed. The grand vision of Frontiers is a world where all people have an equal opportunity to seek, share and generate knowledge. Frontiers provides immediate and permanent online open access to all its publications, but this alone is not enough to realize our grand goals.

Frontiers Journal Series

The Frontiers Journal Series is a multi-tier and interdisciplinary set of open-access, online journals, promising a paradigm shift from the current review, selection and dissemination processes in academic publishing. All Frontiers journals are driven by researchers for researchers; therefore, they constitute a service to the scholarly community. At the same time, the Frontiers Journal Series operates on a revolutionary invention, the tiered publishing system, initially addressing specific communities of scholars, and gradually climbing up to broader public understanding, thus serving the interests of the lay society, too.

Dedication to Quality

Each Frontiers article is a landmark of the highest quality, thanks to genuinely collaborative interactions between authors and review editors, who include some of the world's best academicians. Research must be certified by peers before entering a stream of knowledge that may eventually reach the public - and shape society; therefore, Frontiers only applies the most rigorous and unbiased reviews.
Frontiers revolutionizes research publishing by freely delivering the most outstanding research, evaluated with no bias from both the academic and social point of view. By applying the most advanced information technologies, Frontiers is catapulting scholarly publishing into a new generation.

What are Frontiers Research Topics?

Frontiers Research Topics are very popular trademarks of the Frontiers Journals Series: they are collections of at least ten articles, all centered on a particular subject. With their unique mix of varied contributions from Original Research to Review Articles, Frontiers Research Topics unify the most influential researchers, the latest key findings and historical advances in a hot research area! Find out more on how to host your own Frontiers Research Topic or contribute to one as an author by contacting the Frontiers Editorial Office: frontiersin.org/about/contact

RECENT ADVANCES IN BASIC AND TRANSLATIONAL OSTEOIMMUNOLOGY

Topic Editors:
Rupesh K. Srivastava, All India Institute of Medical Sciences, India
Naibedya Chattopadhyay, Central Drug Research Institute (CSIR), India
Katharina Schmidt-Bleek, Charité University Medicine Berlin, Germany
Pradyumna Kumar Mishra, ICMR-National Institute for Research in Environmental Health, India
Massimo De Martinis, University of L'Aquila, Italy

Citation: Srivastava, R. K., Chattopadhyay, N., Schmidt-Bleek, K., Mishra, P. K., De Martinis, M., eds. (2021). Recent Advances in Basic and Translational Osteoimmunology. Lausanne: Frontiers Media SA.
doi: 10.3389/978-2-88974-014-7

Table of Contents

frontiers in Immunology

EDITORIAL
published: 18 November 2021
doi: 10.3389/fimmu.2021.800508

Editorial: Recent Advances in Basic and Translational Osteoimmunology

Rupesh K. Srivastava[1*], *Katharina Schmidt-Bleek*[2], *Naibedya Chattopadhyay*[3], *Massimo De Martinis*[4] *and Pradyumna Kumar Mishra*[5]

[1] Department of Biotechnology, All India Institute of Medical Sciences (AIIMS), New Delhi, India, [2] Julius Wolff Institut, Berlin Institute of Health at Charité – Universitätsmedizin Berlin, Charitéplatz 1, Berlin, Germany, [3] Division of Endocrinology and Centre for Research in Anabolic Skeletal Targets in Health and Illness (ASTHI), CSIR-Central Drug Research Institute, Lucknow, India, [4] Department of Life, Health and Environmental Sciences, University of L'Aquila, L'Aquila, Italy, [5] Department of Molecular Biology, ICMR-National Institute for Research in Environmental Health (NIREH), Bhopal, India

Keywords: osteoimmunology, immune cells, bone, immunoporosis, cytokines, inflammation

Editorial on the Research Topic

Recent Advances in Basic and Translational Osteoimmunology

The term "Osteoimmunology" was coined to describe the correlation between bone and immune cells (1). Recent findings have highlighted the link between both the bone and immune systems (2), an interrelation further supported by the common developmental niche, Bone Marrow (BM). "Immunoporosis" as an independent field under the umbrella of osteoimmunology was recently proposed in 2018 to highlight the growing importance of the immune system in Osteoporosis (3, 4). The present research topic on 'Recent advances in Basic and Translational Osteoimmunology' comprises research in the emerging field of Osteoimmunology. This Research Topic brings together 17 contributions by 116 authors from across the globe, including the U.S.A. (6), Europe (72), and Asia (38). The compilation of these recent reviews and research articles deepens understanding of the role of the immune system in various skeletal system associated pathologies.

OPEN ACCESS

Edited and reviewed by:
Pietro Ghezzi,
Brighton and Sussex Medical School, United Kingdom

***Correspondence:**
Rupesh K. Srivastava
rupesh_srivastava13@yahoo.co.in; rupeshk@aiims.edu

Specialty section:
This article was submitted to Inflammation, a section of the journal Frontiers in Immunology

Received: *23 October 2021*
Accepted: *27 October 2021*
Published: *18 November 2021*

Citation:
Srivastava RK, Schmidt-Bleek K, Chattopadhyay N, De Martinis M and Mishra PK (2021) Editorial: Recent Advances in Basic and Translational Osteoimmunology. Front. Immunol. 12:800508. doi: 10.3389/fimmu.2021.800508

ROLE OF THE ADAPTIVE IMMUNE SYSTEM IN SKELETAL HOMEOSTASIS

Primarily, osteoimmunology emphasizes the two-way communication between the bone and immune cells. The interrelation between the bone and immune system plays an indispensable role in the maintenance of skeletal homeostasis. The first question that comes to mind is how the immune system can contribute to the differentiation and functional activity of bone cells. Furthermore, Th17 cells play an important role *via* producing interleukin (IL)-17A, which enhances bone resorption by bone degrading osteoclasts cells as reviewed by Tang et al. and Wu et al. in the context of postmenopausal osteoporosis (PMO), psoriatic arthritis (PsA) rheumatoid arthritis (RA), and axial spondylarthritis (axSpA). From their discussion, it appears that targeting the immune-regulatory molecules involved in the modulation of osteoimmune response may be a feasible approach to several inflammatory bone diseases. The role of T-cell protein tyrosine phosphatase (TCPTP), a protein tyrosine phosphatase immune-modulator in osteoporosis has been exhaustively reviewed by Wang et al. Another T cell regulatory molecule butyrophilin

(Btn2a2), a transmembrane protein that suppresses the differentiation and fusion of osteoclasts and reduces the bone resorption process, has been demonstrated by Frech et al. Altogether, these studies highlight the significance of T cells and their associated molecules in regulating osteoclast differentiation with potential applications in osteoimmunology.

The potential of the immune system to regulate bone cells appears to be much more complex as besides T cells, other immune cells are also known to influence the bone remodeling and fracture healing process. Using single cell RNA sequencing (scRNA-seq) Zhang et al. demonstrate that the frequency of B cells is significantly reduced in the early stage of the fracture healing process. This study indicates that B cell is a crucial regulator of the fracture healing process *via* inhibiting excessive regeneration of bone by producing various osteoblast inhibitors. On the other hand, a pioneering study by Sapra et al. is the first to show that IL-10 producing regulatory B cells (Bregs) possess anti-osteoclastogenic properties. Importantly, this study also revealed that reduction in the frequency of Bregs and their reduced tendency to produce IL-10 enhances bone loss in a mouse model of osteoporosis. This study opens novel avenues in the field of cellular immunotherapy for the treatment and management of osteoporosis. Additionally, Breedveld et al. revealed that IgA autoantibodies, by promoting the release of IL-6 and IL-8 by immune cells and osteoclasts, enhance bone resorption in RA patients. Thus, targeting the interactions between IgA and its FcαRI receptor could be a promising therapeutic target in the treatment of RA. Altogether these studies highlight the growing importance of adaptive immunity in modulating bone health.

ROLE OF INNATE IMMUNE CELLS IN SKELETAL HOMEOSTASIS

Accumulating evidence suggests that both the innate and adaptive immune system contributes to inflammatory bone diseases including osteoporosis. Innate immune cells by producing various inflammatory modulators contribute to the pathogenesis of osteoporosis. This group of immune cells, along with modulating osteoclastogenesis, also exhibits the potential of transdifferentiating into multinucleated osteoclasts. Thus, highlighting the importance of innate immune cells in the context of osteoporosis, Saxena et al. review the role of different innate immune cells in osteoporosis in a detailed systematic manner, thereby adding strength to the emerging field of Immunoporosis. Furthermore, to emphasize the role of macrophages in inflammatory bone loss conditions such as osteoarthritis (OA), Thomson and Hilkens comprehensively review the involvement of macrophages in disease progression. Activation of macrophages and osteoclastogenesis is a hallmark of osteolysis and thus can be targeted by the application of local platelet rich fibrin (PRF). Kargarpour et al. demonstrated that PRF has anti-inflammatory potential by mitigating macrophage function and thus exhibits the ability to reduce osteoclastogenesis.

IMPLICATIONS OF CHRONIC INFLAMMATION ON BONE HEALTH

Emerging clinical and molecular evidence suggests that local and systemic inflammation can trigger osteoporosis. Among several conditions, psoriasis (Pso) showed an increased risk of osteoporosis mainly due to the deficiency of vitamin D and chronic inflammatory conditions. Of note, few studies have revealed the close functional association between vitamin D and IL-33/ST2 signaling pathway in the bone remodeling process (5, 6). Based on this close functional link, De Martinis et al. reviewed their crosstalk in the pathogenesis of bone and skin pathologies (7). Chronic inflammation that increases osteoclastogenesis also adversely impacts adipogenesis by increasing adipocyte population in lieu of osteoblasts from the mesenchymal stem cells (MSC). To highlight the significance of chronic inflammation in regulating the adipogenesis process, Furesi et al. demonstrate that higher levels of pro-inflammatory cytokines viz. IL-17 suppresses the adipogenesis process. By employing a bioinformatics tool, Wang et al. report that upregulation of chronic inflammation leads to intervertebral disc (IVD) degeneration and discogenic pain. Further analysis shows that infiltration of $CCR7^{+}CD163^{+}$ macrophages and Tregs is significantly enhanced in the degenerative IVDs. Various anti-inflammatory agents are currently being employed in chronic inflammation of which glucocorticoid (GC) is the first-line anti-inflammatory agent that acts *via* glucocorticoid receptor (GR). Upon binding of GCs, GR dimerizes is essential for aiding the anti-inflammatory potential of GCs. In contrast to the beneficial effects of GR dimerization, Hachemi et al. report on the adverse effects of GR dimerization on the fracture healing process and thus establish the detrimental effect of GCs and GR on fracture healing. The life cycle of osteoblasts and osteoclasts is regulated by key modulators of apoptosis viz., Fas-ligand (FasL) which is a member of the TNF superfamily and plays a fundamental role in the healing of extraction sockets. Alccayhuaman et al. further support the notion that FasL is necessary for bone regeneration and the healing process and showed a significant reduction in bone volume over tissue volume (BV/TV) in a study performed using FasL knock out mice. The involvement of the immune system is now also identified in very rare bone complications like aseptic implant failure (AIF) and periprosthetic joint infections (PJI). It was observed that the expression of immunoregulatory markers viz. sCD28, cCD80, sCTLA4, and sBTLA is significantly altered in the joints of AIF and PJI patients compared to controls and thus could be employed as a promising diagnostic marker for both AIF and PJI (Jubel et al.).

POTENTIAL THERAPIES TO ALLEVIATE BONE HEALTH

Tissue engineering methods utilize progenitor cells as a potential therapy for the treatment of several diseases. Studies demonstrated that chondrogenically primed human MSC (hMSCs) reiterate the methodology of endochondral ossification and in forming mature bone. To further translate this MSCs based approach in bone

formation, Fahy et al. clearly show that implantation of MSCs in an immunocompetent xenogenic model promotes endochondral ossification and provides in-depth mechanistic insights into the osteoimmunological processes that regulate the regeneration of bone and homeostasis.

CONCLUSION

The field of "Osteoimmunology" will provide novel etiologic insights into skeletal system-associated ailments in the near future. This might help in the design of therapeutic strategies for the management of various inflammatory bone pathologies with better translational potential. We (the editors) strongly believe that each article published under this Research Topic on "*Recent Advances in Basic and Translational Osteoimmunology*" will help in the discovery of new molecular candidates and pathways and unravel this complex yet important connection between the bone and immune system.

AUTHORS CONTRIBUTIONS

All the authors have made extensive, direct, and intellectual contributions to the present work and approved it for publication.

REFERENCES

1. Arron JR, Choi Y. Bone Versus Immune System. *Nature* (2000) 408:535–6. doi: 10.1038/35046196
2. Dar HY, Azam Z, Anupam R, Mondal RK, Srivastava RK. Osteoimmunology: The Nexus Between Bone and Immune System. *Front Biosci (Landmark Ed)* (2018) 23. doi: 10.2741/4600
3. Srivastava RK, Dar HY, Mishra PK. Immunoporosis: Immunology of Osteoporosis—Role of T Cells. *Front Immunol* (2018) 9:657. doi: 10.3389/fimmu.2018.00657
4. Sapra L, Azam Z, Rani L, Saini C, Bhardwaj A, Shokeen N, et al. "Immunoporosis": Immunology of Osteoporosis. *Proc Natl Acad Sci India Sect B Biol Sci* (2021) 91:511–9. doi: 10.1007/s40011-021-01238-x
5. De Martinis M, Sirufo MM, Suppa M, Ginaldi L. IL-33/IL-31 Axis in Osteoporosis. *Int J Mol Sci* (2020) 21(4):1239. doi: 10.3390/ijms21041239
6. De Martinis M, Ginaldi L, Sirufo MM, Pioggia G, Calapai G, Gangemi S, et al. Alarmins in Osteoporosis, RAGE, IL-1, and IL-33 Pathways: A Literature Review. *Med (Kaunas)* (2020) 56(3):138. doi: 10.3390/medicina56030138
7. Sirufo MM, De Pietro F, Bassino EM, Ginaldi L, De Martinis M. Osteoporosis in Skin Diseases. *Int J Mol Sci* (2020) 21(13):4749. doi: 10.3390/ijms21134749

Conflict of Interest: The authors declare that the work has been conducted in the absence of any financial and commercial relationships that could lead to a potential conflict of interest.

frontiers in Immunology

REVIEW
published: 08 January 2021
doi: 10.3389/fimmu.2020.604055

IL-33/Vitamin D Crosstalk in Psoriasis-Associated Osteoporosis

Massimo De Martinis[1], Lia Ginaldi[1], Maria Maddalena Sirufo[1], Enrica Maria Bassino[1], Francesca De Pietro[1], Giovanni Pioggia[2†] and Sebastiano Gangemi[3†]*

[1] Department of Life, Health and Environmental Sciences, University of L'Aquila, L'Aquila, Italy, [2] Institute for Biomedical Research and Innovation (IRIB), National Research Council of Italy (CNR), Messina, Italy, [3] School and Operative Unit of Allergy and Clinical Immunology, Department of Clinical and Experimental Medicine, University of Messina, Messina, Italy

Patients with psoriasis (Pso) and, in particular, psoriatic arthritis (PsoA) have an increased risk of developing osteoporosis (OP). It has been shown that OP is among the more common pathologies associated with Pso, mainly due to the well-known osteopenizing conditions coexisting in these patients. Pso and OP share common risk factors, such as vitamin D deficiency and chronic inflammation. Interestingly, the interleukin (IL)-33/ST2 axis, together with vitamin D, is closely related to both Pso and OP. Vitamin D and the IL-33/ST2 signaling pathways are closely involved in bone remodeling, as well as in skin barrier pathophysiology. The production of anti-osteoclastogenic cytokines, e.g., IL-4 and IL-10, is promoted by IL-33 and vitamin D, which are stimulators of both regulatory and Th2 cells. IL-33, together with other Th2 cytokines, shifts osteoclast precursor differentiation towards macrophage and dendritic cells and inhibits receptor activator of nuclear factor kappa-B ligand (RANKL)-induced osteoclastogenesis by regulating the expression of anti-osteoclastic genes. However, while the vitamin D protective functions in OP and Pso have been definitively ascertained, the overall effect of IL-33 on bone and skin homeostasis, because of its pleiotropic action, is still controversial. Emerging evidence suggests a functional link between vitamin D and the IL-33/ST2 axis, which acts through hormonal influences and immune-mediated effects, as well as cellular and metabolic functions. Based on the actions of vitamin D and IL-33 in Pso and OP, here, we hypothesize the role of their crosstalk in the pathogenesis of both these pathologies.

Keywords: osteoporosis, psoriasis, IL-33, vitamin D, osteoimmunology, skin, bone, cytokines

OPEN ACCESS

Edited by:
Joanna Cichy, Jagiellonian University, Poland

Reviewed by:
Christoph Baerwald, Leipzig University, Germany
Nada Pejnovic, University of Belgrade, Serbia

****Correspondence:***
Massimo De Martinis
demartinis@cc.univaq.it

[†]These authors have contributed equally to this work

Specialty section:
This article was submitted to Cytokines and Soluble Mediators in Immunity, a section of the journal Frontiers in Immunology

Received: *08 September 2020*
Accepted: *24 November 2020*
Published: *08 January 2021*

Citation:
De Martinis M, Ginaldi L, Sirufo MM, Bassino EM, De Pietro F, Pioggia G and Gangemi S (2021) IL-33/Vitamin D Crosstalk in Psoriasis-Associated Osteoporosis. Front. Immunol. 11:604055. doi: 10.3389/fimmu.2020.604055

INTRODUCTION

Psoriasis (Pso) is a chronic autoimmune multifactorial disease that is associated with systemic inflammation. It presents with skin erythematous plaques, covered by characteristic white silvery scales (1). It is characterized by increased proliferation of keratinocytes, perivascular skin infiltration by cells belonging to both the adaptive and innate immune system, and imbalances in apoptotic and autophagic pathways (2).

Through the production of inflammatory cytokines, activated and autoreactive immune cells play central roles in its pathogenesis (3). In both skin and blood of psoriatic patients, there are increased levels of various cytokines, growth factors, and chemokines (4). Patients suffering from Pso,

particularly those with psoriatic arthritis (PsoA) or more severe forms of the disease, develop multiple comorbidities in addition to joint diseases, including cardiovascular and rheumatologic disorders, infections, obesity, and diabetes (5–7). The link between these comorbidities is likely systemic inflammation (8). Recently, osteoporosis (OP) is also considered to be a relevant comorbidity in Pso (9). Therefore, patients with Pso are now recognized to be at increased risk of pathologic fractures and OP, so today, it is commonly believed that Pso patients might benefit from increased screening for OP (10).

OP is defined as a generalized disease of the skeleton, characterized by low bone mineral density (BMD) and altered microarchitecture, leading to increased bone fragility and, as a result, increased risk of fractures (11, 12). In addition to senile and postmenopausal OP, secondary OP may also occur as a consequence of various pathologies, including endocrinopathies, rheumatic and neoplastic diseases, malnutrition, chronic inflammatory conditions, and 1,25-dihydroxyvitamin D (vitamin D) deficiency (13–17). Several potential mechanisms may explain the association between Pso and OP, including a low vitamin D level, chronic inflammation, and drug usage (18–20). In particular, proinflammatory cytokines, such as interleukin (IL)-1, IL-6, IL-11, IL-15, IL-17, and tumor necrosis factor (TNF)-alpha, might accelerate bone loss, whereas other cytokines, mostly of the Th2 profile, e.g., IL-4 and IL-33, are usually considered osteoprotective (21).

IL-33 and vitamin D are emerging pathogenetic factors of both Pso and OP. However, their role in the development of these associated pathologies is complex and not yet fully clarified. Here, we hypothesize a mechanistic link between vitamin D and IL-33 in patients with Pso and associated OP.

PATHOGENIC MECHANISMS LINKING PSO AND OP

Several pathogenetic mechanisms link Pso and OP (**Box 1**). Although there are conflicting results in the literature about this association and its pathogenetic mechanisms, the majority of studies describe a decreased BMD in patients with long-term Pso and PsoA (9, 22, 23). Like Pso, OP can also be considered a systemic pathology (21). Although it is mainly linked to menopause and aging (14, 24), OP can also accompany a wide range of pathologies, in particular, those with an important inflammatory substrate, including dermatological disorders (25–28).

BOX 1 | Main pathogenetic mechanisms in Pso and OP.

Key points:
- Vitamin D deficiency
- Overexpression of IL-33/IL-31 axis
- Chronic systemic inflammation
- Increased production of inflammatory and osteoclastogenic cytokines
- Unbalanced RANKL-RANK-OPG signaling pathway
- Overexpression of IL-23/IL-17 axis
- Impaired Th17/Treg cell balance
- Increased secretion of IL-17 and IL-22 from IL-23-stimulated ILC3

Many cytokines are involved in the regulation of bone turnover, and most of them also underlie the inflammatory background of Pso (4, 21, 29). Vitamin D deficiency is among the main risk factors of both pathologies (29–31). The hypothesized mechanisms underlying the potential association between Pso and OP involves enhanced bone resorption secondary to increased concentrations of osteoclastogenic cytokines, such as TNF-alpha, IL-6, IL-12, IL-23, or IL-17 (31, 32). The central signal pathway in bone resorption is the system of the receptor activator of nuclear factor kappa-B (NF-kB) ligand (RANKL), mainly expressed by osteoblasts, that binds to its receptor RANK on the osteoclast precursor cells, inducing their differentiation into mature osteoclasts and thus leading to bone resorption. Osteoprotegerin (OPG), the decoy receptor of RANKL, prevents bone resorption by inhibiting osteoclastogenesis. In the pathogenesis of OP, the RANKL-RANK-OPG axis is unbalanced (12). Inflammatory cytokines, whose production is increased in Pso, exert osteoclastogenic effects mainly through the enhancement of RANKL expression. In particular, IL-17, produced by T helper type 17 (Th17) cells, plays a pivotal role in the bone loss of inflammatory conditions, including Pso, by enhancing RANKL expression on osteoblasts and synovial fibroblasts. Moreover, IL-17 stimulates the production of other inflammatory and osteoclastogenic cytokines, such as TNF-α, IL-1, and IL-6, which accelerate osteoclastogenesis, further facilitating the development of OP. High surface expression of RANKL on Th17 cells characterizes the so-called osteoclast subsets of T lymphocytes, that strongly enhance bone resorption. On the contrary, T regulatory (Treg) cells inhibit osteoclastogenesis and support bone formation. Therefore, while Th17 cells induce osteoclastogenesis, mainly by secreting IL-17, IL-4 enhanced Treg exert anti-osteoclastogenic activity by producing suppressor cytokines, including IL-10, and transforming growth factor-beta (TGF-β) (21). An impaired Th17/Treg cell balance is central in the inflammatory background of both Pso and OP. Treg cells are responsible for the maintenance of self-tolerance, thus inhibiting autoimmune diseases, including Pso, and are also able to suppress RANKL-induced osteoclastogenesis, whereas pro-inflammatory Th17 cells contribute to the induction and propagation of inflammation. Th17 cells, converted from Foxp3+ Treg in inflamed tissues, such as psoriatic skin lesions, comprise the most potent osteoclastogenic T cell subset in inflammatory bone loss (33). In the complex cytokine network involved in Pso, a crucial role is also exerted by IL-12/Th1 and IL-23/Th17 axis, by linking components of adaptive and innate immunity in an inflammatory crosstalk. In the skin, activated dendritic cells (DCs) trigger Th1 and Th17 cells to differentiate and release IFN-γ and TNF-α, and IL-17 and IL-22, respectively, which promote keratinocyte proliferation. IL-23 is a heterodimeric cytokine composed of two subunits, p19 and p40. The latter subunit is shared by the Th1-inducing cytokine IL-12. Upon skin injury, IL-23 produced by activated DCs, stressed keratinocytes and other non-immune cells directly drives expansion and survival of Th17 lymphocytes, stimulates IL-17 production, and induces downregulation of IL-10, involved in

Treg cell function, thus creating a self-amplifying inflammatory response that drives the development of skin lesions infiltrated with a mixture of inflammatory cell populations. Innate lymphoid cells (ILCs) represent a heterogeneous group of immune cells lacking specific antigen receptors or T/B cell markers. ILC3, which express the transcription factor retinoid-related orphan receptor γt (ROR γt) and are characterized by the ability to produce Th17 and IL-22 cytokines, are increased in Pso. ILC3 constitutively express the IL-23 receptor, thus representing a target for IL-23-mediated IL-17 and IL-22 increased production. The secretion of IL-17 and IL-22 from IL-23-stimulated ILC3 promotes the aberrant keratinocyte differentiation and hyperproliferation, typically observed in Pso (34). IL-12 and IL-23 involved in skin inflammation, are also critical to inflammation-induced bone resorption, *via* a number of direct and indirect effects that modulate osteoclast formation. In the bone, IL-23 upregulates RANK on preosteoclasts and induces Th17 cells to produce IL-17, which acts on osteoblasts to secrete RANKL. Th17 cells also secrete RANKL directly and further induce osteoclast formation and secretion of bone-degrading enzymes leading to bone destruction (35). Many other cytokines involved in bone remodeling have recently been shown to also exert roles in the pathogenesis of Pso, including, in particular, IL-33 (36–39). In addition, some treatments used in Pso might contribute to bone loss, for example, corticosteroids and cyclosporin, particularly when used systemically (18–20), whereas treatments at the systemic level aimed at reducing inflammation, e.g., biologics or methotrexate, could reduce the risk associated with osteoporotic fractures (40). Finally, psoriatic patients, especially those with associated inflammatory arthritis, engage less in physical activities and tend to cover affected body surfaces with consequent decreases in osteoformation and vitamin D synthesis (41, 42). In particular, the lack of sun exposure, which may affect mainly psoriatic patients with extensive skin involvement and/or arthritis through vitamin D deficiency, negatively affects calcium metabolism, further increasing bone resorption and leading to the onset of OP (43). Psoriatic patients of both sexes appear to have a high prevalence of OP and vitamin D deficiency (10, 44). Low levels of vitamin D metabolizing enzymes (CYP27A1 and CYP27B1) within psoriatic lesions have also been documented (9, 45), and vitamin-D treatment in psoriatic patients has been associated with clinical improvement of skin lesions (46, 47).

Pso is related to vitamin D deficiency through both inflammation and a lack of sun exposure (48). Interestingly, vitamin D deficiency and OP are frequently recognized in the great majority of associated Pso comorbidities (21, 49) For example, Pso is frequently associated with metabolic syndrome, increased body mass index, and obesity (50). All of these associated conditions are characterized by both an inflammatory background and increased fat deposits, in which vitamin D tends to accumulate because of its liposolubility, consequently reducing its circulating bioavailable levels. In these patients, vitamin D deficiency is commonly related to hyperglycemia and higher levels of cholesterol, low-density lipoprotein, and triglycerides (51, 52). Therefore, despite the tendency for a higher body mass index in patients with Pso, which might have a protective effect against OP, both vitamin D deficiency and systemic inflammation can still induce BMD loss.

Chronic inflammation itself has been related to low vitamin D levels and decreased BMD (53, 54). Under pathological conditions, the equilibrium between bone formation and resorption, which physiologically ensures skeletal homeostasis, is shifted towards osteoclast-mediated bone resorption. Proinflammatory cytokines, such as TNF-alpha and IL-17, are notoriously associated with osteoclastic bone resorption in inflammatory diseases (21). These cytokines trigger osteoclastogenesis through the activation of a series of transcription factors, such as NF-kappa B. In PsoA, synovial inflammation can further facilitate the onset of local and systemic OP (29). In these patients, an increase in osteoclast progenitors (OCP) correlates with the extent of joint erosions and inflammation markers (41).

The association between Pso and OP is therefore supported by the existence of pathophysiological mechanisms, namely, excessive production of proinflammatory cytokines that are able to activate osteoclastogenesis, and the frequent lack of vitamin D characterizing psoriatic patients (55, 56).

However, studies on OP development and the increased risk of fractures in patients with Pso are still somewhat controversial, because of the complexity of the network of interconnected cytokines and the regulatory factors linking the two pathologies.

THE ROLE OF VITAMIN D

Vitamin D has multiple functions, including hormonal and immunological control (**Box 2**). Vitamin D regulates more than 200 genes involved in cell proliferation and differentiation, the secretion of different hormones, and immune cell activity (54, 57). The lack of vitamin D in Pso is widely recognized as an important factor that contributes to the development of OP (58). Vitamin D regulates calcium and phosphorous metabolism and parathyroid hormone (PTH) secretion and function. For these activities, it has important implications for the maintenance of skeletal integrity. As a consequence of vitamin D deficiency, bone mineralization disorders arise, mainly through an imbalance in the calcium/phosphorus ratio. Vitamin D is indispensable for physiological bone turnover. In particular, in order to prevent OP, supplementation with vitamin D is strongly recommended as a support for anti-osteoporotic therapies (12, 15, 53). Moreover, in

BOX 2 | Vitamin D functions.

Key points:
- Calcium/phosphorous metabolism regulation
- Parathyroid hormone secretion and function control
- Regulation of cutaneous barrier homeostasis
- Keratinocyte proliferation, apoptosis and function control
- Th1/Th2 cell development modulation
- Induction of regulatory T cells
- Down-regulation of Th17 cells
- Down-regulation of nflammatory cytokine production

addition to its effects on bone, vitamin D also exerts important functions in skin homeostasis and its deficiency is linked with Pso development (48, 59). Vitamin D is therefore no longer considered to just be an essential factor for the maintenance of a normal skeletal structure, but its extraskeletal effects, including cell cycle regulation and immune modulation, are becoming increasingly known (60–62).

The epidermis is the natural source of vitamin D synthesis through the action of ultraviolet light (53), and in turn, vitamin D functions as a key regulator of cutaneous barrier homeostasis. The skin therefore acts as the site of vitamin D synthesis and also as the target organ for its biologically active form (47). Keratinocytes contain enzymes needed for the production of the active form of vitamin D, 1,25 (OH)2D, and express its receptor, vitamin D receptor (VDR), thus being able to synthesize and also respond to vitamin D. Through this signaling pathway, vitamin D is involved in regulating epidermal development, keratinocyte proliferation, differentiation and apoptosis (54), and the synthesis of keratins, involucrin, transglutaminase, loricrin, and filaggrin, helping to modulate skin barrier function (63, 64). These control mechanisms are partly due to its ability to increase intracellular calcium by inducing the production of phospholipases and calcium receptors needed for calcium-dependent keratinocyte differentiation. After activation, VDRs interact with retinoid X receptor (RXR) to exert their functions. VDRs, as well as enzymes able to synthesize the active form of the vitamin, namely 1,25-dihydroxy-vitamin D, are expressed in several tissues beyond the kidneys and bones, including the skin and the immune system, suggesting that vitamin D is involved in many other functions besides the metabolic ones (53, 65). An association between Pso susceptibility and VDR polymorphisms, as well as between reduced tight-junction proteins and decreased VDR expression in psoriatic skin, has been described (57). It has been shown that vitamin D also exerts central roles in both humoral and cellular regulation by suppressing T-cell proliferation and Th2 cell development and through the induction of regulatory T cells, cytokine production modulation, and dendritic cell regulation (66–69).

Through the downregulation of IL-12 production, vitamin D suppresses the maturation of Th1 cells, leading to increased Th2 lymphocyte proliferation (47, 70). However, vitamin D also promotes regulatory T cell maturation and increases IL-10 synthesis, exerting inhibitory effects on Th2 immune responses (71).

Moreover, vitamin D inhibits proliferation and induces apoptosis in various cell types (54). Following dysregulation of the cell cycle, autophagy and apoptosis have important roles in inflammatory processes (72) underlying both OP and Pso. This could represent a further mechanism through which vitamin D deficiency contributes to their pathogeneses (73–76). In psoriatic skin inflammation, cytokines and chemokines produced by dysregulated T lymphocytes play key roles (77). As in Pso, in the pathogenesis of OP, these immune-mediated mechanisms are strongly involved (21). By inhibiting the production of Th1 and Th17 cytokines and stimulating T cells to secrete anti-inflammatory Th2 cytokines in both the skin and bone immune systems, vitamin D reduces the production of osteoclastogenic cytokines as well as the psoriatic inflammatory process (64, 78, 79). Moreover, since vitamin D promotes Th2 and Treg differentiation rather than Th1 and Th17 proinflammatory lymphocytes (48) and inhibits B cell differentiation, thus interfering with the production of antibodies by plasma cells (70), its deficiency is also associated with an increased risk of developing autoimmune diseases (80–82), including Pso, which is a Th1-Th17-Th22-based inflammatory disease involving innate and acquired immunity (53). Therefore, despite being historically associated with rickets, osteomalacia, and OP, now considered an inflammatory Th1-mediated disease (83), vitamin D deficiency has recently been recognized as a risk factor for chronic systemic diseases, including diabetes, neoplasia, allergies, infections, autoimmune, cardiovascular, and neurodegenerative diseases (76). Pso is histologically characterized by keratinocyte hyperproliferation, derangement of the epidermal barrier function, and infiltration of the skin by multiple activated inflammatory cells (53). As a key modulator of systemic inflammation, vitamin D normalizes the dysregulated distribution of CD26 and ICAM-1 integrins in the dermal–epidermal junction of psoriatic skin and suppresses the inflammatory profile of monocytes/macrophages (55), down-regulating the production of cytokines, such as IL-1β, IL-6, IL-8, and TNF-alpha (48, 80). All of these cytokines are involved in inflammatory processes leading to Pso and OP (47, 83, 84). Indeed, vitamin D and its analogues suppress the proliferation of keratinocytes and their proinflammatory molecule production, therefore improving psoriatic lesions and contributing to skeletal health by suppressing bone resorption and favoring bone formation.

THE ROLE OF IL-33

IL-33 is a cytokine that can promote Th2 response, but also has broad activities (**Box 3**) including the promotion of activated Th1 and CD8+ cytotoxic cells and also Treg cells that express ST2 receptor (85, 86). As well as vitamin D, also IL-33 is involved in various biological processes, including tissue homeostasis and repair, cell proliferation, and the immune response, and it plays key roles in the pathogenetic mechanisms of several diseases, such as allergic, autoimmune, neoplastic, and cardiovascular diseases. In particular, IL-33 is involved in skin diseases, including Pso (39, 87, 88), and in OP through its role in bone remodeling (89–92). Its receptor complex consists of a primary receptor, ST2, and an accessory IL-1 receptor protein. The ST2 receptor exists in two different forms: a transmembrane isoform acts as a cellular receptor, whereas a soluble form (sST2) plays the role of decoy receptor inhibiting IL-33 activity (93, 94). Interestingly, the IL-33/

BOX 3 | IL-33 functions.

Key points:

- Induction of Th2 responses and Th2 cytokine production
- Promotion of activated Th1 and CD8+ cytotoxic cells
- Activation of Treg cells expressing ST2 receptor
- Gene expression regulation
- Activation of inflammation and tissue ripair upon danger signals
- Mast cell and neutrophil activation in inflamed skin
- Enhancement of TNFα induced secretion of IL-6, VEGF, and MCP-1

ST2 axis is involved in both Th2 and Th1/Th17 responses (88) as well as in the activation of Treg and natural killer (NKT) cells, B and NK lymphocytes, neutrophils, and macrophages (91, 95–98). A regulatory feedback axis exists between stromal cells expressing IL-33 and adipose resident ST2+ Tregs (99, 100). Obesity alters this homeostatic cellular network and promotes the inflammatory response (101, 102). Several immune cells involved in the type 2 immune response express ST2. Among others, examples of such immune cells are the group 2 innate lymphoid cells (ILC2), eosinophils, basophils, and DCs, as well as mast cells and Th2 cells (103). Increased amphiregulin (AREG) levels are associated with vitamin D deficiency. The ILC2-associated marker AREG, whose encoding gene is a target of vitamin D, activates IL-33-responsive ST2 T cells and ILC2s (104), which function as key effectors producing Th2 cytokines, including IL-4, IL-5, IL-9, and IL-13 (105), when released from necrotic and/or apoptotic epithelial cells. On the other hand, TNF-alpha, INF-gamma, and IL-17, major effectors of the Th1/Th17 responses in Pso and OP pathogenesis, stimulate the release of IL-33. Both skin lesions and unaffected skin biopsies of Pso patients (36, 37, 95) express high IL-33 levels (103, 106). The rapid IL-33 release from keratinocytes after skin injury could be a crucial mechanism involved in the pathogenesis of Pso (107–110). Once released in the local microenvironment, IL-33 could activate mast cells and neutrophils as well as Th1/Th17 cells, triggering both innate and adaptive immune responses. Mast cells can activate other innate immune cells, such as eosinophils and neutrophils, and, in turn, can recruit and activate keratinocytes. The above-mentioned interactions are pivotal for the emergence of skin inflammation and Pso lesions (111). Both TNF-alpha and INF-gamma in psoriatic skin increase the expression of IL-33 which, in turn, is able to suppress the actions of other cytokines (38). Also, IL-17 upregulates IL-33 expression in normal human epidermal keratinocyte (NHEK) cultures through the activation of the p38/MAPK, ERK, and JAK/STAT pathways (112). IL-33 reinforces the TNF-alpha induced secretion of IL-6, VEGF, and MCP-1. However, data on IL-33 serum levels in Pso are controversial (113). A large number of studies suggest that a localized, rather than a generalized, IL-33 linked inflammatory pattern is evident in Pso (114). IL-33 serum levels are not always increased in the serum of patients with Pso, notwithstanding the increased levels of this cytokine in inflamed skin (103, 111, 114). It has also been suggested that IL-33 expression in the nuclei of keratinocytes following IL-17 stimulation may represent a regulatory mechanism aimed at attenuating immune reactions (110).

The expression levels of both IL-33 and ST2 are up-regulated in psoriasis, likely as a consequence of keratinocyte damage. IL-33/ST2 signals may subsequently trigger the activation of neutrophils and mast cells, leading to Pso development. This pathogenetic hypothesis assumes interplay between keratinocytes and the immune system (88, 107, 108). IL-33 exerts a dual function. It acts as a cytokine or as a nuclear factor when involved extracellularly or intracellularly, respectively, thus participating in both inflammation processes and gene expression regulation (4). Upon cellular stress and tissue damage, released IL-33 functions as an alarmin and activates innate and adaptive immune cells, inflammation, or tissue repair. IL-33 is considered a key alarmin in both Pso and OP, although it exerts contrasting effects in these pathological conditions (115). Continuous alarmin release promotes polarization toward a Th1 phenotype, and this effect contributes to the initial background of the local hyperinflammatory environment that characterizes Pso (92, 107).

The IL-33/ST2 pathway intervenes in the pathogenesis of Th2-related diseases, such as allergies (103), but could also exert some protective effects in other inflammatory pathologies, such as cardiovascular diseases and OP, mainly depending on genetics, disease duration, and the cytokine microenvironment (116). In particular, the role of IL-33 in OP and Pso is still debated. Some authors have reported IL-33 inhibition of osteoclast formation (117), whereas others described an IL-33-induced reduction in osteoprotegerin expression by osteoblasts and an increase in osteoclastogenic factor release (118), thus suggesting an IL-33 mediated bone resorption induction during inflammation (98). IL-33 stimulates mast cells to produce IL-6 and IL-13 *via* the canonical NF-kB signaling and p38 pathways. The MAPK-activated protein kinases MK2 and MK3, function as sensors of cell injury and exert pivotal roles in IL-33-induced cytokine production by mast cells in inflammatory responses (87, 98, 107). Due to its pleiotropic nature, IL-33 exerts contrasting roles in different diseases (87, 88), i.e., IL-33 can either drive the underlying inflammation or promote its resolution (99, 113) according to the individual inflammatory context. Disease severity and changes in relation to hormonal influences contribute to the bone remodeling effects of IL-33. For example, notwithstanding the decreased serum IL-33 levels in women undergoing menopause with OP, its protective effect on the bone disappears as OP progresses, likely due to the interference of other proinflammatory osteoclastogenic cytokines. In particular, IL-33 has controversial roles in bone remodeling (115, 119, 120). The majority of studies suggest prevalent anti-osteoclastogenic and osteoanabolic functions of IL-33, but the reduced expression of OPG by osteoblasts and the induced production of the osteoclastogenic cytokine IL-31 (97), have also been reported, suggesting that in particular inflammatory conditions, including arthritis and Pso, IL-33 can induce bone resorption. This hypothesis seems to be supported by the finding of periarticular bone erosions and systemic OP in PsoA, in which IL-33 plays a pathogenetically important role.

THE RELATIONSHIP BETWEEN VITAMIN D AND THE IL-33/ST2 AXIS IN PSORIASIS-ASSOCIATED OSTEOPOROSIS

Link Between Vitamin D and IL-33

There is a close relationship between vitamin D and the IL-33/ST2 axis in bone and skin homeostasis. Nonetheless, the exact role of vitamin D in IL-33 activities, which creates vicious circles in the pathogenesis of Pso-associated OP, remains controversial (91, 93). It is likely that vitamin D and IL-33 share some signal pathways and need each other to perform some important

immunological and metabolic functions both the skin and bone levels. In particular, there is evidence that, in some biological processes, they act in synergy, while in other cases, they act by controlling and modulating each other (71). Here, we hypothesize a mechanistic link between vitamin D and IL-33 in patients with Pso and associated OP.

Vitamin D and IL-33 Immunological Crosstalk

IL-33 shares many of the immunoregulatory effects of vitamin D, either potentiating or modulating them (**Box 4**). IL-33 is produced by cells regulated by vitamin D, and often their tissue targets and signal pathways are shared. For example, both vitamin D and IL-33 promote the differentiation of Th2 lymphocytes by inhibiting Th1 differentiation and also act as inducers of immunoregulatory cells. Vitamin D can downregulate the production of inflammatory cytokines and chemokines (121). Moreover, vitamin D activity is determined through vitamin D receptors, which are present not only in the skeleton but also in different types of cells, including antigen-presenting-cells, immune cells, and keratinocytes. In particular, DCs, lymphocytes, monocytes/macrophages, neutrophils, and epithelial cells can produce IL-33 and other cytokines involved in both bone remodeling and Pso inflammation, including IL-31, IL-17, and TNF-alpha (29, 62, 107). IL-33 therefore orchestrates the immune cascade of Pso. Moreover, it takes part in the bone remodeling process (115). Vitamin D plays a central role in both bone turnover and immune regulation. In addition, vitamin D is also implicated in skin homeostasis, acting as a potent immune system modulator and suppressing dendritic cell maturation. Serum vitamin D levels are decreased in Pso patients and, in particular, in those with associated OP.

The impact of low vitamin D levels has been widely investigated in both Pso and OP, as has the role of IL-33. Th2-related cytokines, including IL-4, IL-31, and IL-33, have recently been shown to play important roles in bone remodeling as well as in Pso skin inflammation and PsoA (47, 65). IL-33 may act as an alarmin, exerting both repairing and damaging processes and functioning as a nuclear transcription factor. Similarly, the vitamin D receptor, functioning as a ligand-activated transcription factor, regulates the activation or repression of gene transcription (121). Moreover, vitamin D deficiency likely independently contributes to the increased incidence of OP in Pso patients.

The relationship between IL-33 and vitamin D is highly complex and extremely variable. For example, IL-33 contributes to inflammatory reactions involving vitamin D deficiency but could also counteract some of its deleterious effects, mainly depending on the clinical context as well as on the cytokine and hormonal milieu. As a consequence, it is conceivable that although both vitamin D and IL-33 in the bone environment exert protective effects against OP, in inflamed Pso skin and in PsoA, the deleterious effects of vitamin D deficiency and IL-33/ST2 axis activation potentiate each other (85, 100). Decreased vitamin D and increased IL-33 levels are also both associated to Th2 immunity in allergic inflammatory diseases (122), suggesting that they play contrasting roles in allergies (71). Based on these considerations, a potential complex interaction between vitamin D and IL-33 has been hypothesized, not only in allergic diseases but also in other clinical conditions in which their roles have also been demonstrated, including Pso and OP. Vitamin D promotes anti-inflammatory IL-10 synthesis by inducing α-1-antitrypsin expression in CD4+ T cells (123). IL-10, as an immunosuppressive cytokine, directly limits Th2 cell differentiation and survival during allergic airway inflammation (124). On the other hand, IL-33 induces Th2 cytokines, including IL-31, thus exerting a pivotal role in orchestrating the recruitment and activation of effector cells of the allergic response. IL-31 is a cytokine produced by CD4+ T cells which has a potent immunological link with IL-33 and plays important roles in allergic inflammation and atopic dermatitis as well as in Pso (38, 88). A similar close link has been highlighted as being an important factor in the alteration of the bone remodeling process that underlies OP (92). The IL-31 receptor IL-31RA, the oncostatin M receptor, and the IL-33 receptor ST2 are related to the immunopathological mechanisms of Pso and OP. The ST2 receptor of IL-33, which is a critical component of Th2 responses, stimulates the production of IL-31 (88). At the same time, sST2, which is increased in Pso patients and acts as a decoy receptor for IL-33, is a negative modulator of the IL-33/ST2 axis. There is evidence that a perturbation of this axis exerts essential roles in OP (91). Plasma sST2 levels were found to be correlated with decreased cortical BMD and deterioration of the bone microstructure in Pso. Vitamin D enhances the synthesis of the IL-33 inhibitor sST2, counteracting inflammation in psoriatic skin (66). The association between increased sST2 and decreased vitamin D in Pso might synergistically contribute to the effect of inflammatory mediators in inducing compromised bone quality and OP.

Treg activity is influenced by both vitamin D and IL-33. Normal tissue repair, as well as bone and skin homeostasis, requires both vitamin D and IL-33 to locally expand Treg cells. The impact of Foxp3+ Treg cell derangement is involved in the autoimmune inflammatory processes of Pso (125). IL-33 promotes the recruitment of Treg cells into the site of injury, where they suppress inflammation. Through Treg recruitment and inhibition of NF-kB mediated gene transcription, IL-33

BOX 4 | Vitamin D/IL-33 crosstalk.

Key points:

1. *Shared immunoregulatory and homeostatic effects:*
   - Promotion of Th2 lymphocyte differentiation
   - Induction of immunoregulatory cells
   - Downregulation of inflammatory cytokine and chemokine production
   - Regulation of bone remodeling process
   - Modulation of PTH control of bone turnover
2. *Contrasting roles:*
   - Protective role of vitamin D in allergic diseases vs the induction of allergic inflammation by IL-33
   - Enhanced inflammatory osteoclastogenesis by IL-33-induced secretion of IL-31 vs bone protection by vitamin D
   - IL-33 induced and amplified inflammatory circuits vs vitamin D anti-inflammatory activity in Pso

exerts protective effects on bone. Also, vitamin D may exert its immune regulatory properties through the induction of Treg cells. Low levels of vitamin D in Pso patients could dysregulate immunological homeostasis by decreasing the number of circulatory Tregs (46, 80). Vitamin D modulates CD4+ T cell function, reversing the defective induction of IL-10-secreting regulatory T cells. IL-33 induces IL-10-producing regulatory B cells and promotes IL-10 production in macrophages (125, 126).

PTH Regulation by Vitamin D and IL-33

The links between vitamin D and IL-33 are both hormonal and immunological. PTH, the main hormone that regulates bone turnover and whose production is dependent on the levels of calcium and vitamin D in the body, is, in turn, strictly dependent on the IL-33/ST2 axis (127). Calcium metabolism is finely regulated by vitamin D and IL-33 in concert with PTH. The latter elevates calcium levels and reduces phosphorus levels in the blood. Calcium is a major regulator of sequential keratinocyte differentiation through the different layers of the epidermis until the stratum corneum is formed and is involved in signaling pathways that are central to desmosome and tight junction formation. Calcium receptors initiate the intracellular signaling cascade, driving differentiation in response to extracellular calcium. Calcium metabolism is also central to bone turnover. It is an essential component of hydroxyapatite crystals which confer hardness and resistance to the skeleton through deposits in the extracellular bone matrix. Vitamin D deficiency involves modification of calcium–phosphorus metabolism and increased secretion of PTH, which leads to increases in bone resorption and matrix demineralization. However, PTH could also function as an important osteoanabolic factor when administered pharmacologically (120, 128).

IL-33 and its receptors have roles in the PTH control of bone turnover (129). IL-33 mRNA levels in osteoblasts are increased by PTH and M oncostatin (127), and a positive correlation between PTH and IL-33 serum levels in postmenopausal OP has been observed (99). IL-33 production is stimulated by PTH, which contributes to the osteoanabolic effects of such a hormone. Vitamin D deficiency increases PTH secretion (78). As a consequence, IL-33 also increases, thus modulating the effects of PTH on bone remodeling (127). Therefore, the cytokine IL-33 represents a target of PTH and, synergistically with vitamin D, increases bone matrix mineralization by osteoblasts. IL-33 induced expression of the RANKL-encoding gene has been demonstrated in osteoblasts. RANKL, the major osteoclastogenic cytokine, is produced as a transmembrane protein, whose proteolytic processing is promoted by PTH, leading to the release of its soluble form. RANKL secretion, therefore, depends on integrated actions of both IL-33 and PTH (130). Moreover, both vitamin D and PTH control the levels of sST2. Serum sST2 correlates positively with serum phosphorus and negatively with serum calcium. The osteocyte-derived factor FGF-23, which inhibits PTH and promotes renal phosphorus excretion, also antagonizes some vitamin D effects. The IL-33/ST2 axis is, therefore, a PTH target that is able to both promote osteoblastic calcium deposition in the bone matrix and inhibit osteoclastogenesis (36). Increased levels of PTH induce elevation of sST2 (129). These data suggest that sST2 may play important roles in bone metabolism disorders, such as OP, as well as in inflammatory diseases, such as Pso.

THE PARADOX OF THE VITAMIN D AND IL-33 RELATIONSHIP IN PSO-ASSOCIATED OP

Increased bone resorption with consequent appearance of OP is commonly associated with Pso and, in particular, with the more evolutionary forms characterized by systemic inflammation and joint involvement. It has been ascertained that vitamin D exerts protective effects in both Pso and OP (9). On the contrary, IL-33 is considered a pathogenetic cytokine in Pso, whereas its effects on bone are variable. Therefore, the role of IL-33 seems to be contrasting (111). In reality, this apparent contradiction could be explained by the multiplicity of functions of this cytokine which, depending on the type of tissue, the immune environment, and the presence of other associated factors, can have different effects. It could be hypothesized that, notwithstanding increased IL-33 levels, the skeleton is instead more sensitive to a wide range of osteoporotic risk factors that are increased during Pso, including inflammation and vitamin D deficiency, which potentiate each other. Furthermore, most studies have shown compartmentalization of IL-33 in Pso with increased concentrations in skin lesions but not in the serum (114), potentially explaining the lack of protective effects on bone. The final effect of the IL-33/ST2 axis in both Pso and OP therefore depends on the reciprocal relationship between its various components which influence each other through complex regulatory mechanisms and positive and negative feedback circuits (113). For example, the effect of an increase in IL-33 could be counterbalanced by a consensual increase in its decoy receptor sST2 or, on the contrary, it could be enhanced by increased expression of its receptor on different cell types (66). In turn, there are several types of IL-33 target cells, including immune cells, mesenchymal stromal cells, and epithelial cells (85). Therefore, depending on the target cell type, the effect of the cytokine could vary from pro-inflammatory to anti-inflammatory. In the immunopathogenetic processes driving inflammation, the co-operation of IL-33 with IL-17, IL-22, TNF-alpha, IFN-gamma, or other inflammatory factors has been suggested. In this way, the proinflammatory functions of IL-33 could prevail on its immunoregulatory properties, as observed in several autoimmune diseases, including Pso (129).

The bone protective effect of IL-33 could be masked or prevented by concomitant factors characterizing Pso, such as the deficiency of vitamin D and the consequently altered PTH-mediated calcium–phosphorus metabolism, the prevalence of Th1/Th17 systemic inflammation with an increase in osteoclastogenic cytokines, and mechanisms of counter-regulation of IL-33 signaling associated with the inflammatory process (99). On the other hand, IL-33 itself can perform

different and contrasting functions: it can act as a pro-inflammatory factor in some pathological conditions but also as an alarmin with protective functions in response to danger signals, cell injury, and tissue damage (37).

Both vitamin D deficiency and increased circulating sST2 decoy receptor in Pso negatively impact the bone, favoring the production of Th1 rather than Th2 cytokines, suppressing the development of Treg cells and the production of regulatory and anti-inflammatory cytokines, thus promoting osteoclastogenesis and bone resorption (88, 94). The frequent of onset of OP during Pso could also be conditioned by the effective variability of effects of IL-33 on bone remodeling, which are dependent on a wide range of other factors (inflammatory microenvironment, influence of other cytokines, hormones, and vitamins) (9). A vitamin D deficiency could somehow nullify the protective effect of IL-33 on bone through mechanisms that are still unclear (121).

Figure 1 summarizes the complex interaction between vitamin D deficiency and increased IL-33/ST2 axis expression leading to increased bone resorption and OP in Pso.

CONCLUSIONS

In summary, there is clinical evidence that Pso, especially if associated with arthritis and a more advanced age, is associated with hypovitaminosis D, inflammation, and OP, and these factors might shift the effect of IL-33 from osteoprotective to proinflammatory and osteoclastogenic (39). The IL-33 levels in subjects with Pso reflect of increased inflammation, driving OP development. Different hypotheses could explain this paradox. For example, it has been recently demonstrated that the production of the soluble decoy receptor sST2 is enhanced by vitamin D (94). Since sST2 neutralizes the effect of IL-33, it is

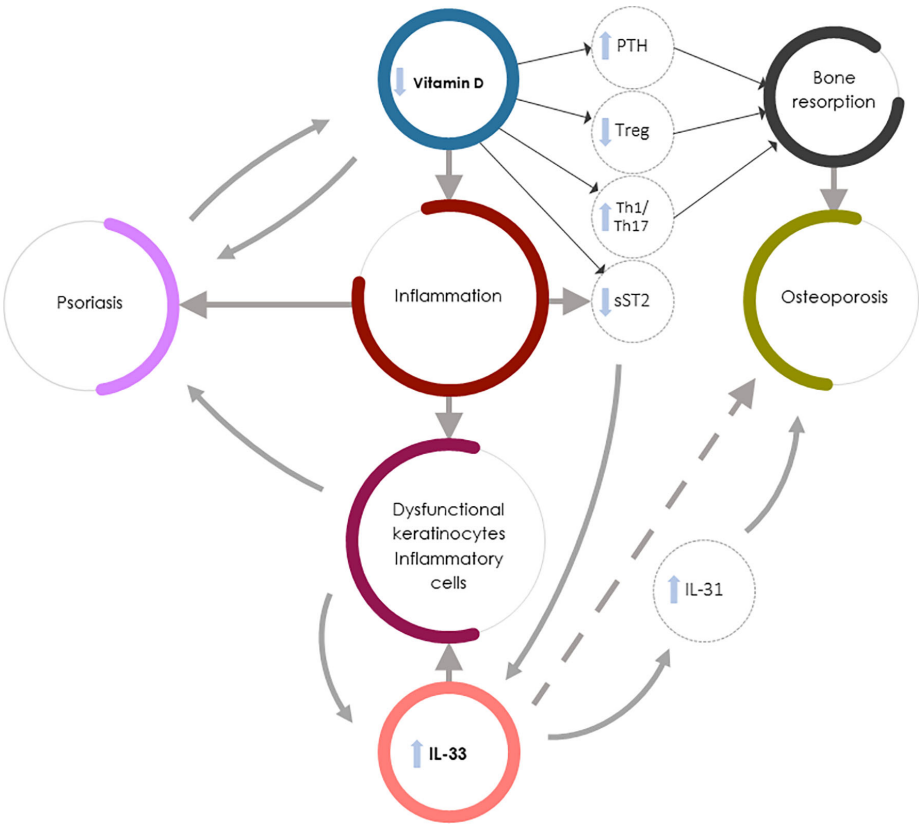

FIGURE 1 | Vitamin D deficiency and increased IL-33/ST2 expression in Pso-associated OP. IL-33 could exert contrasting roles in Pso and OP: it might drive the inflammation underlying Pso by inducing the production of dysfunctional keratinocytes and inflammatory cells but could exert protective effects in OP (dashed arrow). Vitamin D, in synergy with IL-33, regulates bone metabolism through PTH release and function, but also increases the soluble decoy receptor sST2 production, thus regulating IL-33 function. The direct action of vitamin D in inhibiting IL-33 function on bone cells is, however, less important than other vitamin D-mediated osteoprotective mechanisms (e.g., the vitamin D capacity to both inhibit Th1 and Th17 inflammation and induce bone protective Th2-type responses). In Pso-associated OP the complex interaction between vitamin D deficiency and increased IL-33/ST2 expression therefore leads to osteoclastogenesis and bone resorption through several mechanisms: PTH hyperproduction, impaired Treg function, increased Th1 and Th17 inflammatory and osteoclastogenic cytokine production, and decreased sST2 expression by lymphocytes and epithelial cells, resulting in an increase in IL-33 induced skin inflammation. Furthermore, the increase in IL-33 in psoriatic patients leads to an increased production of IL-31 which contributes to the worsening of bone loss.

considered an anti-inflammatory factor in conditions in which IL-33 takes place in the driving inflammatory processes, such as asthma and Pso, and IL-33 neutralization may represent a novel therapeutic approach in these diseases. On the contrary, in the skeleton, the role of IL-33 is likely protective against OP and its sST2 mediated neutralization is detrimental (66). Therefore, in Pso-associated OP, the final effect of vitamin D deficiency and IL-33/ST2 axis overexpression is overall increased bone resorption due to the prevalence of proinflammatory and dysmetabolic processes (9, 66).

AUTHOR CONTRIBUTIONS

All authors contributed to the article and approved the submitted version.

REFERENCES

1. Boehncke WH, Schön MP. Psoriasis. *Lancet* (2015) 386(9997):983–94. doi: 10.1016/S0140-6736(14)61909-7
2. Rendon A, Schäkel K. Psoriasis Pathogenesis and Treatment. *Int J Mol Sci* (2019) 20(6):1475. doi: 10.3390/ijms20061475
3. Veale DJ, Fearon U. The pathogenesis of psoriatic arthritis. *Lancet* (2018) 391(10136):2273–84. doi: 10.1016/S0140-6736(18)30830-4
4. Borsky P, Fiala Z, Andrys C, Beranek M, Hamakova K, Malkova A, et al. Alarmins HMGB1, IL-33, S100A7, and S100A12 in psoriasis vulgaris. *Mediators Inflamm* (2020) 2020:8465083. doi: 10.1155/2020/8465083
5. Boehncke WH. Systemic inflammation and cardiovascular comorbidity in psoriasis patients: causes and consequences. *Front Immunol* (2018) 9:579. doi: 10.3389/fimmu.2018.00579
6. Ciccarelli F, De Martinis M, Sirufo MM, Ginaldi L. Psoriasis Induced by Anti-Tumor Necrosis Factor Alpha Agents: A Comprehensive Review of the Literature. *Acta Dermatovenerol Croat* (2016) 24(3):169–74.
7. Bilal J, Malik SU, Riaz IB, Kurtzman DJB. Psoriasis and psoriatic spectrum disease: a primer for the primary care physician. *Am J Med* (2018) 131 (10):1146–54. doi: 10.1016/j.amjmed.2018.05.013
8. Furue M, Kadono T. Psoriasis: behind the scenes. *J Dermatol* (2016) 43(1):4–8. doi: 10.1111/1346-8138.131865
9. Sirufo MM, De Pietro F, Bassino EM, Ginaldi L, De Martinis M. Osteoporosis in Skin Diseases. *Int J Mol Sci* (2020) 21(13):4749. doi: 10.3390/ijms21134749
10. Lajevardi V, Abedini R, Moghaddasi M, Nassiri S, Goodarzi A. Bone mineral density is lower in male than female patients with plaque-type psoriasis in Iran. *Int J Women's Dermatol* (2017) 3:201–5. doi: 10.1016/j.ijwd.2017.07.007
11. De Martinis M, Sirufo MM, Polsinelli M, Placidi G, Di Silvestre D, Ginaldi L. Gender differences in osteoporosis: A single-center observational study. *WJMH* (2020) 38:e62. doi: 10.5534/wjmh.200099
12. De Martinis M, Sirufo MM, Ginaldi L. Osteoporosis: Current and emerging therapies targeted to immunological checkpoints. *Curr Med Chem* (2020) 27 (37):6356–72. doi: 10.2174/0929867326666190730113123
13. Ginaldi L, Di Benedetto MC, De Martinis M. Osteoporosis, inflammation and ageing. *Immun Ageing* (2005) 2:14. doi: 10.1186/1742-4933-2-14
14. De Martinis M, Di Benedetto MC, Mengoli LP, Ginaldi L. Senile osteoporosis: is it an immune-mediated disease? *Inflammation Res* (2006) 55(10):399–404. doi: 10.1007/s00011-006-6034-x
15. Wacker M, Holick MF. Vitamin D - Effects on skeletal and extraskeletal health and the need for supplementation. *Nutrients* (2013) 5(1):111–48. doi: 10.3390/nu5010111.16
16. Irelli A, Sirufo MM, Scipioni T, De Pietro F, Pancotti A, Ginaldi L, et al. mTOR links tumor immunity and bone metabolism: What are the clinical implications? *Int J Mol Sci* (2019) 20:5841. doi: 10.3390/ijms20235841
17. De Martinis M, Sirufo MM, Nocelli C, Fontanella L, Ginaldi L. Hyperhomocysteinemia is associated with inflammation, bone resorption, vitamin B12 and folate deficiency and MTHFR C677T polymorphism in postmenopausal women with decreased bone mineral density. *Int J Environ Res Public Health* (2020) 17(12):4260. doi: 10.3390/ijerph17124260
18. Kanda J, Izumo N, Furukawa M, Shimakura T, Yamamoto N, Takahashi HE, et al. Effects of the calcineurin inhibitors cyclosporine and tacrolimus on bone metabolism in rats. *BioMed Res* (2018) 39:131–9. doi: 10.2220/biomedres.39.131
19. Ciccarelli F, De Martinis M, Ginaldi L. Glucocorticoids in patients with rheumatic diseases: friends or enemies of bone? *Curr Med Chem* (2015) 22 (5):596–603. doi: 10.2174/0929867321666141106125051
20. Mowad C, Cohen SF, Fussell NF, Martin RE, Ellison CA. Referral patterns to an osteoporosis clinic for dermatology patients undergoing prolonged corticosteroid therapy. *J Am Acad Dermatol* (2018) 78:591–2. doi: 10.1016/j.jaad.2017.01.058
21. Ginaldi L, De Martinis M. Osteoimmunology and Beyond. *Curr Med Chem* (2016) 23(33):3754–74. doi: 10.2174/0929867323666160907162546
22. Ramot Y. Psoriasis and osteoporosis: The debate continues. *Br J Dermatol* (2017) 176:1117–8. doi: 10.1111/bjd.15437
23. Ogdie A, Harter L, Shin D, Baker J, Takeshita J, Choi HK, et al. The risk of fracture among patients with psoriatic arthritis and psoriasis: A population-based study. *Ann Rheum Dis* (2017) 76:882–5. doi: 10.1136/annrheumdis-2016-210441
24. Pedreira PG, Pinheiro MM, Szejnfeld VL. Bone mineral density and body composition in postmenopausal women with psoriasis and psoriatic arthritis. *Arthritis Res* (2011) 13:R16. doi: 10.1186/ar3240
25. Sirufo MM, Suppa M, Ginaldi L, De Martinis M. Does Allergy Break Bones? Osteoporosis and Its Connection to Allergy. *Int J Mol Sci* (2020) 21(3):712. doi: 10.3390/ijms21030712
26. De Martinis M, Ciccarelli F, Sirufo MM, Ginaldi L. An overview of environmental risk factors in systemic sclerosis. *Expert Rev Clin Immunol* (2016) 12(4):465–78. doi: 10.1586/1744666X.2016.1125782
27. Sirufo MM, Ginaldi L, De Martinis M. Successful Treatment With Omalizumab in a Child With Asthma and Urticaria: A Clinical Case Report. *Front Pediatr* (2019) 7:213. doi: 10.3389/fped.2019.00213
28. Sirufo MM, De Martinis M, Ginaldi L. Omalizumab an effective and safe alternative therapy in severe refractory atopic dermatitis: A case report. *Med (Baltimore)* (2018) 97(24):e10897. doi: 10.1097/MD.0000000000010897
29. Raimondo A, Lembo S, Di Caprio R, Donnarumma G, Monfrecola G, Balato N, et al. Psoriatic cutaneous inflammation promotes human monocyte differentiation into active osteoclasts, facilitating bone damage. *Eur J Immunol* (2017) 47:1062–74. doi: 10.1002/eji.201646774
30. Uluçkan Ö, Wagner EF. Chronic systemic inflammation originating from epithelial tissues. *FEBS J* (2017) 284(4):505–16. doi: 10.1111/febs.13904
31. Uluçkan Ö, Wagner EF. Role of IL-17A signalling in psoriasis and associated bone loss. *Clin Exp Rheumatol* (2016) 34(4 Suppl 98):17–20.
32. Mizutani K, Isono K, Matsushima Y, Okada K, Umaoka A, Iida S, et al. Inflammatory skin-derived cytokines accelerate osteoporosis in mice with persistent skin inflammation. *Int J Mol Sci* (2020) 21:3620. doi: 10.3390/ijms21103620
33. Komatsu N, Takayanagi H. Immune-bone interplay in the structural damage in rheumatoid arthritis. *Clin Exp Immunol* (2018) 194(1):1–8. doi: 10.1111/cei.13188
34. Sato Y, Ogawa E, Okuyama R. Role of innate immune cells in psoriasis. *Int J Mol Sci* (2020) 21(18):6604. doi: 10.3390/ijms21186604
35. Michael P, Schön MP, Erpenbeck L. The interleukin-23/interleukin-17 axis links adaptive and innate immunity in psoriasis. *Front Immunol* (2018) 9:1323. doi: 10.3389/fimmu.2018.01323
36. Cannavò SP, Bertino L, Di Salvo E, Papaianni V, Ventura-Spagnolo E, Gangemi S. Possible roles of IL-33 in the innate-adaptive immune crosstalk of psoriasis pathogenesis. *Mediators Inflammation* (2019) 2019:7158014. doi: 10.1155/2019/7158014

37. Sehat M, Talaei R, Dadgostar E, Nikoueinejad H, Akbari H. Evaluating serum levels of IL-33, IL-36, IL-37 and gene expression of IL-37 in patients with psoriasis vulgaris. *Iran J Allergy Asthma Immunol* (2018) 17(2):179–87.
38. Duan Y, Dong Y, Hu H, Wang Q, Guo S, Fu D, et al. IL-33 contributes to disease severity in psoriasis-like models of mouse. *Cytokine* (2019) 119:159–67. doi: 10.1016/j.cyto.2019.02.019
39. Mitsui A, Tada Y, Takahashi T, Shibata S, Kamata M, Miyagaki T, et al. Serum IL-33 levels are increased in patients with psoriasis. *Clin Exp Dermatol* (2016) 41(2):183–9. doi: 10.1111/ced.12670
40. Modalsli EH, Åsvold BO, Romundstad PR, Langhammer A, Hoff M, Forsmo S, et al. Psoriasis, fracture risk and bone mineral density: the HUNT Study, Norway. *Br J Dermatol* (2017) 176(5):1162–9. doi: 10.1111/bjd.15123
41. Kathuria P, Gordon KB, Silverberg JI. Association of psoriasis and psoriatic arthritis with osteoporosis and pathological fractures. *J Am Acad Dermatol* (2017) 76(6):1045–1053.e3. doi: 10.1016/j.jaad.2016.11.046
42. Martinez-Lopez A, Blasco-Morente G, Giron-Prieto MS, Arrabal-Polo MA, Luque-Valenzuela M, Luna-Del Castillo JD, et al. Linking of psoriasis with osteopenia and osteoporosis: A cross-sectional study. *Indian J Dermatol Venereol Leprol* (2019) 85(2):153–9. doi: 10.4103/ijdvl.IJDVL_831_17
43. Attia EA, Khafagy A, Abdel-Raheem S, Fathi S, Saad AA. Assessment of osteoporosis in psoriasis with and without arthritis: correlation with disease severity. *Int J Dermatol* (2011) 50(1):30–5. doi: 10.1111/j.1365-4632.2010.04600.x
44. De Martinis M, Sirufo MM, Suppa M, Di Silvestre D, Ginaldi L. Sex and gender aspects for patient stratification in allergy prevention and treatment. *Int J Mol Sci* (2020) 21(4):1535. doi: 10.3390/ijms21041535
45. Kaukinen A, Pelkonen J, Harvima IT. Mast cells express CYP27A1 and CYP27B1 in epithelial skin cancers and psoriasis. *Eur J Dermatol* (2015) 25 (6):548–55. doi: 10.1684/ejd.2015.2645
46. Zuccotti E, Oliveri M, Girometta C, Ratto D, Di Iorio C, Occhinegro A, et al. Nutritional strategies for psoriasis: current scientific evidence in clinical trials. *Eur Rev Med Pharmacol Sci* (2018) 22(23):8537–51. doi: 10.26355/eurrev-201812-16554
47. Kusuba N, Kitoh A, Dainichi T, Honda T, Otsuka A, Egawa G, et al. Inhibition of IL-17-committed T cells in a murine psoriasis model by a vitamin D analogue. *J Allergy Clin Immunol* (2018) 141(3):972–81.e10. doi: 10.1016/j.jaci.2017.07.033
48. Mattozzi C, Paolino G, Richetta AG, Calvieri S. Psoriasis, vitamin D and the importance of the cutaneous barrier's integrity: An update. *J Dermatol* (2016) 43(5):507–14. doi: 10.1111/1346-8138.13305
49. Takeshita J, Grewal S, Langan SM, Mehta NN, Ogdie A, Van Voorhees AS, et al. Psoriasis and comorbid diseases: Epidemiology. *J Am Acad Dermatol* (2017) 76(3):377–90. doi: 10.1016/j.jaad.2016.07.064
50. Gisondi P, Fostini AC, Fossà I, Girolomoni G, Targher G. Psoriasis and the metabolic syndrome. *Clin Dermatol* (2018) 36(1):21–8. doi: 10.1016/j.clindermatol.2017.09.005
51. Jensen P, Skov L. Psoriasis and obesity. *Dermatology* (2016) 232(6):633–9. doi: 10.1159/000455840
52. Lee SJ, Lee EY, Lee JH, Kim JE, Kim KJ, Rhee Y, et al. Associations of serum 25-hydroxyvitamin D with metabolic syndrome and its components in elderly men and women: the Korean Urban Rural Elderly cohort study. *BMC Geriatr* (2019) 19(1):102. doi: 10.1186/s12877-019-1118-y
53. Barrea L, Savanelli MC, Di Somma C, Napolitano M, Megna M, Colao A, et al. and its role in psoriasis: an overview of the dermatologist and nutritionist. *Rev Endocr Metab Disord* (2017) 18(2):195–205. doi: 10.1007/s11154-017-9411-6
54. Umar M, Sastry KS, Al Ali F, Al-Khulaifi M, Wang E, Chouchane AI. Vitamin D and the pathophysiology of inflammatory skin diseases. *Skin Pharmacol Physiol* (2018) 31(2):74–86. doi: 10.1159/000485132
55. Cubillos S, Krieg N, Norgauer J. Effect of vitamin D on peripheral blood mononuclear cells from patients with psoriasis vulgaris and psoriatic arthritis. *PloS One* (2016) 11(4):e0153094. doi: 10.1371/journal.pone.0153094
56. Kanda N, Hoashi T, Saeki H. Nutrition and psoriasis. *Int J Mol Sci* (2020) 21 (15):E5405. doi: 10.3390/ijms21155405
57. Stefanic M, Rucevic I, Barisic-Drusko V. Meta-analysis of vitamin D receptor polymorphisms and psoriasis risk. *Int J Dermatol* (2013) 52 (6):705–10. doi: 10.1111/j.1365-4632.2012.5813.x
58. Kincse G, Bhattoa PH, Herédi E, Varga J, Szegedi A, Kéri J, et al. Vitamin D3 levels and bone mineral density in patients with psoriasis and/or psoriatic arthritis. *J Dermatol* (2015) 42(7):679–84. doi: 10.1111/1346-8138.12876
59. Hambly R, Kirby B. The relevance of serum vitamin D in psoriasis: a review. *Arch Dermatol Res* (2017) 309(7):499–517. doi: 10.1007/s00403-017-1751-2
60. Morales-Tirado V, Wichlan DG, Leimig TE, Street SE, Kasow KA, Riberdy JM. 1α,25-dihydroxyvitamin D3 (vitamin D3) catalyzes suppressive activity on human natural regulatory T cells, uniquely modulates cell cycle progression, and augments FOXP3. *Clin Immunol* (2011) 138(2):212–21. doi: 10.1016/j.clim.2010.11.003
61. Nair-Shalliker V, Fenech M, Forder PM, Clements MS, Armstrong BK. Sunlight and vitamin D affect DNA damage, cell division and cell death in human lymphocytes: a cross-sectional study in South Australia. *Mutagenesis* (2012) 27(5):609–14. doi: 10.1093/mutage/ges026
62. Janeva-Jovanovska E, Dokic D, Jovkovska-Kaeva B, Breskovska G, Goseva Z, Minov J, et al. Relationship between vitamin D, inflammation and lung function in patients with severe uncontrolled asthma. *Open Access Maced J Med Sci* (2017) 5(7):899–903. doi: 10.3889/oamjms.2017.190
63. Chaiprasongsuk A, Janjetovic Z, Kim TK, Jarrett SG, D'Orazio JA, Holick MF, et al. Protective effects of novel derivatives of vitamin D(3) and lumisterol against UVB-induced damage in human keratinocytes involve activation of Nrf2 and p53 defense mechanisms. *Redox Biol* (2019) 24:101206. doi: 10.1016/j.redox.2019.101206
64. Soleymani T, Hung T, Soung J. The role of vitamin D in psoriasis: a review. *Int J Dermatol* (2015) 54(4):383–92. doi: 10.1111/ijd.12790
65. Gao M, Yao X, Ding J, Hong R, Wu Y, Huang H, et al. Low levels of vitamin D and the relationship between vitamin D and Th2 axis-related cytokines in neuromyelitis optica spectrum disorders. *J Clin Neurosci* (2019) 61:22–7. doi: 10.1016/j.jocn.2018.11.024
66. Pfeffer PE, Chen YH, Woszczek G, Matthews NC, Chevretton E, Gupta A, et al. Vitamin D enhances production of soluble ST2, inhibiting the action of IL-33. *J Allergy Clin Immunol* (2015) 135(3):824–7.e3. doi: 10.1016/j.jaci.2014.09.044
67. Prietl B, Treiber G, Pieber TR, Amrein K, Vitamin D. and immune function. *Nutrients* (2013) 5(7):2502–21. doi: 10.3390/nu5072502
68. Mohammadi-Kordkhayli M, Ahangar-Parvin R, Azizi SV, Nemati M, Shamsizadeh A, Khaksari M, et al. Vitamin D modulates the expression of IL-27 and IL-33 in the central nervous system in experimental autoimmune encephalomyelitis (EAE). *Iran J Immunol* (2015) 12(1):35–49.
69. Jafarzadeh A, Azizi SV, Arabi Z, Ahangar-Parvin R, Mohammadi-Kordkhayli M, Larussa T, et al. Vitamin D down-regulates the expression of some Th17 cell-related cytokines, key inflammatory chemokines, and chemokine receptors in experimental autoimmune encephalomyelitis. *Nutr Neurosci* (2019) 22(10):725–37. doi: 10.1080/1028415X.2018.1436237
70. Skrobot A, Demkow U, Wachowska M. Immunomodulatory role of vitamin D: a review. *Adv Exp Med Biol* (2018) 1108:13–23. doi: 10.1007/5584_2018_246
71. Bonanno A, Gangemi S, La Grutta S, Malizia V, Riccobono L, Colombo P, et al. 25-hydroxyvitamin D, IL-31, and IL-33 in children with allergic disease of the airways. *Mediators Inflammation* (2014) 2014:520241. doi: 10.1155/2014/520241
72. De Martinis M, Franceschi C, Monti D, Ginaldi L. Apoptosis remodeling in immunosenescence: implications for strategies to delay ageing. *Curr Med Chem* (2007) 14(13):1389–97. doi: 10.2174/092986707780831122
73. Guo Y, Zhang X, Wu T, Hu X, Su J, Chen X. Autophagy in skin diseases. *Dermatology* (2019) 235:380–9. doi: 10.1159/000500470
74. Massimini M, Palmieri C, De Maria R, Romanucci M, Malatesta D, De Martinis M, et al. 17-AAG and apoptosis, autophagy, and mitophagy in canine osteosarcoma cell lines. *Vet Pathol* (2014) 54(3):405–12. doi: 10.1177/0300985816681409
75. Sun HQ, Yan D, Wang QN, Meng HZ, Zhang YY, Yin LX, et al. 1,25-Dihydroxyvitamin D3 attenuates disease severity and induces synoviocyte apoptosis in a concentration-dependent manner in rats with adjuvant-induced arthritis by inactivating the NF-κB signaling pathway. *J Bone Miner Metab* (2019) 37(3):430–40. doi: 10.1007/s00774-018-0944-x
76. Marino R, Misra M. Extra-skeletal effects of vitamin D. *Nutrients* (2019) 11 (7):1460. doi: 10.3390/nu110714608–10
77. Deng Y, Chang C, Lu Q. The inflammatory response in psoriasis: a comprehensive review. *Clin Rev Allergy Immunol* (2016) 50(3):377–89. doi: 10.1007/s12016-016-8535-x

78. Goltzman D. Functions of vitamin D in bone. *Histochem Cell Biol* (2018) 149 (4):305–12. doi: 10.1007/s00418-018-1648-y
79. Brembilla NC, Senra L, Boehncke WH. The IL-17 family of cytokines in psoriasis: IL-17A and beyond. *Front Immunol* (2018) 9:1682. doi: 10.3389/fimmu.2018.01682
80. Hau CS, Shimizu T, Tada Y, Kamata M, Takeoka S, Shibata S, et al. The vitamin D(3) analog, maxacalcitol, reduces psoriasiform skin inflammation by inducing regulatory T cells and downregulating IL-23 and IL-17 production. *J Dermatol Sci* (2018) 92(2):117–26. doi: 10.1016/j.jdermsci.2018.08.007
81. Yamamoto EA, Nguyen JK, Liu J, Keller E, Campbell N, Zhang CJ, et al. Low levels of vitamin D promote memory B cells in lupus. *Nutrients* (2020) 12 (2):291. doi: 10.3390/nu12020291
82. Coates LC, FitzGerald O, Helliwell PS, Paul C. Psoriasis, psoriatic arthritis, and rheumatoid arthritis: Is all inflammation the same? *Semin Arthritis Rheumatol* (2016) 46(3):291–304. doi: 10.1016/j.semarthrit.2016.05.012
83. Srivastava RK, Dar HY, Mishra PK. Immunoporosis: immunology of osteoporosis-role of T cells. *Front Immunol* (2018) 9:657. doi: 10.3389/fimmu.2018.00657
84. Zhang J, Fu Q, Ren Z, Wang Y, Wang C, Shen T, et al. Changes of serum cytokines-related Th1/Th2/Th17 concentration in patients with postmenopausal osteoporosis. *Gynecol Endocrinol* (2015) 31(3):183–90. doi: 10.3109/09513590.2014.975683
85. Cayrol C, Girard JP. Interleukin-33 (IL-33): A nuclear cytokine from the IL-1 family. *Immunol Rev* (2018) 281(1):154–68. doi: 10.1111/imr.12619
86. Ding W, Zou GL, Zhang W, Lai XN, Chen HW, Xiong LX. Interleukin-33: its emerging role in allergic diseases. *Molecules* (2018) 23(7):1665. doi: 10.3390/molecules23071665
87. Hueber AJ, Alves-Filho JC, Asquith DL, Michels C, Millar NL, Reilly JH, et al. IL-33 induces skin inflammation with mast cell and neutrophil activation. *Eur J Immunol* (2011) 41(8):2229–37. doi: 10.1002/eji.201041360
88. Vocca L, Di Sano C, Uasuf CG, Sala A, Riccobono L, Gangemi S, et al. IL-33/ST2 axis controls Th2/IL-31 and Th17 immune response in allergic airway diseases. *Immunobiology* (2015) 220(8):954–63. doi: 10.1016/j.imbio.2015.02.005
89. Ginaldi L, De Martinis M, Saitta S, Sirufo MM, Mannucci C, Casciaro M, et al. Interleukin-33 serum levels in postmenopausal women with osteoporosis. *Sci Rep* (2019) 9(1):3786. doi: 10.1038/s41598-019-40212-6
90. Ohori F, Kitaura H, Ogawa S, Shen WR, Qi J, Noguchi T, et al. IL-33 Inhibits TNF-α-Induced Osteoclastogenesis and Bone Resorption. *Int J Mol Sci* (2020) 21(3):1130. doi: 10.3390/ijms21031130
91. De Martinis M, Sirufo MM, Suppa M, Ginaldi L. IL-33/IL-31 Axis in Osteoporosis. *Int J Mol Sci* (2020) 21(4):1239. doi: 10.3390/ijms21041239
92. De Martinis M, Ginaldi L, Sirufo MM, Pioggia G, Calapai G, Gangemi S, et al. Alarmins in Osteoporosis, RAGE, IL-1, and IL-33 Pathways: A Literature Review. *Medicina (Kaunas)* (2020) 56(3):138. doi: 10.3390/medicina56030138
93. Shen J, Shang Q, Wong CK, Li EK, Kun EW, Cheng IT, et al. Carotid plaque and bone density and microarchitecture in psoriatic arthritis: the correlation with soluble ST2. *Sci Rep* (2016) 6:32116. doi: 10.1038/srep32116
94. Haag P, Sharma H, Rauh M, Zimmermann T, Vuorinen T, Papadopoulos NG, et al. Soluble ST2 regulation by rhinovirus and 25(OH)-vitamin D3 in the blood of asthmatic children. *Clin Exp Immunol* (2018) 193(2):207–20. doi: 10.1111/cei.13135
95. Balato A, Di Caprio R, Canta L, Mattii M, Lembo S, Raimondo A, et al. IL-33 is regulated by TNF-α in normal and psoriatic skin. *Arch Dermatol Res* (2014) 306(3):299–304. doi: 10.1007/s00403-014-1447-9
96. Di Salvo E, Ventura-Spagnolo E, Casciaro M, Navarra M, Gangemi S. IL-33/IL-31 Axis: A potential inflammatory pathway. *Mediators Inflammation* (2018) 2018:3858032. doi: 10.1155/2018/3858032
97. Ginaldi L, De Martinis M, Ciccarelli F, Saitta S, Imbesi S, Mannucci C, et al. Increased levels of interleukin 31 (IL-31) in osteoporosis. *BMC Immunol* (2015) 16:60. doi: 10.1186/s12865-015-0125
98. Drube S, Kraft F, Dudeck J, Müller AL, Weber F, Göpfert C, et al. MK2/3 are pivotal for IL-33-induced and mast cell-dependent leukocyte recruitment and the resulting skin inflammation. *J Immunol* (2016) 197(9):3662–8. doi: 10.4049/jimmunol.1600658
99. Spallanzani RG, Zemmour D, Xiao T, Jayewickreme T, Li C, Bryce PJ, et al. Distinct immunocyte-promoting and adipocyte-generating stromal components coordinate adipose tissue immune and metabolic tenors. *Sci Immunol* (2019) 4(35):eaaw3658. doi: 10.1126/sciimmunol.aaw3658
100. Mahlakõiv T, Flamar AL, Johnston LK, Moriyama S, Putzel GG, Bryce PJ, et al. Stromal cells maintain immune cell homeostasis in adipose tissue via production of interleukin-33. *Sci Immunol* (2019) 4(35):eaax0416. doi: 10.1126/sciimmunol.aax0416
101. Dempsey LA. Fat IL-33 sources. *Nat Immunol* (2019) 20:776. doi: 10.1038/s41590-019-0439-5
102. Duffen J, Zhang M, Masek-Hammerman K, Nunez A, Brennan A, Jones JEC, et al. Modulation of the IL-33/IL-13 Axis in Obesity by IL-13Rα2. *J Immunol* (2018) 200(4):1347–59. doi: 10.4049/jimmunol.1701256
103. Murdaca G, Greco M, Tonacci A, Negrini S, Borro M, Puppo F, et al. IL-33/IL-31 axis in immune-mediated and allergic diseases. *Int J Mol Sci* (2019) 20 (23):5856. doi: 10.3390/ijms20235856
104. Wang L, Tang J, Yang X, Zanvit P, Cui K, Ku WL, et al. TGF-β induces ST2 and programs ILC2 development. *Nat Commun* (2020) 11(1):35. doi: 10.1038/s41467-019-13734-w
105. Halvorsen EC, Franks SE, Wadsworth BJ, Harbourne BT, Cederberg RA, Steer CA, et al. IL-33 increases ST2(+) Tregs and promotes metastatic tumour growth in the lungs in an amphiregulin-dependent manner. *Oncoimmunology* (2018) 8 (2):e1527497. doi: 10.1080/2162402X.2018.1527497
106. Li J, Liu L, Rui W, Li X, Xuan D, Zheng S, et al. New interleukins in psoriasis and psoriatic arthritis patients: the possible roles of interleukin-33 to interleukin-38 in disease activities and bone erosions. *Dermatology* (2017) 233(1):37–46. doi: 10.1159/000471798
107. Balato A, Lembo S, Mattii M, Schiattarella M, Marino R, De Paulis A, et al. IL-33 is secreted by psoriatic keratinocytes and induces pro-inflammatory cytokines via keratinocyte and mast cell activation. *Exp Dermatol* (2012) 21 (11):892–4. doi: 10.1111/exd.12027
108. Oshio T, Komine M, Tsuda H, Tominaga SI, Saito H, Nakae S, et al. Nuclear expression of IL-33 in epidermal keratinocytes promotes wound healing in mice. *J Dermatol Sci* (2017) 85(2):106–14. doi: 10.1016/j.jdermsci.2016.10.008
109. Shlomovitz I, Erlich Z, Speir M, Zargarian S, Baram N, Engler M, et al. Necroptosis directly induces the release of full-length biologically active IL-33 in vitro and in an inflammatory disease model. *FEBS J* (2019) 286(3):507–22. doi: 10.1111/febs.14738
110. Nygaard U, van den Bogaard EH, Niehues H, Hvid M, Deleuran M, Johansen C, et al. The "Alarmins" HMBG1 and IL-33 downregulate structural skin barrier proteins and impair epidermal growth. *Acta Derm Venereol* (2017) 97(3):305–12. doi: 10.2340/00015555-2552
111. Meephansan J, Komine M, Tsuda H, Karakawa M, Tominaga S, Ohtsuki M. Expression of IL-33 in the epidermis: The mechanism of induction by IL-17. *J Dermatol Sci* (2013) 71(2):107–14. doi: 10.1016/j.jdermsci.2013.04.014
112. Gruber JV, Holtz R. In vitro expression of NLRP inflammasome-induced active Caspase-1 expression in normal human epidermal keratinocytes (NHEK) by various exogenous threats and subsequent inhibition by naturally derived ingredient blends. *J Inflammation Res* (2019) 12:219–30. doi: 10.2147/JIR.S215776
113. Allegra A, Innao V, Tartarisco G, Pioggia G, Casciaro M, Musolino C, et al. The ST2/Interleukin-33 axis in hematologic malignancies: the IL-33 paradox. *Int J Mol Sci* (2019) 20(20):5226. doi: 10.3390/ijms20205226
114. Talabot-Ayer D, McKee T, Gindre P, Bas S, Baeten DL, Gabay C, et al. Distinct serum and synovial fluid interleukin (IL)-33 levels in rheumatoid arthritis, psoriatic arthritis and osteoarthritis. *Joint Bone Spine* (2012) 79 (1):32–7. doi: 10.1016/j.jbspin.2011.02.011
115. Schulze J, Bickert T, Beil FT, Zaiss MM, Albers J, Wintges K, et al. Interleukin-33 is expressed in differentiated osteoblasts and blocks osteoclast formation from bone marrow precursor cells. *J Bone Miner Res* (2011) 26(4):704–17. doi: 10.1002/jbmr.269
116. Aimo A, Migliorini P, Vergaro G, Franzini M, Passino C, Maisel A, et al. The IL-33/ST2 pathway, inflammation and atherosclerosis: Trigger and target? *Int J Cardiol* (2018) 267:188–92. doi: 10.1016/j.ijcard.2018.05.056
117. Kiyomiya H, Ariyoshi W, Okinaga T, Kaneuji T, Mitsugi S, Sakurai T, et al. IL-33 inhibits RANKL-induced osteoclast formation through the regulation of Blimp-1 and IRF-8 expression. *Biochem Biophys Res Commun* (2015) 460 (2):320–6. doi: 10.1016/j.bbrc.2015.03.033

118. Malcolm J, Awang RA, Oliver-Bell J, Butcher JP, Campbell L, Adrados Planell A, et al. IL-33 exacerbates periodontal disease through Induction of RANKL. *J Dent Res* (2015) 94(7):968–75. doi: 10.1177/0022034515577815
119. Okragly AJ, Hamang MJ, Pena EA, Baker HE, Bullock HA, Lucchesi J, et al. Elevated levels of interleukin (IL)-33 induce bone pathology but absence of IL-33 does not negatively impact normal bone homeostasis. *Cytokine* (2016) 79:66–73. doi: 10.1016/j.cyto.2015.12.011
120. Lima IL, Macari S, Madeira MF, Rodrigues LF, Colavite PM, Garlet GP, et al. Osteoprotective effects of IL-33/ST2 link to osteoclast apoptosis. *Am J Pathol* (2015) 185(12):3338–48. doi: 10.1016/j.ajpath.2015.08.013
121. Annalora AJ, Jozic M, Marcus CB, Iversen PL. Alternative splicing of the vitamin D receptor modulates target gene expression and promotes ligand-independent functions. *Toxicol Appl Pharmacol* (2019) 364:55–67. doi: 10.1016/j.taap.2018.12.009
122. De Martinis M, Sirufo MM, Ginaldi L. Allergy and Aging: An Old/New Emerging Health Issue. *Aging Dis* (2017) 8(2):162–75. doi: 10.14336/AD.2016.0831
123. Dimeloe S, Rice LV, Chen H, Cheadle C, Raynes J, Pfeffer P, et al. Vitamin D (1,25(OH)(2)D3) induces α-1-antitrypsin synthesis by CD4(+) T cells, which is required for 1,25(OH)(2)D3-driven IL-10. *J Steroid Biochem Mol Biol* (2019) 189:1–9. doi: 10.1016/j.jsbmb.2019.01.014
124. Coomes SM, Kannan Y, Pelly VS, Entwistle LJ, Guidi R, Perez-Lloret J, et al. CD4+ Th2 cells are directly regulated by IL-10 during allergic airway inflammation. *Mucosal Immunol* (2017) 10(1):150–61. doi: 10.1038/mi.2016.47
125. Zhang L, Li Y, Yang X, Wei J, Zhou S, Zhao Z, et al. Characterization of Th17 and FoxP3(+) Treg Cells in Paediatric Psoriasis Patients. *Scand J Immunol* (2016) 83(3):174–80. doi: 10.1111/sji.12404
126. Sattler S, Ling GS, Xu D, Hussaarts L, Romaine A, Zhao H, et al. IL-10-producing regulatory B cells induced by IL-33 (Breg(IL-33)) effectively attenuate mucosal inflammatory responses in the gut. *J Autoimmun* (2014) 50(100):107–22. doi: 10.1016/j.jaut.2014.01.032
127. Saleh H, Eeles D, Hodge JM, Nicholson GC, Gu R, Pompolo S, et al. Interleukin-33, a target of parathyroid hormone and oncostatin m, increases osteoblastic matrix mineral deposition and inhibits osteoclast formation in vitro. *Endocrinology* (2011) 152(5):1911–22. doi: 10.1210/en.2010-1268
128. Gruson D, Ferracin B, Ahn SA, Rousseau MF. Soluble ST2, the vitamin D/PTH axis and the heart: new interactions in the air? *Int J Cardiol* (2016) 12:292–4. doi: 10.1016/j.ijcard.2016.03.063
129. Liew FY, Girard JP, Turnquist HR. Interleukin-33 in health and disease. *Nat Rev Immunol* (2016) 16(11):676–89. doi: 10.1038/nri.2016.95
130. Heckt T, Keller J, Peters S, Streichert T, Chalaris A, Rose-John S, et al. Parathyroid hormone induces expression and proteolytic processing of Rankl in primary murine osteoblasts. *Bone* (2016) 92:85–93. doi: 10.1016/j.bone.2016.08.016

Conflict of Interest: The authors declare that the research was conducted in the absence of any commercial or financial relationships that could be construed as a potential conflict of interest.

frontiers in Immunology

REVIEW
published: 04 February 2021
doi: 10.3389/fimmu.2020.625034

Interleukin-17A Interweaves the Skeletal and Immune Systems

Mengjia Tang[1†], *Lingyun Lu*[2†] *and Xijie Yu*[1*]

[1] Department of Endocrinology and Metabolism, Laboratory of Endocrinology and Metabolism, National Clinical Research Center for Geriatrics, West China Hospital, Sichuan University, Chengdu, China, [2] Department of Integrated Traditional Chinese and Western Medicine, Laboratory of Endocrinology and Metabolism, West China Hospital, Sichuan University, Chengdu, China

The complex crosstalk between the immune and the skeletal systems plays an indispensable role in the maintenance of skeletal homeostasis. Various cytokines are involved, including interleukin (IL)-17A. A variety of immune and inflammatory cells produces IL-17A, especially Th17 cells, a subtype of $CD4^+$ T cells. IL-17A orchestrates diverse inflammatory and immune processes. IL-17A induces direct and indirect effects on osteoclasts. The dual role of IL-17A on osteoclasts partly depends on its concentrations and interactions with other factors. Interestingly, IL-17A exerts a dual role in osteoblasts *in vitro*. IL-17A is a bone-destroying cytokine in numerous immune-mediated bone diseases including postmenopausal osteoporosis (PMOP), rheumatoid arthritis (RA), psoriatic arthritis (PsA) and axial spondylarthritis (axSpA). This review will summarize and discuss the pathophysiological roles of IL-17A on the skeletal system and its potential strategies for application in immune-mediated bone diseases.

Keywords: osteoimmunology, interleukin-17A, osteoclasts, osteoblasts, postmenopausal osteoporosis, rheumatoid arthritis, psoriatic arthritis, axial spondyloarthritis

OPEN ACCESS

Edited by:
Rupesh K. Srivastava, All India Institute of Medical Sciences, India

Reviewed by:
Arthur Kavanaugh, University of California, San Diego, United States
Ineke Jansen, VU University Amsterdam, Netherlands

***Correspondence:**
Xijie Yu
xijieyu@scu.edu.cn;
xijieyu@hotmail.com

[†]*These authors have contributed equally to this work*

Specialty section:
This article was submitted to Inflammation, a section of the journal Frontiers in Immunology

Received: *02 November 2020*
Accepted: *23 December 2020*
Published: *04 February 2021*

Citation:
Tang MJ, Lu LY and Yu XJ (2021) Interleukin-17A Interweaves the Skeletal and Immune Systems. Front. Immunol. 11:625034. doi: 10.3389/fimmu.2020.625034

INTRODUCTION

Over the last 20 years, a growing body of research has focused on the relationship between the skeletal and immune systems. Subsequently, the term "osteoimmunology" was defined for this field of study. Accumulating evidence has shown that multiple components of immune systems including immune organs, multiple immune cells, and immune factors, participate in bone metabolism. In turn, bone cells, including osteoclasts, osteoblasts, bone lining cells, and osteocytes, are indispensable for the regulation of immune systems. The interaction between the skeletal and immune systems constitutes a complex network and is involved in the pathological process of many immune-mediated bone diseases. Recent studies have shown that IL-17A as one of the immune-derived cytokines participates in the regulation of bone metabolism. Understanding the effect of IL-17A on bone metabolism is more conducive to develop new-targeted drugs for immune-related bone diseases. This review will summarize the current knowledge of IL-17A in the skeletal system and will discuss the potential clinical value of IL-17A in immune-mediated bone diseases.

IL-17A SIGNALING PATHWAY AND FUNCTION

The IL-17 family includes six major isoforms: IL-17A, IL-17B, IL-17C, IL-17D, IL-17E, and IL-17F. Six of these isoforms interact with the five receptors (IL-17RA-E), respectively (1). IL-17A was the first member discovered and the most studied of the IL-17 family. Thereafter, following large-scale sequencing of the human and other vertebrate genomes, additional isoforms homologous to IL-17A were found (2). In 1993, Rouvier et al. cloned IL-17 for the first time. IL-17 was initially called the murine cytotoxic T lymphocyte-associated antigen-8 (mCTLA8) and was found to share 57% homology with the open reading frame 13 (ORF13) of Herpesvirus saimiri (HVS) (3). Subsequently, Yao et al. and Fossiez et al. cloned IL-17A in 1995 and 1996, respectively. Humans and mice share 25% amino acid sequence homology in IL-17A (4). IL-17A has been reported to be involved in inflammation and hematopoiesis and its secretion might be restricted to activated memory $CD4^+$ T cells (4, 5). Current studies indicate that IL-17A is mainly produced by a special $CD4^+$ T cell subtype, Th17 cells (6). In addition, other types of lymphocytes including $IL\text{-}17^+$ $CD8^+$ T cells (Tc17 cells) (7), invariant natural killer T (8), $Foxp3^+$ Treg cells (9), γδ T cells (10), lymphoid–tissue inducer (LTi)–like cells (11), innate lymphoid cell (ILC3) (12), and NK cells can produce IL-17A. Besides, lymphocytes, myeloid cells including macrophages/monocytes (13), neutrophils (14), mast cells (15), Paneth cells (16) can secret IL-17A. Moreover, fibroblasts can also produce IL-17A (17). Multiple cytokines affect the expression of IL-17A, IL-1β, tumor necrosis factor (TNF)-β, IL-21, and IL-23 stimulate the expression of IL-17A in T cells (18), while interferon (IFN)-α inhibits the expression of IL-17A in T cells (19). Thus, IL-17A is derived from a variety of immune and inflammatory cells and its expression is regulated by a variety of immune factors.

IL-17A interacts with its receptors to activate downstream regulators and trigger cellular responses. Receptors for IL-17A are ubiquitously expressed on the cellular surface including synoviocytes, chondrocytes, fibroblasts, monocytes/macrophages, mast cells (20, 21). Bone cells including osteoclasts and osteoblasts also express IL-17RA (22). The interaction between IL-17RA and IL-17RC forms a complex to mediate the functions of IL-17A. The binding of IL-17A to the related receptor sites of IL-17RA alters the affinity and specificity of the symmetry receptor site. This response promotes the form of IL-17RA/RC heterodimer and makes an optimal response to mediate the functions of IL-17A homodimers (23, 24). Both IL-17RA and IL-17RC are type I transmembrane proteins. IL-17RA includes two extracellular fibronectin II-like domains and two intracellular "SEFIR" domains (25, 26). The SEFIR is homologous to Toll-IL-1R (TIR) domains found in the TLR/IL-1R family and is crucial for triggering downstream signaling events. IL-17A binds to its heterodimeric receptors complex and then recruits Act1 to activate classic IL-17A signaling cascades through receptor-associated factor 6 (TRAF6) proteins. TRAF6 binding subsequently triggers the mitogen-activated protein kinase (MAPK) pathway, extracellular signal–regulated kinase 1/2 (ERK1/2) pathway, and nuclear factor-κB (NF-κB) pathway. Among the non-classical signaling pathways, IL-17A integrates with epidermal growth factor receptor (EGFR), Notch 1, homolog translocation-associated (NOTCH1), C-type lectin receptor components, and interacts with fibroblast growth factor (FGF) signaling to initiate downstream biological responses (27).

In physiological conditions, IL-17A, as an immune and inflammatory-related factor, plays a protective role in host defenses against many bacterial and fungal pathogens (28). IL-17A activates neutrophils to promote neutrophil recruitment and accumulation (29). Meanwhile, IL-17A also affects the activity of B and T cells to act as a bridge between innate and acquired immune responses. Many studies have suggested that IL-17A is involved in the pathophysiological process of multiple diseases, including inflammatory bowel disease, breast cancer (30), lung cancer (31), cardiovascular system (32), uveitis (33), rheumatoid arthritis (RA), and psoriasis.

EFFECTS OF IL-17A ON THE SKELETAL SYSTEM

Osteoclasts

The skeleton maintains physiological function through a dynamic balance of bone formation and resorption. Osteoclasts derive from the monocyte/macrophage lineage and are key players in bone resorption. IL-17A acts directly on osteoclast precursors. Exposure to IL-17A (0.1–1 ng/ml) induces the expression of colony-stimulating factor-1 receptor (c-Fms) and receptor activator of nuclear factor-κB (RANK) on human peripheral blood mononuclear cells (hPBMCs), thereby promoting more hPBMCs to differentiate into functional osteoclasts. The effect is not dose-dependent, but 1 ng/ml of IL-17A shows the best induction (34). The direct effect of IL-17A on osteoclast precursors seems to be dependent on its concentration. A low concentration of IL-17A (0.5ng/ml) promotes autophagy of osteoclast precursors by activating the RANKL-JNK signaling pathway, thereby enhancing RANKL-induced osteoclast differentiation. However, treatment with a high concentration of IL-17A (5–50 ng/ml) inhibits autophagy and decreases osteoclast formation (35). In addition, a low level of IL-17A can reduce the apoptosis of osteoclasts and thus increases the number of osteoclasts by targeting the RANKL-Beclin1-autophagy-TRAF3 pathway (36). In turn, high levels of IL-17A increase apoptosis of osteoclasts and ultimately reduce pro-osteoclast mediators including cathepsin K, tartrate-resistant acid phosphatase (TRAP), and matrix metalloproteinase (MMP)-9 (36, 37). Interestingly, a higher concentration of IL-17A (100 ng/ml) promotes RANKL-induced polynuclear osteoclast formation and increases the expression of RANK and TRAP (38) (**Figure 1**).

Conversely, IL-17A can regulate osteoclast formation by targeting osteoclast-supporting cells. When activated by IL-17A, human bone marrow-derived mesenchymal stem cells

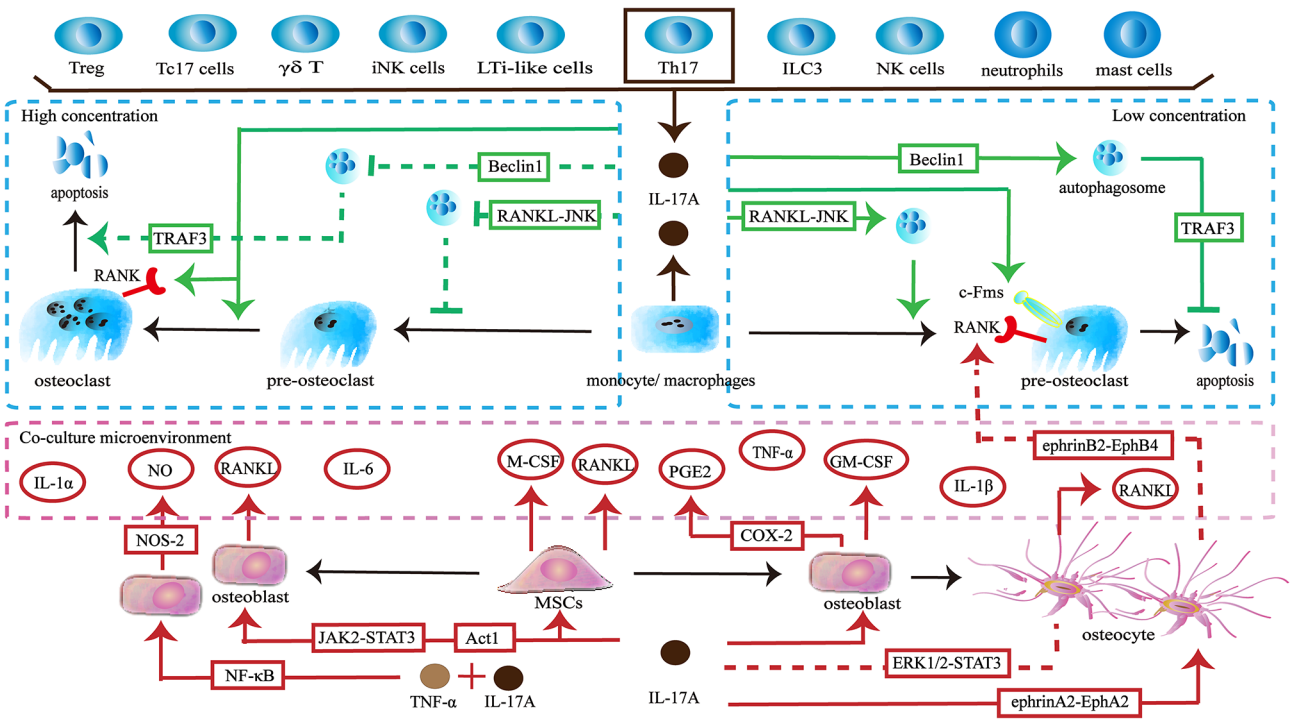

FIGURE 1 | Effects of IL-17A on osteoclasts. ① IL-17A is produced by multiple lymphocytes including Treg cells, IL-17$^+$ CD8$^+$ T cells (Tc17 cells), γδ T cells, invariant natural killer T (iNK cells), and Th17 cells. Myeloid cells including macrophages/monocytes, neutrophils and mast cells can also secrete IL-17A. Th17 cells are the main source of IL-17A. ② Low concentrations of IL-17A promote osteoclastogenesis through the RANKL-JNK signaling pathway and reduces the apoptosis of osteoclasts through the RANKL-Beclin1-autophagy-TRAF3 pathway. IL-17A increases the expression of c-Fms in osteoclast precursors to promote proliferation and differentiation. IL-17A increases the number of RANK$^+$ osteoclast precursors to influence subsequent RANKL-dependent osteoclastogenesis. ③ High concentration of IL-17A (5–50 ng/ml) inhibits osteoclastogenesis through the RANKL-JNK signaling pathway and promotes the apoptosis of osteoclasts through the RANKL-Beclin1-autophagy-TRAF3 pathway. However, a higher concentration of IL-17A (100 ng/ml) increases the number of RANK+ osteoclast precursors and induces polynuclear osteoclast formation. ④ IL-17A acts on osteoclast-supporting cells including mesenchymal stem cells, osteoblasts and osteocytes to produce various cytokines and molecules to regulate osteoclastogenesis indirectly.

(hBM-MSCs) secrete M-CSF and RANKL, thereby supporting osteoclastogenesis (39). When IL-17A binds to its receptors IL-17RA SEFIR/TILL domain on pre-osteoclasts, they trigger Act1 adaptor protein and may activate downstream JAK2-STAT3 signaling to promote the expression of RANKL (40–43). The upregulation of RANKL and the increase the ratio of RANKL/osteoprotegerin (OPG) promotes osteoclastogenesis (44, 45). Moreover, IL-17A stimulates osteoblast precursors to produce cyclooxygenase-2 (COX-2) related-prostaglandin E2 (PGE2), which is a facilitated factor in osteoclasts formation (46). The synergistic effects of IL-17A and TNF-α activate NF-κB-dependent pathways to promote the production of nitric oxide synthase-2 (NOS-2) and nitric oxide (NO). NO triggers the RANKL-RANK pathway to increase osteoclastic bone resorption (47). In addition, IL-17A and TNF-α synergistically induce osteoblast precursors to produce inflammatory factors including IL-1α, IL-1β and IL-6. These cytokines can up-regulate osteoclast activity (48). When activated by IL-17A, osteocytes inhibit the ERK1/2-STAT3 pathway and increase the RANKL/OPG ratio and TNF-α, thereby enhancing osteoclast formation. Furthermore, due to the activation of reversed ephrinA2-EphA2 signaling and suppression of ephrinB2-EphB4 signaling between osteocytes and osteoclast precursors, RANK$^+$ bone marrow macrophages (BMMs) are increased, which influences subsequent RANKL-dependent osteoclastogenesis (49). In addition to providing osteoclastic activating factors, IL-17A can promote the expression of inhibitory factors. IL-17A promotes osteoblasts to produce granulocyte-macrophage colony-stimulating factor (GM-CSF), which in turn reduces the expression of RANK in osteoclast precursors and thus may weaken RANKL-RANK signaling to inhibit osteoclastogenesis (50). Moreover, GM-CSF maintains monocytes in an undifferentiated state by downregulating c-Fos, Fra-1, and nuclear factor of activated T cells 1 (Nfatc1) (51) (**Figure 1**).

The *in vitro* effects of IL-17A on osteoclasts are dual. Recent findings indicate that the direct effects of IL-17A on osteoclastogenesis are related to its concentration, but are not dose-dependent. Low concentration of IL-17A promotes osteoclastogenesis, while IL-17A begins to inhibit the formation of osteoclasts as the concentration increases. Strangely, further increases in the concentrations of IL-17A promote osteoclastogenesis. The precise relationship requires further exploration. In addition, IL-17A is involved in osteoclastogenesis *via* other types of cells and factors. The

integrated network of cells and the factors they produce makes the specific effects attributable to IL-17A difficult to determine. The dominant effect may vary in different states. Thus, the role of IL-17A needs to be explored in more complex environments *in vivo*.

Osteoblasts

The osteoblast is another important player involved in maintaining bone homeostasis. When IL-17A binds receptors on pre-osteoblasts, it promotes their proliferation in a dose-dependent manner (49, 52, 53). When IL-17A activates TRAF6 and Act1 to initiate Ras-related C3 botulinum toxin substrate 1 guanosine triphosphatase (Rac1 GTPase) and NADPH oxidase 1 (Nox1), the expression of reactive oxygen species (ROS) is upregulated to promote pre-osteoblasts proliferation (39).

Slightly confusingly, the effects of IL-17A on osteoblastic differentiation *in vitro* are fraught with contradictions. A study showed that IL−17A promoted the differentiation of murine pre-osteoblastic MC3T3−E1 through the phosphoinositide 3-kinase-serine/threonine kinases (PI3K-AKT) pathway, whereas another study showed that IL−17A of the same concentration inhibited osteoblastic differentiation of MC3T3-E1 (54, 55). IL-17A can cause an increase in the osteoblastic differentiation of murine calvarial osteoblasts by up-regulating the expression of genes involved in osteoblastic differentiation including Runx2, ALP, osterix, osteocalcin and type I collagen (Colla1), osteoprotegerin (OPG), bone sialoprotein (Ibsp), and osteopontin (Spp1) (43, 44). However, IL-17A inhibits osteogenic differentiation of rat calvarial osteoblast cells by down-regulating expression of genes involved in osteoblastic differentiation including Runx2, ALP, osterix, osteocalcin and type I collagen (56, 57). Different species lead to the expressed differential of IL-17R, which might partly explain this opposite effect (56). When activated by IL-17A, mice bone marrow mesenchymal stem cells (BM-MSCs) secrete IL-6 and IL-1β, thereby activating the AKT, STAT3, and ERK1/2 pathways to promote osteoblastic differentiation (55). However, IL-17A inhibits the Wnt signaling, resulting in reduced levels of osteoblast differentiation markers (osterix and osteocalcin) and early osteocyte markers (Dmp1 and Phex), thereby inhibiting osteoblastic differentiation of BM-MSCs (52). Moreover, IL-17A increases the expression of N-cadherin to inhibit PTHR1-LRP-6 interaction in osteoblasts, which also can inhibit the Wnt-signaling pathway (58) (**Figure 2**).

Studies involving human pre-osteoblasts have indicated that IL-17A could promote bone-derived cells to differentiate into osteoblasts through JAK2/STAT3 signaling (59). In addition, IL-17A promotes the differentiation of hBM-MSCs into osteoblasts and promotes the mineralization of osteoblasts by upregulating bone formation-related gene ALP and Runx2 (39). The synergistic effects of IL-17A and bone morphogenetic protein-2 (BMP-2) promote the osteogenic differentiation of hBM-MSCs (60). Besides, the synergistic effects of IL-17A and TNF-α enhance osteogenic differentiation and mineralization of hBM-MSCs by down-regulating Dickkopf-1 (DKK-1), an inhibitor of the Wnt-signaling pathway (61). Osteoblasts and adipocytes are differentiated from a common pluripotent precursor, the mesenchymal stem cell (MSC). Many studies have suggested the differentiation decision of osteoblasts and adipocytes is delicately balanced and may even have a competitive relationship. IL-17A may steer mesenchymal stem cells into an osteogenic fate. IL-17A activates COX-2-induced prostaglandin E2 to inhibit lipid-related proteins include PPAR-γ, FABP4, and adiponectin. Therefore, the differentiation of hBM-MSCs into adipocytes is reduced (62). However, one study indicated that IL-17A inhibited osteogenic differentiation with up-regulated expression of the Wnt antagonist secreted frizzled-related protein 1 (sFRP1) and down-regulated expression of Wnt3 and Wnt6 in hBM-MSCs (63) (**Figure 2**).

The *in vitro* effects of IL-17A on osteoblasts are difficult to be defined. The effects of IL-17A on osteoblasts may not depend on the concentrations. IL-17A probably exerts distinct roles depending on the *in vitro* model used to assess osteoblast development. In addition, different species may also be partly responsible for the controversial results. It is not excluded that the different experimental methods also influence results. To achieve the precise effects of IL-17A on osteoblasts, the type of *in vitro* model, the correspondence between *in vitro* or *in vivo* effects, and the similarity of the effects between animal models and humans should be considered.

EFFECTS OF IL-17A ON BONE DISEASE

The knockout of IL-17A or its receptors in animal models does not affect bone mass, osteoclast numbers, or osteoblast numbers (34, 40, 64–66). Moreover, neutralizing antibodies directed against IL-17A in wild-type mice also do not influence bone mass (65). These results indicate that IL-17A might not have any effect on bone under normal physiological conditions, and it only plays a role in inflammatory conditions or injury. The involvement of IL-17A in immune-mediated bone disease is worthy of exploration.

Postmenopausal Osteoporosis

Women undergoing natural menopause often experience postmenopausal osteoporosis (PMOP) with a decrease in bone mineral density (BMD) and an increased risk of fractures (67). Estrogen deficiency is the pivotal reason for PMOP. Estrogen deficiency increases osteoclast formation by increasing the number of hematopoietic progenitors and recruiting osteoclast progenitors. Likewise, estrogen deficiency allows prolonged survival of osteoclasts, and the net increase in bone resorption leads to bone loss (68, 69). Recent studies show that osteoimmunology is involved in the pathogenesis of PMOP. Furthermore, T-cell activity is increased while B-cell activity is decreased in postmenopausal women (70, 71). Estrogen deficiency can activate T cells and promotes the production of a variety of immune factors. These factors include IL-6 (72), TNF-α (73), IFN-γ (74), IL-1β, and TNF-β (75), all of which enhance bone loss.

Despite one study showing that the level of serum IL-17A in postmenopausal women with low BMD is not significantly different from that in women with normal BMD (76), other studies have indicated that postmenopausal women with

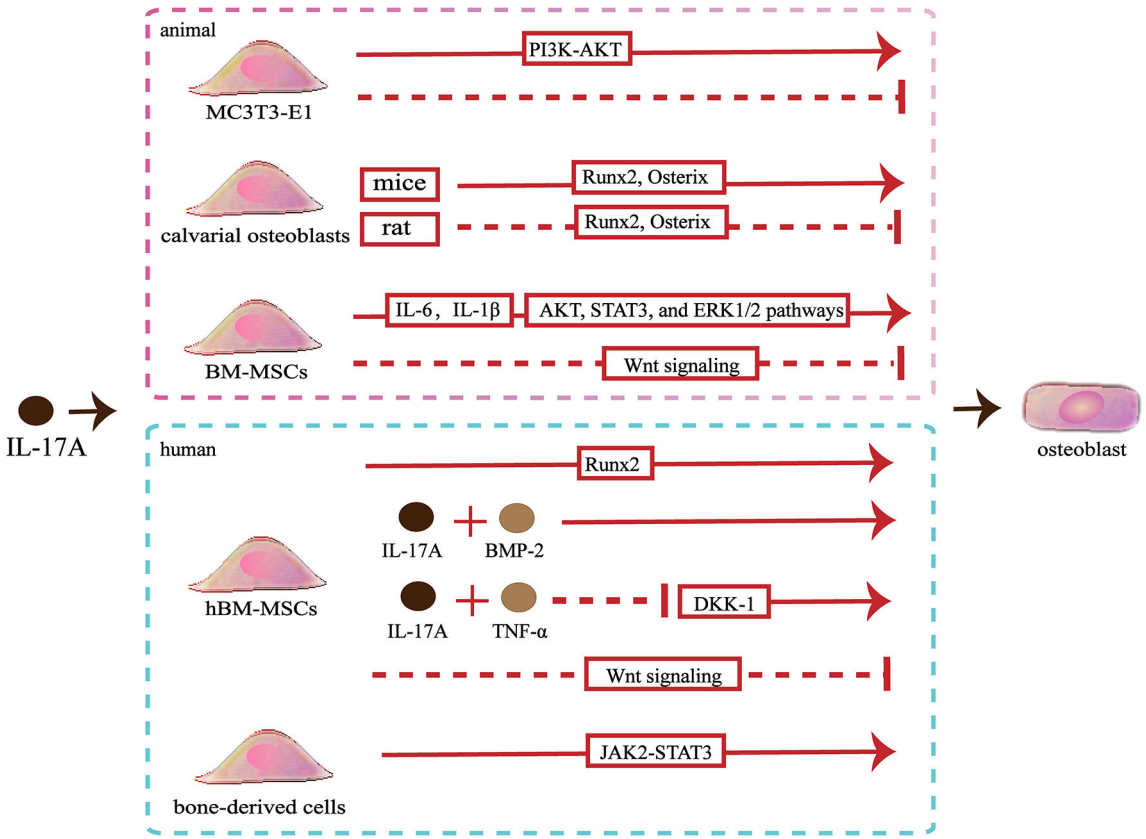

FIGURE 2 | Effects of IL-17A on osteoblasts. ①IL−17A promotes MC3T3-E1 to differentiate into osteoblasts by activating the PI3K-AKT signaling pathways, whereas another study indicated that IL-17A inhibited osteoblastic differentiation of MC3T3-E1. ② IL-17A upregulates Runx2 and osterix expression to promote mice calvarial osteoblast to differentiate into mature osteoblast, whereas downregulates Runx2 and osterix expression to inhibit rat calvarial osteoblast to differentiate into mature osteoblast. ③ IL-17A promotes the secrete of IL-6 and IL-1β to activate the AKT, STAT3, and ERK1/2 pathways and promotes osteoblastic differentiation of bone marrow mesenchymal stem cells (BM-MSCs), whereas IL-17A inhibits osteoblastic differentiation through inhibiting the Wnt signaling pathway.④ IL-17A promotes human BM-MSCs (hBM-MSCs) to differentiate into osteoblasts by upregulating Runx2 expression. IL-17A with bone morphogenetic protein-2 (BMP-2) or with tumor necrosis factor (TNF)-α synergistically enhance osteogenic differentiation. However, IL-17A inhibits osteoblastic differentiation of hBM-MSCs by inhibiting the Wnt signaling pathway. ⑤ IL-17A promotes bone-derived cells to differentiate into osteoblasts by activating the JAK2-STAT3 signaling pathways.

osteoporosis have a higher concentration of serum IL-17A, and have more peripheral blood IL-17-producing $CD4^+$ T-cells (58, 77–80). In postmenopausal women with osteoporosis, the concentration of serum IL-17A is negatively correlated with BMD, but is positively correlated with sRANKL level (78, 79).

In animal studies, ovariectomy (OVX) causes estrogen deficiency and bone loss. The drastic reduction of estrogen increases expression of the differentiation factors of Th17 including STAT3, ROR-α, and ROR-γt, which indicates that more peripheral blood mononuclear cells can differentiate into Th17 and produce IL-17A (80). The level of IL-17A in the bone marrow and blood are increased after OVX (38). IL-17RA knockdown and anti-IL17 antibody injection both protect against bone loss caused by estrogen deficiency (40). Anti-IL-17 antibodies and parathyroid hormone (PTH) can be used in combination to further protect OVX-induced bone loss (58, 81). Anti-IL17 antibodies exert a bone protective effect by inhibiting osteoclast formation, decreasing the apoptosis of osteoblasts and promoting the formation of mineralized nodules. Moreover, the blocking of IL-17A may inhibit osteoblasts to produce osteoclastogenic factors including TNF-α, IL-6, and RANKL in OVX mice (38, 40). Interestingly, anti-IL-17A antibodies have also been reported to reverse the higher frequency of $CD4^+$ T cells and the proliferation of $B220^+$ cells in bone marrow caused by estrogen deficiency. Anti-IL-17A antibodies exert an immuno-protective effect and translate to superior skeletal outcomes (81).

Rheumatoid Arthritis

RA is an autoimmune disease characterized by the upregulation of various immune factors that recruit and activate various immune cells, especially T and B cells to destroy cartilage and bone (82). RA patients have higher levels of IL-17A in synovial tissue and fluid compared with normal subjects (83–85). In a 2-year prospective study, the expression of IL-17A in synovial tissues was associated with increased joint damage progression in RA (86). Except for synovial tissue, RA patients have a higher concentration of serum IL-17A, which is proportional to the

severity of RA (87–90). Moreover, the PBMCs of patients with RA produce more IL-17A (91). The increased levels of IL-17A in synovial fluid, serum, PBMCs are associated with the Disease Activity Score of 28 joints (DAS28), and levels of C-reactive protein (CRP), the erythrocyte sedimentation rate (ESR), and rheumatoid factor (RF) expression (92, 93). In addition, evidence suggests that IL-17A is not only related to the progression of the disease but is also associates with the occurrence of the disease. Studies indicate that IL-17A plays an important role in the pre-onset, early, and chronic stages of RA (94, 95).

Collagen-induced arthritis (CIA) is the most common animal model for studies involving RA (96). High levels of IL-17A are detected in $CD4^+$ T cells and γδT cells located in joints of CIA mice (97). Th17 cells are localized adjacent to osteoclasts in the subarticular cartilage and express IL-17A, indicating the involvement of IL-17A in bone destruction of CIA (97). Local injection of IL-17A in the joint increases the morbidity of CIA and joint damage, while local injection of an adenoviral vector expressing murine IL-17A in the joint also accelerates the initiation of CIA and inflammation (98). Treatment with a soluble IL-17R fusion protein or anti-IL-17A antibody prevents bone erosion and the initiation of CIA (99, 100). In the progression of CIA, the local injection of IL-17A in knee-joint promotes arthritis and exacerbates joint damage (101). Anti-IL-17A antibodies ameliorate the severity of arthritis, cartilage damage, and bone loss (97, 102). Combinations that neutralize both TNF-α and IL-17A can also alleviate CIA progression (103). The combination of anti-IL-1β and anti-IL-17A antibodies significantly reduce the severity of arthritis, alleviates bone and cartilage damage, and down-regulates IL-1β, IL-6, IL-17A, IFN-γ, RANKL, and MMP-3 (104, 105). IL-17A plays an important role not only in the pathogenesis but also in the progression of the disease. Moreover, IL-17A is involved in the pathological process of bone erosion and bone loss.

The pathological mechanism of IL-17A may involve the immune activation and an immune cascade reaction in RA. In addition, the activation of osteoclasts promotes bone erosion in RA. Collagen-specific T cells and collagen-specific IgG2a are involved in the development of CIA. IL-17A is responsible for the priming of collagen-specific T cells and collagen-specific IgG2a production (106). Anti-IL-17A significantly reduces splenocytes proliferation and reduces leukocyte recruitment in CIA (105, 107). Anti-IL-17A also down-regulates IL-1β, IL-1, IL-6, IL-17A, and IFN-γ in the joint (104, 105). Increased osteoclast activity in the subchondral, trabecular, and cortical bone erosion areas is observed after local IL-17A overexpression in joint (98, 101, 102).

Several drugs targeting IL-17A are currently being evaluated in clinical trials, but the benefit seems to be not satisfactory for RA. Brodalumab, a human anti-IL-17 receptor A (IL-17RA) monoclonal antibody, did not demonstrate clinical efficacy in active RA patients (108). The humanized anti-IL-17A monoclonal antibody ixekizumab improved the signs and symptoms of RA patients in a phase II study, but the efficacy was not considered robust sufficient to support continued development (109). Bimekizumab is a monoclonal antibody that selectively neutralizes IL-17A and IL-17F. Bimekizumab plus certolizumab pegol further reduced disease activity score 28-joint count C-reactive protein (DAS28(CRP)) for RA patient in a phase II study, but more messages about the efficacy and safety is lack (110). Secukinumab, a fully human monoclonal antibody directed against IL-17A, has advanced in phase III studies. Secukinumab achieved 20% improvement in the American College of Rheumatology criteria (ACR20) at week 24 among patients with active RA, although, studies have suggested that secukinumab may not provide additional benefit beyond the currently approved therapies to such patients and further development was not pursued due to lack well-pleasing efficacy (111–114).

Psoriatic Arthritis

PsA is an immune-mediated chronic inflammatory arthritis associated with psoriasis. PsA presents synovial inflammation, bone destruction, and juxta-articular new bone formation (115, 116). Aberrant cytokine expression of TNF-α, IL-23, IL-22, IL-9, IL-15 is involved in the pathological mechanisms of PsA (117). Serum IL-17A levels are higher in psoriasis patients (118). $IL\text{-}17^+$ $CD4^+$ T cells and IL-17A secretion increase in peripheral blood and synovial fluid of PsA (119, 120). Besides $CD4^+$ T cells, IL-17A-producing ILCs are present in the synovial fluid of PsA (121). $IL\text{-}17A^+CD8^+$ T cells are enriched in the joints of patients with PsA and have been correlated with disease activity and bone erosion (7).

In the animal model of PsA, increased serum IL-17A is associated with bone loss. The imbalance between osteoblasts and osteoclasts is the main cause for the appearance of PsA in the bone. Skin-resident cells such as keratinocytes, γδT cells, and innate lymphoid cells express IL-17A, which inhibits osteoblasts and osteocytes function through the Wnt signaling (52). In addition, IL-17A may also promote epidermal sheet, keratinocytes and skin resident T cells to produce RANKL (122).

Clinical trials of antagonizing IL-17A in PsA are underway. Secukinumab improves the signs and symptoms of active PsA (123). At the same time, secukinumab inhibits the progression of bone erosions and maintains bone stability (124–127). In 2016, secukinumab became the first targeting IL-17A drug approved by the FDA for the treatment of active PsA. Ixekizumab, an IL-17A specific monoclonal antibody, improved the signs and symptoms of patients with active PsA and inhibited bone damage progression in PsA (128, 129). In 2017, ixekizumab was approved by the FDA for the treatment of PsA. Brodalumab, a fully human monoclonal antibody targeting the IL-17 RA, achieved ACR20 at week 16 among patients with PsA in a phase III study (130). However, the trials were terminated early due to a possible safety concern about suicidal ideation and behavior (131). Bimekizumab, which inhibits both IL-17A and IL-17F, improved ACR50 in patients with active PsA in a phase II trial and phase III trials that are currently underway (132).

Axial Spondyloarthritis

Axial spondyloarthritis (axSpA) is chronic inflammatory bone diseases including non-radiographic axial spondyloarthritis (nr-axSpA) and radiographic axial spondyloarthritis (ankylosing spondylitis [AS]). Bone destruction and new bone formation may occur simultaneously in axSpA. Various types of cytokines

including IL-17A, TNF-α and IL-23 are involved in the pathological processes (133, 134). Many studies have indicated that IL-17 is involved in immunopathogenesis of axSpA (135). IL-17$^+$ CD4$^+$ T cells increase in peripheral blood of axSpA and IL-17A synthesis also increases (120, 136–138). Levels of IL-17A in the synovial fluid are elevated in patients with AS (59). Serum IL-17A levels are also higher in AS and elevated IL-17 serum levels may associate with the development of AS (139, 140). A few studies have focused on the role of IL-17 in the processes of axSpA bone damage. IL-17A promotes local mesenchymal stem cell populations to osteoblast differentiation and increases mineralization in AS by JAK2/STAT3 signaling, which may be a mechanism of ankyloses progression (59). Anti-IL-17A treatment prevented bone loss and induced new bone formation in an animal model of pathogenic SpA, mycobacterium tuberculosis-induced disease in B27/hβ2m-transgenic rats (141).

Several IL-17A targeted drugs are currently in clinical trials. Secukinumab and Ixekizumab are both anti-interleukin-17A monoclonal antibodies and have been reported to improve the signs and symptoms of axSpA (142–148). To date, the FDA has approved both antibodies for the treatment of adults with active AS and nr-axSpA with objective signs of inflammation. Netakimab, a humanized monoclonal antibody targeting IL-17A, significantly achieved 20% improvement in Assessment of Spondyloarthritis International Society (ASAS20) response among patients with AS in a phase II study (149). Bimekizumab, a monoclonal antibody that selectively neutralizes IL-17A and IL-17F, achieved ASAS40 response at week 12 in a phase II trial (150). Phase III trials that aim to assess the efficacy and safety of netakimab and bimekizumab in AS patients are currently underway.

CONCLUSION AND PERSPECTIVES

IL-17A is involved in innate immune responses and adaptive immunity. Meanwhile, IL-17A plays an important role in bone homeostasis *via* activation of complex cellular and molecular interactions. IL-17A may exert direct positive or negative effects on osteoclastogenesis depending on its concentration *in vitro*. Osteoblasts are most closely associated with osteoclasts, which both are involved in bone metabolism. IL-17A indirectly regulates osteoclastogenesis by inducing multiple factors derived from the osteoclast-supporting cells. The effects of IL-17A on osteoblasts may depend on the different experimental models of osteoblast development and species tested *in vitro*. These aforementioned cell studies provide evidence supporting the skeletal-regulatory properties of IL-17A and support the concept that IL-17A acts as the link between the skeletal and the immune systems. Future research should focus on the molecular pathways involved and explore the precise reasons for the dual effects of IL-17A in bone cells.

Mechanistic studies have hinted that IL-17A is a bone-destroying cytokine involved in immune-mediated bone diseases, such as PMOP, RA, PsA, and axSpA. IL-17A exerts a negative effect on bone by promoting osteoclastogenesis, excessively activates bone formation, and initiates an immunologic cascade. Indeed anti-IL-17A therapy has produced promising results in clinical trials of RA, PsA, and axSpA, although, few studies have focused on bone damage. A deeper understanding of the molecular mechanisms of IL-17A involved in bone disease may supply novel therapeutic interventions and provide a new thought to prevent bone loss and osteoporosis associated with immune-mediated bone diseases.

AUTHOR CONTRIBUTIONS

XY provided the conception of the manuscript. MT and LL were contributed to perform the literature search and drafted the work. All authors contributed to the article and approved the submitted version.

FUNDING

This work was supported by grants from the National Natural Science Foundation of China [No. 81770875]; the Sichuan University [No. 2018SCUH0093]; the Post-Doctor Research Project, West China Hospital, Sichuan University [No.19HXBH053]; the Health and Family Planning Commission of Sichuan Province [No. 19PJ096]; and the 1.3.5 project for discipline of excellence, West China Hospital, Sichuan University [No. 2020HXFH008, No. ZYJC18003]; the National Clinical Research Center for Geriatrics of West China Hospital (No. Z2018B05).

REFERENCES

1. Liu S. Structural Insights into the Interleukin-17 Family Cytokines and Their Receptors. *Adv Exp Med Biol* (2019) 1172:97–117. doi: 10.1007/978-981-13-9367-9_5
2. Aggarwal S, Gurney AL. IL-17: prototype member of an emerging cytokine family. *J leukocyte Biol* (2002) 71(1):1–8. doi: 10.1189/jlb.71.1.1
3. Rouvier E, Luciani MF, Mattéi MG, Denizot F, Golstein P. CTLA-8, cloned from an activated T cell, bearing AU-rich messenger RNA instability sequences, and homologous to a herpesvirus saimiri gene. *J Immunol* (1993) 150(12):5445–56.
4. Yao Z, Painter SL, Fanslow WC, Ulrich D, Macduff BM, Spriggs MK, et al. Human IL-17: a novel cytokine derived from T cells. *J Immunol* (1995) 155 (12):5483–6.
5. Fossiez F, Djossou O, Chomarat P, Flores-Romo L, Ait-Yahia S, Maat C, et al. T cell interleukin-17 induces stromal cells to produce proinflammatory and hematopoietic cytokines. *J Exp Med* (1996) 183(6):2593–603. doi: 10.1084/jem.183.6.2593
6. Miossec P. IL-17 and Th17 cells in human inflammatory diseases. *Microbes Infect* (2009) 11(5):625–30. doi: 10.1016/j.micinf.2009.04.003
7. Menon B, Gullick NJ, Walter GJ, Rajasekhar M, Garrood T, Evans HG, et al. Interleukin-17+CD8+ T Cells Are Enriched in the Joints of Patients With Psoriatic Arthritis and Correlate With Disease Activity and Joint Damage Progression. *Arthritis Rheumatol* (2014) 66(5):1272–81. doi: 10.1002/art.38376
8. Venken K, Jacques P, Mortier C, Labadia ME, Decruy T, Coudenys J, et al. RORgammat inhibition selectively targets IL-17 producing iNKT and gammadelta-T cells enriched in Spondyloarthritis patients. *Nat Commun* (2019) 10(1):9. doi: 10.1038/s41467-018-07911-6

9. Zhu L, Song H, Zhang L, Meng H. Characterization of IL-17-producing Treg cells in type 2 diabetes patients. *Immunologic Res* (2019) 67(4-5):443–9. doi: 10.1007/s12026-019-09095-7
10. Coffelt SB, Kersten K, Doornebal CW, Weiden J, Vrijland K, Hau C-S, et al. IL-17-producing γδ T cells and neutrophils conspire to promote breast cancer metastasis. *Nature* (2015) 522(7556):345–8. doi: 10.1038/nature14282
11. Crellin NK, Trifari S, Kaplan CD, Cupedo T, Spits H. Human NKp44+IL-22+ cells and LTi-like cells constitute a stable RORC+ lineage distinct from conventional natural killer cells. *J Exp Med* (2010) 207(2):281–90. doi: 10.1084/jem.20091509
12. Triggianese P, Conigliaro P, Chimenti MS, Biancone L, Monteleone G, Perricone R, et al. Evidence of IL-17 producing innate lymphoid cells in peripheral blood from patients with enteropathic spondyloarthritis. *Clin Exp Rheumatol* (2016) 34(6):1085–93.
13. Okamoto N, Homma M, Kawaguchi Y, Kabasawa N, Uto Y, Hattori N, et al. Increased expression of interleukin-17 is associated with macrophages in chronic immune thrombocytopenia. *Int J Clin Exp Pathol* (2018) 11(5):2419–29.
14. Li L, Huang L, Vergis AL, Ye H, Bajwa A, Narayan V, et al. IL-17 produced by neutrophils regulates IFN-gamma-mediated neutrophil migration in mouse kidney ischemia-reperfusion injury. *J Clin Invest* (2010) 120 (1):331–42. doi: 10.1172/JCI38702
15. Hueber AJ, Asquith DL, Miller AM, Reilly J, Kerr S, Leipe J, et al. Mast cells express IL-17A in rheumatoid arthritis synovium. *J Immunol (Baltimore Md 1950)* (2010) 184(7):3336–40. doi: 10.4049/jimmunol.0903566
16. Takahashi N, Vanlaere I, de Rycke R, Cauwels A, Joosten LAB, Lubberts E, et al. IL-17 produced by Paneth cells drives TNF-induced shock. *J Exp Med* (2008) 205(8):1755–61. doi: 10.1084/jem.20080588
17. Sheibanie AF, Khayrullina T, Safadi FF, Ganea D. Prostaglandin E2 exacerbates collagen-induced arthritis in mice through the inflammatory interleukin-23/interleukin-17 axis. *Arthritis Rheum* (2007) 56(8):2608–19. doi: 10.1002/art.22794
18. Golebski K, Ros XR, Nagasawa M, van Tol S, Heesters BA, Aglmous H, et al. IL-1β, IL-23, and TGF-β drive plasticity of human ILC2s towards IL-17-producing ILCs in nasal inflammation. *Nat Commun* (2019) 10(1):2162. doi: 10.1038/s41467-019-09883-7
19. Chalise J, Narendra S, Paudyal B, Magnusson M. Interferon alpha inhibits antigen-specific production of proinflammatory cytokines and enhances antigen-specific transforming growth factor beta production in antigen-induced arthritis. *Arthritis Res Ther* (2013) 15(5):R143. doi: 10.1186/ar4326
20. Nesmond S, Muller C, Le Naour R, Viguier M, Bernard P, Antonicelli F, et al. Characteristic Pattern of IL-17RA, IL-17RB, and IL-17RC in Monocytes/Macrophages and Mast Cells From Patients With Bullous Pemphigoid. *Front Immunol* (2019) 10:2107:2107. doi: 10.3389/fimmu.2019.02107
21. Zrioual S, Toh ML, Tournadre A, Zhou Y, Cazalis MA, Pachot A, et al. IL-17RA and IL-17RC receptors are essential for IL-17A-induced ELR+ CXC chemokine expression in synoviocytes and are overexpressed in rheumatoid blood. *J Immunol (Baltimore Md 1950)* (2008) 180(1):655–63. doi: 10.4049/jimmunol.180.1.655
22. Shen F, Gaffen SL. Structure-function relationships in the IL-17 receptor: implications for signal transduction and therapy. *Cytokine* (2008) 41(2):92–104. doi: 10.1016/j.cyto.2007.11.013
23. Krstic J, Obradovic H, Kukolj T, Mojsilovic S, Okic-Dordevic I, Bugarski D, et al. An Overview of Interleukin-17A and Interleukin-17 Receptor A Structure, Interaction and Signaling. *Protein Pept Lett* (2015) 22(7):570–8. doi: 10.2174/0929866522666150520145554
24. Liu S, Song X, Chrunyk BA, Shanker S, Hoth LR, Marr ES, et al. Crystal structures of interleukin 17A and its complex with IL-17 receptor A. *Nat Commun* (2013) 4:1888. doi: 10.1038/ncomms2880
25. Gaffen SL. Structure and signalling in the IL-17 receptor family. *Nat Rev Immunol* (2009) 9(8):556–67. doi: 10.1038/nri2586
26. Gaffen S. IL-17 receptor composition. *Nat Rev Immunol* (2016) 16(1):4. doi: 10.1038/nri.2015.2
27. Li X, Bechara R, Zhao J, McGeachy MJ, Gaffen SL. IL-17 receptor-based signaling and implications for disease. *Nat Immunol* (2019) 20(12):1594–602. doi: 10.1038/s41590-019-0514-y
28. Cypowyj S, Picard C, Maródi L, Casanova JL, Puel A. Immunity to infection in IL-17-deficient mice and humans. *Eur J Immunol* (2012) 42(9):2246–54. doi: 10.1002/eji.201242605
29. Zenobia C, Hajishengallis G. Basic biology and role of interleukin-17 in immunity and inflammation. *Periodontol 2000* (2015) 69(1):142–59. doi: 10.1111/prd.12083
30. Fabre JAS, Giustinniani J, Garbar C, Merrouche Y, Antonicelli F, Bensussan A. The Interleukin-17 Family of Cytokines in Breast Cancer. *Int J Mol Sci* (2018) 19(12):3880. doi: 10.3390/ijms19123880
31. Wu F, Xu J, Huang Q, Han J, Duan L, Fan J, et al. The Role of Interleukin-17 in Lung Cancer. *Mediators Inflammation* (2016) 2016:8494079. doi: 10.1155/2016/8494079
32. Robert M, Miossec P. Effects of Interleukin 17 on the cardiovascular system. *Autoimmun Rev* (2017) 16(9):984–91. doi: 10.1016/j.autrev.2017.07.009
33. Guedes MC, Borrego LM, Proença RD. Roles of interleukin-17 in uveitis. *Indian J Ophthalmol* (2016) 64(9):628–34. doi: 10.4103/0301-4738.194339
34. Adamopoulos IE, Chao CC, Geissler R, Laface D, Blumenschein W, Iwakura Y, et al. Interleukin-17A upregulates receptor activator of NF-kappaB on osteoclast precursors. *Arthritis Res Ther* (2010) 12(1):R29. doi: 10.1186/ar2936
35. Ke D, Fu X, Xue Y, Wu H, Zhang Y, Chen X, et al. IL-17A regulates the autophagic activity of osteoclast precursors through RANKL-JNK1 signaling during osteoclastogenesis in vitro. *Biochem Biophys Res Commun* (2018) 497 (3):890–6. doi: 10.1016/j.bbrc.2018.02.164
36. Xue Y, Liang Z, Fu X, Wang T, Xie Q, Ke D. IL-17A modulates osteoclast precursors' apoptosis through autophagy-TRAF3 signaling during osteoclastogenesis. *Biochem Biophys Res Commun* (2019) 508(4):1088–92. doi: 10.1016/j.bbrc.2018.12.029
37. Kitami S, Tanaka H, Kawato T, Tanabe N, Katono-Tani T, Zhang F, et al. IL-17A suppresses the expression of bone resorption-related proteinases and osteoclast differentiation via IL-17RA or IL-17RC receptors in RAW264.7 cells. *Biochimie* (2010) 92(4):398–404. doi: 10.1016/j.biochi.2009.12.011
38. Tyagi AM, Srivastava K, Mansoori MN, Trivedi R, Chattopadhyay N, Singh D. Estrogen deficiency induces the differentiation of IL-17 secreting Th17 cells: a new candidate in the pathogenesis of osteoporosis. *PloS One* (2012) 7 (9):e44552. doi: 10.1371/journal.pone.0044552
39. Huang H, Kim HJ, Chang EJ, Lee ZH, Hwang SJ, Kim HM, et al. IL-17 stimulates the proliferation and differentiation of human mesenchymal stem cells: implications for bone remodeling. *Cell Death Differ* (2009) 16 (10):1332–43. doi: 10.1038/cdd.2009.74
40. DeSelm CJ, Takahata Y, Warren J, Chappel JC, Khan T, Li X, et al. IL-17 mediates estrogen-deficient osteoporosis in an Act1-dependent manner. *J Cell Biochem* (2012) 113(9):2895–902. doi: 10.1002/jcb.24165
41. Zhang F, Wang CL, Koyama Y, Mitsui N, Shionome C, Sanuki R, et al. Compressive force stimulates the gene expression of IL-17s and their receptors in MC3T3-E1 cells. *Connective Tissue Res* (2010) 51(5):359–69. doi: 10.3109/03008200903456942
42. Funaki Y, Hasegawa Y, Okazaki R, Yamasaki A, Sueda Y, Yamamoto A, et al. Resolvin E1 Inhibits Osteoclastogenesis and Bone Resorption by Suppressing IL-17-induced RANKL Expression in Osteoblasts and RANKL-induced Osteoclast Differentiation. *Yonago Acta Med* (2018) 61 (1):8–18. doi: 10.33160/yam.2018.03.002
43. Wang Z, Tan J, Lei L, Sun W, Wu Y, Ding P, et al. The positive effects of secreting cytokines IL-17 and IFN-γ on the early-stage differentiation and negative effects on the calcification of primary osteoblasts in vitro. *Int Immunopharmacol* (2018) 57:1–10. doi: 10.1016/j.intimp.2018.02.002
44. Kim HJ, Seo SJ, Kim J-Y, Kim Y-G, Lee Y. IL-17 promotes osteoblast differentiation, bone regeneration, and remodeling in mice. *Biochem Biophys Res Commun* (2020) 55(4):1044–50. doi: 10.1016/j.bbrc.2020.02.054
45. Li JY, Yu M, Tyagi AM, Vaccaro C, Hsu E, Adams J, et al. IL-17 Receptor Signaling in Osteoblasts/Osteocytes Mediates PTH-Induced Bone Loss and Enhances Osteocytic RANKL Production. *J Bone mineral Res Off J Am Soc Bone Mineral Res* (2019) 34(2):349–60. doi: 10.1002/jbmr.3600
46. Zhang F, Tanaka H, Kawato T, Kitami S, Nakai K, Motohashi M, et al. Interleukin-17A induces cathepsin K and MMP-9 expression in osteoclasts via celecoxib-blocked prostaglandin E2 in osteoblasts. *Biochimie* (2011) 93 (2):296–305. doi: 10.1016/j.biochi.2010.10.001
47. Van Bezooijen RL, Papapoulos SE, Lowik CW. Effect of interleukin-17 on nitric oxide production and osteoclastic bone resorption: is there dependency on nuclear factor-kappaB and receptor activator of nuclear factor kappaB (RANK)/RANK ligand signaling? *Bone* (2001) 28(4):378–86. doi: 10.1016/s8756-3282(00)00457-9

48. Van bezooijen RL, Farih-Sips HC, Papapoulos SE, Lowik CW. Interleukin-17: A new bone acting cytokine in vitro. *J Bone mineral Res Off J Am Soc Bone Mineral Res* (1999) 14(9):1513–21. doi: 10.1359/jbmr.1999.14.9.1513
49. Liao C, Cheng T, Wang S, Zhang C, Jin L, Yang Y. Shear stress inhibits IL-17A-mediated induction of osteoclastogenesis via osteocyte pathways. *Bone* (2017) 101:10–20. doi: 10.1016/j.bone.2017.04.003
50. Balani D, Aeberli D, Hofstetter W, Seitz M. Interleukin-17A stimulates granulocyte-macrophage colony-stimulating factor release by murine osteoblasts in the presence of 1,25-dihydroxyvitamin D(3) and inhibits murine osteoclast development in vitro. *Arthritis Rheum* (2013) 65 (2):436–46. doi: 10.1002/art.37762
51. Atanga E, Dolder S, Dauwalder T, Wetterwald A, Hofstetter W. TNFalpha inhibits the development of osteoclasts through osteoblast-derived GM-CSF. *Bone* (2011) 49(5):1090–100. doi: 10.1016/j.bone.2011.08.003
52. Uluçkan Ö, Jimenez M, Karbach S, Jeschke A, Graña O, Keller J, et al. Chronic skin inflammation leads to bone loss by IL-17-mediated inhibition of Wnt signaling in osteoblasts. *Sci Transl Med* (2016) 8(330):330ra37. doi: 10.1126/scitranslmed.aad8996
53. Huang W, La Russa V, Alzoubi A, Schwarzenberger P. Interleukin-17A: a T-cell-derived growth factor for murine and human mesenchymal stem cells. *Stem Cells (Dayton Ohio)* (2006) 24(6):1512–8. doi: 10.1634/stemcells.2005-0156
54. Tan J-Y, Lei L-H, Chen X-T, Ding P-H, Wu Y-M, Chen L-L. AKT2 is involved in the IL−17A−mediated promotion of differentiation and calcification of murine preosteoblastic MC3T3−E1 cells. *Mol Med Rep* (2017) 16(5):5833–40. doi: 10.3892/mmr.2017.7315
55. Liao C, Zhang C, Jin L, Yang Y. IL-17 alters the mesenchymal stem cell niche towards osteogenesis in cooperation with osteocytes. *J Cell Physiol* (2020) 235(5):4466–80. doi: 10.1002/jcp.29323
56. Kim YG, Park JW, Lee JM, Suh JY, Lee JK, Chang BS, et al. IL-17 inhibits osteoblast differentiation and bone regeneration in rat. *Arch Oral Biol* (2014) 59(9):897–905. doi: 10.1016/j.archoralbio.2014.05.009
57. Zhang J-R, Pang D-D, Tong Q, Liu X, Su D-F, Dai S-M. Different Modulatory Effects of IL-17, IL-22, and IL-23 on Osteoblast Differentiation. *Mediators Inflammation* (2017) 2017:5950395–. doi: 10.1155/2017/5950395
58. Mansoori MN, Shukla P, Singh D. Combination of PTH (1-34) with anti-IL17 prevents bone loss by inhibiting IL-17/N-cadherin mediated disruption of PTHR1/LRP-6 interaction. *Bone* (2017) 105:226–36. doi: 10.1016/j.bone.2017.09.010
59. Jo S, Wang SE, Lee YL, Kang S, Lee B, Han J, et al. IL-17A induces osteoblast differentiation by activating JAK2/STAT3 in ankylosing spondylitis. *Arthritis Res Ther* (2018) 20(1):115–. doi: 10.1186/s13075-018-1582-3
60. Croes M, Öner FC, van Neerven D, Sabir E, Kruyt MC, Blokhuis TJ, et al. Proinflammatory T cells and IL-17 stimulate osteoblast differentiation. *Bone* (2016) 84:262–70. doi: 10.1016/j.bone.2016.01.010
61. Osta B, Lavocat F, Eljaafari A, Miossec P. Effects of Interleukin-17A on Osteogenic Differentiation of Isolated Human Mesenchymal Stem Cells. *Front Immunol* (2014) 425. doi: 10.3389/fimmu.2014.00425
62. Shin JH, Shin DW, Noh M. Interleukin-17A inhibits adipocyte differentiation in human mesenchymal stem cells and regulates pro-inflammatory responses in adipocytes. *Biochem Pharmacol* (2009) 77 (12):1835–44. doi: 10.1016/j.bcp.2009.03.008
63. Wang Z, Jia Y, Du F, Chen M, Dong X, Chen Y, et al. IL-17A Inhibits Osteogenic Differentiation of Bone Mesenchymal Stem Cells via Wnt Signaling Pathway. *Med Sci Monit Int Med J Exp Clin Res* (2017) 23:4095–101. doi: 10.12659/msm.903027
64. Goswami J, Hernandez-Santos N, Zuniga LA, Gaffen SL. A bone-protective role for IL-17 receptor signaling in ovariectomy-induced bone loss. *Eur J Immunol* (2009) 39(10):2831–9. doi: 10.1002/eji.200939670
65. Li JY, D'Amelio P, Robinson J, Walker LD, Vaccaro C, Luo T, et al. IL-17A Is Increased in Humans with Primary Hyperparathyroidism and Mediates PTH-Induced Bone Loss in Mice. *Cell Metab* (2015) 22(5):799–810. doi: 10.1016/j.cmet.2015.09.012
66. Sato K, Suematsu A, Okamoto K, Yamaguchi A, Morishita Y, Kadono Y, et al. Th17 functions as an osteoclastogenic helper T cell subset that links T cell activation and bone destruction. *J Exp Med* (2006) 203(12):2673–82. doi: 10.1084/jem.20061775
67. Compston JE, McClung MR, Leslie WD. Osteoporosis. *Lancet* (2019) 393 (10169):364–76. doi: 10.1016/S0140-6736(18)32112-3
68. Black DM, Rosen CJ. Clinical Practice. Postmenopausal Osteoporosis. *New Engl J Med* (2016) 374(3):254–62. doi: 10.1056/NEJMcp1513724
69. Zhao R. Immune regulation of osteoclast function in postmenopausal osteoporosis: a critical interdisciplinary perspective. *Int J Med Sci* (2012) 9 (9):825–32. doi: 10.7150/ijms.5180
70. Faienza MF, Ventura A, Marzano F, Cavallo L. Postmenopausal osteoporosis: the role of immune system cells. *Clin Dev Immunol* (2013) 2013:575936. doi: 10.1155/2013/575936
71. D'Amelio P, Grimaldi A, Di Bella S, Brianza SZM, Cristofaro MA, Tamone C, et al. Estrogen deficiency increases osteoclastogenesis up-regulating T cells activity: a key mechanism in osteoporosis. *Bone* (2008) 43(1):92–100. doi: 10.1016/j.bone.2008.02.017
72. Zhong Z, Qian Z, Zhang X, Chen F, Ni S, Kang Z, et al. Tetrandrine Prevents Bone Loss in Ovariectomized Mice by Inhibiting RANKL-Induced Osteoclastogenesis. *Front Pharmacol* (2020) 10:1530. doi: 10.3389/fphar.2019.01530
73. Kim B-J, Bae SJ, Lee S-Y, Lee Y-S, Baek J-E, Park S-Y, et al. TNF-α mediates the stimulation of sclerostin expression in an estrogen-deficient condition. *Biochem Biophys Res Commun* (2012) 424(1):170–5. doi: 10.1016/j.bbrc.2012.06.100
74. Xiong Q, Zhang L, Ge W, Tang P. The roles of interferons in osteoclasts and osteoclastogenesis. *Joint bone Spine Rev du rhumatisme* (2016) 83(3):276–81. doi: 10.1016/j.jbspin.2015.07.010
75. Gao Y, Qian WP, Dark K, Toraldo G, Lin AS, Guldberg RE, et al. Estrogen prevents bone loss through transforming growth factor beta signaling in T cells. *Proc Natl Acad Sci USA* (2004) 101(47):16618–23. doi: 10.1073/pnas.0404888101
76. Mannucci C, Calapai G, Gangemi S. Commentary: Circulatory pattern of cytokines, adipokines and bone markers in postmenopausal women with low BMD. *Front Immunol* (2019) 10:2666. doi: 10.3389/fimmu.2019.02666
77. Zhao R, Wang X, Feng F. Upregulated Cellular Expression of IL-17 by CD4+ T-Cells in Osteoporotic Postmenopausal Women. *Ann Nutr Metab* (2016) 68(2):113–8. doi: 10.1159/000443531
78. Zhang J, Fu Q, Ren Z, Wang Y, Wang C, Shen T, et al. Changes of serum cytokines-related Th1/Th2/Th17 concentration in patients with postmenopausal osteoporosis. *Gynecol Endocrinol Off J Int Soc Gynecol Endocrinol* (2015) 31(3):183–90. doi: 10.3109/09513590.2014.975683
79. Molnár I, Bohaty I, Somogyiné-Vári É. IL-17A-mediated sRANK ligand elevation involved in postmenopausal osteoporosis. *Osteoporosis Int* (2014) 25(2):783–6. doi: 10.1007/s00198-013-2548-6
80. Shukla P, Mansoori MN, Singh D. Efficacy of anti-IL-23 monotherapy versus combination therapy with anti-IL-17 in estrogen deficiency induced bone loss conditions. *Bone* (2018) 110:84–95. doi: 10.1016/j.bone.2018.01.027
81. Tyagi AM, Mansoori MN, Srivastava K, Khan MP, Kureel J, Dixit M, et al. Enhanced immunoprotective effects by anti-IL-17 antibody translates to improved skeletal parameters under estrogen deficiency compared with anti-RANKL and anti-TNF-alpha antibodies. *J Bone mineral Res Off J Am Soc Bone Mineral Res* (2014) 29(9):1981–92. doi: 10.1002/jbmr.2228
82. Smolen JS, Aletaha D, McInnes IB. Rheumatoid arthritis. *Lancet (London England)* (2016) 388(10055):2023–38. doi: 10.1016/s0140-6736(16)30173-8
83. Chabaud M, Durand JM, Buchs N, Fossiez F, Page G, Frappart L, et al. Human interleukin-17: A T cell-derived proinflammatory cytokine produced by the rheumatoid synovium. *Arthritis Rheum* (1999) 42 (5):963–70. doi: 10.1002/1529-0131(199905)42:5<963::aid-anr15>3.0.co;2-e
84. Li N, Wang JC, Liang TH, Zhu MH, Wang JY, Fu XL, et al. Pathologic finding of increased expression of interleukin-17 in the synovial tissue of rheumatoid arthritis patients. *Int J Clin Exp Pathol* (2013) 6(7):1375–9.
85. Ziolkowska M, Koc A, Luszczykiewicz G, Ksiezopolska-Pietrzak K, Klimczak E, Chwalinska-Sadowska H, et al. High levels of IL-17 in rheumatoid arthritis patients: IL-15 triggers in vitro IL-17 production via cyclosporin A-sensitive mechanism. *J Immunol (Baltimore Md 1950)* (2000) 164 (5):2832–8. doi: 10.4049/jimmunol.164.5.2832
86. Kirkham BW, Lassere MN, Edmonds JP, Juhasz KM, Bird PA, Lee CS, et al. Synovial membrane cytokine expression is predictive of joint damage progression in rheumatoid arthritis: a two-year prospective study (the DAMAGE study cohort). *Arthritis Rheum* (2006) 54(4):1122–31. doi: 10.1002/art.21749
87. Siloşi I, Boldeanu MV, Cojocaru M, Biciuşcă V, Pădureanu V, Bogdan M, et al. The Relationship of Cytokines IL-13 and IL-17 with Autoantibodies Profile in Early Rheumatoid Arthritis. *J Immunol Res* (2016) 2016:3109135. doi: 10.1155/2016/3109135

88. Costa CM, Santos M, Pernambuco AP. Elevated levels of inflammatory markers in women with rheumatoid arthritis. *J Immunoassay Immunochem* (2019) 40(5):540–54. doi: 10.1080/15321819.2019.1649695
89. Schofield C, Fischer SK, Townsend MJ, Mosesova S, Peng K, Setiadi AF, et al. Characterization of IL-17AA and IL-17FF in rheumatoid arthritis and multiple sclerosis. *Bioanalysis* (2016) 8(22):2317–27. doi: 10.4155/bio-2016-0207
90. Lee YH, Bae SC. Associations between circulating IL-17 levels and rheumatoid arthritis and between IL-17 gene polymorphisms and disease susceptibility: a meta-analysis. *Postgraduate Med J* (1102) 2017) 93:465–71. doi: 10.1136/postgradmedj-2016-134637
91. Kim KW, Cho ML, Park MK, Yoon CH, Park SH, Lee SH, et al. Increased interleukin-17 production via a phosphoinositide 3-kinase/Akt and nuclear factor kappaB-dependent pathway in patients with rheumatoid arthritis. *Arthritis Res Ther* (2005) 7(1):R139–48. doi: 10.1186/ar1470
92. Roşu A, Mărgăritescu C, Stepan A, Muşetescu A, Ene M. IL-17 patterns in synovium, serum and synovial fluid from treatment-naïve, early rheumatoid arthritis patients. *Romanian J Morphol Embryol = Rev roumaine morphologie embryologie* (2012) 53(1):73–80.
93. El-Maghraby HM, Rabie RA, Makram WK. Correlation between Relative Expression of IL 17 and PERP in Rheumatoid Arthritis Patients and Disease Activity. *Egyptian J Immunol* (2019) 26(2):19–29.
94. Kokkonen H, Söderström I, Rocklöv J, Hallmans G, Lejon K, Rantapää Dahlqvist S. Up-regulation of cytokines and chemokines predates the onset of rheumatoid arthritis. *Arthritis Rheum* (2010) 62(2):383–91. doi: 10.1002/art.27186
95. Raza K, Falciani F, Curnow SJ, Ross EJ, Lee CY, Akbar AN, et al. Early rheumatoid arthritis is characterized by a distinct and transient synovial fluid cytokine profile of T cell and stromal cell origin. *Arthritis Res Ther* (2005) 7(4):R784–95. doi: 10.1186/ar1733
96. Wu S, Meng Z, Zhang Y. Correlation between rheumatoid arthritis and immunological changes in a rheumatoid arthritis rat model. *J Biol Regul Homeostatic Agents* (2018) 32(6):1461–6.
97. Pollinger B, Junt T, Metzler B, Walker UA, Tyndall A, Allard C, et al. Th17 cells, not IL-17+ gammadelta T cells, drive arthritic bone destruction in mice and humans. *J Immunol (Baltimore Md 1950)* (2011) 186(4):2602–12. doi: 10.4049/jimmunol.1003370
98. Lubberts E, Joosten LA, van de Loo FA, Schwarzenberger P, Kolls J, van den Berg WB. Overexpression of IL-17 in the knee joint of collagen type II immunized mice promotes collagen arthritis and aggravates joint destruction. *Inflammation Res Off J Eur Histamine Res Soc [et al]* (2002) 51(2):102–4. doi: 10.1007/bf02684010
99. Bush KA, Farmer KM, Walker JS, Kirkham BW. Reduction of joint inflammation and bone erosion in rat adjuvant arthritis by treatment with interleukin-17 receptor IgG1 Fc fusion protein. *Arthritis Rheum* (2002) 46 (3):802–5. doi: 10.1002/art.10173
100. Lubberts E, Joosten LA, Oppers B, van den Bersselaar L, Coenen-de Roo CJ, Kolls JK, et al. IL-1-independent role of IL-17 in synovial inflammation and joint destruction during collagen-induced arthritis. *J Immunol (Baltimore Md 1950)* (2001) 167(2):1004–13. doi: 10.4049/jimmunol.167.2.1004
101. Lubberts E, van den Bersselaar L, Oppers-Walgreen B, Schwarzenberger P, Coenen-de Roo CJ, Kolls JK, et al. IL-17 promotes bone erosion in murine collagen-induced arthritis through loss of the receptor activator of NF-kappa B ligand/osteoprotegerin balance. *J Immunol (Baltimore Md 1950)* (2003) 170(5):2655–62. doi: 10.4049/jimmunol.170.5.2655
102. Lubberts E, Koenders MI, Oppers-Walgreen B, van den Bersselaar L, Coenen-de Roo CJJ, Joosten LAB, et al. Treatment with a neutralizing anti-murine interleukin-17 antibody after the onset of collagen-induced arthritis reduces joint inflammation, cartilage destruction, and bone erosion. *Arthritis Rheumatic* (2004) 50(2):650–9. doi: 10.1002/art.20001
103. Shen F, Verma AH, Volk A, Jones B, Coleman BM, Loza MJ, et al. Combined Blockade of TNF-α and IL-17A Alleviates Progression of Collagen-Induced Arthritis without Causing Serious Infections in Mice. *J Immunol* (2019) 202 (7):2017–26. doi: 10.4049/jimmunol.1801436
104. Zhang Y, Ren G, Guo M, Ye X, Zhao J, Xu L, et al. Synergistic effects of interleukin-1β and interleukin-17A antibodies on collagen-induced arthritis mouse model. *Int Immunopharmacol* (2013) 15(2):199–205. doi: 10.1016/j.intimp.2012.12.010
105. Li Q, Ren G, Xu L, Wang Q, Qi J, Wang W, et al. Therapeutic efficacy of three bispecific antibodies on collagen-induced arthritis mouse model. *Int Immunopharmacol* (2014) 21(1):119–27. doi: 10.1016/j.intimp.2014.04.018
106. Nakae S, Nambu A, Sudo K, Iwakura Y. Suppression of immune induction of collagen-induced arthritis in IL-17-deficient mice. *J Immunol (Baltimore Md 1950)* (2003) 171(11):6173–7. doi: 10.4049/jimmunol.171.11.6173
107. Chao CC, Chen SJ, Adamopoulos IE, Davis N, Hong K, Vu A, et al. Anti-IL-17A therapy protects against bone erosion in experimental models of rheumatoid arthritis. *Autoimmunity* (2011) 44(3):243–52. doi: 10.3109/08916934.2010.517815
108. Martin DA, Churchill M, Flores-Suarez L, Cardiel MH, Wallace D, Martin R, et al. A phase Ib multiple ascending dose study evaluating safety, pharmacokinetics, and early clinical response of brodalumab, a human anti-IL-17R antibody, in methotrexate-resistant rheumatoid arthritis. *Arthritis Res Ther* (2013) 15(5):R164. doi: 10.1186/ar4347
109. Genovese MC, Greenwald M, Cho CS, Berman A, Jin L, Cameron GS, et al. A phase II randomized study of subcutaneous ixekizumab, an anti-interleukin-17 monoclonal antibody, in rheumatoid arthritis patients who were naive to biologic agents or had an inadequate response to tumor necrosis factor inhibitors. *Arthritis Rheumatol* (2014) 66(7):1693–704. doi: 10.1002/art.38617
110. Glatt S, Taylor PC, McInnes IB, Schett G, Landewé R, Baeten D, et al. Efficacy and safety of bimekizumab as add-on therapy for rheumatoid arthritis in patients with inadequate response to certolizumab pegol: a proof-of-concept study. *Ann Rheumatic Dis* (2019) 78(8):1033–40. doi: 10.1136/annrheumdis-2018-214943
111. Genovese MC, Durez P, Richards HB, Supronik J, Dokoupilova E, Aelion JA, et al. One-year Efficacy and Safety Results of Secukinumab in Patients With Rheumatoid Arthritis: Phase II, Dose-finding, Double-blind, Randomized, Placebo-controlled Study. *J Rheumatol* (2014) 41(3):414–21. doi: 10.3899/jrheum.130637
112. Blanco FJ, Möricke R, Dokoupilova E, Codding C, Neal J, Andersson M, et al. Secukinumab in Active Rheumatoid Arthritis: A Phase III Randomized, Double-Blind, Active Comparator- and Placebo-Controlled Study. *Arthritis Rheumatol* (2017) 69(6):1144–53. doi: 10.1002/art.40070
113. Huang Y, Fan Y, Liu Y, Xie W, Zhang Z. Efficacy and safety of secukinumab in active rheumatoid arthritis with an inadequate response to tumor necrosis factor inhibitors: a meta-analysis of phase III randomized controlled trials. *Clin Rheumatol* (2019) 38(10):2765–76. doi: 10.1007/s10067-019-04595-1
114. Dokoupilová E, Aelion J, Takeuchi T, Malavolta N, Sfikakis PP, Wang Y, et al. Secukinumab after anti-tumour necrosis factor-α therapy: a phase III study in active rheumatoid arthritis. *Scand J Rheumatol* (2018) 47(4):276–81. doi: 10.1080/03009742.2017.1390605
115. de Vlam K, Gottlieb AB, Mease PJ. Current concepts in psoriatic arthritis: pathogenesis and management. *Acta Dermato Venereologica* (2014) 94 (6):627–34. doi: 10.2340/00015555-1833
116. Ritchlin CT, Colbert RA, Gladman DD. Psoriatic Arthritis. *New Engl J Med* (2017) 376(10):957–70. doi: 10.1056/NEJMra1505557
117. Veale DJ, Fearon U. The pathogenesis of psoriatic arthritis. *Lancet (London England)* (2018) 391(10136):2273–84. doi: 10.1016/s0140-6736(18)30830-4
118. Coimbra S, Oliveira H, Reis F, Belo L, Rocha S, Quintanilha A, et al. Interleukin (IL)-22, IL-17, IL-23, IL-8, vascular endothelial growth factor and tumour necrosis factor-α levels in patients with psoriasis before, during and after psoralen-ultraviolet A and narrowband ultraviolet B therapy. *Br J Dermatol* (2010) 163(6):1282–90. doi: 10.1111/j.1365-2133.2010.09992.x
119. Benham H, Norris P, Goodall J, Wechalekar MD, FitzGerald O, Szentpetery A, et al. Th17 and Th22 cells in psoriatic arthritis and psoriasis. *Arthritis Res Ther* (2013) 15(5):R136. doi: 10.1186/ar4317
120. Jandus C, Bioley G, Rivals JP, Dudler J, Speiser D, Romero P. Increased numbers of circulating polyfunctional Th17 memory cells in patients with seronegative spondylarthritides. *Arthritis Rheum* (2008) 58(8):2307–17. doi: 10.1002/art.23655
121. Leijten EF, van Kempen TS, Boes M, Michels-van Amelsfort JM, Hijnen D, Hartgring SA, et al. Brief report: enrichment of activated group 3 innate lymphoid cells in psoriatic arthritis synovial fluid. *Arthritis Rheumatol* (2015) 67(10):2673–8. doi: 10.1002/art.39261
122. Raimondo A, Lembo S, Di Caprio R, Donnarumma G, Monfrecola G, Balato N, et al. Psoriatic cutaneous inflammation promotes human monocyte differentiation into active osteoclasts, facilitating bone damage. *Eur J Immunol* (2017) 47(6):1062–74. doi: 10.1002/eji.201646774

123. McInnes IB, Mease PJ, Kirkham B, Kavanaugh A, Ritchlin CT, Rahman P, et al. Secukinumab, a human anti-interleukin-17A monoclonal antibody, in patients with psoriatic arthritis (FUTURE 2): a randomised, double-blind, placebo-controlled, phase 3 trial. *Lancet (London England)* (2015) 386 (9999):1137–46. doi: 10.1016/s0140-6736(15)61134-5
124. Mease P, van der Heijde D, Landewé R, Mpofu S, Rahman P, Tahir H, et al. Secukinumab improves active psoriatic arthritis symptoms and inhibits radiographic progression: primary results from the randomised, double-blind, phase III FUTURE 5 study. *Ann Rheumatic Dis* (2018) 77(6):890–7. doi: 10.1136/annrheumdis-2017-212687
125. Wu D, Li C, Zhang S, Wong P, Cao Y, Griffith JF, et al. Effect of biologics on radiographic progression of peripheral joint in patients with psoriatic arthritis: meta-analysis. *Rheumatol (Oxford England)* (2020) 59(11):3172–80. doi: 10.1093/rheumatology/keaa313
126. Kampylafka E, d'Oliveira I, Linz C, Lerchen V, Stemmler F, Simon D, et al. Resolution of synovitis and arrest of catabolic and anabolic bone changes in patients with psoriatic arthritis by IL-17A blockade with secukinumab: results from the prospective PSARTROS study. *Arthritis Res Ther* (2018) 20(1):153. doi: 10.1186/s13075-018-1653-5
127. Mease PJ, McInnes IB, Kirkham B, Kavanaugh A, Rahman P, van der Heijde D, et al. Secukinumab Inhibition of Interleukin-17A in Patients with Psoriatic Arthritis. *New Engl J Med* (2015) 373(14):1329–39. doi: 10.1056/NEJMoa1412679
128. Nash P, Kirkham B, Okada M, Rahman P, Combe B, Burmester GR, et al. Ixekizumab for the treatment of patients with active psoriatic arthritis and an inadequate response to tumour necrosis factor inhibitors: results from the 24-week randomised, double-blind, placebo-controlled period of the SPIRIT-P2 phase 3 trial. *Lancet (London England)* (2017) 389(10086): 2317–27. doi: 10.1016/s0140-6736(17)31429-0
129. Mease PJ, van der Heijde D, Ritchlin CT, Okada M, Cuchacovich RS, Shuler CL, et al. Ixekizumab, an interleukin-17A specific monoclonal antibody, for the treatment of biologic-naive patients with active psoriatic arthritis: results from the 24-week randomised, double-blind, placebo-controlled and active (adalimumab)-controlled period of the phase III trial SPIRIT-P1. *Ann Rheumatic Dis* (2017) 76(1):79–87. doi: 10.1136/annrheumdis-2016-209709
130. Mease PJ, Helliwell PS, Hjuler KF, Raymond K, McInnes I. Brodalumab in psoriatic arthritis: results from the randomised phase III AMVISION-1 and AMVISION-2 trials. *Ann Rheumatic Dis* (2020) 80(2):185–93. doi: 10.1136/annrheumdis-2019-216835
131. Foulkes AC, Warren RB. Brodalumab in psoriasis: evidence to date and clinical potential. *Drugs context* (2019) 8:212570. doi: 10.7573/dic.212570
132. Ritchlin CT, Kavanaugh A, Merola JF, Schett G, Scher JU, Warren RB, et al. Bimekizumab in patients with active psoriatic arthritis: results from a 48-week, randomised, double-blind, placebo-controlled, dose-ranging phase 2b trial. *Lancet (London England)* (2020) 395(10222):427–40. doi: 10.1016/s0140-6736(19)33161-7
133. Sieper J, Braun J, Dougados M, Baeten D. Axial spondyloarthritis. *Nat Rev Dis Primers* (2015) 1:15013. doi: 10.1038/nrdp.2015.13
134. Ranganathan V, Gracey E, Brown MA, Inman RD, Haroon N. Pathogenesis of ankylosing spondylitis - recent advances and future directions. *Nat Rev Rheumatol* (2017) 13(6):359–67. doi: 10.1038/nrrheum.2017.56
135. Taams LS, Steel KJA, Srenathan U, Burns LA, Kirkham BW. IL-17 in the immunopathogenesis of spondyloarthritis. *Nat Rev Rheumatol* (2018) 14 (8):453–66. doi: 10.1038/s41584-018-0044-2
136. Jansen DT, Hameetman M, van Bergen J, Huizinga TW, van der Heijde D, Toes RE, et al. IL-17-producing CD4+ T cells are increased in early, active axial spondyloarthritis including patients without imaging abnormalities. *Rheumatol (Oxford England)* (2015) 54(4):728–35. doi: 10.1093/rheumatology/keu382
137. Shen H, Goodall JC, Hill Gaston JS. Frequency and phenotype of peripheral blood Th17 cells in ankylosing spondylitis and rheumatoid arthritis. *Arthritis Rheum* (2009) 60(6):1647–56. doi: 10.1002/art.24568
138. Kenna TJ, Davidson SI, Duan R, Bradbury LA, McFarlane J, Smith M, et al. Enrichment of circulating interleukin-17-secreting interleukin-23 receptor-positive γ/δ T cells in patients with active ankylosing spondylitis. *Arthritis Rheum* (2012) 64(5):1420–9. doi: 10.1002/art.33507
139. Mei Y, Pan F, Gao J, Ge R, Duan Z, Zeng Z, et al. Increased serum IL-17 and IL-23 in the patient with ankylosing spondylitis. *Clin Rheumatol* (2011) 30 (2):269–73. doi: 10.1007/s10067-010-1647-4
140. Liu W, Wu YH, Zhang L, Liu XY, Xue B, Wang Y, et al. Elevated serum levels of IL-6 and IL-17 may associate with the development of ankylosing spondylitis. *Int J Clin Exp Med* (2015) 8(10):17362–76.
141. van Tok MN, van Duivenvoorde LM, Kramer I, Ingold P, Pfister S, Roth L, et al. Interleukin-17A Inhibition Diminishes Inflammation and New Bone Formation in Experimental Spondyloarthritis. *Arthritis Rheumatol* (2019) 71 (4):612–25. doi: 10.1002/art.40770
142. Pavelka K, Kivitz A, Dokoupilova E, Blanco R, Maradiaga M, Tahir H, et al. Efficacy, safety, and tolerability of secukinumab in patients with active ankylosing spondylitis: a randomized, double-blind phase 3 study, MEASURE 3. *Arthritis Res Ther* (2017) 19(1):285. doi: 10.1186/s13075-017-1490-y
143. Baraliakos X, Kivitz AJ, Deodhar AA, Braun J, Wei JC, Delicha EM, et al. Long-term effects of interleukin-17A inhibition with secukinumab in active ankylosing spondylitis: 3-year efficacy and safety results from an extension of the Phase 3 MEASURE 1 trial. *Clin Exp Rheumatol* (2018) 36(1):50–5.
144. Ashany D, Stein EM, Goto R, Goodman SM. The Effect of TNF Inhibition on Bone Density and Fracture Risk and of IL17 Inhibition on Radiographic Progression and Bone Density in Patients with Axial Spondyloarthritis: a Systematic Literature Review. *Curr Rheumatol Rep* (2019) 21(5):20. doi: 10.1007/s11926-019-0818-9
145. Deodhar A, Blanco R, Dokoupilová E, Hall S, Kameda H, Kivitz AJ, et al. Secukinumab improves signs and symptoms of non-radiographic axial spondyloarthritis: primary results of a randomized controlled phase III study. *Arthritis Rheumatol* (2020) 73(1):110–20. doi: 10.1002/art.41477
146. van der Heijde D, Cheng-Chung Wei J, Dougados M, Mease P, Deodhar A, Maksymowych WP, et al. Ixekizumab, an interleukin-17A antagonist in the treatment of ankylosing spondylitis or radiographic axial spondyloarthritis in patients previously untreated with biological disease-modifying anti-rheumatic drugs (COAST-V): 16 week results of a phase 3 randomised, double-blind, active-controlled and placebo-controlled trial. *Lancet (London England)* (2018) 392(10163):2441–51. doi: 10.1016/s0140-6736(18)31946-9
147. Dougados M, Wei JC, Landewé R, Sieper J, Baraliakos X, Van den Bosch F, et al. Efficacy and safety of ixekizumab through 52 weeks in two phase 3, randomised, controlled clinical trials in patients with active radiographic axial spondyloarthritis (COAST-V and COAST-W). *Ann Rheumatic Dis* (2020) 79(2):176–85. doi: 10.1136/annrheumdis-2019-216118
148. Deodhar A, van der Heijde D, Gensler LS, Kim TH, Maksymowych WP, Østergaard M, et al. Ixekizumab for patients with non-radiographic axial spondyloarthritis (COAST-X): a randomised, placebo-controlled trial. *Lancet (London England)* (2020) 395(10217):53–64. doi: 10.1016/s0140-6736(19)32971-x
149. Erdes S, Nasonov E, Kunder E, Pristrom A, Soroka N, Shesternya P, et al. Primary efficacy of netakimab, a novel interleukin-17 inhibitor, in the treatment of active ankylosing spondylitis in adults. *Clin Exp Rheumatol* (2020) 38(1):27–34.
150. van der Heijde D, Gensler LS, Deodhar A, Baraliakos X, Poddubnyy D, Kivitz A, et al. Dual neutralisation of interleukin-17A and interleukin-17F with bimekizumab in patients with active ankylosing spondylitis: results from a 48-week phase IIb, randomised, double-blind, placebo-controlled, dose-ranging study. *Ann Rheumatic Dis* (2020) 79(5):595–604. doi: 10.1136/annrheumdis-2020-216980

Conflict of Interest: The authors declare that the research was conducted in the absence of any commercial or financial relationships that could be construed as a potential conflict of interest.

frontiers in Immunology

ORIGINAL RESEARCH
published: 17 February 2021
doi: 10.3389/fimmu.2020.628287

Intact Glucocorticoid Receptor Dimerization Is Deleterious in Trauma-Induced Impaired Fracture Healing

Yasmine Hachemi[1], Anna E. Rapp[2†], Sooyeon Lee[1], Ann-Kristin Dorn[1], Benjamin T. Krüger[2], Kathrin Kaiser[2], Anita Ignatius[2] and Jan Tuckermann[1*]*

[1] Institute of Comparative Molecular Endocrinology, Ulm University, Ulm, Germany, [2] Institute of Orthopedic Research and Biomechanics, Ulm University Medical Center, Ulm, Germany

Following severe trauma, fracture healing is impaired because of overwhelming systemic and local inflammation. Glucocorticoids (GCs), acting *via* the glucocorticoid receptor (GR), influence fracture healing by modulating the trauma-induced immune response. GR dimerization-dependent gene regulation is essential for the anti-inflammatory effects of GCs. Therefore, we investigated in a murine trauma model of combined femur fracture and thoracic trauma, whether effective GR dimerization influences the pathomechanisms of trauma-induced compromised fracture healing. To this end, we used mice with decreased GR dimerization ability (GR^{dim}). The healing process was analyzed by cytokine/chemokine multiplex analysis, flow cytometry, gene-expression analysis, histomorphometry, micro-computed tomography, and biomechanical testing. GR^{dim} mice did not display a systemic or local hyper-inflammation upon combined fracture and thorax trauma. Strikingly, we discovered that GR^{dim} mice were protected from fracture healing impairment induced by the additional thorax trauma. Collectively and in contrast to previous studies describing the beneficial effects of intact GR dimerization in inflammatory models, we report here an adverse role of intact GR dimerization in trauma-induced compromised fracture healing.

Keywords: inflammation, glucocorticoid receptor, fracture, thoracic trauma, bone repair

OPEN ACCESS

Edited by:
Katharina Schmidt-Bleek, Charité – Universitätsmedizin Berlin, Germany

Reviewed by:
Annemarie Lang, Charité Medical University of Berlin, Germany
Oxana Bereshchenko, University of Perugia, Italy

***Correspondence:**
Jan Tuckermann
jan.tuckermann@uni-ulm.de
Anita Ignatius
anita.ignatius@uni-ulm.de

***Present address:**
Anna E. Rapp, Pitzer Laboratory of Osteoarthritis Research, German Rheumatism Research Center (DRFZ) – a Leibniz Institute, Berlin, Germany and Experimental Immunology and Osteoarthritis Research, Department of Rheumatology and Clinical Immunology, Charité - Universitätsmedizin Berlin, Berlin, Germany

Specialty section:
This article was submitted to Inflammation, a section of the journal Frontiers in Immunology

Received: *11 November 2020*
Accepted: *29 December 2020*
Published: *17 February 2021*

Citation:
Hachemi Y, Rapp AE, Lee S, Dorn A-K, Krüger BT, Kaiser K, Ignatius A and Tuckermann J (2021) Intact Glucocorticoid Receptor Dimerization Is Deleterious in Trauma-Induced Impaired Fracture Healing. Front. Immunol. 11:628287. doi: 10.3389/fimmu.2020.628287

INTRODUCTION

Fracture healing is largely impaired in patients suffering from multiple injuries (1, 2). For example, multi-injured patients with tibial fractures exhibit a higher risk for non-union (2). Thoracic trauma particularly represents a critical injury in multi-injured patients and it frequently occurs in association with fractures. Indeed, 50% of patients with a blunt thoracic trauma suffer additional fractures of the extremities (3) and the mortality is markedly elevated in polytraumatized patients with severe thoracic trauma compared to patients with similar severity of injury without thoracic trauma (4). Thoracic trauma is also a strong inducer of the posttraumatic systemic inflammation

with a rapid release of pro-inflammatory cytokines, including interleukin (IL)-6 (5, 6). Thoracic trauma can lead to acute lung injury, a strong inflammatory response in the lungs, which affects a subfraction of patients, leading to a systemic trigger that impacts on the whole organism (7). Several experimental models combining femur fracture and thorax trauma described a systemic inflammation and disturbed fracture healing (6, 8), indicating the interference of the posttraumatic inflammation in the fracture healing process (9). Endogenous glucocorticoids (GCs) are stress hormones that play a crucial role in controlling inflammation and maintaining bone mass (10, 11). We previously demonstrated that endogenous GCs signaling through the glucocorticoid receptor (GR) is critical for efficient fracture healing (12). However, less is known about the function of GCs during bone regeneration in the context of multiple injuries.

Endogenous GCs are released from the adrenal cortex in a circadian and stress-associated manner under the control of the hypothalamic-pituitary-adrenal axis (13). Their effects are mediated by the nuclear receptors for glucocorticoid and mineralocorticoid receptors. Upon binding of GCs, GR translocates into nucleus and acts as a homodimer or a monomer to regulate gene expression (11). The GR dimer can bind to GC-response elements in DNA and induce gene expression by transactivation (11). The GR monomer can bind directly to DNA or indirectly by tethering with transcriptions factors, including nuclear factor kappa-light-chain-enhancer of activated B cells (NF-κB) and activator protein 1 (AP-1), leading to transrepression of genes (14, 15). It was previously considered that transrepression was the major mechanism of GC's anti-inflammatory effects (16). Therefore, a mouse model with impaired dimerization of the GR (GR^{dim}) was generated (17) by introducing a point mutation into the second zinc finger, which encompasses one of the dimerization interfaces. In these GR^{dim} mice, GCs failed to suppress inflammation during allergy (18), acute lung injury (19), and systemic inflammation (20, 21), revealing a critical role for GR dimerization in controlling inflammation by transactivation of gene expression. Moreover, GR^{dim} mice still develop osteoporosis when treated with pharmacological doses of GCs indicating that these effects are mediated through the GR monomer and its transrepression activity (22).

Endogenous GCs signaling is essential for maintaining bone homeostasis, because patients with adrenal insufficiency exhibit an increased fracture risk (23) and mice with selective GR deletion in the osteoblast lineage have a reduced trabecular bone mass (22). Endogenous GCs signaling plays a crucial role in osteoblastogenesis through the activation of Wnt signaling (24). Few studies have addressed the role of endogenous GCs during fracture healing. We and others could demonstrate a critical role for the GR during endochondral ossification (12, 25). Whether intact GR dimerization is important for proper fracture healing remains unknown. Thoracic trauma induces a systemic posttraumatic inflammation that potentially interferes with fracture healing (5, 6). We hypothesize that intact GR dimerization is important for proper fracture healing and for the overall control of the systemic posttraumatic inflammation caused by additional thoracic trauma. To test this hypothesis, we used mice with impaired GR dimerization capacity (GR^{dim}) and subjected them to isolated femur fracture as a model of uncomplicated healing or to combined fracture and thoracic trauma as a model of inflammation-induced disturbed healing.

MATERIAL AND METHODS

Study Design

We performed femur osteotomy with or without thoracic trauma on 14-week old male GR^{dim} mice and littermate wildtype controls (**Supplementary Figure 1A**). Mice were euthanized at different time points during fracture healing (**Supplementary Figure 1B**). At 6 h, 24 h, and 10 days post operation, we analyzed lung tissues by HE staining and qRT-PCR to evaluate the effects of the trauma. At 24 h post operation, blood plasma, bronco-alveolar lavage (BAL) and hematoma samples were processed for cytokine and chemokine measurement by multiplex assay. Immune cell profile from blood and hematoma samples was also analyzed by FACS. Callus of the fractured femur was evaluated at day 10 and day 23 by histology, histomorphometry, microCT and biomechanical analysis.

Sample size of 8 per group was determined by G*Power software (Version 3.1.9.6; Heinrich Heine University, Düsseldorf, Germany) with 80% power and a significance level of 5% based on previous data (12) taking flexural rigidity as the primary readout. We used T-test to compare between two independent groups.

Exclusion criteria included: death following thorax trauma, over-range osteotomy gap size, skins wounds resulting from bites and shattered bone during the osteotomy procedure. The animals were randomly assigned to each group and assessment of the outcome was performed blindly.

Animal Model and Husbandry

The animal experiments were performed in compliance with the international regulations for the care and use of laboratory animals (Directive 2010/63/EU) and with the approval of the local ethical committee (Regierungspräsidium Tübingen, Germany Reg. No. 1225). GR^{dim} mice ($Nr3c1^{tm3Gsc}$) were maintained in the BALB/c background.

Genotypes were determined by polymerase chain reaction (PCR) using DNA from tail biopsies as described previously (22). The mice were housed in groups of up to five animals with a 14-h light, 10-h dark cycle at 23°C and 55 ± 10% humidity. Standard rodent chow and water were available *ad libitum*. Mice were housed in specific pathogen free (SPF) conditions during breeding and transferred to experimental area in individually ventilated caging (IVC).

When aged 14 weeks, male mice received an unilateral femur osteotomy as described previously (26). In brief, under general anesthesia (2 vol% isoflurane, Forene®, Abbott, Wiesbaden Germany), the right femur was exposed and the mid shaft was osteotomized using a 0.4-mm Gigli saw (RISystem, Davos,

Switzerland). The osteotomy was stabilized using an external fixator (axial stiffness 3.2 N/mm, RISystem, Davos, Switzerland) that was fitted to the bone with four mini-Schanz screws. The osteotomy was combined with an additional thoracic trauma as described previously (27) to induce systemic inflammation. The thoracic trauma directly followed the femur osteotomy, while the mice were still under general anesthesia. In brief, a blast wave generator placed 2 cm from the mid-thorax released a blast wave at 13 bar pressure, inducing a standardized bilateral, isolated lung contusion. An analgesic was administered *via* the drinking water from 1 day before to 3 days after surgery (tramadol-hydrochloride, 25 mg/l; Gruenenthal, Aachen, Germany). Prior to surgery, mice received a single dose of antibiotics (clindamycin-2-dihydrogenphosphate, 45 mg/kg; Ratiopharm, Ulm, Germany). Mice were euthanized by intracardial blood withdrawal under deep isoflurane anesthesia after 6 or 24 h, and after 10 or 23 days.

Cytokine and Chemokine Analysis

Blood serum, broncho-alveolar lavage (BAL) fluid, and fracture hematomas harvested 24 h after osteotomy were used for cytokine analysis. Blood was collected in microvettes (Sarstedt AG&Co. Nümbrecht, Germany) and centrifuged at 4,000 *g* for 10 min at 4°C. The obtained plasma was stored at −80°C until use. BAL fluid was obtained, after flushing the lungs with 0.5 ml of ice-cold phosphate-buffered saline solution. In total, 5 µl protease inhibitor mixture were added to the obtained BAL fluid and the samples were stored on ice. The samples were centrifuged at 300 *g* for 15 min and the supernatants were harvested and kept at −80°C until use. The fracture hematoma was directly transferred into lysis buffer (10 mM tris pH 7.5, 10 mM NaCl, 0.5 mM Triton X-100, 0.2 mM phenylmethylsulfonyl fluoride, all from Sigma-Aldrich, Steinheim, Germany) with protease inhibitor cocktail (Halt™ Protease and Phosphatase Inhibitor Cocktail, Fisher Scientific GmbH, Schwerte, Germany) and minced. Following 30 min incubation on ice, the samples were centrifuged at 18,000 *g* for 30 min at 4°C. The protein concentration was determined using the Pierce™ BCA Protein Assay Kit (ThermoFisher Scientific GmbH) according to the manufacturer's instructions. The lysates were stored at −80°C until use. Using a mouse multiplex cytokine and chemokine assay (ProcartaPlex™, eBioscience, San Diego, CA, USA), the levels of the pro-inflammatory mediators IL-6, monocyte chemotactic protein (MCP)-1, macrophage inflammatory protein (MIP)-1α, and keratinocyte chemoattractant (CXCL-1) were determined on a Bio-Plex 200 (Bio-Rad, Hercules, CA, USA). Using standard curves, the cytokine levels were calculated automatically (Bio-Plex Manager™ software).

Flow Cytometry

At 24 h after osteotomy, blood and the fracture hematoma were analyzed for immune cells by flow cytometry. To remove erythrocytes from blood, lysis was performed twice for 5 min on 37°C using lysis buffer (150 mM NH_4Cl, 10 mM $KHCO_3$, 0.125 mM ethylenediamintetraacetic acid (EDTA), all from Sigma-Aldrich). The hematoma between the bone ends was excised and pressed through a cell strainer to obtain a single-cell suspension. Cells of the innate and adaptive immune systems were stained using the following antibodies or respective isotypes: CD11b Alexa Fluor 700 (clone M1/70, eBioscience, 1:400 dilution), Ly-6G V450 (clone 1A8, BD Pharmingen, 1:400 dilution), F4/80 FITC (clone BM8, eBioscience, 1:50 dilution), CD3ϵ PE-Cyanine 7 (clone 145-2C11, eBioscience, 1:100 dilution), CD4 APC-eFluor 780 (clone GK1.5, eBioscience, 1:200 dilution), CD8a APC (clone 53-6.7, eBioscience, 1:800 dilution), and CD19 PE (clone 1D3, eBioscience, 1:400 dilution). 7-AAD (Sigma) was used to distinguish between living and dead cells. A minimum of 10,000 events was measured on an LSRII flow cytometer (BD Biosciences, San Jose, CA, USA) and analyzed using FlowJo software (FlowJo, Ashland, OR, USA). Detailed gating strategy is provided in **Supplementary Figure 1C**.

Histology and Histomorphometry

Harvested lungs at 6 h and 10 days were fixed in 4% formaldehyde, embedded in paraffin, and stained with hematoxylin and eosin (H&E, Mayer's hemalum solution Merck KGaA®, Darmstadt, Germany and Eosin Y, Applichem, Darmstadt, Germany) for morphological investigations.

Femurs harvested at different time points were fixed for 48 h, decalcified in 20% EDTA for 10–12 days, dehydrated, and embedded in paraffin. Sections of 6–8 µm thickness were stained using safranin-O/fast green. Evaluation of the callus composition was performed by light microscopy (Leica DMI6000 B; Software MetaMorph®, Leica Microsystems, Mannheim, Germany) under 50-fold magnification. At all the time points, the entire callus was analyzed for the amount of bone, cartilage, and fibrous tissue. To determine the number of osteoblasts, sections were stained with toluidine blue. For visualization of osteoclasts, tartrate-resistant acid phosphatase (TRAP) activity was determined by naphthol AS-MX phosphate and Fast Red TR-Salt (both Sigma-Aldrich) in 0.2 M acetate buffer pH 5.0. Osteoblast and osteoclast numbers and surface per bone surface were determined using the OsteoMeasure histomorphometry system (OsteoMetrics, Decatur, USA). Analysis was performed according to the recommendations of the American Society for Bone and Mineral Research (28).

RNA Isolation and Gene Expression Analysis

RNA from lung tissue was isolated at 6 h and 10 days after isolated fracture or combined fracture and thoracic trauma using Trizol reagent (Invitrogen, Ambion, USA). Lungs were homogenized in Trizol for 3 min at 1,500 rotations/min using Precellys 24 homogenizer (Bertin Technologies, Montigny-le-Bretonneux, France), incubated at room temperature for 5 min, and 200 µl chloroform was added to the Trizol followed by centrifugation at maximum speed at 4°C. The aqueous phase was mixed with 0.7 volumes of isopropanol and centrifuging at maximum speed to pellet down RNA. The RNA pellet was washed with 500 µl 70% ethanol and dried at room temperature for 5–10min before suspending with RNase free water. RNA quality and amount were determined using the Nanodrop 2000 system (Thermo Scientific, Waltham, USA). cDNA was synthesized from 1–2 µg RNA using RevertAid H Minus reverse transcriptase (M-MulV, Fermentas, MA, USA) with 5× reverse transcriptase reaction buffer, random primers

(200 ng/µl, Invitrogen, Carlsbad, CA, USA), and 10 mM deoxyribonucleotide triphosphate (dNTPs) following the manufacturer's instructions. Quantitative real-time PCR (qRT-PCR) was performed in 10 µl reaction volume using SYBR Green I dye (Invitrogen) on an ABI ViiA-7 system (Applied Biosystems, Foster City, CA, USA). The mRNA abundance of *Nos2, Cd86, Il4, Chil3*, and *Il13* was calculated relative to the expression of the reference gene *Gapdh* and the data analyzed using a model based on correction for exact PCR efficiencies. The primers used are listed in **Supplementary Table 1**.

Micro-Computed Tomography (µCT)

Osteotomized and intact femurs harvested after 23 days were scanned using a µCT device (Skyscan 1172, Bruker, Kontich, Belgium) at a resolution of 8 µm at a peak voltage of 50 kV and 200 µA. Within each scan, two phantoms with defined hydroxyapatite (HA) content (250 and 750 mg/cm^3) were scanned to determine the bone mineral density (BMD). In intact femurs, a volume of interest of 1 mm length below the trochanter major was analyzed for cortical thickness (Ct.Th), mineralization (BMD), and 2nd moment of inertia (Ix). Trabecular bone was analyzed in the distal femur 0.2 mm above the growth plate. In fractured femurs, the former osteotomy gap was analyzed for trabecular parameters. To distinguish between mineralized and non-mineralized tissue, a fixed global threshold set at 643 mg HA/cm^3 was applied (29, 30). Basal bone phenotype was evaluated in intact femur and L5 vertebrae by measuring trabecular and/or cortical parameters at the age of 14 weeks. Analogous to the standard clinical assessment of X-rays to determine the healing outcome, the number of bridged cortices was determined in two perpendicular axes from µCT scans. A fracture was considered to be "healed" when the osteotomy gap was bridged at ≥3 sites (31).

Biomechanical Testing

Intact and osteotomized femurs harvested after 23 days were analyzed for flexural rigidity by nondestructive three-point bending (26). In brief, the proximal end of the femur was fixed to an aluminum cup, which in turn was fixed to a hinge joint of the three-point bending setup in the material testing machine (Z10, Zwick Roell, Ulm, Germany). The femur condyles rested unfixed on a bending support. The bending load was applied to the mid-shaft of intact bones or the middle of the callus up to a maximum load of 4 N. Flexural rigidity (EI) was calculated from the slope (k) of the linear region of the force-displacement curve. The distance of the load vector and the proximal (a) and distal (b) bending supports was considered in the calculation when the force was not applied exactly in the middle between the supports (l/2). For the calculation, the formula $EI=k(a^2b^2)/3l$ was used.

Statistics

Statistical analyses were performed using GraphPad Prism7 (GraphPad Software Inc., La Jolla, CA, USA). Non-parametric Wilcoxon-Mann-Whitney or Kruskal-Wallis with Dunn's multiple comparison test were used. *p<0.05, **p<0.01, ***p<0.005, ****p<0.001, was considered statistically significant.

RESULTS

Trabecular Bone Mass Is Moderately Affected in Mice With Impaired GR Dimerization

Before subjecting GR^{dim} mice to fracture or combined fracture and thoracic trauma, we first analyzed the basal bone phenotype in these mice with a congenital deficiency of the GR dimer when aged 14 weeks. MicroCT analysis of the distal femur revealed a significantly higher bone volume per tissue volume (BV/TV) ratio in GR^{dim} mice compared to wild types (**Figure 1A**). Trabecular number (Tb.N) and thickness (Tb.Th) were significantly increased and accordingly trabecular spacing (Tb.Sp) was reduced in the femurs of GR^{dim} mice (**Figures 1B–D**). Cortical thickness of the femur diaphysis did not differ between mutant and wild type mice (**Figure 1E**). By contrast, in the L5 vertebrae there was no significant difference in the BV/TV, Tb.N, Tb.Th, or Tb.Sp between GR^{dim} and wild type mice (**Figures 1F–I**). Histomorphometry analysis of femur trabecular bone did not show any significant difference in terms of osteoblast or osteoclast parameters between GR^{dim} mice and wild type controls (**Figures 1J–M**). In summary, impairment of GR dimerization moderately increased trabecular bone mass in the femur but not in vertebrae, and this difference cannot be explained by a difference in osteoblast or osteoclast parameters.

Impaired GR Dimerization Moderately Affects Inflammation in a Model of Combined Fracture and Thoracic Trauma

Next, we applied a thoracic trauma concomitant with a femur fracture to analyze the consequences of a severe injury on fracture healing in GR^{dim} mice during different phases of the healing response. Twenty-four hours following isolated fracture (Fx) or combined fracture and thoracic trauma (Fx+TxT), we found that the chemokines CXCL-1, IL-6, and MCP-1 in plasma had increased by trend in wild type mice receiving additional thoracic trauma to the initial fracture compared to the wild type mice that had fracture alone (**Figures 2A–C**). At the fracture site (hematoma), there were no major alteration in levels of CXCL-1, IL-6, and MCP-1 (**Figures 2D–F**) except for MIP-1α that was higher by trend in GR^{dim} compared to wild type mice in the context of combined trauma (**Figure 2G**). The additional thoracic trauma significantly increased the concentration of CXCL-1, IL-6 and MCP-1 in the BAL fluid of wild type mice compared to the mice with fracture alone (**Figures 2H–J**). This effect was more subtle in GR^{dim} mice.

Flow cytometry analysis of immune cells in the blood and hematoma (**Table 1**) revealed no significant changes in polymorphonuclear leukocytes (PMNs) (CD11b$^+$Ly6G$^+$), monocytes/macrophages (CD11b$^+$F4/80$^+$), B-cells (CD19$^+$), or T-cells (CD3$^+$) between the different groups, indicating no substantial inflammation 24 h after fracture or combined trauma (**Table 1**).

Taken together, at the early time points investigated, the impaired GR dimerization had modest effects on the systemic

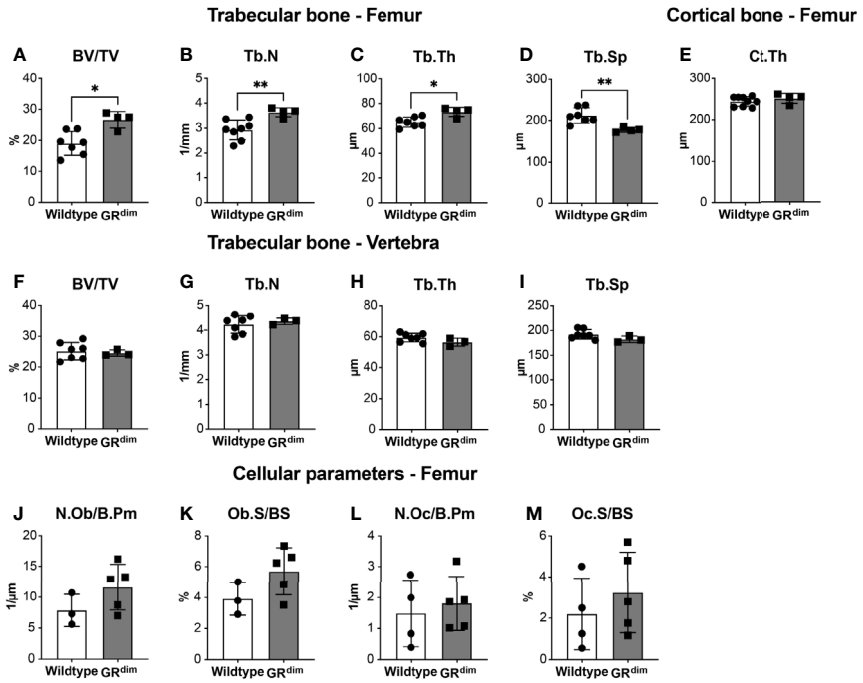

FIGURE 1 | Trabecular but not cortical bone mass is moderately affected in mice with impaired glucocorticoid receptor (GR) dimerization. Bone phenotype of 14-week-old wild type and GR^{dim} mice was analyzed. Bone per tissue volume [BV/TV, **(A)**], trabecular number [Tb.N, **(B)**], trabecular thickness [Tb.Th, **(C)**], and trabecular separation [Tb.Sp, **(D)**] in the distal femur and L5 vertebrae **(F–I)** and cortical thickness of femur diaphysis [Ct.Th, **(E)**] were analyzed by micro-computed tomography. Osteoblast number per bone perimeter [Ob.N/B.Pm, **(J)**], osteoblast surface per bone surface [Ob.S/BS, **(K)**], osteoclast number per bone perimeter [Oc.N/B.Pm, **(L)**], and osteoclast surface per bone surface [Oc.S/BS, **(M)**] were analyzed by histomorphometry in the distal femur. Data are presented as the mean ± standard deviation. n=3–7 per group. *p<0.05, **p<0.01 using Mann-Whitney-Wilcoxon test.

inflammation that were most evident in the context of combined fracture and thoracic trauma.

Additional Thoracic Trauma Differently Affects Lungs of the GR^{dim} Mice

Subsequently, we investigated the consequences of thoracic trauma on the lungs in wild type and GR^{dim} mice. We performed H&E staining to evaluate the lung structure at different time points: 6 h, 24 h, and 10 days (**Figure 3A**). As expected, histological analysis of the lungs from mice with isolated fracture displayed only minor structural signs of inflammation, including alveolar wall thickening, regardless of the genotype and time point, possibly resulting from the isoflurane overdose during sacrifice. In the context of the combined trauma, evident damage to the lung structure was observed in both GR^{dim} and wild type mice at early time points, with more exacerbated inflammatory cell infiltration at 24 h predominantly in GR^{dim} mice (**Figure 3A**). Blunt chest trauma created a non-homogenous injury pattern in the lungs, where some parts displayed massive damage with alveoli disruption and leukocyte infiltration, whereas other parts remained intact (**Supplementary Figure 2**).

To understand the role of macrophages during inflammation and repair, we evaluated the expression of particular marker genes of pro-inflammatory macrophages and anti-inflammatory macrophages in the lung tissue by qRT-PCR. Six hours post-injury, there was reduction, by trend, in *Nos2* gene expression for inducible nitric oxide synthase (iNOS), a marker for pro-inflammatory macrophages, in wild type controls while in GR^{dim} mice levels were high in the context of combined fracture and thoracic trauma (**Figure 3B**). *Cd86*, another pro-inflammatory marker, was also expressed significantly higher in the lung of GR^{dim} mice after combined trauma in comparison with GR^{dim} mice receiving only isolated fracture (**Figure 3C**). Regarding anti-inflammatory macrophage markers, *Il4* was up-regulated, by trend, upon additional thoracic trauma in wild type mice while this upregulation was more modest in GR^{dim} mice in which levels remained lower regardless of the injury type (**Figure 3D**). The anti-inflammatory marker *Chil3*, chitinase-like 3 (Ym1), was reduced by additional thoracic trauma in both wild type and GR^{dim} mice but levels of *Chil3* were lower in GR^{dim} compared to wild type mice, in both, isolated fracture and combined fracture and thoracic trauma (**Figure 3E**). At later healing stages, we did not detect changes in the expression of pro-inflammatory macrophage markers (*Nos2* or *Cd86*) 10 days post isolated fracture or combined fracture and thoracic trauma (**Figures 3F, G**). However, the anti-inflammatory macrophage marker *Il4* coding for the anti-inflammatory cytokine IL-4, was

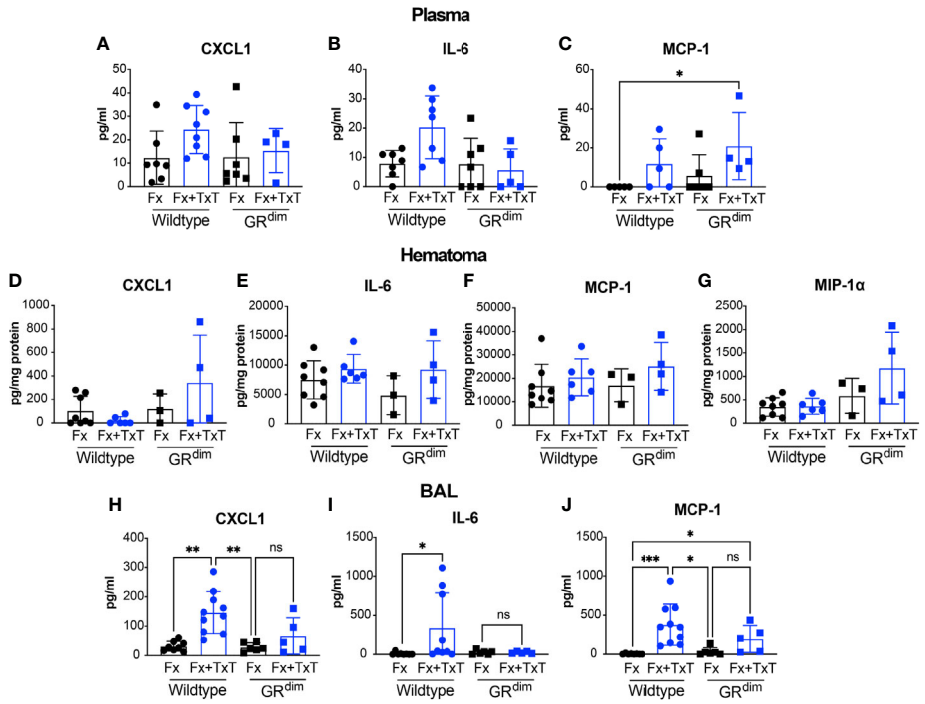

FIGURE 2 | Impaired dimerization of the glucocorticoid receptor (GR) affects inflammation. Cytokine and chemokine levels in plasma, broncho-alveolar lavage (BAL), and callus homogenates were determined by cytokine and chemokine multiplex analysis 24 h after isolated fracture (Fx) or combined fracture and thorax trauma (Fx+TxT) in wild type (WT) and decreased GR dimerization ability (GR^{dim}) mice. Levels of CXCL-1 **(A)**, IL-6 **(B)**, and MCP-1 **(C)** were measured in Plasma, Hematoma **(D–G)** and BAL **(H–J)**. In addition, MIP-1α was measured in the hematoma **(G)**. Data are presented as the mean ± standard deviation. n=4–7 per group Values are present in **Supplementary Data Sheet 1**. *p<0.05, **p<0.01, ns: non signficant, using ANOVA and Kruskal-Wallis tests.

TABLE 1 | Frequency of immune cells in the blood and hematoma after isolated fracture or combined fracture and thorax trauma is not altered in mice with impaired glucocorticoid receptor (GR) dimerization.

Compartment	Cell populations	WT Fx n=3-5	WT Fx+TxT n=5	GR^{dim} Fx. n=2	GR^{dim} Fx+TxT n=3
Hematoma	PMNs ($CD11b^+Ly6G^+$)	8.8 ± 9.1	6.2 ± 4.1	9.7 ± 5.5	4.0 ± 1.8
	Monocytes/macrophages ($CD11b^+F4/80^+$)	3.8 ± 2.3	2.8 ± 3.3	2.6 ± 0.3	1.4 ± 0.3
	B-cells ($CD19^+$)	3.2 ± 4.1	3.3 ± 3.1	6.9 ± 0.4	2.3 ± 1.5
	T-cells ($CD3^+$)	2.9 ± 1.9	1.8 ± 7.5	2.8 ± 1.6	1.3 ± 0.5
	T-helper ($CD3^+CD4^+$)	0.3 ± 0.30	0.19 ± 0.29	0.07 ± 0.06	0.00092 ± 0.001
	Cytotoxic T-cells ($CD3^+CD8^+$)	0.022 ± 0.02	0.010 ± 0.012	0.012 ± 0.0015	0.0042 ± 0.0033
Blood	PMNs ($CD11b^+Ly6G^+$)	39.3 ± 29.8	53.56 ± 16.2	53.6 ± 22.9	59.8 ± 5.0
	Monocytes/macrophages ($CD11b^+F4/80^+$)	1.5 ± 0.7	2.0 ± 1.1	1.9 ± 1.2	1.8 ± 0.9
	B-cells ($CD19^+$)	20.7 ± 12.4	10.2 ± 3.8	17. 9 ± 15.2	10.9 ± 4.8
	T-cells ($CD3^+$)	18.0± 8.9	15.5 ± 6.4	11.2 ± 2.4	9.7 ± 1.6
	T-helper ($CD3^+CD4^+$)	13.4 ± 6.3	11.5 ± 4.83	8.7 ± 1.41	7.59 ± 1.6
	Cytotoxic T-cells ($CD3^+CD8^+$)	4.2 ± 2.5	3.6 ± 2.04	2.1 ± 0.78	1.57 ± 0.4

Data are presented as the mean ± standard deviation.
Immune cell populations circulating in the blood and the fracture hematoma were analyzed by flow cytometry 24 h after isolated fracture (Fx) or combined fracture and thorax trauma (Fx+Txt) in wild type (WT) and decreased GR dimerization ability (GR^{dim}) mice.

less expressed in the lung tissue of GR^{dim} mice both after isolated fracture and combined fracture and thoracic trauma (**Figure 3H**), similarly *Il13* as an anti-inflammatory molecule was not significantly altered (**Figure 3I**).

Overall, these results suggest that the thoracic trauma impaired lung tissue structure regardless of the mouse genotype. In addition, marker genes for pro-inflammatory macrophages appear to be expressed more in the early stage of inflammation whereas anti-inflammatory ones remained low throughout the inflammatory phase in the lungs of GR^{dim} mice.

Impaired GR Dimerization Modulates Callus Formation

To evaluate the intermediate healing response in the femur, we performed histomorphometry analysis on safranin-O/fast green-stained sections of the fracture callus at day 10 (**Figure 4A**).

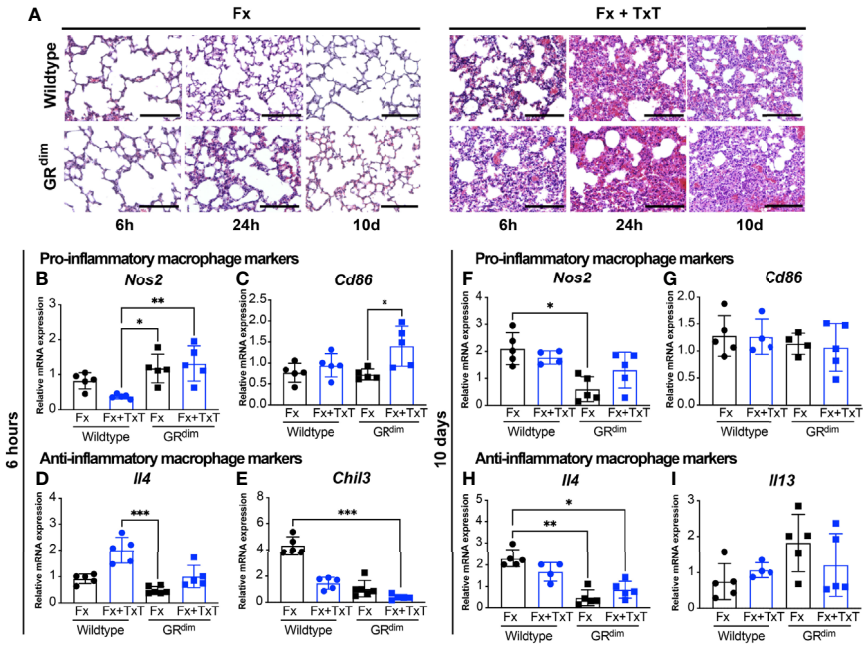

FIGURE 3 | Additional thorax trauma decreases the expression of anti-inflammatory macrophage marker genes in the lungs of mice with impaired GR dimerization. H&E staining of lung sections illustrate the structural damage and the inflammation induced by the thoracic trauma 6 and 24 h and 10 days after isolated fracture (Fx) or combined fracture and thorax trauma (Fx+TxT) in wild type and GR^{dim} mice **(A)** scale bar in all micrographs: 100 µm. Gene expression of inducible nitric oxide synthase (*Nos2*) **(B, F)**, cluster of differentiation 86 (*Cd86*) **(C, G)**, interleukin-4 (*Il4*) **(D, H)**, chitinase-3-like protein 3 (*Chil3*) **(E)**, and *Il13* **(I)** were measured in the lungs 6 h and 10 days after Fx or FX+TxT by qRT-PCR. Data are presented as the mean ± standard deviation. n=4–5 per group, *p<0.05, **p<0.01, ***p<0.001, using ANOVA and Kruskal-Wallis tests.

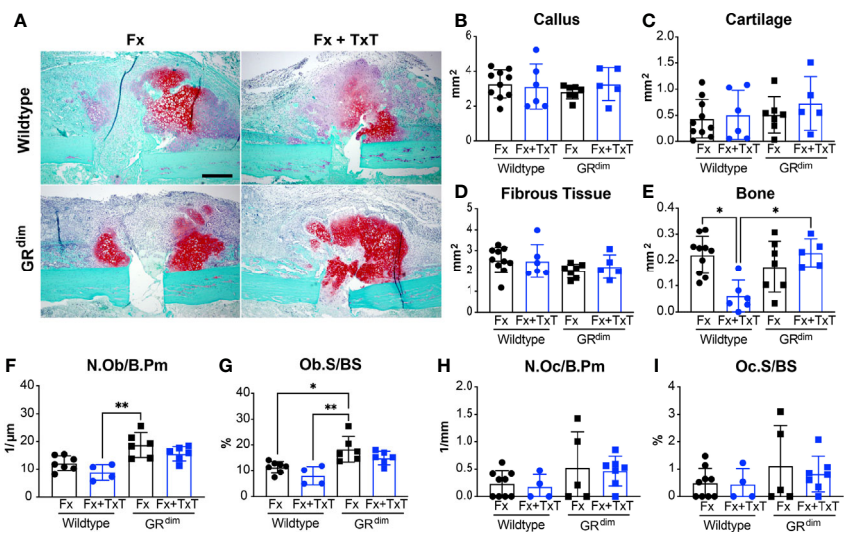

FIGURE 4 | Callus maturation is not impaired while osteoblast number and osteoblast surface are higher in mice with impaired glucocorticoid receptor (GR) dimerization 10 days after combined fracture and thoracic trauma. Sections were stained using safranin-O/fast green to illustrate callus composition at day 10 after isolated fracture (Fx) or combined fracture and thorax trauma (Fx+TxT) **(A)**. In wild type and GR^{dim} mice, the callus area **(B)** and its composition: cartilage area **(C)**, fibrous tissue area **(D)**, and bone area **(E)** were analyzed on day 10 by histomorphometry. Osteoblast number per bone perimeter [Ob.N/B.Pm, **(F)**], osteoblast surface per bone surface [Ob.S/BS, **(G)**], osteoclast number per bone perimeter [Oc.N/B.Pm, **(H)**], and osteoclast surface per bone surface [Oc.S/BS, **(I)**] were assessed in the callus by histomorphometry. Scale bar in all micrographs: 200 µm. Data are presented as the mean ± standard deviation. n=4–10 per group. *p<0.05, **p<0.01 using ANOVA and Kruskal-Wallis tests.

There were no significant differences in the callus size or cartilage or fibrous tissue content between the different groups (**Figures 4B–D**). However, the bone content was, as expected, significantly reduced in wild type mice in the combined trauma compared to the ones with isolated fracture (**Figure 4E**). Strikingly, the bone content in GR^{dim} mice was not reduced by the additional thoracic trauma and remained significantly higher compared to the wild type mice receiving combined trauma (**Figure 4E**). In addition, osteoblast number and surface were significantly higher in the fracture callus of GR^{dim} compared to wild type mice after both, isolated fracture and combined fracture and thoracic trauma (**Figures 4F, G**). By contrast, osteoclast parameters were not significantly different between the groups (**Figures 4H, I**).

Taken together, impaired GR dimerization had no effect on the endochondral ossification phase after isolated fracture. By contrast, the impaired GR dimerization protected against the disturbed callus maturation observed in the wild type mice upon additional thoracic trauma. The greater number of osteoblasts in the callus of GR^{dim} mice may at least in part explain their higher bone content.

Mice With Impaired GR Dimerization Are Protected From the Detrimental Effects of Additional Thorax Trauma

To evaluate the fracture healing outcome after isolated fracture and combined fracture and thoracic trauma in both genotypes, the bending stiffness of the fractured femurs was assessed at day 23. In the context of an isolated fracture, there was no difference between GR^{dim} and wild type mice (**Figure 5A**). However, after additional thoracic trauma, wild type mice displayed a significant reduction in the flexural rigidity, indicating impaired healing, which was not observed in GR^{dim} mice (**Figure 5A**). Accordingly, results of the cortical bridging analysis showed a higher proportion of successfully healed femurs in GR^{dim} compared to wild type mice in the context of combined trauma (**Figure 5B**), whereas in the context of an isolated

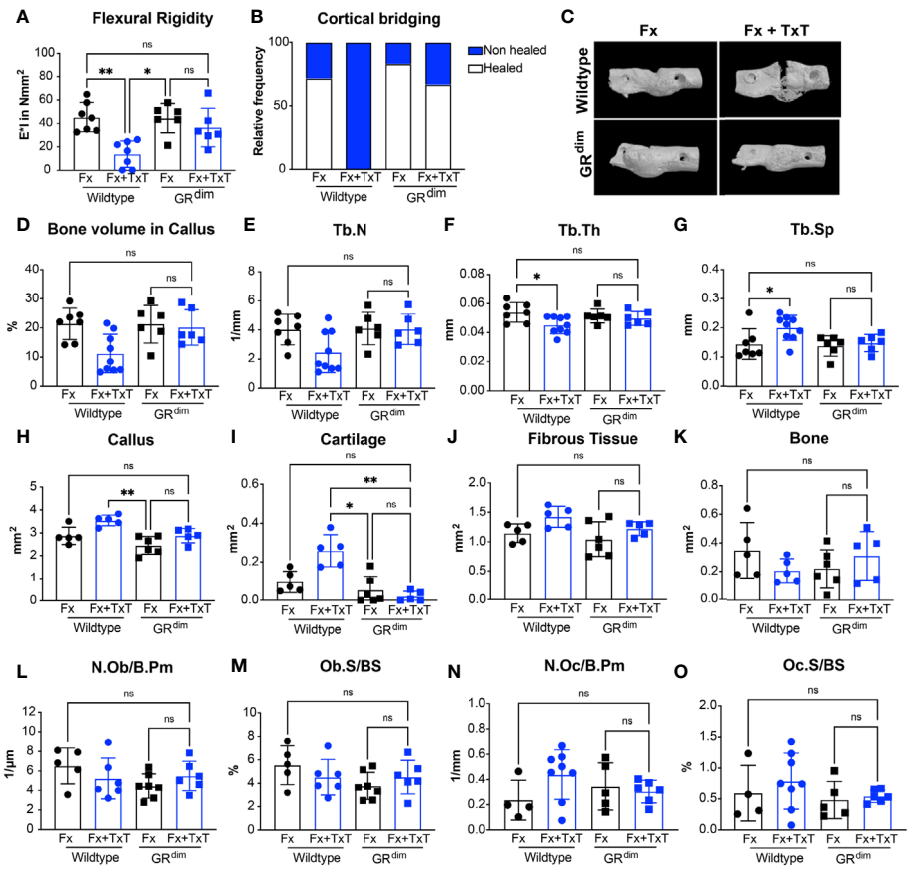

FIGURE 5 | Mice with impaired glucocorticoid receptor (GR) dimerization are protected from the detrimental effect of additional thorax trauma. At day 23 after isolated fracture (Fx) or combined fracture and thorax trauma (Fx+TxT), flexural rigidity of the fracture calli was analyzed by a three-point bending test **(A)**. The healing frequency was assessed from micro-computed tomography (μCT) datasets **(B)** and three-dimensionally reconstructed fracture callus representations were generated **(C)**. Bone volume per tissue volume [BV/TV, **(D)**], trabecular number [Tb.N, **(E)**], trabecular thickness [Tb.Th, **(F)**], and trabecular spacing [Tb.Sp, **(G)**] were determined in the former osteotomy by μCT. Callus **(H)** and cartilage **(I)**, fibrous tissue **(J)**, and bone areas **(K)** were analyzed on day 23 by histomorphometry. Osteoblast number per bone perimeter [Ob.N/B.Pm, **(L)**], osteoblast surface per bone surface [Ob.S/BS, **(M)**], osteoclast number per bone perimeter [Oc.N/B.Pm, **(N)**], and osteoclast surface per bone surface [Oc.S/BS, **(O)**] were assessed in the callus by histomorphometry. Data are presented as the mean ± standard deviation. n=5–8 per group. *p<0.05, **p<0.01, ***p<0.001, ns: non significant using ANOVA and Kruskal-Wallis tests.

fracture, there were no differences in comparison to wild type mice. These results were also reflected in the three-dimensional reconstructions of fracture calli (**Figure 5C**).

MicroCT analysis confirmed a higher bone content, by trend, in the fracture calli in GR^{dim} compared to wild type mice after combined trauma (**Figure 5D**). In agreement with this, the number of the trabeculae was higher and the trabecular spacing was reduced in GR^{dim} compared to wild type mice after combined trauma (**Figures 5E, G**). Additional thoracic trauma reduced trabecular thickness in wild type mice but had no significant effect on GR^{dim} mice (**Figure 5F**).

Histomorphometry of fracture calli at day 23 indicated that additional thoracic trauma tends to induce a larger callus area in wild type mice, whereas GR^{dim} mice exhibited a smaller callus size (**Figure 5H**). The differences in callus size could be due to the higher cartilage content, because there was significantly more cartilage in wild type mice after combined trauma, indicating delayed healing (**Figure 5I**). Additionally, no difference was detected between GR^{dim} and wild type mice in terms of callus size or cartilage content in the context of isolated fracture (**Figures 5H, I**). Fibrous tissue and bone tissue content did not exhibit major alterations in their composition between the different groups at this stage (**Figures 5J, K**). In parallel, osteoblast and osteoclast counts did not significantly differ between GR^{dim} and wild type mice 23 days post isolated fracture or combined trauma (**Figures 5L–O**).

In summary, these data indicate that GR^{dim} mice are protected from the adverse effect of additional thoracic trauma on bone fracture healing, implying an important role for the GR dimer in meditating these effects.

DISCUSSION

The present study investigated the role of endogenous GC signaling through the dimeric GR during both, isolated and compromised fracture healing induced by an additional thoracic trauma. Our results confirm previous findings on the detrimental effect of thoracic trauma on bone healing in wild type mice. In contrast to previous studies describing strong anti-inflammatory effects of intact GR dimerization in inflammatory models, we report here a negative effect of the GR dimer in trauma-induced compromised fracture healing.

GR^{dim} mice carry a point mutation in one of the dimerization interfaces of the GR that leads to a partial disruption of GR dimerization, which although incomplete (32), is still sufficient in the *in vivo* context to display impaired binding to palindromic response elements as demonstrated by Exo-ChIP Seq (33). Moreover, mice with this impaired GR dimerization display induced resistance to the anti-inflammatory effects of both, exogenous and endogenous GCs in several inflammatory models (18–21, 34, 35).

Several clinical and experimental reports confirmed a critical role for endogenous GCs in maintaining bone mass (10, 12, 22, 36–38). The analysis of the basal bone phenotype in GR^{dim} mice used in the present study showed that, although cortical bone was unaffected, trabecular bone was enhanced in the femur but not the vertebrae. This is in part consistent with a previous study reporting no effect of impaired GR dimerization on trabecular bone mass of the vertebrae (22). Osteoblast and osteoclast counts did not differ in the femur between GR^{dim} and wild type mice, suggesting only a modest influence of the GR dimer during bone growth.

We observed in our investigation that thoracic trauma causes a systemic posttraumatic inflammation which confirmed previous studies (2, 9). IL-6 is considered as a hallmark cytokine of posttraumatic inflammation because multi-injured patients xhibit an increased IL-6 level within the first 24 h (39). Accordingly, although not statistically significant, IL-6 levels were increased in wild type mice upon additional thorax trauma. Studies using similar experimental settings in rats recorded increased IL-6 levels after 24 h (5, 9, 40). IL-6 was described to play a pathophysiological role in the impairment of fracture healing induced by severe trauma in mice (41, 42). In the present study, we observed either no or mild effects of thoracic trauma on IL-6 levels in plasma or BAL. This could possibly be explained by the different background strain used in the present study (43, 44). In contrast to our previous studies (41, 42), we here used BALB/c mice, because GR^{dim} mice in the C57BL/6 background do not survive. In the context of trauma-induced compromised fracture healing, plasma IL-6 levels in the GR^{dim} mice were not elevated. This contrasts with previous studies describing a failure to reduce IL-6 in GR^{dim} mice because they were resistant to the anti-inflammatory effects of not only endogenous GCs in sepsis models (21) but also of exogenous GCs treatment in the context of antigen-induced arthritis (34). This could be a characteristic of the combined trauma model resembling a milder inflammation than experimental septic shock models.

In the early fracture hematoma, MIP-1α was elevated in mice with impaired GR dimerization in the context of combined trauma compared to wild type mice. Similarly, fibroblast-like synoviocytes from GR^{dim} mice were resistant to dexamethasone-mediated MIP-1α suppression during experimental serum-induced arthritis (45). Reports on the role of MIP-1α on mesenchymal stem cell homing and migration to the injury site (46) but also on the enhancement of osteoclast differentiation and activation (47–49) suggest a beneficial role of MIP-1α on fracture healing outcome in our model. While systemic inflammation leads to hyper-inflammation in GR^{dim} mice (20, 21, 35), inflammation was not increased in the early fracture hematoma after combined injury. This observation correlates with models of contact allergy and arthritis, where despite the non-responsiveness of GR-deficient mice to exogenous GC treatment, these GR^{dim} mice were not hyper-responsive to inflammation as a response to endogenous GCs (18, 34). In conclusion, impaired GR dimerization affected inflammation in the circulation and marginally in the hematoma.

Flow cytometry analysis of the blood and fracture hematoma in GR^{dim} mice did not reveal major alterations in the immune cell composition 24 h post injury. This observation is partially in accordance with the cytokine measurements in the

same compartments, because we did not observe major systemic inflammation.

In models of acute lung injury, GCs reduced inflammation *via* the induction of anti-inflammatory macrophages (50) and the presence of dimeric GR in macrophages was required to reduce vascular leakage of the endothelium (19). Our investigations indicated an upregulation of genes associated with a pro-inflammatory macrophage phenotype in the injured lungs of GR^{dim} mice (e.g., *Cd86*). Anti-inflammatory associated genes were clearly reduced in the combined treatment. *Il4* induction as an anti-inflammatory marker was less pronounced and *Chil3* was further reduced in GR^{dim} mice. Throughout the healing time, the effects on these markers were less prominent.

Chil3 exhibits anti-inflammatory functions and participates in lung tissue repair (51–53). Likewise, in our model, *Chil3* gene expression was down regulated in mice with impaired GC signaling (GR^{dim}) regardless of injury type, revealing a potential role of the GR dimer in *Chil3* regulation in the lung. This is in agreement with the concept that GCs induce rather an anti-inflammatory phenotype than just suppression of pro-inflammatory mediators (54, 55).

A study in human monocytes suggest that the main GC effects are not the suppression of pro-inflammatory mediators but rather the induction of an anti- inflammatory phenotype in monocytes and the promotion of their survival by prolonging the activation of the ERK/MAPK pathway (54). Moreover, transient presence of the macrophage chemokine MCP-1 was proven to be important for activation of anti-inflammatory macrophages and later on, to be beneficial for the lung contusion outcome (56). In line with these findings, we speculate that reduced expression of anti-inflammatory macrophage markers in GR^{dim} mice is linked to the reduced MCP-1 levels in the BAL.

Our investigations in the lungs provide insights for the function of the GR dimer in the inflammatory response towards thoracic trauma and strengthens its previously established role as mediator of GC-mediated anti-inflammatory effects. Current data do not allow conclusions about the lung repair outcome and further investigations are necessary to understand the effects of endogenous GCs during lung repair and its impact on fracture healing.

We have previously demonstrated a critical role of the GR during endochondral ossification in the context of isolated fracture healing (12). Interestingly, in the present study, impaired GR dimerization did not affect isolated fracture healing, indicating an important role of the GR monomer in mediating GC effects during endochondral ossification. By contrast, the GR dimer had a detrimental role during trauma-induced impaired fracture healing.

Regarding the outcome of impaired fracture healing after concomitant thoracic trauma, our model recapitulates the clinical (2) and experimental observations (5, 9). Indeed, and similarly to previous reports, biomechanical properties, cortical bridging score, and mineralization levels of the fracture callus at day 23 correlated with previous reports describing trauma-induced compromised fracture healing (27, 41, 57), whereas GR^{dim} mice displayed non-compromised healing. In contrast to GR^{dim} mice, wild type mice exhibited high cartilage content after combined injury. Intriguingly, there was no difference in osteoblast or osteoclast counts that could explain the different healing outcomes. Successful bone repair depends on effective cartilage-to-bone transition. Similar to a previous report (41), endochondral ossification in wild type mice was impaired upon combined injury because the callus bone content was significantly reduced 10 days later, whereas GR^{dim} mice did not display a reduced bone content.

Interference of the early inflammatory response with the healing cascade was described to be in part responsible for trauma-induced compromised fracture healing. Indeed, Recknagel et al. reported early alterations in neutrophil and monocyte infiltrations into the fracture callus and subsequent impairment of endochondral ossification (9). However, to what extent intact GR dimerization confers protection against thoracic trauma-impaired fracture healing *via* modulation of inflammation is unclear. Given the rather modest effects on the inflammatory response, this needs further investigation, possibly also in other murine backgrounds.

One possible cause could be that the high bone content observed in GR^{dim} mice upon combined trauma could also result from an accelerated bone-to-cartilage transformation. Accordingly, osteoblast numbers were higher in GR^{dim} mice compared to wild type mice 10 days post-combined trauma. This raises the possibility that GC signaling through the GR dimer would act on osteoblast progenitors and decrease their differentiation and/or proliferation in the context of trauma, thus leading to impaired endochondral ossification. In agreement with this, Rauch et al. reported an influence of dimeric GR on osteoblast proliferation rather than differentiation (22). Although intact GR dimerization was also described to be necessary for GC action on osteoclasts (58), we did not observe any changes in osteoclast numbers or surfaces throughout the investigated time in both genotypes.

A limitation of the study is that we do not clarify the exact molecular interactions and mechanisms that explain the adverse effects by the GR dimer. This requires further studies and may go beyond the regulation of inflammatory mediators or factors of bone cell differentiation. However, building on these data we and others are currently exploiting novel GR dimer gene regulation that is detrimental for trauma impact on fracture healing.

In conclusion, our data demonstrate a redundant role for intact GR dimerization during isolated fracture healing. However, in contrast to previous studies describing beneficial effects of the GR dimer in inflammatory models, we report here a negative effect of the intact GR dimerization in trauma-induced compromised fracture healing potentially by mediating the interaction of the thoracic trauma-induced systemic inflammation with the local inflammatory process at the fracture site. This study demonstrates a partial detrimental role of endogenous GCs/GR action on thoracic trauma-impaired fracture healing.

DATA AVAILABILITY STATEMENT

The original contributions presented in the study are included in the article/**Supplementary Material**, further inquiries can be directed to the corresponding author/s.

ETHICS STATEMENT

The animal study was reviewed and approved by Regierungspräsidium Tübingen.

AUTHOR CONTRIBUTIONS

AI, JT, YH, and AR designed the study. AR, YH, SL, A-KD, BK, and KK conducted the experiments. AI, JT, YH, and AR analyzed and interpreted the data. YH drafted the manuscript. JT and AI revised the paper. All authors contributed to the article and approved the submitted version.

FUNDING

This study was financed by the German Research Foundation in the context of the Collaborative Research Center 1149 – Project-ID 251293561 – "Danger Response, Disturbance Factors and Regenerative Potential after Acute Trauma" (CRC 1149, C02, INST 40/492-2).

ACKNOWLEDGMENTS

The authors thank Miriam Tschaffon, Deniz Ragipoglu, and Kristin Hauff for technical assistance during the surgeries. We acknowledge the excellent technical assistance of Natalja Möbius, Ulrike Kelp, Ursula Maile, Cherise Grieser, and Marion Tomo.

SUPPLEMENTARY MATERIAL

The Supplementary Material for this article can be found online at: https://www.frontiersin.org/articles/10.3389/fimmu.2020.628287/full#supplementary-material

REFERENCES

1. Karladani AH, Granhed H, Karrholm J, Styf J. The influence of fracture etiology and type on fracture healing: a review of 104 consecutive tibial shaft fractures. *Arch Orthop Trauma Surg* (2001) 121:325–8. doi: 10.1007/s004020000252
2. Bhandari M, Tornetta P3, Sprague S, Najibi S, Petrisor B, Guyatt GH. Predictors of reoperation following operative management of fractures of the tibial shaft. *J Orthop Trauma* (2003) 17:353–61. doi: 10.1097/00005131-200305000-00006
3. Shorr RM, Crittenden M, Indeck M, Hartunian SL, Rodriguez A. Blunt thoracic trauma. Analysis of 515 patients. *Ann Surg* (1987) 206:200–5. doi: 10.1097/00000658-198708000-00013
4. Hildebrand F, Giannoudis P, Van Griensven M, Chawda M, Probst C, Harms O, et al. Secondary effects of femoral instrumentation on pulmonary physiology in a standardised sheep model: What is the effect of lung contusion and reaming? *Injury* (2005) 36:544–55. doi: 10.1016/j.injury.2004.10.017
5. Claes L, Ignatius A, Lechner R, Gebhard F, Kraus M, Baumgärtel S, et al. The effect of both a thoracic trauma and a soft-tissue trauma on fracture healing in a rat model. *Acta Orthop* (2011) 82:223–7. doi: 10.3109/17453674.2011.570677
6. Recknagel S, Bindl R, Brochhausen C, Göckelmann M, Wehner T, Schoengraf P, et al. Systemic inflammation induced by a thoracic trauma alters the cellular composition of the early fracture callus. *J Trauma Acute Care Surg* (2013) 74:531–7. doi: 10.1097/TA.0b013e318278956d
7. Herridge MS, Angus DC. Acute lung injury–affecting many lives. *N Engl J Med* (2005) 353:1736–8. doi: 10.1056/NEJMe058205
8. Mangum LH, Avila JJ, Hurtgen BJ, Lofgren AL, Wenke JC. Burn and thoracic trauma alters fracture healing, systemic inflammation, and leukocyte kinetics in a rat model of polytrauma. *J Orthop Surg Res* (2019) 14:58. doi: 10.1186/s13018-019-1082-4
9. Recknagel S, Bindl R, Kurz J, Wehner T, Ehrnthaller C, Knöferl MW, et al. Experimental blunt chest trauma impairs fracture healing in rats. *J Orthop Res* (2011) 29:734–9. doi: 10.1002/jor.21299
10. Kalak R, Zhou H, Street J, Day RE, Modzelewski JRK, Spies CM, et al. Endogenous glucocorticoid signalling in osteoblasts is necessary to maintain normal bone structure in mice. *Bone* (2009) 45:61–7. doi: 10.1016/j.bone.2009.03.673
11. Hartmann K, Koenen M, Schauer S, Wittig-Blaich S, Ahmad M, Baschant U, et al. Molecular Actions of Glucocorticoids in Cartilage and Bone During Health, Disease, and Steroid Therapy. *Physiol Rev* (2016) 96:409–47. doi: 10.1152/physrev.00011.2015
12. Rapp AE, Hachemi Y, Kemmler J, Koenen M, Tuckermann J, Ignatius A. Induced global deletion of glucocorticoid receptor impairs fracture healing. *FASEB J* (2018) 32:2235–45. doi: 10.1096/fj.201700459RR
13. Papadimitriou A, Priftis KN. Regulation of the hypothalamic-pituitary-adrenal axis. *Neuroimmunomodulation* (2009) 16:265–71. doi: 10.1159/000216184
14. Schiller BJ, Chodankar R, Watson LC, Stallcup MR, Yamamoto KR. Glucocorticoid receptor binds half sites as a monomer and regulates specific target genes. *Genome Biol* (2014) 15:1–16. doi: 10.1186/s13059-014-0418-y
15. Baschant U, Tuckermann J. The role of the glucocorticoid receptor in inflammation and immunity. *J Steroid Biochem Mol Biol* (2010) 120:69–75. doi: 10.1016/j.jsbmb.2010.03.058
16. Hübner S, Dejager L, Libert C, Tuckermann JP. The glucocorticoid receptor in inflammatory processes: Transrepression is not enough. *Biol Chem* (2015) 396:1223–31. doi: 10.1515/hsz-2015-0106
17. Reichardt HM, Kaestner KH, Tuckermann J, Kretz O, Wessely O, Bock R, et al. DNA binding of the glucocorticoid receptor is not essential for survival. *Cell* (1998) 93:531–41. doi: 10.1016/S0092-8674(00)81183-6
18. Tuckermann JP, Kleiman A, Moriggl R, Spanbroek R, Neumann A, Illing A, et al. Macrophages and neutrophils are the targets for immune suppression by glucocorticoids in contact allergy. *J Clin Invest* (2007) 117:1381–90. doi: 10.1172/JCI28034
19. Vettorazzi S, Bode C, Dejager L, Frappart L, Shelest E, Klaßen C, et al. Glucocorticoids limit acute lung inflammation in concert with inflammatory stimuli by induction of SphK1. *Nat Commun* (2015) 6:1–12. doi: 10.1038/ncomms8796
20. Vandevyver S, Dejager L, Van Bogaert T, Kleyman A, Liu Y, Tuckermann J, et al. Glucocorticoid receptor dimerization induces MKP1 to protect against TNF-induced inflammation. *J Clin Invest* (2012) 122:2130–40. doi: 10.1172/JCI60006
21. Kleiman A, Hübner S, Rodriguez Parkitna JM, Neumann A, Hofer S, Weigand MA, et al. Glucocorticoid receptor dimerization is required for survival in septic shock via suppression of interleukin-1 in macrophages. *FASEB J* (2012) 26:722–9. doi: 10.1096/fj.11-192112
22. Rauch A, Seitz S, Baschant U, Schilling AF, Illing A, Stride B, et al. Glucocorticoids suppress bone formation by attenuating osteoblast differentiation via the monomeric glucocorticoid receptor. *Cell Metab* (2010) 11:517–31. doi: 10.1016/j.cmet.2010.05.005
23. Bjornsdottir S, Saaf M, Bensing S, Kampe O, Michaelsson K, Ludvigsson JF. Risk of hip fracture in Addison's disease: a population-based cohort study. *J Intern Med* (2011) 270:187–95. doi: 10.1111/j.1365-2796.2011.02352.x
24. Zhou H, Mak W, Zheng Y, Dunstan CR, Seibel MJ. Osteoblasts directly control lineage commitment of mesenchymal progenitor cells through Wnt signaling. *J Biol Chem* (2008) 283:1936–45. doi: 10.1074/jbc.M702687200
25. Tu J, Henneicke H, Zhang Y, Stoner S, Cheng TL, Schindeler A, et al. Disruption of glucocorticoid signaling in chondrocytes delays metaphyseal fracture healing but does not affect normal cartilage and bone development. *Bone* (2014) 69:12–22. doi: 10.1016/j.bone.2014.08.016

26. Röntgen V, Blakytny R, Matthys R, Landauer M, Wehner T, Göckelmann M, et al. Fracture healing in mice under controlled rigid and flexible conditions using an adjustable external fixator. *J Orthop Res* (2010) 28:1456–62. doi: 10.1002/jor.21148
27. Kemmler J, Bindl R, Mccook O, Wagner F, Gröger M. Exposure to 100 % Oxygen Abolishes the Impairment of Fracture Healing after Thoracic Trauma. *PLoS One* (2015) 10:1–19. doi: 10.1371/journal.pone.0131194
28. Dempster DW, Compston JE, Drezner MK, Glorieux FH, Kanis JA, Malluche H, et al. Standardized nomenclature, symbols, and units for bone histomorphometry: a 2012 update of the report of the ASBMR Histomorphometry Nomenclature Committee. *J Bone Miner Res* (2013) 28:2–17. doi: 10.1002/jbmr.1805
29. Morgan EF, Mason ZD, Chien KB, Pfeiffer AJ, Barnes GL, Einhorn TA, et al. Micro-computed tomography assessment of fracture healing: relationships among callus structure, composition, and mechanical function. *Bone* (2009) 44:335–44. doi: 10.1016/j.bone.2008.10.039
30. O'Neill KR, Stutz CM, Mignemi NA, Burns MC, Murry MR, Nyman JS, et al. Micro-computed tomography assessment of the progression of fracture healing in mice. *Bone* (2012) 50:1357–67. doi: 10.1016/j.bone.2012.03.008
31. Risselada M, Winter MD, Lewis DD, Griffith E, Pozzi A. Comparison of three imaging modalities used to evaluate bone healing after tibial tuberosity advancement in cranial cruciate ligament-deficient dogs and comparison of the effect of a gelatinous matrix and a demineralized bone matrix mix on bone healing -. *BMC Vet Res* (2018) 14:1–12. doi: 10.1186/s12917-018-1490-4
32. Presman DM, Ogara MF, Stortz M, Alvarez LD, Pooley JR, Schiltz RL, et al. Live cell imaging unveils multiple domain requirements for in vivo dimerization of the glucocorticoid receptor. *PloS Biol* (2014) 12:e1001813–e1001813. doi: 10.1371/journal.pbio.1001813
33. Lim H, Uhlenhaut NH, Rauch A, Weiner J, Hübner S, Hübner N, et al. Genomic redistribution of GR monomers and dimers mediates transcriptional response to exogenous glucocorticoid in vivo. *Genome Res* (2015) 25:836–44. doi: 10.1101/gr.188581.114
34. Baschant U, Frappart L, Rauchhaus U, Bruns L, Reichardt HM, Kamradt T, et al. Glucocorticoid therapy of antigen-induced arthritis depends on the dimerized glucocorticoid receptor in T cells. *Proc Natl Acad Sci USA* (2011) 108:19317–22. doi: 10.1073/pnas.1105857108
35. Silverman MN, Mukhopadhyay P, Belyavskaya E, Tonelli LH, Revenis BD, Doran JH, et al. Glucocorticoid receptor dimerization is required for proper recovery of LPS-induced inflammation, sickness behavior and metabolism in mice. *Mol Psychiatry* (2013) 18:1006–17. doi: 10.1038/mp.2012.131
36. Koetz KR, Ventz M, Diederich S, Quinkler M. Bone mineral density is not significantly reduced in adult patients on low-dose glucocorticoid replacement therapy. *J Clin Endocrinol Metab* (2012) 97:85–92. doi: 10.1210/jc.2011-2036
37. Sher LB, Woitge HW, Adams DJ, Gronowicz GA, Krozowski Z, Harrison JR, et al. Transgenic Expression of 11β-Hydroxysteroid Dehydrogenase Type 2 in Osteoblasts Reveals an Anabolic Role for Endogenous Glucocorticoids in Bone. *Endocrinology* (2004) 145:922–9. doi: 10.1210/en.2003-0655
38. Sher L-B, Harrison JR, Adams DJ, Kream BE. Impaired Cortical Bone Acquisition and Osteoblast Differentiation in Mice with Osteoblast-Targeted Disruption of Glucocorticoid Signaling. *Calcif Tissue Int* (2006) 79:118–25. doi: 10.1007/s00223-005-0297-z
39. Giannoudis PV, Harwood PJ, Loughenbury P, Van Griensven M, Krettek C, Pape HC. Correlation between IL-6 levels and the systemic inflammatory response score: Can an IL-6 cutoff predict a SIRS state? *J Trauma* (2008) 65:646–52. doi: 10.1097/TA.0b013e3181820d48
40. Fitschen-Oestern S, Lippross S, Klueter T, Weuster M, Varoga D, Tohidnezhad M, et al. A new multiple trauma model of the mouse. *BMC Musculoskelet Disord* (2017) 18:1–12. doi: 10.1186/s12891-017-1813-9
41. Kaiser K, Prystaz K, Vikman A, Haffner-luntzer M, Bergdolt S, Strauss G, et al. Pharmacological inhibition of IL-6 trans-signaling improves compromised fracture healing after severe trauma. *Naunyn Schmiedebergs Arch Pharmacol* (2018) 391:523–36. doi: 10.1007/s00210-018-1483-7
42. Prystaz K, Kaiser K, Kovtun A, Haffner-Luntzer M, Fischer V, Rapp AE, et al. Distinct Effects of IL-6 Classic and Trans-Signaling in Bone Fracture Healing. *Am J Pathol* (2018) 188:474–90. doi: 10.1016/j.ajpath.2017.10.011
43. Magaña-Guerrero FS, Quiroz-Mercado J, Garfias-Zenteno N, Garfias Y. Comparative analysis of inflammatory response in the BALB/c and C57BL/6 mouse strains in an endotoxin-induced uveitis model. *J Immunol Methods* (2020) 476:112677. doi: 10.1016/j.jim.2019.112677
44. Ferreira BL, Ferreira ÉR, de Brito MV, Salu BR, Oliva MLV, Mortara RA, et al. BALB/c and C57BL/6 Mice Cytokine Responses to Trypanosoma cruzi Infection Are Independent of Parasite Strain Infectivity. *Front Microbiol* (2018) 9:553. doi: 10.3389/fmicb.2018.00553
45. Koenen M, Culemann S, Vettorazzi S, Caratti G, Frappart L, Baum W, et al. Glucocorticoid receptor in stromal cells is essential for glucocorticoid-mediated suppression of inflammation in arthritis. *Ann Rheumatol Dis* (2018) 77:1610–8. doi: 10.1136/annrheumdis-2017-212762
46. Ito H. Chemokines in mesenchymal stem cell therapy for bone repair: A novel concept of recruiting mesenchymal stem cells and the possible cell sources. *Mod Rheumatol* (2011) 21:113–21. doi: 10.3109/s10165-010-0357-8
47. Kukita T, Kukita A, Harada H, Iijima T. Regulation of osteoclastogenesis by antisense oligodeoxynucleotides specific to zinc finger nuclear transcription factors Egr-1 and WT1 in rat bone marrow culture system. *Endocrinology* (1997) 138:4384–9. doi: 10.1210/endo.138.10.5466
48. Tsubaki M, Kato C, Manno M, Ogaki M, Satou T, Itoh T, et al. Macrophage inflammatory protein-1alpha (MIP-1alpha) enhances a receptor activator of nuclear factor kappaB ligand (RANKL) expression in mouse bone marrow stromal cells and osteoblasts through MAPK and PI3K/Akt pathways. *Mol Cell Biochem* (2007) 304:53–60. doi: 10.1007/s11010-007-9485-7
49. Wan H, Qian TY, Hu XJ, Huang CY, Yao WF. Correlation of serum ccl3/mip-1α levels with disease severity in postmenopausal osteoporotic females. *Balkan Med J* (2018) 35:320–5. doi: 10.4274/balkanmedj.2017.1165
50. Tu GW, Shi Y, Zheng Y, Ju M, He H, Ma G, et al. Glucocorticoid attenuates acute lung injury through induction of type 2 macrophage. *J Transl Med* (2017) 15:181. doi: 10.1186/s12967-017-1284-7
51. Chang NCA, Hung SII, Hwa KY, Kato I, Chen JE, Liu CH, et al. A Macrophage Protein, Ym1, Transiently Expressed during Inflammation Is a Novel Mammalian Lectin. *J Biol Chem* (2001) 276:17497–506. doi: 10.1074/jbc.M010417200
52. Raes G, De Baetselier P, Noel W, Beschin A, Brombacher F, Hassanzadeh Gh G. Differential expression of FIZZ1 and Ym1 in alternatively versus classically activated macrophages. *J Leukoc Biol* (2002) 71:597–602. doi: 10.1189/jlb.71.4.597
53. Sutherland TE, Rückerl D, Logan N, Duncan S, Wynn TA, Allen JE. Ym1 induces RELMα and rescues IL-4Rα deficiency in lung repair during nematode infection. *PloS Pathog* (2018) 14:1–27. doi: 10.1371/journal.ppat.1007423
54. Barczyk K, Ehrchen J, Tenbrock K, Ahlmann M, Kneidl J, Viemann D, et al. Glucocorticoids promote survival of anti-inflammatory macrophages via stimulation of adenosine receptor A3. *Blood* (2010) 116:446–55. doi: 10.1182/blood-2009-10-247106
55. Escoter-Torres L, Caratti G, Mechtidou A, Tuckermann J, Uhlenhaut NH, Vettorazzi S. Fighting the Fire: Mechanisms of Inflammatory Gene Regulation by the Glucocorticoid Receptor. *Front Immunol* (2019) 10:1–17. doi: 10.3389/fimmu.2019.01859
56. Suresh MV, Yu B, Machado-Aranda D, Bender MD, Ochoa-Frongia L, Helinski JD, et al. Role of macrophage chemoattractant protein-1 in acute inflammation after lung contusion. *Am J Respir Cell Mol Biol* (2012) 46:797–806. doi: 10.1165/rcmb.2011-0358OC
57. Kovtun A, Bergdolt S, Wiegner R, Radermacher P, Ignatius A. The crucial role of neutrophil granulocytes in bone fracture healing. *Eur Cells Mater* (2016) 32:152–62. doi: 10.22203/eCM.v032a10
58. Conaway HH, Henning P, Lie A, Tuckermann J, Lerner UH. Activation of dimeric glucocorticoid receptors in osteoclast progenitors potentiates RANKL induced mature osteoclast bone resorbing activity. *Bone* (2016) 93:43–54. doi: 10.1016/j.bone.2016.08.024

Conflict of Interest: The authors declare that the research was conducted in the absence of any commercial or financial relationships that could be construed as a potential conflict of interest.

frontiers in Immunology

REVIEW
published: 22 February 2021
doi: 10.3389/fimmu.2021.620333

T Cell Protein Tyrosine Phosphatase in Osteoimmunology

Ya-nan Wang[1,2,3†], *Shiyue Liu*[2,3,4†], *Tingting Jia*[1,2,3], *Yao Feng*[1,2,3], *Wenjing Zhang*[1,2,3], *Xin Xu*[1,2,3] *and Dongjiao Zhang*[1,2,3*]

[1] Department of Implantology, School and Hospital of Stomatology, Cheeloo College of Medicine, Shandong University, Jinan, China, [2] Shandong Key Laboratory of Oral Tissue Regeneration, Jinan, China, [3] Shandong Engineering Laboratory for Dental Materials and Oral Tissue Regeneration, Jinan, China, [4] Department of Periodontology, School and Hospital of Stomatology, Cheeloo College of Medicine, Shandong University, Jinan, China

Osteoimmunology highlights the two-way communication between bone and immune cells. T cell protein tyrosine phosphatase (TCPTP), also known as protein-tyrosine phosphatase non-receptor 2 (PTPN2), is an intracellular protein tyrosine phosphatase (PTP) essential in regulating immune responses and bone metabolism *via* dephosphorylating target proteins. *Tcptp* knockout in systemic or specific immune cells can seriously damage the immune function, resulting in bone metabolism disorders. This review provided fresh insights into the potential role of TCPTP in osteoimmunology. Overall, the regulation of osteoimmunology by TCPTP is extremely complicated. TCPTP negatively regulates macrophages activation and inflammatory factors secretion to inhibit bone resorption. TCPTP regulates T lymphocytes differentiation and T lymphocytes-related cytokines signaling to maintain bone homeostasis. TCPTP is also expected to regulate bone metabolism by targeting B lymphocytes under certain time and conditions. This review offers a comprehensive update on the roles of TCPTP in osteoimmunology, which can be a promising target for the prevention and treatment of inflammatory bone loss.

Keywords: T cell protein tyrosine phosphatase (TCPTP), Protein tyrosine phosphatase non-receptor 2 (PTPN2), osteoimmunology, macrophages, T cell, B cell

OPEN ACCESS

Edited by:
Teun J. De Vries,
VU University Amsterdam, Netherlands

Reviewed by:
Maria-Bernadette Madel,
Baylor College of Medicine, United States
Claudine Blin-Wakkach,
UMR7370 Laboratoire de Physio Médecine Moléculaire (LP2M), France

***Correspondence:**
Dongjiao Zhang
djzhang1109@163.com

[†]*These authors have contributed equally to this work*

Specialty section:
This article was submitted to Inflammation, a section of the journal Frontiers in Immunology

Received: *22 October 2020*
Accepted: *04 January 2021*
Published: *22 February 2021*

Citation:
Wang Y-N, Liu S, Jia T, Feng Y, Zhang W, Xu X and Zhang D (2021) T Cell Protein Tyrosine Phosphatase in Osteoimmunology. Front. Immunol. 12:620333. doi: 10.3389/fimmu.2021.620333

INTRODUCTION

Inflammatory bone diseases characterized by severe bone loss, such as osteoarthritis, rheumatoid arthritis, and periodontitis, are a manifestation of imbalance between the skeletal and immune systems (1–3). Their interactions, known as osteoimmunology, were firstly proposed by Choi and Aaron in 2000, which highlights the two-way communication between bone and immune cells (4). With a comprehensive and profound acknowledgment of osteoimmunology, targeting regulatory proteins involved in osteoimmune responses can be a feasible means against inflammatory bone diseases. T-cell protein tyrosine phosphatase (TCPTP), one of the protein tyrosine phosphatases (PTPs) family, was identified by Cool et al. using T-cell-based cDNA library screening (5). There is growing evidence that TCPTP is a critical regulator in immune responses and bone metabolism. Nevertheless, the potential effect of TCPTP in the field of osteoimmunology is less explored. As a result, we intended to offer a comprehensive update on the known and potential roles of TCPTP in osteoimmunology in this review. Our study will lay a theoretical foundation for further basic researches of TCPTP in the field of osteoimmunology and provide references for treatment strategies of inflammatory bone diseases.

OSTEOIMMUNOLOGY

During osteoimmune responses, different immune cells and bone cells interact reciprocally to maintain the homeostasis between the immune and skeletal systems (**Figure 1**). The two-way communication may influence either immune or bone cells *via* cytokine activities in the immune-bone interface. The proposal of screening new targets interfering with osteoimmunology may be feasible for identifying critical targets suppressing immune hyperactivity in inflammatory bone loss diseases.

Influence of Immune Cells on Bone Cells

Immune cells, such as T lymphocytes (Th1, Th2, Treg, and Th17 cells), B lymphocytes, dendritic cells, and macrophages, actively regulate the homeostasis of bone metabolism. Th1 cells secrete interferon-γ (IFN-γ) that has been found to exert controversial

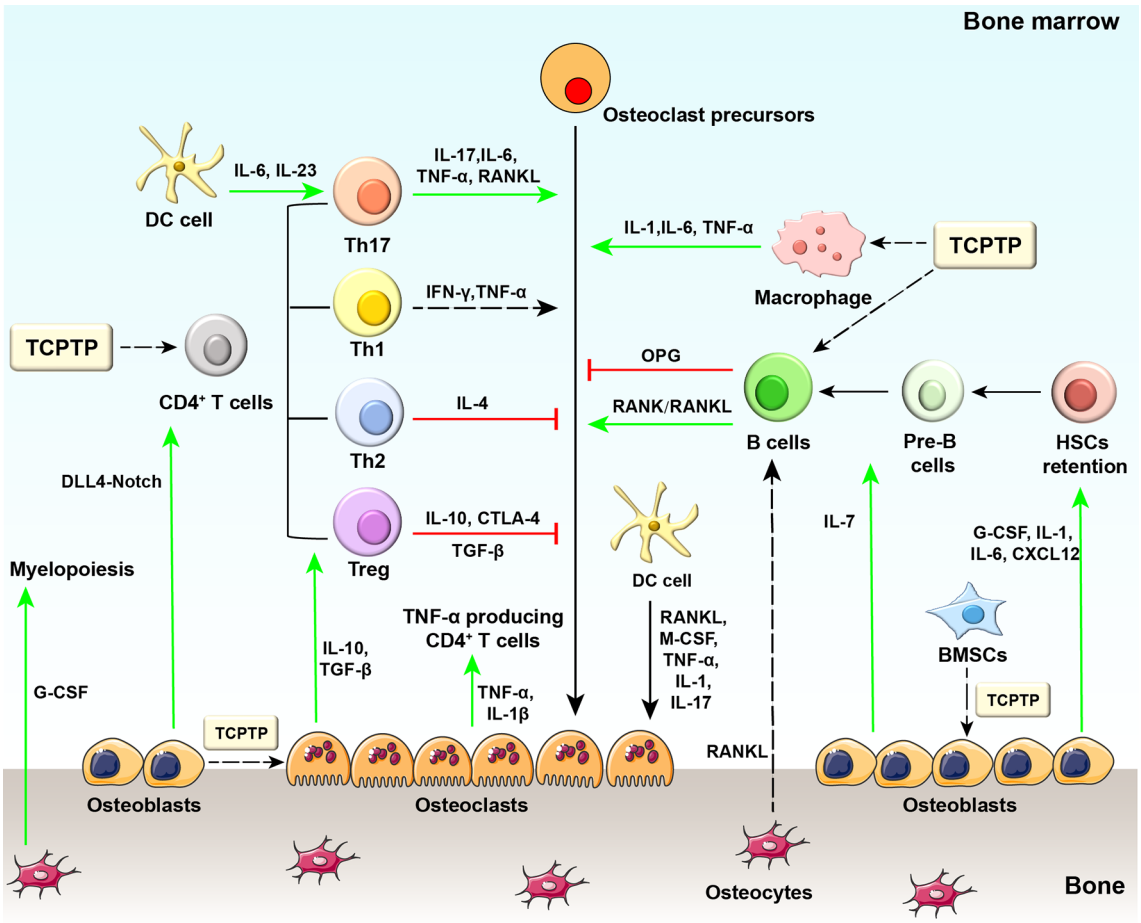

FIGURE 1 | Diagram of osteoimmunology and potential regulatory sites of TCPTP. Regarding the regulation of bone-related cells by immune cells, some $CD4^+$ T cell subsets can produce osteoclastogenic cytokines (e.g., TNF-α from Th1 cells and IL–17 from Th17 cells), while other subsets secrete anti-osteoclastogenic cytokines (e.g., IL–4 from Th2 cells, IL–10 and CTLA4 from Treg cells). IFN-γ released by Th1 cells may exert both pro- and anti-osteoclastogenic effects as reported by previous studies. B cells physiologically inhibit osteoclastogenesis but stimulate osteoclastogenesis through activating the RANK/RANKL axis in the pathological state. Different stages of dendritic cells exhibit distinct properties in immune responses: immature dendritic cells differentiate into osteoclasts in response to M-CSF, RANKL, TNF-α, IL-1, and IL-17, while mature ones drive the activation and expansion of Th17 cells. Macrophages are essential to bone loss with the involvement of TNF-α, IL-1, and IL-6 released by themselves. On the other hand, bone-related cells also provide feedback to immune cells. Osteoblasts secrete G-CSF, IL–1, IL–6, IL–7, and CXCL12, which are required for HSCs maintenance. In addition, osteoblasts secrete IL-7 to support B lymphopoiesis and regulate DLL4-Notch signaling pathway to support T lymphopoiesis. Osteocytes are supposed to mobilize HSCs and are involved in myelopoiesis. Osteocyte-derived RANKL participates in estrogen deficiency-induced bone loss by indirect regulation of B cell development. Osteoclasts are also involved in antigen presentation and T cell activation. Osteoclasts secrete tolerogenic cytokines (e.g., IL-10, TGF-β) and activate regulatory T cells in physiological conditions, while in pathological conditions, osteoclasts secrete inflammatory cytokines (e.g., TNFα, IL-1β) and activate TNF-α producing $CD4^+$ T cells. Generally, TCPTP regulates bone metabolism mainly by changing the biofunction of macrophages, T cells, and B cells. TCPTP, T cell protein tyrosine phosphatase; DC cell, dendritic cell; IL-6, interleukin-6; IL-23, interleukin-23; IL-17, interleukin-17; TNF-α, tumor necrosis factor-α; RANK, receptor activator of nuclear factor–κB; RANKL, receptor activator of nuclear factor–κB ligand; IL-1, interleukin-1; IL-4, interleukin-4; IL-10, interleukin-10; CTLA4, cytotoxic T lymphocyte protein 4; OPG, osteoprotegerin; Th17, T helper 17 cells; Th1, T helper 1 cells; Th2, T helper 2 cells; Treg, regulatory T cells; G-CSF, granulocyte colony-stimulating factor; M-CSF, macrophage colony-stimulating factor; TGF-β, transforming growth factor β; DLL4, Delta-like protein 4; IL-1β, interleukin-1β; IL-7, interleukin-7; CXCL12, CXC-motif chemokine 12; HSCs, hematopoietic stem cells.

effects in bone metabolism (6, 7). Sato et al. demonstrated that Th1 cells generated amounts of IFN-γ and mediated osteoclastogenesis inhibition *in vitro* (8). However, another study reported that IFN-γ could promote osteoclast maturation in the late period of osteoclastogenesis (9). Th1 cells are found to induce orthodontic tooth movement and bone resorption indirectly by upregulating the tumor necrosis factor-alpha (TNF-α) secretion and promoting osteoclastogenesis (10, 11). Th2 cells secrete interleukin-4 (IL-4), interleukin-5 (IL-5), and interleukin-13 (IL-13) leading to the osteoclastogenesis inhibition in a signal transducer and activator of transcription 6 (STAT6)-dependent pathway (12). Cytotoxic T-lymphocyte antigen 4 (CTLA4) secreted by Treg cells can promote apoptosis of osteoclasts *via* binding to CD80/CD86 on osteoclast precursors (13). Besides, Treg cells not only inhibit osteoclastogenesis directly *via* suppressing receptor activator of nuclear factor-κB ligand (RANKL) generation (14) but also suppress osteoclast differentiation and bone resorption by secreting interleukin-10 (IL-10) and transforming growth factor-β (TGF-β) (15). Th17 cells are one of the osteoclastogenic subsets of T cells that participate in various inflammatory diseases, such as rheumatoid arthritis, osteoporosis, inflammatory bowel disease, and periodontal disease (16–18). In the process of osteoclastogenesis and bone loss, higher amounts of osteoclastogenic cytokines, including interleukin-17 (IL-17), interleukin-6 (IL-6), interleukin-1 (IL-1), and TNF-α, are released from Th17 cells (19, 20). Among these cytokines, IL-17 stimulates the synthesis of cyclooxygenase-2 dependent prostaglandin E2 and the gene transcription of osteoclast differentiation factor (ODF) in osteoblasts to induce osteoclastogenesis (21). B cells inhibit osteoclastogenesis *via* secreting osteoprotegerin in the physiological state but stimulate osteoclastogenesis through activating the receptor activator of nuclear factor−κB (RANK)/RANKL axis in the pathological state (22, 23). Human immature dendritic cells differentiate into osteoclasts in response to macrophage colony-stimulating factor (M-CSF), RANKL, TNF-α, IL-1, and IL-17 (24–26), while mature dendritic cells can drive the activation of Th17 cells that produce IL-17, thereby enhancing osteoclastogenesis (27). Macrophages are reported to secrete different proinflammatory cytokines (e.g., TNF-α, IL-1, and IL-6) to enhance bone loss (28).

Influence of Bone Cells on Immune Cells

Bone-related cells (e.g., osteoblasts, osteocytes, osteoclasts) could also regulate the immune system. In this process, numerous cytokines (e.g., granulocyte colony-stimulating factor [G−CSF], IL−1, IL−6, IL−7, and CXC-motif chemokine 12 [CXCL12]) are secreted from osteoblasts for hematopoietic stem cell (HSC) maintenance, lymphoid progenitor cell maintenance, as well as the balance of T cell or B cell generation (29–31). Zhu et al. reported that osteoblasts support all stages of B lymphopoiesis *via* locally secreting interleukin-7 (IL-7) and stromal cell derived factor-1 (SDF-1) (32, 33). Osteoblasts-specific knockout of osteocalcin results in a marked reduction in mature T cells through disrupting the delta-like protein 4-notch signaling (34). Osteocytes are supposed to mobilize hematopoietic stem cells (HSCs) and might also be involved in myelopoiesis. In mice with targeted ablation of osteocytes, the mobilization of HSCs was suppressed in bone marrow (35). Besides, deficiency of the G−protein subunit GSα in osteocytes results in increased G−CSF production and dramatic expansion of myeloid lineage cells (36). RANKL generated by osteocytes participates in estrogen deficiency-induced bone loss by regulating B cell development indirectly (37). Several studies reported that osteoclasts could promote the mobilization of hematopoietic progenitor cells (38), while others revealed that they were dispensable for HSC maintenance and mobilization (39). Osteoclasts are also involved in antigen presentation and T cell activation. In the physiological conditions, osteoclasts secrete tolerogenic cytokines (such as IL-10 and TGF-β) and activate $CD4^+$ and $CD8^+$ regulatory T cells, while in the pathological conditions, osteoclasts activate TNF-α producing $CD4^+$ T cells *via* unleashing myriads of inflammatory cytokines (e.g., TNF-α and IL-1) (26, 40, 41).

TCPTP

Overview of TCPTP

TCPTP is a tyrosine-specific phosphatase that is firstly identified by Cool et al. (5). There are two splice variants of TCPTP: TC45 (45 kDa) which is located in nuclear and TC48 (48 kDa) which is located in the endoplasmic reticulum (42). TC45 is a widely expressed form in various species, including humans and mice, and TC48 is human-specific. In most species, TC45 shuttles between the nucleus and cytoplasm in response to cytokine stimulation (43).

TCPTP regulates diverse signaling pathways related to glucose metabolism, inflammation control, cancer progress, and other biological processes *via* dephosphorylation of distinct substrates (44–50). Experiments *in vitro* and *in vivo* have confirmed that TCPTP could regulate several cytokine signaling pathways by inhibiting Janus activated kinase (JAK)/signal transducer and activator of transcription (STAT) predominantly (51–54). The direct substrates have been recognized as JAK1, JAK3, STAT1, STAT3, and STAT5 (55–59). Some members of the tyrosine kinase receptor (RTK) family, comprising insulin receptors (IRs) (60, 61), epidermal growth factor receptors (EGFRs) (62, 63), vascular endothelial growth factor receptors (VEGFRs) (64), platelet-derived growth factor receptors (PDGFRs) (65, 66) and colony-stimulating factor-1 receptors (CSF-1Rs) are also the specific dephosphorylating substrates of TCPTP (67).

TCPTP and Immunomodulation

Growing evidence has indicated that TCPTP is a key player in regulating innate and acquired immune responses. GWA studies found single nucleotide polymorphisms (SNPs) of TCPTP are associated with the onset of several inflammatory diseases and autoimmunology disorders, such as inflammatory bowel disease (68, 69), ocular Behcet's disease (70), rheumatoid arthritis (53), and juvenile inflammatory arthritis (71). *Tcptp* knockout in the systemic or specific cells can seriously jeopardize immune reactions.

Mice null for *Tcptp* ($Tcptp^{-/-}$) showed a smaller body size, decreased mobility, severe anemia, and diarrhea followed by

death at three to 5 weeks of age (72). From the perspective of histology, *Tcptp*$^{-/-}$ mice showed mononuclear cell infiltration in the salivary gland and gastric mucosa at 1 week of age (72). Dramatic increases in TNF-α and inducible nitric oxide synthase (iNOS) were also detected at 3 weeks of age in *Tcptp*$^{-/-}$ mice (73).

Loss of PTPN2 in T cells (TCPTP-CD4Cre) not only led to increased intestinal inflammation risk but also resulted in T-lymphocyte infiltration in the liver, kidney, and skin (74, 75). This may be caused by the enhanced induction of Th1 cells, Th17 cells, and effector and memory CD8$^+$ T cells, but the impaired induction of Tregs after T cell-specific knockout of *Tcptp*. Myeloid cell-specific loss of TCPTP (TCPTP-LysMCre) also enhanced susceptibility to colitis and serum IL-1β levels in mice (76). Spalinger et al. reported that TCPTP loss in macrophages compromises epithelial cell-macrophage interactions and reduces epithelial barrier integrity (77). Furthermore, TCPTP knockdown in THP-1 cells elevated the IFN-γ-induced secretion of the proinflammatory cytokines IL-6 (78). TCPTP silencing in rheumatoid arthritis synovial fibroblasts could also increase IL-6 production (53).

TCPTP and Hematopoiesis

Although ubiquitously expressed, TCPTP is pronouncedly expressed in hematopoietic tissues and plays a significant role in the development of hematopoietic lineages (5).

TCPTP and Hematopoiesis: Stem Cells

Hematopoietic stem cells (HSCs) are one of the adult stem cells and can differentiate into various mature blood cells (79). Compared with the control group, *Tcptp* knockout resulted in a nine-fold increase of the HSC number in the bone marrow (80). Lymphoid and myeloid precursors were also more abundant in *Tcptp*$^{-/-}$ mice compared with the wide type controls (45). Bourdeau et al. also demonstrated that this effect could be reproduced by TCPTP inhibiting agents and interleukin-18 (IL-18) signaling pathway involved in this process (80). The above results implicated that TCPTP plays an important role in the regulation of HSC proliferation.

TCPTP and Hematopoiesis: Myeloid Cells

Tcptp$^{-/-}$ mice exhibited increased splenic macrophage populations and yielded four times of the macrophage colony-forming unit (CFU-M) number (67). TCPTP is also involved in myeloid progenitor development. *Tcptp*$^{-/-}$ mice had 4 times of the granulocyte/macrophage precursors (GMPs) compared with wildtype mice and CSF-1/CSF-1R signaling may involve in this process (67).

Tcptp$^{-/-}$ mice were reported to suffer from severe anemia which could contribute to their early lethality. You-Ten et al. reported a failure to initiate hematopoietic function in the bone marrow of *Tcptp*$^{-/-}$ animals after 2–3 weeks (72). What's more, the deficiency of bone marrow stromal cell numbers, the impairment of remaining stromal cells, and the inadequate cytokines production by the bone marrow microenvironment could be the possible explanations for the defective hematopoiesis in *Tcptp*$^{-/-}$ mice (72).

TCPTP and Hematopoiesis: Lymphocytes

Tcptp$^{-/-}$ mice exhibited specific defects of B cell lymphopoiesis in the bone marrow, however, T cell development in the thymus was not significantly affected (72). The defects of B cell lymphopoiesis were characterized by fewer pre-B cell colonies and impaired transition to the immature B-cell stage (81). Bourdeau et al. have found that bone marrow stromal cells from *Tcptp*$^{-/-}$ mice could secrete higher levels of IFN-γ resulting in a 2-fold reduction in the mitotic index on IL-7 stimulation of *Tcptp*$^{-/-}$ pre-B cells (81).

TCPTP and Bone Metabolism

Recent studies using gene knockout mice have emphasized the importance of TCPTP in bone metabolism. *Tcptp*$^{-/-}$ BALB/c mice showed significantly reduced femoral length and width, as reflected by the large volume of unabsorbed cartilage at the epiphysis by 14 days of age (82); however the latter was no longer evident at 21 days of age (82). Besides, *Tcptp*$^{-/-}$ mice have a higher incidence of synovitis in the knee joint (83). Loh et al. found that the runted body of neuronal cell-specific *Tcptp* knockout mice is associated with decreased circulating growth hormone (84). However, the precise mechanisms that underlie the bone development in *Tcptp*$^{-/-}$ mice still need further investigation.

Insulin signaling in osteoblast inhibits the expression of osteoprotegerin (OPG), an osteoclastogenesis inhibitory factor (85). TCPTP expressed in osteoblasts regulates insulin receptor phosphorylation, thus activating insulin signaling (86). A classical coculture assay revealed that osteoblasts lacking TCPTP induced more tartrate-resistant acid phosphatase (TRAP) positive osteoclasts than wild-type osteoblasts did (86). Accordingly, osteoclast activity was increased in osteoblasts-specific *Tcptp*$^{-/-}$ mice which was proved by increased serum levels of CTx, a marker of bone resorption (86).

TCPTP IN OSTEOIMMUNOLOGY

As shown in **Figure 1**, TCPTP could influence bone metabolism by regulating the biofunction of macrophages, T cells, and B cells. Besides, TCPTP in osteoblasts and bone marrow stem cells also regulates bone metabolism. The potential roles of TCPTP in osteoimmunology are discussed below.

TCPTP and Macrophages in Osteoimmunology

Macrophages, a significant component of the non-specific immunity, are crucial regulators in bone metabolism and can be regulated by TCPTP (77, 87, 88). The potential influences of TCPTP on osteoimmunology through macrophages can be expounded from four aspects. Firstly, TCPTP negatively regulates macrophages development (45). *Tcptp*$^{-/-}$ animals exhibited significantly impaired bone marrow microenvironment (including impairment of erythropoiesis, the decline of pre-B and mature B cells, and reduced stromal cells) and increased macrophage numbers (89). Secondly, TCPTP participates in the process of macrophage polarization. M1 and M2 macrophages, the two major phenotypes of macrophages, are pro-inflammatory and

anti-inflammatory respectively. A previous study reported that the increased M1/M2 ratio finally promoted osteoclastogenesis (90), and TCPTP could reverse diabetes-mediated high M1/M2 polarization in mice (91). This can be attributed to the fact that macrophages from *Tcptp*$^{-/-}$ mice are inherently hypersensitive to lipopolysaccharide and IFN-γ stimulation, which are two main cytokines that induce M1 differentiation (73, 92). Thirdly, the colony-stimulating factor 1 (CSF-1)/colony-stimulating factor 1 receptor (CSF-1R) signaling has been proven to be downregulated by TCPTP in macrophages. After CSF-1 stimulation, tyrosine phosphorylation of the CSF-1R markedly increased, and the activation of extracellular regulated protein kinases (ERK) was enhanced in *Tcptp*$^{-/-}$ macrophages (67). Zhang et al. ascertained that TCPTP inhibited alveolar bone resorption in diabetic periodontitis *via* dephosphorylating CSF-1R at the Y807 site, thereby prohibiting osteoclast differentiation (93). Fourthly, the dephosphorylating of c-Jun N-terminal kinase (JNK) in macrophages is another means how TCPTP protects against inflammatory response and bone loss caused by inflammasome-mediated interleukin-1β secretion (76). These studies suggest that TCPTP may be a potential treatment target against inflammatory bone loss induced by macrophage-related disorders, for example, periodontitis and synovitis (**Figure 2A**).

TCPTP and T Cells in Osteoimmunology

Undoubtedly, T cells play a critical role in bone homeostasis, wherein the effects of TCPTP on T cell function cannot be neglected (**Figure 2C**). TCPTP negatively regulates T cell activation (94, 95). *Tcptp*$^{-/-}$ T cells show enhanced cell activity *via* the reduction of T cell receptor (TCR) threshold and hyperphosphorylation of the activated tyrosine residue of Lck (75). Furthermore, TCPTP regulates T cell differentiation (91, 96, 97). TCPTP regulated the activation and differentiation of T cells in colonic inflammation (96). Wiede et al. showed that TCPTP attenuates the activity of the STAT5 signaling to regulate αβ TCR versus γδ TCR T cell development (97). Li et al. reported that TCPTP overexpression reversed the high Th1/Treg and Th17/Treg ratios in epididymal white adipose tissue of diabetic mice (91). Spalinger et al. showed that *Tcptp*$^{-/-}$ CD4^{+} T cell reinfusion led to a nearly 3-fold increase in the frequency of Th1 cells, a 2-fold increase in the frequency of Th17 cells, and by contrast, a 3-fold decrease in the frequency of Tregs in colitis animal models (74). In addition, the inhibition of the interleukin-2 (IL-2)/IL-2 receptor pathway mediated by JAK1, JAK3, and STAT5 dephosphorylation was found to be the mechanism of how TCPTP drives Treg differentiation possibly (98). As illustrated above, various cytokines (e.g., IFN-γ and IL-6 from Th1 cells) released from stimulated T cells bridge the two-way communications in osteoimmune responses. These two cytokines, which are closely associated with osteoimmunology, can be regulated by TCPTP. Therefore, the interactions between the two cytokines and TCPTP in bone metabolism were discussed in detail below.

TCPTP and IFN-γ

IFN-γ is a classical cytokine secreted from Th1 cells. On the one hand, IFN-γ promotes osteoclastogenesis *via* promoting the fusion of mononucleated pre-osteoclasts in the late period of osteoclastogenesis directly and stimulating the secretion of osteoclastic factors (such as RANKL and TNF-α)indirectly (9, 99, 100). By contrast, IFN-γ can also intensively suppress osteoclastogenesis by degrading tumor necrosis factor receptor-associated factor 6 and inhibiting the RANK/RANKL signaling pathway (6). TCPTP downregulates the IFN-γ signaling through JAK1, STAT1, and STAT3 dephosphorylation (52, 55, 59, 92). So, a rational thread of targeting TCPTP to suppress IFN-γ activity is expected to regulate osteoclastogenesis, and this hypothesis still needs more validations.

TCPTP and IL-6

IL-6 is an inflammatory cytokine that exerts pathological effects on inflammatory bone loss (101, 102), directly supporting osteoclast formation, stimulating osteoclast differentiation, and accelerating bone resorption (103, 104). IL-6 is associated with Th17 cell differentiation (105), and abnormalities in the IL-6 signaling can disturb the Th17/Treg balance and influence bone homeostasis indirectly (106). Concerning the regulation of IL-6 by TCPTP, TCPTP curbs both IL-6 secretion and signaling. Aradi et al. confirmed that TCPTP silencing significantly increased IL-6 secretion from synovial fibroblasts in rheumatoid arthritis animals (53). TCPTP also dephosphorylate STAT3 at the Y705 site, thereby suppressing IL-6 signaling (107, 108). Besides, TCPTP inhibits the IL-6-driven pathogenic loss of Foxp3 after Tregs have acquired RORγt expression through dephosphorylation of STAT3 (109). Therefore, TCPTP can be expected to inhibit bone resorption through inhibiting IL-6 generation and IL-6 signaling directly or reversing IL-6-induced Th17/Treg imbalance indirectly.

TCPTP and B Cells in Osteoimmunology

B lymphocytes play an extremely vital role in both immune responses and bone metabolism, but the detailed relationship between B lymphocytes and osteoclastogenesis remains some points for debate. Physiologically, B cells produce osteoprotegerin to inhibit osteoclastogenesis but stimulate osteoclastogenesis *via* the RANK/RANKL axis in the pathological state (22, 23, 110). Recently, increasing evidence tended to support that B cell development and proliferation were crucially affected by TCPTP (**Figure 2B**). An impaired transition from pre-B to immature B cell was found in *Tcptp*$^{-/-}$ mice (45, 89), which might be associated with the abnormally increased release of IFN-γ and enhanced STAT1 phosphorylation in the pre-B cell compartment (81). With interleukin-21-induced hyperactivity of the STAT-3 signaling in *Tcptp*$^{-/-}$ mice, B cell proliferation was simultaneously boosted (111). These results ascertain TCPTP as an important regulator of B cells in bone homeostasis. However, concerning the complexity of the two-way effect between B lymphocytes and bone homeostasis or between TCPTP and B lymphocytes, the specific effect and the mechanisms behind each regulation should be confirmed in further explorations.

TCPTP and Bone-Related Cells in Osteoimmunology

TCPTP that is expressed in osteoblasts and bone marrow stem cells participates in the regulation of bone metabolism

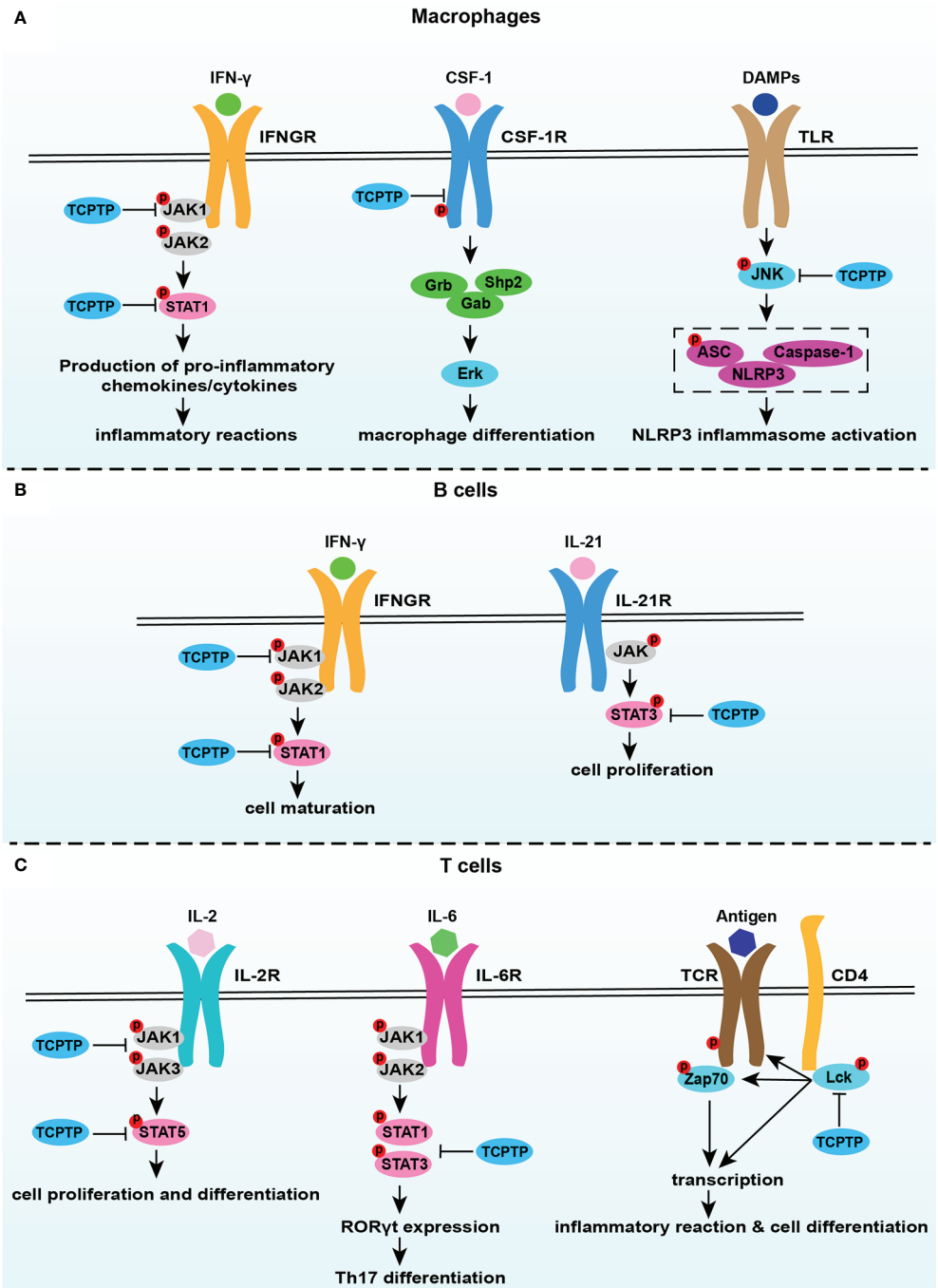

FIGURE 2 | TCPTP-related signaling pathways in macrophages, B cells, and T cells. **(A)** TCPTP downregulates the IFN-γ signaling, the CSF-1/CSF-1R signaling, and inflammasome activation in macrophages. **(B)** TCPTP drives B cell maturation *via* suppressing the IFN-γ signaling and prohibits B cell proliferation by downregulating the IL-21 signaling. **(C)** TCPTP inhibits IL-6-driven pathogenic loss of Foxp3 after Tregs have acquired RORγt expression through dephosphorylation of STAT3. TCPTP negatively regulates the IL-2 receptor signaling by JAK1, JAK3, and STAT5 dephosphorylation, which is an important way related to Treg differentiation. TCPTP inhibits TCR activation and hyperphosphorylation of Lck to inhibit inflammatory reactions and cell differentiation. TCPTP, T cell protein tyrosine phosphatase; JAK1, Janus activated kinase 1; JAK2, Janus activated kinase 2; JAK3, Janus activated kinase 3; STAT1, signal transducer and activator of transcription1; STAT3, signal transducer and activator of transcription3; STAT5, signal transducer and activator of transcription5; IFN-γ, interferon-γ; IFNGR, interferon-γ receptor; CSF-1, colony-stimulating factor 1; CSF-1R, colony-stimulating factor 1 receptor; DAMPs, damage-associated molecular pattern molecules; TLR, toll-like receptor; JNK, c-Jun N-terminal kinase; IL-21, interleukin-21; IL-21R, interleukin-21R; IL-6, interleukin-6; IL-6R, interleukin-6R; TCR, T cell receptor.

(**Figure 1**). Zee et al. demonstrated that TCPTP deficiency in osteoblasts enhanced the activity of osteoclasts by activating insulin signaling and inhibiting the expression of OPG *in vitro* (86). Our previous study found that TCPTP improved the osteogenic differentiation ability *via* ERK dephosphorylation in rat bone marrow stem cells in high glucose conditions (112). However, to our knowledge, no specific studies have reported the impacts of TCPTP in bone-related cells on immune cells which may be a novel aspect in the future, and the underlying mechanism also needs further exploration.

THERAPEUTIC ASPECTS FROM "TCPTP AND OSTEOIMMUNOLOGY" PERSPECTIVE

TCPTP exerts an anti-inflammatory role in innate and adaptive immunity (113). As described in Section *TCPTP and Immunomodulation*, *Tcptp* knockout in systemic or specific immune cells brings about serious immune disorders. TCPTP deficiency also leads to subchondral bone loss and spontaneous synovitis mediated by excessive inflammatory cytokines (83). Loss-of-function variants of TCPTP increase the risk of rheumatoid arthritis due to Treg cell dysfunction (114). Therefore, using TCPTP agonists to overexpress or activate TCPTP seems to be a rational strategy against inflammatory bone resorption. This proposal can be supported by other studies. Zhang P. et al. found that TCPTP alleviated inflammatory responses and bone resorption in periodontal tissues *via* the JAK/STAT pathway in human oral keratinocytes and type 2 diabetes mellitus (T2DM) *db*/*db* mice (115). Zhang D.J. et al. demonstrated that TCPTP inhibited alveolar bone resorption in T2DM C57BL/6 wild-type mice *via* dephosphorylating CSF1 receptor (93). Consistently, our previous study series ascertained that TCPTP improves implant osseointegration in T2DM rats *via* ERK dephosphorylation (112). It is obvious that TCPTP could work as an effective potential target for preventing and treating inflammatory bone resorption. However, concerning the ubiquitous distribution and wide regulation of TCPTP related to glucose metabolism, immunoregulation, oncogenesis, and other various life processes in a cell or tissue-specific way, designing specific agents targeting TCPTP in specific cells, tissues or organs is a promising research direction and a novel aspect of osteoimmunology in the future.

CONCLUSION

TCPTP bridges the two-way communication between immune cells and bone cells and it could work as a potential target for the prevention and treatment of inflammatory bone diseases, such as periodontitis, synovitis, and osteoarthritis. The proposal of identifying whether TCPTP can be used as an independent therapeutic target is feasible for the development of TCPTP agonists binding to a target of interest. This review provides clear insights into the potential roles of TCPTP in osteoimmunology, which may pave the way for further bone studies on osteoimmunological aspects.

AUTHOR CONTRIBUTIONS

Y-NW, SL, TJ, YF, and DZ made substantial contributions to conception, design, and acquisition of data. Y-NW, SL, WZ, and XX drafted the initial manuscript. XX and DZ critically reviewed it for important intellectual content. All authors contributed to the article and approved the submitted version.

FUNDING

This work was supported by the National Natural Science Foundation of China (no. 82071148; no. 82001055), the Construction Engineering Special Fund of Taishan Scholars (TS201511106), the Key Project of Chinese National Programs for Research and Development (2016YFC1102705), the Shandong Provincial Natural Science Foundation (ZR2020QH158), the Fundamental Research Funds of Shandong University (2018GN024), the China Postdoctoral Science Foundation (2019M662371), and the Youth scientific research funds of School of Stomatology, Shandong University (2019QNJJ03).

REFERENCES

1. Orsolini G, Bertoldi I, Rossini M. Osteoimmunology in rheumatoid and psoriatic arthritis: potential effects of tofacitinib on bone involvement. *Clin Rheumatol* (2020) 39:727–36. doi: 10.1007/s10067-020-04930-x
2. Gruber R. Osteoimmunology: Inflammatory osteolysis and regeneration of the alveolar bone. *J Clin Periodontol* (2019) 46 Suppl 21:52–69. doi: 10.1111/jcpe.13056
3. Chen Z, Bozec A, Ramming A, Schett G. Anti-inflammatory and immune-regulatory cytokines in rheumatoid arthritis. *Nat Rev Rheumatol* (2019) 15:9–17. doi: 10.1038/s41584-018-0109-2
4. Arron JR, Choi Y. Bone versus immune system. *Nature* (2000) 408:535–6. doi: 10.1038/35046196
5. Cool DE, Tonks NK, Charbonneau H, Walsh KA, Fischer EH, Krebs EG. cDNA isolated from a human T-cell library encodes a member of the protein-tyrosine-phosphatase family. *Proc Natl Acad Sci USA* (1989) 86:5257–61. doi: 10.1073/pnas.86.14.5257
6. Takayanagi H, Ogasawara K, Hida S, Chiba T, Murata S, Sato K, et al. T-cell-mediated regulation of osteoclastogenesis by signalling cross-talk between RANKL and IFN-gamma. *Nature* (2000) 408:600–5. doi: 10.1038/35046102
7. Tang M, Tian L, Luo G, Yu X. Interferon-Gamma-Mediated Osteoimmunology. *Front Immunol* (2018) 9:1508:1508. doi: 10.3389/fimmu.2018.01508
8. Sato K, Suematsu A, Okamoto K, Yamaguchi A, Morishita Y, Kadono Y, et al. Th17 functions as an osteoclastogenic helper T cell subset that links T cell activation and bone destruction. *J Exp Med* (2006) 203:2673–82. doi: 10.1084/jem.20061775
9. Kim JW, Lee MS, Lee CH, Kim HY, Chae SU, Kwak HB, et al. Effect of interferon-γ on the fusion of mononuclear osteoclasts into bone-resorbing osteoclasts. *BMB Rep* (2012) 45:281–6. doi: 10.5483/bmbrep.2012.45.5.281

10. Yan Y, Liu F, Kou X, Liu D, Yang R, Wang X, et al. T Cells Are Required for Orthodontic Tooth Movement. *J Dent Res* (2015) 94:1463–70. doi: 10.1177/0022034515595003
11. Marahleh A, Kitaura H, Ohori F, Kishikawa A, Ogawa S, Shen WR, et al. TNF-α Directly Enhances Osteocyte RANKL Expression and Promotes Osteoclast Formation. *Front Immunol* (2019) 10:2925:2925. doi: 10.3389/fimmu.2019.02925
12. Palmqvist P, Lundberg P, Persson E, Johansson A, Lundgren I, Lie A, et al. Inhibition of hormone and cytokine-stimulated osteoclastogenesis and bone resorption by interleukin-4 and interleukin-13 is associated with increased osteoprotegerin and decreased RANKL and RANK in a STAT6-dependent pathway. *J Biol Chem* (2006) 281:2414–29. doi: 10.1074/jbc.M510160200
13. Wing K, Yamaguchi T, Sakaguchi S. Cell-autonomous and -non-autonomous roles of CTLA-4 in immune regulation. *Trends Immunol* (2011) 32:428–33. doi: 10.1016/j.it.2011.06.002
14. Wang J, Jiang H, Qiu Y, Wang Y, Sun G, Zhao J. Effector memory regulatory T cells were most effective at suppressing RANKL but their frequency was downregulated in tibial fracture patients with delayed union. *Immunol Lett* (2019) 209:21–7. doi: 10.1016/j.imlet.2019.03.018
15. Luo CY, Wang L, Sun C, Li DJ. Estrogen enhances the functions of CD4(+) CD25(+)Foxp3(+) regulatory T cells that suppress osteoclast differentiation and bone resorption in vitro. *Cell Mol Immunol* (2011) 8:50–8. doi: 10.1038/cmi.2010.54
16. Miossec P, Korn T, Kuchroo VK. Interleukin-17 and type 17 helper T cells. *N Engl J Med* (2009) 361:888–98. doi: 10.1056/NEJMra0707449
17. Yasuda K, Takeuchi Y, Hirota K. The pathogenicity of Th17 cells in autoimmune diseases. *Semin Immunopathol* (2019) 41:283–97. doi: 10.1007/s00281-019-00733-8
18. Dey I, Bishayi B. Role of Th17 and Treg cells in septic arthritis and the impact of the Th17/Treg -derived cytokines in the pathogenesis of S. aureus induced septic arthritis in mice. *Microb Pathog* (2017) 113:248–64. doi: 10.1016/j.micpath.2017.10.033
19. Samuel RO, Ervolino E, de Azevedo Queiroz ÍO, Azuma MM, Ferreira GT, Cintra LTA. Th1/Th2/Th17/Treg Balance in Apical Periodontitis of Normoglycemic and Diabetic Rats. *J Endod* (2019) 45:1009–15. doi: 10.1016/j.joen.2019.05.003
20. Li JY, Yu M, Tyagi AM, Vaccaro C, Hsu E, Adams J, et al. IL-17 Receptor Signaling in Osteoblasts/Osteocytes Mediates PTH-Induced Bone Loss and Enhances Osteocytic RANKL Production. *J Bone Miner Res* (2019) 34:349–60. doi: 10.1002/jbmr.3600
21. Kotake S, Udagawa N, Takahashi N, Matsuzaki K, Itoh K, Ishiyama S, et al. IL-17 in synovial fluids from patients with rheumatoid arthritis is a potent stimulator of osteoclastogenesis. *J Clin Invest* (1999) 103:1345–52. doi: 10.1172/jci5703
22. Li Y, Toraldo G, Li A, Yang X, Zhang H, Qian WP, et al. B cells and T cells are critical for the preservation of bone homeostasis and attainment of peak bone mass in vivo. *Blood* (2007) 109:3839–48. doi: 10.1182/blood-2006-07-037994
23. Weitzmann MN. T-cells and B-cells in osteoporosis. *Curr Opin Endocrinol Diabetes Obes* (2014) 21:461–7. doi: 10.1097/med.0000000000000103
24. Rivollier A, Mazzorana M, Tebib J, Piperno M, Aitsiselmi T, Rabourdin-Combe C, et al. Immature dendritic cell transdifferentiation into osteoclasts: a novel pathway sustained by the rheumatoid arthritis microenvironment. *Blood* (2004) 104:4029–37. doi: 10.1182/blood-2004-01-0041
25. Speziani C, Rivollier A, Gallois A, Coury F, Mazzorana M, Azocar O, et al. Murine dendritic cell transdifferentiation into osteoclasts is differentially regulated by innate and adaptive cytokines. *Eur J Immunol* (2007) 37:747–57. doi: 10.1002/eji.200636534
26. Madel MB, Ibáñez L, Wakkach A, de Vries TJ, Teti A, Apparailly F, et al. Immune Function and Diversity of Osteoclasts in Normal and Pathological Conditions. *Front Immunol* (2019) 10:1408:1408. doi: 10.3389/fimmu.2019.01408
27. Dhodapkar KM, Barbuto S, Matthews P, Kukreja A, Mazumder A, Vesole D, et al. Dendritic cells mediate the induction of polyfunctional human IL17-producing cells (Th17-1 cells) enriched in the bone marrow of patients with myeloma. *Blood* (2008) 112:2878–85. doi: 10.1182/blood-2008-03-143222
28. Kwan Tat S, Padrines M, Théoleyre S, Heymann D, Fortun Y. IL-6, RANKL, TNF-alpha/IL-1: interrelations in bone resorption pathophysiology. *Cytokine Growth Factor Rev* (2004) 15:49–60. doi: 10.1016/j.cytogfr.2003.10.005
29. Mercier FE, Ragu C, Scadden DT. The bone marrow at the crossroads of blood and immunity. *Nat Rev Immunol* (2011) 12:49–60. doi: 10.1038/nri3132
30. Taichman RS, Emerson SG. Human osteoblasts support hematopoiesis through the production of granulocyte colony-stimulating factor. *J Exp Med* (1994) 179:1677–82. doi: 10.1084/jem.179.5.1677
31. Nakamura Y, Arai F, Iwasaki H, Hosokawa K, Kobayashi I, Gomei Y, et al. Isolation and characterization of endosteal niche cell populations that regulate hematopoietic stem cells. *Blood* (2010) 116:1422–32. doi: 10.1182/blood-2009-08-239194
32. Zhu J, Garrett R, Jung Y, Zhang Y, Kim N, Wang J, et al. Osteoblasts support B-lymphocyte commitment and differentiation from hematopoietic stem cells. *Blood* (2007) 109:3706–12. doi: 10.1182/blood-2006-08-041384
33. Wu JY, Purton LE, Rodda SJ, Chen M, Weinstein LS, McMahon AP, et al. Osteoblastic regulation of B lymphopoiesis is mediated by Gs{alpha}-dependent signaling pathways. *Proc Natl Acad Sci USA* (2008) 105:16976–81. doi: 10.1073/pnas.0802898105
34. Yu VW, Saez B, Cook C, Lotinun S, Pardo-Saganta A, Wang YH, et al. Specific bone cells produce DLL4 to generate thymus-seeding progenitors from bone marrow. *J Exp Med* (2015) 212:759–74. doi: 10.1084/jem.20141843
35. Asada N, Katayama Y, Sato M, Minagawa K, Wakahashi K, Kawano H, et al. Matrix-embedded osteocytes regulate mobilization of hematopoietic stem/progenitor cells. *Cell Stem Cell* (2013) 12:737–47. doi: 10.1016/j.stem.2013.05.001
36. Azab E, Chandler KB, Uda Y, Sun N, Hussein A, Shuwaikan R, et al. Osteocytes control myeloid cell proliferation and differentiation through Gsα-dependent and -independent mechanisms. *FASEB J* (2020) 34:10191–211. doi: 10.1096/fj.202000366R
37. Fujiwara Y, Piemontese M, Liu Y, Thostenson JD, Xiong J, O'Brien CA. RANKL (Receptor Activator of NFκB Ligand) Produced by Osteocytes Is Required for the Increase in B Cells and Bone Loss Caused by Estrogen Deficiency in Mice. *J Biol Chem* (2016) 291:24838–50. doi: 10.1074/jbc.M116.742452
38. Kollet O, Dar A, Shivtiel S, Kalinkovich A, Lapid K, Sztainberg Y, et al. Osteoclasts degrade endosteal components and promote mobilization of hematopoietic progenitor cells. *Nat Med* (2006) 12:657–64. doi: 10.1038/nm1417
39. Miyamoto K, Yoshida S, Kawasumi M, Hashimoto K, Kimura T, Sato Y, et al. Osteoclasts are dispensable for hematopoietic stem cell maintenance and mobilization. *J Exp Med* (2011) 208:2175–81. doi: 10.1084/jem.20101890
40. Kiesel JR, Buchwald ZS, Aurora R. Cross-presentation by osteoclasts induces FoxP3 in CD8+ T cells. *J Immunol* (2009) 182:5477–87. doi: 10.4049/jimmunol.0803897
41. Ibáñez L, Abou-Ezzi G, Ciucci T, Amiot V, Belaïd N, Obino D, et al. Inflammatory Osteoclasts Prime TNFα-Producing CD4(+) T Cells and Express CX(3) CR1. *J Bone Miner Res* (2016) 31:1899–908. doi: 10.1002/jbmr.2868
42. Bussieres-Marmen S, Hutchins AP, Schirbel A, Rebert N, Tiganis T, Fiocchi C, et al. Characterization of PTPN2 and its use as a biomarker. *Methods* (2014) 65:239–46. doi: 10.1016/j.ymeth.2013.08.020
43. Tiganis T, Kemp BE, Tonks NK. The protein-tyrosine phosphatase TCPTP regulates epidermal growth factor receptor-mediated and phosphatidylinositol 3-kinase-dependent signaling. *J Biol Chem* (1999) 274:27768–75. doi: 10.1074/jbc.274.39.27768
44. Sharp RC, Abdulrahim M, Naser ES, Naser SA. Genetic Variations of PTPN2 and PTPN22: Role in the Pathogenesis of Type 1 Diabetes and Crohn's Disease. *Front Cell Infect Microbiol* (2015) 5:95. doi: 10.3389/fcimb.2015.00095
45. Doody KM, Bourdeau A, Tremblay ML. T-cell protein tyrosine phosphatase is a key regulator in immune cell signaling: lessons from the knockout mouse model and implications in human disease. *Immunol Rev* (2009) 228:325–41. doi: 10.1111/j.1600-065X.2008.00743.x
46. Stuible M, Doody KM, Tremblay ML. PTP1B and TC-PTP: regulators of transformation and tumorigenesis. *Cancer Metastasis Rev* (2008) 27:215–30. doi: 10.1007/s10555-008-9115-1
47. LaFleur MW, Nguyen TH. PTPN2 regulates the generation of exhausted CD8(+) T cell subpopulations and restrains tumor immunity. *Nat Immunol* (2019) 20:1335–47. doi: 10.1038/s41590-019-0480-4

48. Manguso RT, Pope HW, Zimmer MD, Brown FD, Yates KB, Miller BC, et al. In vivo CRISPR screening identifies Ptpn2 as a cancer immunotherapy target. *Nature* (2017) 547:413–18. doi: 10.1038/nature23270
49. Wiede F, Lu K-H, Du X, Liang S, Hochheiser K, Dodd GT, et al. PTPN2 phosphatase deletion in T cells promotes anti-tumour immunity and CAR T-cell efficacy in solid tumours. *EMBO J* (2020) 39:e103637–e37. doi: 10.15252/embj.2019103637
50. Wiede F, Brodnicki TC. T-Cell-Specific PTPN2 Deficiency in NOD Mice Accelerates the Development of Type 1 Diabetes and Autoimmune Comorbidities. *Diabetes* (2019) 68:1251–66. doi: 10.2337/db18-1362
51. Scharl M, McCole DF, Weber A, Vavricka SR, Frei P, Kellermeier S, et al. Protein tyrosine phosphatase N2 regulates TNFalpha-induced signalling and cytokine secretion in human intestinal epithelial cells. *Gut* (2011) 60:189–97. doi: 10.1136/gut.2010.216606
52. Scharl M, Hruz P, McCole DF. Protein tyrosine phosphatase non-receptor Type 2 regulates IFN-gamma-induced cytokine signaling in THP-1 monocytes. *Inflammation Bowel Dis* (2010) 16:2055–64. doi: 10.1002/ibd.21325
53. Aradi B, Kato M, Filkova M, Karouzakis E, Klein K, Scharl M, et al. Protein tyrosine phosphatase nonreceptor type 2: an important regulator of lnterleukin-6 production in rheumatoid arthritis synovial fibroblasts. *Arthritis Rheumatol* (2015) 67:2624–33. doi: 10.1002/art.39256
54. Parlato M, Nian Q, Charbit-Henrion F, Ruemmele FM, Rodrigues-Lima F, Cerf-Bensussan N. Loss-of-Function Mutation in PTPN2 Causes Aberrant Activation of JAK Signaling Via STAT and Very Early Onset Intestinal Inflammation. *Gastroenterology* (2020) 159:1968–71. doi: 10.1053/j.gastro.2020.07.040
55. Simoncic PD, Lee-Loy A, Barber DL, Tremblay ML, McGlade CJ. The T cell protein tyrosine phosphatase is a negative regulator of janus family kinases 1 and 3. *Curr Biol* (2002) 12:446–53. doi: 10.1016/s0960-9822(02)00697-8
56. Krishnan M, McCole DF. T cell protein tyrosine phosphatase prevents STAT1 induction of claudin-2 expression in intestinal epithelial cells. *Ann New Y Acad Sci* (2017) 1405:116–30. doi: 10.1111/nyas.13439
57. Fukushima A, Loh K, Galic S, Fam B, Shields B, Wiede F, et al. T-cell protein tyrosine phosphatase attenuates STAT3 and insulin signaling in the liver to regulate gluconeogenesis. *Diabetes* (2010) 59:1906–14. doi: 10.2337/db09-1365
58. Gurzov EN, Tran M, Fernandez-Rojo MA, Merry TL, Zhang X, Xu Y, et al. Hepatic oxidative stress promotes insulin-STAT-5 signaling and obesity by inactivating protein tyrosine phosphatase N2. *Cell Metab* (2014) 20:85–102. doi: 10.1016/j.cmet.2014.05.011
59. ten Hoeve J, de Jesus Ibarra-Sanchez M, Fu Y, Zhu W, Tremblay M, David M, et al. Identification of a nuclear Stat1 protein tyrosine phosphatase. *Mol Cell Biol* (2002) 22:5662–68. doi: 10.1128/mcb.22.16.5662-5668.2002
60. Galic S, Klingler-Hoffmann M, Fodero-Tavoletti MT, Puryer MA, Meng TC, Tonks NK, et al. Regulation of insulin receptor signaling by the protein tyrosine phosphatase TCPTP. *Mol Cell Biol* (2003) 23:2096–108. doi: 10.1128/mcb.23.6.2096-2108.2003
61. Dodd GT, Lee-Young RS, Bruning JC, Tiganis T. TCPTP Regulates Insulin Signaling in AgRP Neurons to Coordinate Glucose Metabolism With Feeding. *Diabetes* (2018) 67:1246–57. doi: 10.2337/db17-1485
62. Tiganis T, Bennett AM, Ravichandran KS, Tonks NK. Epidermal growth factor receptor and the adaptor protein p52Shc are specific substrates of T-cell protein tyrosine phosphatase. *Mol Cell Biol* (1998) 18:1622–34. doi: 10.1128/mcb.18.3.1622
63. Stanoev A, Mhamane A, Schuermann KC, Grecco HE, Stallaert W, Baumdick M, et al. and Phosphatases Spatially Established by Vesicular Dynamics Generates a Growth Factor Sensing and Responding Network. *Cell Syst* (2018) 7:295–309.e11. doi: 10.1016/j.cels.2018.06.006
64. Mattila E, Auvinen K, Salmi M, Ivaska J. The protein tyrosine phosphatase TCPTP controls VEGFR2 signalling. *J Cell Sci* (2008) 121:3570–80. doi: 10.1242/jcs.031898
65. Persson C, Sävenhed C, Bourdeau A, Tremblay ML, Markova B, Böhmer FD, et al. Site-selective regulation of platelet-derived growth factor beta receptor tyrosine phosphorylation by T-cell protein tyrosine phosphatase. *Mol Cell Biol* (2004) 24:2190–201. doi: 10.1128/mcb.24.5.2190-2201.2004
66. Kramer F, Dernedde J, Mezheyeuski A, Tauber R, Micke P, Kappert K. Platelet-derived growth factor receptor β activation and regulation in murine myelofibrosis. *Haematologica* (2020) 105:2083–94. doi: 10.3324/haematol.2019.226332
67. Simoncic PD, Bourdeau A, Lee-Loy A, Rohrschneider LR, Tremblay ML, Stanley ER, et al. T-cell protein tyrosine phosphatase (Tcptp) is a negative regulator of colony-stimulating factor 1 signaling and macrophage differentiation. *Mol Cell Biol* (2006) 26:4149–60. doi: 10.1128/MCB.01932-05
68. Lees CW, Barrett JC, Parkes M, Satsangi J. New IBD genetics: common pathways with other diseases. *Gut* (2011) 60:1739–53. doi: 10.1136/gut.2009.199679
69. Marcil V, Mack DR, Kumar V, Faure C, Carlson CS, Beaulieu P, et al. Association between the PTPN2 gene and Crohn's disease: dissection of potential causal variants. *Inflammation Bowel Dis* (2013) 19:1149–55. doi: 10.1097/MIB.0b013e318280b181
70. Zhang Q, Li H, Hou S, Yu H, Su G, Deng B, et al. Association of genetic variations in PTPN2 and CD122 with ocular Behcet's disease. *Br J Ophthalmol* (2018) 102:996–1002. doi: 10.1136/bjophthalmol-2017-310820
71. Killock D. Genetics: Etiological insight into the genetic association of TCPTP with RA and JIA? *Nat Rev Rheumatol* (2011) 7:683. doi: 10.1038/nrrheum.2011.167
72. You-Ten KE, Muise ES, Itié A, Michaliszyn E, Wagner J, Jothy S, et al. Impaired bone marrow microenvironment and immune function in T cell protein tyrosine phosphatase-deficient mice. *J Exp Med* (1997) 186:683–93. doi: 10.1084/jem.186.5.683
73. Heinonen KM, Nestel FP, Newell EW, Charette G, Seemayer TA, Tremblay ML, et al. T-cell protein tyrosine phosphatase deletion results in progressive systemic inflammatory disease. *Blood* (2004) 103:3457–64. doi: 10.1182/blood-2003-09-3153
74. Spalinger MR, Kasper S, Chassard C, Raselli T, Frey-Wagner I, Gottier C, et al. PTPN2 controls differentiation of CD4(+) T cells and limits intestinal inflammation and intestinal dysbiosis. *Mucosal Immunol* (2015) 8:918–29. doi: 10.1038/mi.2014.122
75. Wiede F, Shields BJ, Chew SH, Kyparissoudis K, van Vliet C, Galic S, et al. T cell protein tyrosine phosphatase attenuates T cell signaling to maintain tolerance in mice. *J Clin Invest* (2011) 121:4758–74. doi: 10.1172/JCI59492
76. Spalinger MR, Manzini R, Hering L, Riggs JB, Gottier C, Lang S, et al. PTPN2 Regulates Inflammasome Activation and Controls Onset of Intestinal Inflammation and Colon Cancer. *Cell Rep* (2018) 22:1835–48. doi: 10.1016/j.celrep.2018.01.052
77. Spalinger MR, Sayoc-Becerra A, Santos AN, Shawki A, Canale V, Krishnan M, et al. PTPN2 Regulates Interactions Between Macrophages and Intestinal Epithelial Cells to Promote Intestinal Barrier Function. *Gastroenterology* (2020) 159:1763–77. doi: 10.1053/j.gastro.2020.07.004
78. Zheng L, Zhang W, Li A, Liu Y, Yi B, Nakhoul F, et al. PTPN2 Downregulation Is Associated with Albuminuria and Vitamin D Receptor Deficiency in Type 2 Diabetes Mellitus. *J Diabetes Res* (2018) 2018:3984797. doi: 10.1155/2018/3984797
79. Dzierzak E, Bigas A. Blood Development: Hematopoietic Stem Cell Dependence and Independence. *Cell Stem Cell* (2018) 22:639–51. doi: 10.1016/j.stem.2018.04.015
80. Bourdeau A, Trop S, Doody KM, Dumont DJ, Tremblay ML. Inhibition of T cell protein tyrosine phosphatase enhances interleukin-18-dependent hematopoietic stem cell expansion. *Stem Cells* (2013) 31:293–304. doi: 10.1002/stem.1276
81. Bourdeau A, Dube N, Heinonen KM, Theberge JF, Doody KM, Tremblay ML. TC-PTP-deficient bone marrow stromal cells fail to support normal B lymphopoiesis due to abnormal secretion of interferon-{gamma}. *Blood* (2007) 109:4220–8. doi: 10.1182/blood-2006-08-044370
82. Wiede F, Chew SH, van Vliet C, Poulton IJ, Kyparissoudis K, Sasmono T, et al. Strain-dependent differences in bone development, myeloid hyperplasia, morbidity and mortality in ptpn2-deficient mice. *PloS One* (2012) 7:e36703. doi: 10.1371/journal.pone.0036703
83. Doody KM, Bussières-Marmen S, Li A, Paquet M, Henderson JE, Tremblay ML. T cell protein tyrosine phosphatase deficiency results in spontaneous synovitis and subchondral bone resorption in mice. *Arthritis Rheumatism* (2012) 64:752–61. doi: 10.1002/art.33399
84. Loh K, Fukushima A, Zhang X, Galic S, Briggs D, Enriori Pablo J, et al. Elevated Hypothalamic TCPTP in Obesity Contributes to Cellular Leptin Resistance. *Cell Metab* (2011) 14:684–99. doi: 10.1016/j.cmet.2011.09.011

85. Ferron M, Wei J, Yoshizawa T, Del Fattore A, DePinho RA, Teti A, et al. Insulin signaling in osteoblasts integrates bone remodeling and energy metabolism. *Cell* (2010) 142:296–308. doi: 10.1016/j.cell.2010.06.003
86. Zee T, Settembre C, Levine RL. Karsenty G. T-cell protein tyrosine phosphatase regulates bone resorption and whole-body insulin sensitivity through its expression in osteoblasts. *Mol Cell Biol* (2012) 32:1080–88. doi: 10.1128/MCB.06279-11
87. Sinder BP, Pettit AR, McCauley LK. Macrophages: Their Emerging Roles in Bone. *J Bone Miner Res* (2015) 30:2140–9. doi: 10.1002/jbmr.2735
88. Spalinger MR, Sayoc-Becerra A, Ordookhanian C, Canale V, Santos AN, King SJ, et al. The JAK inhibitor tofacitinib rescues intestinal barrier defects caused by disrupted epithelial-macrophage interactions. *J Crohns Colitis* (2020) jjaa182. doi: 10.1093/ecco-jcc/jjaa182
89. You-Ten KE, Muise ES, Itié A, Michaliszyn E, Wagner J, Jothy S, et al. Impaired bone marrow microenvironment and immune function in T cell protein tyrosine phosphatase-deficient mice. *J Exp Med* (1997) 186:683–93. doi: 10.1084/jem.186.5.683
90. He D, Kou X, Luo Q, Yang R, Liu D, Wang X, et al. Enhanced M1/M2 macrophage ratio promotes orthodontic root resorption. *J Dent Res* (2015) 94:129–39. doi: 10.1177/0022034514553817
91. Li Y, Zhou HM, Wang F, Han L, Liu MH, Li YH, et al. Overexpression of PTPN2 in Visceral Adipose Tissue Ameliorated Atherosclerosis via T Cells Polarization Shift in Diabetic Apoe(-/-) Mice. *Cell Physiol Biochem* (2018) 46:118–32. doi: 10.1159/000488415
92. Heinonen KM, Bourdeau A, Doody KM, Tremblay ML. Protein tyrosine phosphatases PTP-1B and TC-PTP play nonredundant roles in macrophage development and IFN-gamma signaling. *Proc Natl Acad Sci USA* (2009) 106:9368–72. doi: 10.1073/pnas.0812109106
93. Zhang D, Jiang Y, Song D, Zhu Z, Zhou C, Dai L, et al. Tyrosine-protein phosphatase non-receptor type 2 inhibits alveolar bone resorption in diabetic periodontitis via dephosphorylating CSF1 receptor. *J Cell Mol Med* (2019) 23:6690–99. doi: 10.1111/jcmm.14545
94. Rhee I, Veillette A. Protein tyrosine phosphatases in lymphocyte activation and autoimmunity. *Nat Immunol* (2012) 13:439–47. doi: 10.1038/ni.2246
95. Flosbach M, Oberle SG, Scherer S, Zecha J, von Hoesslin M, Wiede F, et al. PTPN2 Deficiency Enhances Programmed T Cell Expansion and Survival Capacity of Activated T Cells. *Cell Rep* (2020) 32:107957. doi: 10.1016/j.celrep.2020.107957
96. Pike KA, Tremblay ML. Protein Tyrosine Phosphatases: Regulators of CD4 T Cells in Inflammatory Bowel Disease. *Front Immunol* (2018) 9:2504:2504. doi: 10.3389/fimmu.2018.02504
97. Wiede F, Dudakov JA, Lu K-H, Dodd GT, Butt T, Godfrey DI, et al. PTPN2 regulates T cell lineage commitment and αβ versus γδ specification. *J Exp Med* (2017) 214:2733–58. doi: 10.1084/jem.20161903
98. Yi Z, Lin WW, Stunz LL, Bishop GA. The adaptor TRAF3 restrains the lineage determination of thymic regulatory T cells by modulating signaling via the receptor for IL-2. *Nat Immunol* (2014) 15:866–74. doi: 10.1038/ni.2944
99. Cenci S, Toraldo G, Weitzmann MN, Roggia C, Gao Y, Qian WP, et al. Estrogen deficiency induces bone loss by increasing T cell proliferation and lifespan through IFN-gamma-induced class II transactivator. *Proc Natl Acad Sci USA* (2003) 100:10405–10. doi: 10.1073/pnas.1533207100
100. Gao Y, Grassi F, Ryan MR, Terauchi M, Page K, Yang X, et al. IFN-gamma stimulates osteoclast formation and bone loss in vivo via antigen-driven T cell activation. *J Clin Invest* (2007) 117:122–32. doi: 10.1172/jci30074
101. Lazzaro L, Tonkin BA, Poulton IJ, McGregor NE, Ferlin W, Sims NA. IL-6 trans-signalling mediates trabecular, but not cortical, bone loss after ovariectomy. *Bone* (2018) 112:120–27. doi: 10.1016/j.bone.2018.04.015
102. Kuroyanagi G, Adapala NS, Yamaguchi R, Kamiya N, Deng Z, Aruwajoye O, et al. Interleukin-6 deletion stimulates revascularization and new bone formation following ischemic osteonecrosis in a murine model. *Bone* (2018) 116:221–31. doi: 10.1016/j.bone.2018.08.011
103. Udagawa N, Takahashi N, Katagiri T, Tamura T, Wada S, Findlay DM, et al. Interleukin (IL)-6 induction of osteoclast differentiation depends on IL-6 receptors expressed on osteoblastic cells but not on osteoclast progenitors. *J Exp Med* (1995) 182:1461–8. doi: 10.1084/jem.182.5.1461
104. Wu Q, Zhou X, Huang D, Ji Y, Kang F. IL-6 Enhances Osteocyte-Mediated Osteoclastogenesis by Promoting JAK2 and RANKL Activity In Vitro. *Cell Physiol Biochem* (2017) 41:1360–69. doi: 10.1159/000465455
105. Yamashita T, Iwakura T, Matsui K, Kawaguchi H, Obana M, Hayama A, et al. IL-6-mediated Th17 differentiation through RORγt is essential for the initiation of experimental autoimmune myocarditis. *Cardiovasc Res* (2011) 91:640–8. doi: 10.1093/cvr/cvr148
106. Aqel SI, Kraus EE, Jena N, Kumari V, Granitto MC, Mao L, et al. Novel small molecule IL-6 inhibitor suppresses autoreactive Th17 development and promotes T(reg) development. *Clin Exp Immunol* (2019) 196:215–25. doi: 10.1111/cei.13258
107. Zhang Y, Ding H, Wang X, Ye SD. Modulation of STAT3 phosphorylation by PTPN2 inhibits naive pluripotency of embryonic stem cells. *FEBS Lett* (2018) 592:2227–37. doi: 10.1002/1873-3468.13112
108. Yamamoto T, Sekine Y, Kashima K, Kubota A, Sato N, Aoki N, et al. The nuclear isoform of protein-tyrosine phosphatase TC-PTP regulates interleukin-6-mediated signaling pathway through STAT3 dephosphorylation. *Biochem Biophys Res Commun* (2002) 297:811–7. doi: 10.1016/s0006-291x(02)02291-x
109. Svensson MN, Doody KM, Schmiedel BJ, Bhattacharyya S, Panwar B, Wiede F, et al. Reduced expression of phosphatase PTPN2 promotes pathogenic conversion of Tregs in autoimmunity. *J Clin Invest* (2019) 129:1193–210. doi: 10.1172/JCI123267
110. Onal M, Xiong J, Chen X, Thostenson JD, Almeida M, Manolagas SC, et al. Receptor activator of nuclear factor κB ligand (RANKL) protein expression by B lymphocytes contributes to ovariectomy-induced bone loss. *J Biol Chem* (2012) 287:29851–60. doi: 10.1074/jbc.M112.377945
111. Wiede F, Sacirbegovic F, Leong YA, Yu D, Tiganis T. PTPN2-deficiency exacerbates T follicular helper cell and B cell responses and promotes the development of autoimmunity. *J Autoimmun* (2017) 76:85–100. doi: 10.1016/j.jaut.2016.09.004
112. Wang YN, Jia T, Zhang J, Lan J, Zhang D, Xu X. PTPN2 improves implant osseointegration in T2DM via inducing the dephosphorylation of ERK. *Exp Biol Med (Maywood)* (2019) 244:1493–503. doi: 10.1177/1535370219883419
113. Niechcial A, Butter M, Manz S, Obialo N, Bäbler K, van der Lely L, et al. Presence of PTPN2 SNP rs1893217 Enhances the Anti-inflammatory Effect of Spermidine. *Inflammation Bowel Dis* (2020) 26:1038–49. doi: 10.1093/ibd/izaa013
114. Hsieh WC, Svensson MN, Zoccheddu M, Tremblay ML, Sakaguchi S, Stanford SM, et al. PTPN2 links colonic and joint inflammation in experimental autoimmune arthritis. *JCI Insight* (2020) 5:e141868. doi: 10.1172/jci.insight.141868
115. Zhang P, Zhang W, Zhang D, Wang M, Aprecio R, Ji N, et al. 25-Hydroxyvitamin D3 -enhanced PTPN2 positively regulates periodontal inflammation through the JAK/STAT pathway in human oral keratinocytes and a mouse model of type 2 diabetes mellitus. *J Periodontal Res* (2018) 53:467–77. doi: 10.1111/jre.12535

Conflict of Interest: The authors declare that the research was conducted in the absence of any commercial or financial relationships that could be construed as a potential conflict of interest.

frontiers in Immunology

ORIGINAL RESEARCH
published: 09 April 2021
doi: 10.3389/fimmu.2021.636427

Liquid PRF Reduces the Inflammatory Response and Osteoclastogenesis in Murine Macrophages

*Zahra Kargarpour[1], Jila Nasirzade[1], Layla Panahipour[1], Richard J. Miron[2] and Reinhard Gruber[1,2]**

[1] Department of Oral Biology, Medical University of Vienna, Vienna, Austria, [2] Department of Periodontology, School of Dental Medicine, University of Bern, Bern, Switzerland

OPEN ACCESS

Edited by:
Pradyumna Kumar Mishra, ICMR-National Institute for Research in Environmental Health, India

Reviewed by:
Radha Dutt Singh, University of Calgary, Canada
Rajaneesh Anupam, Dr. Hari Singh Gour University, India
Rajesh Kumar Mondal, National Institute of Research in Tuberculosis (ICMR), India

***Correspondence:**
Reinhard Gruber
reinhard.gruber@meduniwien.ac.at

Specialty section:
This article was submitted to Inflammation, a section of the journal Frontiers in Immunology

Received: 01 December 2020
Accepted: 08 March 2021
Published: 09 April 2021

Citation:
Kargarpour Z, Nasirzade J, Panahipour L, Miron RJ and Gruber R (2021) Liquid PRF Reduces the Inflammatory Response and Osteoclastogenesis in Murine Macrophages. Front. Immunol. 12:636427. doi: 10.3389/fimmu.2021.636427

Macrophage activation and osteoclastogenesis are hallmarks of inflammatory osteolysis and may be targeted by the local application of liquid platelet-rich fibrin (PRF). Liquid PRF is produced by a hard spin of blood in the absence of clot activators and anticoagulants, thereby generating an upper platelet-poor plasma (PPP) layer, a cell-rich buffy coat layer (BC; termed concentrated-PRF or C-PRF), and the remaining red clot (RC) layer. Heating PPP has been shown to generate an albumin gel (Alb-gel) that when mixed back with C-PRF generates Alb-PRF having extended working properties when implanted *in vivo*. Evidence has demonstrated that traditional solid PRF holds a potent anti-inflammatory capacity and reduces osteoclastogenesis. Whether liquid PRF is capable of also suppressing an inflammatory response and the formation of osteoclasts remains open. In the present study, RAW 264.7 and primary macrophages were exposed to lipopolysaccharides (LPS), lactoferrin, and agonists of Toll-like receptors (TLR3 and TLR7) in the presence or absence of lysates prepared by freeze-thawing of liquid PPP, BC, Alb-gel, and RC. For osteoclastogenesis, primary macrophages were exposed to receptor activator of nuclear factor kappa B ligand (RANKL), macrophage colony-stimulating factor (M-CSF), and human transforming growth factor-β1 (TGF-β1) in the presence or absence of PPP, BC, Alb-gel, RC lysates and hemoglobin. We show here that it is mainly the lysates prepared from PPP and BC that consistently reduced the agonist-induced expression of interleukin 6 (IL6) and cyclooxygenase-2 (COX2) in macrophages, as determined by RT-PCR and immunoassay. With respect to osteoclastogenesis, lysates from PPP and BC but also from RC, similar to hemoglobin, reduced the expression of osteoclast marker genes tartrate-resistant acid phosphatase (TRAP) and cathepsin K, as well as TRAP histochemical staining. These findings suggest that liquid PRF holds a potent *in vitro* heat-sensitive anti-inflammatory activity in macrophages that goes along with an inhibition of osteoclastogenesis.

Keywords: platelet-rich fibrin, inflammation, lipopolysaccharides, lactoferrin, Toll-like receptors, hemoglobin, osteoclastogenesis, osteoimmunology

INTRODUCTION

Osteoimmunology was coined at the edge of the millennium when lymphocytes were discovered to drive the differentiation of hematopoietic progenitors into bone-resorbing osteoclasts (1). This process essentially depends on the activation of the RANKL-RANK signaling cascade that ultimately culminates in the expression of the genes not only characteristic of osteoclast, but also dictating their function; which is the tartrate-resistant acid phosphatase (TRAP) and the cathepsin K, removing phosphate from their substrate and the digestion of collagen of the previously solubilized mineralized extracellular matrix, respectively (2). Osteoimmunology not only provides insights into how the delicate balance of bone turnover and its shifting towards a pathological bone loss in osteoporosis and other metabolic disorders is regulated (3), but also the cross-talk of the cells representing the immune system with bone cells. Particularly, the osteoclasts was discovered to be responsible for the catabolic changes of the inflammation-induced bone loss, what we consider today as inflammatory osteolysis, a pathological process that is of significant importance in periodontitis (4, 5) and rheumatoid arthritis (6, 7).

Inflammatory osteolysis is pharmacologically targeted at the level of cytokines to interrupt the link between the activated macrophages and other immune cells to produce the inflammatory mediators, which in turn stimulate the RANKL-dependent osteoclastogenesis (8). While, rheumatoid arthritis is successfully treated with biologicals, including blocking of the major inflammatory cytokines TNFα and IL6, causing a reduction of the inflammatory symptoms (8, 9), this systemic therapeutically strategy is not feasible in oral diseases such as chronic periodontitis; an inflammation of the periodontal tissue caused by the virulence factors of the biofilm and other local mediators (4, 10). Chronic periodontitis therefore requires local therapeutic strategies, in concert with removing of the bacterial biofilm and calculus by scaling and root planning (11), to target the chronic inflammation in periodontitis with the overall aim to diminish the activation of inflammatory macrophages by their virulence factors such as LPS, and thereby reduce the formation and activation of osteoclasts.

Solid platelet-rich fibrin (PRF), which is basically the coagulated plasma-rich fraction of blood upon centrifugation, was introduced as a local therapy to support wound healing and potentially also tissue regeneration in oral indications including treatment of gingival recessions (12), increasing the width of keratinized mucosa around implants (13), to prevent atrophic bone resorption following tooth extraction (14), and to lower the symptoms that come along with inflammation such as pain and swelling upon third molar surgery (15). Support for the beneficial clinical performance of PRF application comes from *in vitro* studies showing that lysates of PRF membranes are capable of reducing the LPS-induced inflammatory response of macrophages indicated by an M1-to-M2 shift of IL6 and arginase 1 expression, respectively (16, 17), and also reduce the formation of osteoclasts in murine bone marrow cultures shown by histochemical staining of TRAP and the reduced expression of the respective gene and cathepsin K (18). Considering that both, macrophage activation (19) and osteoclastogenesis (20) require activation of the NFκB signaling pathway, and that both cells originate from the same hematopoietic progenitors (21), it might be possible that solid PRF, by reducing NFκB signaling, directly affects macrophage polarization and osteoclastogenesis. Similar data for liquid PRF are not available thus far.

Liquid PRF obtained by high-speed fractionation of blood without clot activators was termed concentrated PRF (C-PRF) (22), in contrast to injectable PRF prepared with low-speed and short-time protocols using clot activator tubes (23). Centrifugation separates the blood in a large liquid platelet-poor plasma (PPP) layer that is almost devoid of cells and the buffy coat layer accumulating the platelets and leucocytes termed concentrated PRF or C-PRF (22). It is particularly the C-PRF that is utilized to support tissue regeneration (22) and therefore used to reconstitute albumin gels (Alb-gel) prepared from heated PPP (24). The Alb-PRF gel (combination of PPP and Alb-gel) maintains volume stability for at least 4 months (25). The clinical applications of liquid PRF are thus manifold and include the production of transplantable conglomerates of fragmented solid PRF, autografts and liquid PRF (26), direct injection into a soft tissue, for example in facial esthetics (27), or to produce a growth factor-enriched matrix, exemplified by Alb-PRF (24). The impact of liquid PRF on the cellular aspects related to inhibition of inflammation and osteoclastogenesis have not been determined.

There is a rational to investigate the possible inflammatory activity of liquid PRF, as reported by us for solid PRF in a macrophage setting (16, 17) and on osteoclastogenesis (18). However, considering that the previous research on solid PRF has not considered the fractions (16–18), it remains unclear if liquid PRF produced at high speed in non-ridged (pull cap) plastic tubes exerts an anti-inflammatory activity and reduction in osteoclastogenesis, and if yes, which fraction (PPP and BC, the latter being a synonym for C-PRF) is responsible for this effect. Moreover, it is relevant to determine the possible anti-inflammatory and osteoclastogenic activity of the Alb-gel prepared from heated PPP and the remaining red clot. Here we provide data demonstrating that lysates prepared from PPP and BC exert an anti-inflammatory and together with lysates of the red clot also a reduction of osteoclastogenesis.

MATERIALS AND METHODS

Isolation and Culture of Murine Bone Marrow-Derived Macrophages and RAW 264.7 Cells

RAW 264.7 macrophage-like cells (LGC Standards, Wesel, Germany) were expanded in growth Dulbecco's Modified Eagle Medium (DMEM, Sigma Aldrich, St. Louis, MO, USA), 10% fetal calf serum (Bio&Sell GmbH, Nuremberg, Germany) and 1% antibiotics (Sigma Aldrich, St. Louis, MO, USA) and seeded at 2×10^5 cells/cm^2 into 24-well plates. Primary bone marrow cells were collected from the femora and tibiae of BALB/c mice, 6- to 8-weeks (Animal Research Laboratories, Himberg, Austria). Bone marrow cells were seeded at 4×10^6 cells/cm^2 into

24-well plates and grown for 5 days in DMEM supplemented with 10% fetal bovine serum, antibiotics and with 20 ng/mL macrophage colony-stimulating factor (M-CSF; ProSpec-Tany TechnoGene Ltd, Ness-Ziona, Israel). Bone marrow macrophages and RAW 264.7 were exposed to the respective treatments for another 24 hours under standard conditions at 37°C, 5% CO_2, and 95% humidity. The cells were treated with LPS from *Escherichia coli* 0111: B41 (Sigma Aldrich, St. Louis, MO) at 100 ng/mL, lactoferrin at 50 ng/mL, poly (1:C) HMW (InvivoGen, Toulouse, France) at 10 μg/mL, imiquimod (InvivoGen, Toulouse, France) at 5 μg/mL, recombinant mouse IL4 (ProSpec, Ness Ziona, Israel) at 120 ng/mL in the respective experiments. All the fractions PPP, BC, Alb-gel and RC and serum were added to the cells at 10% (v/v). After overnight incubation, expression changes of respective genes were determined.

Preparation of PPP, Buffy Coat, and Red Clot

Volunteers signed informed consent and the ethics committee of the Medical University of Vienna (1644/2018) approved the preparation of PRF. For preparing PRF gels, venous blood was collected from healthy volunteers, three females and three males from 23 to 35 years, in non-ridged (pull cap) plastic tubes ("No Additive", Greiner Bio-One GmbH, Kremsmünster, Austria) and centrifuged at 2000 g for 8 min (swing-out rotor; Z 306 Hermle, Universal Centrifuge, Wehingen, Germany). The uppermost 2 mL PPP, the 1 mL buffy coat (BC or C-PRF), and the 1 mL erythrocyte fraction (RC) were collected. To generate Alb-gels, PPP was immediately heated at 75°C for 10 min (Eppendorf, Thermomixer F1.5, Hamburg, Germany) before being placed on ice. Every 1-ml fraction of the solid Alb-gel was then transferred into 1 ml of serum-free media. For preparation of liquid serum obtained from solid PRF, blood samples were collected into plain glass tubes (Bio-PRF, Venice, FL, USA) and centrifuged at 2000 g for 8 minutes. The solid PRF clot was squeezed out by pressing plate (Bio-PRF, Venice, FL, USA) to generate serum. The remaining PRF membrane was then divided into two parts, equivalent to PPP and BC. All fractions and the Alb-gel were subjected to dual freeze-thawing at -80°C and room temperature, respectively, followed by sonication (Sonopuls 2000.2, Bandelin electronic, Berlin, Germany) for 30 seconds. After centrifugation (Eppendorf, Hamburg, Germany) at 15,000 g for 10 min, aliquots of lysates were stored at −20°C for not longer than one month. The lysates were thawed and cells were exposed as indicated above.

Growing Osteoclasts in Bone Marrow Cultures

Extracted bone marrow cells from femora and tibia of mice were seeded at 4×10^6 cells/cm^2 into 48-well plates and grown for 5 days in Minimum Essential Medium Eagle-Alpha Modification (αMEM) supplemented with 10% fetal calf serum (FCS) and 1% antibiotic. Receptor activator of nuclear factor kappa B ligand (ProSpec, Ness-Ziona, Israel) at 30 ng/mL, M-CSF (Cell Signaling Technology Europe, B.V., Frankfurt am Main, Germany) at 20 ng/mL, and TGF-β1 (Cell Signaling Technology Europe, B.V., Frankfurt am Main, Germany) at 10 ng/mL were used to induce osteoclastogenesis. If not otherwise indicated, 10% of PPP, BC, Alb-gel and RC or hemoglobin (Sigma Aldrich, St. Louis, MO) at 20 mM were used in the culture medium. After 6 days, histochemical staining for TRAP was performed following the instructions of the manufacturer (Sigma Aldrich, St. Louis, MO). Images were captured under a light microscope with 10X magnification (Echorevolve microscope, Euromex, Arnheim, Netherlands).

Reverse Transcription Quantitative Real-Time PCR (RT-qPCR) and Immunoassay

For RT-qPCR (28), after overnight stimulation total RNA was isolated with the ExtractMe total RNA kit (Blirt S.A., Gdańsk, Poland) followed by reverse transcription (LabQ, Labconsulting, Vienna, Austria) and polymerase chain reaction (LabQ, Labconsulting, Vienna, Austria) on a CFX Connect™ Real-Time PCR Detection System (Bio-Rad Laboratories, Hercules, CA). Primer sequences were mIL6-F: GCTACCAA ACTGGATATAATCAGGA, mIL6-R: CCAGGTAGCT ATGGTACTCCAGAA; mCOX2-F: CAGACAACATA AAACTGCGCCTT, mCOX2-R: GATACACCTCTCC ACCAATGACC; mCXCL2-F: CATCCAGAGCTTGAGTGT GACG, mCXCL2-R: GGCTTCAGGGTCAAGGCAAAC; mCCL2-F: GCTACAAGAGGATCACCAGCAG, mCCL2-R: GTCTGGACCCATTCCTTCTTGG; mCCL5-F: CCTGCT GCTTTGCCTACCTC, mCCL5-R: ACACACTTGGC GGTTCCTTC; mGAPDH-F: AACTTTGGCATTGTGGAAGG, mGAPDH-R: GGATGCAGGGATGATGTTCT; mARG1-F: GAATCTGCATGGGCAACC, mARG1-R: GAATCCTGGT ACATCTGGGAAC; mYM1-F: CATTCCAAGGCTGC TACTCA, mYM1-R: TCATGACCTGAATATAGTCGA GAGA; mcathepsin K-F: TGTATAACGCCACGGCAAA, mcathepsin K-R: GGTTCACATTATCACGGTCACA; m TRAP-F: AAGCGCAAACGGTAGTAAGG, mTRAP-R: CGTCTCTGCACAGATTGCAT. The mRNA levels were calculated by normalizing to the housekeeping gene GAPDH using the ΔΔCt method. Supernatants were analyzed for IL6 secretion by immunoassay according to the manufacturer's instruction (R&D Systems, Minneapolis, MN). RT-PCR data are represented compared to the untreated control, which was considered 1.0 in all the measurements so there was no need to show it as a separate group. However, in IL6 ELISA the absolute amount of secreted protein (ρg/mL) from the cells were reported, so untreated cells were also considered to show the amount of protein in all the samples and compare the protein concentration.

Immunofluorescence

The immunofluorescent analysis of p65 nuclear translocation were performed in RAW 264.7 cells plated onto Millicell® EZ slides (Merck KGaA, Darmstadt, Germany) at 15,000 cells/cm^2. Cells were exposed to 10% of PPP, BC, Alb-gel and RC for 1 hour following overnight serum starvation. Thereafter the cells were exposed to LPS from *Escherichia coli* 0111: B41 (Sigma Aldrich,

St. Louis, MO) for another 1 hour. The cells were fixed with 4% paraformaldehyde, blocked with 1% bovine serum albumin (Sigma Aldrich, St. Louis, MO) and permeabilized with 0.3% TritonX-100 (Sigma Aldrich, St. Louis, MO). We used NF-κB p65 antibodies (IgG, 1:800, Cell Signaling Technology, #8242), at 4°C overnight. Detection was with the goat anti-rabbit Alexa 488 secondary antibody (1:1000, Cell Signaling Technology, #4412). Images were captured under a fluorescent microscope with a single filter block 455 nm (Oxion fluorescence, Euromex, Arnheim, Netherlands).

Western Blot

RAW 264.7 cells were seeded at 50,000 cells/cm^2 into 6-well plates. The following day cells were exposed to 10% of PPP, BC, Alb-gel and RC for 30 minutes and then they were exposed to LPS for 40 minutes. Extracts containing SDS buffer with protease and phosphatase inhibitors (cOmplete ULTRA Tablets and PhosSTOP; Roche, Mannheim, Germany) were separated by SDS-PAGE and transferred onto PVDF membranes (Roche Diagnostics, Mannheim, Germany). Membranes were blocked and the binding of the first antibody NF-κB p65 antibodies (IgG, 1:1000, Cell Signaling Technology, #8242), phospho-p65 antibody (IgG, 1:1000, Cell Signaling Technology, #3031), was detected with the second antibody labelled with HRP anti-rabbit (IgG, 1:10,000, Cell Signaling Technology, #7074). After exposure to the Clarity Western ECL Substrate (Bio-Rad Laboratories, Inc., Hercules, CA) chemiluminescence signals were visualized with the ChemiDoc imaging system (Bio-Rad Laboratories). For blot densitometric analysis images were analyzed using Image Lab software (Bio-Rad Laboratories).

Statistical Analysis

All experiments were performed four times. Every single data point is representative for an independent experiment, which is individually obtained from a different blood donor in the treatment groups. Statistical analysis of the IL6 expression and immunoassay was performed with Friedman test for multiple comparison and paired t test for single comparison. All the groups were compared with LPS, lactoferrin, poly (1:C) HMW, imiquimod, or MRT group as the positive control in the respective experiments. Analyses were performed using Prism v8 (GraphPad Software, La Jolla, CA). Significance was set at $p < 0.05$.

RESULTS

The Anti-inflammatory Effect of PPP and BC Is Dose-Dependent in RAW 264.7 Cells

To determine the most appropriate experimental concentration of PPP and BC, we evaluated the effect of various concentrations of both fractions (0, 1, 3, 10, and 30%) on IL6 gene expression. RAW 264.7 macrophage cells were exposed to 100 ng/mL LPS either with or without aforementioned concentrations of PPP and BC. Dose-response curves revealed that concentrations above 10% could significantly suppress the LPS-induced inflammation indicated by IL6 gene expression (**Figures 1A, B**). MTT results for RC indicated that concentrations above 10% of RC were cytotoxic (data not shown). The RC fraction at 10% had no effect on the basal expression of inflammatory marker genes including IL6 and COX2 in RAW264.7 cells (data not shown).

PPP and BC Can Suppress LPS-Induced Inflammatory Effect in RAW 264.7 Cells

To evaluate the anti-inflammatory effect of different fractions of liquid PRF (22, 26), the RAW 264.7 macrophage cell line was exposed to LPS either without or with 10% of PPP, BC, Alb-gel and RC. Gene expression analysis showed that PPP and BC fractions are both able to notably reduce the LPS-induced inflammatory effects. Alb-gel and RC fractions, however, failed to significantly reduce expression of IL6 and COX2 (**Figures 2A, B**). To confirm these findings obtained by gene expression analysis, we measured the levels of IL6 protein in the supernatant of RAW264.7 cells. Consistently, PPP and BC, but not Alb-gel and RC, reduced the production of IL6 (**Figure 2C**). To additionally approve the anti-inflammatory effect of PPP and BC, we measured the expression of LPS-induced chemokines

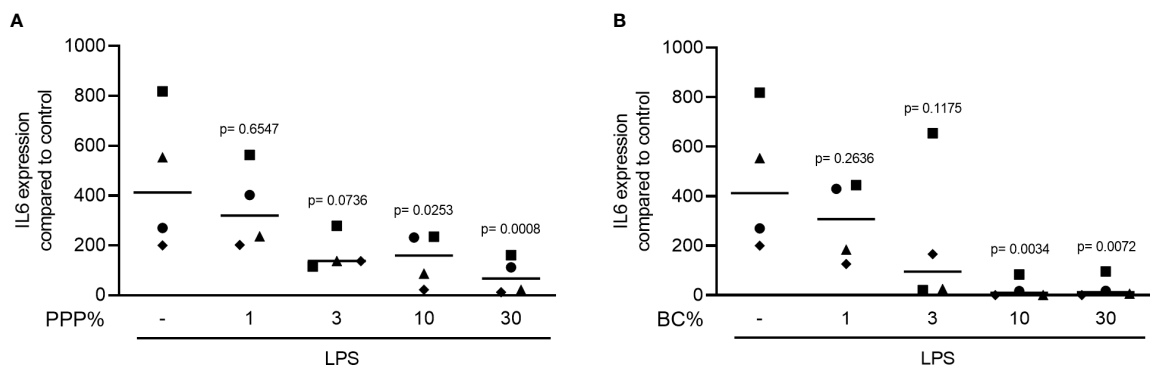

FIGURE 1 | The anti-inflammatory effect of PPP and BC is dose-dependent. RAW 264.7 cells were incubated with various concentrations of PPP and BC in the presence of LPS. **(A, B)** Data represent the x-fold changes in IL6 gene expression compared to untreated control, N = 4. Statistical analysis was based on Friedman test, and P values are indicated compared to the LPS group. Significance was set at $p < 0.05$.

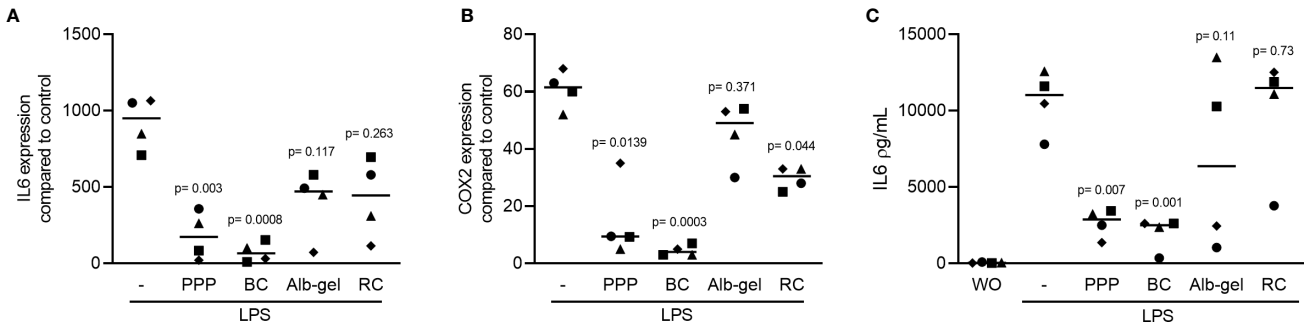

FIGURE 2 | Liquid PRF fractions PPP and BC can reduce LPS-induced inflammation. RAW 264.7 cells were exposed to 10% PPP, BC, Alb-gel and RC fractions in the presence of 100 ng/mL LPS. **(A, B)** Data show the x-fold changes of IL6 and COX2 gene expression **(C)** and the IL6 levels in the cell supernatant, N = 4. Statistical analysis was based on Friedman test, and P values are indicated compared to the LPS group. Significance was set at $p < 0.05$.

CXCL2, CCL2 and CCL5 in the RAW 264.7 cells. Consistently, expression of all chemokines was significantly suppressed by PPP and BC (**Figures 3A–C**).

PPP and BC Can Reduce Lactoferrin and TLR Agonist-Induced Inflammation in RAW 264.7 Cells

To understand if the anti-inflammatory activity of PPP and BC is limited to LPS, and considering that LPS is possibly scavenged by the HDL, we have generated an inflammatory response in RAW 264.7 by lactoferrin (29). We report here that in the presence of lactoferrin, all the fractions including PPP, BC, Alb-gel and RC are able to reduce the expression of IL6 and COX2 in RAW 264.7, but only PPP and BC could reach the significant level of reduction (**Figures 4A, B**). In support with the gene expression data, PPP and BC greatly reduced the IL6 protein levels provoked by lactoferrin in the macrophage cell line (**Figure 4C**). Furthermore, RAW264.7 cells were treated with poly (1: C) HMW and imiquimod, agonist of TLR3 and TLR7, respectively, and also in this setting, PPP and BC significantly reduced the expression of IL6 and COX2 (**Figures 5A, B**).

Serum From Solid PRF Can Reduce LPS-Induced Inflammation in RAW 264.7 Cells

To see if the serum produced from solid PRF (30) also holds an anti-inflammatory activity, solid PRF clots was squeezed out to collect the serum. The remaining PRF membrane was cut into a PPP and a BC part and lysates were prepared as described recently (17). RAW 264.7 macrophage cell line was exposed to 100 ng/mL LPS either without or with 10% of the solid PPP, solid BC and serum. All the fractions substantially lowered LPS-induced inflammation indicated by the expression of IL6 and COX2 (**Figures 6A, B**). To confirm the findings obtained by gene expression analysis, we measured accumulation of IL6 protein in the supernatant of RAW264.7 cells (**Figure 6C**).

PPP and BC Can Suppress Phosphorylation and Nuclear Translocation of p65 in RAW 264.7

To confirm the anti-inflammatory activity of PPP and BC, Western blot analysis was carried out for phospho-p65. PPP and BC suppressed the phosphorylation of p65 and even caused a gel shift of p65 in RAW 264.7 (**Figure 7A**) being quantified by

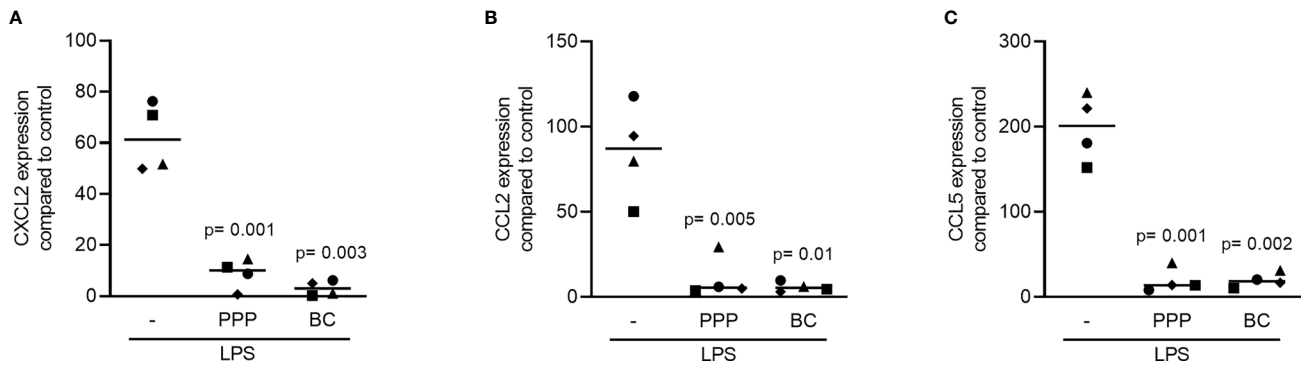

FIGURE 3 | Liquid PRF fractions PPP and BC can suppress LPS-induced chemokines. RAW 264.7 cells were treated with 10% PPP and BC fractions in the presence of 100 ng/mL LPS to evaluate expression changes of LPS-induced chemokines. **(A–C)** Data show the x-fold changes of CXCL2, CCL2 and CCL5 in the presence of PPP and BC, N = 4. Statistical analysis was based on Friedman test, and P values are indicated compared to the LPS group. Significance was set at $p < 0.05$.

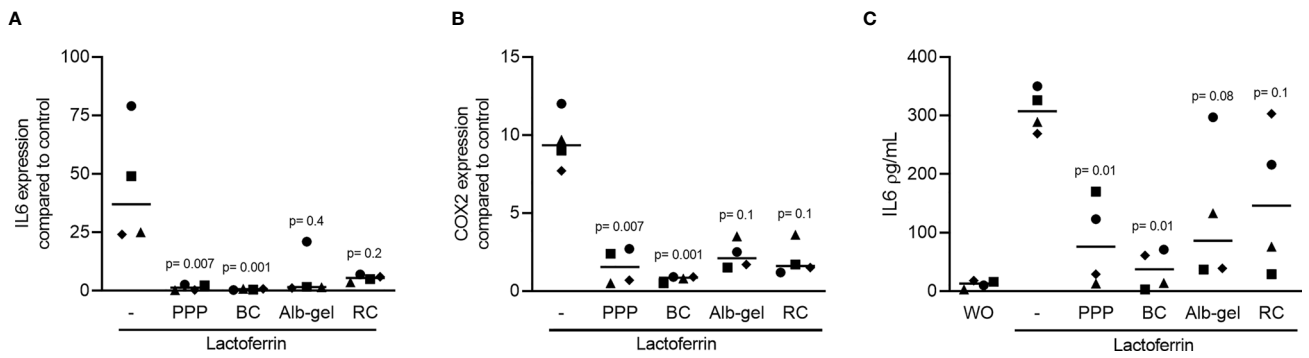

FIGURE 4 | PPP and BC can suppress lactoferrin-induced inflammation in RAW 264.7. The cells were exposed to 10% PPP, BC, Alb-gel and RC fractions in the presence of 50 μg/mL lactoferrin. **(A, B)** Data show the x-fold changes of IL6 and COX2 gene expression and **(C)** the IL6 levels in the cell supernatant, N = 4. Statistical analysis was based on Friedman test, and P values are indicated compared to the lactoferrin group. Significance was set at $p < 0.05$. WO means without and represents unstimulated cells.

densitometry (**Figure 7B**). To further evaluate the inhibitory effect of PPP and BC on NF-κB signaling, we performed an immunofluorescent analysis of NF-κB nuclear translocation. LPS caused a clear p65 nuclear staining that was however not observed in the presence of PPP and BC (**Figure 8A**). Histogram analysis of the signal intensity support the visual impression of the nuclear staining (**Figure 8B**). Thus, the anti-inflammatory activity of PPP and BC is associated with a reduction of p65 phosphorylation and its nuclear translocation.

PPP and BC Can Provoke an M1-to-M2 Polarization Shift in Murine Bone Marrow Cells

To confirm the findings observed in the RAW 264.7 cells, primary macrophages from murine bone marrow were similarly exposed to LPS in the presence or absence of 10% PPP, BC, Alb-gel and RC. Consistently, PPP and BC but not Alb-gel and RC strongly suppressed the LPS-provoked inflammation in primary macrophages indicated by the reduced expression of IL6 (**Figure 9A**). Interestingly all the fractions but Alb-gel could significantly reduce expression of COX2 (**Figure 9B**). In line with the gene expression data, PPP and BC but not Alb-gel and RC substantially reduced the IL6 protein levels induced by LPS the supernatant of primary macrophages (**Figure 9C**). Moreover, as with IL4 (31), PPP and BC induced an M2 macrophage polarization indicated by robust expression of arginase 1 (ARG1; **Figure 10A**) and chitinase-like protein 3 (Chil3; YM1; **Figure 10B**). Thus, PPP and BC provoke a macrophage polarization from pro-inflammatory M1 toward pro-resolving M2 phenotypes that can, for example, suppress osteoclast differentiation in a periodontitis model (32).

Osteoclast Formation Was Suppressed in the Presence of PPP, BC and RC but Not Alb-Gel

We then assessed the direct role of liquid PRF fractions in osteoclast differentiation. Murine bone marrow cells cultivated by M-CSF, RANKL and TGF-β (MRT) were treated with or without 10% of PPP, BC, Alb-gel and RC fractions. We showed that PPP, BC and RC fractions can decrease the size and number of TRAP-positive multinucleated cells using TRAP histochemical staining (**Figure 11A**). In line with this observation, PPP, BC and RC reduced the expression of TRAP and cathepsin K significantly, both enzymes required for bone resorption (**Figure 11B**). Alb-gel failed to substantially reduce the number of osteoclasts and the expression of osteoclast marker genes (**Figure 11B**). PPP, BC and RC had no impact on the expression of INFγ and IL12, both osteoclastogenesis inhibitors (data not shown). Hemoglobin also reduced osteoclast formation what may explain the findings obtained with the RC lysates (**Figures 12A, B**).

DISCUSSION

Liquid PRF prepared in regular plastic tubes at high-speed centrifugation (22, 26) provides the cell-rich buffy coat layer of C-PRF (22) and the platelet-poor plasma (PPP), the latter being a rich source of fibrinogen to prepare conglomerates of bone grafts (26) or albumin gels (Alb-gel) upon heating (24). It is thus the C-PRF but also the PPP that is clinically applied in regenerative dentistry. The proposed beneficial activity of liquid PRF that includes the lowering of the local inflammation and the reduction of osteoclastogenesis is supposed to be caused by the C-PRF being a rich-source of platelets and leucocytes (33), however, if also PPP being almost devoid of cells exerts an anti-inflammatory and anti-osteoclastogenic activity remains unclear. Even more enigmatic is the possible anti-inflammatory and anti-osteoclastogenic activity of the heated PPP, the Alb-gel. Here we provide some basal insights into the possible anti-inflammatory and anti-osteoclastogenic activity of the various fractions and preparations of liquid PRF based on murine bone marrow *in vitro* models.

The first main finding of the present study was that not only BC lysates have the expected anti-inflammatory activity (17), but

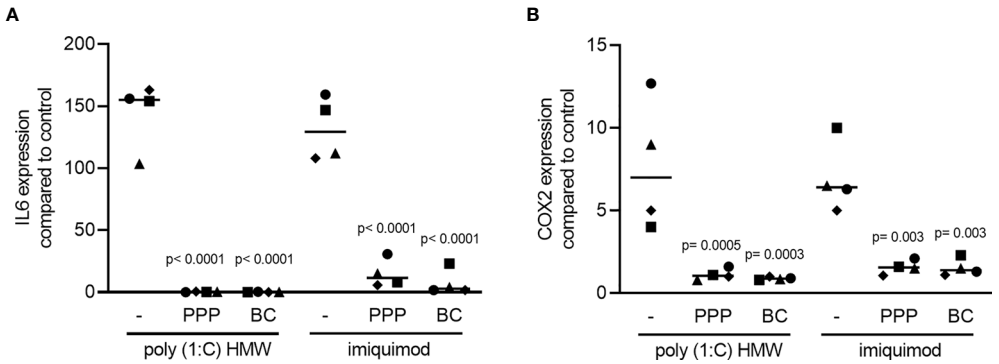

FIGURE 5 | PPP and BC can significantly reduce inflammation induced by TLR agonists. The cells were exposed to 10% PPP, BC in the presence of 10 μg/mL poly (1:C) HMW and 5 μg/mL imiquimod, agonists of TLR3 and TLR7 respectively. **(A, B)** Data show the x-fold changes of IL6 and COX2 gene expression, N = 4. Statistical analysis was based on Friedman test, and P values are indicated compared to the TLR agonists group. Significance was set at $p < 0.05$.

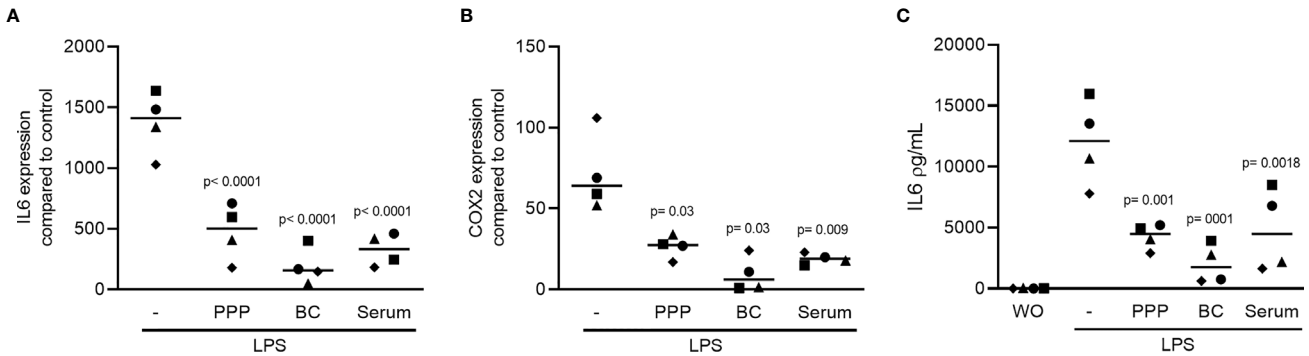

FIGURE 6 | The solid PPP, solid BC and serum are able to reduce LPS-induced inflammation. To confirm that also the serum produced from solid PRF hold an anti-inflammatory activity, jelly solid PRF was squeezed out to collect the PRF serum. RAW 264.7 cells were exposed to 10% solid PPP, solid BC, and serum in the presence of 100 ng/mL LPS. **(A, B)** Data show the x-fold changes of IL6 and COX2 gene expression and **(C)** the IL6 levels in the cell supernatant, N = 4. Statistical analysis was based on Friedman test, and P values are indicated compared to the LPS group. WO means without and represents unstimulated cells.

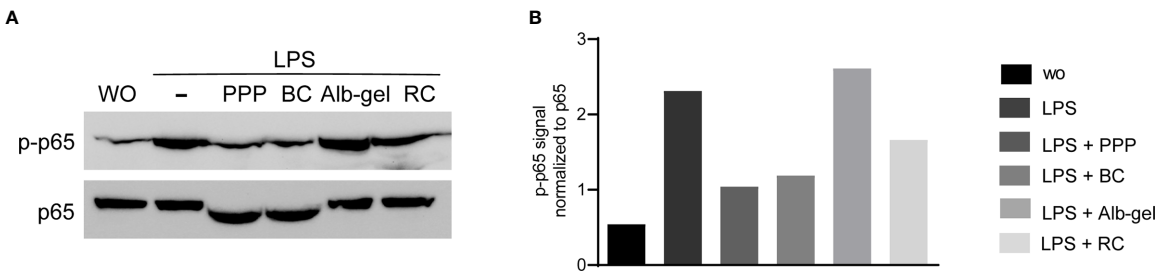

FIGURE 7 | PPP and BC layers can suppress phosphorylation of p65 in RAW 264.7. Western blot analysis was carried out for phospho-p65 and total p65. **(A)** Raw cells were treated with LPS in the presence or absence of 10% of PPP, BC, Alb-gel and RC. **(B)** Data indicate the relative changes normalized to p65 and unstimulated control cells.

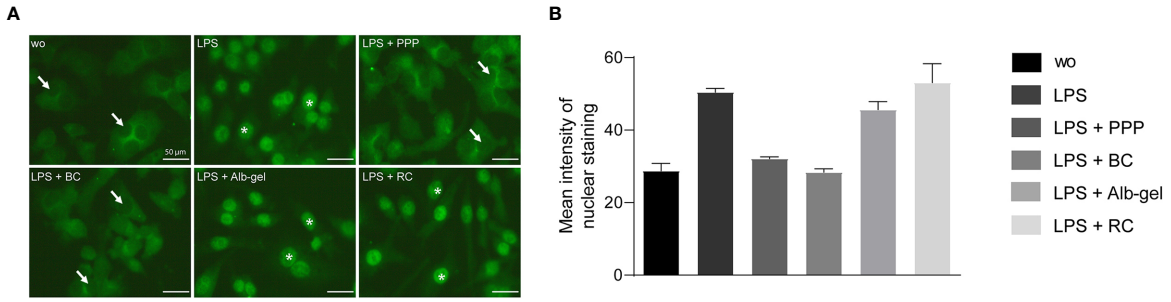

FIGURE 8 | PPP and BC attenuate the translocation of NFkB from the cytoplasm into the nucleus. Raw 264.7 cells were exposed to LPS with or without PPP, BC, Albgel and RC. **(A)** Immunofluorescence analysis of intracellular translocation of NFkB p65 into the nucleus, induced by LPS in RAW 264.7. WO means without and represents unstimulated cells. Stars represent stained nuclei and arrows represent non-stained nuclei for more clarity. **(B)** Data indicate the mean signal intensity of nuclear staining by obtained by ImageJ software.

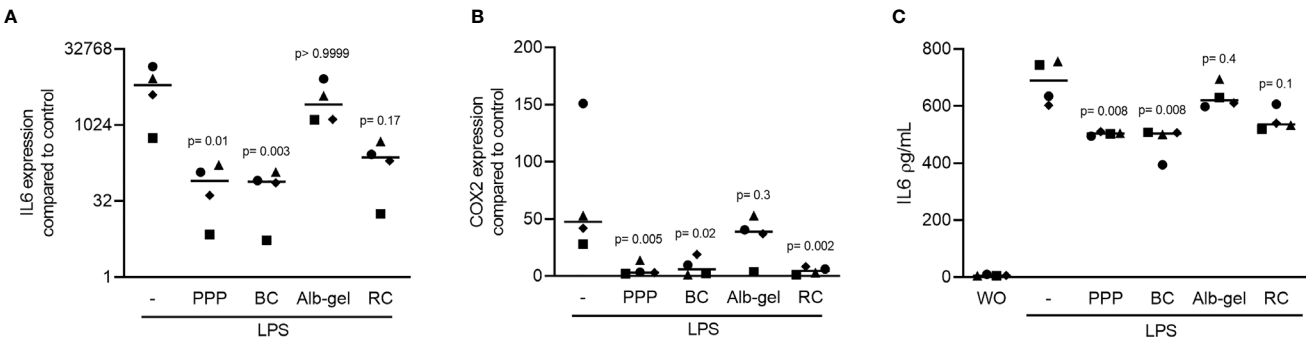

FIGURE 9 | Liquid PRF fractions PPP and BC suppress LPS-induced inflammation in macrophages. Bone marrow macrophages were exposed to 10% PPP, BC, Alb-gel and RC fractions in the presence of 100 ng/mL LPS. **(A, B)** Data show the x-fold changes of IL6 and COX2 gene expression and **(C)** the IL6 levels in the cell supernatant, N = 4. Statistical analysis was based on Friedman test, and P values are indicated compared to the LPS group. WO means without and represents unstimulated cells.

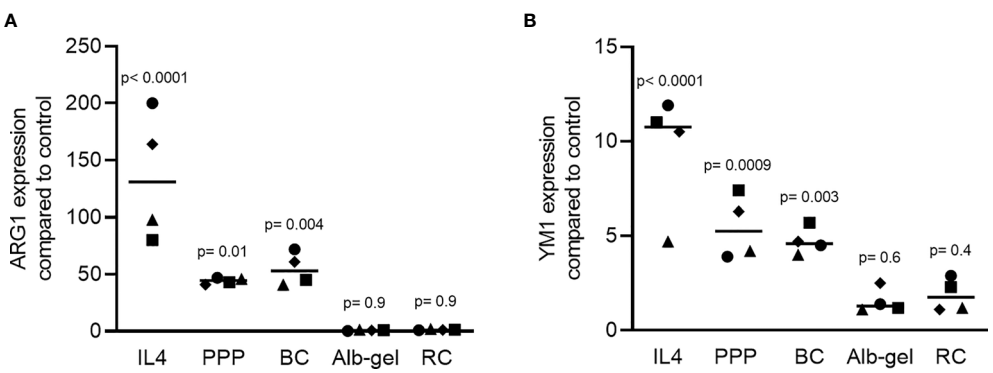

FIGURE 10 | PPP and BC but not Alb-gel and RC induce the formation of M2 pro-resolving macrophages. Bone marrow macrophages were exposed to 120 ng/mL IL4 or 10% PPP, BC, Alb-gel and RC. **(A–B)** Data show the x-fold changes of ARG1 and YM1 expression in bone marrow cultures; N = 4. Statistical analysis was based on Friedman test, and P values are indicated comparing mean of each group with the mean of untreated control group.

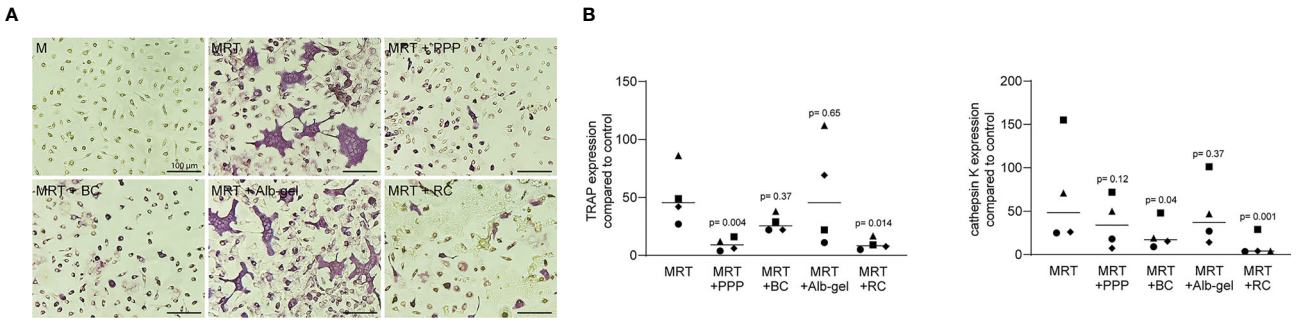

FIGURE 11 | Osteoclast formation is suppressed in the presence of PPP, BC and RC. Murine Bone marrow cells were grown in the presence of 10% PPP, BC, Alb-gel and RC to modify osteoclastogenesis induced by M-CSF, RANKL and TGF-β (MRT). **(A)** Representative images of TRAP$^+$ multinucleated osteoclasts in the control group M-CSF (M) and in the absence or presence of PPP, BC, Alb-gel and RC. **(B)** Data represent the x-fold changes in expression of osteoclast marker genes, TRAP and cathepsin K compared to an M-CSF control, N=4. Statistical analysis was based on Friedman test.

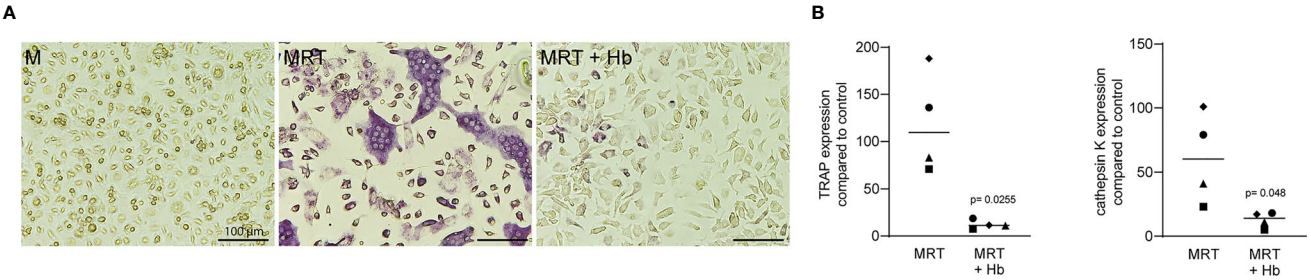

FIGURE 12 | Osteoclast formation is suppressed in the presence of hemoglobin. Murine Bone marrow cells were grown in the presence of 20 mM hemoglobin (Hb) to modify osteoclastogenesis induced by M-CSF, RANKL and TGF-β (MRT). **(A)** Representative images of TRAP$^+$ multinucleated osteoclasts in the control group M-CSF (M) and in the absence or presence of Hb. **(B)** Data represent the x-fold changes in expression of osteoclast marker genes, TRAP and cathepsin K compared to an M-CSF control, N=4. Statistical analysis was based on Paired t test.

also PPP lysates caused a robust inhibition of the inflammatory response of macrophages exposed to the classical TLR4 agonist LPS that goes along with a reduced p65 phosphorylation and nuclear translocation, overall suggesting a diminished NFκB signaling. The same is true when macrophages are stimulated with another TLR4 agonist namely lactoferrin (34), and poly (1:C) HMW and imiquimod, agonists of TLR3 and TLR7, respectively. Thus, the inhibition of inflammation caused by the PRF lysates is not specific for any TLRs. Moreover, the anti-inflammatory activity reported herein, indicated by the cytokine IL6 and COX2 the key enzyme of prostaglandin E_2 production, was also shown for a chemokine panel, CXCL2, CCL2 and CCL5.

The second main finding was that lysates of BC and PPP induce an M1-to-M2 polarization switch. For that, the anti-inflammatory activity BC and PPP was confirmed in macrophages generated from murine bone marrow. In extension of this information, we investigated the potential that the macrophages are not only suppressed in their M1-inflammatory status but shifted towards the M2-resolving status. Indeed, lysates of BC and PPP increased the expression of ARG1 and YM1, both being markers for M2 macrophages. These findings support our previous observation that lysates of solid PRF cause an M1-to-M2 polarization switch (17), and are partially consistent with PPP prepared with an apheresis system, where PPP reduced nitric oxide but not TNFα and COX2 expression of LPS-stimulated RAW 264.7 macrophages (33). Thus, our data suggest that it is not only the cell-rich BC but also the PPP that holds a potent anti-inflammatory activity that extends towards an M2-polarisation of macrophages in murine bone marrow cultures.

The third main finding of the current research was that lysates of the BC thus C-PRF and PPP reduced the formation of osteoclasts *in vitro* – similar to what we have shown for lysates of solid PRF (18). Again, it seems that the inhibition of osteoclastogenesis is not necessity caused by platelets, but more likely by parts of the PPP that are also present in BC and consequently C-PRF. Moreover, activated platelets depleted for leucocytes and freed from plasma components support osteoclastogenesis in murine bone marrow cultures (35), and it was the serum that reduced osteoclastogenesis *in vitro* (36).

However, we have not expected the robust inhibition of osteoclastogenesis by lysates of the RC. Searching for possible explanations, we show here that also hemoglobin alone can suppress osteoclastogenesis. These findings are supported by observations that oxidized ferryl hemoglobin greatly abolished osteoclastogenesis *in vitro* (37). In vivo, upon hemolysis hemoglobin is released from red blood cells to the circulation and give a rise to heme which has pro-inflammatory properties (38). Even though, hemoglobin is linked to TLR4 signaling in the epithelium (39) and TLR4 signaling suppresses osteoclastogenesis in murine bone marrow cultures (40, 41) (42), this mechanism is unlikely in our model because RC lysates failed to activate TLR4 signaling in RAW 264.7 cells.

Our findings observed with heated PPP that turns into Alb-gel are also interesting. Compared to the lysates of PPP, the lysates of Alb-gel are considerably less potent to lower the LPS and lactoferrin-induced IL6 expression. These findings suggest that the molecules responsible for the anti-inflammatory activity of PPP are heat sensitive. Nevertheless, in RAW 264.7 macrophages exposed to LPS or lactoferrin, there is a remaining anti-inflammatory activity on Alb-gel, even though not reaching a level of significance. This observation may help to identify which components in PPP, and presumably also BC, are responsible for the lowering of IL6 and COX2 expression in macrophages. There are candidate molecules such as apolipoprotein A-I of HDL to adsorb and thereby lower the LPS-induced inflammatory response (43). Also serum components such as high-density lipoprotein (44, 45) and the content of apolipoprotein A-I exert an anti-inflammatory activity by interfering with the TLR system (46). From a clinical perspective, not only the C-PRF but also PPP is useful, maybe not as a primary source of platelet-derived growth factors, but because of its osteoimmunological activity on macrophages and osteoclasts (24).

Taken together, we report here that not only lysates prepared from the cell-rich BC or C-PRF but also from the plasma PPP layer of liquid PRF exert an anti-inflammatory as well as an anti-osteoclastogenic response in macrophage cultures, presumably involving heat sensitive components lowering the NFκB signaling. Whether or not that the anti-inflammatory as well as the anti-osteoclastogenic response are mediated by the same or different plasma-derived components and pathways remains to be determined. Also understanding the possible role of the platelets and the leucocytes in this context is an inspiration for future research. The study provides another novel aspect to PRF research namely that the lysates of RC similar to hemoglobin suppressed osteoclastogenesis.

DATA AVAILABILITY STATEMENT

The original contributions presented in the study are included in the article/supplementary material. Further inquiries can be directed to the corresponding author.

ETHICS STATEMENT

The studies involving human participants were reviewed and approved by ethics committee of the Medical University of Vienna (1644/2018). The patients/participants provided their written informed consent to participate in this study.

AUTHOR CONTRIBUTIONS

ZK contributed to conceptualization and design, methodology, acquisition, analysis, software, validation and interpretation, critically revised manuscript, gave final approval, agreed to be accountable for all aspects of work. JN contributed to acquisition, analysis, interpretation, critically revised manuscript, gave final approval, agreed to be accountable for all aspects of work. LP contributed to acquisition, analysis, interpretation, critically revised manuscript, gave final approval, agreed to be accountable for all aspects of work. RM critically revised manuscript, gave final approval, agreed to be accountable for all aspects of work. RG contributed to conception and design, acquisition, analysis, and interpretation, drafted manuscript, critically revised manuscript, gave final approval, agreed to be accountable for all aspects of work. All authors contributed to the article and approved the submitted version.

FUNDING

This research was funded in part by a grant from the Osteology Foundation, Switzerland (17-125 and 17-219). ZK and JN received support from the Austrian Science Fund (FWF) (4072-B28).

REFERENCES

1. Takayanagi H. Osteoimmunology: shared mechanisms and crosstalk between the immune and bone systems. *Nat Rev Immunol* (2007) 7:292–304. doi: 10.1038/nri2062
2. Teitelbaum SL. Bone resorption by osteoclasts. *Science* (2000) 289:1504–8. doi: 10.1126/science.289.5484.1504
3. Tsukasaki M, Takayanagi H. Osteoimmunology: evolving concepts in bone-immune interactions in health and disease. *Nat Rev Immunol* (2019) 19:626–42. doi: 10.1038/s41577-019-0178-8
4. Gruber R. Osteoimmunology: Inflammatory osteolysis and regeneration of the alveolar bone. *J Clin Periodontol* (2019) 46 Suppl 21:52–69. doi: 10.1111/jcpe.13056
5. Tsukasaki M, Komatsu N, Nagashima K, Nitta T, Pluemsakunthai W, Shukunami C, et al. Host defense against oral microbiota by bone-damaging T cells. *Nat Commun* (2018) 9:701. doi: 10.1038/s41467-018-03147-6
6. Mbalaviele G, Novack DV, Schett G, Teitelbaum SL. Inflammatory osteolysis: a conspiracy against bone. *J Clin Invest* (2017) 127:2030–9. doi: 10.1172/JCI93356

7. Chen Z, Bozec A, Ramming A, Schett G. Anti-inflammatory and immune-regulatory cytokines in rheumatoid arthritis. *Nat Rev Rheumatol* (2019) 15:9–17. doi: 10.1038/s41584-018-0109-2
8. McInnes IB, Schett G. Pathogenetic insights from the treatment of rheumatoid arthritis. *Lancet* (2017) 389:2328–37. doi: 10.1016/S0140-6736(17)31472-1
9. McInnes IB, Schett G. Cytokines in the pathogenesis of rheumatoid arthritis. *Nat Rev Immunol* (2007) 7:429–42. doi: 10.1038/nri2094
10. Kinane DF, Stathopoulou PG, Papapanou PN. Periodontal diseases. *Nat Rev Dis Primers* (2017) 3:17038. doi: 10.1038/nrdp.2017.38
11. Caffesse RG, Echeverria JJ. Treatment trends in periodontics. *Periodontol 2000* (2019) 79:7–14. doi: 10.1111/prd.12245
12. Miron RJ, Moraschini V, Del Fabbro M, Piattelli A, Fujioka-Kobayashi M, Zhang Y, et al. Use of platelet-rich fibrin for the treatment of gingival recessions: a systematic review and meta-analysis. *Clin Oral Investig* (2020) 24:2543–57. doi: 10.1007/s00784-020-03400-7
13. Temmerman A, Cleeren GJ, Castro AB, Teughels W, Quirynen M. L-PRF for increasing the width of keratinized mucosa around implants: A split-mouth, randomized, controlled pilot clinical trial. *J Periodontal Res* (2018) 53:793–800. doi: 10.1111/jre.12568
14. Temmerman A, Vandessel J, Castro A, Jacobs R, Teughels W, Pinto N, et al. The use of leucocyte and platelet-rich fibrin in socket management and ridge preservation: a split-mouth, randomized, controlled clinical trial. *J Clin Periodontol* (2016) 43:990–9. doi: 10.1111/jcpe.12612
15. Zhu J, Zhang S, Yuan X, He T, Liu H, Wang J, et al. Effect of platelet-rich fibrin on the control of alveolar osteitis, pain, trismus, soft tissue healing, and swelling following mandibular third molar surgery: an updated systematic review and meta-analysis. *Int J Oral Maxillofac Surg* (2020) 50:398–406. doi: 10.1016/j.ijom.2020.08.014
16. Zhang J, Yin C, Zhao Q, Zhao Z, Wang J, Miron RJ, et al. Anti-inflammation effects of injectable platelet-rich fibrin via macrophages and dendritic cells. *J BioMed Mater Res A* (2020) 108:61–8. doi: 10.1002/jbm.a.36792
17. Nasirzade J, Kargarpour Z, Hasannia S, Strauss FJ, Gruber R. Platelet-rich fibrin elicits an anti-inflammatory response in macrophages in vitro. *J Periodontol* (2020) 91:244–52. doi: 10.1002/JPER.19-0216
18. Kargarpour Z, Nasirzade J, Strauss FJ, Di Summa F, Hasannia S, Muller HD, et al. Platelet-rich fibrin suppresses in vitro osteoclastogenesis. *J Periodontol* (2020) 91:413–21. doi: 10.1002/JPER.19-0109
19. Porta C, Rimoldi M, Raes G, Brys L, Ghezzi P, Di Liberto D, et al. Tolerance and M2 (alternative) macrophage polarization are related processes orchestrated by p50 nuclear factor kappaB. *Proc Natl Acad Sci USA* (2009) 106:14978–83. doi: 10.1073/pnas.0809784106
20. Yamashita T, Yao Z, Li F, Zhang Q, Badell IR, Schwarz EM, et al. NF-kappaB p50 and p52 regulate receptor activator of NF-kappaB ligand (RANKL) and tumor necrosis factor-induced osteoclast precursor differentiation by activating c-Fos and NFATc1. *J Biol Chem* (2007) 282:18245–53. doi: 10.1074/jbc.M610701200
21. Fierro FA, Nolta JA, Adamopoulos IE. Concise Review: Stem Cells in Osteoimmunology. *Stem Cells* (2017) 35:1461–7. doi: 10.1002/stem.2625
22. Miron RJ, Chai J, Zhang P, Li Y, Wang Y, Mourao C, et al. A novel method for harvesting concentrated platelet-rich fibrin (C-PRF) with a 10-fold increase in platelet and leukocyte yields. *Clin Oral Investig* (2020) 24:2819–28. doi: 10.1007/s00784-019-03147-w
23. Wend S, Kubesch A, Orlowska A, Al-Maawi S, Zender N, Dias A, et al. Reduction of the relative centrifugal force influences cell number and growth factor release within injectable PRF-based matrices. *J Mater Sci Mater Med* (2017) 28:188. doi: 10.1007/s10856-017-5992-6
24. Fujioka-Kobayashi M, Schaller B, Mourao C, Zhang Y, Sculean A, Miron RJ. Biological characterization of an injectable platelet-rich fibrin mixture consisting of autologous albumin gel and liquid platelet-rich fibrin (Alb-PRF). *Platelets* (2020) 32:1–8. doi: 10.1080/09537104.2020.1717455
25. Gheno E, Mourao C, Mello-Machado RC, Stellet Lourenco E, Miron RJ, Catarino KFF, et al. In vivo evaluation of the biocompatibility and biodegradation of a new denatured plasma membrane combined with liquid PRF (Alb-PRF). *Platelets* (2020) 32:1–13. doi: 10.1080/09537104.2020.1775188
26. Andrade C, Camino J, Nally M, Quirynen M, Martinez B, Pinto N. Combining autologous particulate dentin, L-PRF, and fibrinogen to create a matrix for predictable ridge preservation: a pilot clinical study. *Clin Oral Investig* (2020) 24:1151–60. doi: 10.1007/s00784-019-02922-z
27. Wang X, Yang Y, Zhang Y, Miron RJ. Fluid platelet-rich fibrin stimulates greater dermal skin fibroblast cell migration, proliferation, and collagen synthesis when compared to platelet-rich plasma. *J Cosmet Dermatol* (2019) 18:2004–10. doi: 10.1111/jocd.12955
28. Bustin SA, Benes V, Garson JA, Hellemans J, Huggett J, Kubista M, et al. The MIQE guidelines: minimum information for publication of quantitative real-time PCR experiments. *Clin Chem* (2009) 55:611–22. doi: 10.1373/clinchem.2008.112797
29. Meilhac O, Tanaka S, Couret D. High-Density Lipoproteins Are Bug Scavengers. *Biomolecules* (2020) 10:598. doi: 10.3390/biom10040598
30. Kargarpour Z, Nasirzade J, Panahipour L, Miron RJ, Gruber R. Liquid Platelet-Rich Fibrin and Heat-Coagulated Albumin Gel: Bioassays for TGF-beta Activity. *Mater (Basel)* (2020) 13:3466. doi: 10.3390/ma13163466
31. Sheldon KE, Shandilya H, Kepka-Lenhart D, Poljakovic M, Ghosh A, Morris SMJr. Shaping the murine macrophage phenotype: IL-4 and cyclic AMP synergistically activate the arginase I promoter. *J Immunol* (2013) 191:2290–8. doi: 10.4049/jimmunol.1202102
32. Miao Y, He L, Qi X, Lin X. Injecting Immunosuppressive M2 Macrophages Alleviates the Symptoms of Periodontitis in Mice. *Front Mol Biosci* (2020) 7:603817. doi: 10.3389/fmolb.2020.603817
33. Renn TY, Kao YH, Wang CC, Burnouf T. Anti-inflammatory effects of platelet biomaterials in a macrophage cellular model. *Vox Sang* (2015) 109:138–47. doi: 10.1111/vox.12264
34. Na YJ, Han SB, Kang JS, Yoon YD, Park SK, Kim HM, et al. Lactoferrin works as a new LPS-binding protein in inflammatory activation of macrophages. *Int Immunopharmacol* (2004) 4:1187–99. doi: 10.1016/j.intimp.2004.05.009
35. Gruber R, Karreth F, Fischer MB, Watzek G. Platelet-released supernatants stimulate formation of osteoclast-like cells through a prostaglandin/RANKL-dependent mechanism. *Bone* (2002) 30:726–32. doi: 10.1016/s8756-3282(02)00697-x
36. Agis H, Schrockmair S, Skorianz C, Fischer MB, Watzek G, Gruber R. Platelets increase while serum reduces the differentiation and activity of osteoclasts in vitro. *J Orthop Res* (2013) 31:1561–9. doi: 10.1002/jor.22386
37. Zavaczki E, Gall T, Zarjou A, Hendrik Z, Potor L, Toth CZ, et al. Ferryl Hemoglobin Inhibits Osteoclastic Differentiation of Macrophages in Hemorrhaged Atherosclerotic Plaques. *Oxid Med Cell Longev* (2020) 2020:3721383. doi: 10.1155/2020/3721383
38. Bozza MT, Jeney V. Pro-inflammatory Actions of Heme and Other Hemoglobin-Derived DAMPs. *Front Immunol* (2020) 11:1323. doi: 10.3389/fimmu.2020.01323
39. Merle NS, Paule R, Leon J, Daugan M, Robe-Rybkine T, Poillerat V, et al. P-selectin drives complement attack on endothelium during intravascular hemolysis in TLR-4/heme-dependent manner. *Proc Natl Acad Sci USA* (2019) 116:6280–5. doi: 10.1073/pnas.1814797116
40. Takami M, Kim N, Rho J, Choi Y. Stimulation by toll-like receptors inhibits osteoclast differentiation. *J Immunol* (2002) 169:1516–23. doi: 10.4049/jimmunol.169.3.1516
41. Zou W, Bar-Shavit Z. Dual modulation of osteoclast differentiation by lipopolysaccharide. *J Bone Miner Res* (2002) 17:1211–8. doi: 10.1359/jbmr.2002.17.7.1211
42. Muller HD, Caballe-Serrano J, Lussi A, Gruber R. Inhibitory effect of saliva on osteoclastogenesis in vitro requires toll-like receptor 4 signaling. *Clin Oral Investig* (2017) 21:2445–52. doi: 10.1007/s00784-016-2041-7
43. Beck WH, Adams CP, Biglang-Awa IM, Patel AB, Vincent H, Haas-Stapleton EJ, et al. Apolipoprotein A-I binding to anionic vesicles and lipopolysaccharides: role for lysine residues in antimicrobial properties. *Biochim Biophys Acta* (2013) 1828:1503–10. doi: 10.1016/j.bbamem.2013.02.009
44. Fotakis P, Kothari V, Thomas DG, Westerterp M, Molusky MM, Altin E, et al. Anti-Inflammatory Effects of HDL (High-Density Lipoprotein) in Macrophages Predominate Over Proinflammatory Effects in Atherosclerotic Plaques. *Arterioscler Thromb Vasc Biol* (2019) 39:e253–72. doi: 10.1161/ATVBAHA.119.313253
45. Pajkrt D, Doran JE, Koster F, Lerch PG, Arnet B, van der Poll T, et al. Antiinflammatory effects of reconstituted high-density lipoprotein during human endotoxemia. *J Exp Med* (1996) 184:1601–8. doi: 10.1084/jem.184.5.1601
46. Zhang M, Zhao GJ, Yin K, Xia XD, Gong D, Zhao ZW, et al. Apolipoprotein A-1 Binding Protein Inhibits Inflammatory Signaling Pathways by Binding to

Apolipoprotein A-1 in THP-1 Macrophages. *Circ J* (2018) 82:1396–404. doi: 10.1253/circj.CJ-17-0877

Conflict of Interest: The authors declare that the research was conducted in the absence of any commercial or financial relationships that could be construed as a potential conflict of interest.

frontiers in Immunology

ORIGINAL RESEARCH
published: 27 May 2021
doi: 10.3389/fimmu.2021.666355

Revealing the Immune Infiltration Landscape and Identifying Diagnostic Biomarkers for Lumbar Disc Herniation

*Linbang Wang[1], Tao He[1], Jingkun Liu[2], Jiaojiao Tai[2], Bing Wang[3], Lanyue Zhang[4] and Zhengxue Quan[1]**

[1] Department of Orthopedic Surgery, The First Affiliated Hospital of Chongqing Medical University, Chongqing, China, [2] Honghui Hospital, Xi'an Jiaotong University, Xi'an, China, [3] Laboratory of Environmental Monitoring, Shaanxi Province Health Inspection Institution, Xi'an, China, [4] Traditional Chinese Medicine Department, Chongqing Medical University, Chongqing, China

Intervertebral disc (IVD) degeneration and its inflammatory microenvironment ultimately led to discogenic pain, which is thought to originate in the nucleus pulposus (NP). In this study, key genes involved in NP tissue immune infiltration in lumbar disc herniation (LDH) were identified by bioinformatic analysis. Gene expression profiles were downloaded from the Gene Expression Omnibus (GEO) database. The CIBERSORT algorithm was used to analyze the immune infiltration into NP tissue between the LDH and control groups. Hub genes were identified by the WGCNA R package in Bioconductor and single-cell sequencing data was analyzed using R packages. Gene expression levels were evaluated by quantitative real-time polymerase chain reaction. The immune infiltration profiles varied significantly between the LDH and control groups. Compared with control tissue, LDH tissue contained a higher proportion of regulatory T cells and macrophages, which are associated with the macrophage polarization process. The most significant module contained three hub genes and four subclusters of NP cells. Functional analysis of these genes was performed, the hub gene expression pattern was confirmed by PCR, and clinical features of the patients were investigated. Finally, we identified TGF-β and MAPK signaling pathways as crucial in this process and these pathways may provide diagnostic markers for LDH. We hypothesize that the hub genes expressed in the specific NP subclusters, along with the infiltrating macrophages play important roles in the pathogenesis of IVD degeneration and ultimately, disc herniation.

Keywords: intervertebral disc degeneration, lumbar disc herniation, macrophages, nucleus pulposus, single-cell sequencing (SCS)

OPEN ACCESS

Edited by:
Katharina Schmidt-Bleek, Charité – Universitätsmedizin Berlin, Germany

Reviewed by:
Claudia Schlundt, Charité – Universitätsmedizin Berlin, Germany
Cristhopher Mazuret, Hospital Sotero Del Rio, Chile

****Correspondence:***
Zhengxue Quan
quanzx18@163.com

Specialty section:
This article was submitted to Inflammation, a section of the journal Frontiers in Immunology

Received: *10 February 2021*
Accepted: *04 May 2021*
Published: *27 May 2021*

Citation:
Wang L, He T, Liu J, Tai J, Wang B, Zhang L and Quan Z (2021) Revealing the Immune Infiltration Landscape and Identifying Diagnostic Biomarkers for Lumbar Disc Herniation. Front. Immunol. 12:666355. doi: 10.3389/fimmu.2021.666355

INTRODUCTION

Low back pain is a widespread and complex clinical condition affecting 70%–85% of the population worldwide. However, in more than 40% of chronic lower back pain cases, there is no evidence of nerve compression (1). Therefore, intervertebral disc (IVD) degeneration is believed to be the main cause of pain (2).

The IVD has been identified as an immune privilege organ because its unique structure isolates the nucleus pulposus (NP) from the immune system of the host (3), in which the annulus fibrosus (AF), cartilaginous endplate, and immunosuppressive molecular factors consist of the blood-NP barrier (4). The NP triggers an immune response when the blood-NP barrier is damaged. This process plays a crucial role in IVD degeneration and leads to multiple pathological processes, in which the NP loses proteoglycans and becomes more fibrotic (5). Meanwhile, matrix metalloproteinases and inflammatory mediators, such as interleukin-1β (IL-1β) and tumor necrosis factor-alpha (TNF-α), are upregulated in the disc micro environment. These cytokines are produced by IVD cells and immune cells, such as macrophages and CD8 T cells (6–8). However, the immune landscape and the role of epigenetic regulation in the pathological process of IVD degeneration remains unclear.

In this study, we first determined the specific types of immune cells that are involved in IVD degeneration by using gene expression matrices. Then, the hub genes involved in this process were screened. Single-cell analysis uncovered the expression patterns of hub genes in NP cell clusters, and the prospective clinical experiment confirmed the prognostic value of hub gene expression.

MATERIALS AND METHODS

Data Collection and Preprocessing

The microarray data and corresponding clinical information, including 30 human disc tissues, were downloaded and filtered from the GEO dataset (GSE124272, GSE147383, and GSE153761). The single-cell transcriptome data from intervertebral discs were obtained from GEO (GSE154884). Multiple datasets of gene expression matrices were merged and the inter-batch differences were removed for further processing.

Differentially Expressed Genes (DEGs)

The edgeR package was used to screen for DEGs in stage IV lumbar disc herniation (LDH) tissues and controls, including spondylolisthesis and LDH stages I to III. The selection criteria were $|\log2\ FC| > 1.5$, and false discovery rate (FDR) < 0.05. The volcano plot and heatmap of DEGs were generated by the pheatmap R package.

Immune Cell Infiltration Estimation

The CIBERSORT deconvolution algorithm was applied to quantify the degree of infiltration of 22 types of immune cells through the transcriptome data. Investigated immune cells included plasma cells, resting memory CD4+ T cells, CD8+ T cells, naive CD4+ T cells, T follicular helper cells, regulatory T cells (Tregs), activated memory CD4+ T cells, gamma delta T cells, naive B cells, memory B cells, monocytes, M0 macrophages, M1 macrophages, M2 macrophages, resting natural killer (NK) cells, activated NK cells, activated mast cells, eosinophils, neutrophils, resting dendritic cells, activated dendritic cells, and resting mast cells. The differences between the two groups were compared using the wilcox test and the results were visualized by applying the vioplot package. Finally, the correlation between infiltration rate of each types of immune cells was determined by the corrplot package.

Identification of Immune Cell Infiltration-Related Genes

Immune cell infiltration-related genes were identified using the WGCNA R package. First, the gene expression matrices outliers were filtered by hierarchical cluster analysis. Then, the correlation coefficient of genes was constructed and transformed into a weighted adjacency matrix. Next, these genes were allocated into minimum-sized modules and a cluster dendrogram was drawn, and then merged with a height cutoff (cutoff < 0.3). The correlation between gene expression and sample trait (immune cell infiltration score) was determined by the criterion of gene significance (GS) > 0.5 and module membership (MM) > 0.8. The relevant genes in the module were then tested for correlation with all other genes, the screening conditions were set at cor > 0.7 and $p < 0.01$, the regulatory network was visualized using cytoscape. Finally, matascape was used to conducted functional analysis to the selected genes.

Single-Cell Analysis

Single-cell RNA sequencing data sets from IVD tissue (GSE154884) were obtained. The Seurat pipeline was used for data reprocessing and to classify the cell groups, SingleR identified the cell type, and Monocle was used to analyze the cell differentiation trajectory.

Functional Correlation Analysis

The clusterProfiler package (9) was used for performing gene ontology (GO) enrichment analyses on cell cluster marker genes, where $p < 0.05$ and FDR < 0.25 were considered significantly enriched.

Patients

Nine patients who underwent posterior open discectomy for radiating pain due to single-level LDH (classified as Pfirrmann grade IV by MRI) were included. Six patients were female and three were male (10). The mean duration between onset of symptoms and operation was 13.5 weeks. Patients with degenerative spondylolisthesis or a history of diabetes mellitus or renal disease were excluded. As a control, 14 patients, including 8 females and 6 males, who underwent posterior

Abbreviations: IVD, intervertebral disc; NP, nucleus pulposus; AF, annulus fibrosus; DEGs, differentially expressed genes; LDH, lumbar disc herniation; FDR, false discovery rate; NK, natural killer; GO, gene ontology; ELISA, enzyme-linked immunosorbent assay; qRT-PCR, quantitative real-time polymerase chain reaction; t-SNE, t-distributed stochastic neighbor embedding; PLET1, placenta expressed transcript 1; ID1, inhibitor of DNA binding 1.

open discectomy for neurological symptoms due to single-level lumbar disc herniation (classified as Pfirrmann grades I to III by MRI) were selected for this study. Patient immune responses were evaluated as either "high" or "low" and the results are shown in **Table 1**, to be specific, the immune status of each individual is evaluated by whether the percentage of total lymphocytes higher than the median level of 32 or the percentage of CD4-CD8- lymphocytes is lower than median level of 6. Tissues were excised and transferred to liquid nitrogen for RNA and protein extraction. Written informed consent was obtained from all patients. Clinical data were acquired from hospital records and pathology reports. The study protocol (approval number: 2020–171) was approved by The Ethics Committee of the Affiliated Hospital of Chongqing Medical University.

Total Protein and RNA Extraction

IVD specimens obtained from patients were first homogenized in phosphate-buffered saline (Tissue Tearor kits, Racine, model 985–370). The supernatant was obtained by centrifugation at 15,000 rpm at 4°C for 30 min. The Bradford protein assay method (#500–0006; Biorad, Hercules, CA, USA) was used for protein quantification and the results were used for measurement of TNF-α and TGF-β. IVD specimens were also used for RNA extraction using the UNIQ-10 Column Total RNA Purification Kit (Sangon Biotech, China). The quality and concentration of RNA were evaluated using a SMA4000 microspectrophotometer (Merinton Instrument, Inc. MI, USA).

ELISA

IVD extracts were quantitatively analyzed for TNF-α and TGF-β using an enzyme-linked immunosorbent assay (ELISA) kit (Beijing Jingmei Biological Engineering Co, Ltd, China) and measurement at 450 nm. TNF-α and TGF-β concentrations were extrapolated from the standard curve.

Reverse Transcription and Quantitative Real-Time Polymerase Chain Reaction (qRT-PCR)

The RR047A cDNA synthesis kit (TaKaRa, China) was used to perform the reverse-transcription of the extracted RNA and the 2X SG Fast qPCR Master Mix (High Rox, B639273, BBI) was used for quantitative PCR of hub genes on an ABI PRISM 3700 instrument (Foster, CA, USA). GAPDH was used as an internal control and primers are as follows:

ID1-F: 5' CTCAGCACCCTCAACGG 3',
ID1-R: 5' GATCGGTCTTGTTCTCCCTC 3',
RAP2C-F: 5' CCCTCCGTGCTGGAAATTCT 3',
RAP2C-R: 5 'CCATGAAAGGACAGCCCCAT 3',
PTPRK-F: 5' ACAGAGTGGTGAAAATAGCAGGAA 3',
PTPRK-R: 5' TGACAACTAGGAGAAGGAGGATGA 3',
GAPDH-F: 5' TGGGTGTGAACCATGAGAAGT 3', and
GAPDH-R: 5' TGAGTCCTTCCACGATACCAA 3'.

TABLE 1 | Results of immune function quality of patients in different groups.

item	patient 1	patient 2	patient 3	patient 4	patient 5	patient 6	patient 7	patient 8	patient 9	patient 10	patient 11	patient 12	patient 13	patient 14	reference range
ZLBXB-FZ1	18.74	22.06	17.12	26.33	21.2	36.42	19.24	48.2	36.63	38.27	21.87	24.24	25.22	26.83	27.90~37.3
CD3+	66.23	85.43	84.9	78.27	73.18	69.48	53.91	62.94	67.12	82.01	72.32	76.81	74.29	74.21	26.00-76.80
CD3+ CD4+ CD8-	37.78	52.67	58.32	41.89	36.67	42.74	45.21	43.62	41.37	47.91	46.68	46.37	42.24	47.52	30-46
CD3+ CD4- CD8+	28.42	27.69	27.12	34.31	34.13	24.31	16.33	26.25	23.9	27.12	23.88	26.16	27.22	24.89	19.2-33.6
CD4+ CD8+	1.13	1.45	0.77	1.82	0.23	0.43	0.19	3.11	0.31	0.86	0.13	0.43	0.71	0.22	0-2.00
CD4- CD8-	6.42	5.36	3.78	3.26	10.17	4.12	2.45	1.72	1.23	3.90	2.91	1.99	2.03	2.46	0-12.00
CD3- CD19+	12.76	5.69	6.51	3.31	5.23	18.92	23.65	17.13	23.72	10.56	11.87	22.15	19.88	16.41	8.50-14.50
CD3- CD16/56+	14.91	112.13	10.98	16.89	22	15.12	11.17	16.83	9.92	8.23	10.56	11.77	6.93	8.59	9.50-23.50
CD3+ CD16/56+	3.82	7.87	5.34	3.66	6.92	0.76	2.31	3.98	7.23	4.81	1.54	1.57	1.21	2.66	/
High or low flag	L	L	L	L	L	L	L	H	H	H	H	H	H	H	/

RESULTS

Research Design Summary

A flow diagram showing the research design is shown in **Figure 1**. In brief, DEGs in the LDH were screened from microarray data of samples in the GEO database. CIBERSORT was then applied to DEGs for identifying LDH-related immune cells. Next, WGCNA and correlation test were used to find hub genes associated with the identified immune cells. The expression pattern of these hub genes was then examined at the single-cell level and several LDH-related NP cells were recognized. Finally, qRT-PCR and ELISAs were performed to verify the relationship between hub gene expression levels and clinical characteristics in LDH patients.

Screening of DEGs

Batch correction, normalization, and difference analysis of RNA-seq data from GSE124272, GSE147383, and GSE153761 were performed to screen for DEGs in IVD samples. A total of 410 DEGs, including 195 downregulated and 215 upregulated genes were identified. The results were visualized using a volcano plot (**Figure 2A**), which identifies important genes.

Immune Microenvironment Characteristics of Degenerated IVDs

In order to further reveal the immune microenvironment in degenerated IVDs, the CIBERSORT method was used to analyze specific immune cell types that infiltrated into IVD tissue. Among the 22 types of immune cells investigated, the results showed that Tregs and macrophage levels were significantly higher in degenerated IVD ($p<0.05$) (**Figure 2B**), As is shown in **Figure 2C**, by further analyzing the CIBERSORT scores, there was a positive strong correlation between Mast cells, neutrophils and M1 macrophages, On the other hand, there was a negative correlation between the infiltration of plasma cells, regulatory T cells and M1 macrophages.

Identification of Immune Cell-Related Genes

WGCNA was applied to identify differentially expressed immune cell-related genes from 410 DEGs, as shown in **Figures 3A–D**. These DEGs were then divided into modules and merged with different colors (**Figures 3A, B**). Five merged modules were analyzed and three gene modules were significantly correlated with immune cells (**Figure 3C**). Among them, we selected the green module, which was the most significant module that was related to macrophages M0, with a positive correlation of 0.58 and $p<0.001$ (**Figure 3D**). 15 genes were screened according to the criteria, of which 12 were selected by correlation test. The expression pattern of these key genes was then analyzed accordingly (**Figures 3E, F**). Cytoscape constructed the interaction network between these 12 genes and their target genes (**Figure 3G**). Next, to acquire more information about these genes we performed functional analysis using Matascape, as shown in **Figure 3H**, genes were enriched in critical biological processes, such as interleukin signaling and the regulation of cytokine production.

scRNA-Seq Data Revealed High Cell Heterogeneity in IVD Tissue

To determine the single-cell level transcriptomic landscape of IVD compartments, we employed scRNA-sequencing data from healthy, non-degenerated rat IVDs. We first conducted quality control of the gene expression matrix (**Figure 4A**). Then, normalization of scRNA-seq data was performed and 20 principal components ($p<0.05$) were screened for subsequent analysis (**Figure 4B**). Reduced dimension process analysis was achieved by using Discriminative Dimensionality Reduction Tree (**Figure 4E**). Unsupervised analysis was then conducted for cell clustering using the t-distributed stochastic neighbor embedding (t-SNE) method (**Figures 4C, D**). The result showed high cell heterogeneity, in which IVD cells were segregated into four major distinct clusters, including chondrocytes (NP cells), fibroblasts (AF cells), adipocytes, and epithelial cells, which were

FIGURE 1 | A flowchart showing the steps in this study.

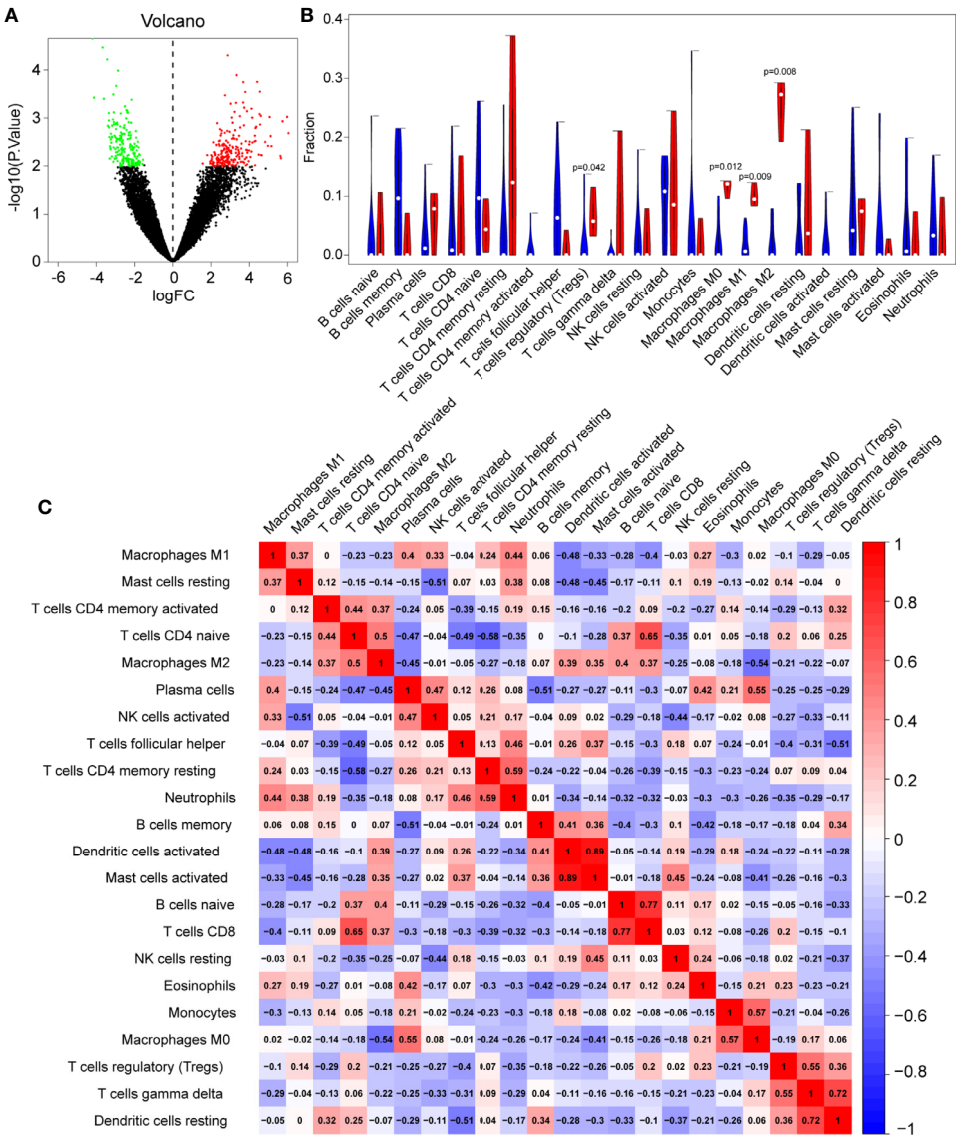

FIGURE 2 | The differentially expressed genes (DEGs) and immune infiltration landscape in nucleus pulposus (NP) tissue. **(A)** Volcano map of DEGs, where red represents upregulated genes and green represents downregulated genes. **(B)** Immune infiltration differences between intervertebral disc grade IV degenerative tissue and control tissue. **(C)** Correlation matrix of 22 immune cell type proportions.

determined using singleR and cell markers. Next, we tested the expression pattern of the hub genes in these cell clusters. As expected, most of the key genes were highly expressed in NP cells, with the key gene *ID1* found to be highly expressed in the AF cells (**Figure 4F**).

Identification of NP Cell Clusters in IVD Tissue

To uncover the detailed heterogeneity of NP cells, we re-subclustered the scRNA-seq data by upregulating the resolution value. Four cell clusters, including clusters 1, 2, 4, and 5, were identified according to their gene expression pattern (**Figure 5A**). Trajectory analysis was then performed to illustrate the degree of cell differentiation. All cells were projected onto one root and two branches. Interestingly, cells in cluster 5 were mainly located in the root, whereas cells in clusters 1, 4 were mostly located in the left, and most cells in cluster 2 were located in the right (**Figure 5C**). Based on the hub gene markers, clusters 1, 2, 4, and 5 were defined as RBB7+Pdlim5-, RBB7+ Pdlim5+, RBB7- ID1+, and RBB7- Pdlim5+ cell groups (**Figure 5B**). Next, we defined the molecular features of these NP cell groups by tracking their gene markers (**Figure 5D**). Among them, *TOMM20*, *TOMM22*, and *CXCL2* were recognized as specific marker genes in cluster 1 (**Figures 6A–C**). *TOMM20* has been

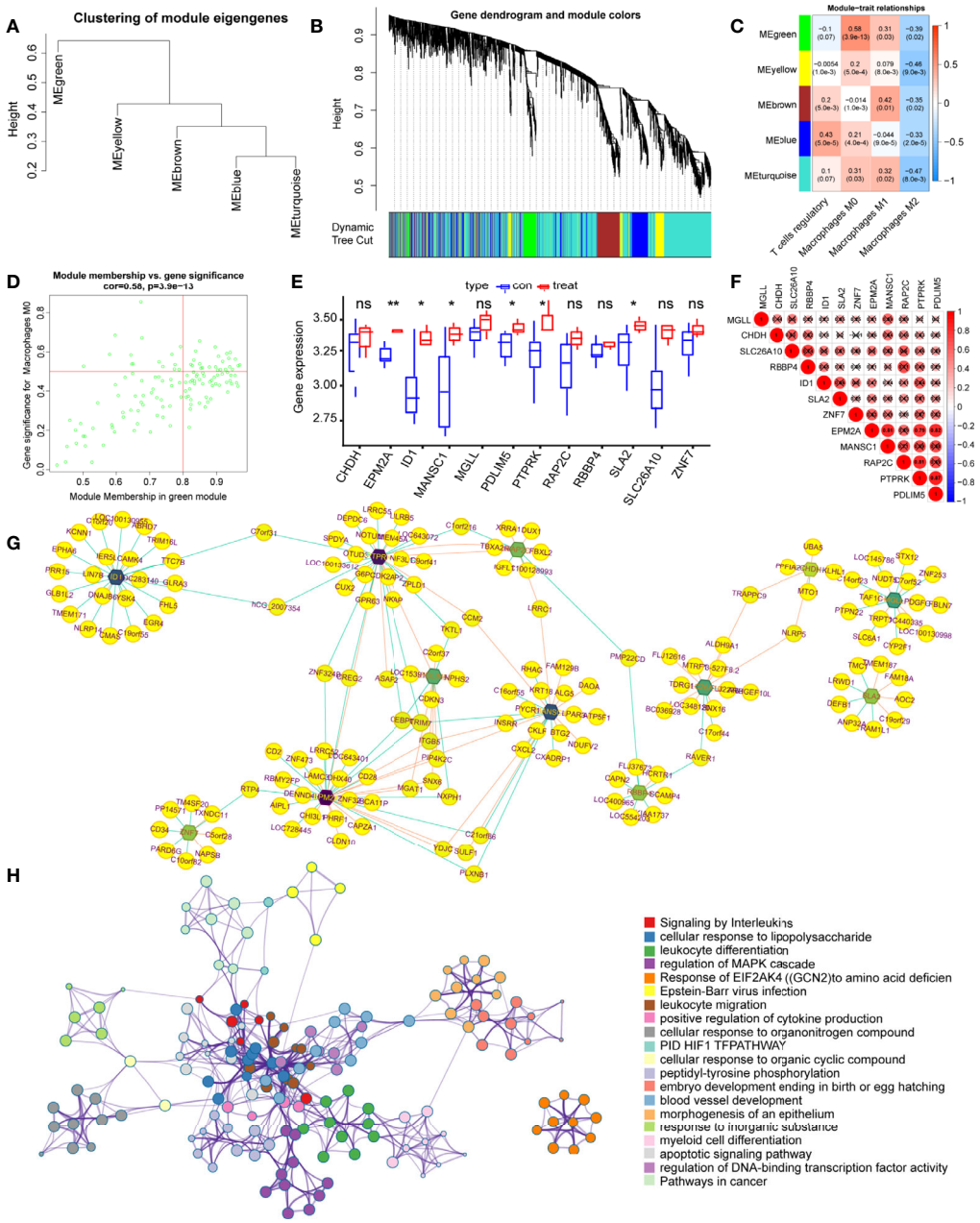

FIGURE 3 | Identification of the key modules and genes that relate to immune infiltration features in intervertebral disc degeneration. **(A, B)** The construction of the co-expression network module clustering tree based on the 1-tom matrix. **(C)** Feature of each merged module relationship, with different colors representing different modules. Each row corresponds to a module and columns represent their correlations with the traits. Each unit includes the correlation coefficient and p-value. **(D)** Genes of the selected green module. **(E)** The hub gene expression levels in different groups. **(F)** Expression correlation matrix of each hub gene in lumbar disc herniation. **(G)** The gene regulation networks are constructed to identify the hub genes. The edge represents the protein binding conditions and the node represents each gene. Darkness of the node represents the edge number of each gene. **(H)** The functional enrichment of the correlated genes by using metascape. Symbol "*", "**", and "ns" respectively stand for P value under 0.05, P value under 0.01, and non-significance.

shown to induce tissue inflammation responses in adipose and muscle tissue (11). *CXCL2* is reported to promote tumor cell migration through the induction of M2-like macrophage polarization. Therefore, we named cluster 1 "NP inflammatory response cells". Genes, including *TOMM7* and placenta expressed transcript 1 (*PLET1*), are specifically expressed in cluster 2. *PLET1* encodes for a cell surface protein that is specifically expressed in trophoblast stem cells. Of interest, functions enriched in cluster 2 included regulation of extrinsic apoptotic pathway and responses to metal ions, suggesting that

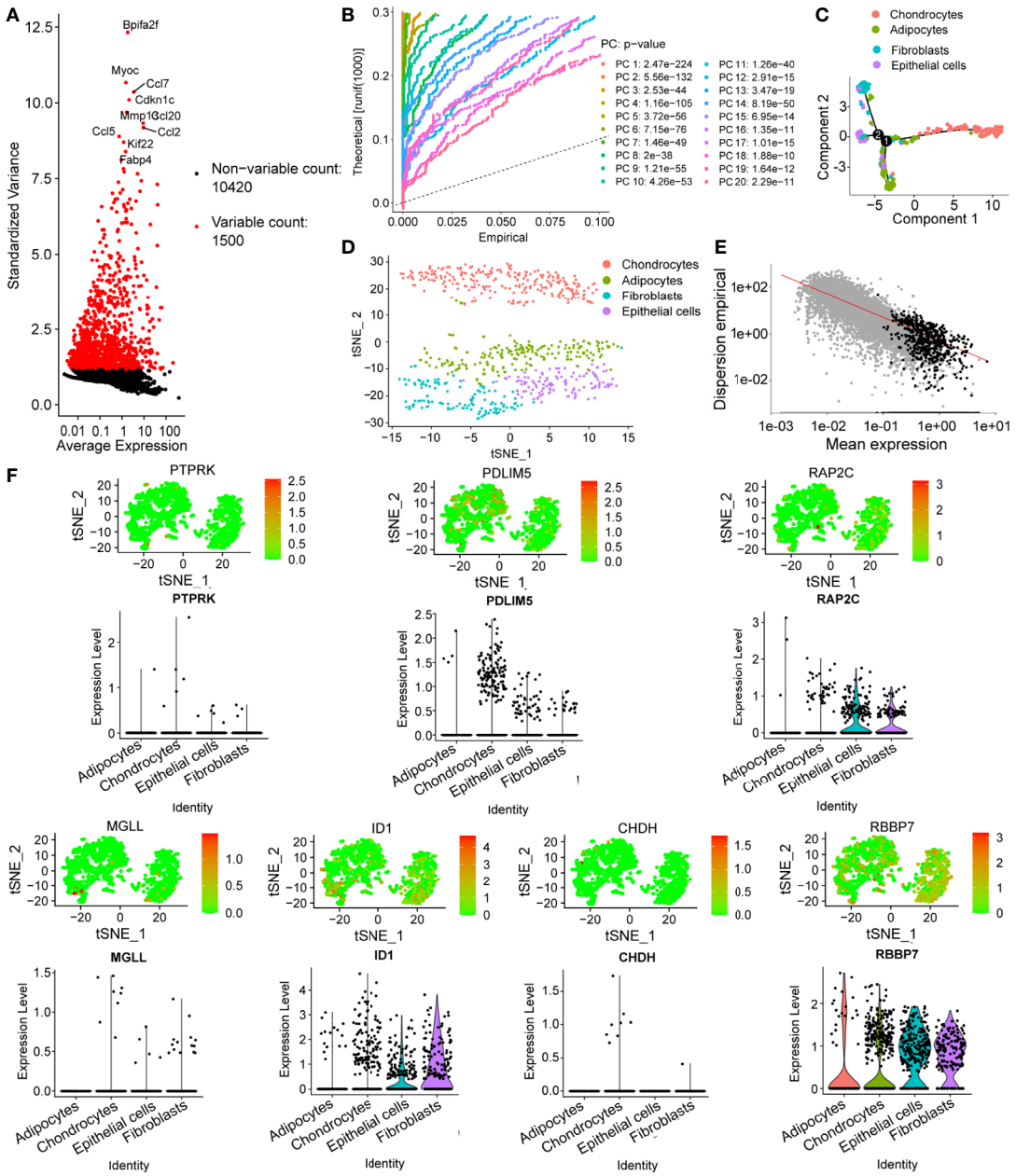

FIGURE 4 | Preprocessing of the single-cell sequencing data and cell cluster identification. **(A, B)** Gene filtering and PCA clustering of the gene expression matrix. **(C)** t-SNE projections and cell subset annotation of intervertebral disc (IVD) tissue. **(D)** Quality control process for the trajectory analysis using the DDRTree method. **(E)** Cell trajectory analysis of single cells in IVDs shows distinct lineage cells in different clusters. **(F)** Expression pattern of key genes at the single-cell level, shown in t-SNE figures and violin maps.

cluster 2 cells are involved in multidirectional maintenance and differentiation of chondroid cells (**Figures 6B–D**). Therefore, cluster 2 was named "NP repair cells". *BNIP3*, *SOD2*, and other genes are highly expressed in cluster 4. Functional enrichment results from cluster 4 marker genes showed that these cells function to response to oxygen levels. Cluster 4 cells provide extracellular matrix structural constituents, which confer resistance to compression (**Figures 7A, C**). Thus, we named cluster 4 "extracellular matrix NP cells". Cluster 5 cells have highly expressed genes, including *CLU*, *MEF2A*, *MCAM57*, and *FAM162A*, which are known markers of mesenchymal stem cells and NP progenitor cells (**Figures 7B–D**). The trajectory result showed that cluster 4 cells were mostly populated in the root of two branches. We speculate that this cell group of the IVD contains NP progenitor cells, which other researchers have suggested. Thus, we refer to this group as the "stem-like NP cells".

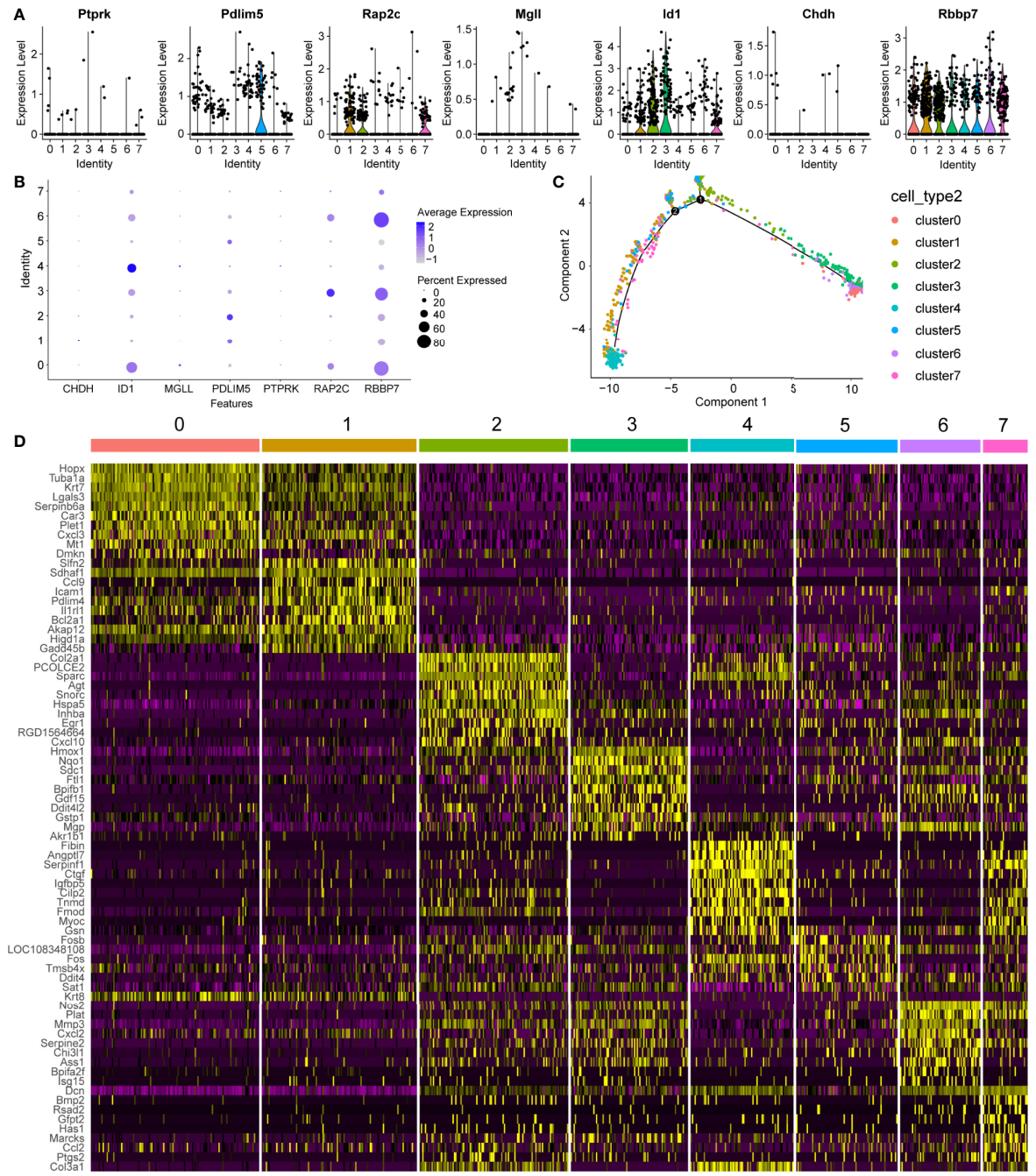

FIGURE 5 | Clustering of nucleus pulposus (NP) cells, revealing key gene expression patterns. **(A, B)** The expression pattern of key genes in each NP cluster is shown in the violin maps and dot plot. Clusters 1, 2, 4, and 5 refer to each NP subcluster. In the dot plot, the average expression of each cluster is represented by a color gradient, in which lower expression is represented by a lighter color and higher expression is represented by darker color. The percentage of cells is indicated by dot size. **(C)** Cell trajectory analysis of the clusters, including NP cells. Noted that NP cells in cluster 5 are mainly located in the root, while other cells in clusters are distributed in branches. **(D)** The heatmap shows the marker genes in each cluster.

Hub Gene Expression Validation and Cytokine Levels in LDH Patients

The Pfirrmann grade for each study group is represented by a set of lumbar intervertebral disc MRIs, as shown in **Figures 8A, B**. qRT-PCR results showed that the expression levels of ID1, RAP2C, and PTPRK were all significantly higher in NP tissues of the grade IV disc degeneration and high immunity groups (**Figures 8C–E**). ELISA results also showed that the expression of

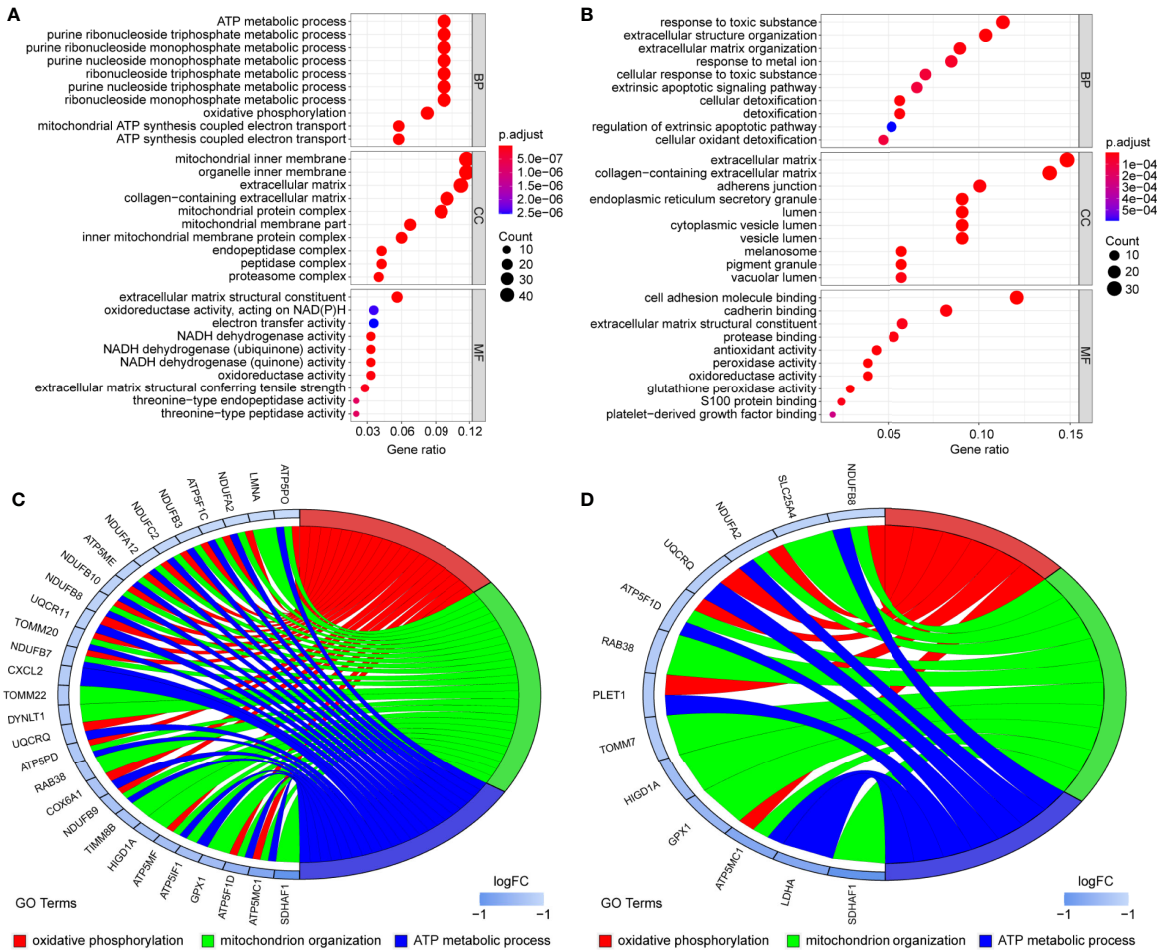

FIGURE 6 | Gene markers and functional analysis of each nucleus pulposus (NP) cell cluster. Bubble plots showing GO/pathway analysis results of marker genes in NP cell cluster 1 **(A)** and cluster 2 **(B)**. The chord plots reveal highly relevant functions and genes assigned to NP cell cluster 1 **(C)** and cluster 2 **(D)**.

these genes was positively correlated with TNF-α (**Figures 8G–I**) but not with TGF-β ($p<0.05$, $r=0.492$). We believe that the expression of hub genes may play a role in chronic disorders such as IVD degeneration (**Figure 8F**).

DISCUSSION

IVD degeneration is one of the major contributors to radicular back and neck pain. However, structural degeneration of discs is not necessarily accompanied by pain (12). Therefore, the pain is likely a secondary event of leakage or injury to NP material through annular fissures caused by the recruitment of immune cells to the area with the structural deficit (13). IVD degeneration has been characterized by the infiltration of CD68 macrophages, T cells (CD4, CD8), and neutrophils in herniated discs. It is also accompanied by the appearance of invading blood vessels and nociceptive nerve fibers (14). NP, AF cells, and immune cells, such as macrophages, T cells, and neutrophils, have been reported to release cytokines like TNF-α, IL-1 α/β, IL-6, IL-17, IL-8, IL-2, IL-4, IL-10, and IFN-γ, as well as neurogenic factors, which promote discogenic pain and reinforce disc cell pathogenic processes, including senescence and autophagy (15).

In our study, infiltration of macrophages and Tregs was found to be increased in the degenerative IVDs compared with that in the control group. It is reported that the accumulation of macrophages is significantly higher with the progression of IVD degenerative grade. The presence of multiple macrophage markers, including CCR7+ and CD163+, is significantly higher in the NP, AF, and endplate regions of degenerative IVD with structural defects (16). Th17/Treg cells were reported to be involved in the pathogenesis of chronic low back pain through an immune response. The number of anti-inflammatory Tregs is higher in chronic lower back pain patients, along with alterations in the Th17/Treg ratio (17).

A great number of researches have demonstrated the involvement of aberrant epigenetic modification in many diseases, including Alzheimer's disease and many other age-related diseases (18), as for the epigenetic modification in the

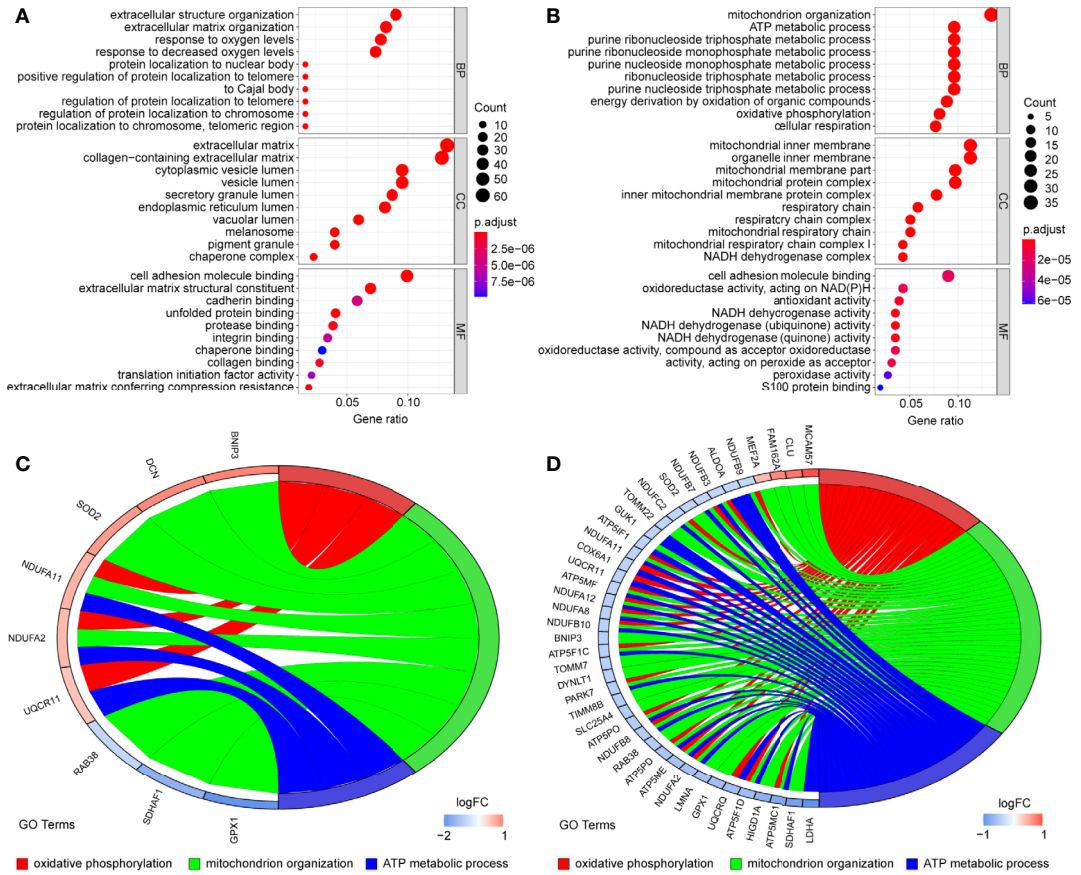

FIGURE 7 | Gene markers and functional analysis of each nucleus pulposus (NP) cell cluster. Bubble plots showing GO/pathway analysis results of marker genes in NP cell cluster 4 **(A)** and cluster 5 **(B)**. The chord plots reveal highly relevant functions and genes assigned to NP cell cluster 4 **(C)** and cluster 5 **(D)**.

IVD, we detected a relatively high expression of the inhibitor of DNA binding 1 protein (ID1) in both NP (mostly in cluster 4) and AF cells. ID1 is a nuclear protein that regulates cell growth by binding to DNA and preventing gene transcription. ID1 can inhibit the DNA binding and transcriptional activation ability of Helix-loop-helix (HLH) proteins with which it interacts. the latter of which are dimeric transcription factors that deposit or erase epigenetic marks, activate noncoding transcription, and sequester chromatin remodelers across the chromatin landscape. Its expression level is found to be correlated with multiple signaling pathways, including EGFR, K-Ras, MAPK, PI3K/Akt, and TGF-β, in various tumor types while facilitating angiogenesis (19). ID1 also plays an important role in tissue inflammation during orchestration (20). In fibroblasts, ID1 inhibits collagen expression through the TGF-β signaling pathway (21). ID1 production in rheumatoid arthritis synovial fibroblasts is mostly contained within exosomes, which could be affected by endothelial progenitor cells, leading to JNK signaling pathway activation in human dermal microvascular endothelial cells (20). We also noticed that IVD tissue expression of PTPRK is correlated with the pathological process of IVD degeneration. High PTPRK expression mediates homophilic intercellular interaction with adhesion junctions through its interaction with β and γ-catenin (22). RAP2C has also been reported to be involved in TNF-α-induced colorectal cancer metastasis (23). PCR results from IVD tissues showed that ID1, PTPRK, and RAP2C were highly expressed in stage IV tissues, which was consistent with our bioinformatics data. Our results also revealed that these genes were highly expressed in the high immune group. Combined with the results that hub gene expression was positively correlated with TNF secretion, we confirmed that with more IVD tissue degeneration, there was higher immune cell infiltration and higher hub gene expression, combining with previous studies and present results, we speculate that the pathological process of IVD degeneration has generated a special types of immune microenvironment that recruit regulatory T cells and multiple types of macrophages, the latter of which interact with NP cells, adipocytes, and fibroblasts through cytokines like TGF-β and IL-10, and brought abnormal gene expressions of ID1, PTPRK, and RAP2C in NP cells and promote the IVD pathological changes (**Figure 8I**).

The general cell components of the IVD includes cells of the NP and AF cells (24). However, the IVD cell type subclassification has been unrevealed. Despite similarities shared by these cells, there is

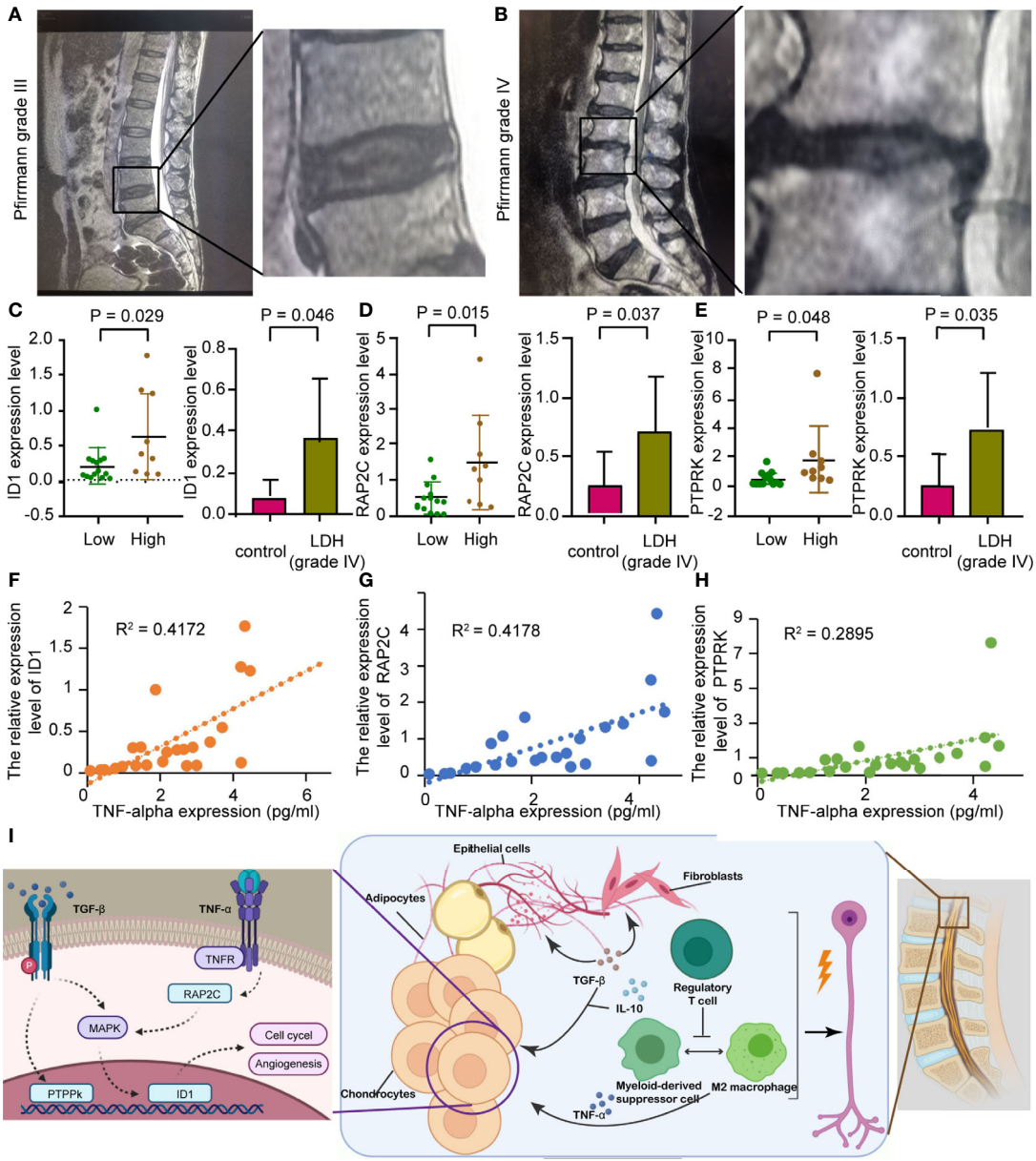

FIGURE 8 | Prospective clinical experiment confirms the bioinformatic results. **(A, B)** The MRI image shows lumbar disc herniation in patients from different groups which are divided by Pfirrmann grades I-III or IV. **(C, E)** Comparison of preoperative hub gene expression levels. The box plots on the right show hub genes expression in in vertebral disc tissue from different groups, divided by the Pfirrmann disc grade; The left honeycomb map show hub genes expression levels in the high and low immunity groups, coffee color represent high immunity group and green represent low immunity group. **(C)** *ID1*, **(D)** *RAP2C*, **(E)** *PTPRK*. **(F)** Schematic showing that the extrusion of the nucleus pulposus in a degenerating intervertebral disc could cause multiple inflammatory responses, resulting in radicular pain. **(G–I)** Correlation between TNF-α level assessed by ELISA and hub genes expression, as previously described. R represents Pearson's correlation coefficient. **(G)** *ID1*, **(H)** *RAP2C*, **(I)** *PTPRK*.

high heterogeneity in terms of molecular phenotypic characteristics, extracellular matrix, and biomechanical behavior (25). In this study, we took advantage of single-cell sequencing technology to classify the IVD cells into four categories including NP, AF, adipocytes, and epithelial cells. The corresponding gene markers of each cluster were also elucidated, indicating new targets for the treatment of IVD-related disorders. Next, we performed a detailed cluster analysis for NP cells. NP cells were separated into two branches with distinct differentiation features, according to trajectory analysis. Four clusters of NP cells were identified and we speculated that the different roles for each cluster were influenced by the expression of certain genes. The cells in cluster 1 were inferred to be responsible for the inflammatory process through immune cells such as macrophages. The cells in cluster 4 are also worth investigating since their stem-like characteristics have great therapeutic potential (26). The marker genes in clusters 2 and 3 are mainly related to stress and fibrotic

changes. The relationships between the various populations of NP and AF cells require further investigation.

CONCLUSION

Our research shows that immune cell infiltration, including Tregs and macrophages, is involved in the pathological process of IVD degeneration. Through single-cell sequencing and clinical experiments, we identified *ID1*, *PTPRK*, and *RAP2C* as hub genes, which may serve as molecular targets for prognostic evaluation and treatment of LDH.

DATA AVAILABILITY STATEMENT

Publicly available datasets were analyzed in this study. This data can be found here: https://www.ncbi.nlm.nih.gov/geo/query/acc.cgi?acc=GSE154884.

ETHICS STATEMENT

The studies involving human participants were reviewed and approved by The Ethics Committee of the Affiliated Hospital of Chongqing Medical University. The patients/participants provided their written informed consent to participate in this study. Written informed consent was obtained from the individual(s) for the publication of any potentially identifiable images or data included in this article.

AUTHOR CONTRIBUTIONS

Conception and design: ZQ. Acquisition of data: LW. Analysis and interpretation of data: LW. Writing, review, and/or revision of the manuscript: JL, JT, and LZ. Study supervision: BW and JL. All authors have read and approved the final manuscript.

REFERENCES

1. Berman BM, Langevin HM, Witt CM, Dubner R. Acupuncture for Chronic Low Back Pain. *New Engl J Med* (2010) 363(5):454–61. doi: 10.1056/NEJMct0806114
2. Diagnostic and Therapeutic Technology Assessment. Chemonucleolysis for Herniated Lumbar Disk. *JAMA* (1989) 262(7):953–6. doi: 10.1001/jama.262.7.953
3. Di Martino A, Merlini L, Faldini C. Autoimmunity in Intervertebral Disc Herniation: From Bench to Bedside. *Expert Opin Ther Targets* (2013) 17 (12):1461–70. doi: 10.1517/14728222.2013.834330
4. Sun Z, Liu B, Luo ZJ. The Immune Privilege of the Intervertebral Disc: Implications for Intervertebral Disc Degeneration Treatment. *Int J Med Sci* (2020) 17(5):685–92. doi: 10.7150/ijms.42238
5. Bridgen DT, Fearing BV, Jing L, Sanchez-Adams J, Cohan MC, Guilak F, et al. Regulation of Human Nucleus Pulposus Cells by Peptide-Coupled Substrates. *Acta Biomater* (2017) 55:100–8. doi: 10.1016/j.actbio.2017.04.019
6. Wang Y, Che M, Xin J, Zheng Z, Li J, Zhang S. The Role of IL-1β and TNF-α in Intervertebral Disc Degeneration. *Biomedicine Pharmacother = Biomedecine Pharmacotherapie* (2020) 131:110660. doi: 10.1016/j.biopha.2020.110660
7. Gorth DJ, Ottone OK, Shapiro IM, Risbud MV. Differential Effect of Long-Term Systemic Exposure of Tnfα on Health of the Annulus Fibrosus and Nucleus Pulposus of the Intervertebral Disc. *J Bone Mineral Res Off J Am Soc Bone Mineral Res* (2020) 35(4):725–37. doi: 10.1002/jbmr.3931
8. Silva AJ, Ferreira JR, Cunha C, Corte-Real JV, Bessa-Gonçalves M, Barbosa MA, et al. Macrophages Down-Regulate Gene Expression of Intervertebral Disc Degenerative Markers Under a Pro-inflammatory Microenvironment. *Front Immunol* (2019) 10:1508. doi: 10.3389/fimmu.2019.01508
9. Yu G, Wang LG, Han Y, He QY. clusterProfiler: An R Package for Comparing Biological Themes Among Gene Clusters. *Omics A J Integr Biol* (2012) 16 (5):284–7. doi: 10.1089/omi.2011.0118
10. Wang R, Ji X, Liu L, Chen H, Jia P, Bao L, et al. Changes of MRI in Inter-Spinal Distraction Fusion for Lumbar Degenerative Disease: A Retrospective Analysis Covering 3 Years. *J Clin Neurosci Off J Neurosurgical Soc Australasia* (2020) 81:455–61. doi: 10.1016/j.jocn.2020.10.011
11. Martinez Cantarin MP, Whitaker-Menezes D, Lin Z, Falkner B. Uremia Induces Adipose Tissue Inflammation and Muscle Mitochondrial Dysfunction. *Nephrol Dialysis Transplant Off Publ Eur Dialysis Transplant Assoc - Eur Renal Assoc* (2017) 32(6):943–51. doi: 10.1093/ndt/gfx050
12. Tong W, Lu Z, Qin L, Mauck RL, Smith HE, Smith LJ, et al. Cell Therapy for the Degenerating Intervertebral Disc. *Trans Res J Lab Clin Med* (2017) 181:49–58. doi: 10.1016/j.trsl.2016.11.008
13. Norbertczak HT, Ingham E, Fermor HL, Wilcox RK. Decellularized Intervertebral Discs: A Potential Replacement for Degenerate Human Discs. *Tissue Eng Part C Methods* (2020) 26(11):565–76. doi: 10.1089/ten.TEC.2020.0104
14. Nakazawa KR, Walter BA, Laudier DM, Krishnamoorthy D, Mosley GE, Spiller KL, et al. Accumulation and Localization of Macrophage Phenotypes With Human Intervertebral Disc Degeneration. *Spine J Off J North Am Spine Soc* (2018) 18(2):343–56. doi: 10.1016/j.spinee.2017.09.018
15. Risbud MV, Shapiro IM. Role of Cytokines in Intervertebral Disc Degeneration: Pain and Disc Content. *Nat Rev Rheumatol* (2014) 10(1):44–56. doi: 10.1038/nrrheum.2013.160
16. Proto JD, Doran AC, Gusarova G, Yurdagul AJr., Sozen E, Subramanian M, et al. Regulatory T Cells Promote Macrophage Efferocytosis During Inflammation Resolution. *Immunity* (2018) 49(4):666–77.e6. doi: 10.1016/j.immuni.2018.07.015
17. Luchting B, Rachinger-Adam B, Zeitler J, Egenberger L, Möhnle P, Kreth S, et al. Disrupted TH17/Treg Balance in Patients With Chronic Low Back Pain. *PloS One* (2014) 9(8):e104883. doi: 10.1371/journal.pone.0104883
18. Karagiannis TC, Maulik N. Factors Influencing Epigenetic Mechanisms and Related Diseases. *Antioxid Redox Signal* (2012) 17(2):192–4. doi: 10.1089/ars.2012.4562
19. Su Y, Gao L, Teng L, Wang Y, Cui J, Peng S, et al. Id1 Enhances Human Ovarian Cancer Endothelial Progenitor Cell Angiogenesis Via PI3K/Akt and NF-κb/MMP-2 Signaling Pathways. *J Trans Med* (2013) 11:132. doi: 10.1186/1479-5876-11-132
20. Edhayan G, Ohara RA, Stinson WA, Amin MA, Isozaki T, Ha CM, et al. Inflammatory Properties of Inhibitor of DNA Binding 1 Secreted by Synovial Fibroblasts in Rheumatoid Arthritis. *Arthritis Res Ther* (2016) 18:87. doi: 10.1186/s13075-016-0984-3
21. Je YJ, Choi DK, Sohn KC, Kim HR, Im M, Lee Y, et al. Inhibitory Role of Id1 on TGF-β-Induced Collagen Expression in Human Dermal Fibroblasts. *Biochem Biophys Res Commun* (2014) 444(1):81–5. doi: 10.1016/j.bbrc.2014.01.010
22. Fearnley GW, Young KA, Edgar JR, Antrobus R, Hay IM, Liang WC, et al. The Homophilic Receptor PTPRK Selectively Dephosphorylates Multiple JunctionalRegulators to Promote Cell-Cell Adhesion. *eLife* (2019) 8:1–41. doi: 10.7554/eLife.44597
23. Shen Z, Zhou R, Liu C, Wang Y, Zhan W, Shao Z, et al. MicroRNA-105 is Involved in TNF-α-Related Tumor Microenvironment Enhanced Colorectal Cancer Progression. *Cell Death Dis* (2017) 8(12):3213. doi: 10.1038/s41419-017-0048-x
24. Du L, Yang Q, Zhang J, Zhu M, Ma X, Zhang Y, et al. Engineering a Biomimetic Integrated Scaffold for Intervertebral Disc Replacement. *Materials*

Sci Eng C Materials Biol Appl (2019) 96:522–9. doi: 10.1016/j.msec.2018.11.087

25. Fernandes LM, Khan NM, Trochez CM, Duan M, Diaz-Hernandez ME, Presciutti SM, et al. Single-Cell RNA-seq Identifies Unique Transcriptional Landscapes of Human Nucleus Pulposus and Annulus Fibrosus Cells. *Sci Rep* (2020) 10(1):15263. doi: 10.1038/s41598-020-72261-7
26. Li XC, Tang Y, Wu JH, Yang PS, Wang DL, Ruan DK. Characteristics and Potentials of Stem Cells Derived From Human Degenerated Nucleus Pulposus: Potential for Regeneration of the Intervertebral Disc. *BMC Musculoskeletal Disord* (2017) 18(1):242. doi: 10.1186/s12891-017-1567-4

Conflict of Interest: The authors declare that the research was conducted in the absence of any commercial or financial relationships that could be construed as a potential conflict of interest.

frontiers in Immunology

ORIGINAL RESEARCH
published: 31 May 2021
doi: 10.3389/fimmu.2021.678873

FasL Is Required for Osseous Healing in Extraction Sockets in Mice

Karol Alí Apaza Alccayhuaman[1,2], *Patrick Heimel*[2,3,4], *Jung-Seok Lee*[1,5], *Stefan Tangl*[2,4], *Franz J. Strauss*[1,6,7], *Alexandra Stähli*[8], *Eva Matalová*[9] *and Reinhard Gruber*[1,4,8*]

[1] Department of Oral Biology, Medical University of Vienna, Vienna, Austria, [2] Karl Donath Laboratory for Hard Tissue and Biomaterial Research, School of Dentistry, Medical University of Vienna, Vienna, Austria, [3] Ludwig Boltzmann Institute for Experimental and Clinical Traumatology, Vienna, Austria, [4] Austrian Cluster for Tissue Regeneration, Medical University of Vienna, Vienna, Austria, [5] Department of Periodontology, Research Institute for Periodontal Regeneration, College of Dentistry, Yonsei University, Seoul, South Korea, [6] Clinic of Reconstructive Dentistry, University of Zurich, Zurich, Switzerland, [7] Department of Conservative Dentistry, School of Dentistry, University of Chile, Santiago, Chile, [8] Department of Periodontology, School of Dental Medicine, University of Bern, Bern, Switzerland, [9] Institute of Animal Physiology and Genetics, Czech Academy of Sciences, Brno, Czechia

Fas ligand (FasL) is a member of the tumor necrosis factor (TNF) superfamily involved in the activation of apoptosis. Assuming that apoptosis is initiated after tooth extraction it is reasonable to suggest that FasL may play a pivotal role in the healing of extraction sockets. Herein, we tested the hypothesis of whether the lack of FasL impairs the healing of extraction sockets. To this end, we extracted upper right incisors of FasL knockout (KO) mice and their wildtype (WT) littermates. After a healing period of two weeks, bone volume over total volume (BV/TV) *via* µCT and descriptive histological analyses were performed. µCT revealed that BV/TV in the coronal region of the socket amounted to 39.4% in WT and 21.8% in KO, with a significant difference between the groups (p=0.002). Likewise, in the middle region of the socket, BV/TV amounted to 50.3% in WT and 40.8% in KO (p<0.001). In the apical part, however, no difference was noticed. Consistently, WT mice displayed a significantly higher median trabecular thickness and a lower trabecular separation when compared to the KO group at the coronal and central region of the socket. There was the overall tendency that in both, female and male mice, FasL affects bone regeneration. Taken together, these findings suggest that FasL deficiency may reduce bone regeneration during the healing process of extraction sockets.

Keywords: dentistry, bone regenaration, tooth extraction, fasl, knockout (KO), µCT, histology

OPEN ACCESS

Edited by:
Pradyumna Kumar Mishra, ICMR-National Institute for Research in Environmental Health, India

Reviewed by:
Prasant Kumar Jena, Cedars Sinai Medical Center, United States
Mary A. Markiewicz, University of Kansas Medical Center, United States
Sriram Seshadri, Nirma University, India

***Correspondence:**
Reinhard Gruber
reinhard.gruber@meduniwien.ac.at

Specialty section:
This article was submitted to Inflammation, a section of the journal Frontiers in Immunology

Received: *10 March 2021*
Accepted: *10 May 2021*
Published: *31 May 2021*

Citation:
Apaza Alccayhuaman KA, Heimel P, Lee J-S, Tangl S, Strauss FJ, Stähli A, Matalová E and Gruber R (2021) FasL Is Required for Osseous Healing in Extraction Sockets in Mice. Front. Immunol. 12:678873. doi: 10.3389/fimmu.2021.678873

INTRODUCTION

FasL (CD178; CD95L; APO1L and TNF ligand superfamily member 6) belongs to the tumor necrosis factor (TNF) family and interacts with Fas (CD95; APO-1; TNFRSF6) receptor (1). The FasL/Fas pathway is the common initiator of an extrinsic apoptotic machinery engaged in the immune system (2–4) having the potential to affect the development of teeth (5) and bones (6–8). Fas and Fas ligand are present in the jaw bone and tooth germs of human fetuses (9). Moreover, mice homozygous for the FasL point mutation display an osteopetrotic phenotype in their long bones (10). These mice even showed an enhanced bone formation upon stimulation with demineralized bone and BMP-2 when compared to wildtype mice (11, 12). FasL when expressed

by osteoblast controls osteoclast apoptosis (13, 14), number and activity (15). Considering that bone regeneration involves the coordinated activity of osteoclasts and particularly of osteoblasts, there is reason to suggest that FasL is required for the healing of tooth extraction sockets.

Healing of extraction sockets has become an important issue in dentistry particularly due to the increasing demand of dental implants as a therapy to replace missing teeth (16). The alveolar bone usually undergoes atrophy upon the tooth extraction (17–19), and various treatment regimens were developed and introduced for extraction socket grafting. However, histologic bone quality differs with varying degrees of new bone formation (20). Therefore, there has been a great interest to understand bone regeneration and the healing process of extraction sockets. Bone regeneration is a sequential process of events that partially recapitulates bone development involving cell apoptosis and the coordinated action of osteoblast and osteoclasts (21–23). Accumulating evidence suggests that the FasL/Fas system is involved in bone regeneration. For example, mice lacking Fas show delayed cartilage resorption and less bone in the fracture calluses (24). With respect to wound healing, the lack of FasL/Fas signaling impairs apoptosis in granulation tissue and mononuclear cells (25, 26). Thus, it seems conceivable that FasL is involved in the healing of extraction sockets.

The aim of the present study was, therefore, to examine whether or not the lack of FasL impairs the healing of extraction sockets. To test this assumption, we took advantage of the established FasL knockout mice along with a recent established tooth extraction model in mice (27). Based on a segmentation of the alveolar socket, it is possible to measure new bone formation, that in combination with histology of undecalcified thin ground sections, provides insights into the overall healing situation of the extraction socket. Based on this approach, we identified FasL as a molecular target involved in the bone regeneration and healing process of extraction sockets in rodents.

MATERIAL AND METHODS

Study Design

The Medical University of Vienna ethical review board for animal research approved the study protocol (GZ BMWFW-66.009/0359-V/3b/2018). The study was performed at the Department of Biomedical Research of the Medical University of Vienna in accordance with the NC3Rs ARRIVE guidelines. Mice homozygous for the Fas*lgld* mutation (B6Smn.C3-Faslgld/J) were purchased from The Jackson Laboratory (Bar Harbor, ME) and housed in the Medical University of Vienna, Institute of Biomedical Research under specific-pathogen-free (SPF) conditions. FasL knockout mice and littermate controls (8-12 weeks, around 22 g) underwent tooth extraction of the upper right incisor. The animals were maintained according to the animal welfare guidelines with free access to water and a standard diet (28).

Tooth Extraction Model

The tooth extraction model was performed as recently described (27). In brief, all animals received ketamine 100 mg/kg (AniMedica, Senden, Erlangen, Germany) and xylazine hydrochloride 5mg/kg (Bayer Austria, Vienna, Austria) by intramuscular injection. Then, the head of the mouse was stabilized by holding the contralateral tooth with a tweezer. Next, with the aid of a stereomicroscope (Leica M651, Leica Microsystems, Wetzlar, Germany) under 16X magnification, the upper right incisor was luxated using disposable needles (HSW FINE-JECT®, Tuttlingen, Germany) of different diameters (0.4 mm, 0.6 mm and 0.8 mm) as periotomes. After a proper luxation, the tooth was carefully extracted to avoid any root fracture using an Adson tweezer (Aesculap, Tuttlingen, Germany) and checked for integrity. For pain relief, buprenorphine 0.06 mg/kg s.c. (Temgesic®, Reckitt and Colman Pharm., Hull, UK) and piritramide in drinking water ad lib was administered. The first 72 hours after surgery soft diet was provided. Mice were euthanized on day fourteen by cervical dislocation and each alveolar socket was subjected to micro computed tomographic (μCT) and histological analysis.

MicroCT Analysis

After euthanasia, the heads were fixed in phosphate-buffered formalin (Roti-Histofix 4%, Carl Roth, Karlsruhe, Germany). MicroCT scans were made using a Scanco μCT 50 (Scanco Medical AG, Bruttisellen, Switzerland) at 90 kV/200 μA with an isotropic resolution of 10 μm and an integration time of 500 ms. Using Amira 6.1.1 (Thermo Fisher Scientific, Waltham, USA), The image stacks were imported into Fiji for the posterior analysis (29, 30). The region of interest (ROI) was drawn using the polygon and freehand selection tools and saved using the ROI manager. To have a standardized position of the ROIs from all samples, four anatomical landmarks were set up, thereby dividing the alveolar socket in three regions (coronal, middle and apical) from the rearmost point to the most frontal point (**Figure 1A**). The percentage of Bone volume per Tissue volume (BV/TV), Trabecular thickness (Tb.Th) and Trabecular separation (Tb.Sp) were measured in the ROI with a threshold of 254 mgHA/cm^3.

Histological Analysis

Ten samples were dehydrated with ascending alcohol grades and embedded in light-curing resin (Technovit 7200 VLC + BPO; Kulzer & Co., Wehrheim, Germany). Blocks were further processed using Exakt cutting and grinding equipment (Exakt Apparatebau, Norderstedt, Germany). Thin-ground sections from all samples were prepared (31), in a plane parallel to the sagittal suture and through the middle of the alveolar socket and stained with Levai–Laczko dye (**Figure 1B**). The slices of around 100 μm were scanned using an Olympus BX61VS digital virtual microscopy system (DotSlide 2.4, Olympus, Tokyo, Japan) with a 20x objective resulting in a resolution of 0.32 μm per pixel and then evaluated.

Statistical Analysis

Statistical analysis was based on the data obtained from the microCT analysis. Median values and confidence intervals (CI) of the primary endpoint, bone volume (BV/TV) and secondary endpoints (Tb.Th and Tb.Sp) in the alveolar socket, between the two groups were compared with Mann-Whitney U test. Further analyses were performed comparing the mice gender and

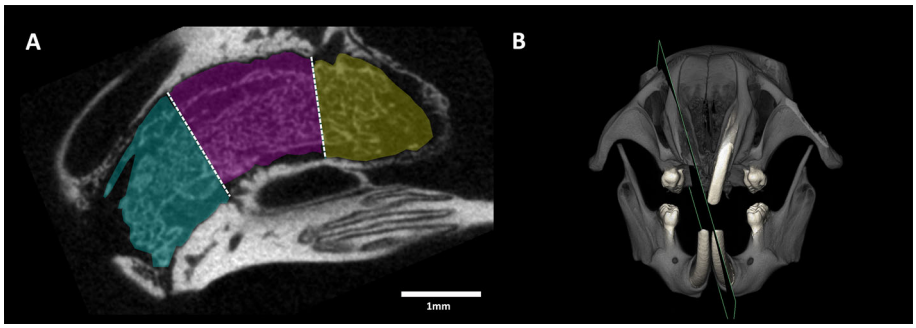

FIGURE 1 | Region of interests (ROI) of the extraction socket for the μCT analysis. **(A)** The ROIs for the microCT analysis comprised the coronal (cyan), middle (purple) and apical (yellow) region through the entire volume of the tooth extraction site. **(B)** The plane oriented along the central alveolar socket was the reference for preparing the histological ground sections.

intragroup between WT and FasL KO using the Mann-Whitney U test. All the analyses were performed using Prism v7 (GraphPad Software, La Jollia, CA). Significance was set at $p<0.05$.

RESULTS

Micro CT Analysis of Bone Volume Per Tissue Volume (BV/TV)

For the analysis a total of ten WT and ten FasL KO mice were used comprising five males and females in each group (**Figure 2**). Statistical analysis revealed that the median BV/TV in the coronal region of the socket was significantly higher ($p=0.002$) in the WT than in the KO group, with 39.4% (22.1 min; 52.3 max) *versus* 21.8% (2.0 min; 41.0 max), respectively (**Figures 2A–C**). Likewise, in the middle region of the socket, the BV/TV in the WT was significantly higher ($p<0.001$) than in the KO group, with 50.3% (39.57 min; 66.31 max) and 40.8% (30.20 min; 46.81 max), respectively (**Figure 2D**). The median changes of BV/TV in the apical part of the socket failed to reach the level of significance ($p=0.796$; **Figure 2E**). Further analysis was performed comparing female and male mice. In the coronal and center region, the WT female ($p=0.016$; $p=0.008$) and WT male mice ($p=0.032$; $p=0.056$) displayed higher bone formation compared to the respective FasL KO mice. Intragroup comparisons revealed in the middle region a remarkable difference ($p=0.008$) between the male and female WT mice (**Figure 2D**), while in the other groups there were no gender differences. These findings suggest that FasL is involved in the formation of new bone volume in the extraction socket of female and male mice.

Micro CT Analysis of Trabecular Thickness (TbTh) and Trabecular Separation (TbSp)

In support of the bone volume fraction, the median trabecular thickness (TbTh) in the coronal region of the socket was significantly ($p=0.002$) higher in WT than in KO, with 0.04 mm (0.02 min; 0.06 max) *versus* 0.02 mm (0.002 min; 0.04 max), respectively (**Figure 3A**). This significant difference ($p<0.001$) was also observed in the middle part of the socket, with 0.05 mm (0.04 min; 0.07 max) in WT and 0.04 mm (0.03 min; 0.04 max) in KO, respectively (**Figure 3B**) but not in the apical part of the socket (**Figure 3C**). Consistently, coronal trabecular separation (TbSp) was significant higher ($p=0.003$) in WT than in KO mice, with 0.09 mm (0.06 min; 0.14 max) and 0.17 mm (0.07 min; 0.23 max), respectively (**Figure 3A**). Similarly, this difference was also significant ($p=0.004$) in the middle part, 0.07 mm (0.04 min; 0.13 max) *versus* 0.09 mm (0.06 min; 0.15 max), respectively (**Figure 3B**). In the apical part, nonetheless, there were no significant differences (**Figure 3C**). Considering mouse gender, there was the overall tendency that female and male mice, were similarly affected by the lack of FasL in the coronal and middle part of the extraction sockets (**Figures 3A, B**). Intragroup comparisons revealed that WT and KO female mice when compared to their male littermates, have a denser trabecular network reaching the level of significance in the middle region (**Figure 3B**). Taken together, these observations indicate that FasL is partially required for the proper formation of trabecular structures in both genders.

Histological Analyses

Newly generated woven bone was observed in the WT and FasL KO mice (**Figure 4**). This woven bone formed a trabecular network with random orientation surrounded either by thin layers of parallel fibered bone or thin layers of unmineralized matrix osteoid. Newly formed bone was located next to the coronally bone walls and in the middle, filling almost completely the alveolar defect, while the FasL KO mice exhibited a trabecular bone enclosing bigger spaces formed between. We also observed signs of growing teeth denoted by the formation of new dentine and enamel in both, the FasL KO and WT mice (**Figure 5**). These structures, nevertheless, were excluded from the μCT analysis by segmentation.

DISCUSSION

The present pre-clinical study revealed that the lack of FasL attenuates the healing process of extraction socket in female and male mice. This research was inspired by the fact that FasL is a

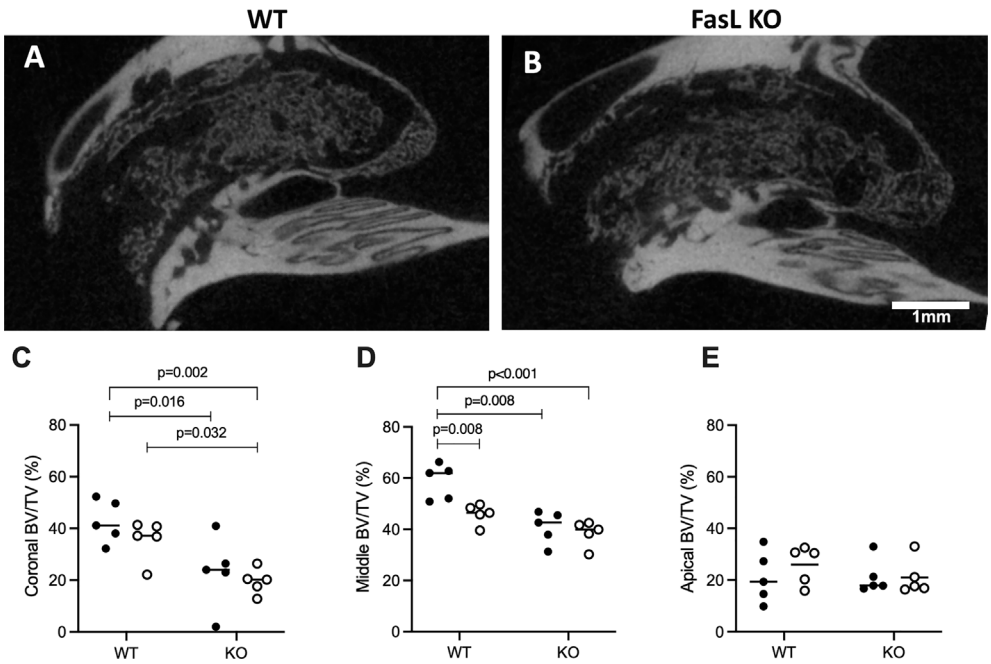

FIGURE 2 | Lack of FasL attenuates regeneration of the extraction socket. Sagittal view of the alveolar socket depicts the WT **(A)** and FasL KO mice **(B)**. Quantitative analysis of the bone volume per tissue volume (BV/TV) displayed higher amounts of new bone volume in the WT mice in the coronal **(C)** and middle part **(D)** of the extraction socket compared to FasL KO mice. The apical region revealed no significant differences in BV/TV between WT and FasL KO mice **(E)**. Statistical analysis was based on Mann-Whitney U test, P values are given where there was significant differences. The bars show the median and female (black dots) and male mice (white dots) are distributed in the dot plots for the WT and KO group.

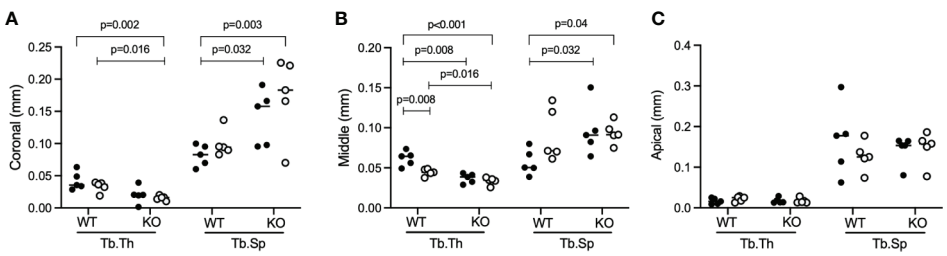

FIGURE 3 | Trabecular thickness (TbTh) and trabecular separation (TbSp) in the extraction sockets. FasL KO mice shows lower Tb.Th and higher Tb.Sp compared to WT mice in the coronal **(A)** and middle part **(B)** while no differences were observed in the apical part **(C)**. Statistical analysis was based on Mann-Whitney U test, P values are given where was found significant differences. The bars show the median with female (black dots) and male mice (white dots) are distributed in the dot plots.

central regulator of apoptosis (2–4) having a major impact on bone cells life cycle thereby affecting osteoblasts and osteoclasts during bone remodeling. FasL is a key target for estrogen to control osteoblast-mediated osteoclast apoptosis (13–15). FasL was reported to delay cartilage resorption and bone formation in the fracture calluses (24) and wound healing. Moreover, FasL/Fas signaling controls apoptosis in granulation tissue and mononuclear cells (25, 26). To the best of the authors knowledge, the impact of FasL on bone regeneration, and in particular the intramembranous ossification upon tooth extraction inside the remaining alveolus, had not been investigated. Assuming that dying cells upon tooth extraction are presumably responsible for triggering the signals for repair and regeneration, we raised the hypothesis that the lack of FasL impairs the overall capacity of bone regeneration. Hereby we report that female and male mice deficient in FasL, show less bone formation in extraction sockets as compared to WT mice. This finding supports the notion that FasL is required for the bone healing process of extraction sockets.

If we compare the present findings to those of others, our data are in line with the critical involvement of FasL in bone formation. For example, embryonic and early 6-week postnatal FasL knockout mice showed less mandibular and alveolar bone compared to WT littermates (32, 33). Consistently, in 22-week old mice, whole genome FasL KO mice have less trabecular and

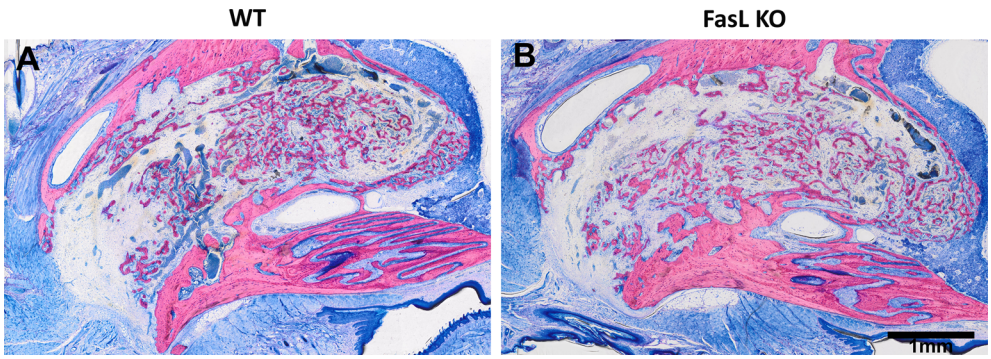

FIGURE 4 | The features of the newly formed bone were similar for the WT **(A)** and the FasL KO mice **(B)**. Overview photomicrographs (2x) depicting the woven network.

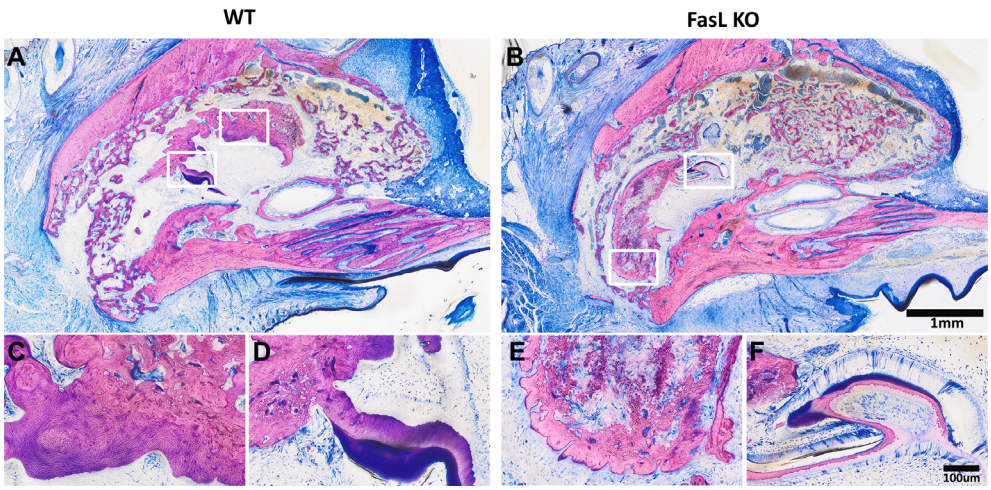

FIGURE 5 | The WT **(A)** and The FasL KO **(B)** mice revealed a structure like a growing tooth located at different areas of the alveolar socket in the overview image (2x). A higher magnification (20x) evidenced the "osteodentin mass" with dentin tubules **(C, E)** and enamel structure **(D, F)**.

cortical bone in the axial and appendicular skeleton compared to their WT littermates (34). Even osteoblast progenitor/osteoblast-specific FasL-deficient mice showed markedly reduced bone density and structural parameters in the femurs (15). Our findings that FasL knockout mice showed less bone formation in the alveolar socket upon tooth extraction compared to the WT littermates are consistent with the relevance of FasL in bone formation. Furthermore, these findings are largely in agreement with the observation that already after two weeks healing, the extraction socket of incisors is almost completely filled with an immature woven bone-like tissue (27, 35).

The present study has a number of limitations. In the knockout mice, FasL is missing in all cells, meaning that we cannot draw conclusions whether or not the observed effects are caused by osteoblast or osteoclasts. It is plausible that the lack of FasL affects angiogenesis, implying that the impaired bone regeneration observed in the KO mice, is rather a consequence of a reduced supply of osteogenic progenitor cells (36). Future studies should therefore take advantage of conditional knockout models where FasL is deleted in specific cells types, for example with osteoblast progenitor/osteoblast-specific FasL-deficient mice (15). Thus, the origin of FasL capable of driving the FasL-dependent apoptosis- or other apoptosis-independent responses during bone regeneration remains to be elucidated. Another study limitation was that we could not avoid sites with new tooth formation. The present findings might also serve for researchers asking if overexpression of FasL can support bone regeneration, for example by implementing the respective agonists (37) or using a transgenic FasL mouse model (38). It would also be interesting to know why female compared to male WT mice, show more a pronounced healing of extraction sockets. This was unexpected since male muscle-derived stem cells regenerated more bone than female cells in a calvaria defect (39). Nevertheless, the estrogen receptor beta is required for proper healing in female mice that

however, does not rule out that it is also required in male mice (40). Moreover, ovariectomy impairs bone formation in drill-hole defects, but this setting does not allow a gender comparison (41). Hence, future research could focus more on the impact of gender on the healing of extraction sockets.

Future research should further use the FasL model to investigate fracture healing, as the impact of FasL on endochondral bone formation is not necessarily reflected by the tooth extraction model of intramembranous ossification that was used (21, 23). In fact, it is unclear whether a tooth extraction model represents intramembranous ossification in other anatomical regions that are perhaps more representative for the appendicular skeleton, beyond the field of dentistry. Our model, however, seems to be suitable to better understand the biology of the healing of extraction sockets and presumably also the osseointegration of dental implants that follow the same conserved sequence of events (42). It can be speculated that targeting the FasL system could be a therapeutic option to boost osseointegration, nevertheless, this would require data showing that pushing physiological FasL signaling enhances the bone regeneration (37). Certainly, the present research is a further step towards FasL-signaling in bone regeneration.

In conclusion, these data suggest that FasL is required for bone regeneration during the healing process of tooth extraction sockets.

DATA AVAILABILITY STATEMENT

The original contributions presented in the study are included in the article/supplementary material. Further inquiries can be directed to the corresponding author.

ETHICS STATEMENT

The animal study was reviewed and approved by Austrian Federal Ministry of Education, Science and Research.

AUTHOR CONTRIBUTIONS

RG and EM contributed to the conception and design of the study. KAAA and PH work on the measurements of the data and organized the database. RG and KAAA wrote the first draft of the manuscript. FS, ST, and JL wrote sections of the manuscript. All authors contributed to the article and approved the submitted version.

FUNDING

This research project is funded by a grant from the Austrian Science Fund (FWF) (4072-B28) joint with the Czech Science Foundation (GACR) (19-29667L). KAAA is supported by an Osteology Research Scholarship.

ACKNOWLEDGMENTS

Authors thank Prof. Ulrike Kuchler for taking responsibility for the animal experiment.

REFERENCES

1. Suda T, Takahashi T, Golstein P, Nagata S. Molecular Cloning and Expression of the Fas Ligand, A Novel Member of the Tumor Necrosis Factor Family. *Cell* (1993) 75:1169–78. doi: 10.1016/0092-8674(93)90326-L
2. Tsutsui H, Nakanishi K, Matsui K, Higashino K, Okamura H, Miyazawa Y, et al. IFN-Gamma-Inducing Factor Up-Regulates Fas Ligand-Mediated Cytotoxic Activity of Murine Natural Killer Cell Clones. *J Immunol* (1996) 157:3967–73.
3. Griffith TS, Brunner T, Fletcher SM, Green DR, Ferguson TA. Fas Ligand-Induced Apoptosis as a Mechanism of Immune Privilege. *Science* (1995) 270:1189–92. doi: 10.1126/science.270.5239.1189
4. Nagata S. Apoptosis by Death Factor. *Cell* (1997) 88:355–65. doi: 10.1016/S0092-8674(00)81874-7
5. Matalova E, Svandova E, Tucker AS. Apoptotic Signaling in Mouse Odontogenesis. *OMICS* (2012) 16:60–70. doi: 10.1089/omi.2011.0039
6. Kovacic N, Lukic IK, Grcevic D, Katavic V, Croucher P, Marusic A. The Fas/Fas Ligand System Inhibits Differentiation of Murine Osteoblasts But has a Limited Role in Osteoblast and Osteoclast Apoptosis. *J Immunol* (2007) 178:3379–89. doi: 10.4049/jimmunol.178.6.3379
7. Josefsen D, Myklebust JH, Lynch DH, Stokke T, Blomhoff HK, Smeland EB. Fas Ligand Promotes Cell Survival of Immature Human Bone Marrow CD34+ CD38- Hematopoietic Progenitor Cells by Suppressing Apoptosis. *Exp Hematol* (1999) 27:1451–9. doi: 10.1016/S0301-472X(99)00073-9
8. Rippo MR, Babini L, Prattichizzo F, Graciotti L, Fulgenzi G, Tomassoni Ardori F, et al. Low FasL Levels Promote Proliferation of Human Bone Marrow-Derived Mesenchymal Stem Cells, Higher Levels Inhibit Their Differentiation Into Adipocytes. *Cell Death Dis* (2013) 4:e594. doi: 10.1038/cddis.2013.115
9. Hatakeyama S, Tomichi N, Ohara-Nemoto Y, Satoh M. The Immunohistochemical Localization of Fas and Fas Ligand in Jaw Bone and Tooth Germ of Human Fetuses. *Calcif Tissue Int* (2000) 66:330–7. doi: 10.1007/s002230010069
10. Katavic V, Lukic IK, Kovacic N, Grcevic D, Lorenzo JA, Marusic A. Increased Bone Mass Is a Part of the Generalized Lymphoproliferative Disorder Phenotype in the Mouse. *J Immunol* (2003) 170:1540–7. doi: 10.4049/jimmunol.170.3.1540
11. Katavic V, Grcevic D, Lukic IK, Vucenik V, Kovacic N, Kalajzic I, et al. Non-Functional Fas Ligand Increases the Formation of Cartilage Early in the Endochondral Bone Induction by rhBMP-2. *Life Sci* (2003) 74:13–28. doi: 10.1016/j.lfs.2003.06.031
12. Mori S, Nose M, Chiba M, Narita K, Kumagai M, Kosaka H, et al. Enhancement of Ectopic Bone Formation in Mice With a Deficit in Fas-Mediated Apoptosis. *Pathol Int* (1997) 47:112–6. doi: 10.1111/j.1440-1827.1997.tb03729.x
13. Krum SA, Miranda-Carboni GA, Hauschka PV, Carroll JS, Lane TF, Freedman LP, et al. Estrogen Protects Bone by Inducing Fas Ligand in Osteoblasts to Regulate Osteoclast Survival. *EMBO J* (2008) 27:535–45. doi: 10.1038/sj.emboj.7601984
14. Nakamura T, Imai Y, Matsumoto T, Sato S, Takeuchi K, Igarashi K, et al. Estrogen Prevents Bone Loss Via Estrogen Receptor Alpha and Induction of Fas Ligand in Osteoclasts. *Cell* (2007) 130:811–23. doi: 10.1016/j.cell.2007.07.025
15. Wang L, Liu S, Zhao Y, Liu D, Liu Y, Chen C, et al. Osteoblast-Induced Osteoclast Apoptosis by Fas Ligand/FAS Pathway Is Required for Maintenance of Bone Mass. *Cell Death Differ* (2015) 22:1654–64. doi: 10.1038/cdd.2015.14
16. Jung RE, Zembic A, Pjetursson BE, Zwahlen M, Thoma DS. Systematic Review of the Survival Rate and the Incidence of Biological, Technical, and Aesthetic Complications of Single Crowns on Implants Reported in Longitudinal Studies With a Mean Follow-Up of 5 Years. *Clin Oral Implants Res* (2012) 23(Suppl 6):2–21. doi: 10.1111/j.1600-0501.2012.02547.x
17. Couso-Queiruga E, Stuhr S, Tattan M, Chambrone L, Avila-Ortiz G. Post-Extraction Dimensional Changes: A Systematic Review and Meta-Analysis. *J Clin Periodontol* (2021) 48:126–44. doi: 10.1111/jcpe.13390

18. Tan WL, Wong TL, Wong MC, Lang NP. A Systematic Review of Post-Extractional Alveolar Hard and Soft Tissue Dimensional Changes in Humans. *Clin Oral Implants Res* (2012) 23(Suppl 5):1–21. doi: 10.1111/j.1600-0501.2011.02375.x
19. Schropp L, Wenzel A, Kostopoulos L, Karring T. Bone Healing and Soft Tissue Contour Changes Following Single-Tooth Extraction: A Clinical and Radiographic 12-Month Prospective Study. *Int J Periodontics Restorative Dent* (2003) 23:313–23. doi: 10.1016/j.prosdent.2003.10.022
20. Koo TH, Song YW, Cha JK, Jung UW, Kim CS, Lee JS. Histologic Analysis Following Grafting of Damaged Extraction Sockets Using Deproteinized Bovine or Porcine Bone Mineral: A Randomized Clinical Trial. *Clin Oral Implants Res* (2020) 31:93–102. doi: 10.1111/clr.13557
21. Einhorn TA, Gerstenfeld LC. Fracture Healing: Mechanisms and Interventions. *Nat Rev Rheumatol* (2015) 11:45–54. doi: 10.1038/nrrheum.2014.164
22. Gruber R, Koch H, Doll BA, Tegtmeier F, Einhorn TA, Hollinger JO. Fracture Healing in the Elderly Patient. *Exp Gerontol* (2006) 41:1080–93. doi: 10.1016/j.exger.2006.09.008
23. Claes L, Recknagel S, Ignatius A. Fracture Healing Under Healthy and Inflammatory Conditions. *Nat Rev Rheumatol* (2012) 8:133–43. doi: 10.1038/nrrheum.2012.1
24. Al-Sebaei MO, Daukss DM, Belkina AC, Kakar S, Wigner NA, Cusher D, et al. Role of Fas and Treg Cells in Fracture Healing as Characterized in the Fas-Deficient (Lpr) Mouse Model of Lupus. *J Bone Miner Res* (2014) 29:1478–91. doi: 10.1002/jbmr.2169
25. Li Y, Takemura G, Kosai K, Takahashi T, Okada H, Miyata S, et al. Critical Roles for the Fas/Fas Ligand System in Postinfarction Ventricular Remodeling and Heart Failure. *Circ Res* (2004) 95:627–36. doi: 10.1161/01.RES.0000141528.54850.bd
26. Guan DW, Ohshima T, Kondo T. Immunohistochemical Study on Fas and Fas Ligand in Skin Wound Healing. *Histochem J* (2000) 32:85–91. doi: 10.1023/A:1004058010500
27. Strauss FJ, Stähli A, Kobatake R, Tangl S, Heimel P, Apaza Alccayhuaman KA, et al. miRNA-21 Deficiency Impairs Alveolar Socket Healing in Mice. *J Periodontol* (2020) 91(12):1664–72. doi: 10.1002/JPER.19-0567
28. Kilkenny C, Browne WJ, Cuthill IC, Emerson M, Altman DG. Improving Bioscience Research Reporting: The ARRIVE Guidelines for Reporting Animal Research. *PloS Biol* (2010) 8:e1000412. doi: 10.1371/journal.pbio.1000412
29. Schindelin J, Arganda-Carreras I, Frise E, Kaynig V, Longair M, Pietzsch T, et al. Fiji: An Open-Source Platform for Biological-Image Analysis. *Nat Methods* (2012) 9:676–82. doi: 10.1038/nmeth.2019
30. Schindelin J, Rueden CT, Hiner MC, Eliceiri KW. The ImageJ Ecosystem: An Open Platform for Biomedical Image Analysis. *Mol Reprod Dev* (2015) 82:518–29. doi: 10.1002/mrd.22489
31. Donath K, Breuner G. A Method for the Study of Undecalcified Bones and Teeth With Attached Soft Tissues. The Sage-Schliff (Sawing and Grinding) Technique. *J Oral Pathol* (1982) 11:318–26. doi: 10.1111/j.1600-0714.1982.tb00172.x
32. Svandova E, Sadoine J, Vesela B, Djoudi A, Lesot H, Poliard A, et al. Growth-Dependent Phenotype in FasL-Deficient Mandibular/Alveolar Bone. *J Anat* (2019) 235:256–61. doi: 10.1111/joa.13015
33. Svandova E, Vesela B, Lesot H, Sadoine J, Poliard A, Matalova E. Fasl Modulates Expression of Mmp2 in Osteoblasts. *Front Physiol* (2018) 9:1314. doi: 10.3389/fphys.2018.01314
34. Kim HN, Ponte F, Nookaew I, Ucer Ozgurel S, Marques-Carvalho A, Iyer S, et al. Estrogens Decrease Osteoclast Number by Attenuating Mitochondria Oxidative Phosphorylation and ATP Production in Early Osteoclast Precursors. *Sci Rep* (2020) 10:11933. doi: 10.1038/s41598-020-68890-7
35. Vieira AE, Repeke CE, Ferreira Junior Sde B, Colavite PM, Biguetti CC, Oliveira RC, et al. Intramembranous Bone Healing Process Subsequent to Tooth Extraction in Mice: Micro-Computed Tomography, Histomorphometric and Molecular Characterization. *PloS One* (2015) 10:e0128021. doi: 10.1371/journal.pone.0128021
36. Sivaraj KK, Adams RH. Blood Vessel Formation and Function in Bone. *Development* (2016) 143:2706–15. doi: 10.1242/dev.136861
37. Chodorge M, Zuger S, Stirnimann C, Briand C, Jermutus L, Grutter MG, et al. A Series of Fas Receptor Agonist Antibodies That Demonstrate an Inverse Correlation Between Affinity and Potency. *Cell Death Differ* (2012) 19:1187–95. doi: 10.1038/cdd.2011.208
38. Yang J, Jones SP, Suhara T, Greer JJ, Ware PD, Nguyen NP, et al. Endothelial Cell Overexpression of Fas Ligand Attenuates Ischemia-Reperfusion Injury in the Heart. *J Biol Chem* (2003) 278:15185–91. doi: 10.1074/jbc.M211707200
39. Scibetta AC, Morris ER, Liebowitz AB, Gao X, Lu A, Philippon MJ, et al. Characterization of the Chondrogenic and Osteogenic Potential of Male and Female Human Muscle-Derived Stem Cells: Implication for Stem Cell Therapy. *J Orthop Res* (2019) 37:1339–49. doi: 10.1002/jor.24231
40. He YX, Liu Z, Pan XH, Tang T, Guo BS, Zheng LZ, et al. Deletion of Estrogen Receptor Beta Accelerates Early Stage of Bone Healing in a Mouse Osteotomy Model. *Osteoporos Int* (2012) 23:377–89. doi: 10.1007/s00198-011-1812-x
41. He YX, Zhang G, Pan XH, Liu Z, Zheng LZ, Chan CW, et al. Impaired Bone Healing Pattern in Mice With Ovariectomy-Induced Osteoporosis: A Drill-Hole Defect Model. *Bone* (2011) 48:1388–400. doi: 10.1016/j.bone.2011.03.720
42. Vasak C, Busenlechner D, Schwarze UY, Leitner HF, Munoz Guzon F, Hefti T, et al. Early Bone Apposition to Hydrophilic and Hydrophobic Titanium Implant Surfaces: A Histologic and Histomorphometric Study in Minipigs. *Clin Oral Implants Res* (2014) 25:1378–85. doi: 10.1111/clr.12277

Conflict of Interest: The authors declare that the research was conducted in the absence of any commercial or financial relationships that could be construed as a potential conflict of interest.

frontiers in Immunology

ORIGINAL RESEARCH
published: 02 June 2021
doi: 10.3389/fimmu.2021.665208

Rodent Models of Spondyloarthritis Have Decreased White and Bone Marrow Adipose Tissue Depots

*Giulia Furesi[1], Ingrid Fert[2,3,4], Marie Beaufrère[2,3,4], Luiza M. Araujo[2,3,4], Simon Glatigny[2,3,4], Ulrike Baschant[1], Malte von Bonin[5], Lorenz C. Hofbauer[1], Nicole J. Horwood[6], Maxime Breban[2,3,4] and Martina Rauner[1]**

[1] Department of Medicine III & Center for Healthy Aging, Technische Universität Dresden, Dresden, Germany, [2] Laboratoire Infection et inflammation, UMR U1173 INSERM/Université de Versailles-Saint-Quentin-Paris-Saclay, Montigny-le-Bretonneux, France, [3] Laboratoire d'Excellence Inflamex, Université Paris Descartes, Paris, France, [4] Service de Rhumatologie, Hôpital Ambroise Parè, AP-HP, Boulogne, France, [5] Department of Medicine I, Technische Universität Dresden, Dresden, Germany, [6] Norwich Medical School, University of East Anglia, Norwich, United Kingdom

OPEN ACCESS

Edited by:
Katharina Schmidt-Bleek, Charité – Universitätsmedizin Berlin, Germany

Reviewed by:
Erica L. Scheller, Washington University in St. Louis, United States
Tim Schulz, German Institute of Human Nutrition Potsdam-Rehbruecke (DIfE), Germany

***Correspondence:**
Martina Rauner
martina.rauner@ukdd.de

Specialty section:
This article was submitted to Inflammation, a section of the journal Frontiers in Immunology

Received: 07 February 2021
Accepted: 11 May 2021
Published: 02 June 2021

Citation:
Furesi G, Fert I, Beaufrère M, Araujo LM, Glatigny S, Baschant U, von Bonin M, Hofbauer LC, Horwood NJ, Breban M and Rauner M (2021) Rodent Models of Spondyloarthritis Have Decreased White and Bone Marrow Adipose Tissue Depots. Front. Immunol. 12:665208. doi: 10.3389/fimmu.2021.665208

Bone marrow adipose tissue (BMAT) has recently been recognized as a distinct fat depot with endocrine functions. However, if and how it is regulated by chronic inflammation remains unknown. Here, we investigate the amount of white fat and BMAT in HLA-B27 transgenic rats and curdlan-challenged SKG mice, two well-established models of chronic inflammatory spondyloarthritis (SpA). Subcutaneous and gonadal white adipose tissue and BMAT was reduced by 65-70% and by up to 90% in both experimental models. Consistently, B27 rats had a 2-3-fold decrease in the serum concentrations of the adipocyte-derived cytokines adiponectin and leptin as well as a 2-fold lower concentration of triglycerides. The bone marrow of B27 rats was further characterized by higher numbers of neutrophils, lower numbers of erythroblast precursors, and higher numbers of IL-17 producing $CD4^+$ T cells. IL-17 concentration was also increased in the serum of B27 rats. Using a cell culture model, we show that high levels of IL-17 in the serum of B27 rats negatively impacted adipogenesis (-76%), an effect that was reversed in the presence of neutralizing anti-IL-17 antibody. In summary, these findings show BMAT is severely reduced in two experimental models of chronic inflammatory SpA and suggest that IL-17 is involved in this process.

Keywords: spondyloarthritis, HLA-B27 transgenic rat, SKG mouse, bone marrow fat, IL-17

INTRODUCTION

Bone marrow adipose tissue (BMAT) has been recently recognized as a unique fat depot (1, 2). While white adipose tissue is crucial for systemic metabolic homeostasis and brown adipose tissue controls adaptive thermogenesis, the role of BMAT remains incompletely understood. Previous studies have shown that bone marrow adipocytes (BMAds) are morphologically similar to white adipocytes with large unilocular lipid droplets, albeit transcriptional analysis revealed a detectable expression of brown adipocyte markers as well (3, 4). Also, BMAds have been recognized as metabolically active cells that secrete adipokines, growth factors, and proinflammatory cytokines

(5, 6). As such, BMAds may participate in the immune response and tissue remodeling. In fact, BMAds have been recently shown to control bone remodeling and bone mass maintenance (7, 8). In adulthood, BMAT can account for up to 70% of the bone marrow cavity, and it is further increased in diverse clinical conditions, including obesity, type 2 diabetes, anorexia, and osteoporosis (9, 10).

Although dysregulation of white adipose tissue is a common feature of chronic inflammatory disorders, the impact of long-term inflammation on BMAT remains elusive. In this study, we used spondyloarthritis (SpA) as prototypical chronic inflammatory disorders to investigate how BMAds are affected by chronic inflammation. SpA is a group of chronic inflammatory rheumatic diseases that affect the axial skeleton, peripheral joints, and entheses, leading to bone erosions followed by bony ankylosis (10). In addition, the spectrum of SpA comprises frequent extra-articular features, including anterior uveitis, psoriasis, and inflammatory bowel disease (IBD) (11). The exact etiology and pathogenesis of SpA are still under investigation. Among various genetic (e.g. HLA-B27 association) and immunological factors that trigger the disease, adaptive immune cells such as $CD4^+$ T cells have been recognized as key drivers of chronicity in SpA (12). Of note, numerous studies confirmed the critical role of interleukin-17 (IL-17) and T helper (Th) 17 cell subset in joint inflammation and disruption of bone remodeling in arthritis *via* the modulation of matrix metalloproteinases and stimulation of RANKL (13–15). In particular by attracting neutrophils and macrophages to the site of inflammation and enhancing the production of pro-inflammatory cytokines, IL-17 plays a significant role in the pathogenesis of SpA (13, 16). Recently, antibodies neutralizing IL-17, such as secukinumab and ixekizumab, became clinically available to treat SpA, thereby providing new efficacious therapeutic regimens for these disorders (17).

To assess how chronic inflammation may affect BMAT, we utilized HLA-B27 transgenic rats (B27) and curdlan-challenged SKG mice, two well-established models of SpA (18). Both models recapitulate typical features of human SpA, including chronic systemic inflammation and accelerated bone loss and reduced bone strength due to stimulation of osteoclastogenesis and suppression of bone formation (19–21). Our results show that chronic inflammation in these models is associated with a decreased amount of white adipose tissue and BMAT, with a significant decrease of adipokines, such as leptin and adiponectin. Moreover, we show in a cell culture model that high levels of pro-inflammatory IL-17, which is detected in the serum of B27 rats, may contribute to the suppression of adipogenesis. Thus, chronic inflammation has a significant negative impact on BMAT. Whether the loss of BMAT is due to inhibition of BMAT expansion or depletion of existing stores remains to be investigated.

METHODS

Animals

Two and six months old non-transgenic (NTG) and disease-prone HLA-B27/ hβ_2m transgenic rats (33-3 line, Fischer (F344) background) of mixed gender were used in this study. Rat lines were bred and maintained under conventional conditions at University of Versailles-St-Quentin. Rats were kept at 21 degree Celsius with a hygrometry of 41%. The 12 hours light cycle is with light on 8AM to 8 PM and off 8PM to 8AM. Two to three rats were kept in cages. All animals received water and food ad libitum (chow: M25, Special Diet Service, Paris, France). Study procedures were approved by the institutional animal care committee (APAFIS-8910). After sacrifice, rats were weighed. Subcutaneous and peri-gonadal fat mass was excised and weighed. Disease activity score was graded from 0-3: 0=no inflammation, 1=arthritis on one leg, 2=arthritis on both legs, 3=arthritis, and other clinical manifestations (orchitis, alopecia, gut inflammation).

Experiments for the SKG model of AS were conducted under a UK Home Office project license (PBFB4BA22) as previously described (22). Mice were kept on a 12 hour light/12 hour dark cycle at 21°C+/- 2°C with 55% humidity +/- 10%. Up to 5 mice were kept per cage with a mixture of control and curdlan-challenged mice in each cage. All animals received water and food ad libitum (chow: RM3 from Special Diet Service; LBS Biotech, UK). BALB/c ZAP-70^{W163C}-mutant (SKG) mice were a kind gift from S. Sakaguchi (University of Kyoto, Kyoto, Japan), bred in house and maintained under specific pathogen-free conditions. Disease was induced in 10-week-old female mice using a single dose of 3 mg curdlan (β-1,3-glucan derived from *Alcaligenes faecalis* variety *myxogenes*; Wako, Japan) administered intraperitoneally (i.p.). Arthritis was scored twice a week using the following defined criteria: 0, no joint swelling; 0.5, mild swelling of wrist or ankle, 1.0, pronounced swelling of wrist or ankle, 1.5 including swelling of at least one digit, 2 including swelling of all digits, 3 severe swelling with ankylosis. All paws for each mouse were scored and were summed per mouse to give an overall clinical grade for each mouse ranging from 0 to 12. Ankle diameter and weight were measured twice weekly. After 3 and 6 weeks, mice were sacrificed for organ collection.

Hematologic Analysis

Peripheral blood was collected from rats by heart puncture into heparinized capillary tubes, and complete blood counts were performed (Sysmex, Paris, France). Hematopoietic cells in the bone marrow were assessed using a bone marrow smear. For that purpose, bone marrow was flushed from the tibia and transferred to an objective slide. Bone marrow was spread using a coverslip and after staining with May-Grünwald, cells were counted in a blinded fashion by two experienced technicians from the hematology department according to their cytomorphological appearance.

Histology

Subcutaneous and gonadal fat pads, the liver, and the decalcified femur and fourth lumbar vertebrae were fixed in 4% PBS-buffered paraformaldehyde, dehydrated using an ascending ethanol series, and embedded with paraffin. Sections (4 μm) were prepared and stained for hematoxylin/eosin (HE) to assess tissue structures. Adipocyte area and number of adipocytes were

quantified using the Osteomeasure software (Osteometrics, Decatur, USA).

µCT Analysis of Bone Marrow Adipose Tissue Content

BMAT content was analyzed at the distal femur using osmium staining and subsequent µCT analysis (vivaCT40, Scanco Medical, Brüttisellen, Switzerland). Femurs from mice and rats were fixed with 10% PBS-buffered formalin for 24 h and decalcified in Osteosoft (Merck, Darmstadt, Germany). After decalcification, bones were scanned using the vivaCT40 using a standard protocol to ensure complete demineralization. Afterward, bones were incubated with 2% osmium tetroxide (Sigma-Aldrich, Mannheim, Germany) dissolved in 0.1 M sodium cacodylate buffer (Sigma-Aldrich, Mannheim, Germany) for 1 h at room temperature. Specimens were washed and immediately scanned using the µCT with an X-ray energy of 55 keV, 300 ms integration time, and an isotropic voxel size of 10.5 µm. The fat volume (FV) in the rats was calculated from 700 slices using manual contouring and the Scanco bone evaluation software. The threshold was set to 448 mg HA/cm^3. In mice, 400 slices were used with a threshold of 180 mg HA/cm^3.

Flow Cytometric Analysis

Mesenteric lymph nodes and bone marrow from one tibia were collected from NTG and B27 rats. Cell suspensions were prepared and resuspended in RPMI 1640 media (Gibco) containing 10% fetal bovine serum, 2% sodium pyruvate, 0.05 mM 2-mercaptoethanol, and 5 mM HEPES. To determine intracellular cytokine production, cells were stimulated with PMA and ionomycin (both at 500 ng/ml) in the presence of brefeldin A (10 µg/ml) for 4 hours. First, cells were stained with live-dead fixable reagent (Thermo Fisher) to exclude dead cells from the analysis. Second, surface markers were labeled using antibody mixtures prior to fixation and permeabilization with Foxp3/Transcription Factor Staining Buffer Kit according to the manufacturer instructions (Tonbo Biosciences). Surface marker antibodies were CD45 (OX-1 clone, BD-Biosciences), CD3 (1F4 clone, BD-Biosciences), TCRαβ (R73 clone, BD-Biosciences), and CD4 (Ox35 clone, Invitrogen). Then, cells were stained for intracellular IL-17 (TC11-18H10 clone, BD Horizon) and Foxp3 (FJK-16S clone, Invitrogen) for 30 minutes at 4°C. Eight-parameter cytometry was performed on an LSR III Fortessa flow cytometer (BD Biosciences) with FACSDiva software and analyzed with FlowJo software version 10.6.2.

Adipocyte Cell Culture

3T3-L1 adipogenic cells were obtained from ATCC and maintained in DMEM supplemented with 10% FCS and 1% penicillin/streptomycin. Cells were deposited on glass coverslips at 70% confluence and differentiated into adipocytes using maintenance medium supplemented with 174 nM insulin, 0.5 mM 3-Isobutyl-1-methylxanthine (IBMX), 250 nM dexamethasone, and 2 µM rosiglitazone. Cells were kept in this medium for 3 days. Afterward, cells were switched to maintenance medium plus 174 nM insulin for another 3 days (post-differentiation). Thereafter, cells were kept in maintenance medium until day 10. Adipocytes were stained with LipidTox (Thermo Fisher Scientific) according to the manufacturer's instructions.

To determine the effects of IL-17 on adipogenic differentiation, recombinant mouse IL-17A (R&D Systems) was added at the start of the differentiation protocol at various concentrations (10-100 ng/ml) for the entire differentiation period.

To determine the effect of IL-17 stemming from the serum of B27 transgenic rats, we added 5% of serum from NTG or B27 rats on day 3 of adipogenic differentiation for 4 days or on day 2 post-differentiation for 2 days. Additionally, some wells received 5 µg/ml of a neutralizing anti-mouse-IL-17A antibody or anti-IgG (both from R&D Systems). The percentage of rat serum was determined beforehand using a dose-response curve of NTG serum (0-5-25-50%) by assessing its effects on adipogenesis.

Gene Expression Analysis

Long bones of NTG and B27 rats were flushed and bone marrow was harvested for total RNA isolation using TRIzol reagent (Invitrogen, Germany) following the manufacturer's instructions. Total RNA from murine 3T3-L1 adipogenic cells was isolated with the High Pure RNA Isolation Kit (Roche, Germany) according to the manufacturer's protocol and quantified using the NanoDrop spectrophotometer (Peqlab, Erlangen, Germany). Five hundred nanograms of RNA were reverse transcribed using M-MLV RT RNase (H-) Point Mutant (Promega, Mannheim, Germany) followed by SYBR Green-based quantitative real-time PCR according to established protocols (ABI7500 Fast; Applied Biosystems, Carlsbad, CA). The primer sequences were: *rActb* S: GCTACAGCTTCA CCACCACA, *rActb* AS: AGGGCAACATAGCACAGCTT; *mActb* S: GATCTGGCACCACACCTTCT, *mActb* AS: GGGGTGTTGAAGGTCTCAAA; *rAdipoq* S: AGGAAACTT GTGCAGGTTGG, *rAdipoq* AS: CCTGTCATTCCAGC ATCTCC; *mAdipoq* S: AAAGGAGAGCCTGGAGAAGC, *mAdipoq* AS: GTAGAGTCCCGGAATGTTGC; *rAdipor1* S: CTTCTACTGCTCCCCACAGC, *rAdipor1* S: ACACCACTC AAGCCAAGTCC; *mAp2* S: GATGCCTTTGTGGGAACCTG; *mAp2 AS:* GAATTCCACGCCCAGTTTGA; *mCebpa S:* CTGAGAGCTCCTTGGTCAAG, *mCebpa AS:* GAATCTCCTA GTCCTGGCTTG; *rPparg* S: CCGAGAAGGAGAAGCTGTTG, *rPparg* AS: TCAGCGGGAAGGACTTTATG; *mPparg* S: CACTCGCATTCCTTTGACATC, *mPparg AS*: CGCACTT TGGTATTCTTGGAG; (r = rat; m = mouse). PCR conditions were: 95°C for 2 min followed by 40 cycles with 95°C for 15 sec and 60°C for 1 min. Melting curves were assessed to confirm the amplification of one PCR product by increasing the temperature from 65°C to 95°C. Results were calculated based on the ΔΔCT method and are depicted in x-fold change normalized to the housekeeping gene *Actb*.

Serum Analysis

Serum levels of glucose, triglycerides, cholesterol, and high- and low-density lipoprotein (HDL, LDL) were measured in B27 rats using a Roche ModularPPEanalyzer. Serum IL-17 and adiponectin levels in B27 rats were quantified using Quantikine ELISAs from R&D Systems.

Adipokine Profiling

Rat serum was further used to quantify obesity-related cytokines using the Proteome Profiler Rat Adipokine Array Kit from R&D Systems according to the manufacturer's protocol.

Statistical Analysis

Results are presented as individual dots with the mean indicated as horizontal line. Comparisons were performed using unpaired Student's *t*-test, two way ANOVA, and one-way ANOVA followed by Tukey's *post hoc* test as appropriate, by using GraphPad Prism version 7.0. P-values ≤ 0.05 were considered statistically significant.

RESULTS

Loss of Bone Marrow Adipocytes in HLA-B27 Transgenic Rats and SKG Mice

In the course of previous analyses that were aimed at investigating the rate of bone loss during disease progression in B27 rats (23), we observed that BMAds were strongly reduced along with disease development. To investigate this further, we examined the BMAT content in 2-and 6-month-old B27 rats with a low degree of inflammation and established disease (**Figure 1A**), respectively, using histology and osmium-based μCT, in which osmium stains lipid droplets and due to its heavy metal characteristics can be quantified using μCT. Histological analysis revealed no difference in the number of adipocytes in the femur of 2-month-old B27 rats, while 90% of BMAT reduction was observed in the 6-month-old cohort (**Figure 1B**). Analysis of the lumbar vertebral body also showed diminished BMAT in B27 rats before and after the onset of the disease (**Figure 1C**). Interestingly, loss of adipocytes was accompanied by an increased immune cell infiltration in the femur (6-month-old group) and lumbar vertebral body (2- and 6-month-old groups) of B27 rats (**Figures 1D, E**). μCT analysis revealed a more than a three-fold reduction in BMAT in the bone marrow of 6-month-old B27 rats compared to NTG rats (**Figure 1F, G**). Furthermore, the mRNA expression of adipocyte markers including peroxisome proliferator-activated receptor gamma (*Pparg*), adiponectin (*Adipoq*), and adiponectin receptor 1 (*Adipor1*) was strongly downregulated in the bone marrow of 6-month-old B27 rats (**Figure 1H**).

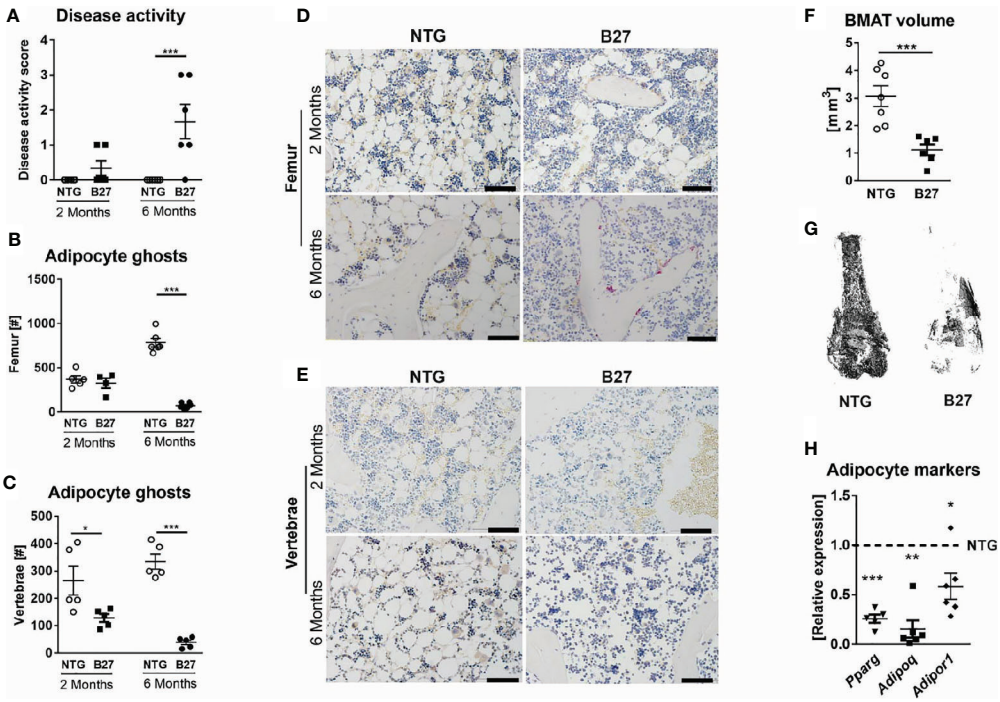

FIGURE 1 | Decreased numbers of bone marrow adipocytes in B27 transgenic rats. **(A)** Clinical score of 2 and 6 months old NTG and B27 rats. Disease level was graded from 0-3: 0=no inflammation, 1=arthritis on one leg, 2=arthritis on both legs, 3=severe arthritis, and other organ manifestation. **(B)** Number of bone marrow adipocytes ghosts from the femur of 2- and 6 months old NTG and B27 (n=5-6 per group). **(C)** Number of bone marrow adipocytes ghosts from the vertebrae of 2- and 6 months old NTG and B27 (n=5 per group). **(D, E)** Representative histology sections from femur and vertebrae of 2-and 6 months old NTG and B27 rats stained with von Kossa/toluidine blue (scale bar: 100 μm) **(F, G)** Osmium tetroxide staining for bone marrow adipose tissue (BMAT) followed by micro-computed tomography (μCT) analysis. Quantification of fat volume **(F)** and representative images **(G)** of stained lipids in femora of NTG and B27 rats (n=6-7 per group). **(H)** Relative expression of PPARγ, adiponectin, and adiponectin receptor in the bone marrow of NTG and B27 rats. Results are presented as individual dots with the mean indicated as horizontal line (n=5-6 per group). *p < 0.05; **p < 0.01 and ***p ≤ 0.001 *vs.* controls *via* unpaired Student's t-test.

To investigate if a similar phenotype occurs in another murine model of SpA, we assessed the BMAT in curdlan-challenged SKG mice. SKG mice developed severe inflammatory arthritis (**Figures 2A, B**) that was associated with a marked reduction in BMAT content (**Figure 2C**) and BMAd number (**Figure 2D**) at three weeks post curdlan challenge that remained low until six weeks. Thus, BMAT is severely reduced in two characteristic murine models of chronic inflammatory SpA.

Chronic Inflammation in Murine Models of SpA Is Associated With Loss of Adipose Tissue and an Altered Metabolic Profile

To further investigate whether the decreased amount of adipocytes in the bone marrow from B27 rats is site-specific, we measured in these rats body weight and subcutaneous and peri-gonadal fat weight. We observed a significant loss of body weight (**Table 1**) as well as a marked reduction of subcutaneous and peri-gonadal fat mass compared to NTG rats (**Figures 3A, B**). Histological analysis of these fat pads showed that adipocyte number was similar, but that adipocyte size was significantly reduced in B27 rats compared to NTG rats (**Figures 3A, B**). Furthermore, HE staining showed massive inflammatory infiltrates into the adipose tissue at both sites in B27 rats (**Figures 3C, D**). Importantly, these results were corroborated in arthritic SKG mice, showing weight loss (**Figure 3E**) and reduced subcutaneous fat mass (**Figure 3F**). Thus, loss of BMAT is not bone marrow-specific, but also white adipose tissue undergoes destruction during chronic inflammation, underscoring the consumptive or catabolic nature of unopposed chronic inflammation. In addition to adipose tissue loss, B27 rats showed significant reduction in serum triglycerides, cholesterol, LDL as well as HDL (**Table 1**). Moreover, blood glucose levels were decreased by 20% (**Table 1**). To further examine the levels of adipokines, we performed a proteome profiler assay on NTG and B27 rat sera. This analysis showed that adiponectin and leptin levels, two cytokines produced mainly by adipocytes, were highly reduced in B27 rats (**Figures 4A, B**). In addition, CD26, IGF-1, LIF, and RAGE were also significantly reduced (**Figure 4B**). Representative blots for cytokine expression in NTG and B27 are shown in **Figure 4C**. Of note, the abundance of all other

TABLE 1 | Body weight and serum fat parameters in no-transgenic and HLA-B27 transgenic rats.

Parameters	NTG N = 8	B27 N = 6	p-value
Weight (g)	349 ± 101	248 ± 50.0	0.046
Serum glucose (mmol/L)	14.7 ± 2.25	11.8 ± 1.67	0.031
Triglycerides (mmol/L)	1.93 ± 0.87	1.00 ± 0.46	0.036
Cholesterol (mmol/L)	2.99 ± 0.98	1.65 ± 0.29	0.007
LDL (mmol/L)	0.37 ± 0.09	0.23 ± 0.11	0.032
HDL (mmol/L)	1.75 ± 0.36	1.04 ± 0.25	0.002

NTG, non-transgenic rat; B27, HLA-B27 transgenic rat; LDL, low-density lipoprotein; HDL, high-density lipoprotein. Data are represented as mean ± SD.

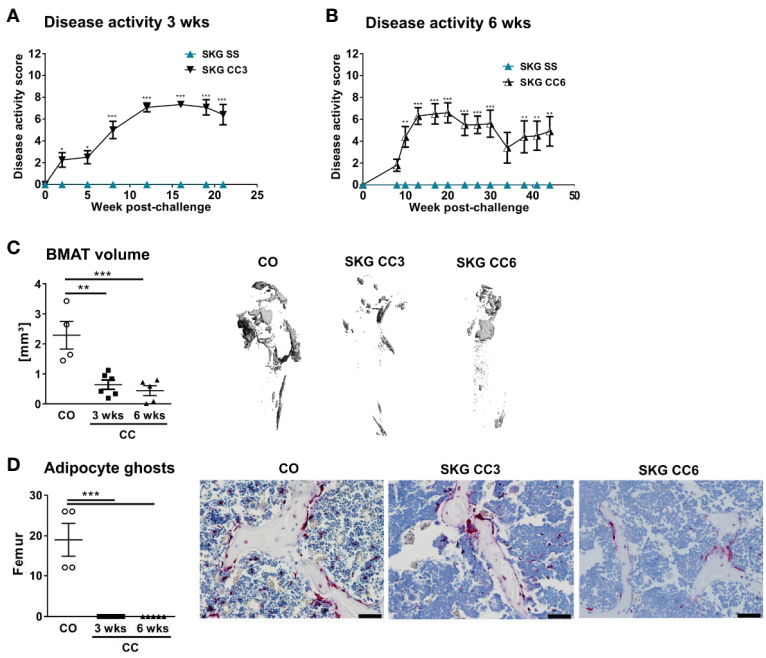

FIGURE 2 | Decreased numbers of bone marrow adipocytes in SKG mice. **(A, B)** Clinical score of SKG animals at steady-state (SS) or curdlan-challenged (CC) for 3 and 6 weeks. **(C)** Osmium tetroxide staining for BMAT followed by µCT analysis. Quantification of fat volume (left) and representative images (right) of stained lipids in femora of SKG mice at 3- and 6-weeks post-curdlan challenge *vs.* control group. **(D)** Number of bone marrow adipocytes ghosts (left) and representative histology sections (right) from femur in SKG mice at 3 and 6 weeks post-curdlan challenge *vs.* control group stained with von Kossa/toluidine blue (scale bar: 100 µm). Results are presented as individual dots with the mean indicated as horizontal line (n=4-6 per group). *p < 0.05, **p ≤ 0.01, and ***p ≤ 0.001 *vs.* controls *via* two-way ANOVA with Tukey's *post hoc* test **(A, B)** and one-way ANOVA with Tukey's *post hoc* test **(C, D)**.

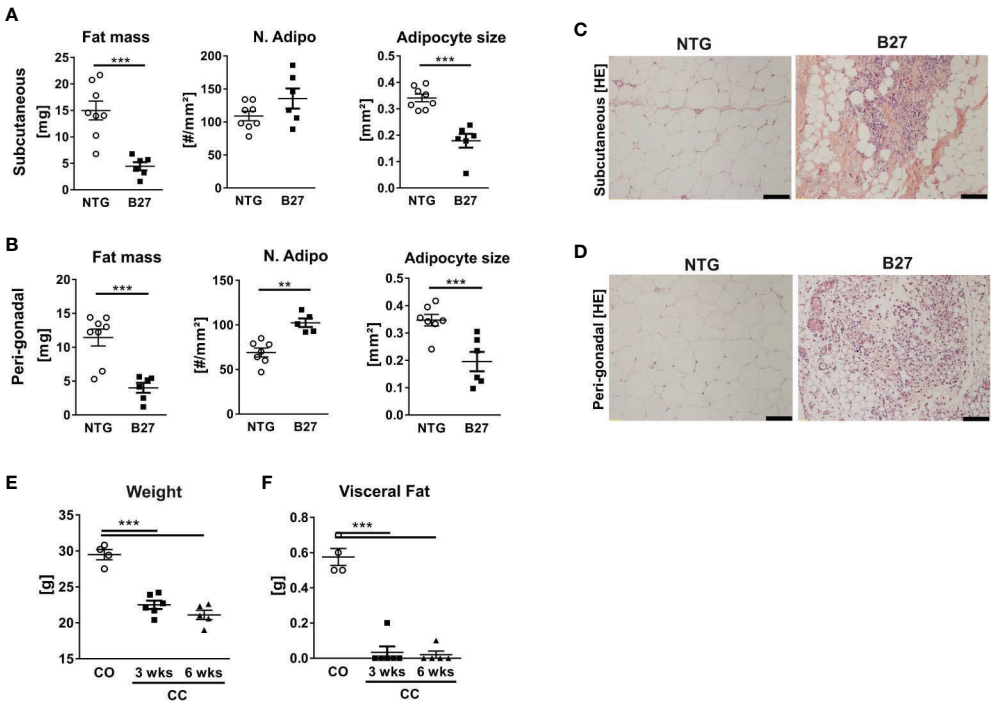

FIGURE 3 | Chronic inflammation in rodent models of SpA leads to loss of white adipose tissue. **(A, B)** Fat mass, number, and size of adipocytes in subcutaneous (top) and peri-gonadal (bottom) adipose tissue of NTG and B27 rats. **(C, D)** Representative histology sections stained with hematoxylin/eosin staining. Scale bars: 100 µm (n=6-8 per group). **(E, F)** Bodyweight and visceral fat weight of SKG mice at 3- and 6-weeks post-curdlan challenge vs. control group (n=4-6 per group). Results are presented as individual dots with the mean indicated as horizontal line. **p ≤ 0.01, and ***p ≤ 0.001 *vs* controls *via* unpaired Student´s t-test **(A, B)** and one-way ANOVA with Tukey's *post hoc* test **(E, F)**.

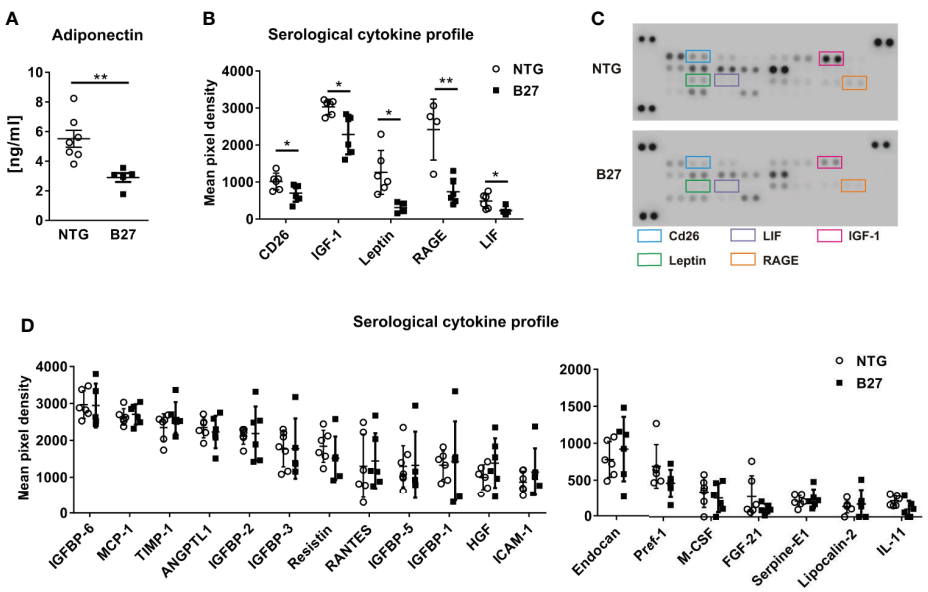

FIGURE 4 | Altered metabolic profile in B27 transgenic rats. **(A)** Serum concentrations of adiponectin in NTG and B27 rats (n=5-7 per group). **(B)** Significantly regulated cytokines in the serum of NTG and B27 rats. **(C)** Representative image of cytokine profiler array results from serum of NTG and B27 rats. Significant ones are highlighted. **(D)** Relative levels of not-regulated obesity-related cytokines in NTG and B27 rats (B,D n=6-8 per group). Data are presented as mean ± SD. *p ≤ 0.05 and **p ≤ 0.001 NTG *vs.* B27 *via* unpaired Student's t-test.

obesity-related cytokines investigated in the serum was not altered (**Figure 4D**).

Hematopoietic Composition of the Bone Marrow and Blood of B27 Rats

As dysregulated hematopoiesis occurs in several chronic inflammatory diseases, we analyzed immune cell populations present in the bone marrow and assessed hematological parameters in the blood. The frequency of neutrophils was significantly increased in the bone marrow, mostly due to an increase in the promyeloid stage and the segmented neutrophils (**Supplementary Figure 1A**). In contrast, lymphocytes and monocytes frequencies were decreased (**Supplementary Figure 1B**). Leukocyte numbers were increased by 3-fold in the peripheral blood of B27 animals, showing significantly increased numbers in neutrophils, eosinophils, monocytes, and platelets (**Table 2**). As expected, erythroid precursors in the bone marrow were significantly reduced, as was the hematocrit and the mean corpuscular volume, indicating that anemia of inflammation had developed in B27 rats (**Figure 1** and **Table 2**). Thus, during inflammation, neutrophils appear to account for most of the inflammatory cells in the bone marrow of B27 rats.

Elevated Levels of IL-17 May Contribute to the Loss of Adipocytes in B27 Rats

As B27 rats have been shown to have an increased prevalence of $CD4^+$ T-helper 17 (Th17) cells and elevated serum levels of IL-17 (24, 25), we investigated the absolute number of $CD4^+$ T present in the bone marrow and used mesenteric lymph nodes (mLN) as a control with a known expansion of Th17 cells. Absolute numbers of $CD4^+$ T cells were significantly higher in mLN of spondyloarthritic B27 compared to the healthy NTG rats (**Figure 5A**), while similar numbers were found in the bone marrow (**Figure 5B**). Importantly, the frequency of IL-17-producing $CD4^+$ T cells was significantly increased in both mLN and bone marrow of B27 rats compared to NTG rats (**Figures 5C, D**). Accordingly, B27 rats showed an 8-fold higher serum level of IL-17 than NTG (**Figure 6A**). Given that IL-17 reduces preadipocyte differentiation and alters adipogenesis (26, 27), we examined whether this cytokine could be involved in the depletion of BMAT in our model. For this, we first tested whether IL-17 indeed suppresses adipogenesis of 3T3 adipocytes. Treatment of 3T3 cells with IL-17 during the differentiation period reduced in a dose-dependent manner adipocyte numbers (**Figure 6B**). Importantly, treatment of 3T3 cells with 5% serum from B27 rats starting at day 3 of differentiation reduced adipocyte number and the mRNA expression of adipocyte markers compared to cells treated with 5% NTG serum (**Figures 6C, D**). This effect with sera was reversed when cells were incubated with a neutralizing IL-17 antibody confirming the critical role of IL-17 in the regulation of adipocyte differentiation (**Figure 6E**). Notably, treating adipocyte cultures on day 2 post-differentiation with rat serum did not result in altered adipocyte numbers (NTG: 120.7 ± 13.7 *vs.* B27: 101.3 ± 38.9 adipocytes, p=0.43). Thus, these data suggest that the high amount of IL-17 present in the serum of B27 reduces adipogenesis.

TABLE 2 | Blood differential in no-transgenic and HLA-B27 transgenic rats.

Parameters	NTG N = 8	B27 N = 5	p-value
Hematocrit (%)	**47.6 ± 4.37**	**41.4 ± 3.50**	**0.025**
Hemoglobin (g/dl)	14.8 ± 2.68	14.2 ± 2.87	0.787
MCV (fl)	**53.4 ± 1.98**	**50.4 ± 2.07**	**0.029**
MCH (pg)	16.6 ± 2.00	16.4 ± 0.55	0.813
MCHC (g/dl)	31.4 ± 3.82	32.4 ± 1.34	0.567
Erythrocytes (10^5 #/mm³)	88.9 ± 6.99	81.3 ± 9.08	0.117
Leucocytes (10^3 #/mm³)	**4.22 ± 2.50**	**11.6 ± 1.35**	**<0.001**
Neutrophils (10^3 #/mm³)	1.50 ± 1.30	20.6 ± 15.4	0.053
Eosinophils (#/mm³)	**26.5 ± 27.1**	**115 ± 13.7**	**<0.001**
Basophils (#/mm³)	22.5 ± 48.5	24.6 ± 55.0	0.944
Lymphocytes (10^3 #/mm³)	2.36 ± 1.26	3.52 ± 0.96	0.109
Monocytes (#/mm³)	**59.3 ± 56.3**	**425 ± 241**	**0.002**
Platelets (10^5 #/mm³)	**7.10 ± 1.31**	**9.60 ± 1.06**	**0.006**

NTG, non-transgenic rat; B27, HLA-B27 transgenic rat; MCV, mean corpuscular volume; MCH, mean corpuscular hemoglobin; MCHC,: mean corpuscular hemoglobin content. Data are represented as mean ± SD.
Bold values mean they are statistically significant.

DISCUSSION

The ability of BMAds to concurrently influence bone remodeling and hematopoiesis (7, 8) places them in a crucial position in the regulation of bone and immune cell fate. Notably, recent evidence demonstrated that BMAds play a decisive role in regulating immune responses, contributing to increased levels of pro-inflammatory cytokines and oxidative stress (6). However, how chronic inflammation affects BMAT is currently unknown. We previously observed a drastic reduction of BMAd with disease duration in B27 rat, while studying the impact of chronic inflammation on bone in this model of SpA (23). Here, we examined in more detail the femoral and vertebral BMAT content in 2 and 6 months old B27 rats. Using 3D μCT and histology, we showed that BMAT was reduced by up to 90% in 6-month-old B27 rats with established disease in the femur and vertebral body compared to control NTG. This finding was not restricted to the B27 rat model of SpA, since similar findings were also observed in curdlan-challenged SKG mice, suggesting that depletion of BMAT is a common characteristic of SpA rodent models.

Weight loss and decrease in lean mass have been commonly described in individuals with inflammatory rheumatic disorders, reflecting their consumptive nature (28, 29). Based on this clinical evidence, we quantified total body weight as well as subcutaneous and peri-gonadal fat weight to assess whether the loss of BMAds is site-specific. Both B27 rats and SKG mice showed a significant body weight and overall fat mass loss. Thus, these data show that the decreased amount of BMAT is not a localized, but rather a systemic phenomenon, and that also white adipose tissue decreases during chronic inflammation. Consistently, proteomic analyses showed low serum levels of adipokines in B27 rats compared to NTG. Interestingly, reduction of both adiponectin and leptin has been associated

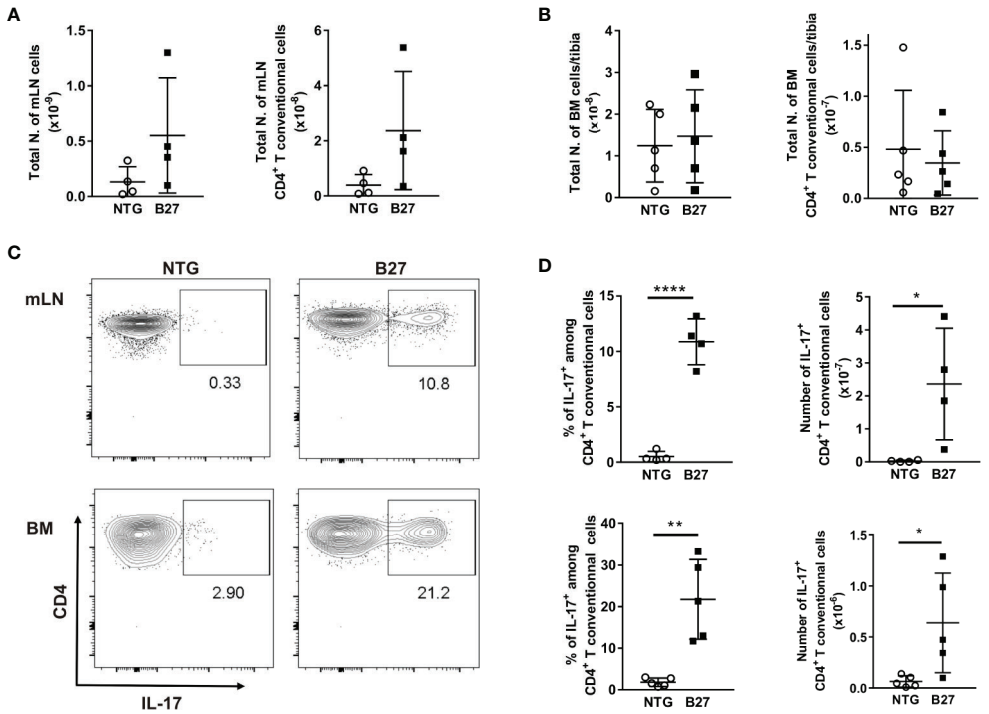

FIGURE 5 | Expansion of IL17+ producing CD4+ T cells in the bone marrow from B27 transgenic rats. **(A)** Absolute number of live cells and $CD4^+$ T cells in mesenteric lymph nodes (mLN) from NTG (grey) and B27 (white) rats were determined using flow cytometry. **(B)** Absolute number of live cells and $CD4^+$ T cells in bone marrow (BM) from NTG and B27 rats. **(C)** Representative plots of intracellular IL-17 staining gated on $CD4^+$ $Foxp3^-$ T cells in mLN (top) and BM (bottom) from NTG (left panel) or B27 (right panel) rats. **(D)** Frequencies of IL-17^+ cells among $CD4^+$ T cells (left) and their absolute numbers (right) in mLN (top) and BM (bottom) from NTG and B27 rats (A-D n=4-5 per group). Results are presented as individual dots with the mean indicated as horizontal line. Data were analyzed by unpaired Student's t-test (*p<0.05, **p < 0.01 and ****p < 0.0001).

with increased inflammatory responses and enhanced susceptibility to the toxicity of proinflammatory stimuli, respectively (29, 30).

In addition, high inflammation reduces circulating levels of lipids (31–33). Analysis of the serum lipid profile in B27 rats revealed marked dyslipidemia with decreased triglycerides, cholesterol, and associated lipoproteins as compared to the controls. Reduction in HDL cholesterol levels in our rat model appeared consistent with clinical observations previously reported (34). Indeed, patients affected by axial SpA and psoriatic arthritis present with an abnormal lipid profile and low HDL levels, which have been linked to accelerated manifestations of cardiovascular diseases and reduced lifespan (35). Nevertheless, the molecular factors that potentially mediate the interaction between inflammatory disease and altered lipid metabolism require further investigations. A plausible explanation is that proinflammatory cytokines may redirect energy consumption in favor of hematopoietic cells at the expense of fat tissue, thereby guaranteeing that enough energy can be provided to immune cells in states of high demand, such as during inflammation (36). Thus, cytokines might have direct effects on lipid metabolism as well as glucose metabolism, which can also explain the significant reduction of blood glucose levels in B27 rats as compared to the healthy controls.

Although the immune cell network that drives SpA is still unclear, experimental evidence supports a central role for HLA-B27 expressing hematopoietic cells in disease development (37). Therefore, to gain a greater understanding of the hematopoietic cell composition and explore which other cells inhabit the bone marrow instead of the BMAds, we analyzed immune cell populations in B27 rats. Systemic inflammation was associated with an increased number of mature neutrophils, which was mirrored by decreased erythroid precursors. These data support previous findings, in which non-resolving joint and intestinal inflammation in the SKG mouse model of SpA was accompanied by dysregulated hematopoietic stem cell activity and biased differentiation toward myeloid progenitors, culminating in an invasion of target organs by activated neutrophils (38). Within the same study, the authors demonstrated that $CD4^+$ T-cell depletion was not required for the development of SpA in this model, supporting the critical function of innate versus adaptive immune response in inflammation (38). Nevertheless, the critical contribution of adaptive cells to the disease has been shown in other situations such as in HLA-B27 transgenic rats (12). This leads to the production of proinflammatory cytokines implicated in the pathogenesis of SpA. In particular, IL-17 derived from $CD4^+$Th17 has been found to positively correlate with disease severity. Indeed, serum concentrations of IL-17 were higher in patients with SpA

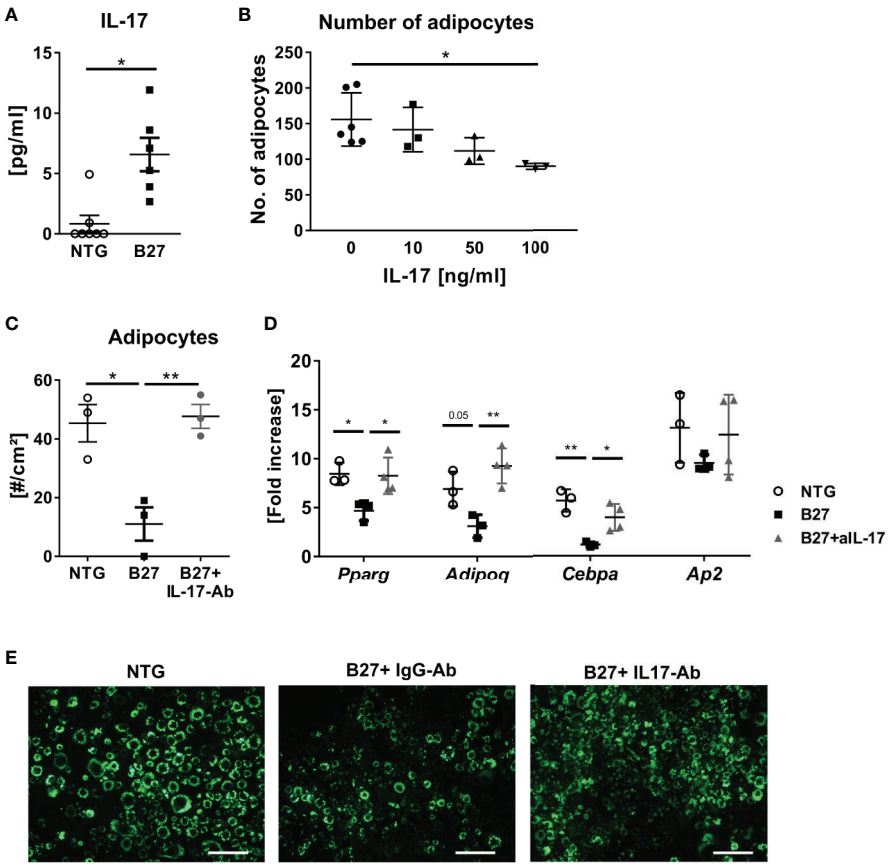

FIGURE 6 | IL-17 from B27 transgenic rat serum inhibits adipogenesis in vitro. **(A)** IL-17 levels in sera of in B27 and NTG rats (n=6-7 per group). **(B)** Absolute numbers of 3T3 adipocytes after exposure to control medium or increasing doses of IL-17 during adipocyte differentiation (n=3-6 per group). **(C, D)** Absolute numbers of 3T3 adipocytes and relative expression of the most representative adipocyte markers after 48 h exposure to 5% serum from NTG rats, B27 rats + IgG antibody (IgG-Ab), or B27 rats + neutralizing anti-IL-17 antibody (IL-17-Ab) treatment (n=3-6 per group). **(E)** Representative fluorescence microscopy pictures of LipidTOX stained 3T3 cells. Scale bar: 50 µm. All experiments were performed independently three times. Results are presented as individual dots with the mean indicated as horizontal line. *p ≤ 0.05 and **p ≤ 0.01 NTG *vs.* B27 *via* unpaired Student's t-test **(A)**. and one-way ANOVA with Tukey's *post hoc* test **(B–D)**.

than in age and sex-controlled healthy individuals (39, 40). These observations are congruent with our analysis, where B27 rats displayed higher levels of IL-17 in the serum as compared to the NTG controls. In addition, insights into the molecular regulation of bone homeostasis revealed that IL-17 steers mesenchymal stem cells into an osteogenic fate and promote osteoclastogenesis in a RANKL-dependent manner (16, 41). Further, *in vivo* studies implicate IL-17 in the regulation of adipogenesis by inhibiting preadipocyte differentiation, hampering metabolic function of mature adipocytes, and consequentially reducing white adipose tissue accumulation (16, 42). Accordingly, our *in vitro* experiment confirmed a significant reduction in the number of adipocytes after treatment with recombinant IL-17 as well as after treatment with B27 rat serum. This effect was only observed, however, when starting the treatment early during the differentiation process. The reduction of adipocytes was dependent on the IL-17 present in the serum of B27 rats, as suppression of adipogenesis was reversed when IL-17 was neutralized using antibodies. Whether IL-17 mediates the reduction of BMAT during chronic inflammation in SpA *in vivo* and whether this is driven by suppression of BMAT expansion and/or loss of mature BMAds remains to be investigated.

Besides its prominent role in the regulation of adipose tissue and energy homeostasis, IL-17 has been shown to activate innate immune mechanisms, including the recruitment and survival of neutrophils (13, 43, 44). Thus, the high levels of IL-17 could explain the reduction of BMAds and the increase of neutrophils within the bone marrow in our rat model. In fact, the abundance of IL-17-producing $CD4^+$ T cells observed in the bone marrow of B27 rats may promote the accumulation of neutrophils and, simultaneously, induce lipolysis in the surrounded adipocytes to provide energy for the immune system. Clearly, further investigations are necessary to thoroughly address this hypothesis and clarify the mechanisms and purpose of BMAd reduction during chronic inflammation.

Despite strong evidence that BMAT is reduced in rodent models of SpA, our study has potential limitations. First, our animal models do not fully reflect the spectrum of spine manifestations found in

patients with SpA. For example, osteophytes and fatty streaks at the vertebral column are rarely observed. Moreover, we evaluated adipokines in the serum. However, other fat depots such as white adipose tissue also produce adipokines that are released into the circulation. Therefore, it would be interesting to analyze adipokine concentrations directly in the bone marrow microenvironment to better address which adipokines are locally altered by chronic inflammation.

CONCLUSIONS

Our results show a significant reduction of white adipose tissue and BMAT in two relevant rodent models of SpA. Elevated serum levels of IL-17 suggest a potential role of $IL17^{+}CD4^{+}$ T cells in sustaining inflammation by disrupting BMAT.

DATA AVAILABILITY STATEMENT

The raw data supporting the conclusions of this article will be made available by the authors, without undue reservation.

ETHICS STATEMENT

The animal study was reviewed and approved by APAFIS-8910 and UK Home Office project license (PBFB4BA22).

AUTHOR CONTRIBUTIONS

MR, LA, MBr, and LH designed the experiments. GF, MR, UB, IF, MBe, SG, MvB, and LA performed all experiments and analyzed the data. MBr, SG, and MvB evaluated bone marrow. NH performed SKG mouse experiments. All authors contributed to data discussion and interpretation. GF and MR drafted the manuscript. All authors contributed to the article and approved the submitted version.

FUNDING

This work was supported by grants from the Deutsche Forschungsgemeinschaft and the European Union's Horizon 2020 research and innovation programme under the Marie Skłodowska-Curie grant agreement No 860898 to MR and LH, as well as NH, supported by Versus Arthritis Grant No. 20372.

ACKNOWLEDGMENTS

We would like to thank Ina Gloe, Tina Dybek, and Sophie Pählig for their excellent technical assistance.

SUPPLEMENTARY MATERIAL

The Supplementary Material for this article can be found online at: https://www.frontiersin.org/articles/10.3389/fimmu.2021.665208/full#supplementary-material

Supplementary Figure 1 | Effect of chronic inflammation on blood cells in the bone marrow of B27 rats. Percentage of neutrophil subpopulations **(A)**, other leucocyte populations **(B)**, and erythroblast populations **(C)** in the bone marrow of NTG and B27 rats (n=6-8 per group). Data are presented as mean ± SD. *$p \leq 0.05$, **$p \leq 0.01$, and ***$p \leq 0.001$ NTG *vs.* B27 *via* unpaired Student´s t-test.

REFERENCES

1. Suchacki KJ, Tavares AAS, Mattiucci D, Scheller EL, Papanastasiou G, Gray C, et al. Bone Marrow Adipose Tissue Is a Unique Adipose Subtype With Distinct Roles in Glucose Homeostasis. *Nat Commun* (2020) 11:3097. doi: 10.1038/s41467-020-16878-2
2. Scheller EL, Cawthorn WP, Burr AA, Horowitz MC, MacDougald OA. Marrow Adipose Tissue: Trimming the Fat. *Trends Endocrinol Metab TEM* (2016) 27:392–403. doi: 10.1016/j.tem.2016.03.016
3. Sulston RJ, Learman BS, Zhang B, Scheller EL, Parlee SD, Simon BR, et al. Increased Circulating Adiponectin in Response to Thiazolidinediones: Investigating the Role of Bone Marrow Adipose Tissue. *Front Endocrinol* (2016) 7:128. doi: 10.3389/fendo.2016.00128
4. Krings A, Rahman S, Huang S, Lu Y, Czernik PJ, Lecka-Czernik B. Bone Marrow Fat Has Brown Adipose Tissue Characteristics, Which Are Attenuated With Aging and Diabetes. *Bone* (2012) 50:546–52. doi: 10.1016/j.bone.2011.06.016
5. Chen Q, Shou P, Zheng C, Jiang M, Cao G, Yang Q, et al. Fate Decision of Mesenchymal Stem Cells: Adipocytes or Osteoblasts? *Cell Death Differ* (2016) 23:1128–39. doi: 10.1038/cdd.2015.168
6. Miggitsch C, Meryk A, Naismith E, Pangrazzi L, Ejaz A, Jenewein B, et al. Human Bone Marrow Adipocytes Display Distinct Immune Regulatory Properties. *EBioMedicine* (2019) 46:387–98. doi: 10.1016/j.ebiom.2019.07.023
7. Zhong L, Yao L, Tower RJ, Wei Y, Miao Z, Park J, et al. Single Cell Transcriptomics Identifies a Unique Adipose Lineage Cell Population That Regulates Bone Marrow Environment. *eLife* (2020) 9:e54695. doi: 10.7554/eLife.54695
8. Zou W, Rohatgi N, Brestoff JR, Li Y, Barve RA, Tycksen E, et al. Ablation of Fat Cells in Adult Mice Induces Massive Bone Gain. *Cell Metab* (2020) 32:801–13.e6. doi: 10.1016/j.cmet.2020.09.011
9. Tratwal J, Labella R, Bravenboer N, Kerckhofs G, Douni E, Scheller EL, et al. Reporting Guidelines, Review of Methodological Standards, and Challenges Toward Harmonization in Bone Marrow Adiposity Research. Report of the Methodologies Working Group of the International Bone Marrow Adiposity Society. *Front Endocrinol* (2020) 11:65. doi: 10.3389/fendo.2020.00065
10. Sieper J, Poddubnyy D. Axial Spondyloarthritis. *Lancet* (2017) 390:73–84. doi: 10.1016/S0140-6736(16)31591-4
11. Fragoulis GE, Liava C, Daoussis D, Akriviadis E, Garyfallos A, Dimitroulas T. Inflammatory Bowel Diseases and Spondyloarthropathies: From Pathogenesis to Treatment. *World J Gastroenterol* (2019) 25:2162–76. doi: 10.3748/wjg.v25.i18.2162
12. Breban M, Fernández-Sueiro JL, Richardson JA, Hadavand RR, Maika SD, Hammer RE, et al. T Cells, But Not Thymic Exposure to HLA-B27, Are Required for the Inflammatory Disease of HLA-B27 Transgenic Rats. *J Immunol Baltim Md 1950* (1996) 156:794–803.
13. Lubberts E. The IL-23–IL-17 Axis in Inflammatory Arthritis. *Nat Rev Rheumatol* (2015) 11:415–29. doi: 10.1038/nrrheum.2015.53
14. Raychaudhuri SP, Raychaudhuri SK. Mechanistic Rationales for Targeting Interleukin-17A in Spondyloarthritis. *Arthritis Res Ther* (2017) 19:51. doi: 10.1186/s13075-017-1249-5

15. Glatigny S, Fert I, Blaton MA, Lories RJ, Araujo LM, Chiocchia G, et al. Proinflammatory Th17 Cells are Expanded and Induced by Dendritic Cells in Spondylarthritis-Prone HLA-B27-transgenic Rats. *Arthritis Rheum* (2012) 64:110–20. doi: 10.1002/art.33321
16. Lee Y. The Role of interleukin-17 in Bone Metabolism and Inflammatory Skeletal Diseases. *BMB Rep* (2013) 46:479–83. doi: 10.5483/BMBRep.2013.46.10.141
17. Yin Y, Wang M, Liu M, Zhou E, Ren T, Chang X, et al. Efficacy and Safety of IL-17 Inhibitors for the Treatment of Ankylosing Spondylitis: A Systematic Review and Meta-Analysis. *Arthritis Res Ther* (2020) 22:111. doi: 10.1186/s13075-020-02208-w
18. Breban M, Glatigny S, Cherqaoui B, Beaufrère M, Lauraine M, Rincheval-Arnold A, et al. Lessons on SpA Pathogenesis From Animal Models. *Semin Immunopathol* (2021) 43(2):207–19. doi: 10.1007/s00281-020-00832-x
19. Keller KK, Lindgaard LM, Wogensen L, Dagnæs-Hansen F, Thomsen JS, Sakaguchi S, et al. SKG Arthritis as a Model for Evaluating Therapies in Rheumatoid Arthritis With Special Focus on Bone Changes. *Rheumatol Int* (2013) 33:1127–33. doi: 10.1007/s00296-012-2500-7
20. Fakhreldin S, Abdallah MM, Al-tohamy MY, Zayed HS. Bone Mineral Density in Ankylosing Spondylitis: Relation to Disease Activity, Functional Capacity, Spinal Mobility and Radiological Damage. *Egypt Rheumatol* (2020) 42:297–301. doi: 10.1016/j.ejr.2020.07.009
21. Rauner M, Stupphann D, Haas M, Fert I, Glatigny S, Sipos W, et al. The HLA-B27 Transgenic Rat, a Model of Spondyloarthritis, Has Decreased Bone Mineral Density and Increased RANKL to Osteoprotegerin mRNA Ratio. *J Rheumatol* (2009) 36:120–6. doi: 10.3899/jrheum.080475
22. Ruutu M, Thomas G, Steck R, Degli-Esposti MA, Zinkernagel MS, Alexander K, et al. β-Glucan Triggers Spondylarthritis and Crohn's Disease-Like Ileitis in SKG Mice. *Arthritis Rheum* (2012) 64:2211–22. doi: 10.1002/art.34423
23. Rauner M, Thiele S, Fert I, Araujo LM, Layh-Schmitt G, Colbert RA, et al. Loss of Bone Strength in HLA-B27 Transgenic Rats Is Characterized by a High Bone Turnover and Is Mainly Osteoclast-Driven. *Bone* (2015) 75:183–91. doi: 10.1016/j.bone.2015.02.024
24. Jansen DTSL, Hameetman M, van Bergen J, Huizinga TWJ, van der Heijde D, Toes REM, et al. Il-17-producing Cd4+ T Cells Are Increased in Early, Active Axial Spondyloarthritis Including Patients Without Imaging Abnormalities. *Rheumatology* (2015) 54:728–35. doi: 10.1093/rheumatology/keu382
25. Gullick NJ, Abozaid HS, Jayaraj DM, Evans HG, Scott DL, Choy EH, et al. Enhanced and Persistent Levels of Interleukin (IL)17CD4 T Cells and Serum IL17 in Patients With Early Inflammatory Arthritis. *Clin Exp Immunol* (2013) 174(2):292–301. doi: 10.1111/cei.12167
26. Shin JH, Shin DW, Noh M. Interleukin-17A Inhibits Adipocyte Differentiation in Human Mesenchymal Stem Cells and Regulates Pro-Inflammatory Responses in Adipocytes. *Biochem Pharmacol* (2009) 77:1835–44. doi: 10.1016/j.bcp.2009.03.008
27. Ahmed M, Gaffen SL. Il-17 Inhibits Adipogenesis in Part Via C/Ebpα, Pparγ and Krüppel-like Factors. *Cytokine* (2013) 61:898–905. doi: 10.1016/j.cyto.2012.12.007
28. Briot K. Body Weight, Body Composition, and Bone Turnover Changes in Patients With Spondyloarthropathy Receiving Anti-Tumour Necrosis Factor Treatment. *Ann Rheum Dis* (2005) 64:1137–40. doi: 10.1136/ard.2004.028670
29. Toussirot E, Grandclément E, Gaugler B, Michel F, Wendling D, Saas P, et al. Cbt-506. Serum Adipokines and Adipose Tissue Distribution in Rheumatoid Arthritis and Ankylosing Spondylitis. A Comparative Study. *Front Immunol* (2013) 4:453. doi: 10.3389/fimmu.2013.00453
30. Fantuzzi G. Adipose Tissue, Adipokines, and Inflammation. *J Allergy Clin Immunol* (2005) 115:911–9. doi: 10.1016/j.jaci.2005.02.023
31. Lakatos J, Hárságyi Á. Serum total HDL. LDL Cholesterol, and Triglyceride Levels in Patients With Rheumatoid Arthritis. *Clin Biochem* (1988) 21:93–6. doi: 10.1016/S0009-9120(88)80094-8
32. van Halm VP, van Denderen JC, Peters MJL, Twisk JWR, van der Paardt M, van der Horst-Bruinsma IE, et al. Increased Disease Activity Is Associated With a Deteriorated Lipid Profile in Patients With Ankylosing Spondylitis. *Ann Rheum Dis* (2006) 65:1473–7. doi: 10.1136/ard.2005.050443
33. Myasoedova E, Crowson CS, Kremers HM, Fitz-Gibbon PD, Therneau TM, Gabriel SE. Total Cholesterol and LDL Levels Decrease Before Rheumatoid Arthritis. *Ann Rheum Dis* (2010) 69:1310–4. doi: 10.1136/ard.2009.122374
34. Jones S, Harris C, Lloyd J, Stirling C, Reckless J, McHugh N. Lipoproteins and Their Subfractions in Psoriatic Arthritis: Identification of an Atherogenic Profile With Active Joint Disease. *Ann Rheum Dis* (2000) 59:904–9. doi: 10.1136/ard.59.11.904
35. Papagoras C, Markatseli TE, Saougou I, Alamanos Y, Zikou AK, Voulgari PV, et al. Cardiovascular Risk Profile in Patients With Spondyloarthritis. *Joint Bone Spine* (2014) 81:57–63. doi: 10.1016/j.jbspin.2013.03.019
36. Wang H, Ye J. Regulation of Energy Balance by Inflammation: Common Theme in Physiology and Pathology. *Rev Endocr Metab Disord* (2015) 16:47–54. doi: 10.1007/s11154-014-9306-8
37. Breban M, Hammer RE, Richardson JA, Taurog JD. Transfer of the Inflammatory Disease of HLA-B27 Transgenic Rats by Bone Marrow Engraftment. *J Exp Med* (1993) 178:1607–16. doi: 10.1084/jem.178.5.1607
38. Regan-Komito D, Swann JW, Demetriou P, Cohen ES, Horwood NJ, Sansom SN, et al. Gm-CSF Drives Dysregulated Hematopoietic Stem Cell Activity and Pathogenic Extramedullary Myelopoiesis in Experimental Spondyloarthritis. *Nat Commun* (2020) 11:155. doi: 10.1038/s41467-019-13853-4
39. Romero-Sanchez C, Jaimes DA, Londoño J, De Avila J, Castellanos JE, Bello JM, et al. Association Between Th-17 Cytokine Profile and Clinical Features in Patients With Spondyloarthritis. *Clin Exp Rheumatol* (2011) 29:828–34.
40. Chen W-S, Chang Y-S, Lin K-C, Lai C-C, Wang S-H, Hsiao K-H, et al. Association of Serum Interleukin-17 and Interleukin-23 Levels With Disease Activity in Chinese Patients With Ankylosing Spondylitis. *J Chin Med Assoc* (2012) 75:303–8. doi: 10.1016/j.jcma.2012.05.006
41. Kotake S, Udagawa N, Takahashi N, Matsuzaki K, Itoh K, Ishiyama S, et al. Il-17 in Synovial Fluids From Patients With Rheumatoid Arthritis Is a Potent Stimulator of Osteoclastogenesis. *J Clin Invest* (1999) 103:1345–52. doi: 10.1172/JCI5703
42. Zúñiga LA, Shen W-J, Joyce-Shaikh B, Pyatnova EA, Richards AG, Thom C, et al. IL-17 Regulates Adipogenesis, Glucose Homeostasis, and Obesity. *J Immunol* (2010) 185:6947–59. doi: 10.4049/jimmunol.1001269
43. Flannigan KL, Ngo VL, Geem D, Harusato A, Hirota SA, Parkos CA, et al. Il-17A-mediated Neutrophil Recruitment Limits Expansion of Segmented Filamentous Bacteria. *Mucosal Immunol* (2017) 10:673–84. doi: 10.1038/mi.2016.80
44. Griffin GK, Newton G, Tarrio ML, Bu D, Maganto-Garcia E, Azcutia V, et al. Il-17 and Tnfα Sustain Neutrophil Recruitment During Inflammation Through Synergistic Effects on Endothelial Activation. *J Immunol Baltim Md 1950* (2012) 188:6287–99. doi: 10.4049/jimmunol.1200385

Conflict of Interest: The authors declare that the research was conducted in the absence of any commercial or financial relationships that could be construed as a potential conflict of interest.

frontiers in Immunology

MINI REVIEW
published: 15 June 2021
doi: 10.3389/fimmu.2021.678757

Synovial Macrophages in Osteoarthritis: The Key to Understanding Pathogenesis?

Amanda Thomson and Catharien M. U. Hilkens *

Immunotherapy Research Group, Translational and Clinical Research Institute, Faculty of Medical Sciences, Newcastle University, Newcastle Upon Tyne, United Kingdom

Effective treatment of osteoarthritis (OA) remains a huge clinical challenge despite major research efforts. Different tissues and cell-types within the joint contribute to disease pathogenesis, and there is great heterogeneity between patients in terms of clinical features, genetic characteristics and responses to treatment. Inflammation and the most abundant immune cell type within the joint, macrophages, have now been recognised as possible players in disease development and progression. Here we discuss recent findings on the involvement of synovial inflammation and particularly the role of synovial macrophages in OA pathogenesis. Understanding macrophage involvement may hold the key for improved OA treatments.

Keywords: osteoarthritis, pathogenesis, macrophage subsets, synovial tissue, inflammation

OPEN ACCESS

Edited by:
Katharina Schmidt-Bleek, Charité – Universitätsmedizin Berlin, Germany

Reviewed by:
Carla R. Scanzello, University of Pennsylvania, United States
Simon Mastbergen, University Medical Center Utrecht, Netherlands

***Correspondence:**
Catharien M. U. Hilkens
catharien.hilkens@newcastle.ac.uk

Specialty section:
This article was submitted to Inflammation, a section of the journal Frontiers in Immunology

Received: *10 March 2021*
Accepted: *30 April 2021*
Published: *15 June 2021*

Citation:
Thomson A and Hilkens CMU (2021) Synovial Macrophages in Osteoarthritis: The Key to Understanding Pathogenesis? Front. Immunol. 12:678757. doi: 10.3389/fimmu.2021.678757

INTRODUCTION

Osteoarthritis (OA) is the most common form of arthritis, characterised by pain, swelling and stiffness of the joint. It is also multifactorial in nature, with associated risk factors such as age, sex, ethnicity and obesity. Primary locations affected are synovial joints, including the knee, hip and hands, with knee OA being most frequently observed. OA affects 7% of the global population and it is estimated that one third of people over the age of 65 suffer with the disease. This equates to approximately 500 million individuals, a figure which has risen by 48% from 1990-2019 (1–3). Even though OA is a leading cause of disability, the 15th highest cause of years lived with disability globally, no cure or disease modifying treatments are available (1). Symptoms are typically managed through a combination of non-pharmacological methods and non-steroidal anti-inflammatory drugs (NSAIDS). Surgical intervention through joint replacement still remains the only option for end-stage disease, emphasising the need for better treatment strategies. Here, we provide a short overview of the role of inflammation in OA pathogenesis, with a specific focus on the involvement of synovial macrophages. Unravelling the role of these cells may lead to improved stratification of OA patients for anti-inflammatory treatments and/or the identification of novel therapeutic targets.

OA PATHOGENESIS: CARTILAGE AND SUBCHONDRAL BONE

OA can affect the entire joint, including cartilage, synovial tissue, subchondral bone and the joint capsule, as well as ligaments and periarticular muscles (4). Cartilage degeneration is probably the most well-known hallmark of OA, and many studies have focused on understanding and preventing its destruction (5). The cartilage provides an important lubricated covering to the bone surfaces where the femur, tibia and patella articulate with each other. This absorbs stress created during movement and importantly, creates a smooth platform to allow for efficient joint motions. It comprises an extracellular matrix (ECM), composed mostly of type II collagen and aggrecan proteoglycans, which bring strength and flexibility to the tissue respectively (6, 7).

Chondrocytes constitute the cellular component (7) and maintain homeostasis through synthesis and degradation of the cartilage proteins. In OA, this equilibrium shifts to catabolism and chondrocytes adopt an activated state characterised by increased cell proliferation, molecular alterations and production of ECM degrading enzymes. This leads to cartilage damage (8–10). MMP family proteins and aggrecanases, the most widely studied ECM degrading enzymes, are both able to degrade native collagen and aggrecan (11–13). This breakdown of the ECM leads to fibrillation and subsequent fissure development within the cartilage layers and as a result, the subchondral bone (SB), situated directly beneath, is exposed to the articular cavity. The joint therefore becomes unable to function normally with regards to gliding movements and is incapable of effectively absorbing mechanical stress. Composed of the SB plate and underlying trabecular and subarticular bone, the SB functions as a shock absorber and helps distribute the mechanical load of the joint. Structural changes to SB can also be seen in OA, and include increased bone turnover, the development of microfractures and increased angiogenesis. Bone sclerosis, osteophytes, bone cysts and bone marrow lesions, detected *via* MRI can also be seen.

Inflammatory mediators have long been known to play a role in the breakdown of the cartilage ECM. In particular, OA patients have increased levels of IL-1β, TNF-α and IL-6. IL-1β is an essential mediator of joint inflammation and its overexpression by chondrocytes can be seen in early osteoarthritic cartilage (14, 15). Such levels cause an abnormal chondrocyte phenotype, which directly interferes with the synthesis of ECM collagen and aggrecan proteins. An associated increased release of MMP and aggracanase enzymes such as MMP-1, MMP-3 and MMP-13 is also seen, with destructive effects on cartilage components (16, 17). Functioning in an autocrine manner, IL-1β can induce its own secretion and stimulate the synthesis of other inflammatory mediators, again such as TNF-α and IL-6. Often found working in synergy with IL-1β, TNF-α binding to its receptors induces a similar NF-κB signalling cascade to increase inflammation and catabolism through enhancing adhesion molecule expression, the synthesis of further cytokines, and promoting the expression of more MMP family enzymes able to degrade the ECM (18, 19). Other cytokines such as IL-8, IL-18, IL-17 and IL-22 are increased when comparing human inflamed and non-inflamed synovial tissue (20). In particular such cytokines are associated with Th17 and NK22 cells, along with the recruitment of neutrophils into the tissue, all of which are capable of further promoting synovitis (20). IL-6, produced by cells such as chondrocytes, osteoblasts, fibroblasts, macrophages and adipocytes can also synergise with other cytokines to affect the ECM. However, evidence indicates IL-6 is the key cytokine to affect the SB layer of the joint by promoting the formation of osteoclasts to increase bone absorption within the joint (21, 22). Also associated with the bone itself, high TGF-β has been reported *via in vitro* and *in vivo* studies to promote the production of osteophytes, as well as increasing chondrocyte hypertrophy *via* alternative signalling pathways (23). Further descriptions of cytokines involved in OA are beyond the scope of this mini review, but such information has been discussed elsewhere (24).

OA PATHOGENESIS: SYNOVIAL TISSUE

The synovium lines the joint cavity. Its main function is to produce synovial fluid to equip the joint for efficient movement. Concentrations of synovial fluid components (lubrican and hyaluronic acid) are often altered in OA, influencing cartilage integrity. The synovium is composed of two main regions: the lining and sublining layers. Synovial lining consists mainly of macrophage and fibroblast cell types. The sublining contains additional fibroblasts, macrophages, adipose cells and blood vessels, with low numbers of lymphocytes also detectable (25).

Low-grade synovial inflammation has been observed in over half of OA patients at both early and late stages of disease (26–33) which has led to the notion that OA is not simply caused by an age-related wear and tear of the joint. Unlike more typical inflammatory arthritides [e.g., rheumatoid arthritis (RA)] OA synovitis is usually not accompanied by overt systemic inflammation. In RA, the inflamed synovium is characterised by vasculitis and a mixed immune cell infiltrate. This infiltrate predominantly consists of lymphocytes but also includes myeloid cells such as macrophages. Inflammation and angiogenesis in RA are further exacerbated due to antigen presentation and cytokine release. Subsequently, cartilage degradation and bone erosion arises over time in response to protease (e.g. MMPs) and cytokine release (e.g. TNF-α and IL-6) (34). A role for macrophages, with their associated inflammatory cytokines (IL-6 and TNF-α), has also been recognised in RA (35).

In OA, synovial inflammation is less pronounced, but there is ample evidence to support its pathogenic role (26, 30, 36). Histopathological studies since the 1980s have identified inflammatory signatures (cellular hyperproliferation, increased angiogenesis and lymphocyte aggregate appearance) within OA synovium (37–39). The degree of inflammation is highly heterogenous between patients, but nevertheless, has been associated with pain and disease progression. As highlighted in the previous section, inflammatory molecules, including IL-1β and TNF-α, are able to induce protease secretion by chondrocytes, highlighting possible crosstalk between the synovium and other

joint tissues (40). It has also been reported that the quantity of activated macrophages within patient OA synovium correlates with disease severity and progression (41). Synovitis confers a 9-fold greater risk of individuals presenting with painful knee OA (30). Elevated inflammatory markers have been detected in the serum and synovial fluid of OA patients and levels of serum TNF-α correlate with OA kellgren-lawrence X-ray grades (42). However, whilst treatments to dampen inflammation in RA have shown success (43), trials with anti-inflammatory drugs in OA have been disappointing thus far. A possible reason may be that the inflammatory players and processes differ greatly between patients; a notion that is supported by heterogeneity of the immune cell infiltrate in the OA synovium. For example, bi-compartmental OA is characterised by higher infiltration of $CD4^+$ T cells into the synovium than uni-compartmental disease (44) and we recently demonstrated highly variable numbers of macrophages as well as other immune cell subsets in the OA synovium (45). Therefore, we argue that a better understanding of the inflammatory players in OA would benefit the development of improved therapeutic strategies; either through stratification of OA patients for the most suitable disease-modifying treatments and/or the identification of novel targets.

SYNOVIAL MACROPHAGES

The most abundant immune cell type in the OA synovium is the macrophage. Macrophages are often described as displaying an M1 or M2 phenotype. Activated by environmental factors such as IFN-γ, TNF-α and LPS, M1 macrophages secrete pro-inflammatory cytokines and low levels of IL-10. M2 macrophages display an anti-inflammatory profile and possess tissue-repair functions (46). However, such M1/M2 descriptions are now regarded as extreme poles of a spectrum in many fields, with macrophage phenotype varying greatly depending on the tissue environment. High macrophage numbers are detected in OA patients compared to healthy controls and quantities of activated macrophages correlate with clinical symptoms (41, 47). Furthermore, increases in macrophage associated molecules (sCD163 and sCD14) and chemoattractants such as CCL2 and CX_3CL_1 in OA patient synovial fluid are linked with clinical outcome in OA (48, 49). It is thought that synovial macrophages respond to danger-associated molecular associated patterns, including cartilage fragments and intracellular proteins from necrotic cells, consequently contributing to cartilage damage and bone alterations through the release of cytokines such as IL-1β, TNF-α and TGF-β (**Figure 1**). In support of this, *in vitro* studies have highlighted that depletion of $CD14^+$ macrophages from synovial cell cultures results in a reduction of IL-1β, TNF-α, MMPs and aggrecanase enzymes which are able to degrade joint cartilage (50). Latest research investigating joint macrophages under normal and disease conditions (RA and OA) has led to the identification of multiple synovial macrophage subsets in the same joint. In a setting were inflammation aids disease, it's probable that the abundance of distinct macrophage subsets could perpetuate or indeed help to resolve OA.

NOVEL SYNOVIAL MACROPHAGE SUBSETS IN INFLAMMATORY ARTHRITIS

To carry out comprehensive investigations of joint macrophages Culemann and colleagues utilised transgenic mice and models of inflammatory arthritis (51). Exploring the origin of increased

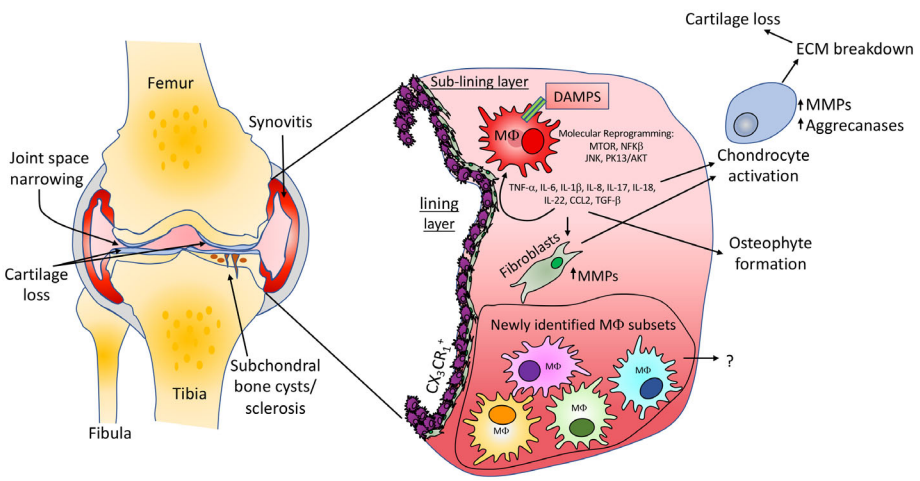

FIGURE 1 | Knee osteoarthritis pathology and macrophage involvement. Common features of OA including cartilage loss, narrowing of the joint space, synovitis and the development of subchondral bone cysts and sclerosis are shown. Macrophages in the synovium can contribute to OA *via* the release of inflammatory molecules which are able to stimulate resident fibroblast populations to produce cartilage extracellular matrix degrading enzymes. Inflammatory molecules are also able to activate chondrocytes, promoting an abnormal molecular and cellular phenotype, again promoting cartilage loss. We suggest that the same or similar macrophage populations newly identified in inflammatory arthritis studies will be found in OA tissues, may differ between clinical states and could provide therapeutic targets for subgroups of patients. The identification and impact of such populations in OA development is yet to be determined.

macrophage numbers during arthritis, the authors identified a CX_3CR_1+ macrophage subset in direct proximity with collagen VI expressing synovial fibroblast cells. This subset expressed tight junctional protein markers usually associated with that of endothelial cells (F11r, ZO-1 and claudin-5), was maintained by a distinct Ki67+ CX_3CR_1- interstitial macrophage population and formed a dense barrier between the synovial capillary network and the intra-articular space. At the onset of arthritis CX_3CR_1+ macrophages underwent altered morphology, and their cell-to-cell contacts were abrogated. Consequently, there was a breakdown of the "macrophage barrier" and CX_3CR_1- macrophage populations were found to rapidly proliferate in response. Coincidingly blood-derived macrophages infiltrated the tissue. The CX_3CR_1+ macrophage subset may therefore promote an important synovial regulatory function to seclude and protect intra-articular structures. Work to identify macrophage populations capable of promoting a "macrophage barrier" and the downstream implications of this in human OA could prove to be highly advantageous. Comparing RNA sequencing of mouse macrophage populations the authors also showed that CX_3CR_1+ macrophages expressed immune related genes (TREM2 and VSIG4) and that additional heterogeneity existed within CX_3CR_1- macrophages (51). This is a significant observation as mouse macrophage expression profiles correlate with recent sc-RNA sequencing data sets from human RA patients. Exploring human synovial macrophages within RA, and using OA tissue as a comparison, Zhang and colleagues identified four transcriptionally distinct subsets (SCM1-M4) (52). In particular, the presence of IL-1β+ pro-inflammatory macrophages (SCM1 subset) were upregulated in "leukocyte-rich" RA tissue compared to OA samples. Conversely, a SCM2 subset, which express VSIG4 similar to mouse CX_3CR_1+ macrophages, were upregulated in OA, suggesting they too are a resident synovial population.

In line with this, Alivernini and colleagues recently identified that clinically distinct states of RA can be characterised by relative proportions of particular macrophage populations. Firstly, healthy donor macrophages and those from patients in remission phenotypically were MerTK+ and CD206+. Patients with active RA had higher amounts of MerTK- CD206- and fewer MerTK+ CD206+ macrophages (53). Delving further to unravel the heterogeneity of these two populations, sc-RNA sequencing revealed nine distinct synovial macrophage clusters that could be classified into again four subpopulations: TREM2+, $FOLR2^{high}$, HLA+ and CD48+. Comparing relative gene ontology pathways of the nine macrophage clusters with clinical state revealed that MerTK+ TREM2+ and MerTK+ FOLR2+ macrophages were predominantly in healthy tissue. They also showed gene expression (ALDH1A1 and VSIG4) that would promote regulation of adaptive immunity through inhibition of T effector cells. Patients with sustained remission showed an increase in MerTK+ $FOLR2^{high}$ LYVE1+ macrophages which link this subset to tissue remodelling and homeostasis. In comparison, treatment naïve and active RA had increased proportions of MerTK- CD48- SPP1+ and MerTK- CD48- S100A12+ clusters which showed a pro-inflammatory transcriptome phenotype. The authors further showed that the MerTK- CD206- and MerTK+ CD206+ macrophage clusters were able to induce proinflammatory responses and repair synovial fibroblasts phenotypes, respectively. An overview of all novel synovial macrophages can be seen in **Table 1**.

SYNOVIAL MACROPHAGE SUBSETS IN OA

Macrophages in OA are not completely understood and most studies to date refer to macrophages as M1/M2, as comprehensively reviewed by Fernandes and colleagues (54). M1 macrophages in OA are linked with destructive processes: down regulation of collagen type II and aggrecan synthesis, and upregulation of enzymes such as MMP-1, -3, -9 and -13 (55). In comparison, there is murine evidence that "tissue repairing" M2 macrophage associated cytokines IL-4 and IL-10 are induced with moderate physical activity within the OA synovium, potentially promoting a protective environment (56). Macrophage-related chemokine CCL2, produced in response to inflammatory stimuli by chondrocytes, and its receptor CCR2 has also been noted. Depletion of CCL2/CCR2 is associated with decreased pain severity and older knockout mice show reduced structural disease after joint de-stabilisation (57). The upstream inducer of CCL2, TGF-α has been identified as a possible gene candidate for determining human OA risk and cartilage thickness. TGF-α inhibition in models also shows reduced structural disease, making this an interesting macrophage-related therapeutic target (58). In other mouse studies, contradictory results are reported. Macrophage depletion has been shown to reduce OA symptoms such as osteophyte formation in some cases, but in others increased synovitis can be seen due to $CD3^+$ T cell and neutrophil infiltration (59, 60). Discrepancies of macrophage manipulation in mouse models however could relate to the mechanism of disease onset used e.g., obesity, surgical etc., something which may suggest the presence of possible OA phenotypes.

With new knowledge of RA synovial macrophage subsets emerging that goes beyond the classical M1/M2 concept, there is further potential to generate new therapeutic strategies to promote the resolution of synovitis in OA, specifically targeting patients that would likely benefit most. Whether the same cellular populations and mechanisms exist in OA remains unclear and is currently under investigation. Nevertheless, the first study to explore and characterise the cellular and transcriptional heterogeneity on a single cell level in matched synovial and cartilage from OA patients was recently published by the Kraus laboratory (61). Here the authors identify twelve synovial cellular populations, including two distinct macrophage populations, and show that key OA mediators (TNF, IL-6 and IL-1β) are released into the joint space *via* HLA-DRA+ macrophages and DCs. Cytokine expression was 25-fold higher within the synovium compared to damaged cartilage areas and no cytokine was exclusively expressed by chondrocytes themselves. This emphasises the possible crosstalk between

TABLE 1 | Recently Identified novel macrophage subsets.

Reference	Species	Macrophage subset	Sub-populations	Clusters identified	Associated disease or clinical state	Associated surface marker or gene expression	Location in Synovium	Additional information
(52)	Human	SC-M1: IL-1β^{pos}, NR4A2^{pos} HBEGF^{pos} PLAUR^{pos} RGS2^{pos} ATF3^{pos}	–	–	↑ leukocyte-rich RA	Mass cytometry: CD11C+ CD38+ RNA-seq: CD14+ CD11C+++ CD38+++	Not specified	–
		SC-M2: MerTK^{pos} HTRA1^{pos}	–	–	↓ leukocyte-rich RA ↑ OA	Mass cytometry: CD11C- RNA-seq: CD14+ CD11C+ CD38-	Not specified	Possibly equivalent to mouse resident macrophage populations.
		SC-M3: CD14^{pos} C1QA^{pos} MARCO^{pos}	–	–	Marginally ↑ OA	–	Not specified	Possibly equivalent to mouse resident macrophage populations.
		SC-M4: LY6E^{pos} IFITM3^{pos} IFI6^{pos} SPP1^{pos}	–	–	↑ leukocyte-rich RA	Mass cytometry: CD11C+ CD38+	Not specified	
(53)	Human	MerTK^{pos} CD206^{pos}	TREM2^{pos} FOLR2^{pos}	TREM2^{pos} TimD4^{pos} CD163^{high}	↑ Healthy donors ↑ RA remission ↓ Active RA ↓Treatment naive	–	MerTK^{pos} TREM2^{pos} cells form a neat lining layer in healthy and RA remission synovium. The cells are dispersed in active RA. TREM2^{high} macrophages are homologs of mouse TREM2^{pos} CX3CR1^{pos} lining layer cells.	Gene expression suggests a role for microbe, apoptotic cell and oxysterol clearance as well as restraining inflammation. TREM2^{high} cells express tight junctional protein genes suggesting barrier functions.
				TREM2^{low}	↑ Healthy ↑ RA remission ↑ UPA ↓ Active RA	–	–	
			FOLR2^{high} TREM2^{neg}	D2^{pos}	Similar proportions in healthy and RA tissues.	–	Not specified	Possible equivalent to mouse M-CSF-driven *in situ* precursors of resident macrophages.
				LYVE1^{pos}	↑ Healthy ↑ RA remission ↓ Active RA ↓ Treatment naive	–	Localised to lining layer in healthy and remission RA. Localised round sublining layer blood vessels in active RA.	Express genes related to collagen turnover, antiprotease enzymes, coagulation factors and regulators of VEGF.
				ICAM1^{pos}	Similar proportions in healthy and RA tissues.	–	Not specified	High expression of proinflammatory cytokine genes e.g., TNF.
		MerTK^{neg} CD206^{neg}	HLA^{high} CD48^{pos}	ISG15^{pos}	↑ Active RA	–	Not specified	–
				CLEC10A^{pos}	Similar proportions in healthy and RA tissues identified by SCRNA-seq, but flow cytometry suggests increases in active RA.	–	Exclusively located in the sublining layer, located adjacent to TREM2^{pos} macrophages in all samples.	Enriched in antigen-presentation pathway genes, DC markers and transcription factors suggesting this is a tissue-resident antigen presenting population. Has high

(Continued)

TABLE 1 | Continued

Reference	Species	Macrophage subset	Sub-populations	Clusters identified	Associated disease or clinical state	Associated surface marker or gene expression	Location in Synovium	Additional information
								HBEGF expression, shown to promote fibroblast invasiveness.
			$CD48^{pos}$	$S100A12^{pos}$	↑ Active RA ↑ Treatment naïve	–	Located in sublining layer	Abundance of alarmins acting as chemoattractants for neutrophils and monocyte/fibroblast production of TNF and IL-6.
				$SPP1^{pos}$	↑ Active RA ↑ Treatment naïve ↓RA remission	–	Located in sublining layer	Osteopontin is highly expressed in this cluster and has proinflammatory and bone reabsorbing properties.
(51)	Mouse	CD45+ CD11b+ Ly6G+ $CX3CR1^{pos}$ lining macrophages	–	–	Spatial location and morphology alter upon inflammatory arthritis onset	SC-RNA-seq: $TREM2^{pos}$ $VSIG4^{pos}$ $Sparc^{pos}$	Membrane-forming lining macrophages located between synovial capillary network and intra-articular space.	Express tight junctional proteins e.g., ZO-1, claudin-5 and JAM-1.
		CD45+ CD11b+ Ly6G+ $CX3CR1^{neg}$ interstitial macrophages	$MHCII^{pos}$	–	–	SC-RNA-seq: $H2\text{-}EB1^{pos}$ $H2\text{-}AB1^{pos}$	Located within synovial interstitium	Proliferate to contribute to the pool of $CX3CR1^{pos}$ lining macrophages. Proliferation is enhanced during arthritis onset.
			RELM-α^{pos}	–	–	SC-RNA-seq: $MRC1^{pos}$ $CD163^{pos}$ $CCL8^{pos}$ $CCL7^{pos}$		
			$AQP1^{pos}$	–	–	SC-RNA-seq: $FXYD2^{pos}$ $LYVE1^{pos}$		

joint tissues in OA development. Such cytokine upregulation in the synovium may have synergistic effects on signalling pathways within other joint tissues to increase inflammation and in turn promote cartilage breakdown (62). This study again displays a potential for tissue specific targeting of pathogenic molecules or cells within the synovium itself in order to treat OA (61).

A recent study from our own laboratory identified distinct human knee OA endotypes (where insights of the pathogenic mechanism of disease are given) based on gene expression profiles of synovial macrophages. One of these endotypes displayed increased numbers of synovial CD14+ macrophages that closely aligned with synovial macrophages from inflammatory arthritis patients and displayed a cell proliferation signature and high Ki67 expression (45). However, whether this finding is in any way comparable with Ki67-expressing CX_3CR_1- macrophages in mice remains to be answered. The discovery of multiple synovial macrophage subsets may help to explain the contradicting results derived from *in vivo* macrophage-depletion studies of OA, and it is thought that macrophage subset identification could be used to aid the stratification of patients for treatment. Understanding the impact of specific synovial macrophage subsets is a research priority, with fundamental questions remaining. Do the same macrophage subsets exist in OA as in RA? Do macrophage subsets differ between OA disease stages? Do particular macrophage subsets associate with clinical symptoms? And importantly, what other cells within the synovial environment do macrophage subsets communicate with or influence? Unearthing such information could prove crucial for understanding OA pathogenesis and importantly reveal new therapeutic targets. Identification of several macrophage subsets within joint tissue truly advocates for an alternative assessment of how this cellular population is involved in OA.

FUTURE DIRECTIONS

New directions for OA research are imperative as clinical trials for disease-modifying treatments thus far have been largely disappointing. Disease heterogeneity often is suggested as a possible explanation. In 2016 Dell'Isola and colleagues provided evidence for the existence of six major OA clinical phenotypes (where observable traits are used to define disease clusters), reporting that 84% of subjects across twenty-four studies could be classified in this manner (63). 12% of OA patients could be classified into an "inflammatory" phenotype,

whilst the others were characterised into chronic pain, metabolic syndrome, bone and cartilage metabolism, mechanical overload and minimal disease phenotypes. Regardless of such classifications, trials of anti-IL-1 agents that specifically focused on patients with synovitis (the inflammatory phenotype) still resulted in limited improvement in pain scores and synovial inflammation (64). This implies factors other than IL-1 are at play in this patient subgroup. The ability to further classify patients more effectively could significantly transform and enhance OA clinical trial efficiency. Such approaches have already been applied in other settings such as in RA and asthma, as a method for identifying "clinicopathobiologic clusters" (65–67). By selecting patients based on particular OA molecular features, such as signalling pathways or other distinct molecular mechanisms as opposed to only by clinical phenotype, such as the presence of synovitis, patient subgroups most likely to benefit from particular therapies may be more easily identified. Of course, revealing molecular endotypes of OA is an extremely complex task. Advancements in imaging techniques, identification of novel OA biomarkers and increased knowledge of cellular communications (like that of macrophage subsets) within joint tissues will be of great importance. Ultimately, this approach could facilitate the development of better treatment strategies for OA patients.

AUTHOR CONTRIBUTIONS

AT and CH conceived the idea of the manuscript and performed literature searches. AT wrote the manuscript. CH reviewed and edited the manuscript. All authors contributed to the article and approved the submitted version.

FUNDING

This work was funded by the JGW Patterson Foundation.

REFERENCES

1. Hunter DJ, March L, Chew M. Osteoarthritis in 2020 and Beyond: A Lancet Commission. *Lancet* (2020) 396:1711–2. doi: 10.1016/10.1001/jamapediatrics.2020.4573
2. Hunter DJ, Bierma-Zeinstra S. Osteoarthritis. *Lancet* (2019) 393:1745–59. doi: 10.1016/S0140-6736(19)30417-9
3. Martel-Pelletier J, Barr AJ, Cicuttini FM, Conaghan PG, Cooper C, Goldring MB, et al. Osteoarthritis. *Nat Rev Dis Primers* (2016) 2:1–18. doi: 10.1038/nrdp.2016.72
4. Loeser RF, Goldring SR, Scanzello CR, Goldring MB. Osteoarthritis: A Disease of the Joint as An Organ. *Arthritis Rheum* (2012) 64(6):1697–707. doi: 10.1002/art.34453
5. Young DA, Barter MJ, Wilkinson DJ. Recent Advances in Understanding the Regulation of Metalloproteinases. *F1000 Res* (2019) 8:195. doi: 10.12688/f1000research.17471.1
6. Buckwalter JA, Mankin HJ. Articular Cartilage: Tissue Design and Chondrocyte-Matrix Interactions. *Instr Course Lectures* (1998) 47:477–86. doi: 10.2106/00004623-199704000-00021
7. Bhosale AM, Richardson JB. Articular Cartilage: Structure, Injuries and Review of Management. *Br Med Bull* (2008) 87:77–95. doi: 10.1093/bmb/ldn025
8. Goldring MB, Marcu KB. Cartilage Homeostasis in Health and Rheumatic Diseases. *Arthritis Res Ther* (2009) 11:224. doi: 10.1186/ar2592
9. Katsara O, Attur M, Ruoff R, Abramson SB, Kolupaeva V. Increased Activity of the Chondrocyte Translational Apparatus Accompanies Osteoarthritic Changes in Human and Rodent Knee Cartilage. *Arthritis Rheumatol* (2017) 69(3):586–97. doi: 10.1002/art.39947
10. Mitchell PG, Magna HA, Reeves LM, Lopresti-Morrow LL, Yocum SA, Rosner PJ, et al. Cloning, Expression, and Type II Collagenolytic Activity of Matrix Metalloproteinase-13 From Human Osteoarthritic Cartilage. *J Clin Invest* (1996) 97(3):761–8. doi: 10.1172/JCI118475
11. Sandy JD. A Contentious Issue Finds Some Clarity: On the Independent and Complementary Roles of Aggrecanase Activity and MMP Activity in Human Joint Aggrecanolysis. *Osteoarthr Cartil* (2006) 14:95–100. doi: 10.1016/j.joca.2005.09.004
12. Rengel Y, Ospelt C, Gay S. Proteinases in the Joint: Clinical Relevance of Proteinases in Joint Destruction. *Arthritis Res Ther* (2007) 9:22. doi: 10.1186/ar2304
13. Cawston TE, Wilson AJ. Understanding the Role of Tissue Degrading Enzymes and Their Inhibitors in Development and Disease. *Best Pract Res Clin Rheumatol* (2006) 20:983–1002. doi: 10.1016/j.berh.2006.06.007
14. Fan Z, Bau B, Yang H, Soeder S, Aigner T. Freshly Isolated Osteoarthritic Chondrocytes are Catabolically More Active Than Normal Chondrocytes, But Less Responsive to Catabolic Stimulation With Interleukin-1? *Arthritis Rheum* (2005) 52(1):136–43. doi: 10.1002/art.20725
15. Towle CA, Hung HH, LJ B, Treadwell BV, Mangham DC. Detection of Interleukin-1 in the Cartilage of Patients With Osteoarthritis: A Possible Autocrine/Paracrine Role in Pathogenesis. *Osteoarthr Cartil* (1997) 5(5):293–300. doi: 10.1016/S1063-4584(97)80008-8
16. Vincenti MP, Brinckerhoff CE. Transcriptional Regulation of Collagenase (MMP-1, MMP-13) Genes in Arthritis: Integration of Complex Signalling Pathways for the Recruitment of Gene-Specific Transcription Factors. *Arthritis Res* (2002) 4:157–64. doi: 10.1186/ar401
17. Mengshol JA, Vincenti MP, Coon CI, Barchowsky A, Brinckerhoff CE. Interleukin-1 Induction of Collagenase 3 (Matrix Metalloproteinase 13) Gene Expression in Chondrocytes Requires p38, C-Jun N-terminal Kinase, and Nuclear Factor κB: Differential Regulation of Collagenase 1 and Collagenase 3. *Arthritis Rheum* (2000) 43(4):801–11. doi: 10.1002/1529-0131(200004)43:4<801::AID-ANR10>3.0.CO;2-4
18. Roman-Blas JA, Jimenez SA. Nf-κB as A Potential Therapeutic Target in Osteoarthritis and Rheumatoid Arthritis. *Osteoarthr Cartil* (2006) 14:839–48. doi: 10.1016/j.joca.2006.04.008
19. Marcu K B, Otero M, Olivotto E, Maria Borzi R, B. Goldring M. NF-κB Signaling: Multiple Angles to Target OA. *Curr Drug Targets* (2010) 11(5):599–613. doi: 10.2174/138945010791011938
20. Deligne C, Casulli S, Pigenet A, Bougault C, Campillo-Gimenez L, Nourissat G, et al. Differential Expression of Interleukin-17 and Interleukin-22 in Inflamed and Non-Inflamed Synovium From Osteoarthritis Patients. *Osteoarthr Cartil* (2015) 23(11):1843–52. doi: 10.1016/j.joca.2014.12.007
21. Steeve KT, Marc P, Sandrine T, Dominique H, Yannick F. IL-6, RANKL, TNF-Alpha/IL-1: Interrelations in Bone Resorption Pathophysiology. *Cytokine Growth Factor Rev* (2004) 15:49–60. doi: 10.1016/j.cytogfr.2003.10.005
22. Chenoufi HL, Diamant M, Rieneck K, Lund B, Stein GS, Lian JB. Increased mRNA Expression and Protein Secretion of Interleukin-6 in Primary Human Osteoblasts Differentiated *In Vitro* From Rheumatoid and Osteoarthritic Bone. *J Cell Biochem* (2001) 81(4):666–78. doi: 10.1002/jcb.1104
23. van der Kraan PM. Differential Role of Transforming Growth Factor-Beta in an Osteoarthritic or a Healthy Joint. *J Bone Metab* (2018) 25(2):65. doi: 10.11005/jbm.2018.25.2.65
24. Chow YY, Chin K-Y. The Role of Inflammation in the Pathogenesis of Osteoarthritis. *Mediators Inflamm* (2020) 2020:8293921. doi: 10.1155/2020/8293921

25. Smith M D. The Normal Synovium. *Open Rheumatol J* (2012) 5(1):100–6. doi: 10.2174/1874312901105010100
26. Haywood L, McWilliams DF, Pearson CI, Gill SE, Ganesan A, Wilson D, et al. Inflammation and Angiogenesis in Osteoarthritis. *Arthritis Rheum* (2003) 48 (8):2173–7. doi: 10.1002/art.11094
27. Benito MJ, Veale DJ, FitzGerald O, Van Den Berg WB, Bresnihan B. Synovial Tissue Inflammation in Early and Late Osteoarthritis. *Ann Rheum Dis* (2005) 64(9):1263–7. doi: 10.1136/ard.2004.025270
28. Torres L, Dunlop DD, Peterfy C, Guermazi A, Prasad P, Hayes KW, et al. The Relationship Between Specific Tissue Lesions and Pain Severity in Persons With Knee Osteoarthritis. *Osteoarthr Cartil* (2006) 14(10):1033–40. doi: 10.1016/j.joca.2006.03.015
29. Hill CL, Hunter DJ, Niu J, Clancy M, Guermazi A, Genant H, et al. Synovitis Detected on Magnetic Resonance Imaging and Its Relation to Pain and Cartilage Loss in Knee Osteoarthritis. *Ann Rheum Dis* (2007) 66(12):1599–603. doi: 10.1136/ard.2006.067470
30. Baker K, Grainger A, Niu J, Clancy M, Guermazi A, Crema M, et al. Relation of Synovitis to Knee Pain Using Contrast-Enhanced MRIs. *Ann Rheum Dis* (2010) 69(10):1779–83. doi: 10.1136/ard.2009.121426
31. Conaghan PG, D'Agostino MA, Le Bars M, Baron G, Schmidely N, Wakefield R, et al. Clinical and Ultrasonographic Predictors of Joint Replacement for Knee Osteoarthritis: Results From a Large, 3-Year, Prospective EULAR Study. *Ann Rheum Dis* (2010) 69(4):644–7. doi: 10.1136/ard.2008.099564
32. Roemer FW, Guermazi A, Felson DT, Niu J, Nevitt MC, Crema MD, et al. Presence of MRI-Detected Joint Effusion and Synovitis Increases the Risk of Cartilage Loss in Knees Without Osteoarthritis at 30-Month Follow-Up: The MOST Study. *Ann Rheum Dis* (2011) 70(10):1804–9. doi: 10.1136/ard.2011.150243
33. Scanzello CR, McKeon B, Swaim BH, Dicarlo E, Asomugha EU, Kanda V, et al. Synovial Inflammation in Patients Undergoing Arthroscopic Meniscectomy: Molecular Characterization and Relationship to Symptoms. *Arthritis Rheum* (2011) 63(2):391–400. doi: 10.1002/art.30137
34. Smolen JS, Aletaha D, McInnes IB. Rheumatoid Arthritis. *Lancet* (2016) 388:2023–38. doi: 10.1016/S0140-6736(16)30173-8
35. Kurowska-Stolarska M, Alivernini S. Synovial Tissue Macrophages: Friend or Foe? *RMD Open* (2017) 3:e000527. doi: 10.1136/rmdopen-2017-000527
36. Mathiessen A, Conaghan PG. Synovitis in Osteoarthritis: Current Understanding With Therapeutic Implications. *Arthritis Res Ther* (2017) 19:18. doi: 10.1186/s13075-017-1229-9
37. Goldenberg DL, Egan MS, Cohen AS. Inflammatory Synovitis in Degenerative Joint Disease. *J Rheumatol* (1982) 9(2):204-9.
38. Lindblad S, Hedfors E. Arthroscopic and Immunohistologic Characterization of Knee Joint Synovitis in Osteoarthritis. *Arthritis Rheum* (1987) 30(10):1081–8. doi: 10.1002/art.1780301001
39. Revell PA, Mayston V, Lalor P, Mapp P. The Synovial Membrane in Osteoarthritis: A Histological Study Including the Characterisation of the Cellular Infiltrate Present in Inflammatory Osteoarthritis Using Monoclonal Antibodies. *Ann Rheum Dis* (1988) 47(4):300–7. doi: 10.1136/ard.47.4.300
40. Milner JM, Kevorkian L, Young DA, Jones D, Wait R, Donell ST, et al. Fibroblast Activation Protein Alpha Is Expressed by Chondrocytes Following a Pro-Inflammatory Stimulus and Is Elevated in Osteoarthritis. *Arthritis Res Ther* (2006) 8(1):R23. doi: 10.1186/ar1877
41. Kraus VB, McDaniel G, Huebner JL, Stabler TV, Pieper CF, Shipes SW, et al. Direct In Vivo Evidence of Activated Macrophages in Human Osteoarthritis. *Osteoarthr Cartil* (2016) 24(9):1613–21. doi: 10.1016/j.joca.2016.04.010
42. Özler K, Aktas E, Atay Ç, Yilmaz B, Arikan M, Güngör S. Serum and Knee Synovial Fluid Matrix Metalloproteinase-13 and Tumor Necrosis Factor-Alpha Levels in Patients With Late-Stage Osteoarthritis. *Acta Orthop Traumatol Turc* (2016) 50(3):356–61. doi: 10.1016/j.aott.2015.11.003
43. Burmester GR, Pope JE. Novel Treatment Strategies in Rheumatoid Arthritis. *Lancet* (2017) 389:2338–48. doi: 10.1016/S0140-6736(17)31491-5
44. Moradi B, Rosshirt N, Tripel E, Kirsch J, Barié A, Zeifang F, et al. Unicompartmental and Bicompartmental Knee Osteoarthritis Show Different Patterns of Mononuclear Cell Infiltration and Cytokine Release in the Affected Joints. *Clin Exp Immunol* (2015) 180(1):143–54. doi: 10.1111/cei.12486
45. Wood MJ, Leckenby A, Reynolds G, Spiering R, Pratt AG, Rankin KS, et al. Macrophage Proliferation Distinguishes 2 Subgroups of Knee Osteoarthritis Patients. *JCI Insight* (2019) 4(2):e125325. doi: 10.1172/jci.insight.125325
46. Mills CD, Kincaid K, Alt JM, Heilman MJ, Hill AM. M-1/M-2 Macrophages and the Th1/Th2 Paradigm. *J Immunol* (2000) 164(12):6166–73. doi: 10.4049/jimmunol.164.12.6166
47. Liu B, Zhang M, Zhao J, Zheng M, Yang H. Imbalance of M1/M2 Macrophages Is Linked to Severity Level of Knee Osteoarthritis. *Exp Ther Med* (2018) 16(6):5009–14. doi: 10.3892/etm.2018.6852
48. Daghestani HN, Pieper CF, Kraus VB. Soluble Macrophage Biomarkers Indicate Inflammatory Phenotypes in Patients With Knee Osteoarthritis. *Arthritis Rheumatol* (2015) 67(4):956–65. doi: 10.1002/art.39006
49. Huo LW, Ye YL, Wang GW, Ye YG. Fractalkine (CX3CL1): A Biomarker Reflecting Symptomatic Severity in Patients With Knee Osteoarthritis. *J Investig Med* (2015) 63(4):626–31. doi: 10.1097/JIM.0000000000000158
50. Bondeson J, Wainwright SD, Lauder S, Amos N, Hughes CE. The Role of Synovial Macrophages and Macrophage-Produced Cytokines in Driving Aggrecanases, Matrix Metalloproteinases, and Other Destructive and Inflammatory Responses in Osteoarthritis. *Arthritis Res Ther* (2006) 8(6): R187. doi: 10.5772/28284
51. Culemann S, Grüneboom A, Nicolás-Ávila JÁ, Weidner D, Lämmle KF, Rothe T, et al. Locally Renewing Resident Synovial Macrophages Provide A Protective Barrier for the Joint. *Nature* (2019) 572:670–5. doi: 10.1038/s41586-019-1471-1
52. Zhang F, Wei K, Slowikowski K, Fonseka CY, Rao DA, Kelly S, et al. Defining Inflammatory Cell States in Rheumatoid Arthritis Joint Synovial Tissues by Integrating Single-Cell Transcriptomics and Mass Cytometry. *Nat Immunol* (2019) 20(7):928–42. doi: 10.1038/s41590-019-0378-1
53. Alivernini S, MacDonald L, Elmesmari A, Finlay S, Tolusso B, Gigante MR, et al. Distinct Synovial Tissue Macrophage Subsets Regulate Inflammation and Remission in Rheumatoid Arthritis. *Nat Med* (2020) 26:1295–306. doi: 10.1038/s41591-020-0939-8
54. Fernandes TL, Gomoll AH, Lattermann C, Hernandez AJ, Bueno DF, Amano MT. Macrophage: A Potential Target on Cartilage Regeneration. *Front Immunol* (2020) 11:111. doi: 10.3389/fimmu.2020.00111
55. Fahy N, de Vries-van Melle ML, Lehmann J, Wei W, Grotenhuis N, Farrell E, et al. Human Osteoarthritic Synovium Impacts Chondrogenic Differentiation of Mesenchymal Stem Cells *Via* Macrophage Polarisation State. *Osteoarthr Cartil* (2014) 22(8):1167–75. doi: 10.1016/j.joca.2014.05.021
56. Castrogiovanni P, Di Rosa M, Ravalli S, Castorina A, Guglielmino C, Imbesi R, et al. Moderate Physical Activity as a Prevention Method for Knee Osteoarthritis and the Role of Synoviocytes as Biological Key. *Int J Mol Sci* (2019) 20(3):511. doi: 10.3390/ijms20030511
57. Raghu H, Lepus CM, Wang Q, Wong HH, Lingampalli N, Oliviero F, et al. CCL2/CCR2, But Not CCL5/CCR5, Mediates Monocyte Recruitment, Inflammation and Cartilage Destruction in Osteoarthritis. *Ann Rheum Dis* (2017) 76(5):914–22. doi: 10.1136/annrheumdis-2016-210426
58. Appleton CTG, Usmani SE, Pest MA, Pitelka V, Mort JS, Beier F. Reduction in Disease Progression by Inhibition of Transforming Growth Factor α-CCL2 Signalling in Experimental Posttraumatic Osteoarthritis. *Arthritis Rheumatol (Hoboken NJ)* (2015) 67(10):2691–701. doi: 10.1002/art.39255
59. Blom AB, van Lent PLEM, Holthuysen AEM, van der Kraan PM, Roth J, van Rooijen N, et al. Synovial Lining Macrophages Mediate Osteophyte Formation During Experimental Osteoarthritis. *Osteoarthr Cartil* (2004) 12(8):627–35. doi: 10.1016/j.joca.2004.03.003
60. Wu CL, McNeill J, Goon K, Little D, Kimmerling K, Huebner J, et al. Conditional Macrophage Depletion Increases Inflammation and Does Not Inhibit the Development of Osteoarthritis in Obese Macrophage FAS-Induced Apoptosis–Transgenic Mice. *Arthritis Rheumatol* (2017) 69(9):1772–83. doi: 10.1002/art.40161
61. Chou CH, Jain V, Gibson J, Attarian DE, Haraden CA, Yohn CB, et al. Synovial Cell Cross-Talk With Cartilage Plays a Major Role in the Pathogenesis of Osteoarthritis. *Sci Rep* (2020) 10(1):1–14. doi: 10.1038/s41598-020-67730-y
62. Wojdasiewicz P, Poniatowski ŁA, Szukiewicz D. The Role of Inflammatory and Anti-Inflammatory Cytokines in the Pathogenesis of Osteoarthritis. *Mediators Inflamm* (2014) 2014:1–19. doi: 10.1155/2014/561459
63. Dell'Isola A, Allan R, Smith SL, Marreiros SSP, Steultjens M. Identification of Clinical Phenotypes in Knee Osteoarthritis: A Systematic Review of the Literature. *BMC Musculoskelet Disord* (2016) 17(1):1–12. doi: 10.1186/s12891-016-1286-2

64. Fleischmann RM, Bliddal H, Blanco FJ, Schnitzer TJ, Peterfy C, Chen S, et al. A Phase II Trial of Lutikizumab, an Anti–Interleukin-1α/β Dual Variable Domain Immunoglobulin, in Knee Osteoarthritis Patients With Synovitis. *Arthritis Rheumatol* (2019) 71(7):1056–69. doi: 10.1002/art.40840
65. Blair JPM, Bager C, Platt A, Karsdal M, Bay-Jensen AC. Identification of Pathological RA Endotypes Using Blood-Based Biomarkers Reflecting Tissue Metabolism. A Retrospective and Explorative Analysis of Two Phase III RA Studies. *PloS One* (2019) 14(7):e0219980. doi: 10.1371/journal.pone.0219980
66. Hinks TSC, Brown T, Lau LCK, Rupani H, Barber C, Elliott S, et al. Multidimensional Endotyping in Patients With Severe Asthma Reveals Inflammatory Heterogeneity in Matrix Metalloproteinases and Chitinase 3–Like Protein 1. *J Allergy Clin Immunol* (2016) 138(1):61–75. doi: 10.1016/j.jaci.2015.11.020
67. Svenningsen S, Nair P. Asthma Endotypes and An Overview of Targeted Therapy for Asthma. *Front Med* (2017) 4:158. doi: 10.3389/fmed.2017.00158

Conflict of Interest: The authors declare that the research was conducted in the absence of any commercial or financial relationships that could be construed as a potential conflict of interest.

frontiers in Immunology

REVIEW
published: 30 June 2021
doi: 10.3389/fimmu.2021.687551

T-Cell Mediated Inflammation in Postmenopausal Osteoporosis

*Di Wu, Anna Cline-Smith, Elena Shashkova, Ajit Perla, Aditya Katyal and Rajeev Aurora**

Department of Molecular Microbiology and Immunology, Saint Louis University School of Medicine, St. Louis, MO, United States

Osteoporosis is the most prevalent metabolic bone disease that affects half the women in the sixth and seventh decade of life. Osteoporosis is characterized by uncoupled bone resorption that leads to low bone mass, compromised microarchitecture and structural deterioration that increases the likelihood of fracture with minimal trauma, known as fragility fractures. Several factors contribute to osteoporosis in men and women. In women, menopause – the cessation of ovarian function, is one of the leading causes of primary osteoporosis. Over the past three decades there has been growing appreciation that the adaptive immune system plays a fundamental role in the development of postmenopausal osteoporosis, both in humans and in mouse models. In this review, we highlight recent data on the interactions between T cells and the skeletal system in the context of postmenopausal osteoporosis. Finally, we review recent studies on the interventions to ameliorate osteoporosis.

Keywords: T cell, postmenopausal osteoporosis, estrogen loss, osteoimmunology, chronic inflammation

OPEN ACCESS

Edited by:
Massimo De Martinis, University of L'Aquila, Italy

Reviewed by:
Kripa Elizabeth Cherian, Christian Medical College & Hospital, India
Luigi Gennari, University of Siena, Italy

***Correspondence:**
Rajeev Aurora
rajeev.aurora@health.slu.edu

Specialty section:
This article was submitted to Inflammation, a section of the journal Frontiers in Immunology

Received: *29 March 2021*
Accepted: *04 June 2021*
Published: *30 June 2021*

Citation:
Wu D, Cline-Smith A, Shashkova E, Perla A, Katyal A and Aurora R (2021) T-Cell Mediated Inflammation in Postmenopausal Osteoporosis. Front. Immunol. 12:687551. doi: 10.3389/fimmu.2021.687551

INTRODUCTION

A great achievement of modern medicine is the increased lifespan of the human population. Unfortunately, the comorbidities of aging have created a large economic and health burden on society. The current challenge is to improve the healthspan and thus to reduce the burden. Osteoporosis is the most prevalent metabolic bone disease that affects half the women and one third of men, typically, in the sixth and seventh decade of life (1, 2). Osteoporosis is characterized by uncoupled bone resorption that leads to low bone mass, compromised microarchitecture and structural deterioration that increases the likelihood of fracture with minimal trauma. These fragility fractures lead to disproportionally high mortality rate and a drastic decline in quality of life for those affected.

Bone remodeling occurs th0roughout life and is a coordinated process to repair microfractures and maintain bone mass. Imbalances in the bone remodeling process underscore the pathophysiology of osteoporosis. Bone remodeling is a tightly coupled: resorption precedes formation and the amount of bone formed is balanced with the amount resorbed. Remodeling can be initiated by hormonal, environmental and nutritional factors (3). The major cell types involved in bone remodeling are bone resorbing osteoclasts (OC) and bone forming osteoblasts (OB). Over the last decade the bone-embedded osteocytes (Ocy) have also emerged as a key regulators. OC are multinucleated cells from the monocytic lineage whose differentiation depends on receptor activator of NF-κB (RANK) and its ligand (RANKL). OB differentiate from the mesenchymal stem cell (MSC) lineage and is regulated by several signaling pathways such as WNT/β-catenin and BMP. During remodeling the OC and OB form the bone remodeling unit (BRU).

Ocy are stellate like cells enclosed within mineralized bone. They serve as mechanosensors within the bone and play a key regulatory role in bone homeostasis, directing and coordinating repair by regulating the BRU.

It was recognized nearly eight decades ago that involutional osteoporosis in postmenopausal women is mediated by loss of estrogen (E2) (4). The mechanism for how E_2 loss leads to increased bone resorption has remained, despite intense focus of investigations (5). Decreased calcium absorption (6, 7), decline in renal function (8) and impaired vitamin D metabolism (9, 10) with aging and menopause. Over the past three decades there has been growing appreciation that the adaptive immune system plays a fundamental role in the development of postmenopausal osteoporosis (PMOP), both in humans and in mouse models. The recognition that T-cell derived cytokines affect bone has given rise to the field of osteoimmunology, a word was first coined in 2000 by Arron and Choi (11). There have been major advances in our understanding of the pro-resorptive effects of pro-inflammatory cytokine, in particular TNFα and interleukine IL-17A made by T cell. In this review, we highlight recent data on the interactions between T cells and the skeletal system in the context of PMOP. We also review recent studies on the interventions to ameliorate osteoporosis, with insights into immunomodulatory options. Finally, we highlight some questions that still remain unanswered.

POSTMENOPAUSAL OSTEOPOROSIS

While dietary, lifestyle and other factors impact bone health (12, 13), in general there are two main reasons for the decline of bone mass. The skeletal system grows rapidly postnatally and through puberty and peak bone mass is attained by mid to late 20s (14). Both men and women gradually loss bone mass as they age (15) and the rate of loss varies by anatomical site (16). In addition to aging, loss of sex hormones and in particular estrogen (E_2) contribute to skeletal homeostasis (5, 17, 18).

Sex hormones increase during puberty and are maintained during reproductive age. While testosterone (T) decreases linearly with age in men, women experience a sharp decline in E_2 at menopause. Menopause, is the cessation of ovarian function, is one of the leading causes of primary osteoporosis. Early studies suggested that E_2 directly regulates OC (19–22) and OB (23, 24) and its loss results in long lived OC and impaired OB leading to uncoupled bone resorption (25). Accordingly, PMOP has been traditionally regarded as an endocrinal, E_2 deficiency mediated disease. While epidemiological observation suggest that E_2 loss is responsible for osteoporosis in both sexes, the mechanism in males remains unclear. The role of estrogen and androgens on the bone have been extensively reviewed previously (25–27). In the next section, we will focus on the role of the immune system in the pathogenesis of PMOP.

THE CROSSTALK BETWEEN THE BONE AND THE IMMUNE SYSTEM

In the past few decades, evidence has emerged supporting the notion that E_2 loss promotes persistent inflammation that promote osteoporosis and perhaps other comorbidities. The mechanistic studies for linking E_2 loss at menopause and activation of the T cells has come from ovariectomy (OVX) of rodents and key outcomes have been validated in human studies. In this section, we highlight recent advances in our understanding on how T cells and proinflammatory cytokines, namely TNFα and IL-17A, contribute to the pathogenesis of PMOP (**Figure 1**).

Inflammation Tips the Balance in Favor of Bone Resorption Through Osteoclasts

Takayanagi et al. were the first to report the bone-immune cross talk, demonstrating that T-cell produced IFN-γ can inhibit RANKL signaling during OC differentiation (28). Because Th1 are major producers of IFN-γ, inflammatory bone loss was thought as a Th1 mediated pathology. It was later demonstrated that Th17 cells are key drivers of bone erosion (29) and IL-17A is a potent promoter of bone destruction, particularly in the context of autoimmune pathologies (30–32). TNFα has also been shown to directly act on OC and its precursors in synergy with RANKL to promote osteoclastogenesis (33–36). Bone appears to be sensitive to T-cell derived cytokines even at distal anatomical sites. For instance, decline in bone mass is observed in patients with chronic HIV (37, 38), Hepatitis B and C (39) infections. Hepatic viruses also affect conversion of vitamin D3 to the metabolically active form calcitriol because they infect hepatocytes and affect calcium absorption in addition to increased IL-17A production by T-cells (40, 41). Increased prevalence of fracture are also observed in patients with rheumatoid arthritis (RA), inflammatory bowel disease (IBD) and chronic obstructive pulmonary disease (COPD) (42–45). The local cytokine milieu can contextually promote or protect against bone loss and the mechanism for how TNFα and IL-17A favor bone resorption *via* OC have been reviewed extensively (46, 47).

In the past decade, several studies showed that the immune system and inflammation play a critical pathogenic role in uncoupled bone loss in the context of E_2 loss (30, 48–52). OVX of sexually mature mice that were T-cell deficient showed decreased bone loss, demonstrating that T-cells are required for promoting bone resorption (53–57). Recently, our lab has described a new pathway where E_2 loss leads to chronic low-grade production of the proinflammatory cytokines TNFα and IL-17 by converting memory T-cells (T_M) to effector T_M (T_{EM}). We showed that there us increased levels of IL-7 and IL-15. Both these cytokines are produced by bone marrow dendritic cells (BMDCs). E_2 induces Fas ligand and apoptosis of BMDC and also T_M. In the absence of E_2, the BMDC become long-lived, which leads to higher IL-7 and IL-15 and to antigen-independent activation of a subset of T_M to produce TNFα and IL-17A (58) (**Figure 2**). The canonical activation of T_M and subsequent conversion to T_{EM} are antigen-dependent (59), thus the activation observed by E_2-loss does not follow the established paradigm. OVX of IL15Rα$^{\Delta T\text{-cells}}$ mice, where T_M cannot convert into T_{EM}, did not result in bone loss (58). Our results uncovered another aspect of how E_2 is anti-inflammatory, as it maintains T_M homeostasis and limits their conversion to T_{EM} in the absence of antigen.

The gut microbiome (GMB) plays an important role in regulating bone mass. A number of studies have shown an

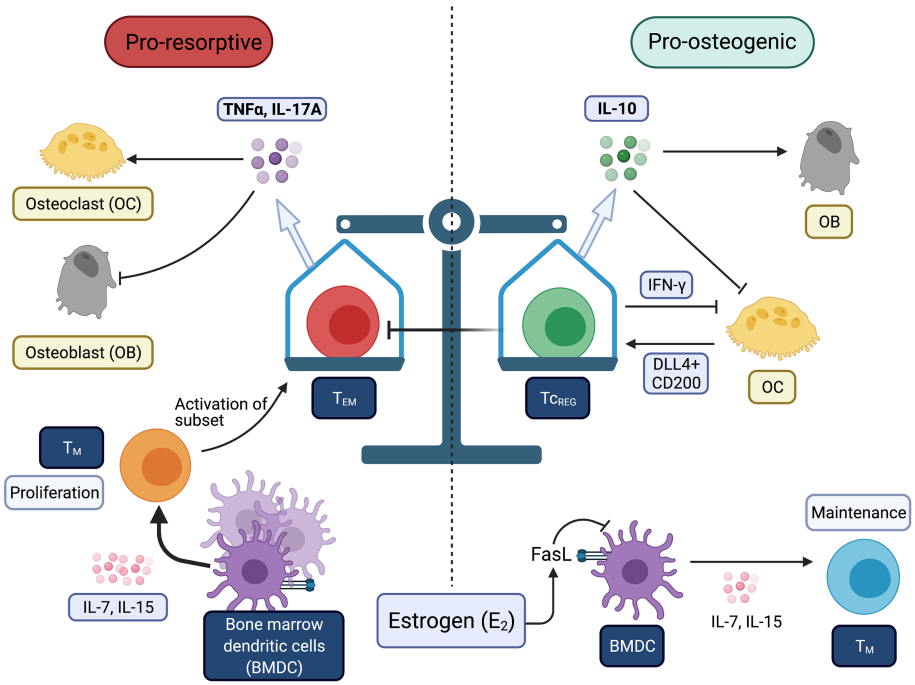

FIGURE 1 | Balance between immunogenic and tolergenic states is linked with resorptive and osteogenic states of the bone. Chronic inflammation may be derived by increases in effector T-cells (T_{EFF}) and effector memory T-cells (T_{EM}). Bone is very sensitive to TNFα and IL-17A produced by T-cells. Estrogen (E_2) prevents the conversion of T_M to T_{EM}. Tolerogenic T-cells (i.e., T_{REG} and Tc_{REG}) promote bone formation through direct and indirect mechanisms. All Figures were created with (BioRender.com).

association between GBM and bone health in both animal models (60, 61) and in humans (13). Germfree (GF) mice have increased bone mass compared to conventionally raised (CONV-R) mice, and restoration of GBM normalized bone mass in GF mice (62). E_2 loss increases gut permeability (63–65), which leads to increased priming and activation of inflammation in the gut mucosa, leading to the generation Th17 cells (66). GF mice do not lose bone post-OVX, and probiotics can prevent OVX-induced bone loss (67, 68). Recent studies have suggested GMB produce microbial metabolites that have regulatory function on distal organs, including the bone. GMB derived butyrate, polyamines and short-chain fatty acids have been shown to induce regulatory T cell (T_{REG}) generation in the colon and be able to directly regulate the BRU (69–71). Thus, there appear to be several mechanisms by which GMB modulate bone health: first, GMB produce metabolites that directly modulate bone mass. Second GBM induce Th17 cell to promote bone loss or T_{REG} to limit bone loss. Finally, GBM not only induce Th17 cells but many of these effector T-cells become T_M. A subset of T_M migrate to the bone marrow to become bone marrow resident T_M (72). Thus prior exposures of pathogens and commensals are encoded in the T_M. This may explain (at the population level) why only about half of postmenopausal women develop osteoporosis. Women who have more exposure to Th17 inducing microbes through their life would have a larger pool of T_M that convert to T_{EM} that produce IL-17 and TNFα postmenopause.

How Does Inflammation or Resolution of Inflammation Regulate Bone Mass?

The field has primarily focused on the effect of inflammation on OC as discussed above. How inflammation restrains bone formation is less well studied. Under coupled bone remodeling conditions, the increase in resorption is accompanied by recruitment of mesenchymal stromal cells (MSC) and their conversion to OB. However, in the presence of inflammatory cytokine (i.e., TNFα, IL-17 and IL-1β) this process appears to be impaired. Thus, bone formation lags behind bone resorption. Next, we discuss how proinflammatory cytokines effects the osteolineage.

Early *in vitro* culture studies showed that TNFα inhibited MSC to OB transition by regulating RUNX2 expression, a master transcription factor that commits MSC into osteogenic pathway. TNFα also targets Osterix (OSX; SP7) expression, a key transcription necessary for osteoblast maturation (73–75). Osteoblastogenesis is sensitive to glucose levels (76) and OB differentiation is regulated *via* mTOR pathway (77–80). While not clearly established in OB, there is precedence that TNFα regulates cellular metabolism in adipocytes and muscles cells (81–83). Since these three cell types all originate from MSC *via* different developmental pathway, it is likely that TNFα targets mTOR complexes in OB to alter cellular metabolism. Indeed, *in vitro* evidence demonstrated that TNFα can modulate autophagy and apoptosis *via* NF-κB signaling in OB (84–86) both of which

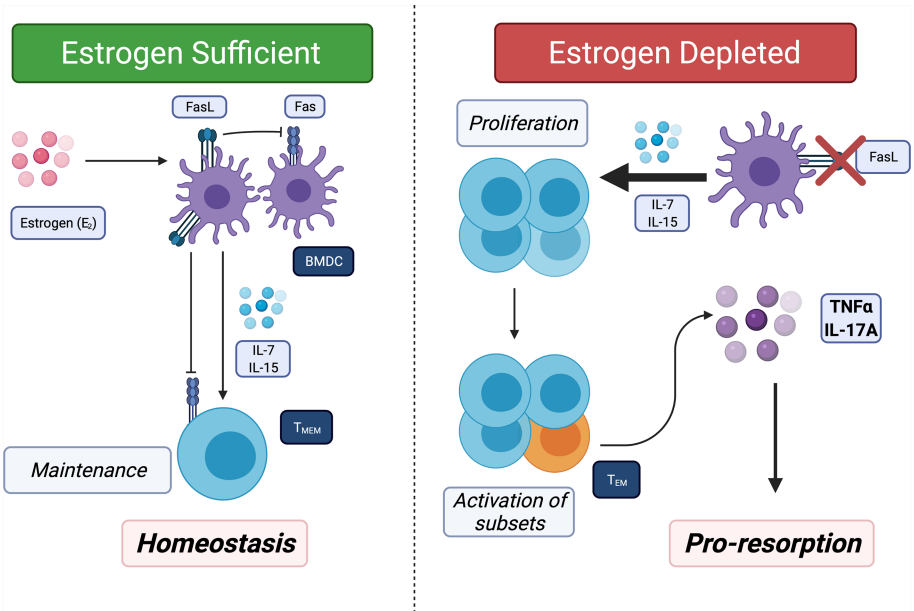

FIGURE 2 | Estrogen (E_2) regulates bone marrow resident memory T-cells (T_{BRM}) homeostasis and E_2 loss promotes conversion of T_{BRM} to T_{EM}. T_M migrate to and take up long-term residence in the bone marrow. *Left panel*: Bone marrow resident dendritic cells (BMDC) secrete IL-7, IL-15 or both to promote survival of T_M. In E_2 replete females, BMDC have a short lifespan because E_2 induces FasL in the BMDC. In addition, IL-15 induces Fas in proliferating T_M in response to IL-7 and IL-15 thus maintain a homeostatic pool of T_{BRM}. *Right*: In absence of E_2, Fas ligand (FasL) is no longer induced leading to increased lifespans of BMDC and high concentrations of IL-7 and IL-15. In the presence of high IL-7 and IL-15 and absence of FasL, all T_M proliferate and a subset (~5 to 10%) produce TNFα and IL-17A, which then promotes bone resorption and also limits bone formation.

are controlled by mTOR. While these results are controversial, there are reports indicating that IL-17A is able to affect MSC to OB differentiation as well as mature OB function and is summarized in a recent review (47). Understanding the effects of TNFα and IL-17A on OB will provide further insight into the imbalance between bone resorption and bone formation.

The effect of inflammation on Ocy is largely unknown. Ocy are regulators of bone homeostasis (87). Ocy produce RANKL that predominantly regulates osteoclastogenesis during remodeling (88, 89). In the presence of TNFα a much lower concentration of RANKL is needed to initiate osteoclastogenesis (90). Ablation of RANKL in Ocy *via* Dmp1-Cre protected against vertebral bone loss (91). TNFα and IL-17A can target Ocy to produce RANKL and thus contribute to increased resorption (92, 93). Furthermore, IL-17A can target Ocy to increase osteogenic differentiation of MSC in cooperation with OB (94). All evidence taken together, suggest that Ocy are at the center of BRU balance and regulate bone resorption and formation according to biological needs. OVX induced Ocy apoptosis (95) possibly *via* TNFα, IL-17A or both, suggesting that inflammation regulates bone health not just through OC or OB. Interestingly during lactation, where there is E_2 loss triggers the same BMDC induced uncoupled bone resorption as OVX, Ocy have been shown to undergo a process called osteocytic osteolysis that promotes bone resorption to release calcium from cortical bone (96). Further investigation is need to understand the role Ocy play in PMOP.

It is clear that the skeletal system is exquisitely sensitive to chronic inflammation suggesting that the skeletal system is "a canary in the coal mine" – a sensor of overall persistent inflammatory burden. All currently available data is consistent with the observation that PMOP is mediated by inflammation. Specifically, E_2 loss induces the conversion of bone marrow resident T_M to T_{EM} that secrete TNFα and IL-17A. These cytokines promote osteoclastogenesis and bone resorption and most likely also limit bone formation. However, the effect of TNFα and IL-17A on MSC, mature OB or Ocy is much less well understood. Future therapies for the treatment of PMOP should also address the underlying inflammation, which we will discuss in the following section.

THERAPEUTIC INTERVENTIONS

A number of therapies have been developed to treat osteoporosis in postmenopausal women. The traditional therapies fall into two classes: anti-resorptive and bone anabolics. Each has been used independently and in some clinical trials also used in combination.

Antiresorptive

The most commonly prescribed medication for osteoporosis are antiresorptives, notably bisphosphonates and denosumab. It has been reported that antiresorptives can interact with the immune

system. Bisphosphonates have been shown to boost B-cell function and promote humoral immunity (97). Denosumab has been associated with increased risks of infection (98) and more recently, being investigated for oncology alongside immune checkpoint inhibitors (99). One drawback with this class of medications are potential severe adverse effects. Osteonecrosis of the jaw (ONJ) is observed in 1-3% of patients on anti-resorptive therapies with certain predisposing factors (i.e., after tooth extraction or in people with type 2 diabetes) (100–102). Atypical femoral fractures have also been reported in patients on bisphosphonates (103) while denosumab discontinuation have been associated with higher risk of vertebral fractures (104). Another disadvantage of anti-resorptive treatment is that there is a specific window where they are most effective. In addition, inhibition of bone resorption prevents bone remodeling and repair leading to effete bone that fractures from minimal trauma (105). As a result, while the patient may maintain BMD, it does not reflect that whether they have improved bone quality.

Anabolics

The second class of therapies are bone anabolics. A commonly used bone anabolic is teriparatide, derived from parathyroid hormone (PTH) (106). More recently romosozumab that targets sclerostin (product of the SOST gene) (107) has been approved as a bone anabolic biologic. Neutralization of sclerostin increases OB numbers and simultaneously suppresses bone resorption thus promoting bone formation. However, due to adaptive changes in bone and potential adverse effects with prolonged use, bone anabolic therapies are limited in their use (108–110), particularly in special populations (111). Antiresorptive therapies (RANKL blockade or bisphosphonates) in postmenopausal women did not increase bone mass in the SHOTZ clinical trial (112, 113) indicating that deficit in OB activity remains. Remarkably, while bone anabolic therapy improve bone mineral density, bone microarchitecture did not improve unless both antiresorptive and anabolic agents were combined (114–116). These results suggest that efficacy is obtained by using both antiresorptive (brakes on OC) and anabolics as accelerator. Since sclerostin is primarily (but not exclusively) produced by Ocy, the action and mechanism of action on Ocy remains to be understood.

All current therapies target the cells of the BRU, either to suppress resorption or to promote bone formation. Furthermore, the current therapies have shortcomings and adverse effects with prolonged use necessitating drug holidays (117).

Immunomodulatory Options

Therapeutic option that target the immune system has recently gained interested as treatment option for PMOP. Given that a number of inflammatory conditions lead to bone destruction, inhibition of specific cytokine signaling have also been used to disrupt the cell-cell signaling and to protect against bone destruction. Blockade of TNFα (118) and IL-17A (119) in mice have shown to prevent OVX-induced bone loss. Etanercept (anti-TNFα) have been used to treat PMOP patients and showed decreases in serum markers of bone resorption (120), which warrant further investigation whether it is safer and better than current therapies (121). A recent study showed that neutralization of IL-17A induces compensatory increase of other Th17 cytokines, including IL-17F, IL-22 and GM-CSF (122). While secukinumab (anti-IL-17A) has not been evaluated for the treatment of osteoporosis, this finding highlights the complex nature of targeting cytokines in preventing bone loss.

Probiotic supplementation can be considered as an immunomodulatory therapy, given the role of GMB in regulating bone health as mentioned in this review. Bone loss in OVX mice can be prevented with supplementation of probiotics (68). While randomized controlled trial were conducted (123) and showed reduction in bone loss in particular with *Lactobacillus reuteri* (124), these results should be interpreted with caution and further studies are needed to evaluate the benefits of probiotics.

Our laboratory discovered that OC are antigen presenting cells during bone resorption that express DLL4, CD200 and MHC I and induce naïve $CD8^+$ T cells to become $FoxP3^+$ regulatory T cells (Tc_{REG}) (**Figure 3**). Tc_{REG} express Eomes and T-bet, have increased the surface expression of CD25 and CTLA-4, and produce IFN-γ and IL-10 (125, 126). Bone resorbing OC induce Tc_{REG} which in turn suppress bone resorption, forming a negative feedback loop (127). Tc_{REG} are also immunosuppressive in addition to regulating OC (128). Both *in vivo* induction by low dose pulsed RANKL (pRANKL) and adoptive transfer of *ex vivo* generated Tc_{REG} suppressed bone resorption, TNFα and IL-17A levels and promoted bone formation (129) to ameliorate osteoporosis in OVX mice. In unpublished studies, IL-10 directly regulate OB at the gene expression level and OVX of IL-10 deficient mice were unresponsive to the anabolic effects of pRANKL. However, Tc_{REG} retained its ability to inhibit TNFα production in T_{EM}. Induction of Tc_{REG} has two facets: first, regulatory T-cells promote a tolerogenic environment by reducing the overall inflammatory burden; second, induction of regulatory T-cells is not expected to immunocompromise the host, unlike targeting inflammatory cytokines with antibodies (i.e., TNF blockade) or by JAK inhibitors. Targeting inflammatory cytokines represses both chronic and acute inflammation and thus increases risk of opportunistic infections. In contrast, inducing antigen-specific regulatory T-cells can precisely target chronic inflammation. Furthermore, while cytokine blockade may slow disease progression, regulatory T-cells promote resolution of inflammation to restore immune homeostasis (130–132). Taken together, our observations indicate that the immune system plays a fundamental role in modulating bone homeostasis, able to tip the balance either in favor of uncoupled bone resorption or bone formation.

CONCLUSION AND PERSPECTIVES

In this review we highlighted how T_M have emerged to be at the center of the pathophysiology of PMOP. These results demonstrate that E_2 loss promotes inflammation leading to the acute phase bone erosion. We also underscore that none of the currently approved therapies for PMOP target inflammation but were intended to act directly on the BRU. The therapies also underscore that increasing bone mass may not be sufficient to reduce risk of fractures. How the proinflammatory cytokines

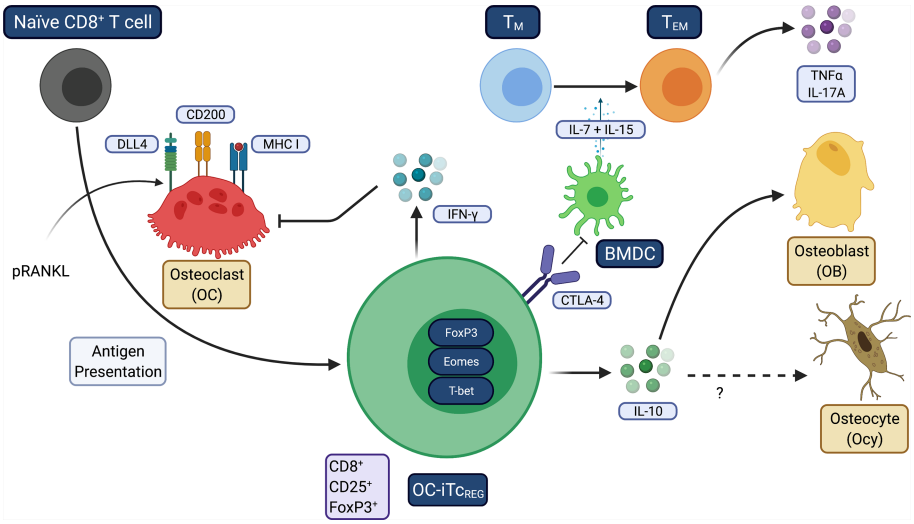

FIGURE 3 | Osteoclasts induce tolerogenic Tc_{REG}. This figure summarizes how OC induce Tc_{REG} to promote restore homeostasis under inflammatory conditions. OC use three signals: antigen-loaded MHC I that ligates TCR on CD8 T-cells, CD200 (a costimulation molecule that activates NF-κB) and the Notch ligand DLL4 that engages Notch1 and Notch4 on the T-cells. TNFα and/or IL-17A downregulate DLL4 expression on OC. Treatment with pRANKL leads to increased expression DLL4. Tc_{REG} secrete IFN-γ that suppress osteoclastogenesis by degrading TRAF6 and also suppress resorption by mature OC. Tc_{REG} also secrete IL-10, which is required for the bone anabolic activity but not resolution of inflammation. IL-10 may also target Ocy to improve cortical bone mass. Resolution of inflammation appears to be mediated by CTLA4 expressed on Tc_{REG}.

TNFα, IL-17A and IL-1β leads to increased OC differentiation and increased resorption are well understood. In contrast, we do not have a similar level of understanding on the action of inflammation on OB and Ocy. We also highlighted how resolution of inflammation leads to increased bone formation. Additional studies are needed to understand the mechanism and the targets. In this context, better therapies will emerge from efforts to understand how Ocy sense bone quality and promote the repair process to produce bone that is resilient and less likely to fail. The correlation between bone mass (primarily by mineralization) to improving bone quality, with improved biomechanical properties needs to be further defined. Research in current decade is likely to provide new insights and mechanisms into the crosstalk. Revealing the mechanistic details on immune regulation on bone homeostasis will provide exciting new targets for therapies.

AUTHOR CONTRIBUTIONS

RA conceived of the manuscript. DW and RA drafted the manuscript. AP and AK created figures and helped with edits. AC-S and ES provided literature search and edits. All authors were involved in scientific discussion of the review. All authors contributed to the article and approved the submitted version.

FUNDING

Research reported in this study was partially supported by National Institute of Arthritis and Musculoskeletal and Skin Disease of the NIH under Award Number RO1AR064821 and RO1AR068438. Washington University Musculoskeletal Research Core (NIH P30 AR057235) also partially supported this study.

ACKNOWLEDGMENTS

We thank Daniel Goering, Yiyi Zhang and Lizzie Geerling for contributing to additional unpublished experiments referenced herein.

REFERENCES

1. Melton LJ. The Prevalence of Osteoporosis: Gender and Racial Comparison. *Calcif Tissue Int* (2001) 69(4):179. doi: 10.1007/s00223-001-1043-9
2. Wright NC, Looker AC, Saag KG, Curtis JR, Delzell ES, Randall S, et al. The Recent Prevalence of Osteoporosis and Low Bone Mass in the United States Based on Bone Mineral Density at the Femoral Neck or Lumbar Spine. *J Bone Miner Res* (2014) 29(11):2520–6. doi: 10.1002/jbmr.2269
3. Kenkre JS, Bassett J. The Bone Remodelling Cycle. *Ann Clin Biochem* (2018) 55(3):308–27. doi: 10.1177/0004563218759371
4. Albright F, Smith PH, Richardson AM. Postmenopausal Osteoprosis: its Clinical Feature. *JAMA* (1941) 116(22):2465–74. doi: 10.1001/jama.1941.02820220007002
5. Riggs BL, Khosla S, Melton LJ3rd. A Unitary Model for Involutional Osteoporosis: Estrogen Deficiency Causes Both Type I and Type II Osteoporosis in Postmenopausal Women and Contributes to Bone Loss

in Aging Men. *J Bone Miner Res* (1998) 13(5):763–73. doi: 10.1359/jbmr.1998.13.5.763
6. Fujita T. Calcium Intake, Calcium Absorption, and Osteoporosis. *Calcif Tissue Int* (1996) 58(4):215. doi: 10.1007/BF02508637
7. Avioli LV, McDonald JE, Lee SW. The Influence of Age on the Intestinal Absorption of 47-Ca Absorption in Post-Menopausal Osteoporosis. *J Clin Invest* (1965) 44(12):1960–7. doi: 10.1172/JCI105302
8. Ledger GA, Burritt MF, Kao PC, O'Fallon WM, Riggs BL, Khosla S. Role of Parathyroid Hormone in Mediating Nocturnal and Age-Related Increases in Bone Resorption. *J Clin Endocrinol Metab* (1995) 80(11):3304–10. doi: 10.1210/jcem.80.11.7593443
9. Eastell R, Yergey AL, Vieira NE, Cedel SL, Kumar R, Riggs BL. Interrelationship Among Vitamin D Metabolism, True Calcium Absorption, Parathyroid Function, and Age in Women: Evidence of an Age-Related Intestinal Resistance to 1,25-Dihydroxyvitamin D Action. *J Bone Miner Res* (1991) 6(2):125–32. doi: 10.1002/jbmr.5650060205
10. Francis RM, Peacock M, Taylor GA, Storer JH, Nordin BE. Calcium Malabsorption in Elderly Women With Vertebral Fractures: Evidence for Resistance to the Action of Vitamin D Metabolites on the Bowel. *Clin Sci (Lond)* (1984) 66(1):103–7. doi: 10.1042/cs0660103
11. Arron JR, Choi Y. Bone Versus Immune System. *Nature* (2000) 408 (6812):535–6. doi: 10.1038/35046196
12. Aurora R. Confounding Factors in the Effect of Gut Microbiota on Bone Density. *Rheumatology (Oxford)* (2019) 58(12):2089–90. doi: 10.1093/rheumatology/kez347
13. Das M, Cronin O, Keohane DM, Cormac EM, Nugent H, Nugent M, et al. Gut Microbiota Alterations Associated With Reduced Bone Mineral Density in Older Adults. *Rheumatology (Oxford)* (2019) 58(12):2295–304. doi: 10.1093/rheumatology/kez302
14. Burr DB. Muscle Strength, Bone Mass, and Age-Related Bone Loss. *J Bone Miner Res* (1997) 12(10):1547–51. doi: 10.1359/jbmr.1997.12.10.1547
15. Bonnick SL. Osteoporosis in Men and Women. *Clin Cornerstone* (2006) 8 (1):28–39. doi: 10.1016/s1098-3597(06)80063-3
16. Aerssens J, Boonen S, Joly J, Dequeker J. Variations in Trabecular Bone Composition With Anatomical Site and Age: Potential Implications for Bone Quality Assessment. *J Endocrinol* (1997) 155(3):411–21. doi: 10.1677/joe.0.1550411
17. Nelson HD. Postmenopausal Osteoporosis and Estrogen. *Am Fam Physician* (2003) 68(4):606.
18. Riggs BL, Khosla S, Atkinson EJ, Dunstan CR, Melton LJ3rd. Evidence That Type I Osteoporosis Results From Enhanced Responsiveness of Bone to Estrogen Deficiency. *Osteoporos Int* (2003) 14(9):728–33. doi: 10.1007/s00198-003-1437-9
19. Nakamura T, Imai Y, Matsumoto T, Sato S, Takeuchi K, Igarashi K, et al. Estrogen Prevents Bone Loss Via Estrogen Receptor Alpha and Induction of Fas Ligand in Osteoclasts. *Cell* (2007) 130(5):811–23. doi: 10.1016/j.cell.2007.07.025
20. Oursler MJ, Landers JP, Riggs BL, Spelsberg TC. Oestrogen Effects on Osteoblasts and Osteoclasts. *Ann Med* (1993) 25(4):361–71. doi: 10.3109/07853899309147298
21. Oursler MJ, Osdoby P, Pyfferoen J, Riggs BL, Spelsberg TC. Avian Osteoclasts as Estrogen Target Cells. *Proc Natl Acad Sci U S A* (1991) 88 (15):6613–7. doi: 10.1073/pnas.88.15.6613
22. Oursler MJ, Pederson L, Pyfferoen J, Osdoby P, Fitzpatrick L, Spelsberg TC. Estrogen Modulation of Avian Osteoclast Lysosomal Gene Expression. *Endocrinology* (1993) 132(3):1373–80. doi: 10.1210/endo.132.3.8440193
23. Kovacic N, Lukic IK, Grcevic D, Katavic V, Croucher P, Marusic A. The Fas/Fas Ligand System Inhibits Differentiation of Murine Osteoblasts But has a Limited Role in Osteoblast and Osteoclast Apoptosis. *J Immunol* (2007) 178 (6):3379–89. doi: 10.4049/jimmunol.178.6.3379
24. Krum SA, Miranda-Carboni GA, Hauschka PV, Carroll JS, Lane TF, Freedman LP, et al. Estrogen Protects Bone by Inducing Fas Ligand in Osteoblasts to Regulate Osteoclast Survival. *EMBO J* (2008) 27(3):535–45. doi: 10.1038/sj.emboj.7601984
25. Vanderschueren D, Gaytant J, Boonen S, Venken K. Androgens and Bone. *Curr Opin Endocrinol Diabetes Obes* (2008) 15(3):250–4. doi: 10.1097/MED.0b013e3282fe6ca9
26. Almeida M, Laurent MR, Dubois V, Claessens F, O'Brien CA, Bouillon R, et al. Estrogens and Androgens in Skeletal Physiology and Pathophysiology. *Physiol Rev* (2017) 97(1):135–87. doi: 10.1152/physrev.00033.2015
27. Clarke BL, Khosla S. Physiology of Bone Loss. *Radiol Clin North Am* (2010) 48(3):483–95. doi: 10.1016/j.rcl.2010.02.014
28. Takayanagi H, Ogasawara K, Hida S, Chiba T, Murata S, Sato K, et al. T-Cell-Mediated Regulation of Osteoclastogenesis by Signalling Cross-Talk Between RANKL and IFN-Gamma. *Nature* (2000) 408(6812):600–5. doi: 10.1038/35046102
29. Sato K, Suematsu A, Okamoto K, Yamaguchi A, Morishita Y, Kadono Y, et al. Th17 Functions as an Osteoclastogenic Helper T Cell Subset That Links T Cell Activation and Bone Destruction. *J Exp Med* (2006) 203(12):2673–82. doi: 10.1084/jem.20061775
30. Tyagi AM, Srivastava K, Mansoori MN, Trivedi R, Chattopadhyay N, Singh D. Estrogen Deficiency Induces the Differentiation of IL-17 Secreting Th17 Cells: A New Candidate in the Pathogenesis of Osteoporosis. *PloS One* (2012) 7(9):e44552. doi: 10.1371/journal.pone.0044552
31. Komatsu N, Okamoto K, Sawa S, Nakashima T, Oh-hora M, Kodama T, et al. Pathogenic Conversion of Foxp3+ T Cells Into TH17 Cells in Autoimmune Arthritis. *Nat Med* (2014) 20(1):62–8. doi: 10.1038/nm.3432
32. Zhao R, Wang X, Feng F. Upregulated Cellular Expression of IL-17 by CD4+ T-Cells in Osteoporotic Postmenopausal Women. *Ann Nutr Metab* (2016) 68(2):113–8. doi: 10.1159/000443531
33. Zhao B, Grimes SN, Li S, Hu X, Ivashkiv LB. TNF-Induced Osteoclastogenesis and Inflammatory Bone Resorption are Inhibited by Transcription Factor RBP-J. *J Exp Med* (2012) 209(2):319–34. doi: 10.1084/jem.20111566
34. Azuma Y, Kaji K, Katogi R, Takeshita S, Kudo A. Tumor Necrosis Factor-α Induces Differentiation of and Bone Resorption by Osteoclasts. *J Biol Chem* (2000) 275(7):4858–64. doi: 10.1074/jbc.275.7.4858
35. Kobayashi K, Takahashi N, Jimi E, Udagawa N, Takami M, Kotake S, et al. Tumor Necrosis Factor α Stimulates Osteoclast Differentiation by a Mechanism Independent of the Odf/Rankl–Rank Interaction. *J Exp Med* (2000) 191(2):275–86. doi: 10.1084/jem.191.2.275
36. Lam J, Takeshita S, Barker JE, Kanagawa O, Ross FP, Teitelbaum SL. TNF-α Induces Osteoclastogenesis by Direct Stimulation of Macrophages Exposed to Permissive Levels of RANK Ligand. *J Clin Invest* (2000) 106(12):1481–8. doi: 10.1172/JCI11176
37. Moran CA, Weitzmann MN, Ofotokun I. Bone Loss in HIV Infection. *Curr Treat Options Infect Dis* (2017) 9(1):52–67. doi: 10.1007/s40506-017-0109-9
38. Ofotokun I, McIntosh E, Weitzmann MN. HIV: Inflammation and Bone. *Curr HIV/AIDS Rep* (2012) 9(1):16–25. doi: 10.1007/s11904-011-0099-z
39. Biver E, Calmy A, Rizzoli R. Bone Health in HIV and Hepatitis B or C Infections. *Ther Adv Musculoskelet Dis* (2017) 9(1):22–34. doi: 10.1177/1759720X16671927
40. Hoan NX, Tong HV, Song LH, Meyer CG, Velavan TP. Vitamin D Deficiency and Hepatitis Viruses-Associated Liver Diseases: A Literature Review. *World J Gastroenterol* (2018) 24(4):445–60. doi: 10.3748/wjg.v24.i4.445
41. Askari A, Naghizadeh MM, Homayounfar R, Shahi A, Afsarian MH, Paknahad A, et al. Increased Serum Levels of IL-17A and IL-23 are Associated With Decreased Vitamin D3 and Increased Pain in Osteoarthritis. *PloS One* (2016) 11 (11):e0164757. doi: 10.1371/journal.pone.0164757
42. Blaschke M, Koepp R, Cortis J, Komrakova M, Schieker M, Hempel U, et al. IL-6, IL-1beta, and TNF-alpha Only in Combination Influence the Osteoporotic Phenotype in Crohn's Patients Via Bone Formation and Bone Resorption. *Adv Clin Exp Med* (2018) 27(1):45–56. doi: 10.17219/acem/67561
43. Sapir-Koren R, Livshits G. Postmenopausal Osteoporosis in Rheumatoid Arthritis: The Estrogen Deficiency-Immune Mechanisms Link. *Bone* (2017) 103:102–15. doi: 10.1016/j.bone.2017.06.020
44. Klingberg E, Geijer M, Gothlin J, Mellstrom D, Lorentzon M, Hilme E, et al. Vertebral Fractures in Ankylosing Spondylitis are Associated With Lower Bone Mineral Density in Both Central and Peripheral Skeleton. *J Rheumatol* (2012) 39(10):1987–95. doi: 10.3899/jrheum.120316
45. Piodi LP, Poloni A, Ulivieri FM. Managing Osteoporosis in Ulcerative Colitis: Something New? *World J Gastroenterol* (2014) 20(39):14087–98. doi: 10.3748/wjg.v20.i39.14087

46. Zhao B. TNF and Bone Remodeling. *Curr Osteoporos Rep* (2017) 15(3):126–34. doi: 10.1007/s11914-017-0358-z
47. Tang M, Lu L, Yu X. Interleukin-17A Interweaves the Skeletal and Immune Systems. *Front Immunol* (2021) 11:625034(3841). doi: 10.3389/fimmu.2020.625034
48. Duque G, Huang DC, Dion N, Macoritto M, Rivas D, Li W, et al. Interferon-γ Plays a Role in Bone Formation In Vivo and Rescues Osteoporosis in Ovariectomized Mice. *J Bone Miner Res* (2011) 26(7):1472–83. doi: 10.1002/jbmr.350
49. Osta B, Benedetti G, Miossec P. Classical and Paradoxical Effects of TNF-α on Bone Homeostasis. *Front Immunol* (2014) 5(48):14–22. doi: 10.3389/fimmu.2014.00048
50. Tyagi AM, Mansoori MN, Srivastava K, Khan MP, Kureel J, Dixit M, et al. Enhanced Immunoprotective Effects by Anti-IL-17 Antibody Translates to Improved Skeletal Parameters Under Estrogen Deficiency Compared With Anti-RANKL and Anti-TNF-α Antibodies. *J Bone Miner Res* (2014) 29 (9):1981–92. doi: 10.1002/jbmr.2228
51. Ginaldi L, De Martinis M, Ciccarelli F, Saitta S, Imbesi S, Mannucci C, et al. Increased Levels of Interleukin 31 (IL-31) in Osteoporosis. *BMC Immunol* (2015) 16(1):60. doi: 10.1186/s12865-015-0125-9
52. Du D, Zhou Z, Zhu L, Hu X, Lu J, Shi C, et al. TNF-Alpha Suppresses Osteogenic Differentiation of MSCs by Accelerating P2Y2 Receptor in Estrogen-Deficiency Induced Osteoporosis. *Bone* (2018) 117:161–70. doi: 10.1016/j.bone.2018.09.012
53. Cenci S, Toraldo G, Weitzmann MN, Roggia C, Gao Y, Qian WP, et al. Estrogen Deficiency Induces Bone Loss by Increasing T Cell Proliferation and Lifespan Through IFN-gamma-induced Class II Transactivator. *Proc Natl Acad Sci U S A* (2003) 100(18):10405–10. doi: 10.1073/pnas.1533207100
54. Cenci S, Weitzmann MN, Roggia C, Namba N, Novack D, Woodring J, et al. Estrogen Deficiency Induces Bone Loss by Enhancing T-Cell Production of TNF-Alpha. *J Clin Invest* (2000) 106(10):1229–37. doi: 10.1172/jci11066
55. Roggia C, Gao Y, Cenci S, Weitzmann MN, Toraldo G, Isaia G, et al. Up-Regulation of TNF-Producing T Cells in the Bone Marrow: A Key Mechanism by Which Estrogen Deficiency Induces Bone Loss In Vivo. *Proc Natl Acad Sci U S A* (2001) 98(24):13960–5. doi: 10.1073/pnas.251534698
56. Roggia C, Tamone C, Cenci S, Pacifici R, Isaia GC. Role of TNF-alpha Producing T-Cells in Bone Loss Induced by Estrogen Deficiency. *Minerva Med* (2004) 95(2):125–32.
57. Weitzmann MN, Pacifici R. Estrogen Deficiency and Bone Loss: An Inflammatory Tale. *J Clin Invest* (2006) 116(5):1186–94. doi: 10.1172/JCI28550
58. Cline-Smith A, Axelbaum A, Shashkova E, Chakraborty M, Sanford J, Panesar P, et al. Ovariectomy Activates Chronic Low-Grade Inflammation Mediated by Memory T-Cells Which Promotes Osteoporosis in Mice. *J Bone Miner Res* (2020) 35(6):1174–87. doi: 10.1002/jbmr.3966
59. MacLeod MK, Kappler JW, Marrack P. Memory CD4 T Cells: Generation, Reactivation and Re-Assignment. *Immunology* (2010) 130(1):10–5. doi: 10.1111/j.1365-2567.2010.03260.x
60. Ohlsson C, Engdahl C, Fåk F, Andersson A, Windahl SH, Farman HH, et al. Probiotics Protect Mice From Ovariectomy-Induced Cortical Bone Loss. *PloS One* (2014) 9(3):e92368. doi: 10.1371/journal.pone.0092368
61. Britton RA, Irwin R, Quach D, Schaefer L, Zhang J, Lee T, et al. Probiotic L. Reuteri Treatment Prevents Bone Loss in a Menopausal Ovariectomized Mouse Model. *J Cell Physiol* (2014) 229(11):1822–30. doi: 10.1002/jcp.24636
62. Sjögren K, Engdahl C, Henning P, Lerner UH, Tremaroli V, Lagerquist MK, et al. The Gut Microbiota Regulates Bone Mass in Mice. *J Bone Miner Res* (2012) 27(6):1357–67. doi: 10.1002/jbmr.1588
63. Sabui S, Skupsky J, Kapadia R, Cogburn K, Lambrecht NW, Agrawal A, et al. Tamoxifen-Induced, Intestinal-Specific Deletion of Slc5a6 in Adult Mice Leads to Spontaneous Inflammation: Involvement of NF-kappaB, NLRP3, and Gut Microbiota. *Am J Physiol Gastrointest Liver Physiol* (2019) 317(4): G518–30. doi: 10.1152/ajpgi.00172.2019
64. Roomruangwong C, Carvalho AF, Geffard M, Maes M. The Menstrual Cycle may Not be Limited to the Endometrium But Also may Impact Gut Permeability. *Acta Neuropsychiatr* (2019) 31(6):294–304. doi: 10.1017/neu.2019.30
65. Rizzetto L, Fava F, Tuohy KM, Selmi C. Connecting the Immune System, Systemic Chronic Inflammation and the Gut Microbiome: The Role of Sex. *J Autoimmun* (2018) 92:12–34. doi: 10.1016/j.jaut.2018.05.008
66. Ivanov II, Atarashi K, Manel N, Brodie EL, Shima T, Karaoz U, et al. Induction of Intestinal Th17 Cells by Segmented Filamentous Bacteria. *Cell* (2009) 139(3):485–98. doi: 10.1016/j.cell.2009.09.033
67. Pacifici R. Bone Remodeling and the Microbiome. *Cold Spring Harb Perspect Med* (2018) 8:a031203 1–13. doi: 10.1101/cshperspect.a031203
68. Li JY, Chassaing B, Tyagi AM, Vaccaro C, Luo T, Adams J, et al. Sex Steroid Deficiency-Associated Bone Loss is Microbiota Dependent and Prevented by Probiotics. *J Clin Invest* (2016) 126(6):2049–63. doi: 10.1172/jci86062
69. Furusawa Y, Obata Y, Fukuda S, Endo TA, Nakato G, Takahashi D, et al. Commensal Microbe-Derived Butyrate Induces the Differentiation of Colonic Regulatory T Cells. *Nature* (2013) 504(7480):446–50. doi: 10.1038/nature12721
70. Smith PM, Howitt MR, Panikov N, Michaud M, Gallini CA, Bohlooly YM, et al. The Microbial Metabolites, Short-Chain Fatty Acids, Regulate Colonic Treg Cell Homeostasis. *Science* (2013) 341(6145):569–73. doi: 10.1126/science.1241165
71. Chevalier C, Kieser S, Colakoglu M, Hadadi N, Brun J, Rigo D, et al. Warmth Prevents Bone Loss Through the Gut Microbiota. *Cell Metab* (2020) 32 (4):575–90 e7. doi: 10.1016/j.cmet.2020.08.012
72. Pascutti MF, Geerman S, Collins N, Brasser G, Nota B, Stark R, et al. Peripheral and Systemic Antigens Elicit an Expandable Pool of Resident Memory CD8+ T Cells in the Bone Marrow. *Eur J Immunol* (2019) 49 (6):853–72. doi: 10.1002/eji.201848003
73. Gilbert L, He X, Farmer P, Boden S, Kozlowski M, Rubin J, et al. Inhibition of Osteoblast Differentiation by Tumor Necrosis Factor-α*. *Endocrinology* (2000) 141(11):3956–64. doi: 10.1210/endo.141.11.7739
74. Gilbert L, He X, Farmer P, Rubin J, Drissi H, van Wijnen AJ, et al. Expression of the Osteoblast Differentiation Factor RUNX2 (Cbfa1/Aml3/Pebp2alpha A) is Inhibited by Tumor Necrosis Factor-Alpha. *J Biol Chem* (2002) 277(4):2695–701. doi: 10.1074/jbc.M106339200
75. Lu X, Gilbert L, He X, Rubin J, Nanes MS. Transcriptional Regulation of the Osterix (Osx, Sp7) Promoter by Tumor Necrosis Factor Identifies Disparate Effects of Mitogen-Activated Protein Kinase and NF Kappa B Pathways. *J Biol Chem* (2006) 281(10):6297–306. doi: 10.1074/jbc.M507804200
76. Wei J, Shimazu J, Makinistoglu MP, Maurizi A, Kajimura D, Zong H, et al. Glucose Uptake and Runx2 Synergize to Orchestrate Osteoblast Differentiation and Bone Formation. *Cell* (2015) 161(7):1576–91. doi: 10.1016/j.cell.2015.05.029
77. Chen J, Long F. mTORC1 Signaling Promotes Osteoblast Differentiation From Preosteoblasts. *PloS One* (2015) 10(6):e0130627. doi: 10.1371/journal.pone.0130627
78. Chen J, Holguin N, Shi Y, Silva MJ, Long F. mTORC2 Signaling Promotes Skeletal Growth and Bone Formation in Mice. *J Bone Miner Res* (2015) 30 (2):369–78. doi: 10.1002/jbmr.2348
79. Fitter S, Matthews MP, Martin SK, Xie J, Ooi SS, Walkley CR, et al. mTORC1 Plays an Important Role in Skeletal Development by Controlling Preosteoblast Differentiation. *Mol Cell Biol* (2017) 37(7):e00668–16. doi: 10.1128/mcb.00668-16
80. Schaub T, Gurgen D, Maus D, Lange C, Tarabykin V, Dragun D, et al. mTORC1 and mTORC2 Differentially Regulate Cell Fate Programs to Coordinate Osteoblastic Differentiation in Mesenchymal Stromal Cells. *Sci Rep* (2019) 9(1):20071. doi: 10.1038/s41598-019-56237-w
81. Ciaraldi TP, Carter L, Mudaliar S, Kern PA , Henry RR. Effects of Tumor Necrosis Factor-α on Glucose Metabolism in Cultured Human Muscle Cells From Nondiabetic and Type 2 Diabetic Subjects**This Work was Supported by Funds From the American Diabetes Association, the Whittier Institute for Diabetes Research, Medical Research Service, the Department of Veterans Affairs, and the Veteran Affairs Medical Center-San Diego (to R.R.H.); Grant MO1-RR-00827 From the General Clinical Research Branch, Division of Research Resources, NIH, and the Medical Research Service, Department of Veterans Affairs and Veteran Affairs Medical Center-Little Rock (to P.A.K.); and NIH Grant Dk-39176. *Endocrinology* (1998) 139 (12):4793–800. doi: 10.1210/endo.139.12.6368
82. Plomgaard P, Bouzakri K, Krogh-Madsen R, Mittendorfer B, Zierath JR, Pedersen BK. Tumor Necrosis Factor-α Induces Skeletal Muscle Insulin

Resistance in Healthy Human Subjects Via Inhibition of Akt Substrate 160 Phosphorylation. *Diabetes* (2005) 54(10):2939–45. doi: 10.2337/diabetes.54.10.2939
83. Hauner H, Petruschke T, Russ M, Röhrig K, Eckel J. Effects of Tumour Necrosis Factor Alpha (Tnfα) on Glucose Transport and Lipid Metabolism of Newly-Differentiated Human Fat Cells in Cell Culture. *Diabetologia* (1995) 38(7):764–71. doi: 10.1007/s001250050350
84. Chen L, Bao J, Yang Y, Wang Z, Xia M, Tan J, et al. Autophagy was Involved in Tumor Necrosis Factor-Alpha-Inhibited Osteogenic Differentiation of Murine Calvarial Osteoblasts Through Wnt/beta-catenin Pathway. *Tissue Cell* (2020) 67:101401. doi: 10.1016/j.tice.2020.101401
85. Zheng LW, Wang WC, Mao XZ, Luo YH, Tong ZY, Li D. TNF-alpha Regulates the Early Development of Avascular Necrosis of the Femoral Head by Mediating Osteoblast Autophagy and Apoptosis Via the P38 MAPK/NF-kappaB Signaling Pathway. *Cell Biol Int* (2020) 44(9):1881–9. doi: 10.1002/cbin.11394
86. Zheng L, Wang W, Ni J, Mao X, Song D, Liu T, et al. Role of Autophagy in Tumor Necrosis Factor-Alpha-Induced Apoptosis of Osteoblast Cells. *J Investig Med* (2017) 65(6):1014–20. doi: 10.1136/jim-2017-000426
87. Nakashima T, Hayashi M, Fukunaga T, Kurata K, Oh-Hora M, Feng JQ, et al. Evidence for Osteocyte Regulation of Bone Homeostasis Through RANKL Expression. *Nat Med* (2011) 17(10):1231–4. doi: 10.1038/nm.2452
88. O'Brien CA, Nakashima T, Takayanagi H. Osteocyte Control of Osteoclastogenesis. *Bone* (2013) 54(2):258–63. doi: 10.1016/j.bone.2012.08.121
89. Xiong J, Piemontese M, Onal M, Campbell J, Goellner JJ, Dusevich V, et al. Osteocytes, Not Osteoblasts or Lining Cells, are the Main Source of the RANKL Required for Osteoclast Formation in Remodeling Bone. *PloS One* (2015) 10(9):e0138189. doi: 10.1371/journal.pone.0138189
90. Xing L, Schwarz EM, Boyce BF. Osteoclast Precursors, RANKL/RANK, and Immunology. *Immunol Rev* (2005) 208:19–29. doi: 10.1111/j.0105-2896.2005.00336.x
91. Fujiwara Y, Piemontese M, Liu Y, Thostenson JD, Xiong J, O'Brien CA. RANKL (Receptor Activator of NFkappaB Ligand) Produced by Osteocytes is Required for the Increase in B Cells and Bone Loss Caused by Estrogen Deficiency in Mice. *J Biol Chem* (2016) 291(48):24838–50. doi: 10.1074/jbc.M116.742452
92. Kim JH, Kim AR, Choi YH, Jang S, Woo GH, Cha JH, et al. Tumor Necrosis Factor-Alpha Antagonist Diminishes Osteocytic RANKL and Sclerostin Expression in Diabetes Rats With Periodontitis. *PloS One* (2017) 12(12):e0189702. doi: 10.1371/journal.pone.0189702
93. Li JY, Yu M, Tyagi AM, Vaccaro C, Hsu E, Adams J, et al. IL-17 Receptor Signaling in Osteoblasts/Osteocytes Mediates PTH-Induced Bone Loss and Enhances Osteocytic RANKL Production. *J Bone Miner Res* (2019) 34(2):349–60. doi: 10.1002/jbmr.3600
94. Liao C, Zhang C, Jin L, Yang Y. IL-17 Alters the Mesenchymal Stem Cell Niche Towards Osteogenesis in Cooperation With Osteocytes. *J Cell Physiol* (2020) 235(5):4466–80. doi: 10.1002/jcp.29323
95. Emerton KB, Hu B, Woo AA, Sinofsky A, Hernandez C, Majeska RJ, et al. Osteocyte Apoptosis and Control of Bone Resorption Following Ovariectomy in Mice. *Bone* (2010) 46(3):577–83. doi: 10.1016/j.bone.2009.11.006
96. Tsourdi E, Jähn K, Rauner M, Busse B, Bonewald LF. Physiological and Pathological Osteocytic Osteolysis. *J Musculoskelet Neuronal Interact* (2018) 18(3):292–303.
97. Tonti E, Jiménez de Oya N, Galliverti G, Moseman EA, Di Lucia P, Amabile A, et al. Bisphosphonates Target B Cells to Enhance Humoral Immune Responses. *Cell Rep* (2013) 5(2):323–30. doi: 10.1016/j.celrep.2013.09.004
98. Diker-Cohen T, Rosenberg D, Avni T, Shepshelovich D, Tsvetov G, Gafter-Gvili A. Risk for Infections During Treatment With Denosumab for Osteoporosis: A Systematic Review and Meta-Analysis. *J Clin Endocrinol Metab* (2020) 105(5):1641–58. doi: 10.1210/clinem/dgz322
99. Deligiorgi M V, Panayiotidis MI, Trafalis DT. Combining Immune Checkpoint Inhibitors With Denosumab: A New Era in Repurposing Denosumab in Oncology? *J BUON* (2020) 25(1):1–14.
100. Ruggiero SL. Bisphosphonate-Related Osteonecrosis of the Jaws. *Compend Contin Educ Dent* (2008) 29(2):96–8.
101. Kim J, Lee DH, Dziak R, Ciancio S. Bisphosphonate-Related Osteonecrosis of the Jaw: Current Clinical Significance and Treatment Strategy Review. *Am J Dent* (2020) 33(3):115–28.
102. Gupta M, Gupta N. Bisphosphonate Related Jaw Osteonecrosis. In: *StatPearls*. Treasure Island (FL): Stat Pearls Publishing (2020).
103. Jain TP, Thorn M. Atypical Femoral Fractures Related to Bisphosphonate Therapy. *Indian J Radiol Imaging* (2012) 22(3):178–81. doi: 10.4103/0971-3026.107178
104. Tripto-Shkolnik L, Rouach V, Marcus Y, Rotman-Pikielny P, Benbassat C, Vered I. Vertebral Fractures Following Denosumab Discontinuation in Patients With Prolonged Exposure to Bisphosphonates. *Calcif Tissue Int* (2018) 103(1):44–9. doi: 10.1007/s00223-018-0389-1
105. Novack DV, Teitelbaum SL. The Osteoclast: Friend or Foe? *Annu Rev Pathol* (2008) 3:457–84. doi: 10.1146/annurev.pathmechdis.3.121806.151431
106. Hodsman AB, Bauer DC, Dempster DW, Dian L, Hanley DA, Harris ST, et al. Parathyroid Hormone and Teriparatide for the Treatment of Osteoporosis: A Review of the Evidence and Suggested Guidelines for its Use. *Endocr Rev* (2005) 26(5):688–703. doi: 10.1210/er.2004-0006
107. Lim SY, Bolster MB. Profile of Romosozumab and its Potential in the Management of Osteoporosis. *Drug Des Dev Ther* (2017) 11:1221. doi: 10.2147/DDDT.S127568
108. Fixen C, Tunoa J. Romosozumab: A Review of Efficacy, Safety, and Cardiovascular Risk. *Curr Osteoporos Rep* (2021) 19(1):15–22. doi: 10.1007/s11914-020-00652-w
109. Saag KG, Zanchetta JR, Devogelaer JP, Adler RA, Eastell R, See K, et al. Effects of Teriparatide Versus Alendronate for Treating Glucocorticoid-Induced Osteoporosis: Thirty-Six-Month Results of a Randomized, Double-Blind, Controlled Trial. *Arthritis Rheum* (2009) 60(11):3346–55. doi: 10.1002/art.24879
110. Tashjian AHJr., Gagel RF. Teriparatide [Human PTH(1-34)]: 2.5 Years of Experience on the Use and Safety of the Drug for the Treatment of Osteoporosis. *J Bone Miner Res* (2006) 21(3):354–65. doi: 10.1359/JBMR.051023
111. Brandenburg VM, Verhulst A, Babler A, D'Haese PC, Evenepoel P, Kaesler N. Sclerostin in Chronic Kidney Disease-Mineral Bone Disorder Think First Before You Block it! *Nephrol Dial Transplant* (2019) 34(3):408–14. doi: 10.1093/ndt/gfy129
112. Dempster DW, Zhou H, Recker RR, Brown JP, Recknor CP, Lewiecki EM, et al. Remodeling- and Modeling-Based Bone Formation With Teriparatide Versus Denosumab: A Longitudinal Analysis From Baseline to 3 Months in the AVA Study. *J Bone Miner Res* (2018) 33(2):298–306. doi: 10.1002/jbmr.3309
113. Dempster DW, Zhou H, Recker RR, Brown JP, Bolognese MA, Recknor CP, et al. A Longitudinal Study of Skeletal Histomorphometry at 6 and 24 Months Across Four Bone Envelopes in Postmenopausal Women With Osteoporosis Receiving Teriparatide or Zoledronic Acid in the SHOTZ Trial. *J Bone Miner Res* (2016) 31(7):1429–39. doi: 10.1002/jbmr.2804
114. Edwards WB, Simonian N, Haider IT, Anschel AS, Chen D, Gordon KE, et al. Effects of Teriparatide and Vibration on Bone Mass and Bone Strength in People With Bone Loss and Spinal Cord Injury: A Randomized, Controlled Trial. *J Bone Miner Res* (2018) 33(10):1729–40. doi: 10.1002/jbmr.3525
115. Tsai JN, Nishiyama KK, Lin D, Yuan A, Lee H, Bouxsein ML, et al. Effects of Denosumab and Teriparatide Transitions on Bone Microarchitecture and Estimated Strength: The DATA-Switch HR-pQCT Study. *J Bone Miner Res* (2017) 32(10):2001–9. doi: 10.1002/jbmr.3198
116. Eastell R, O'Neill TW, Hofbauer LC, Langdahl B, Reid IR, Gold DT, et al. Postmenopausal Osteoporosis. *Nat Rev Dis Primers* (2016) 2:16069. doi: 10.1038/nrdp.2016.69
117. Fink HA, MacDonald R, Forte ML, Rosebush CE, Ensrud KE, Schousboe JT, et al. Long-Term Drug Therapy and Drug Holidays for Osteoporosis Fracture Prevention: A Systematic Review. In: *AHRQ Comparative Effectiveness Reviews*. Rockville (MD): Agency for Health Research and Quality (AHRQ.gov) (2019).
118. Kimble RB, Bain S, Pacifici R. The Functional Block of TNF But Not of IL-6 Prevents Bone Loss in Ovariectomized Mice. *J Bone Miner Res* (1997) 12(6):935–41. doi: 10.1359/jbmr.1997.12.6.935
119. Deselm CJ, Takahata Y, Warren J, Chappel JC, Khan T, Li X, et al. IL-17 Mediates Estrogen-Deficient Osteoporosis in an Act1-dependent Manner. *J Cell Biochem* (2012) 113(9):2895–902. doi: 10.1002/jcb.24165
120. Charatcharoenwitthaya N, Khosla S, Atkinson EJ, McCready LK, Riggs BL. Effect of Blockade of TNF-alpha and Interleukin-1 Action on Bone

Resorption in Early Postmenopausal Women. *J Bone Miner Res* (2007) 22 (5):724–9. doi: 10.1359/jbmr.070207
121. Kawai VK, Stein CM, Perrien DS, Griffin MR. Effects of Anti-Tumor Necrosis Factor α Agents on Bone. *Curr Opin Rheumatol* (2012) 24 (5):576–85. doi: 10.1097/BOR.0b013e328356d212
122. Chong WP, Mattapallil MJ, Raychaudhuri K, Bing SJ, Wu S, Zhong Y, et al. The Cytokine IL-17a Limits Th17 Pathogenicity Via a Negative Feedback Loop Driven by Autocrine Induction of IL-24. *Immunity* (2020) 53(2):384–97.e5. doi: 10.1016/j.immuni.2020.06.022
123. Yu J, Cao G, Yuan S, Luo C, Yu J, Cai M. Probiotic Supplements and Bone Health in Postmenopausal Women: A Meta-Analysis of Randomised Controlled Trials. *BMJ Open* (2021) 11(3):e041393. doi: 10.1136/bmjopen-2020-041393
124. Nilsson AG, Sundh D, Bäckhed F, Lorentzon M. Lactobacillus Reuteri Reduces Bone Loss in Older Women With Low Bone Mineral Density: A Randomized, Placebo-Controlled, Double-Blind, Clinical Trial. *J Intern Med* (2018) 284(3):307–17. doi: 10.1111/joim.12805
125. Buchwald ZS, Kiesel JR, DiPaolo R, Pagadala MS, Aurora R. Osteoclast Activated Foxp3+ CD8+ T-Cells Suppress Bone Resorption In Vitro. *PloS One* (2012) 7(6):e38199–12. doi: 10.1371/journal.pone.0038199
126. Buchwald ZS, Yang C, Nellore S, Shashkova EV, Davis JL, Cline A, et al. A Bone Anabolic Effect of RANKL in a Murine Model of Osteoporosis Mediated Through FoxP3 +CD8 T Cells. *J Bone Miner Res* (2015) 30 (8):1508–22. doi: 10.1002/jbmr.2472
127. Buchwald ZS, Aurora R. Osteoclasts and CD8 T Cells Form a Negative Feedback Loop That Contributes to Homeostasis of Both the Skeletal and Immune Systems. *Clin Dev Immunol* (2013) 2013:429373. doi: 10.1155/2013/429373
128. Buchwald ZS, Kiesel J, Yang C, DiPaolo R, Novack D, Aurora R. Osteoclast-Induced Foxp3+ CD8 T-Cells Limit Bone Loss in Mice. *Bone* (2013) 56:163–73. doi: 10.1016/j.bone.2013.05.024
129. Cline-Smith A, Gibbs J, Shashkova E, Buchwald ZS, Aurora R. Pulsed Low-Dose RANKL as a Potential Therapeutic for Postmenopausal Osteoporosis. *JCI Insight* (2016) 1(13):433–12. doi: 10.1172/jci.insight.88839
130. Chen Z, Bozec A, Ramming A, Schett G. Anti-Inflammatory and Immune-Regulatory Cytokines in Rheumatoid Arthritis. *Nat Rev Rheumatol* (2019) 15 (1):9–17. doi: 10.1038/s41584-018-0109-2
131. Laumet G, Edralin JD, Chiang AC-A, Dantzer R, Heijnen CJ, Kavelaars A. Resolution of Inflammation-Induced Depression Requires T Lymphocytes and Endogenous Brain interleukin-10 Signaling. *Neuropsychopharmacology* (2018) 43(13):2597–605. doi: 10.1038/s41386-018-0154-1
132. Reina-Couto M, Carvalho J, Valente MJ, Vale L, Afonso J, Carvalho F, et al. Impaired Resolution of Inflammation in Human Chronic Heart Failure. *Eur J Clin Invest* (2014) 44(6):527–38. doi: 10.1111/eci.12265

Conflict of Interest: The authors declare that the research was conducted in the absence of any commercial or financial relationships that could be construed as a potential conflict of interest.

frontiers in Immunology

ORIGINAL RESEARCH
published: 30 June 2021
doi: 10.3389/fimmu.2021.691081

Regulatory B Cells (Bregs) Inhibit Osteoclastogenesis and Play a Potential Role in Ameliorating Ovariectomy-Induced Bone Loss

*Leena Sapra[1], Asha Bhardwaj[1], Pradyumna Kumar Mishra[2], Bhavuk Garg[3], Bhupendra Verma[1], Gyan C. Mishra[4] and Rupesh K. Srivastava[1]**

[1] Department of Biotechnology, All India Institute of Medical Sciences (AIIMS), New Delhi, India, [2] Department of Molecular Biology, ICMR-National Institute for Research in Environmental Health, Bhopal, India, [3] Department of Orthopaedics, All India Institute of Medical Sciences (AIIMS), New Delhi, India, [4] National Centre for Cell Science (NCCS), Pune, India

OPEN ACCESS

Edited by:
Giamila Fantuzzi,
University of Illinois at Chicago,
United States

Reviewed by:
Hyun Sook Hong,
Kyung Hee University, South Korea
Roberta Okamoto,
São Paulo State University (UNESP),
Brazil

***Correspondence:**
Rupesh K. Srivastava
rupesh_srivastava13@yahoo.co.in;
rupeshk@aiims.edu

Specialty section:
This article was submitted to Inflammation, a section of the journal Frontiers in Immunology

Received: 05 April 2021
Accepted: 12 May 2021
Published: 30 June 2021

Citation:
Sapra L, Bhardwaj A, Mishra PK, Garg B, Verma B, Mishra GC and Srivastava RK (2021) Regulatory B Cells (Bregs) Inhibit Osteoclastogenesis and Play a Potential Role in Ameliorating Ovariectomy-Induced Bone Loss. Front. Immunol. 12:691081. doi: 10.3389/fimmu.2021.691081

Increasing evidence in recent years has suggested that regulatory B cells (Bregs) are one of the crucial modulators in various inflammatory disease conditions. However, no study to date has investigated the significance of Bregs in modulating osteoclastogenesis. To the best of our knowledge, in the present study, we for the first time examined the anti-osteoclastogenic potential of Bregs under *in vitro* conditions and observed that Bregs suppress RANKL-induced osteoclastogenesis in a dose-dependent manner. We further elucidated the mechanism behind the observed suppression of osteoclasts differentiation *via* Bregs. Our results clearly suggested that the observed anti-osteoclastogenic property of Bregs is mediated *via* the production of IL-10 cytokine. Next, we explored whether Bregs have any role in mediating inflammatory bone loss under post-menopausal osteoporotic conditions in ovx mice. Remarkably, our *in vivo* data clearly suggest that the frequencies of both $CD19^{+}IL\text{-}10^{+}$ Bregs and $CD19^{+}CD1d^{hi}CD5^{+}IL\text{-}10^{+}$ "B10" Bregs were significantly reduced in case of osteoporotic mice model. Moreover, we also found a significant reduction in serum IL-10 cytokine levels in osteoporotic mice, thereby further supporting our observations. Taken together, the present study for the first time establishes the direct role of regulatory B cells in modulating osteoclastogenesis *in vitro*. Further, our *in vivo* data suggest that modulations in the percentage of Bregs population along with its reduced potential to produce IL-10 might further exacerbate the observed bone loss in ovx mice.

Keywords: regulatory B cells, Bregs, osteoclast, osteoporosis, bone health

Abbreviations: Bregs, Regulatory B cells; RANKL, Receptor activator of nuclear factor kappa B; TLR, Toll like receptor; LPS, Lipopolysaccharide; IL, Interleukin; TGF, Transforming growth factor; RA, Rheumatoid arthritis; SLE, Systemic lupus erythematosus; EAE, Experimental autoimmune encephalitis; PMA, Phorbol 12-myristate 13-acetate; BMCs, Bone marrow cells; M-CSF, Monocyte colony stimulating factor; TRAP, Tartrate resistant acid phosphatase; BMD, Bone mineral density; SEM, Scanning electron microscopy; Tregs, Regulatory T cells CIA; Collagen induced arthritis.

INTRODUCTION

B cells are classically characterized by their potential to produce and secrete antibodies. They also function as antigen-presenting cells (APCs) and secrete several immunomodulatory cytokines. Nevertheless, B cells with immunosuppressive functions, called Regulatory B cells or "Bregs", have also been reported. It is known that the microenvironment plays a crucial role in directing the development and differentiation of Bregs (1, 2). It has also been observed that antigen and B cell receptor (BCR) signaling are crucial for the development of Bregs. In the presence of toll-like receptor (TLR) ligands, such as lipopolysaccharide (LPS), CpG, and CD40L, the development of Bregs can be optimized (3, 4). These Bregs exhibit the ability to regulate various disease conditions including inflammatory bone loss diseases such as rheumatoid arthritis (RA), collagen-induced arthritis (CIA), etc. (5, 6). Bregs *via* the production of interleukin (IL)-10, IL-35, and transforming growth factor (TGF)-β suppress several immunopathologies by barring the expansion of various immune cells, including T lymphocytes (7). Given that IL-10 producing B cells play a crucial role in immune regulation, Tedder et al. defined a subset of Bregs named "B10 cells" whose anti-inflammatory potential is only attributable to the production of IL-10 cytokine in various disease models such as cancer, autoimmune diseases, and infectious diseases. The co-expression of CD1d and CD5 has later been utilized to characterize splenic B10 cells to inhibit the progression of inflammation upon stimulation for 5h with LPS, phorbol 12-myristate 13-acetate (PMA), ionomycin, and monensin under *ex vivo* conditions (8, 9). Various studies demonstrated that the adoptive transfer of splenic B10 cells dampened the autoimmune reactions in several models of experimental autoimmune encephalitis (EAE), CIA, intestinal inflammation, and systemic lupus erythematosus (SLE) (5, 10–12). Thus, multiple studies in both humans and mice highlighted that Bregs suppress inflammatory reactions *via* IL-10 cytokine.

Osteoporosis is a systemic skeletal disease that is mainly characterized by deterioration of bone tissue and low bone mass. Various factors act synergistically to enhance the likelihood of developing osteoporosis viz. age, sex, hormonal imbalance, dietary factors, and the immune system. Accumulating evidence has supported the theory that bone destruction observed in osteoporosis caused by osteoclasts is due to impairment or loss of homeostatic balance of inflammatory and anti-inflammatory cells viz. Th17 and Tregs (13, 14). Various studies proposed that $CD4^+Foxp3^+$ Treg cells *via* secretion of IL-10 cytokine suppress osteoclastogenesis and thus bone resorption (13–16). It has also been reported that numerical defect in the Tregs population along with its efficacy to produce IL-10 cytokine results in the development of various inflammatory bone loss conditions, including osteoporosis. IL-10 is thus not just a signature cytokine for Bregs but also a potent modulator of the immune response that further contributes to the maintenance of bone health *via* inhibition of osteoclast-mediated bone resorption (17). Interestingly, a study reported that Breg cells mediate their immunosuppressive functions by inducing differentiation of naïve T cells into Tregs (18). Nevertheless, the role of Bregs and their secretory cytokines on the differentiation of osteoclasts has not been investigated to date. With the growing involvement of the immune system in the pathology of osteoporosis, our group has recently coined the term "Immunoporosis" that emphasizes the specific role of immune cells in osteoporosis (19).

In the present study, we report that under *in vitro* conditions, IL-10 producing Bregs inhibit the differentiation of osteoclasts. In addition, we also report that the frequencies of Bregs ($CD19^+IL\text{-}10^+$ and $CD19^+CD1d^{hi}CD5^+IL\text{-}10^+$ "B10 cells") are significantly reduced in both bone marrow and spleen in ovariectomy-induced post-menopausal osteoporotic mice model. Altogether our results suggest that numerical defects in Bregs along with its inability to secrete IL-10 cytokine might be a contributing factor towards the establishment of pro-inflammatory conditions in the case of postmenopausal osteoporosis. In summary, our results for the first time explore the "Immunoporotic" role of Bregs in bone health.

MATERIALS AND METHODS

Reagents and Antibodies

The following antibodies/kits were obtained from eBiosciences (USA): PerCp-Cy5.5 Anti-Mouse-CD19 (1D3) (45-0193-82), PE-Cy7 Anti-Mouse-CD5 (53-7.3) (25-0051-81), APC Anti-Mouse-CD1d (1B1) (17-0011-82), Foxp3/Transcription factor staining buffer (0-5523-00), and RBC lysis buffer (00-4300-54). FITC Anti-Mouse-IL-10 (JES5-16E3) (505005) was purchased from Biolegend (USA). *InVivo*MAb anti-mouse IL-10 antibody (BE0049) and *InVivo*MAb Rat IgG1 isotype control were purchased from BioXcell (USA). Protein transport inhibitor cocktail and the Mouse TNF-α (560478) ELISA kit were procured from BD (USA). The following ELISA kits were brought from R&D and Elabscience: Mouse IL-10 (M1000B) (E-EL-M0046) and Mouse IL-17 (M1700). PMA, Ionomycin, LPS (*Escherichia coli* serotype 0111: B4), FITC-Phalloidin (P5282), DAPI, and Acid phosphatase leukocyte (TRAP) kit (387A) were procured from Sigma-Aldrich (USA). Macrophage-colony stimulating factor (M-CSF) (300-25) and Receptor activator of nuclear factor κB-ligand (sRANKL) (310-01) were procured from PeproTech (USA). α-Minimal essential media (MEM) and RPMI-1640 were obtained from Gibco (Thermo Fisher Scientific, USA).

B Cell Purification and Activation

Splenic B cells from C57BL/6 mice were purified by magnetic separation according to the manufacturer's instructions. Briefly, after RBC lysis, the resulting cells were subjected to a biotinylated mouse B cell enrichment cocktail (BD, USA) and incubated for 20-30 min at 4°C. Labeled cells were then washed carefully with washing buffer and incubated with streptavidin particles plus-DM for 30 min at 4°C. Further, cells underwent magnetic separation using a cell separation magnet, and a negative fraction comprised of resulting B cells was assessed for purity (>95%) by flow cytometric analysis. Purified B cells (>95%) were then cultured in 24-well plates (2×10^6) in 1ml/well in the presence and absence of LPS (10 ug/ml) for different time periods

(5h and 24h) at 37°C in 5% humidified CO_2 incubator. At the end of incubation, LPS induced Bregs were harvested and washed thrice with 1X PBS containing 2% fetal bovine serum (FBS), especially to remove the traces of LPS before co-culturing with bone marrow cells (BMCs) for osteoclasts differentiation.

Co-Culture of Bregs With BMCs for Osteoclastogenesis

Generation of osteoclasts from mouse BMCs was performed as previously described (16). Briefly, BMCs were harvested from femur and tibiae of 8–10 wks old mice and RBC lysis was performed with 1X RBC lysis buffer. After RBC lysis, cells were cultured overnight in T-25 flask in endotoxin-free α-MEM media supplemented with 10% heat-inactivated FBS and M-CSF (35 ng/ml). On the following day, non-adherent cells (BMCs) ($1 X 10^6$ cells/well) were collected and co-cultured with either Bregs or non-activated B cells ($1X10^5$-$1X10^6$ cells/well) in 24 well plate in different ratios (10:1, 5:1 and 1:1) in the presence of M-CSF (30 ng/ml) and RANKL (100 ng/ml) for 4 days. At an interval of 2 days, media was replenished with fresh media supplemented with M-CSF and RANKL factors. After 4 days of incubation, tartrate-resistant acid phosphatase (TRAP) staining was performed.

For the transwell experimental setup, transwell chambers with 8 μM pore size membranes were employed to physically separate Bregs or B cells from BMCs. Bregs or B cells were seeded in the upper chamber and BMCs in the lower chamber at different cell ratios. After 4 days of incubation, cells were processed for evaluating osteoclastogenesis *via* TRAP staining.

For the IL-10 neutralization experimental setup, neutralizing monoclonal antibody against IL-10 (10 ug/ml) was added in the cocultures of BMCs and Bregs at a 1:1 ratio in the presence of M-CSF (30 ng/ml) and RANKL (100 ng/ml). Isotype control for anti-IL-10 was also added in the control group. After 4 days of incubation, cells were processed for evaluating osteoclastogenesis *via* either TRAP staining or F-actin ring formation assay (described later).

Tartrate Resistant Acid Phosphatase (TRAP) Staining

For evaluating the generation of mature multinucleated osteoclasts TRAP staining was performed according to the manufacturer's instructions. Briefly, at the end of incubation cells were washed thrice with 1X PBS and fixed with a fixative solution comprised of citrate, acetone, and 3.7% formaldehyde for 10 min at 37°C. After washing twice with 1X PBS, fixed cells were stained for TRAP at 37° C in dark for 5–15 min. Multinucleated TRAP-positive cells with ≥ 3 nuclei were considered as mature osteoclasts. TRAP-positive multinucleated cells were further counted and imaged using an inverted microscope (ECLIPSE, TS100, Nikon). The area of TRAP-positive cells was quantified with the help of Image J software (NIH, USA).

F-Actin Ring Formation Assay

F-actin ring formation assay was performed as described previously (16). Briefly, Bregs and BMCs were co-cultured on glass coverslips in a 12-well plate, and after 4 days of incubation, cells were processed for F-actin ring staining. At the end of incubation, after washing cells twice with 1X PBS, cells were fixed with 4% paraformaldehyde (PFA) for 20 min and permeabilized with 0.1% triton X-100 for 5 min. Furthermore, to block non-specific binding, cells were blocked with 1% BSA for 30 min. After the blocking step, cells were stained with FITC-labelled-phalloidin for 1h at room temperature in dark. Finally, after washing nuclei were stained with DAPI (10 ug/ml) and incubated for 5 min in the dark. Subsequently, after mounting slides were observed under an immunofluorescence microscope (Imager.Z2, Zeiss) for F-actin ring formation at 10X magnification.

Flow Cytometric Analysis

Cells were harvested and stained with antibodies specific to Bregs. For analysis of intracellular IL-10 cytokine by B cells, isolated splenocytes or purified B cells were resuspended in RPMI-1640 complete media comprised of 10% FBS and 0.1% mercaptoethanol (ME) at a density of $2 X 10^6$ cells/ml in 24-well plates. Cells were then activated with LPS (10 ug/ml), PMA (50 ng/ml, Sigma Aldrich), Ionomycin (500 ng/ml, Sigma Aldrich), and a protein transport inhibitor cocktail (BD, USA) for 5h. For surface marker staining, cells were first incubated with anti-CD19-PerCP-Cy5.5, anti-CD5-PE-Cy7, and anti-CD1d-APC and incubated for 30 min in dark on ice. After washing, cells were fixed and permeabilized with 1X fixation-permeabilization-buffer for 30 min on ice in dark. Further, cells were stained with anti-IL-10-FITC for 45 min. After washing, cells were acquired on either BD FACS-AriaIII or BD-LSRFortessa (USA). Flowjo-10 (TreeStar, USA) software was used to analyze the samples, and gating strategy was done as per previously defined protocols.

Post-Menopausal Osteoporotic Mice Model

All *in vivo* experiments were carried out in 8-10 wks old female C57BL/6 mice. All the mice were housed under specific pathogen-free conditions at the animal facility of All India Institute of Medical Sciences (AIIMS), New-Delhi-India. Following groups were taken for the present study viz. sham (control) and ovariectomized (ovx) (n=6/grp). A healthy control group (sham) was subjected to sham surgery. In the ovx group, mice were exposed to bilateral-ovariectomy after anesthetizing them with ketamine (100-150 mg/kg) and xylazine (5-16 mg/kg) intraperitoneally. Both the groups were maintained on a 12-h light/dark cycle in polycarbonate cages and fed with sterilized food and autoclaved water *ad-libitum*. At the end of the experiment (6 wks), mice were euthanized by carbon dioxide asphyxiation, and blood, bones, and lymphoid tissues were harvested for further analysis. All the procedures were performed in accordance with the principles, the recommendation, and after the due approval of protocol submitted to the Institutional Animal Ethics Committee of AIIMS, New Delhi, India (85/IAEC-1/2018 and 196/IAEC-1/2019).

Scanning Electron Microscopy (SEM)

SEM was performed for scanning the surface of the femur cortical region of bones (13). Briefly, for 2-3 days bone samples were stored

in 1%-Triton-X-100, and, later on, bones were transferred in 1X PBS buffer till the analysis was carried out. After the preparation of bone slices, samples were dried and sputter coating was performed. Subsequently, bones were scanned and imaged using Quanta 200 FEG SEM. SEM images were digitally photographed at 50,000 X magnification to capture the best cortical region of bones. The SEM images were further analyzed through MATLAB software (Mathworks, Natick, MA, USA).

Micro-Computed Tomography (μ-CT) and Bone Mineral Density (BMD) Measurements

μ-CT scanning and BMD analysis were performed as described previously (13, 14). Briefly, after placing all the samples at the correct orientation, scanning was carried out at 50 kV, 201 mA using a 0.5 mm aluminum filter, and exposure was set to 590 ms. For reconstruction of images NRecon software was used. For trabecular region analysis, ROI was drawn at a total of 100 slices in secondary spongiosa at 1.5 mm from the distal border of growth plates excluding the parts of cortical bone and primary spongiosa. For measuring and calculating the microarchitectural parameters of bone samples CTAn software was employed. Several 3D-histomorphometric indices were obtained such as bone volume/tissue volume ratio (BV/TV); trabecular thickness (Tb. Th); trabecular number (Tb. No.); connectivity density (Conn. Den); trabecular separation (Tb. Sep.); trabecular pattern factor (Tb. Pf.); total cross-sectional area (Tt. Ar.); total cross-sectional perimeter (T. Pm); cortical bone area (Ct. Ar); bone perimeter (B. Pm); and average cortical thickness (Ct. Th). The volume of interest (VOI) of μ-CT scans was used to calculate the BMD of lumbar vertebrae-5 (LV-5), femoral, and tibial bones. BMD was measured by using hydroxyapatite phantom rods of 4 mm diameter with known BMD (0.25 g/cm^3 and 0.75 g/cm^3) as a calibrator.

Enzyme-Linked Immunosorbent Assay (ELISA)

ELISA was carried out for quantitative estimation of the following cytokines viz. IL-10, IL-17, and TNF-α in blood serum using commercially available kits as per the manufacturer's instructions. Secretion of IL-10 cytokine was also evaluated in the culture supernatants of LPS induced purified B cells and co-cultures of Bregs and BMCs under various conditions. Supernatants were collected and stored at -80^{0}C until being measured by ELISA.

Statistical Analysis

Statistical differences between sham and ovx mice groups were assessed by using analysis of variance (ANOVA) with succeeding comparisons *via* student t-test paired or unpaired as appropriate. We performed an analysis of significance in Sigma Plot (Systat Software, Inc., Germany). All the data values are articulated as Mean ± SEM (n=6). Statistical significance was determined as $p \leq 0.05$ (*$p < 0.05$, **$p < 0.01$, ***$p < 0.001$) with respect to the indicated group.

RESULTS

Induction of IL-10 Producing Bregs

In the present study, we made an attempt to dissect the role of Bregs in modulating osteoclastogenesis. To determine whether Bregs possess the potential to modulate osteoclasts differentiation, we first induced Bregs under *in vitro* conditions. Bregs were thus generated as per established literature (9, 20). Firstly, B cells were purified from splenocytes of mice *via* negative selection through magnetic beads (**Figure 1A**). After assessing the purity of isolated B cells (>95%), we stimulated these purified B cells with LPS (10 ug/ml) for different time periods (5h and 24h). Since Bregs have already been reported to express IL-10, we too evaluated the frequency of $CD19^+IL\text{-}10^+$ Bregs in our study. Our flow cytometric data indicates that the frequency of total IL-10 producing B cells, i.e., $CD19^+IL\text{-}10^+$ Bregs was significantly enhanced by LPS stimulation in a time-dependent manner in comparison to the control group ($p < 0.001$) (**Figures 1B, C**). B10 Bregs with a characteristic phenotype of $CD19^+CD1d^{hi}CD5^+IL\text{-}10^+$ were also significantly enhanced after LPS stimulation with respect to control group (**Figure 1D**). In addition, our ELISA results also indicate that IL-10 cytokine levels were significantly enhanced in culture supernatant harvested from LPS stimulated Bregs in comparison to the control group (**Figure 1E**). These results thus clearly indicate towards the successful generation of IL-10 producing Bregs in our culture conditions.

Bregs Inhibit Differentiation and Functional Activity of Osteoclasts

Next, we wanted to investigate whether Bregs exhibit the potential to suppress osteoclast differentiation from BMCs under *in vitro* conditions. To confirm this, we co-cultured BMCs with Bregs at different cell ratios (BMC : Bregs:: 10:1, 5:1, and 1:1) in the presence of M-CSF (30 ng/ml) and RANKL (100 ng/ml). After incubation for 4 days, cells were fixed and stained for TRAP to identify differentiated multinucleated osteoclasts (**Figure 2A**). Interestingly, we observed that BMCs co-cultured with Bregs at different cell ratios showed a significant reduction in osteoclasts differentiation (3-fold), i.e., TRAP-positive osteoclasts (**Figures 2B–D**). Moreover, area measurement analysis of TRAP-positive multinucleated osteoclasts using Image J software also showed significant reduction (30-folds) in the area of osteoclasts in treated groups (**Figure 2E**). Thereby, our results clearly demonstrated that Bregs possess the potential to inhibit RANKL induced osteoclastogenesis in a dose-dependent manner.

Extensive literature suggests that the F-actin ring observed in mature osteoclasts is a characteristic functional phenotype that aids toward the bone-resorbing potential of osteoclasts. Moving ahead, we next asked the question of whether Bregs have the potential to inhibit the functional activity of osteoclasts along with inhibiting their differentiation. In order to examine the same, Bregs and BMCs were co-cultured at different ratios on glass coverslips for 4 days. At the end of the experiment, after fixation and permeabilization, cells were stained for F-actin (FITC-labelled-phalloidin) and nuclei (DAPI). Remarkably, we observed that in comparison to the control group, Bregs significantly suppressed both the number of

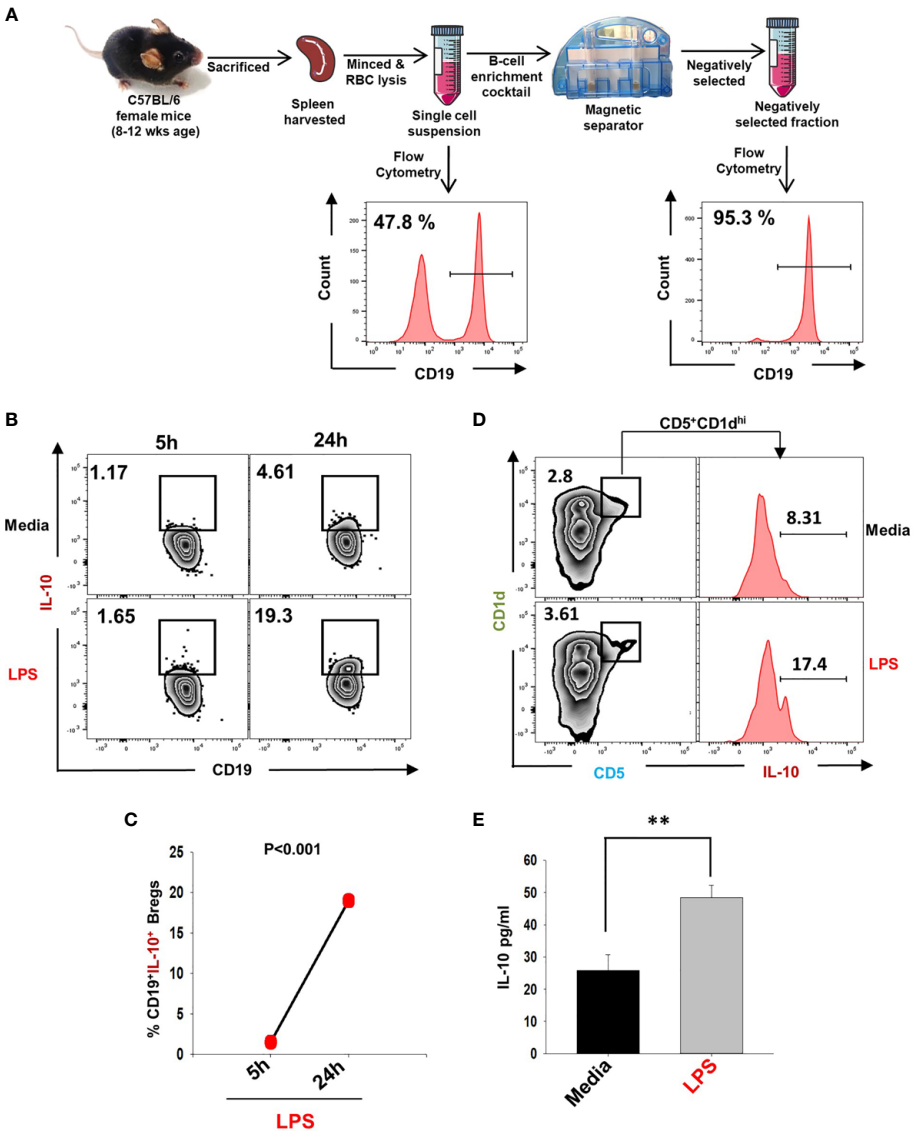

FIGURE 1 | Induction of IL-10 producing Bregs. **(A)** Spleen was harvested and processed for negative selection of $CD19^+$ B cells. After estimation of B cells purity (>95 %), cells were stimulated with LPS (10 ug/ml) for different time periods (5h and 24h). **(B)** Zebra plot depicting the percentages of $CD19^+IL\text{-}10^+$ in media and LPS after 5h and 24h of stimulation. **(C)** Line plot showing $CD19^+IL\text{-}10^+$ B cells after 5h and 24h of LPS stimulation. **(D)** Zebra plot depicting the percentages of $CD19^+CD5^+CD1d^{hi}$ B10 cells and histograms depicting IL-10 production by these cells. **(E)** ELISA results of culture supernatants showing levels of IL-10 cytokine. The above images are indicative of one experiment and similar results were obtained in three independent experiments. The results were evaluated by ANOVA with subsequent comparisons by Student t-test for paired or nonpaired data. Statistical significance was considered as $p \leq 0.05$ ($^*p \leq 0.05$, $^{**}p \leq 0.01$, $^{***}p \leq 0.001$) with respect to indicated groups (Mouse Image courtesy: Ms. Leena Sapra).

F-actin rings and the area of F-actin ring in matured osteoclasts (**Figures 3A–E**). These results of ours thus clearly establish the role of Bregs in significantly impairing not only the differentiation but also the functional capacity of osteoclasts.

Bregs Inhibits Osteoclast Differentiation *via* IL-10

To dissect whether the suppressive effect of Bregs is mediated *via* either a cell-contact-dependent (soluble factors) or cell-contact-independent manner, we co-cultured BMCs and Bregs in trans-wells that prohibit direct cellular interactions. Remarkably, Bregs also significantly inhibited osteoclastogenesis in a dose-dependent manner (5-fold) even in a trans-well setup, thereby clearly establishing the role of soluble factors in mediating inhibitory anti-osteoclastogenic potential of Bregs (**Figures 4A–E**). These data clearly establish that Bregs inhibit osteoclast differentiation *via* soluble mediators.

Various studies have shown that LPS-induced Bregs mediate their immunosuppressive functions *via* IL-10 cytokine (20). Also, among various subtypes of Bregs, $CD19^+CD1d^{hi}CD5^+$

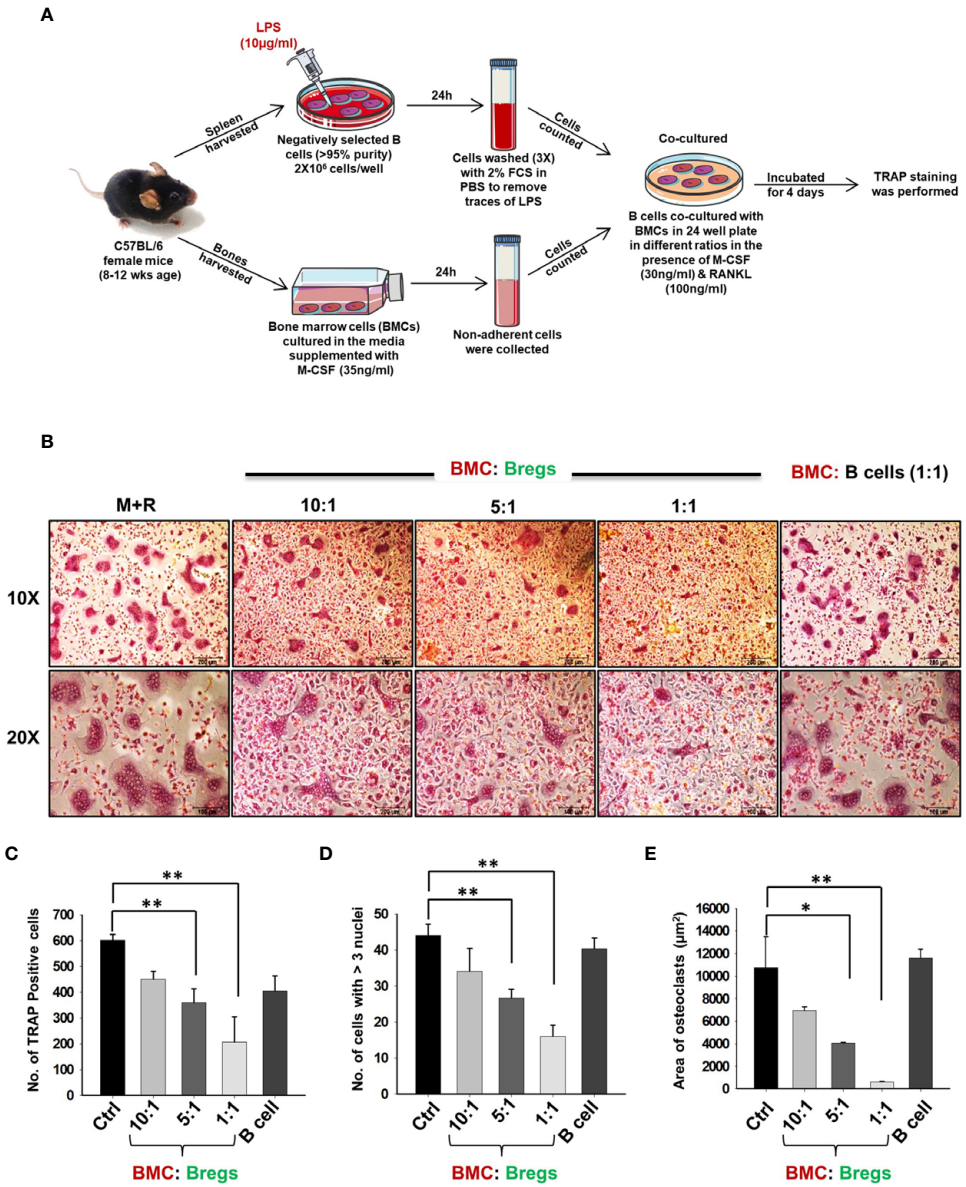

FIGURE 2 | Bregs suppress osteoclastogenesis. **(A)** BMCs and LPS stimulated and non-stimulated B cells were co-cultured in cell culture plate (cell-contact) in the presence of M-CSF (30 ng/ml) and RANKL (100 ng/ml) for 4 days. B cells were induced with LPS (10 ug/ml) for 24h prior to co-cultures. **(B)** Bregs significantly inhibited the generation of multinucleated osteoclasts in a dose-dependent manner. **(C)** Graphical representation showing the number of TRAP-positive cells. **(D)** Bar graphs representing the number of cells with more than three nuclei. **(E)** Bar graphs representing the area of multinucleated TRAP-positive cells. Control denotes BMCs culture only. The above images are indicative of one experiment and similar results were obtained in three independent experiments. The results were evaluated by ANOVA with subsequent comparisons by Student t-test for paired or nonpaired data. Statistical significance was considered as $p \leq 0.05$ (*$p \leq 0.05$, **$p \leq 0.01$, ***$p \leq 0.001$) with respect to indicated groups (Mouse Image courtesy: Ms. Leena Sapra).

(B10) Bregs are known to play a crucial role in preventing immunopathogenesis associated with various autoimmune diseases. Thus, it may be possible that the higher expression of IL-10 by these Bregs could contribute towards the inhibition of osteoclastogenesis in our co-cultures. Therefore, to confirm the significance of IL-10 in Bregs mediated suppression of osteoclastogenesis, we next assessed the percentages of total IL-10 producing B cells ($CD19^{+}IL\text{-}10^{+}$) along with B10 Bregs ($CD19^{+}CD1d^{hi}CD5^{+}IL\text{-}10^{+}$) in our LPS induced Bregs *via* flow cytometric analysis. Intriguingly, we observed that percentages of IL-10 producing Breg populations were significantly enhanced in the LPS induced group with respect to the control group (**Figures 5A–H**). Importantly, the anti-osteoclastogenic effect of Bregs was further found to be correlated with the significant

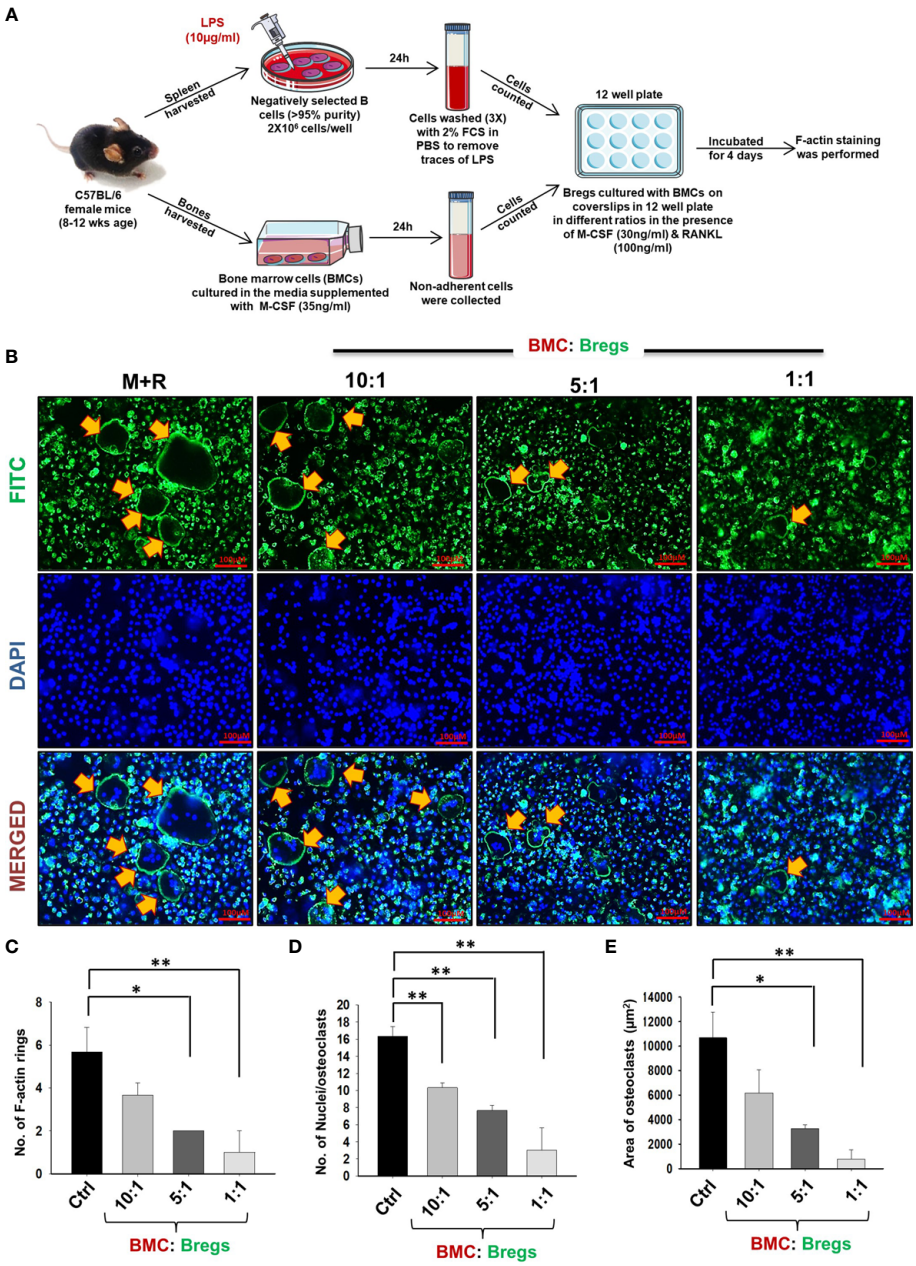

FIGURE 3 | Bregs suppress F-actin formation in osteoclasts. **(A)** BMCs and Bregs were co-cultured in the presence of M-CSF (30 ng/ml) and RANKL (100 ng/ml) at different ratios for 4 days and at the end of incubation F-actin staining was performed. B cells were stimulated with LPS (10 ug/ml) for 24h prior to co-cultures. **(B)** F-actin and nuclei were stained with FITC conjugated phalloidin and DAPI respectively. Images were captured in a fluorescence microscope (Imager.Z2 Zeiss microscope) at 10 X magnification. **(C)** Number of F-actin rings **(D)** Number of nuclei per osteoclasts **(E)** Area of F-actin rings. The above images are indicative of one experiment and similar results were obtained in three independent experiments. The results were evaluated by ANOVA with subsequent comparisons by Student t-test for paired or nonpaired data. Statistical significance was considered as $p \leq 0.05$ (*$p \leq 0.05$, **$p \leq 0.01$, ***$p \leq 0.001$) with respect to indicated groups (Mouse Image courtesy: Ms. Leena Sapra).

enhancement in IL-10 cytokine levels in co-cultures supernatants in comparison to the control group (**Figure 5I**).

To confirm whether the observed inhibitory effects of Bregs on osteoclastogenesis are mediated by IL-10 alone, we next performed an IL-10 neutralization assay. For the same, we employed anti-IL-10 MAb (10 ug/ml) to neutralize the anti-osteoclastogenic potential of Bregs in BMCs and Bregs cell co-cultures. Excitingly, we observed that anti-IL-10 significantly abolished the anti-osteoclastogenic potential of Bregs. Isotype control for anti-IL-10 was also set up to confirm these results (**Figures 6A–D**). Altogether, our results for

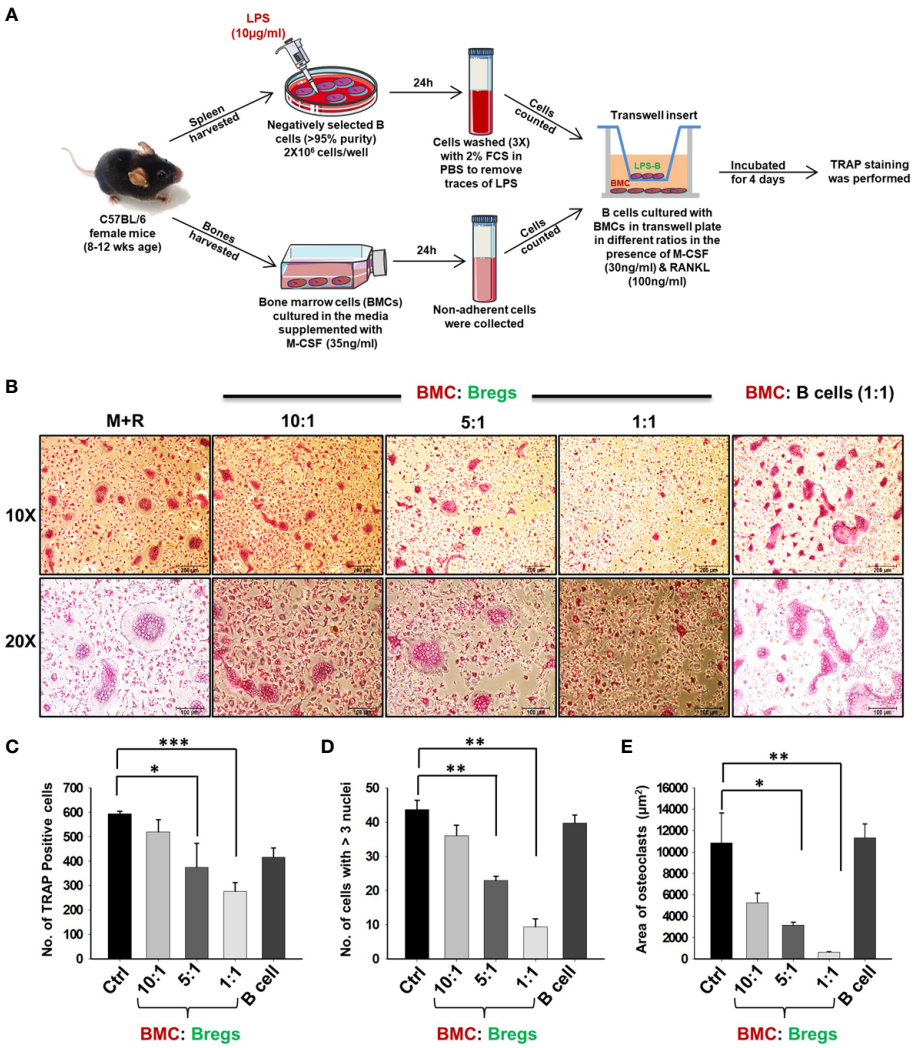

FIGURE 4 | Bregs suppress osteoclastogenesis via soluble molecules. **(A)** BMCs and LPS stimulated and non-stimulated B cells were co-cultured in transwell insert in the presence of M-CSF (30 ng/ml) and RANKL (100 ng/ml) for 4 days. B cells were stimulated with LPS (10 ug/ml) for 24h prior to being added to co-cultures. **(B)** Bregs significantly inhibited the generation of multinucleated osteoclasts in a dose-dependent manner. **(C)** Graphical representation depicting the number of TRAP-positive cells. **(D)** Bar graphs representing the number of cells with more than three nuclei. **(E)** Bar graphs representing the area of multinucleated TRAP-positive cells. Control denotes BMCs culture only. The above images are indicative of one independent experiment and similar results were obtained in three independent experiments. The results were evaluated by ANOVA with subsequent comparisons by Student t-test for paired or nonpaired data. Statistical significance was considered as $p \leq 0.05$ (*$p \leq 0.05$, **$p \leq 0.01$, ***$p \leq 0.001$) with respect to indicated groups (Mouse Image courtesy: Ms. Leena Sapra).

the first time establish the direct role of Bregs in inhibiting *in vitro* osteoclastogenesis in an IL-10-dependent manner.

Successful Development of Postmenopausal Osteoporotic Mice Model

Next, to investigate the likely contribution of regulatory B cells in modulating bone health under normal and osteoporotic conditions, we firstly developed and authenticated a postmenopausal osteoporotic mice model, a prime requirement for our study. For accomplishing the same, female C57BL/6 mice were divided into two groups viz. sham and ovx. At the end of the experiment, blood serum was analyzed for estradiol levels, and bones were harvested for assessing the effect of estrogen deficiency on bone loss (**Figure 7A**). Our results clearly indicated a significant reduction in estradiol levels from 29 pg/ml (sham) to 9 pg/ml (3-fold) in the ovx group ($p < 0.01$) (**Figure 7B**).

After the successful development of a postmenopausal osteoporotic mice model, we next investigated the effect of estrogen loss on bone resorption and bone histomorphometric parameters. Scanning electron microscopy (SEM) and micro-computed tomography (µ-CT) analysis (a gold standard for determining bone health) were next performed. SEM analysis

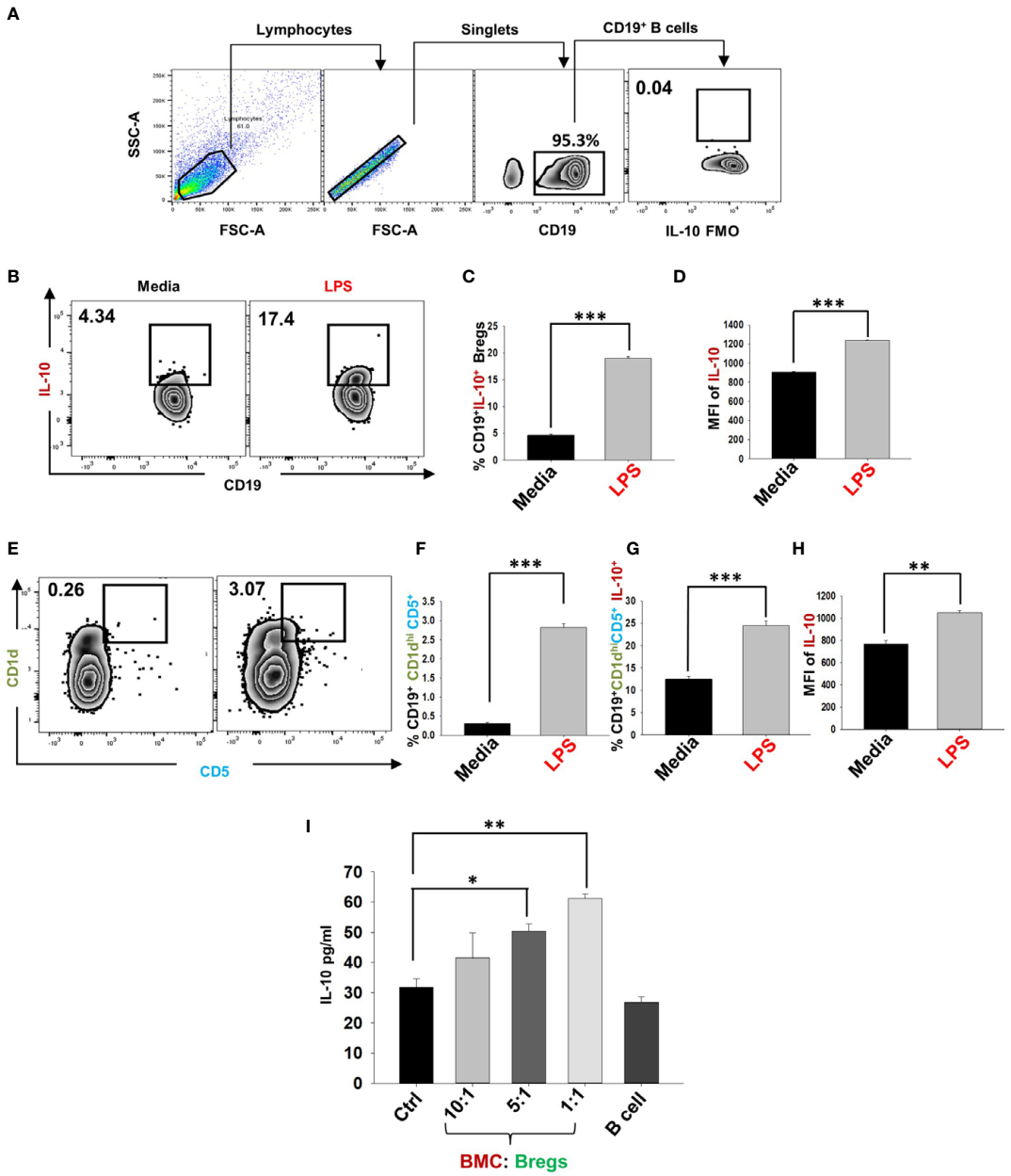

FIGURE 5 | IL-10 producing Bregs inhibits osteoclastogenesis. After 24h of LPS stimulation cells were harvested and evaluated for estimating the expression of markers that may be associated with anti-osteoclastogenic function of B cells. **(A)** Gating strategy followed for data analysis. **(B)** Zebra plot depicting the percentages of $CD19^{+}IL\text{-}10^{+}$ Bregs in media and LPS induced Bregs. **(C)** Graphical representations depicting percentages of $CD19^{+}IL\text{-}10^{+}$ Bregs. **(D)** MFI of IL-10. **(E)** Zebra plot highlighting the percentages of $CD19^{+}CD1d^{hi}CD5^{+}$ (B10) Bregs. **(F)** Graphical representation of $CD19^{+}CD1d^{hi}CD5^{+}$ B10 Bregs. **(G)** Bar graph representing $CD19^{+}CD1d^{hi}CD5^{+}IL\text{-}10^{+}$ B10 Breg **(H)** MFI of IL-10 on $CD19^{+}CD1d^{hi}CD5^{+}$. **(I)** ELISA results of supernatant harvested from co-cultures of BMCs and Bregs showing levels of IL-10 cytokine. The above images are indicative of one independent experiment and similar results were obtained in three independent experiments. The results were evaluated by ANOVA with subsequent comparisons by Student t-test for paired or nonpaired data. Statistical significance was considered as $p \leq 0.05$ ($^{*}p \leq 0.05$, $^{**}p \leq 0.01$, $^{***}p \leq 0.001$) with respect to indicated groups.

of cortical region (femoral bone) demonstrated an enhanced number of lacunae or resorption pits in the ovx group with respect to the control group (**Figure 7C**). To further analyze the SEM 2D-images in a statistical manner, we performed MATLAB (matrix-laboratory) analysis to determine the correlation between bone mass and bone loss in both groups. The MATLAB analysis specifies the degree of homogeneity where a red color indicates higher correlation values (high bone mass), and blue symbolizes lower correlation values (more bone loss). Outcomes of MATLAB analysis clearly showed that the ovx

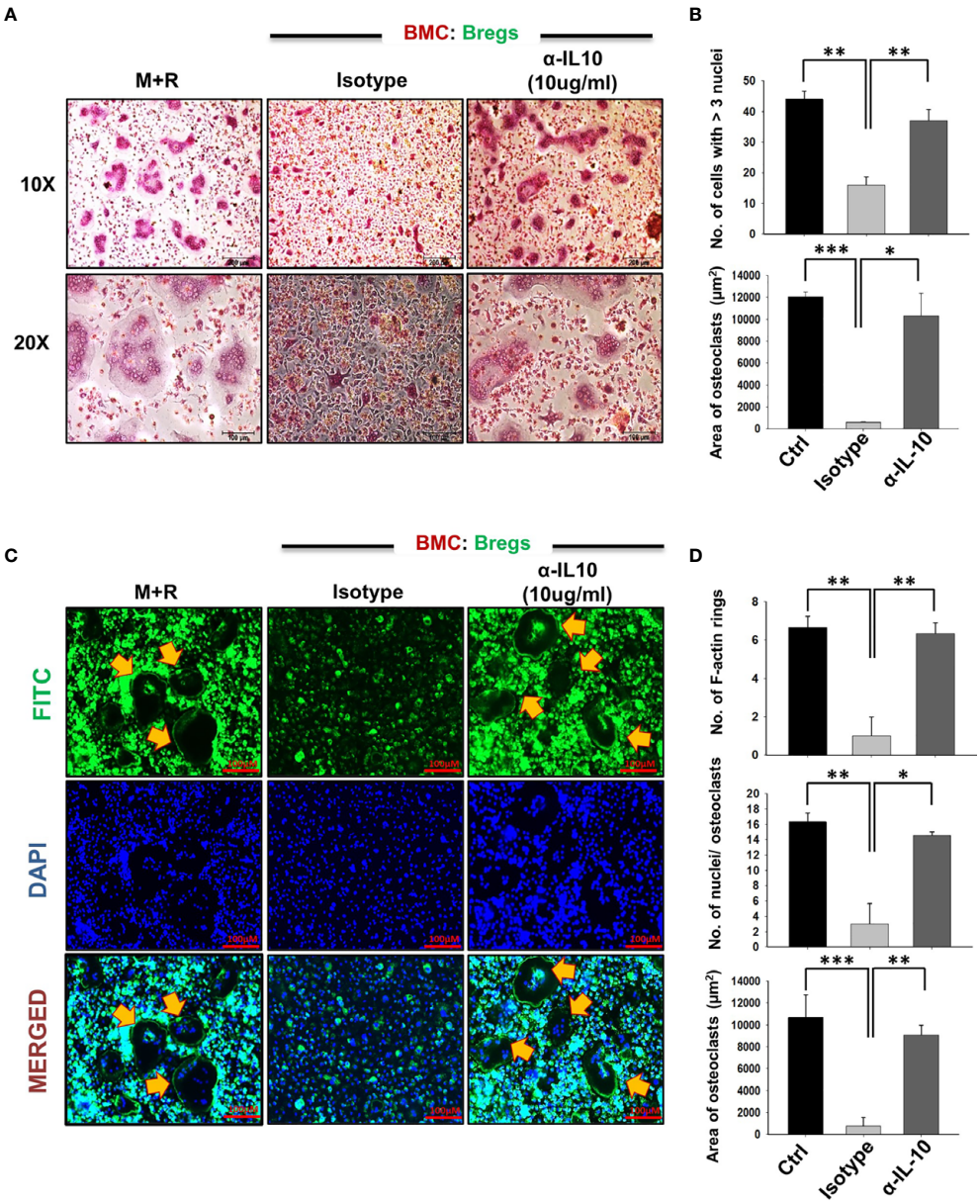

FIGURE 6 | Bregs inhibit osteoclastogenesis in an IL-10 dependent manner. Osteoclastogenesis was evaluated after neutralization of IL-10 cytokine with antibodies against IL-10 in BMCs and Bregs co-cultures. **(A)** BMCs and LPS stimulated B cells were co-cultured (1:1) in 24 well plates in the presence of M-CSF (30 ng/ml) and RANKL (100 ng/ml) along with the presence or absence of α-IL10 & isotype control for 4 days. **(B)** Graphical representation of the number of cells with more than three nuclei and area of multinucleated TRAP-positive cells. **(C)** F-actin and nuclei were stained with FITC conjugated phalloidin and DAPI respectively. **(D)** Number of F-actin rings, Number of nuclei per osteoclasts, and Area of F-actin rings. The above images are indicative of one experiment and similar results were obtained in three independent experiments. The results were evaluated by ANOVA with subsequent comparisons by Student t-test for paired or nonpaired data. Statistical significance was considered as $p \leq 0.05$ (*$p \leq 0.05$, **$p \leq 0.01$, ***$p \leq 0.001$) with respect to indicated groups.

group has lesser correlation values or higher bone loss in the ovx group in comparison to the sham group (**Figure 7D**).

Moving ahead, we next authenticated the successful development of osteoporotic conditions in our model *via* μ-CT analysis. As lumbar-vertebrae-5 (LV-5) is one of the peculiar regions to diagnose osteoporotic conditions (16). Therefore, we analyzed the effect of estrogen deficiency on the LV-5 trabecular region along with the trabecular region of femoral and tibial bones. Interestingly, μ-CT data revealed that estrogen deficiency significantly impaired the micro-architecture of LV-5, femoral, and tibial bones in the ovx group in comparison to the sham group (**Figure 8A**). Moreover, an ameliorated bone loss

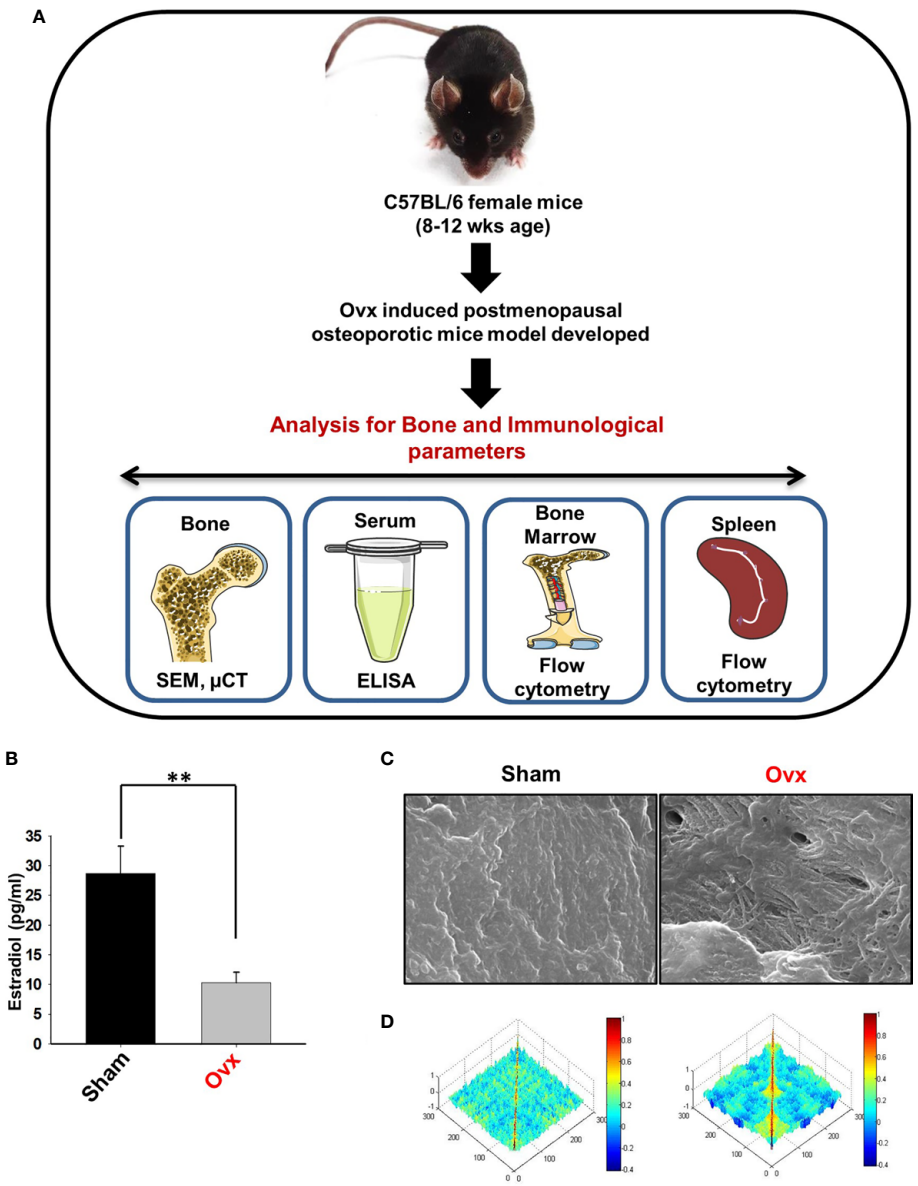

FIGURE 7 | Development of postmenopausal osteoporotic mice model. **(A)** Experimental layout followed for *in vivo* study. **(B)** Estrogen level was estimated in blood serum of the sham and ovx mice groups. Mice were sacrificed at the end of the experiment and cortical bones of both the groups were collected for SEM analysis. **(C)** 2D SEM images. **(D)** MATLAB analysis of SEM images. The above images are indicative of one independent experiment and comparable results were obtained in two different independent experiments with n=6 mice/group/experiment. The results were evaluated by ANOVA with subsequent comparisons by Student t-test for paired or non-paired data. Values are reported as mean ± SEM. Similar results were obtained in two different independent experiments with n=6. Statistical significance was considered as $p \leq 0.05$ (*$p \leq 0.05$, **$p \leq 0.01$, ***$p \leq 0.001$) with respect to indicated Sham group. (Mouse Image courtesy: Ms. Leena Sapra).

condition in the ovx group is further supported by significantly reduced bone mineral density (BMD) in the ovx group with respect to sham group (**Figure 8B**). The quantitative analysis of trabecular and cortical bones which provides an overview of the utmost fundamental histomorphometric indices that were derived from bone micro-architecture 3D images is shown in **Table 1**. Altogether, our results clearly established the successful development of the postmenopausal osteoporotic mice model.

Bregs Play an Important Role in Ameliorating Ovariectomy-Induced Bone Loss

Estrogen-deficiency-induced bone loss is mediated by various factors viz. immunological, biochemical, etc. Also, the role of cytokine imbalance in regulating bone health is well established. Results from our lab (13, 14) along with others have reported significantly reduced levels of osteoprotective cytokine IL-10

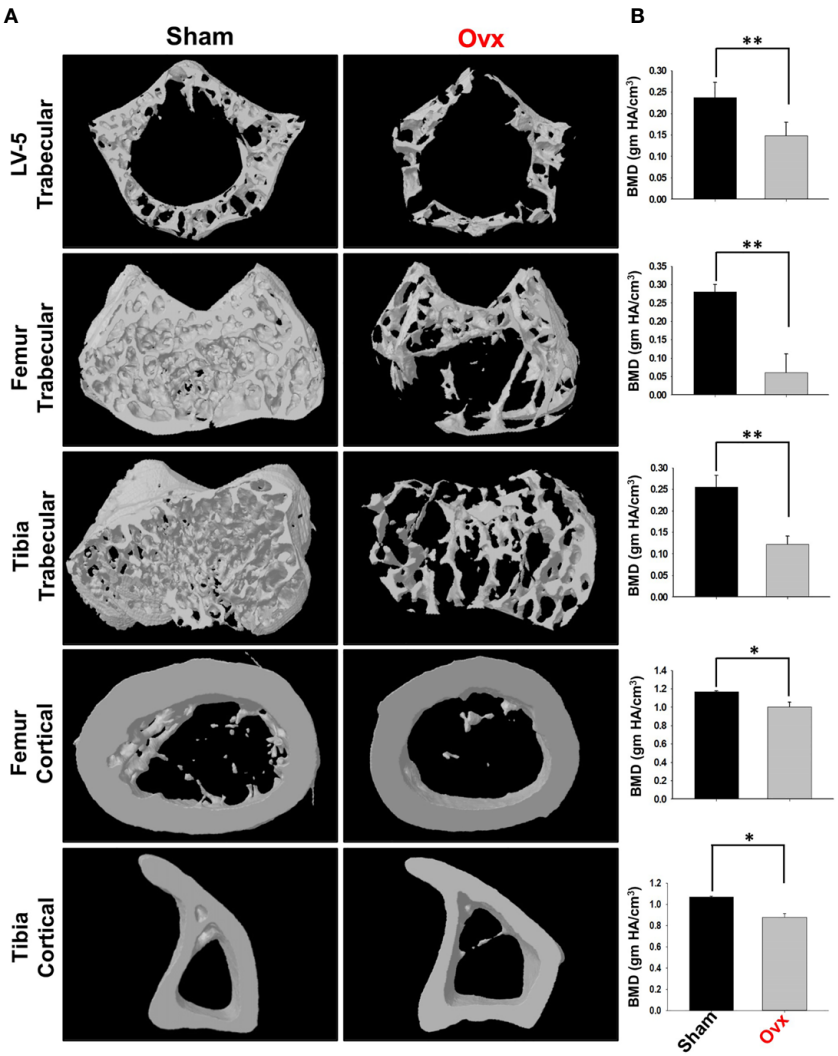

FIGURE 8 | Micro-CT analysis of trabecular and cortical regions of Lumbar Vertebrae-5 (LV-5), Femoral and Tibial bones. **(A)** 3D micro-CT reconstructions of LV-5 trabecular region, Femur trabecular region, Tibia trabecular, Femur cortical, and Tibia cortical regions of the sham and ovx groups. **(B)** Graphical representations of Bone Mineral Density (BMD) of LV-5 trabecular region, Femur trabecular region, Tibia trabecular, Femur cortical, and Tibia cortical regions of the sham and ovx groups. The results were evaluated by ANOVA with subsequent comparisons by Student t-test for paired or non-paired data. Values are reported as mean ± SEM. Similar results were obtained in two different independent experiments with n=6. Statistical significance was considered as $p \leq 0.05$ (*$p \leq 0.05$, **$p \leq 0.01$, ***$p \leq 0.001$) with respect to indicated Sham group.

along with higher levels of osteoclastogenic cytokines viz. IL-17 and TNF-α under ovx conditions (**Figures 9A, B**). Extensive literature suggests that the major source of IL-10 is immune cells. Recently, several studies have reported that apart from Tregs, Bregs are also a major source of IL-10 under physiological conditions (6, 21). Therefore, a strong possibility exists that the observed reduction of IL-10 levels under osteoporotic conditions may not be primarily due to dysregulation of Tregs alone. Based on these studies we strongly believe and propose that alteration in the Bregs population could also be one of the major contributing factors for observed significant reduction in IL-10 levels observed under ovx conditions. Thus, we next asked the question: are the observed significantly reduced levels of IL-10 in ovx mice due to dysregulation of the Bregs population? We thus analyzed the frequency of Bregs in both the BM (prime site of osteoclastogenesis) and spleen (main site of Bregs induction) in mice. Interestingly, the frequencies of total IL-10 producing B cells, i.e., $CD19^{+}IL\text{-}10^{+}$ cells were significantly reduced in the ovx group in comparison to the control group ($p < 0.01$) in both BM and spleen (**Figures 10A–C**). Notably, the population of "B10" Bregs, i.e., $CD19^{+}CD1d^{hi}CD5^{+}IL\text{-}10^{+}$ were also observed to be significantly reduced in both BM and spleen of the ovx group in comparison to th sham group ($p < 0.05$) (**Figures 10D–H**). Taken together, our results clearly point towards a crucial role of Bregs in modulating bone loss under postmenopausal osteoporotic conditions.

TABLE 1 | Bone Histomorphometric Parameters in Ovx mice.

Bone Parameters	Sham	Ovx
LV5		
BV/TV (%)	92.07 ± 2.84	60.87 ±6.62**
Tb. Th (mm)	0.06 ± 0.001	0.04 ± 0.001**
Tb. No (mm^{-1})	11.8 ± 0.86	2.49 ± 0.08**
Conn. Den (mm^{-3})	183.05 ± 43	89.66 ± 6.1
Tb. Sp. (mm)	0.01 ± 0.00	0.27 ± 0.003***
Tb. Pf (mm^{-1})	18.4 ± 0.22	29.7 ± 0.64*
Femur Trabecular		
BV/TV (%)	60.93 ± 3.21	8.24 ±1.18**
Tb. Th (mm)	0.068 ± 0.005	0.04± 0.003*
Tb. No (mm^{-1})	13.6 ± 0.8	1.44 ± 0.18**
Conn. Den (mm^{-3})	227 ± 29.6	58.4 ± 6.02**
Tb. Sp. (mm)	0.07 ± 0.01	0.66 ± 0.03**
Tb. Pf (mm^{-1})	11.12± 1.54	26.11 ± 0.80**
Tibia Trabecular		
BV/TV (%)	88.93 ± 0.09	5.23 ± 0.15***
Tb. Th (mm)	0.07 ± 0.001	0.05 ± 0.0006**
Tb. No (mm^{-1})	13.1 ± 0.45	1.1 ± 0.15***
Conn. Den (mm^{-3})	60.24 ± 3.88	24.79 ± 0.95**
Tb. Sp. (mm)	0.04 ± 0.002	0.53 ± 0.01***
Tb. Pf (mm^{-1})	15.14 ± 1.01	26.43 ± 0.78**
Femur Cortical		
Tt. Ar (mm^2)	2.22 ± 0.05	1.5 ± 0.19*
T. Pm (mm)	5.69 ± 0.09	4.95 ± 0.06*
Ct. Ar (mm^2)	0.85 ± 0.007	0.63 ± 0.04*
B. Pm (mm)	10.33 ± 0.17	8.95 ± 0.15*
Ct. Th (mm)	0.17 ± 0.001	0.12 ± 0.01*
Tibia Cortical		
Tt. Ar (mm^2)	1.46 ± 0.012	1.23 ± 0.02**
T. Pm (mm)	7.4 ± 0.79	5.7 ± 0.25
Ct. Ar (mm^2)	0.70 ± 0.012	0.58 ± 0.02*
B. Pm (mm)	10.4 ± 0.2	9.06 ± 0.25*
Ct. Th (mm)	0.15 ± 0.001	0.11 ± 0.004**

*BV/TV, Bone volume/tissue volume ratio; Tb. Th, trabecular thickness; Tb. No., trabecular number; Conn. Den, connectivity density; Tb. Sep., trabecular separation; Tb. Pf., trabecularpattern factor; Tt. Ar., total cross-sectional area; T. Pm, total cross-sectional perimeter; Ct. Ar, cortical bone area; B. Pm, bone perimeter; Ct. Th, average cortical thickness. The results were evaluated by ANOVA with subsequent comparisons by Student t-test for paired or nonpaired data. Values are reported as mean ± SEM. Similar results were obtained in two different independent experiments with n=6. Statistical significance was considered as p≤0.05 (*p ≤ 0.05, **p ≤ 0.01, ***p ≤ 0.001) with respect to indicated Sham group.*

Histomorphometric indices of LV-5 trabecular, femur trabecular, tibia trabecular, femur cortical, and tibia cortical of the sham and ovx mice groups.

DISCUSSION

Studies from our lab along with others have highlighted the relevance of the immune system in maintaining bone health under both physiological and osteoporotic conditions (13, 19, 22, 23). These studies laid the foundation for the importance of the immune system in osteoporosis, i.e., "Immunoporosis" (19). Various studies demonstrated that the homeostatic balance between anti-inflammatory (Tregs) and inflammatory (Th17) cells is of utmost importance in various diseases including osteoporosis (13, 16, 24). Apart from Tregs, there are also other regulatory lymphocytes with established immunosuppressive functions. Most important among these are the recently discovered "Bregs".

Bregs with immunoregulatory potential have been observed in several disease models of autoimmunity, such as RA, SLE, experimental autoimmune hepatitis (EAH), etc. (6, 21, 25). Bregs perform their regulatory functions *via* secreting soluble cytokines (viz. IL-10) or expressing membrane-bound surface molecules (TGF-β). Nevertheless, the primary regulatory mechanism of Bregs is based on the immunoregulatory cytokine IL-10. Multiple studies demonstrated that IL-10 is an anti-osteoclastogenic cytokine that maintains bone health by inhibiting osteoclastogenesis (26, 27). Moreover, the significance of IL-10 is further highlighted in IL-10 deficient mice in which all the hallmarks of osteoporosis i.e. decreased bone mass, enhanced mechanical fragility, and reduced bone formation was observed (28). Moreover, Tregs *via* secreting IL-10 and other cytokines viz. IL-4 along with membrane-bound receptors, such as cytotoxic T lymphocyte antigen (CTLA)-4 abrogates osteoclastogenesis (15). IL-10 is a pivotal immunomodulator in infectious diseases, autoimmune disorders, inflammatory bone loss conditions including osteoporosis, but no study to date has ever investigated the significance of IL-10 secreting Bregs in regulating bone health in both *in vitro* and *in vivo* conditions. Multiple studies suggested that Bregs mediate its immunosuppressive functions by promoting the differentiation of naïve $CD4^+$ T cells into Tregs (29, 30). Importantly, a study also suggested that even in the absence of Tregs, Bregs suppressed arthritis thereby highlighting towards the independent function of Bregs (31).

IL-10 is an established regulatory molecule of Bregs; but the expression of IL-10 cytokine is quite low in resting B cells, thus to enhance the expression of IL-10, *in vitro* stimulation of B cells is required. A study reported by Yang et al. (32), demonstrated that LPS stimulation for 24h leads to enhancement of IL-10 producing Bregs (32). Thus, we chose this particular method for the generation of Bregs in our experiments. Next, we activated purified B cells (>95%) with LPS for different time periods (5h and 24h) and, in consistence with previously reported studies, we too observed a time-dependent induction of IL-10 producing Bregs. Moving ahead in our study, we were further interested in investigating the role of Bregs in modulating RANKL induced osteoclastogenesis under *in vitro* conditions. Excitingly, we observed that Bregs inhibited the differentiation of osteoclasts from BMCs in a dose-dependent manner. Also, our *in vitro* data suggested that Bregs exhibit the potential of suppressing F-actin ring formation in osteoclasts: a vital characteristic phenotype of mature osteoclasts responsible for their functional activity (bone resorption). We were further keen to know whether the observed suppression of osteoclastogenesis by Bregs is cytokine dependent (soluble factors) or requires cell-to-cell contact. Thus, we employed a trans-well system for our cultures and observed that the anti-osteoclastogenic potential of Bregs is primarily mediated by soluble factors. In addition to this, both our ELISA results (co-culture supernatant) along with flow cytometric data of cells harvested from the co-cultures of BMCs and Bregs clearly establish the role of IL-10 secreting Bregs in suppressing osteoclastogenesis. Moreover, our anti-IL-10 neutralizing antibody experiment clearly showed restoration of osteoclastogenesis in BMCs even in the presence of Bregs, thereby establishing the role of IL-10 in Bregs mediated regulation of osteoclastogenesis. Altogether, these findings of ours for the first time establish the direct role of Bregs in inhibiting osteoclastogenesis under *in vitro* conditions.

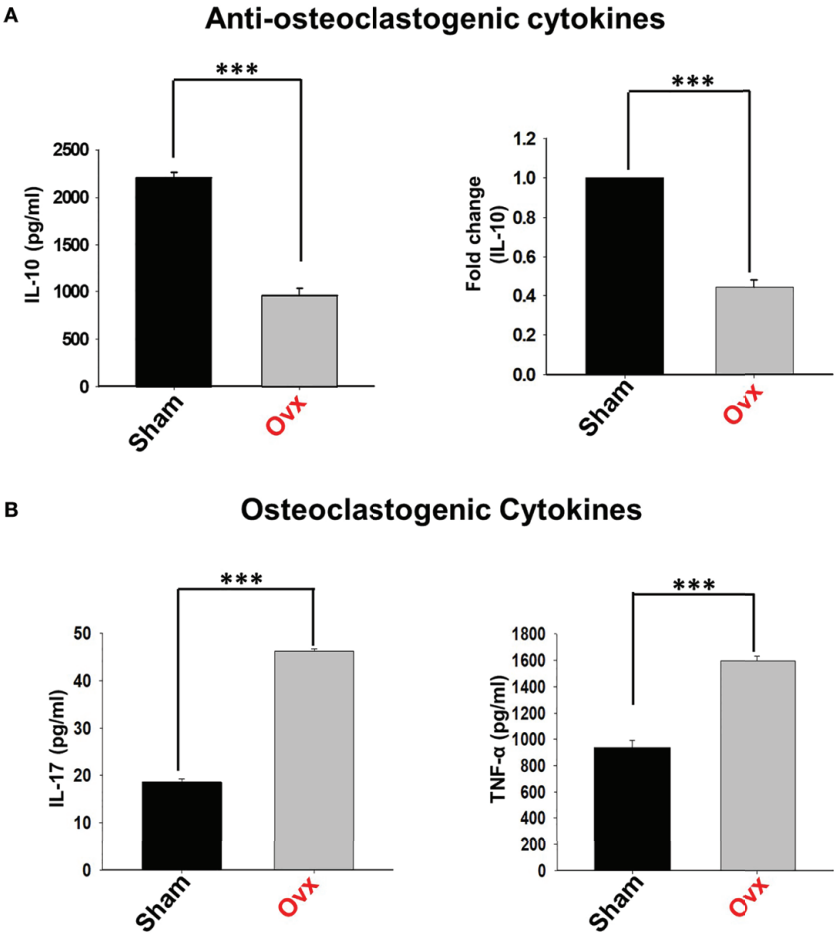

FIGURE 9 | Osteoclastogenic and anti-osteoclastogenic cytokine levels in ovx mice. Cytokines were analyzed in serum samples of mice by ELISA. **(A)** Levels of IL-10 cytokine. **(B)** Levels of IL-17 and TNF-α cytokines in the sham and ovx groups. The results were evaluated by using ANOVA with subsequent comparisons by Student t-test for paired or non-paired data, as appropriate. Values are expressed as mean ± SEM (n=6) and similar results were obtained in two independent experiments. Statistical significance was defined as $p \leq 0.05$, $^{*}p \leq 0.05$, $^{**}p < 0.01$ $^{***}p \leq 0.001$ with respect to indicated mice group.

A study reported in 2013 by the Flores et al. group demonstrated that numerical defects or profound reduction in frequencies of Bregs as a major causative factor for RA in humans (6). In the beginning of 2020, our group also highlighted the probable contribution of IL-10 producing regulatory B cells in the case of osteoporosis and found that IL-10 producing Bregs are significantly reduced in the post-menopausal osteoporotic mice model (unpublished data) (1). As is consistent with our data, recently, one study also suggested that Bregs exhibit osteoprotective potential in case of post-menopausal osteoporosis as adoptive transfer of IL-10 producing Bregs into ovx-mice-reduced bone deterioration (33). In line with these findings, our present study, reports the modulation of IL-10 secreting Bregs not only in the spleen but also in BM, the prime site of osteoclastogenesis. Furthermore, our *in vivo* flow cytometric data clearly indicates a numerical defect in both $CD19^{+}IL\text{-}10^{+}$ Bregs and $CD19^{+}CD1d^{hi}CD5^{+}IL\text{-}10^{+}$ "B10" cells in both BM and spleen (main site of Bregs generation). Furthermore, our serum cytokine data corroborate our flow cytometric data with significant reduction of IL-10 levels in osteoporotic group with respect to control group.

Taken together, our present study for the first time establishes that Bregs exhibits anti-osteoclastogenic potential *in vitro*. Moreover, reduction in Bregs number observed *in vivo* may also be one of the prime contributing factors towards inflammatory bone loss observed in the postmenopausal osteoporotic mice model. These results thus provide novel insight into Bregs biology in the context of osteoporosis (**Figure 11**). Moreover, apart from these Bregs populations (viz. $CD19^{+}IL\text{-}10^{+}$ and $CD19^{+}CD1d^{hi}CD5^{+}IL\text{-}10^{+}$ Bregs), we also observed that other Bregs populations with characteristic phenotypes of $CD19^{+}FOXP3^{+}$ Bregs and $CD19^{+}CD11b^{+}$ Bregs were also found to be decreased in the case of an osteoporotic mice model (unpublished observation). Thus, further studies are need of the hour to fully dissect and establish the role of various

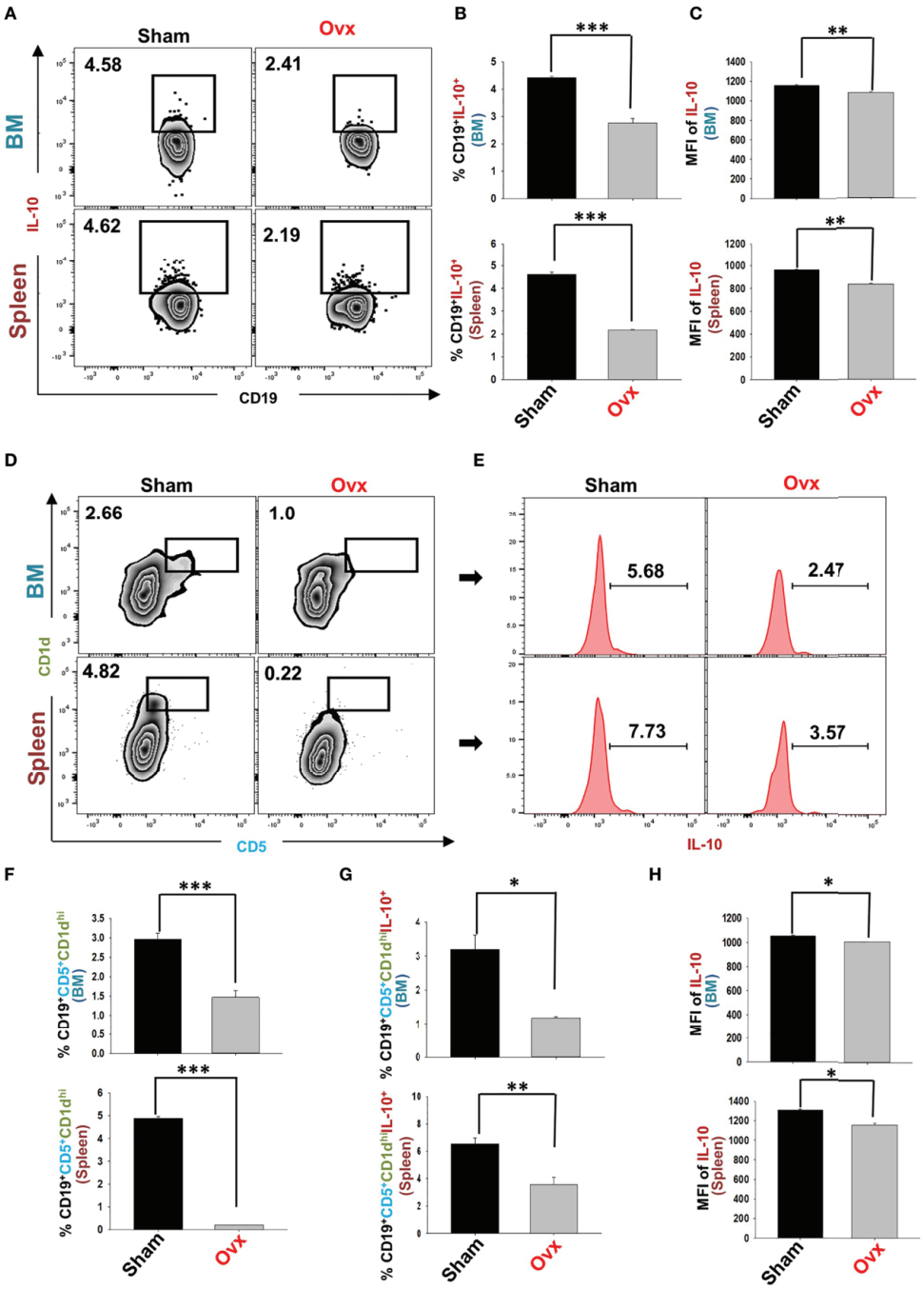

FIGURE 10 | Ovariectomy results in modulation of Bregs population in vivo. Cells from Bone Marrow (BM) and spleen of the sham and ovx groups were harvested and analyzed by flow cytometry for the percentage of Breg **(A)** Zebra plot depicting percentages of $CD19^{+}IL\text{-}10^{+}$ B cells in BM and spleen of sham and ovx. **(B)** Bar graph representing percentages $CD19^{+}IL\text{-}10^{+}$ Bregs in sham and ovx. **(C)** Bar graphs representing the MFI of IL-10 in BM and spleen. **(D)** Zebra plot depicting percentages of $CD19^{+}CD1d^{hi}CD5^{+}$ B10 cells in BM and spleen. **(E)** Histograms representing IL-10 cytokine levels in the sham and ovx groups. **(F)** Graphical representation of $CD19^{+}CD1d^{hi}CD5^{+}$ Bregs in sham and ovx mice. **(G)** Graphical representation of the percentage of $CD19^{+}CD1d^{hi}CD5^{+}IL\text{-}10^{+}$ B10 cells in sham and ovx mice. **(H)** Graphical representation of MFI of IL-10 in sham and ovx. The results were evaluated by using ANOVA with subsequent comparisons by Student t-test for paired or non-paired data, as appropriate. Values are expressed as mean ± SEM (n=6) and similar results were obtained in two independent experiments. Statistical significance was defined as $p \leq 0.05$, $^{*}p \leq 0.05$, $^{**}p < 0.01$ $^{***}p \leq 0.001$ with respect to indicated mice group.

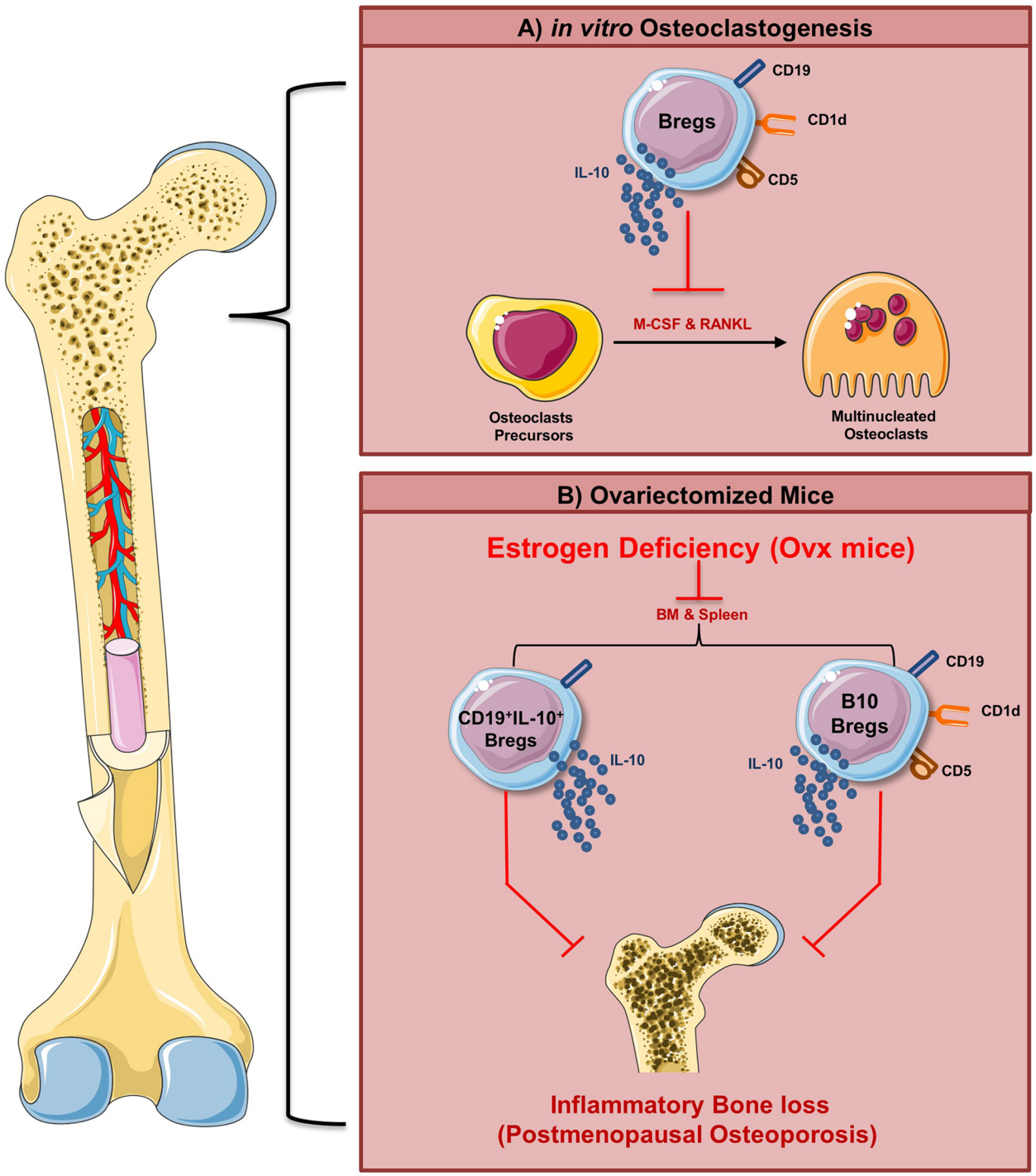

FIGURE 11 | Summary of results. **(A)** Regulatory B cells inhibit RANKL induced osteoclastogenesis under *in vitro* conditions via IL-10 cytokine. **(B)** Our *in vivo* data suggest that modulation of the Bregs population (both bone marrow and spleen) along with its reduced potential to produce IL-10 ameliorates inflammatory bone loss observed under postmenopausal conditions in ovx mice (Image illustrated using Medical Art https://smart.servier.com/).

populations of Bregs in post-menopausal osteoporotic conditions, which would thereby lead to future employment of Bregs-based cellular therapy in ameliorating inflammatory bone loss observed in osteoporosis.

DATA AVAILABILITY STATEMENT

The raw data supporting the conclusions of this article will be made available by the authors, without undue reservation.

ETHICS STATEMENT

The animal study was reviewed and approved by Institutional Animal Ethics Committee of AIIMS, New Delhi, India (85/IAEC-1/2018 and 196/IAEC-1/2019).

AUTHOR CONTRIBUTIONS

RS contributed to the conceptualization and investigation of the study. LS and AB contributed to the methodology and formal analysis of data. PM carried out cytokine analysis. RS and LS contributed to the writing and editing of the manuscript. GM, BG, and BV provided valuable inputs in the study design. All authors reviewed the manuscript. All authors contributed to the article and approved the submitted version.

FUNDING

This work was financially supported by projects: DST-SERB (EMR/2016/007158), Govt. of India and intramural project from All India Institute of Medical Sciences (AIIMS, A-798), New Delhi-India sanctioned to RS; National Academy of Sciences (NASI), Allahabad-India sanctioned to GM.

ACKNOWLEDGMENTS

LS, AB, PM, BG, BV, and RS acknowledge the Department of Biotechnology AIIMS, New Delhi-India for providing infrastructural facilities. GM acknowledges National Centre for Cell Science (NCCS), Pune-India, for providing infrastructural facilities. The authors thank the CCRF shared FACS Facility, AIIMS, for the acquisition of samples. LS thanks UGC for the research fellowship, and AB thanks the DST SERB project for the research fellowship. Figures were created with the help of https://smart.servier.com/.

REFERENCES

1. Dar HY, Rani L, Sapra L, Azam Z, Shokeen N, Bhardwaj A, et al. A Chronological Journey of Breg Subsets: Implications in Health and Disease. In: *Systems and Synthetic Immunology*. Singapore: Springer Singapore (2020). p. 125–52. doi: 10.1007/978-981-15-3350-1_5
2. Ben Nasr M, Usuelli V, Seelam AJ, D'Addio F, Abdi R, Markmann JF, et al. Regulatory B Cells in Autoimmune Diabetes. *J Immunol* (2021) 206:1117–25. doi: 10.4049/jimmunol.2001127
3. Tedder TF. B10 Cells: A Functionally Defined Regulatory B Cell Subset. *J Immunol* (2015) 194:1395–401. doi: 10.4049/jimmunol.1401329
4. Rosser EC, Mauri C. Regulatory B Cells: Origin, Phenotype, and Function. *Immunity* (2015) 42:607–12. doi: 10.1016/j.immuni.2015.04.005
5. Yang M, Deng J, Liu Y, Ko K-H, Wang X, Jiao Z, et al. Il-10–Producing Regulatory B10 Cells Ameliorate Collagen-Induced Arthritis Via Suppressing Th17 Cell Generation. *Am J Pathol* (2012) 180:2375–85. doi: 10.1016/j.ajpath.2012.03.010
6. Flores-Borja F, Bosma A, Ng D, Reddy V, Ehrenstein MR, Isenberg DA, et al. Cd19+Cd24hicd38hi B Cells Maintain Regulatory T Cells While Limiting TH1 and TH17 Differentiation. *Sci Transl Med* (2013) 5:173ra23. doi: 10.1126/scitranslmed.3005407
7. Ran Z, Yue-Bei L, Qiu-Ming Z, Huan Y. Regulatory B Cells and Its Role in Central Nervous System Inflammatory Demyelinating Diseases. *Front Immunol* (2020) 11:1884–904. doi: 10.3389/fimmu.2020.01884
8. Yanaba K, Bouaziz J-D, Haas KM, Poe JC, Fujimoto M, Tedder TF. A Regulatory B Cell Subset With a Unique Cd1dhicd5+ Phenotype Controls T Cell-Dependent Inflammatory Responses. *Immunity* (2008) 28:639–50. doi: 10.1016/j.immuni.2008.03.017
9. Yanaba K, Bouaziz J-D, Matsushita T, Tsubata T, Tedder TF. The Development and Function of Regulatory B Cells Expressing Il-10 (B10 Cells) Requires Antigen Receptor Diversity and TLR Signals. *J Immunol* (2009) 182:7459–72. doi: 10.4049/jimmunol.0900270
10. Matsushita T, Yanaba K, Bouaziz J-D, Fujimoto M, Tedder TF. Regulatory B Cells Inhibit EAE Initiation in Mice While Other B Cells Promote Disease Progression. *J Clin Invest* (2008) 118:3420–30. doi: 10.1172/JCI36030
11. Watanabe R, Ishiura N, Nakashima H, Kuwano Y, Okochi H, Tamaki K, et al. Regulatory B Cells (B10 Cells) Have a Suppressive Role in Murine Lupus: CD19 and B10 Cell Deficiency Exacerbates Systemic Autoimmunity. *J Immunol* (2010) 184:4801–9. doi: 10.4049/jimmunol.0902385
12. Yanaba K, Yoshizaki A, Asano Y, Kadono T, Tedder TF, Sato S. Il-10–Producing Regulatory B10 Cells Inhibit Intestinal Injury in a Mouse Model. *Am J Pathol* (2011) 178:735–43. doi: 10.1016/j.ajpath.2010.10.022
13. Dar HY, Shukla P, Mishra PK, Anupam R, Mondal RK, Tomar GB, et al. Lactobacillus Acidophilus Inhibits Bone Loss and Increases Bone Heterogeneity in Osteoporotic Mice *Via* Modulating Treg-Th17 Cell Balance. *Bone Rep* (2018) 8:46–56. doi: 10.1016/j.bonr.2018.02.001
14. Dar HY, Pal S, Shukla P, Mishra PK, Tomar GB, Chattopadhyay N, et al. Bacillus Clausii Inhibits Bone Loss by Skewing Treg-Th17 Cell Equilibrium in Postmenopausal Osteoporotic Mice Model. *Nutrition* (2018) 54:118–28. doi: 10.1016/j.nut.2018.02.013
15. Zaiss MM, Axmann R, Zwerina J, Polzer K, Gückel E, Skapenko A, et al. Treg Cells Suppress Osteoclast Formation: A New Link Between the Immune System and Bone. *Arthritis Rheum* (2007) 56:4104–12. doi: 10.1002/art.23138
16. Sapra L, Dar HY, Bhardwaj A, Pandey A, Kumari S, Azam Z, et al. Lactobacillus Rhamnosus Attenuates Bone Loss and Maintains Bone Health by Skewing Treg-Th17 Cell Balance in Ovx Mice. *Sci Rep* (2021) 11:1807. doi: 10.1038/s41598-020-80536-2
17. Zhang Q, Chen B, Yan F, Guo J, Zhu X, Ma S, et al. Interleukin-10 Inhibits Bone Resorption: A Potential Therapeutic Strategy in Periodontitis and Other Bone Loss Diseases. *BioMed Res Int* (2014) 2014:1–5. doi: 10.1155/2014/284836
18. Mielle J, Audo R, Hahne M, Macia L, Combe B, Morel J, et al. Il-10 Producing B Cells Ability to Induce Regulatory T Cells Is Maintained in Rheumatoid Arthritis. *Front Immunol* (2018) 9:961. doi: 10.3389/fimmu.2018.00961
19. Srivastava RK, Dar HY, Mishra PK. Immunoporosis: Immunology of Osteoporosis—Role of T Cells. *Front Immunol* (2018) 9:567–9. doi: 10.3389/fimmu.2018.00657
20. Wang Y-H, Tsai D-Y, Ko Y-A, Yang T-T, Lin I-Y, Hung K-H, et al. Blimp-1 Contributes to the Development and Function of Regulatory B Cells. *Front Immunol* (2019) 10:1909. doi: 10.3389/fimmu.2019.01909

21. Blair PA, Noreña LY, Flores-Borja F, Rawlings DJ, Isenberg DA, Ehrenstein MR, et al. Cd19+Cd24hicd38hi B Cells Exhibit Regulatory Capacity in Healthy Individuals But Are Functionally Impaired in Systemic Lupus Erythematosus Patients. *Immunity* (2010) 32:129–40. doi: 10.1016/j.immuni.2009.11.009
22. Okamoto K, Nakashima T, Shinohara M, Negishi-Koga T, Komatsu N, Terashima A, et al. Osteoimmunology: The Conceptual Framework Unifying the Immune and Skeletal Systems. *Physiol Rev* (2017) 97:1295–349. doi: 10.1152/physrev.00036.2016
23. Yu M, Malik Tyagi A, Li J-Y, Adams J, Denning TL, Weitzmann MN, et al. PTH Induces Bone Loss Via Microbial-Dependent Expansion of Intestinal TNF+ T Cells and Th17 Cells. *Nat Commun* (2020) 11:468. doi: 10.1038/s41467-019-14148-4
24. Shokeen N, Saini C, Sapra L, Azam Z, Bhardwaj A, Ahmad A, et al. Role of Regulatory T Lymphocytes in Health and Disease. In: *Systems and Synthetic Immunology*. Singapore: Springer Singapore (2020). p. 201–43. doi: 10.1007/978-981-15-3350-1_8
25. Liu X, Jiang X, Liu R, Wang L, Qian T, Zheng Y, et al. B Cells Expressing CD11b Effectively Inhibit CD4+ T-Cell Responses and Ameliorate Experimental Autoimmune Hepatitis in Mice. *Hepatology* (2015) 62:1563–75. doi: 10.1002/hep.28001
26. Evans KE, Fox SW. Interleukin-10 Inhibits Osteoclastogenesis by Reducing NFATc1 Expression and Preventing its Translocation to the Nucleus. *BMC Cell Biol* (2007) 8:4. doi: 10.1186/1471-2121-8-4
27. Park-Min K-H, Ji J-D, Antoniv T, Reid AC, Silver RB, Humphrey MB, et al. Il-10 Suppresses Calcium-Mediated Costimulation of Receptor Activator NF-Kappa B Signaling During Human Osteoclast Differentiation by Inhibiting TREM-2 Expression. *J Immunol* (2009) 183:2444–55. doi: 10.4049/jimmunol.0804165
28. Dresner-Pollak R, Gelb N, Rachmilewitz D, Karmeli F, Weinreb M. Interleukin 10-Deficient Mice Develop Osteopenia, Decreased Bone Formation, and Mechanical Fragility of Long Bones. *Gastroenterology* (2004) 127:792–801. doi: 10.1053/j.gastro.2004.06.013
29. Olkhanud PB, Damdinsuren B, Bodogai M, Gress RE, Sen R, Wejksza K, et al. Tumor-Evoked Regulatory B Cells Promote Breast Cancer Metastasis by Converting Resting CD4 + T Cells to T-Regulatory Cells. *Cancer Res* (2011) 71:3505–15. doi: 10.1158/0008-5472.CAN-10-4316
30. Tarique M, Naz H, Kurra SV, Saini C, Naqvi RA, Rai R, et al. Interleukin-10 Producing Regulatory B Cells Transformed Cd4+Cd25– Into Tregs and Enhanced Regulatory T Cells Function in Human Leprosy. *Front Immunol* (2018) 9:1636–48. doi: 10.3389/fimmu.2018.01636
31. Evans JG, Chavez-Rueda KA, Eddaoudi A, Meyer-Bahlburg A, Rawlings DJ, Ehrenstein MR, et al. Novel Suppressive Function of Transitional 2 B Cells in Experimental Arthritis. *J Immunol* (2007) 178:7868–78. doi: 10.4049/jimmunol.178.12.7868
32. Yang X, Yang J, Chu Y, Xue Y, Xuan D, Zheng S, et al. T Follicular Helper Cells and Regulatory B Cells Dynamics in Systemic Lupus Erythematosus. *PloS One* (2014) 9:e88441. doi: 10.1371/journal.pone.0088441
33. Wang Y, Zhang W, Lim S-M, Xu L, Jin J-O. Interleukin-10-Producing B Cells Help Suppress Ovariectomy-Mediated Osteoporosis. *Immune Netw* (2020) 2020:20.e50–61. doi: 10.4110/in.2020.20.e50

Conflict of Interest: The authors declare that the research was conducted in the absence of any commercial or financial relationships that could be construed as a potential conflict of interest.

frontiers in Immunology

ORIGINAL RESEARCH
published: 01 July 2021
doi: 10.3389/fimmu.2021.651049

IgA Immune Complexes Induce Osteoclast-Mediated Bone Resorption

Annelot C. Breedveld[1,2†], Melissa M. J. van Gool[1,2†], Myrthe A. M. van Delft[1,2], Conny J. van der Laken[2,3], Teun J. de Vries[4], Ineke D. C. Jansen[4] and Marjolein van Egmond[1,2,5]*

[1] Department of Molecular Cell Biology and Immunology, Amsterdam UMC, Vrije Universiteit Amsterdam, Amsterdam, Netherlands, [2] Amsterdam institute for Infection and Immunity, Amsterdam UMC, Amsterdam, Netherlands, [3] Department of Rheumatology, Amsterdam UMC, Amsterdam, Netherlands, [4] Department of Periodontology, Academic Centre for Dentistry Amsterdam (ACTA), Vrije Universiteit Amsterdam and University of Amsterdam, Amsterdam, Netherlands, [5] Department of Surgery, Amsterdam UMC, Vrije Universiteit Amsterdam, Amsterdam, Netherlands

Objective: Autoantibodies are detected in most patients with rheumatoid arthritis (RA) and can be of the IgM, IgG or IgA subclass. Correlations between IgA autoantibodies and more severe disease activity have been previously reported, but the functional role of IgA autoantibodies in the pathogenesis of RA is ill understood. In this study, we explored the effect of IgA immune complexes on osteoclast mediated bone resorption.

Methods: Anti-citrullinated peptide antibody (ACPA) and anti-carbamylated protein (anti-CarP) antibody levels of the IgA and IgG isotype and rheumatoid factor (RF) IgA were determined in synovial fluid (SF) of RA patients. Monocytes, neutrophils, and osteoclasts were stimulated with precipitated immune complexes from SF of RA patients or IgA- and IgG-coated beads. Activation was determined by neutrophil extracellular trap (NET) release, cytokine secretion, and bone resorption.

Results: NET formation by neutrophils was enhanced by SF immune complexes compared to immune complexes from healthy or RA serum. Monocytes stimulated with isolated SF immune complexes released IL-6 and IL-8, which correlated with the levels of ACPA IgA levels in SF. Osteoclasts cultured in the presence of supernatant of IgA-activated monocytes resorbed significantly more bone compared to osteoclasts that were cultured in supernatant of IgG-activated monocytes ($p=0.0233$). Osteoclasts expressed the Fc receptor for IgA (FcαRI; CD89) and Fc gamma receptors. IgA-activated osteoclasts however produced significantly increased levels of IL-6 ($p<0.0001$) and IL-8 ($p=0.0007$) compared to IgG-activated osteoclasts. Both IL-6 ($p=0.03$) and IL-8 ($p=0.0054$) significantly enhanced bone resorption by osteoclasts.

Conclusion: IgA autoantibodies induce release of IL-6 and IL-8 by immune cells as well as osteoclasts, which enhances bone resorption by osteoclasts. We anticipate that this will result in more severe disease activity in RA patients. Targeting IgA-FcαRI interactions therefore represents a promising novel therapeutic strategy for RA patients with IgA autoantibodies.

Keywords: ACPA, autoantibodies, bone resorption, IgA, osteoclast, rheumatoid arthritis

OPEN ACCESS

Edited by:
Katharina Schmidt-Bleek, Charité – Universitätsmedizin Berlin, Germany

Reviewed by:
Ulrike Steffen, University of Erlangen Nuremberg, Germany
Guy Serre, Université Toulouse 1 Capitole, France

***Correspondence:**
Marjolein van Egmond
m.vanegmond@amsterdamumc.nl

[†]These authors have contributed equally to this work

Specialty section:
This article was submitted to Inflammation, a section of the journal Frontiers in Immunology

Received: *08 January 2021*
Accepted: *07 June 2021*
Published: *01 July 2021*

Citation:
Breedveld AC, van Gool MMJ, van Delft MAM, van der Laken CJ, de Vries TJ, Jansen IDC and van Egmond M (2021) IgA Immune Complexes Induce Osteoclast-Mediated Bone Resorption. Front. Immunol. 12:651049. doi: 10.3389/fimmu.2021.651049

INTRODUCTION

Rheumatoid arthritis (RA) is a heterogeneous chronic inflammatory disease that is mainly characterized by swelling and pain in the joints. Approximately 0.5-1% of the population is affected and the incidence in women is higher compared to men. Distinct clinical phenotypes of RA can develop, which are thought to be a consequence of interactions between genetic and environmental factors (1). Autoantibodies often appear long before any signs of joint inflammation emerge (2–5). The majority of RA patients develop antibodies against the Fc region of IgG (rheumatoid factor; RF). However, RF autoantibodies can also be found in patients with other rheumatic diseases and in non-rheumatic patients. Only IgM RF (and not IgG RF) is used in serological tests for RA. Antibodies against post-translationally modified proteins including anti-citrullinated protein antibodies (ACPAs) and anti-carbamylated protein (anti-CarP) antibodies are highly specific. ACPAs can be locally produced by plasma cells in joints of RA patients and are detected in sera of up to 70% of RA patients (6). They recognize citrullinated proteins or peptides, which can be found throughout the body including cartilage and bone. Anti-CarP antibodies are detected in sera of 45% of RA patients and recognize carbamylated proteins (7).

Currently, presence of ACPA and RF in serum are the most commonly used diagnostic markers for RA. Tested antibodies are predominantly of the IgG and IgM isotype. RF, ACPA and anti-CarP antibodies have been associated with bone loss in patients with established RA, suggesting a pathogenic role (3, 7, 8). Notably, bone loss has also been reported in ACPA-positive individuals who did not have joint inflammation, suggesting an adverse effect of ACPA on bone (9).

Bone remodeling is a process in which osteoblasts generate new bone and osteoclasts resorb bone to maintain bone homeostasis. This balance is lost in RA patients (10). Osteoclasts are large multinucleated cells, which form by fusion of mononuclear progenitors from the $CD14^+$ monocyte/macrophage lineage. Differentiation, survival and activity of osteoclasts depends on the presence of receptor activator of NF-κB ligand (RANK-L) and macrophage colony-stimulating factor (M-CSF) (11). Osteoclasts and their precursors express RANK, which interacts with RANK-L. The formation of osteoclasts is enhanced in an inflammatory environment by several cytokines, including interleukin (IL)-1β, IL-6, IL-8 and, in low doses by transforming growth factor (TGF)-β, which triggers RANK expression on osteoclast precursors (12, 13). Increased levels of these cytokines have been found in synovial fluid of RA patients and have been reported to contribute to RA disease activity (14). These cytokines can be produced by inflammatory cells in the joint, such as monocytes and macrophages. Additionally, neutrophils are abundantly present and have been reported to express RANK-L. Their contribution in osteoclast activation is however debated (15, 16). In the presence of autoantibodies neutrophils can form NETs and contribute to tissue damage by releasing their granule content (17).

Interestingly, neutrophils are particularly potently activated by IgA antibodies (18). Although they are not routinely tested in RA, more attention has been payed to IgA autoantibodies in RA in the last decade. A considerable proportion (~30%) of RA patients is negative for ACPA IgG and RF IgM (19). About one third of ACPA IgG and/or RF IgM seronegative patients had IgA autoantibody levels in their sera (RF, ACPA or anti-CarP) (3, 7, 19, 20). Several studies have reported a correlation between the amount of IgA and disease severity in RA patients (21). Elevated levels of serum RF IgA were associated with extra-articular manifestations in RA patients and worse disease outcome (22, 23). Moreover, patients having erosions in the bones of their hands had higher serum levels of RF IgA (24). Similarly, presence of anti-CarP IgA was associated with more severe disease (7). Nonetheless, the role of IgA autoantibodies on bone erosion is currently unknown. In this study we investigated the effect of IgA complexes and immune complexes isolated from synovial fluid of RA patients on bone resorption.

MATERIALS AND METHODS

Patients

Synovial fluid from the knee (n=26) and serum (n=20) of RA patients was anonymously collected during their visit to the rheumatology department at the Leiden University Medical Center or the Amsterdam University Medical Center. Patients gave their written informed consent in accordance with the guidelines of the Medial Ethical Committee of the Leiden University Medical Center (reference no. B15.003) or the Amsterdam University Medical Center (reference no. 2013.234).

Precipitation of Immune Complexes from Synovial Fluid and Serum

Synovial fluids or sera were centrifuged at 3300x*g* for 5 minutes before use. Supernatants were mixed with an equal volume of 10% PEG6000 (Sigma Aldrich, St. Louis, MO) and incubated overnight at 4°C. Precipitates were collected after centrifugation for 10 minutes at 9500x*g* and resuspended in phosphate buffered saline (PBS; B.Braun, Melsungen, Germany) to the original volume of the synovial fluid/serum.

Serum Collection and Isolation of Human Monocytes and PMN

Serum was collected from healthy donors. Monocytes and polymorphonuclear leukocytes (PMNs) were isolated from peripheral blood obtained from healthy donors or from buffy coats (Sanquin, Amsterdam, The Netherlands). Monocytes were isolated using MACS CD14 MicroBeads (Miltenyi Biotec, Bergisch Gladbach, Germany) according the manufacturer's protocol. In brief, peripheral blood mononuclear cells (PBMCs) and PMNs were collected after Lymphoprep (Axis-Shield, Oslo, Norway) density gradient centrifugation. PBMCs were washed in PBS and incubated with MACS CD14 MicroBeads after which $CD14^+$ monocytes were isolated.

Erythrocytes present in the PMN fraction were lysed with ammonium chloride buffer (155mM NH4Cl, 10mM KHCO3 and 0.11mM EDTA). Cells were resuspended in RPMI 1640 (Gibco BRL, Paisley, UK) supplemented with 1% heat-inactivated fetal calf serum (FCS), glutamine and antibiotics. PMN were incubated for 30 minutes (37°C, 5% CO2) prior to use.

Coating of Beads With BSA, IgA or IgG

Latex beads (carboxylate-modified polystyrene, green fluorescent (1.0 μm); Sigma Aldrich) were washed with sterile 2-(N-morpholino) ethanesulfonic (MES) buffer (30 mM, pH 6.1) and resuspended in MES buffer with 2 mg/ml endotoxin free bovine serum albumin (BSA) (Akron Biotech, Boca Raton, FL), human serum IgA (Cappel, MP Biomedicals, Santa Ana, CA) or human serum IgG (Sigma Aldrich) in the presence of N-(3-Dimethylaminopropyl)-N'-acid ethylcarbodimide hydrochlorid (Sigma Aldrich) and incubated overnight at room temperature in an overhead shaker. Beads were resuspended in sterile PBS containing 0.5% BSA.

Monocyte Stimulation With Immune Complexes

$CD14^+$ monocytes ($2x10^6$/ml) were stimulated for 24 hours with BSA-, IgA-, or IgG coated beads in an effector target (ET) ratio of 1:100. Alternatively, $1x10^5$ monocytes were stimulated for 24 hours with 10, 20 or 40 μl of immune complexes isolated from synovial fluid of RA patients. Supernatants were harvested and stored at -20°C.

NETs Release After Stimulation With Immune Complexes

PMNs ($1x10^5$) were incubated in RPMI with 1% FCS in black 96 well plates (FLUORTRAC 200, Greiner Bio-One) with 10 μl precipitated immune complexes from synovial fluid or serum from RA patients or healthy controls for 3 hours at 37°C. Release of extracellular DNA was detected by adding nucleic acid label SYTOX green (2,5 μg/ml; Invitrogen Life Technologies). Optical density was measured using a fluorimeter (FLUOstar/POLARstar BMG Labtech GmbH, Offenburg, Germany) at 480nm excitation and 520nm emission.

Dectection of Nuclei, αVβ3 & Fc Receptors on Osteoclasts

Isolated $CD14^+$ monocytes ($2x10^6$/ml) were resuspended in minimum essential medium, α modification (α-MEM) (Gibco BRL), supplemented with 10% FCS, 25 ng/ml M-CSF (ImmunoTools, Friesoythe, Germany), and 50 ng/ml RANKL (BioLegend, San Diego, CA). Cells were seeded in 3 well ibidi slides (removable chamber) (Ibidi, Gräfelfing, Germany) for microscopy imaging or 48 well plates for flow cytometry analysis and cultured for 7 days at 37°C, 5% CO_2. Medium was changed twice weekly. Tartrate-resistant acid phosphatase (TRAcP) activity in osteoclasts on ibidi slides was measured with the leukocyte acid phosphatase kit 386A (Sigma Aldrich) according to the manufacturer's instruction and as previously described (25) with slight modifications. Cells were washed with PBS, fixed using 1% paraformaldehyde (PFA) for 10 minutes, washed with MilliQ and incubated with 1 mM tartrate solution for 60 minutes at 37°C. Cells were stained with anti-human CD14-AF488 (Clone HCD14, Biolegend), anti-human CD51/CD61-APC (αVβ3, Clone 23C6, Miltenyi Biotec), and anti-human CD89-PE-Cy7 (Clone A59, Biolegend) for 1 hour at room temperature. Nuclei and cell membranes were stained with 4′,6-diamidino-2-phenylindole (DAPI) and Wheat germ agglutinin (WGA)-AF488 (both ThermoFisher, Waltham, MA), respectively. Osteoclasts were visualized with microscopy (Leica DM6000, Leica, Wetzlar, Germany).

For flow cytometry analysis osteoclasts were detached from the 48 wells plates detached by scraping after 7 day culture. Cells were washed in PBS and stained with fixable viability dye eFluor506 (ThermoFisher) for 20 minutes on ice after which cells were blocked in 5% PBSA for 30 minutes. Cells were stained with anti-human CD14-AF488 (Clone HCD14, Biolegend) and anti-human CD51/CD61-APC (Clone 23C6, Miltenyi Biotec) for 30 minutes on ice. To investigate Fc receptor expression, cells were stained with anti-human CD14-AF488 combined with anti-human CD89-PE-Cy7 (Clone A59, Biolegend), anti-human CD16-APC-eFluor780 (Clone 3G8, ThermoFisher), anti-human CD32-PE-Cy7 (Clone 6C4, ThermoFisher) or anti-human CD64-APC (Clone 10.1, ThermoFisher) for 30 minutes on ice. To determine the number of nuclei, cells were stained with 5 μg/ml Hoechst 33342 (ThermoFisher) for 20 minutes at room temperature. Integrin and Fc receptor expression was analyzed with flow cytometry (LSRFortessa™ X-20, BD Biosciences). Data was processed in FlowJo version 10.6.2. (Tree Star, Inc., Ashland, OR).

Bone Resorption Assay

Bovine cortical bone was cut in slices of 0.5 mm thick and cut to fit in 96 well plates. Bone slices were sonicated, washed with PBS and incubated in α-MEM (Gibco BRL) for 30 minutes at 37°C after which $0.5x10^6$ $CD14^+$ monocytes resuspended in α-MEM supplemented with 10% FCS, 25 ng/ml M-CSF (ImmunoTools) and 50 ng/ml RANKL (BioLegend) were seeded in 96 well plates for 21 days. Supernatant of unstimulated monocytes or monocytes that had been stimulated with BSA-, IgA-, or IgG-coated beads for 24 hours was added (1:1) when indicated. Supernatants and medium were replaced twice weekly and when indicated, medium was supplemented with 25 ng/ml IL-6 (ImmunoTools), 10 ng/ml IL-8 or 5 ng/ml TNF-α (both Peprotech, Rocky Hill, NJ). After 21 days bone slices were stored in water (4°C) and bone resorption was visualized as previously described (26). In brief, bone slices were sonicated for 30 minutes in 10% NH_4OH, washed in distilled water, shortly dried on filter paper and transferred to new wells containing water saturated aluminium potassium sulfate dodecahydrate (Merck Millipore, Burlington, MA) for 10 minutes. Bone slices were washed twice in distilled water, after which they were washed once under a strong current of distilled water and dried between filter paper. Bone slices were stained with Coomassie brilliant blue solution (PhastGel® blue R, PlusOne Coomassie tablets, Pharmacia, Uppsala Sweden) for 1 minute,

and dried between filter paper. Bone resorption pits were visualized with an inverted microscope (Nikon TE-300, Nikon, Tokyo, Japan) and quantified with Image J version 1.49v.

Purification and Stimulation of CD14 Negative Osteoclasts

Generated osteoclasts (7 day culture) were scraped from 48 well plates and incubated with MACS CD14 MicroBeads human (Miltenyi Biotec) according the manufacturer's instruction. The flow through containing CD14 negative cells was collected. To confirm purity of CD14 negative cells, cells were washed in 0.5% PBSA, blocked in 5% PBSA for 30 minutes on ice and stained with anti-human CD14-AF488 (Clone HCD14, Cat#325610, Biolegend) for 30 minutes on ice. Cells were measured with flow cytometry (LSRFortessa™ X-20, BD Biosciences) and data was analyzed with FlowJo version 10.6.2 (Tree Star, Inc.). CD14 negative cells were resuspended in α-MEM supplemented with 10% FCS, 25 ng/ml M-CSF (ImmunoTools) and 50 ng/ml RANKL (BioLegend) and plated in 48 well plates for 24 hours. Medium was refreshed and cells were stimulated with 5 µl of BSA-, IgA-, or IgG-coated beads or 40 µl of immune complexes isolated from synovial fluid of RA patients for 24 hours, after which supernatants were collected and stored at -20°C. To determine the morphology of the sorted osteoclasts, TRAcP activity was measured and nuclei were stained with DAPI as described above.

IL-6 and IL-8 ELISA

Levels of IL-6 and IL-8 were measured with enzyme-linked immunosorbent assay (ELISA) following the manufacturer's protocol (Human uncoated ELISA kits, Invitrogen, ThermoFisher).

Anti-Citrullinated Protein Antibody (ACPA) ELISA

ACPA IgA and IgG levels were determined in synovial fluids of RA patients according to the protocol previously described (20) with minor adaptations. Microtiter ELISA plates (Nunc MaxiSorp™ flat-bottom plates; ThermoFisher) were coated with 50 µl of 1 µg/ml streptavidin (ThermoFisher) and incubated overnight at 4°C after which 50 µl of 1 µg/ml biotinylated CCP2-cittruline or CCP2-arginine (kindly provided by Dr. J.W. Drijfhout, Department of Immunohematology and Blood Transfusion (Leiden University Medical Center)) was added for 1 hour at RT. Synovial fluid (1:10 diluted) was added for 1 hour at 37°C. Wells were washed and incubated with F(ab')2 goat anti-human IgA-HRP (1:4000, ThermoFisher) or F(ab')2 goat anti-human IgG-HRP (1:4000, ThermoFisher) for 1 hour at 37°C. Fifty µl of 3,3′,5,5′-Tetramethylbenzidine (TMB) substrate was added after which the reaction was stopped with 50 µl of sulfuric acid (10% H_2SO_4). Absorbance was measured with a microplate reader (Bio-Rad, Berkeley, CA) at 450nm.

Anti-Carbamylated Protein (anti-CarP) Antibody ELISA

Anti-Carp IgA and IgG were determined in synovial fluids of RA patients according to protocols previously described (7) with minor adaptations. Microtiter ELISA plates (ThermoFisher) were coated with 50 µl of 10 µg/ml carbamylated bovine serum albumin (Ca-BSA) or non-modified BSA and incubated overnight at 4°C after which wells were blocked with 1% PBSA for 6 hours at 4°C. Synovial fluid (1:10 diluted) was added for 1 hour overnight at 4°C. Wells were washed and incubated with F(ab')2 goat anti-human IgA-HRP (1:4000, ThermoFisher) or F(ab')2 goat anti-human IgG-HRP (1:4000, ThermoFisher) for 1 hour at 37°C. Fifty µl of TMB substrate was added after which the reaction was stopped with 50 µl of 10% H_2SO_4. Absorbance was measured with a microplate reader (Bio-Rad, Berkeley, CA) at 450nm.

Rheumatoid Factor (RF) Antibody ELISA

RF IgA levels were determined in synovial fluid of RA patients. Microtiter ELISA plates (ThermoFisher) were coated with 50 µl of 50 µg/ml human serum IgG (Sigma Aldrich) and incubated overnight at 4°C after which wells were blocked with 1% PBSA for 1h at 37°C. Synovial fluid (1:10 diluted) was added for 1 hour at 37°C. Wells were washed and incubated with F(ab')2 goat anti-human IgA-HRP (1:4000, ThermoFisher) for 1 hour at 37°C. Fifty µl of TMB substrate was added after which the reaction was stopped with 50 µl of 10% H_2SO_4. Absorbance was measured with a microplate reader (Bio-Rad, Berkeley, CA) at 450nm.

Statistical Analysis

Statistical analysis were performed with GraphPad Prism version 8.2.1 (GraphPad, San Diego, CA). Statistical differences were determined with unpaired Student two-tailed t tests (two groups) or one-way ANOVA (more than two groups) for normally distributed data. Mann-Whitney U tests (two groups) or Kruskall-Wallis tests (more than two groups) were applied to not normally distributed data. Correlations were determined with nonparametric Spearman correlation coefficients. P values <0.05 were considered statistically significant.

RESULTS

Autoantibodies in Synovial Fluid Induce Immune Cell Activation

To investigate whether local autoantibodies have a potential pathogenic role in RA, we first determined ACPA and anti-CarP IgA and IgG levels in synovial fluid of 26 RA patients (**Figure 1A**). Since we previously demonstrated that RF IgA levels were significantly elevated in RA patients (27), we therefore additionally determined RF IgA in this study. Both IgA and IgG autoantibody levels showed great inter-patient variation. For every patient a profile of IgA and IgG autoantibodies present in their synovial fluid was created (**Figure 1B**).

When neutrophils were stimulated with immune complexes isolated from synovial fluid of RA patients they formed NETs (**Figure 2A**). The level of NET formation varied greatly between samples. Immune complexes isolated from serum of either healthy controls or RA patients did not induced NET release (**Figure 2A**), which may have been due to lower concentrations

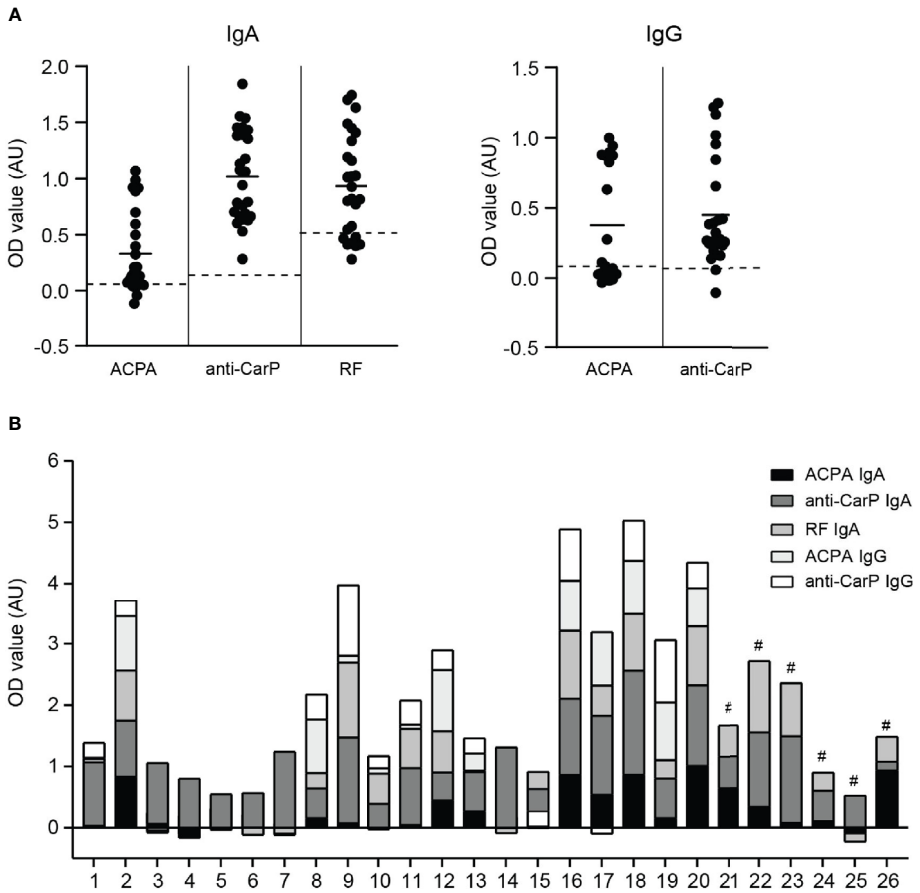

FIGURE 1 | IgA and IgG autoantibody levels in synovial fluid of RA patients **(A)** left panel; ACPA, anti-CarP and RF IgA levels and right panel; ACPA and anti-CarP IgG levels in synovial fluid of RA patients (expressed as OD value). Dotted lines represent blanc OD values of each independent ELISA. **(B)** Synovial fluid profile of ACPA, anti-CarP and RF IgA and IgG levels of 26 RA patients [# IgG levels not determined]. AU, arbitrary units.

of complexes in serum compared to SF. Of note, concentration of immune complexes in sera and SF of RA patients could not be determined due to limited patient material. NET release induced by SF immune complexes significantly positively correlated with ACPA IgA, ACPA IgG and anti-CarP IgG levels present in SF (**Supplementary Figures 1A, B**). Neither anti-CarP IgA nor RF IgA levels in SF correlated with NET release (**Supplementary Figures 1B, C**).

Next, monocytes were activated with immune complexes isolated from synovial fluid of RA patients and IL-6 production was determined (**Figure 2B**). Monocytes were not stimulated with immune complexes isolated from serum of RA patients as neutrophils were not activated by serum immune complexes. Addition of a higher volume of SF immune complexes to monocytes resulted in increased IL-6 release. Furthermore, monocyte IL-8 production after stimulation with 40 µl of immune complexes was enhanced compared to unstimulated monocytes (**Figure 2C**) and positively correlated with IL-6 release (p=0.0003) (**Supplementary Figure 2A**). Immune complexes are large aggregates of autoantibodies and contain multiple antibody isotypes. ACPA IgA levels significantly correlated (p=0.0197) with monocyte IL-6 release induced by these immune complexes (**Figure 2D**). Anti-CarP IgA and RF IgA followed a similar trend, but did not significantly correlate with IL-6 release (**Supplementary Figure 2B**). Neither ACPA nor anti-CarP IgG autoantibodies correlated with IL-6 release (**Supplementary Figure 2C**). Significant positive correlations between ACPA IgA (p=0.0011), ACPA IgG (p=0.0397) and RF IgA (p=0.0015) with monocyte IL-8 release induced by synovial fluid immune complexes were found (**Figure 2E**). While anti-CarP IgA and anti-CarP IgG did not significantly correlate with monocyte IL-8 release (**Supplementary Figure 2D**).

Osteoclasts formation and activity

In vitro generated osteoclasts (OCs) are defined as large multinucleated cells, which express the enzyme tartrate-resistant acid phosphatase (TRAcP) and can resorb bone (28).

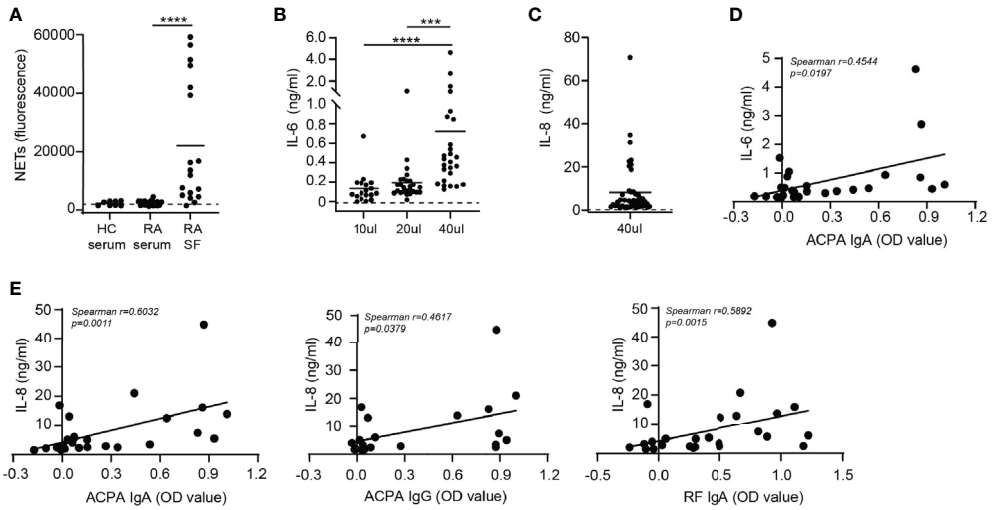

FIGURE 2 | Cytokine release after synovial fluid immune complex stimulation correlates with IgA autoantibody levels in synovial fluid. **(A)** NET release by neutrophils stimulated with immune complexes isolated from healthy control (HC) serum, rheumatoid arthritis (RA) serum or synovial fluid of RA patients (RA SF). Dotted line represents unstimulated neutrophils. **(B, C)** Monocyte **(B)** IL-6 and **(C)** IL-8 release (pooled data from 2 independent experiments) after stimulation with immune complexes isolated from RA SF. Dotted lines represent unstimulated monocytes. **(D)** Correlation between immune complex-induced monocyte IL-6 release with ACPA IgA levels. **(E)** Correlations between monocyte IL-8 release induced by immune complexes isolated from RA SF with (left) ACPA IgA levels, (middle) ACPA IgG levels or (right) RF IgA levels Average cytokine release is displayed (n=2). Data was analyzed using two way ANOVA with Bonferroni post-hoc or using the Spearman correlation coefficient; ***$p \leq 0.001$, ****$p \leq 0.0001$.

When osteoclasts mature, CD14 expression is lost and the expression of TRAcP increases (29, 30). We generated multinucleated cells by culturing $CD14^+$ monocytes for 7 days in the presence of M-CSF and RANK-L which expressed TRAcP (**Figure 3A**). We defined osteoclasts as multinucleated CD14 negative cells with at least 3 nuclei and expressing high levels of TRAcP and αVβ3. The αVβ3 integrin enables the osteoclast to connect to the bone matrix (31). Not all multinucleated cells differentiated into osteoclasts as TRAcP and the αVβ3 integrin were absent. These cells were likely multinucleated giant cells of macrophage origin. Since TGF-β is an important modulator of osteoclasts, we analyzed whether TGF-β influenced osteoclast formation. Addition of TGF-β to the 7 day culture resulted in formation of larger OCs with increased TRAcP expression (**Figure 3A**). Moreover, presence of TGF-β resulted in the formation of more $CD14^-$ cells (~80%) compared to absence of TGF-β (~20%) (**Figure 3B**). Approximately 19% of the $CD14^-$ population was classified as mature osteoclasts as they contained 3 or more nuclei (**Figure 3C**). The formed OCs expressed high levels of the αVβ3 integrin independently of TGF-β presence (**Figure 3D**).

OCs cultured on bone slices for 21 days in presence of M-CSF and RANK-L resorbed bone as visualized by formed bone resorption pits and tracks (**Figure 3E**, left panel). Presence of TGF-β significantly increased bone resorption by OCs (**Figure 3E**, right panel). OCs in absence of TGF-β resorbed ~5000 μm^2 bone, while OCs in presence of TGF-β resorbed significantly more bone (~15000 μm^2) (p=0.0445) (**Figure 3F**).

IgA Activated Monocytes Induce Osteoclast-Mediated Bone Resorption

Supernatant of (activated) monocytes was added to osteoclasts which were plated on bone slices to study its effect on bone resorption. Unstimulated and BSA-activated monocytes supernatant served as control conditions and only induced little bone resorption by osteoclasts (respectively ~3300 μm^2 and ~7300 μm^2) as visualized by dark bone resorption pits (**Figure 4A**). Supernatant of monocytes that had been activated with IgA complexes enhanced osteoclast induced bone resorption compared to supernatant of IgG-activated monocytes (**Figure 4A**). OCs in presence of supernatant of IgA-activated monocytes resorbed on average ~15000 μm^2 of the bone slices, while supernatant of IgG-activated monocytes only induced resorption of ~2600 μm^2 bone by OCs (p=0.0233) (**Figure 4B**).

Osteoclasts Express FcαRI and Are Activated by IgA

Next, we questioned whether presence of IgA autoantibodies also directly affects osteoclast activation. Human osteoclasts expressed intermediated levels CD16 (FcγRIII), CD64 (FcγRIII), CD89 (FcαRI), and low levels of CD32 (FcγRII) (**Figure 5A**, upper panels). Subsequently, CD89 expression on multinuclear $CD14^-\alpha v\beta 3^+$ osteoclasts was confirmed with microscopy (**Figure 5B**). Remaining $CD14^+$ cells expressed high levels of CD16, CD32 and CD89, and intermediate levels of CD64 (**Figure 5A**, lower panels).

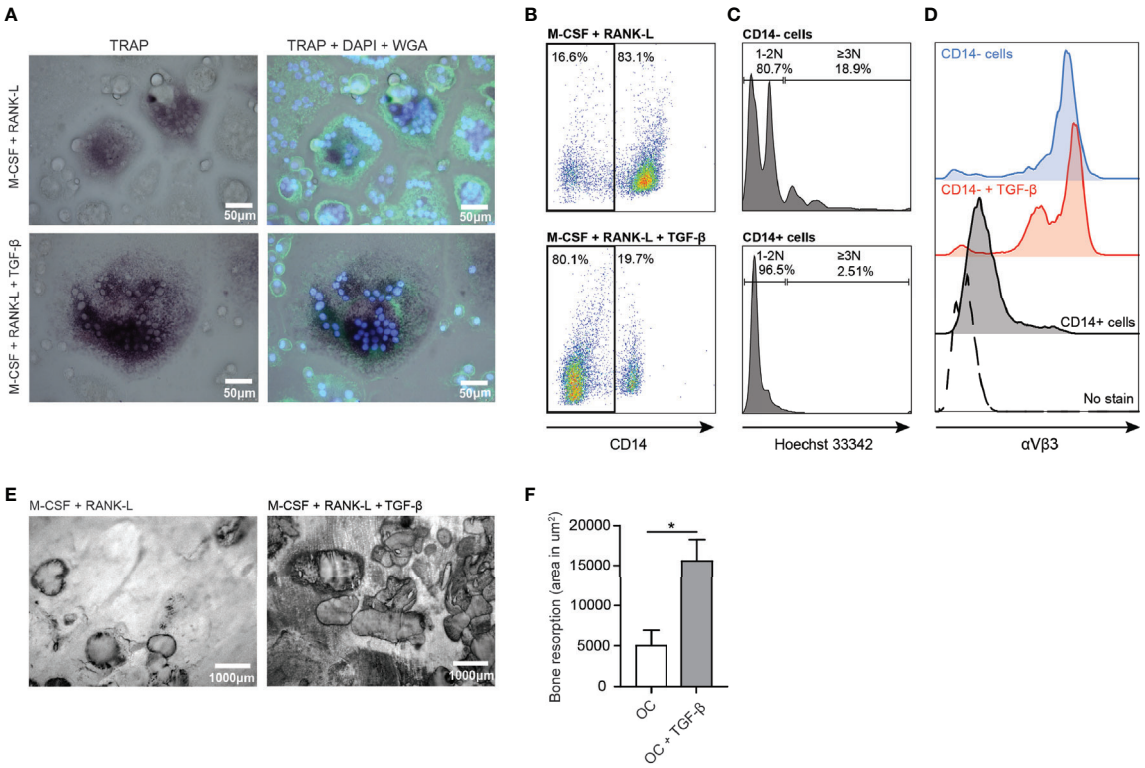

FIGURE 3 | Enhanced osteoclast formation and activity in presence of TGF-β. **(A)** Osteoclast TRAcP expression (purple) in presence of M-CSF and RANK-L (upper left panel) and in presence of M-CSF, RANK-L and TGF-β (lower left panel) after 7 days culture. [Blue (DAPI) = nuclei, green (WGA) = cell membrane]. **(B)** CD14 expression on osteoclasts in absence (upper panel) or presence of TGF-β (lower panel) after 7 days culture. **(C)** Number of nuclei present in CD14- (upper panel) and CD14+ (lower panel) cells after 7 days of culture in presence of M-CSF and RANK-L. **(D)** Expression of αVβ3 on formed osteoclasts in absence (blue (top) histogram) or presence of TGF-β (red (second) histogram) after 7 days culture. Residing $CD14^+$ cells (black histogram) and non-stained cells (dotted histogram) served as controls. **(E)** Bone resorption by human osteoclasts after 21 days in presence of M-CSF and RANK-L (left panel) or M-CSF, RANK-L and TGF-β (right panel) (representative of n=2 experiments). **(F)** Quantification of bone resorption by osteoclasts in absence of TGF-β (white bar) or presence of TGF-β (grey bar) presented as area in μm^2 bone resorption. Data was analyzed using unpaired student's two-tailed T test; $^*p \leq 0.05$.

To investigate the effect of IgA-FcαRI interactions on the bone resorptive capacity of osteoclasts, we separated CD14 negative osteoclasts from the remaining CD14 positive cells. Of the sorted osteoclasts >80% was alive and >95% was CD14 negative (**Supplementary Figure 3A**). The majority of sorted OC were multinucleated and express TRAcP (**Supplementary Figure 3B**). OCs activated with immune complexes isolated from synovial fluid of RA patients produced IL-8 (**Figure 5C**). However, similar levels of IL-8 were released by unstimulated osteoclasts. Production of IL-6 by osteoclasts after stimulation with SF immune complexes varied a lot between samples, but was not produced by unstimulated osteoclasts (**Figure 5D**). To investigate whether cytokine production was mediated by IgA or IgG, we stimulated OCs with IgA-, or IgG-coated beads. IgA-activated OCs produced significantly higher levels of IL-8 compared to unstimulated, BSA or IgG-activated OCs (**Figure 5E**). IL-6 was only produced by OCs after IgA activation (**Figure 5F**). Bone resorptive capacity of osteoclasts was significantly enhanced in the presence of IL-8 (p=0.0054) or IL-6 (p=0.03) (**Figure 5G**). These results support previous findings that IgA autoantibody levels in RA patients correlate with increased bone resorption. We now show that this can be a direct consequence of IgA-mediated activation of osteoclasts through the enhanced release of IL-8 and IL-6.

DISCUSSION

Bone remodeling in RA patients is disturbed, resulting in bone loss and eventually loss of function (10). In this study we demonstrated that IgA enhanced bone resorption through cytokines released by immune cells and by activating osteoclasts through FcαRI crosslinking. Our results show that IgA has a significant effect on bone resorption and in this way is likely responsible for worse pathology in RA patients.

The exact process of bone remodeling in RA patients is incompletely understood. It has been reported that multinucleated cells that express typical osteoclast lineage markers including TRAcP and cathepsin K are found at sites of bone erosion in RA patients (32). Multiple *in vivo* studies with

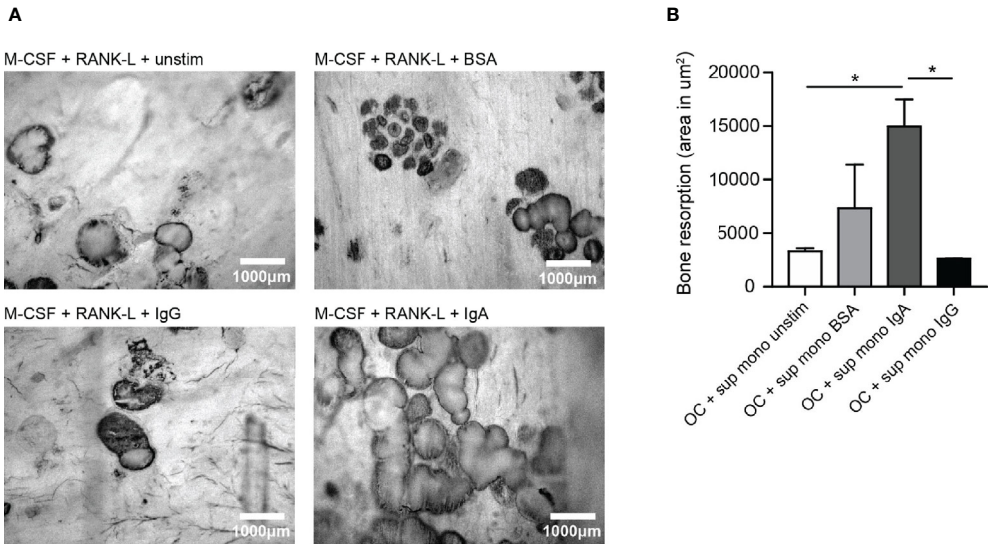

FIGURE 4 | Significantly enhanced bone resorption in presence of supernatant of IgA-activated monocytes. **(A)** Bone resorption by osteoclasts in the presence of supernatant of unstimulated monocytes (upper left panel), BSA-stimulated monocytes (upper right panel), IgG-activated monocytes (lower left panel), or IgA-activated monocytes (lower right panel). **(B)** Quantification of bone resorption (area in um^2) induced by osteoclasts in presence of supernatant of unstimulated monocytes (white bar), BSA-activated monocytes (light grey bar), IgA-activated monocytes (dark grey bar) or IgG-activated monocytes (black bar). Data was analyzed using one way ANOVA with Tukey post-hoc; $^*p \leq 0.05$.

osteoclast deficient mice support the critical role of osteoclasts in bone loss (33, 34). Bone loss in RA patients was strongly associated with presence of ACPA or anti-CarP antibodies (7, 35–37). In contrast to our results, it was shown that bone resorption was enhanced by ACPA IgG containing immune complexes *in vitro* (38). Increased numbers of bone resorbing cells were responsible for this enhanced bone resorption and was also observed in presence of non-ACPA IgG containing immune complexes (38). Presence of ACPA IgA or IgG and anti-CarP antibodies in sera were predictive for the development of RA (3, 7, 39), whereas only ACPA-IgA levels were associated with more active disease (40).

Next to osteoclasts, inflammatory cells present in the joint can indirectly contribute to bone resorption. Neutrophils are the most abundant immune cells present in the inflamed joint and can get highly activated by IgA and IgG resulting in the formation of NETs (18, 41). NET release was induced by immune complexes isolated from synovial fluid of RA patients. Variations in the abundancy of NET formation is likely due to different levels of autoantibodies in SF, influencing the level of neutrophil activation. NET release was not induced by immune complexes derived from serum, which may be due to less presence of immune complexes compared to synovial fluid. NETs can contribute to the autoimmune profile of RA patients, as myeloperoxidase can convert thiocyanate into cyanate, which is essential for carbamylation (42). Previously it was shown that NET formation was significantly increased in neutrophils stimulated with synovial fluid containing ACPAs compared to stimulation with ACPA-negative synovial fluids (43). Similarly we reported positive correlations between NET release and ACPA IgA and IgG levels. NETs may further contribute to the pathogenesis of RA as source of citrullinated autoantigens. In complex with ACPAs they can enhance the production of pro-inflammatory cytokines IL-6 and IL-8 by local (immune) cells (41). Recently a humanized anti-ACPA therapeutic antibody was described to inhibit NET formation by human neutrophils activated with SF of gout patients (44), supporting the importance of this autoantibody in the pathology of RA as well.

Deposition of immune complexes is a common pathogenic feature of several autoimmune diseases, including RA (45). Immune complexes containing antibodies against altered proteins are suggested to initiate a state of non-resolving inflammation in the synovial cavity, followed by RF containing immune complexes reactive to these initial immune complexes (46). However, in animal models it has been shown that immune complexes do not have to be specific against altered proteins to be able to initiate synovitis (47). In the synovium immune complexes can augment inflammation through complement activation (48), Fc receptor engagement (49), toll-like receptor binding (50), and stromal cell activation (51). Furthermore, ACPA containing immune complexes are suggested to be recognized by membrane epitopes (e.g. citrullinated vimentin) expressed by osteoclasts which promotes osteoclastogenesis (38). The glycosylation status of autoantibodies present in immune complexes, such as ACPA sialylation, additionally enhances the capacity to promote inflammation (52). We showed that incubation of monocytes stimulated with SF immune

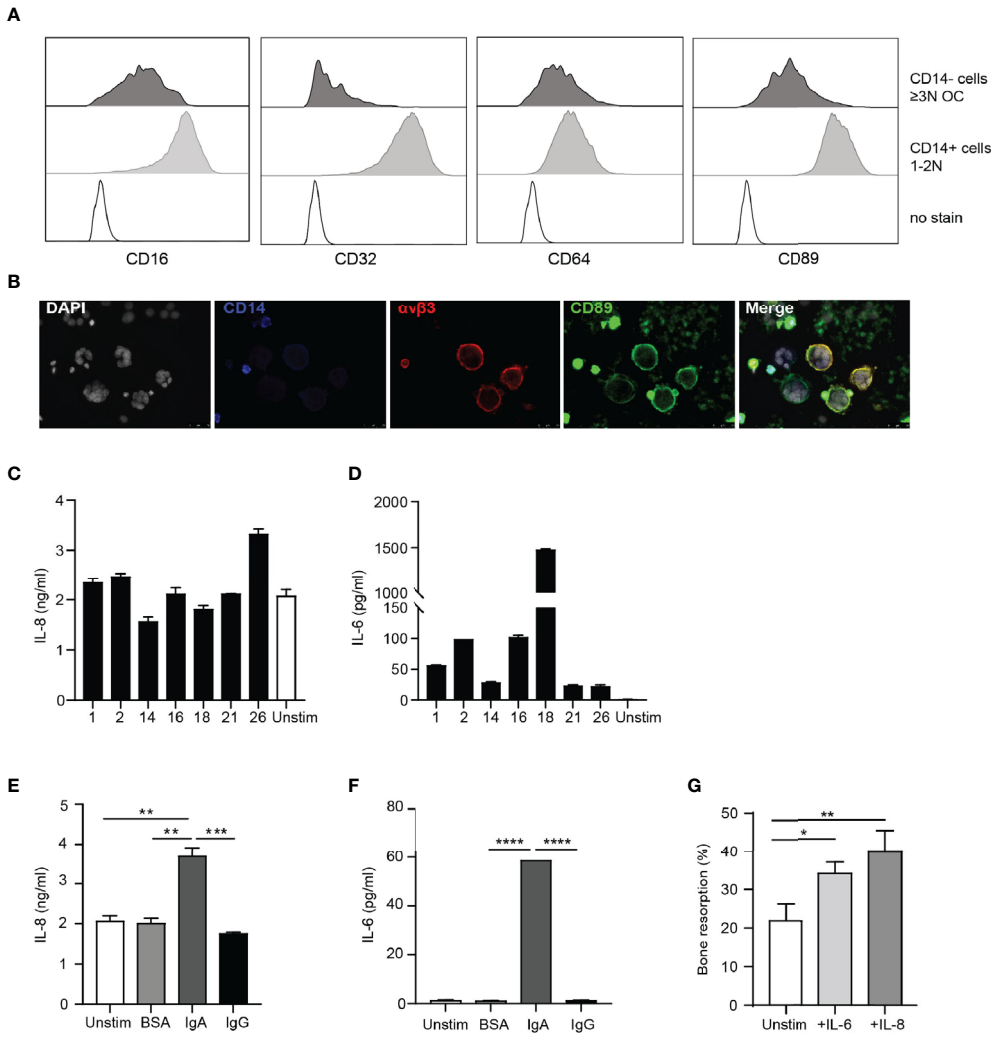

FIGURE 5 | Osteoclasts are activated by IgA immune complexes. **(A)** Expression of CD16, CD32, CD64 and CD89 on CD14 negative OCs (upper panels; dark grey histograms) and remaining CD14$^+$ cells (middle panels; light grey histograms) compared to no stain (lower panels; dotted black line histograms). **(B)** CD89 expression on CD14$^-$αVβ3$^+$ OCs. [White (DAPI) = nuclei, blue = CD14, red = αVβ3, green = CD89]. **(C, D)** IL-8 **(C)** and IL-6 **(D)** release by OCs stimulated with immune complexes isolated from synovial fluid of RA patients. **(E, F)** IL-8 **(E)** and IL-6 **(F)** release by unstimulated OCs (white bar) and after stimulation with BSA- (light grey bar), IgA- (dark grey bar) or IgG- (black bar) coated beads. **(G)** Quantification of bone resorption by OCs in presence of M-CSF and RANK-L (unstim, white bar) and added cytokines IL-6 (25 ng/ml, light grey bar) or IL-8 (10 ng/ml, dark grey bar). Data was analyzed using one way ANOVA with Tukey post-hoc; *$p \leq 0.05$; **$p \leq 0.01$; ***$p \leq 0.001$; ****$p \leq 0.0001$.

complexes resulted in the production of IL-6 and IL-8. The variable levels of cytokine release can be explained by the different levels of autoantibodies present in the immune complexes. IL-8 is an important chemokine for neutrophils (53) and positively correlated with the amount of infiltrated neutrophils in the inflamed synovium of RA patients (43). IL-8 levels produced by monocytes correlated with both IgA and IgG autoantibodies. These results are supported by previous work from our lab demonstrating that IL-8 is produced by monocytes after IgA or IgG activation (own unpublished data). Interestingly, osteoclasts produced significantly elevated levels of IL-6 and IL-8 after stimulation with SF complexes. The direct effect of IgA autoantibodies on osteoclast activity by blocking of FcαRI could not be formally determined, as FcαRI is continuously internalized and re-expressed. Blocking FcαRI during long term culture of osteoclasts is therefore not feasible. Nonetheless, only stimulation of osteoclasts with IgA-, but not IgG complexes resulted in enhanced production of IL-6 and IL-8, supporting that IgA autoantibodies in SF were responsible for the observed IL-6 and IL-8 production.

IL-8 after IgA, compared to IgG activation. Human CD14$^+$ osteoclasts are described to express multiple Fc gamma receptors (54) and autoantibodies can bind osteoclasts specifically, thereby promoting osteolytic function *in vitro* (38). In this study we

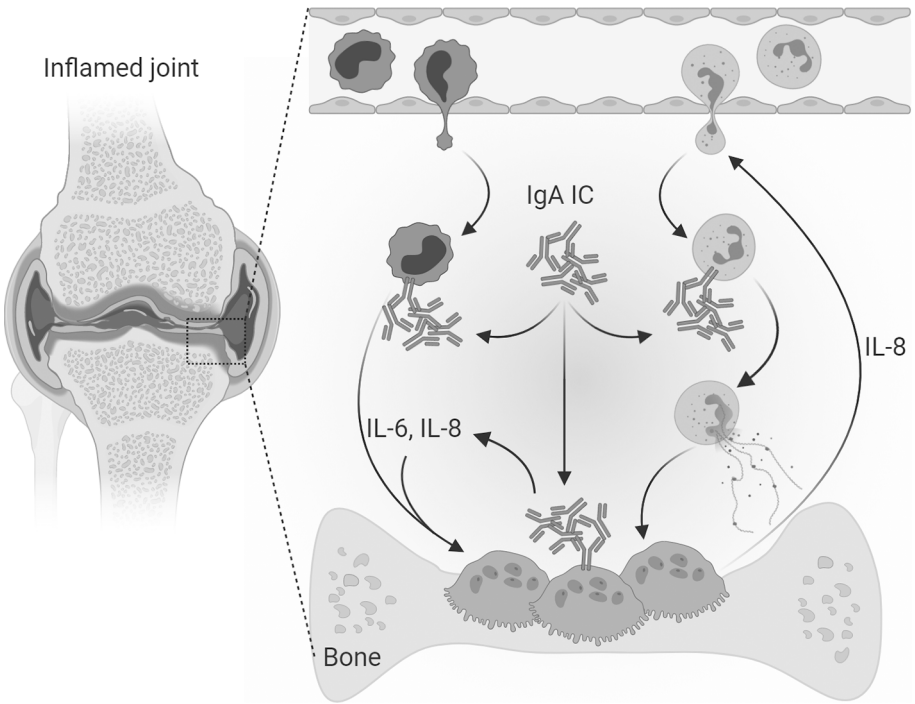

FIGURE 6 | Mechanism of direct and indirect IgA-mediated osteoclast activation. In the inflamed joints of RA patients' immune complexes consisting of IgA autoantibodies are present. Infiltrated neutrophils can form neutrophil extracellular traps (NETs) when activated with IgA-containing immune complexes. Monocytes activated with IgA-containing immune complexes produce high levels of IL-6 and IL-8 and enhance the bone resorptive capacity of osteoclasts. IgA-containing immune complexes can also directly target osteoclasts which express the Fc receptor for IgA (FcαRI). After IgA activation osteoclasts secrete IL-8 and IL-6, which are osteoclastogenic cytokines known to contribute to the formation of osteoclasts. Furthermore, IL-8 contributes to the chemoattraction and infiltration of neutrophils thereby enhancing the pro-inflammatory environment in the inflamed synovium of RA patients. Osteoclast secreted IL-8 could therefore both lead to auto stimulation and attraction of neutrophils to the inflamed area. [Created with BioRender.com].

focused on CD14 negative osteoclasts, as the most mature bone resorbing cells (29), which have intermediate expression of FcγRI, FcγRIII, FcαRI, and low expression of FcγRII compared to $CD14^+$ mononuclear cells.

IgG autoantibodies were described to enhance the production of osteoclastogenic factors, including IL-6, IL-8, TNF-α and IL-1β by monocytes and macrophages (13, 49). However, IgA-activation of monocytes induced higher levels of pro-inflammatory cytokines compared to IgG-activation (own unpublished data). Synovial fluid levels of IL-8 and IL-6 were significantly elevated in patients with high ACPA levels in their synovial fluid (43). ACPA-induced differentiation of osteoclasts was inhibited *in vitro* by a neutralizing IL-8 antibody. Furthermore, *in vivo* IL-8 inhibition reversed ACPA-induced bone loss in mice (55), supporting the importance of IL-8 in the pathology of RA in ACPA positive patients.

IL-6 production by monocytes only positively correlated with levels of ACPA IgA, but not ACPA IgG. These results are in line with previous work showing IL-6 release by monocytes upon IgA, but not IgG activation (own unpublished data). Similarly, osteoclasts only produced IL-6 after IgA activation. IL-6 significantly increased bone resorption by osteoclasts. *In vitro*, IL-6 was shown to enhance osteoclastogenesis through activation of RANKL on osteocytes and osteoblasts (56, 57). *In vivo*, IL-6 was necessary for inducing osteoclast activity and bone resorption (58, 59). Several clinical trials have shown the potential of the human anti-IL-6 blocking antibody tocilizumab in treating RA patients (60–62).

In conclusion, we propose that IgA-FcαRI interactions on both infiltrated immune cells in the synovium and osteoclasts have an essential role in the pathogenesis of RA (**Figure 6**). IL-6 production after IgA activation of monocytes and osteoclasts can contribute to osteoclast formation, activity and their bone resorptive capacity. Elevated IL-8 production after IgA stimulation of monocytes and osteoclasts can contribute to the infiltration of neutrophils, thereby promoting an inflammatory environment. Furthermore it promotes osteoclast activity resulting in increased bone resorption. We anticipate that targeting IgA-FcαRI interactions is a promising therapeutic strategy to diminish bone resorption in RA patients.

DATA AVAILABILITY STATEMENT

The original contributions presented in the study are included in the article/**Supplementary Material**. Further inquiries can be directed to the corresponding author.

ETHICS STATEMENT

The studies involving human participants were reviewed and approved by The Medial Ethical Committee of the Leiden University Medical Center (reference no. B15.003) and the Medical Ethical Committee of the Amsterdam University Medical Center (reference no. 2013.234). The patients/participants provided their written informed consent to participate in this study.

AUTHOR CONTRIBUTIONS

AB, MG, MD, and ME designed the experiments. AB, MG, and MD conducted the experiments. IJ contributed to the bone resorption assays. AB, MG, and MD analyzed the data. CL, TV, and ME provided scientific input. AB wrote the first draft of the manuscript. MG, MD, CL, TV, IJ, and ME revised the manuscript. ME supervised during the entire process. All authors contributed to the article and approved the submitted version.

FUNDING

Netherlands Organization for Scientific Research (VICI 91814650).

ACKNOWLEDGMENTS

We thank V.F.A.M. Derksen and R.E.M. Toes (LUMC) for providing synovial fluid and sera from RA patients.

SUPPLEMENTARY MATERIAL

The Supplementary Material for this article can be found online at: https://www.frontiersin.org/articles/10.3389/fimmu.2021.651049/full#supplementary-material

Supplementary Figure 1 | Correlation between NET release after stimulation of neutrophils with immune complexes isolated from synovial fluid of RA patients with OD values of **(A)** ACPA IgA (left) or ACPA IgG (right), **(B)** anti-CarP IgA (left) or anti-CarP IgG (right) and **(C)** RF IgA measured in synovial fluid of RA patients.

Supplementary Figure 2 | (A) Correlation between monocyte IL-6 and IL-8 release induced by immune complexes of RA SF. **(B, C)** Correlation between monocyte IL-6 release and **(B)** (left) anti-CarP IgA levels or (right) RF IgA, or **(C)** (left) ACPA IgG levels and (right) anti-CarP IgG levels. **(D)** Correlation between monocyte IL-8 release and (left) anti-CarP IgA levels and (right) anti-CarP IgG levels.

Supplementary Figure 3 | (A) Gating strategy to check the purity of sorted osteoclasts. (left) Location of osteoclasts (OCs) on forward-side scatter area with adjusted laser settings to visualize large cells; (middle) viability of the OCs; (left) CD14 negative OCs. **(B)** Multinucleated osteoclast TRAcP expression (purple) 24 hours after sorting [Blue (DAPI) = nuclei].

REFERENCES

1. Lin YJ, Anzaghe M, Schulke S. Update on the Pathomechanism, Diagnosis, and Treatment Options for Rheumatoid Arthritis. *Cells* (2020) 9(4):880. doi: 10.3390/cells9040880
2. Brink M, Hansson M, Mathsson L, Jakobsson PJ, Holmdahl R, Hallmans G, et al. Multiplex Analyses of Antibodies Against Citrullinated Peptides in Individuals Prior to Development of Rheumatoid Arthritis. *Arthritis Rheum* (2013) 65(4):899–910. doi: 10.1002/art.37835
3. Brink M, Verheul MK, Ronnelid J, Berglin E, Holmdahl R, Toes RE, et al. Anti-Carbamylated Protein Antibodies in the Pre-Symptomatic Phase of Rheumatoid Arthritis, Their Relationship With Multiple Anti-Citrulline Peptide Antibodies and Association With Radiological Damage. *Arthritis Res Ther* (2015) 17:25. doi: 10.1186/s13075-015-0536-2
4. Shi J, van de Stadt LA, Levarht EW, Huizinga TW, Hamann D, van Schaardenburg D, et al. Anti-Carbamylated Protein (Anti-Carp) Antibodies Precede the Onset of Rheumatoid Arthritis. *Ann Rheum Dis* (2014) 73 (4):780–3. doi: 10.1136/annrheumdis-2013-204154
5. Aho K, Heliovaara M, Maatela J, Tuomi T, Palosuo T. Rheumatoid Factors Antedating Clinical Rheumatoid Arthritis. *J Rheumatol* (1991) 18(9):1282–4.
6. De Rycke L, Peene I, Hoffman IE, Kruithof E, Union A, Meheus L, et al. Rheumatoid Factor and Anticitrullinated Protein Antibodies in Rheumatoid Arthritis: Diagnostic Value, Associations With Radiological Progression Rate, and Extra-Articular Manifestations. *Ann Rheum Dis* (2004) 63(12):1587–93. doi: 10.1136/ard.2003.017574
7. Shi J, Knevel R, Suwannalai P, van der Linden MP, Janssen GM, van Veelen PA, et al. Autoantibodies Recognizing Carbamylated Proteins Are Present in Sera of Patients With Rheumatoid Arthritis and Predict Joint Damage. *Proc Natl Acad Sci USA* (2011) 108(42):17372–7. doi: 10.1073/pnas.1114465108
8. Hecht C, Englbrecht M, Rech J, Schmidt S, Araujo E, Engelke K, et al. Additive Effect of Anti-Citrullinated Protein Antibodies and Rheumatoid Factor on Bone Erosions in Patients With RA. *Ann Rheum Dis* (2015) 74(12):2151–6. doi: 10.1136/annrheumdis-2014-205428
9. Kleyer A, Finzel S, Rech J, Manger B, Krieter M, Faustini F, et al. Bone Loss Before the Clinical Onset of Rheumatoid Arthritis in Subjects With Anticitrullinated Protein Antibodies. *Ann Rheum Dis* (2014) 73(5):854–60. doi: 10.1136/annrheumdis-2012-202958
10. Haynes DR, Crotti TN, Loric M, Bain GI, Atkins GJ, Findlay DM. Osteoprotegerin and Receptor Activator of Nuclear Factor Kappab Ligand (RANKL) Regulate Osteoclast Formation by Cells in the Human Rheumatoid Arthritic Joint. *Rheumatol (Oxford)* (2001) 40(6):623–30. doi: 10.1093/rheumatology/40.6.623
11. Felix R, Cecchini MG, Hofstetter W, Elford PR, Stutzer A, Fleisch H. Impairment of Macrophage Colony-Stimulating Factor Production and Lack of Resident Bone Marrow Macrophages in the Osteopetrotic Op/Op Mouse. *J Bone Miner Res* (1990) 5(7):781–9. doi: 10.1002/jbmr.5650050716
12. Karst M, Gorny G, Galvin RJ, Oursler MJ. Roles of Stromal Cell RANKL, OPG, and M-CSF Expression in Biphasic TGF-Beta Regulation of Osteoclast Differentiation. *J Cell Physiol* (2004) 200(1):99–106. doi: 10.1002/jcp.20036
13. Bozec A, Luo Y, Engdahl C, Figueiredo C, Bang H, Schett G. Abatacept Blocks Anti-Citrullinated Protein Antibody and Rheumatoid Factor Mediated Cytokine Production in Human Macrophages in IDO-Dependent Manner. *Arthritis Res Ther* (2018) 20(1):24. doi: 10.1186/s13075-018-1527-x
14. Bertazzolo N, Punzi L, Stefani MP, Cesaro G, Pianon M, Finco B, et al. Interrelationships Between Interleukin (IL)-1, IL-6 and IL-8 in Synovial Fluid of Various Arthropathies. *Agents Actions* (1994) 41(1-2):90–2. doi: 10.1007/BF01986402
15. Poubelle PE, Chakravarti A, Fernandes MJ, Doiron K, Marceau AA. Differential Expression of RANK, RANK-L, and Osteoprotegerin by Synovial Fluid Neutrophils From Patients With Rheumatoid Arthritis and by Healthy Human Blood Neutrophils. *Arthritis Res Ther* (2007) 9(2):R25. doi: 10.1186/ar2137
16. Moonen CGJ, de Vries TJ, Rijkschroeff P, Poubelle PE, Nicu EA, Loos BG. The Possible Role of Neutrophils in the Induction of Osteoclastogenesis. *J Immunol Res* (2019) 2019:8672604. doi: 10.1155/2019/8672604
17. Short KR, von Kockritz-Blickwede M, Langereis JD, Chew KY, Job ER, Armitage CW, et al. Antibodies Mediate Formation of Neutrophil Extracellular Traps in the Middle Ear and Facilitate Secondary Pneumococcal Otitis Media. *Infect Immun* (2014) 82(1):364–70. doi: 10.1128/IAI.01104-13
18. Aleyd E, van Hout MWM, Ganzevles SH, Hoeben KA, Everts V, Bakema JE, et al. Iga Enhances Netosis and Release of Neutrophil Extracellular Traps by

Polymorphonuclear Cells *Via* Fcα Receptor I. *J Immunol* (2016) 192(5):2374–83. doi: 10.4049/jimmunol.1300261
19. Sieghart D, Platzer A, Studenic P, Alasti F, Grundhuber M, Swiniarski S, et al. Determination of Autoantibody Isotypes Increases the Sensitivity of Serodiagnostics in Rheumatoid Arthritis. *Front Immunol* (2018) 9:876. doi: 10.3389/fimmu.2018.00876
20. van Delft MAM, Verheul MK, Burgers LE, Derksen V, van der Helm-van Mil AHM, van der Woude D, et al. The Isotype and Igg Subclass Distribution of Anti-Carbamylated Protein Antibodies in Rheumatoid Arthritis Patients. *Arthritis Res Ther* (2017) 19(1):190. doi: 10.1186/s13075-017-1392-z
21. Karimifar M, Moussavi H, Babaei M, Akbari M. The Association of Immunoglobulin a, Immunoglobulin G and Anti-Cyclic Citrullinated Peptide Antibodies With Disease Activity in Seronegative Rheumatoid Arthritis Patients. *J Res Med Sci* (2014) 19(9):823–6.
22. Jonsson T, Arinbjarnarson S, Thorsteinsson J, Steinsson K, Geirsson AJ, Jonsson H, et al. Raised Iga Rheumatoid Factor (RF) But Not Igm RF or Igg RF Is Associated With Extra-Articular Manifestations in Rheumatoid Arthritis. *Scand J Rheumatol* (1995) 24(6):372–5. doi: 10.3109/03009749509095183
23. He Y, Zha Q, Liu D, Lu A. Relations Between Serum Iga Level and Cartilage Erosion in 436 Cases of Rheumatoid Arthritis. *Immunol Invest* (2007) 36 (3):285–91. doi: 10.1080/08820130601069731
24. Jonsson T, Thorsteinsson J, Kolbeinsson A, Jonasdottir E, Sigfusson N, Valdimarsson H. Population Study of the Importance of Rheumatoid Factor Isotypes in Adults. *Ann Rheum Dis* (1992) 51(7):863–8. doi: 10.1136/ard.51.7.863
25. Sprangers S, Schoenmaker T, Cao Y, Everts V, de Vries TJ. Different Blood-Borne Human Osteoclast Precursors Respond in Distinct Ways to IL-17A. *J Cell Physiol* (2016) 231(6):1249–60. doi: 10.1002/jcp.25220
26. ten Harkel B, Schoenmaker T, Picavet DI, Davison NL, de Vries TJ, Everts V. The Foreign Body Giant Cell Cannot Resorb Bone, But Dissolves Hydroxyapatite Like Osteoclasts. *PLoS One* (2015) 10(10):e0139564. doi: 10.1371/journal.pone.0139564
27. Aleyd E, Al M, Tuk CW, van der Laken CJ, van Egmond M. Iga Complexes in Plasma and Synovial Fluid of Patients With Rheumatoid Arthritis Induce Neutrophil Extracellular Traps *Via* Fcalphari. *J Immunol* (2016) 197 (12):4552–9. doi: 10.4049/jimmunol.1502353
28. Cody JJ, Rivera AA, Liu J, Liu JM, Douglas JT, Feng X. A Simplified Method for the Generation of Human Osteoclasts *In Vitro*. *Int J Biochem Mol Biol* (2011) 2(2):183–9.
29. Sorensen MG, Henriksen K, Schaller S, Henriksen DB, Nielsen FC, Dziegiel MH, et al. Characterization of Osteoclasts Derived From CD14+ Monocytes Isolated From Peripheral Blood. *J Bone Miner Metab* (2007) 25(1):36–45. doi: 10.1007/s00774-006-0725-9
30. Athanasou NA, Quinn J. Immunophenotypic Differences Between Osteoclasts and Macrophage Polykaryons: Immunohistological Distinction and Implications for Osteoclast Ontogeny and Function. *J Clin Pathol* (1990) 43 (12):997–1003. doi: 10.1136/jcp.43.12.997
31. Nakamura I, Duong LT, Rodan SB, Rodan GA. Involvement of Alpha(V) Beta3 Integrins in Osteoclast Function. *J Bone Miner Metab* (2007) 25(6):337–44. doi: 10.1007/s00774-007-0773-9
32. Gravallese EM, Manning C, Tsay A, Naito A, Pan C, Amento E, et al. Synovial Tissue in Rheumatoid Arthritis Is a Source of Osteoclast Differentiation Factor. *Arthritis Rheum* (2000) 43(2):250–8. doi: 10.1002/1529-0131 (200002)43:2<250::AID-ANR3>3.0.CO;2-P
33. Pettit AR, Ji H, von Stechow D, Muller R, Goldring SR, Choi Y, et al. TRANCE/RANKL Knockout Mice Are Protected From Bone Erosion in a Serum Transfer Model of Arthritis. *Am J Pathol* (2001) 159(5):1689–99. doi: 10.1016/S0002-9440(10)63016-7
34. Stolina M, Dwyer D, Ominsky MS, Corbin T, Van G, Bolon B, et al. Continuous RANKL Inhibition in Osteoprotegerin Transgenic Mice and Rats Suppresses Bone Resorption Without Impairing Lymphorganogenesis or Functional Immune Responses. *J Immunol* (2007) 179(11):7497–505. doi: 10.4049/jimmunol.179.11.7497
35. Hafstrom I, Ajeganova S, Forslind K, Svensson B. Anti-Citrullinated Protein Antibodies Are Associated With Osteopenia But Not With Pain at Diagnosis of Rheumatoid Arthritis: Data From the BARFOT Cohort. *Arthritis Res Ther* (2019) 21(1):45. doi: 10.1186/s13075-019-1833-y
36. Orsolini G, Caimmi C, Viapiana O, Idolazzi L, Fracassi E, Gatti D, et al. Titer-Dependent Effect of Anti-Citrullinated Protein Antibodies on Systemic Bone Mass in Rheumatoid Arthritis Patients. *Calcif Tissue Int* (2017) 101(1):17–23. doi: 10.1007/s00223-017-0253-8
37. Sargin G, Kose R, Senturk T. Relationship Between Bone Mineral Density and Anti-Citrullinated Protein Antibody and Rheumatoid Factor in Patients With Rheumatoid Arthritis. *Eur J Rheumatol* (2019) 6(1):29–33. doi: 10.5152/eurjrheum.2018.18099
38. Harre U, Georgess D, Bang H, Bozec A, Axmann R, Ossipova E, et al. Induction of Osteoclastogenesis and Bone Loss by Human Autoantibodies Against Citrullinated Vimentin. *J Clin Invest* (2012) 122(5):1791–802. doi: 10.1172/JCI60975
39. Kokkonen H, Mullazehi M, Berglin E, Hallmans G, Wadell G, Ronnelid J, et al. Antibodies of Igg, Iga and Igm Isotypes Against Cyclic Citrullinated Peptide Precede the Development of Rheumatoid Arthritis. *Arthritis Res Ther* (2011) 13(1):R13. doi: 10.1186/ar3237
40. Svard A, Kastbom A, Soderlin MK, Reckner-Olsson A, Skogh T. A Comparison Between Igg- and Iga-Class Antibodies to Cyclic Citrullinated Peptides and to Modified Citrullinated Vimentin in Early Rheumatoid Arthritis and Very Early Arthritis. *J Rheumatol* (2011) 38(7):1265–72. doi: 10.3899/jrheum.101086
41. Khandpur R, Carmona-Rivera C, Vivekanandan-Giri A, Gizinski A, Yalavarthi S, Knight JS, et al. Nets Are a Source of Citrullinated Autoantigens and Stimulate Inflammatory Responses in Rheumatoid Arthritis. *Sci Transl Med* (2013) 5 (178):178ra40. doi: 10.1126/scitranslmed.3005580
42. Shi J, van Veelen PA, Mahler M, Janssen GM, Drijfhout JW, Huizinga TW, et al. Carbamylation and Antibodies Against Carbamylated Proteins in Autoimmunity and Other Pathologies. *Autoimmun Rev* (2014) 13(3):225–30. doi: 10.1016/j.autrev.2013.10.008
43. Gorlino CV, Dave MN, Blas R, Crespo MI, Lavanchy A, Tamashiro H, et al. Association Between Levels of Synovial Anti-Citrullinated Peptide Antibodies and Neutrophil Response in Patients With Rheumatoid Arthritis. *Eur J Immunol* (2018) 48(9):1563–72. doi: 10.1002/eji.201847477
44. Chirivi RGS, van Rosmalen JWG, van der Linden M, Euler M, Schmets G, Bogatkevich G, et al. Therapeutic ACPA Inhibits NET Formation: A Potential Therapy for Neutrophil-Mediated Inflammatory Diseases. *Cell Mol Immunol* (2020) 17:1–17. doi: 10.1038/s41423-020-0381-3
45. van Delft MAM, Huizinga TWJ. An Overview of Autoantibodies in Rheumatoid Arthritis. *J Autoimmun* (2020) 110:102392. doi: 10.1016/j.jaut.2019.102392
46. Tan EM, Smolen JS. Historical Observations Contributing Insights on Etiopathogenesis of Rheumatoid Arthritis and Role of Rheumatoid Factor. *J Exp Med* (2016) 213(10):1937–50. doi: 10.1084/jem.20160792
47. Firestein GS, McInnes IB. Immunopathogenesis of Rheumatoid Arthritis. *Immunity* (2017) 46(2):183–96. doi: 10.1016/j.immuni.2017.02.006
48. Holers VM, Banda NK. Complement in the Initiation and Evolution of Rheumatoid Arthritis. *Front Immunol* (2018) 9:1057. doi: 10.3389/fimmu.2018.01057
49. Laurent L, Clavel C, Lemaire O, Anquetil F, Cornillet M, Zabraniecki L, et al. Fcgamma Receptor Profile of Monocytes and Macrophages From Rheumatoid Arthritis Patients and Their Response to Immune Complexes Formed With Autoantibodies to Citrullinated Proteins. *Ann Rheum Dis* (2011) 70(6):1052–9. doi: 10.1136/ard.2010.142091
50. Sokolove J, Zhao X, Chandra PE, Robinson WH. Immune Complexes Containing Citrullinated Fibrinogen Costimulate Macrophages *Via* Toll-Like Receptor 4 and Fcgamma Receptor. *Arthritis Rheum* (2011) 63(1):53–62. doi: 10.1002/art.30081
51. Dakin SG, Coles M, Sherlock JP, Powrie F, Carr AJ, Buckley CD. Pathogenic Stromal Cells as Therapeutic Targets in Joint Inflammation. *Nat Rev Rheumatol* (2018) 14(12):714–26. doi: 10.1038/s41584-018-0112-7
52. Rombouts Y, Ewing E, van de Stadt LA, Selman MH, Trouw LA, Deelder AM, et al. Anti-Citrullinated Protein Antibodies Acquire a Pro-Inflammatory Fc Glycosylation Phenotype Prior to the Onset of Rheumatoid Arthritis. *Ann Rheum Dis* (2015) 74(1):234–41. doi: 10.1136/annrheumdis-2013-203565
53. Navegantes KC, de Souza Gomes R, Pereira PAT, Czaikoski PG, Azevedo CHM, Monteiro MC. Immune Modulation of Some Autoimmune Diseases: The Critical Role of Macrophages and Neutrophils in the Innate and Adaptive Immunity. *J Transl Med* (2017) 15(1):36. doi: 10.1186/s12967-017-1141-8

54. Seeling M, Hillenhoff U, David JP, Schett G, Tuckermann J, Lux A, et al. Inflammatory Monocytes and Fcgamma Receptor IV on Osteoclasts are Critical for Bone Destruction During Inflammatory Arthritis in Mice. *Proc Natl Acad Sci USA* (2013) 110(26):10729–34. doi: 10.1073/pnas.1301001110
55. Krishnamurthy A, Joshua V, Haj Hensvold A, Jin T, Sun M, Vivar N, et al. Identification of a Novel Chemokine-Dependent Molecular Mechanism Underlying Rheumatoid Arthritis-Associated Autoantibody-Mediated Bone Loss. *Ann Rheum Dis* (2016) 75(4):721–9. doi: 10.1136/annrheumdis-2015-208093
56. Wu Q, Zhou X, Huang D, Ji Y, Kang F. IL-6 Enhances Osteocyte-Mediated Osteoclastogenesis by Promoting JAK2 and RANKL Activity *In Vitro*. *Cell Physiol Biochem* (2017) 41(4):1360–9. doi: 10.1159/000465455
57. Liu XH, Kirschenbaum A, Yao S, Levine AC. Cross-Talk Between the Interleukin-6 and Prostaglandin E(2) Signaling Systems Results in Enhancement of Osteoclastogenesis Through Effects on the Osteoprotegerin/Receptor Activator of Nuclear Factor-κB (RANK) Ligand/RANK System. *Endocrinology* (2005) 146 (4):1991–8. doi: 10.1210/en.2004-1167
58. De Benedetti F, Rucci N, Del Fattore A, Peruzzi B, Paro R, Longo M, et al. Impaired Skeletal Development in Interleukin-6-Transgenic Mice: A Model for the Impact of Chronic Inflammation on the Growing Skeletal System. *Arthritis Rheum* (2006) 54(11):3551–63. doi: 10.1002/art.22175
59. Ohshima S, Saeki Y, Mima T, Sasai M, Nishioka K, Nomura S, et al. Interleukin 6 Plays a Key Role in the Development of Antigen-Induced Arthritis. *Proc Natl Acad Sci USA* (1998) 95(14):8222–6. doi: 10.1073/pnas.95.14.8222
60. Maini RN, Taylor PC, Szechinski J, Pavelka K, Broll J, Balint G, et al. Double-Blind Randomized Controlled Clinical Trial of the Interleukin-6 Receptor Antagonist, Tocilizumab, in European Patients With Rheumatoid Arthritis Who Had An Incomplete Response to Methotrexate. *Arthritis Rheum* (2006) 54(9):2817–29. doi: 10.1002/art.22033
61. Nishimoto N, Hashimoto J, Miyasaka N, Yamamoto K, Kawai S, Takeuchi T, et al. Study of Active Controlled Monotherapy Used for Rheumatoid Arthritis, an IL-6 Inhibitor (SAMURAI): Evidence of Clinical and Radiographic Benefit From an X Ray Reader-Blinded Randomised Controlled Trial of Tocilizumab. *Ann Rheum Dis* (2007) 66(9):1162–7. doi: 10.1136/ard.2006.068064
62. Smolen JS, Beaulieu A, Rubbert-Roth A, Ramos-Remus C, Rovensky J, Alecock E, et al. Effect of Interleukin-6 Receptor Inhibition With Tocilizumab in Patients With Rheumatoid Arthritis (OPTION Study): A Double-Blind, Placebo-Controlled, Randomised Trial. *Lancet* (2008) 371 (9617):987–97. doi: 10.1016/S0140-6736(08)60453-5

Conflict of Interest: The authors declare that the research was conducted in the absence of any commercial or financial relationships that could be construed as a potential conflict of interest.

frontiers in Endocrinology

ORIGINAL RESEARCH
published: 04 August 2021
doi: 10.3389/fendo.2021.685060

RANKL-Induced Btn2a2 – A T Cell Immunomodulatory Molecule – During Osteoclast Differentiation Fine-Tunes Bone Resorption

Michael Frech[1,2], *Gregor Schuster*[1,2], *Fabian T. Andes*[1,2], *Georg Schett*[1,2], *Mario M. Zaiss*[1,2] *and Kerstin Sarter*[1,2*†]

[1] Department of Internal Medicine 3, Rheumatology and Immunology, Friedrich-Alexander-University Erlangen-Nürnberg (FAU) and Universitätsklinikum Erlangen, Erlangen, Germany, [2] Deutsches Zentrum für Immuntherapie (DZI), Friedrich-Alexander-University Erlangen-Nürnberg (FAU) and Universitätsklinikum Erlangen, Erlangen, Germany

OPEN ACCESS

Edited by:
Katharina Schmidt-Bleek, Charité – Universitätsmedizin Berlin, Germany

Reviewed by:
Irma Machuca-Gayet, Centre National de la Recherche Scientifique (CNRS), France
Hamid Yousf Dar, Emory University, United States

***Correspondence:**
Kerstin Sarter
kerstin.sarter-zaiss@uk-erlangen.de

[†]These authors have contributed equally to this work

Specialty section:
This article was submitted to Bone Research, a section of the journal Frontiers in Endocrinology

Received: 24 March 2021
Accepted: 05 July 2021
Published: 04 August 2021

Citation:
Frech M, Schuster G, Andes FT, Schett G, Zaiss MM and Sarter K (2021) RANKL-Induced Btn2a2 – A T Cell Immunomodulatory Molecule – During Osteoclast Differentiation Fine-Tunes Bone Resorption. Front. Endocrinol. 12:685060. doi: 10.3389/fendo.2021.685060

Butyrophilins, which are members of the extended B7 family of immunoregulators structurally related to the B7 family, have diverse functions on immune cells as co-stimulatory and co-inhibitory molecules. Despite recent advances in the understanding on butyrophilins' role on adaptive immune cells during infectious or autoimmune diseases, nothing is known about their role in bone homeostasis. Here, we analyzed the role of one specific butyrophilin, namely Btn2a2, as we have recently shown that Btn2a2 is expressed on the monocyte/macrophage lineage that also gives rise to bone degrading osteoclasts. We found that expression of Btn2a2 on monocytes and pre-osteoclasts is upregulated by the receptor activator of nuclear factor κ-B ligand (RANKL), an essential protein required for osteoclast formation. Interestingly, in Btn2a2-deficient osteoclasts, typical osteoclast marker genes (Nfatc1, cathepsin K, TRAP, and RANK) were downregulated following RANKL stimulation. *In vitro* osteoclast assays resulted in decreased TRAP positive osteoclast numbers in Btn2a2-deficient cells. However, Btn2a2-deficient osteoclasts revealed abnormal fusion processes shown by their increased size. *In vivo* steady state μCT and histological analysis of bone architecture in complete Btn2a2-deficient mice showed differences in bone parameters further highlighting the fine-tuning effect of BTN2a2. Moreover, in rheumatoid arthritis patients and experimental arthritis, we detected significantly decreased serum levels of the secreted soluble Btn2a2 protein. Taken together, we identified the involvement of the immunomodulatory molecule Btn2a2 in osteoclast differentiation with potential future implications in basic and translational osteoimmunology.

Keywords: osteoclast (OC), RANKL (receptor activator for nuclear factor k B ligand), bone homeostasis, bone resorption, T cell

INTRODUCTION

Bone loss and musculoskeletal diseases are playing an increasingly important role in medicine (1). Bone is a living organ that is subject to constant change in the form of remodeling processes (2). Bone homeostasis is determined by the activity of osteoclasts (OC) that break down bone matrix and osteoblasts that synthesize bone matrix. Disturbance in this homeostasis can lead to systemic or local bone loss and the development of osteoporosis and bone erosions, respectively (3, 4). Monocyte-colony-stimulating factor (M-CSF) and the receptor activator of NF-κB Ligand (RANKL) are of primary importance for OC differentiation. M-CSF is primarily secreted by osteoblasts (5), and RANKL is mainly synthesized by osteocytes in the context of bone homeostasis, but many other cells such as osteoblasts and T cells can do so as well. Various signal cascades were identified that are triggered by the RANK-RANKL interaction and that induce osteoclast activity and survival such as the inhibitor of NF-kB kinase (IKK), c-jun n-terminal kinase (JNK), p38, or tyrosine kinase SRC (C-Src), Nuclear factor of activated T-cells, cytoplasmic 1 (Nfatc1), the osteoclast-associated receptors (OSCAR) or epidermal growth factor receptors (EGFR) (6–10). Surface receptors that modulate osteoclast activity and regulate such intracellular signaling pathways are of particular interest in bone biology as their manipulation affects bone homeostasis.

Butyrophilins (BTN) comprise a group of transmembrane proteins belonging to the immunoglobulin superfamily. Due to their very similar structure, BTN are seen as members of the B7 protein family. Only 5 proteins of the family have been detected in both humans and mice (11). Members of the protein family are associated with immunological processes such as the activation of B and T cells and are also expressed on immune cells (12–17). Even if the role of BTN proteins in the immune response is not dominant, they could be one of many factors that, e.g. through mutation, that favor the development of inflammatory disease (18–20). The protein Btn2a2 is particularly expressed on thymic epithelial cells and antigen-presenting cells such as dendritic cells, monocytes, and B cells. In recent years, the contribution of Btn2a2 in the context of T-cell activation has been highlighted (13, 21), and in a mouse model with Btn2a2-deficient animals, it was shown that its main function is a negative co-stimulatory effect on T-cell activation (22).

T cells play a special role in osteoclastogenesis, osteoclast activity and recruitment (23). RANKL is expressed on certain T helper cells (Th), Th17 cells, and some of their cytokines, like IL-17, promote osteoclast differentiation (24). In addition, other downstream effector cytokines such as IL-6 and TNF-alpha induce osteoclasts and promote recruitment of osteoclast precursor cells (25). On the other hand, it was shown that regulatory T cells (Treg) can suppress the differentiation of osteoclasts (26) (27). The RANK receptor and its ligand RANKL are also found in various structures of the immune system such as the thymus (28), the lymph nodes (29), or the microfold cells of the intestine (30). Based on the role of T cells in osteoclast differentiation and the effect of Btn2a2 on T cell costimulation we considered to investigate the influence of Btn2a2 on bone homoeostasis. In our data, we can show that Btn2a2 is involved in the differentiation and fusion processes of bone degrading OC.

MATERIAL AND METHODS

Mice

$Btn2a2^{-/-}$ mice and wild-type littermates were housed and experiments were conducted under specific pathogen-free conditions and housed in a room at 23 ± 2°C, with 50 ± 10% humidity and a 12hour light/dark. $Btn2a2^{-/-}$ mice were generated by the Wellcome Trust Sanger Institute (Cambridge). Mice were allowed free access to water and regular rodent chow. All of the protocols for animal experiments were approved by the local ethics authorities of the Regierung von Unterfranken.

Cell Culture

Bone marrow-derived monocytes (BMMs) were isolated and differentiated into Osteoclast precursors (OCP) and mature Osteoclasts (OC) as previously described with modifications indicated (31). Briefly, bone marrow of 8-14-week-old $Btn2a2^{-/-}$ mice and their littermate controls was isolated by flushing femoral and humeral diaphyseal bones. Cells were seeded into 10 cm petri dishes and cultured overnight in complete medium (αMEM, supplemented with 10% L929 conditioned medium, 10% fetal calf serum (FCS) and 1% penicillin/streptomycin). After 24h 2 x 10^5 cells/well were seeded into 96-well culture plates and grown for 4 days in complete medium containing 50 ng/ml RANKL (R&D Systems, Wiesbaden-Nordenstadt, Germany), unless otherwise stated. Medium was replenished after 72h. Osteoclast differentiation was evaluated by staining fixed cells for TRAP using Leukocyte Acid Phosphatase Kit (Sigma-Aldrich, Taufkirchen, Germany), according to the manufacturer's instructions.

Osteoclast Assay

BMMs from $Btn2a2^{-/-}$ and littermate control mice were isolated and differentiated in osteoclast precursors (OCP) and mature osteoclasts (OC) as described previously (31). The TRAP stain of the differentiated and grown OC was performed 5 days after the isolation. Images were taken by Keyence BZ-X710 in 12 sections per well and got joined digitally to create an image of the complete well. Digital measurement technique (Adobe Photoshop®) was used to quantify osteoclast growth on *in vitro* images. TRAP-positive, multinucleated OC (with 3 or more nuclei) were designated and counted as OC. The contours of those OC were outlined and the enclosed area was calculated with Adobe Photoshop®.

In-Vitro Scratch Assay

For horizontal migration analysis BMMs from $Btn2a2^{-/-}$ and littermate control mice were seeded into 10 cm petri dishes and cultured overnight in complete medium. After 24h, 137.5 × 10^5

cells/well were seeded into a 35 mm 2-well culture insert (ibidi) in complete medium containing 50 ng/ml RANKL (R&D Systems, Wiesbaden-Nordenstadt, Germany) for additional 12h allowing cells to adhere and spread on the substrate. Subsequently, the culture insert was removed and cells were washed five times with growth medium to remove floating cells. Cells were allowed to migrate back into the scratched area for 24h and counted.

Bone Resorption Assay

The mineral resorption activity of osteoclasts was conducted using 24-well Corning Osteo Assay Surface Plates (Sigma-Aldrich). BMMs were seeded at a density of 8 × 105 cells/well in complete medium supplemented with RANKL (50 ng/ml) and cultured for 5 days, with medium exchange after 96h. After removing cells with deionized water, resorption pit formation was visualized by von Kossa staining and the resorptive area was quantified using ImageJ (National Institutes of Health, Bethesda, MD, USA).

RT-PCR Analysis

Samples were lysed with TriFast™ (Peqlab) and RNA was isolated following the instructions of the manufacturer. cDNA was generated using the High Capacity cDNA Reverse Transcription Kit (Applied Biosystems™) and analyzed using SYBR® Select Master Mix (Thermo Fisher Scientific) on a QuantStudio™ 6 Flex Real-Time PCR Instrument (Thermo Fisher Scientific). Gene expression results were expressed as arbitrary units relative to expression of the house keeping gene Glycerinaldehyd-3-phosphat-Dehydrogenase (GAPDH), unless indicated otherwise. Primer sequences are as follows;

GAPDH: 5'-GGGTGTGAACCACGAGAAAT-3' and 5'-CCTTCCACAATGCCAAAGTT-3',

Btn2a2: 5'-ATGACCAGGCAACCATGAAGC-3' and 5'-TCATAGGGGTCTCTCCACA-3',

RANK: 5'-GCCCAGTCTCATCGTTCTGC-3' and 5'-GCAAGCATCATTGACCCAATTC-3',

OPN: 5'-TCCTTAGACTCACCGCTCTT-3' and 5'-TCTCCTTGCGCCACAGAATG-3',

Cathepsin K: 5'-AGGGCCAACTCAAGAAGAAAACT-3' and 5'-TGCCATAGCCCACCACCAACACT-3',

TRAP: 5'-GGCCGGCCACTACCCCATCT-3' and 5'-CACCGTAGCCACAAGCAGGACTCT-3',

C-SRC: 5'-CGTGGCTGTCACCAAGGACCC-3' and 5'-TGGTGCTTTCCCGCACGAGG-3',

Nfatc1: 5'-CGGCGCAAGTACAGTCTCAATGGCG-3' and 5'-GGATGGTGTGGGTGAGTGGT-3',

ATP6v0d2: 5'-TCAGATCTCTTCAAGGCTGTGCTG-3' and 5'-GTGCCAAATGAGTTCAGAGTGATG-3',

Dcstamp: 5'-TTTGCCGCTGTGGACTATCTGC-3' and 5'-GCAGAATCATGGACGACTCCTTG-3',

Ocstamp: 5'-TTGCTCCTGTCCTACAGTGC3-3' and 5'-GCCCTCAGTAACACAGCTCA-3',

Csf1r: 5'-TGGATGCCTGTGAATGGCTCTG-3' and 5'-GTGGGTGTCATTCCAAACCTGC-3',

Cd44: 5'-TGGATCCGAATTAGCTGGAC-3' and 5'-AGCTTTTTCTTCTGCCCACA-3',

cfos: 5'-CTCTGGGAAGCCAAGGTC-3' and 5'-CGAAGGGAACGGAATAAG-3'.

Transcriptome Analysis of Osteoblasts

For transcriptome profiling of primary osteoblasts public RNA-seq data (32) was obtained from the sequence read archive (SRA, BioProject accession: PRJNA648106). Transcript-level abundances were quantified using Salmon (v1.3.0) (33) using the reference transcriptome GRCm39 from ensemble database. Differential expression analysis was performed with DESeq2 (v1.28.1) (34) with default parameters.

Micro-Computed Tomography Analysis (μCT)

For μCT imaging, 12-week old male Btn2a2$^{-/-}$ and littermate controls were used. μCT imaging was performed using the cone-beam Desktop Micro Computer Tomograph "μCT 40" (SCANCO Medical AG, Bruettisellen, Switzerland). The settings were optimized for calcified tissue visualization at 55 kVp with a current of 145 μA and 200 ms integration time for 500 projections/180°. For the segmentation of 3D-Volumes, an isotropic voxel size of 8.4 μm and an evaluation script with adjusted greyscale thresholds of the operating system "Open VMS" (SCANCO Medical) were used.

Histology

For histological analysis, tibial bones were fixed in Histofix (Roth) for 12h and decalcified in EDTA (Sigma-Aldrich). Serial paraffin sections (2 μm) were stained for H&E and tartrate resistant acid phosphatase (TRAP) using a Leukocyte Acid Phosphatase Kit (Sigma) according as to the manufacturer's instructions. Undecalcified bones were embedded in methacrylate and 5μm section were cut. Toluidine blue staining was performed for quantification of osteoblasts. Osteoclast and osteoblast numbers were quantified using a microscope (Nikon) equipped with a digital camera and an image analysis system for performing histomorphometry (Osteomeasure; OsteoMetrics).

Flow Cytometry

Single-cell suspensions of whole bone marrow were incubated on ice with conjugated antibodies in PBS containing 2% FCS and 5 mM EDTA (Merck). Dead cells were excluded with Fixable Aqua Dead Cell Stain (Thermo Fisher Scientific). For detection of the progenitor populations granulocyte-macrophage progenitors (GMP), common myeloid progenitors (CMP) and megakaryocyte erythrocyte progenitors (MEP), cells were stained with fluorochrome-conjugated anti-lineage (CD3, clone 17A2; Ly-6G, clone M1/70; CD11b, clone RB6-8C5; CD45R (B220), clone RA3-6B2; Ter-119, clone Ter-119, cat. #133311, Biolegend), anti-CD117 (clone 2B8, Biolegend), anti-CD127 (clone A7R34, Biolegend), anti-Ly6A/E (clone D7, Biolegend), anti-CD16/32 (clone 93, Biolegend) and anti-CD34 (clone RAM34, BD). Flow cytometry analysis was performed on the cytoflex platform (Beckman Coulter) and analyzed with FLowJo v.10 software (TreeStar).

Measurement of Serum Cytokines and Serum Btn2a2

Serum levels of osteocalcin (Nordic Bioscience), C-terminal telopeptide α1 chain of type I collagen (CTX-I) (RatLaps; Nordic Bioscience), and Btn2a2 (MyBioSource) were measured by enzyme-linked immunosorbent assay according to the manufacturer's instructions.

Collagen-Induced Arthritis (CIA)

CIA was induced in 8-week-old female DBA/1J mice by s.c. injection of 100 µl containing 0,25 mg chicken type II collagen (CII; Chondrex, Redmond, WA) in complete Freund adjuvant (CFA; Difco Laboratory, Detroit, MI), and 5 mg/mL killed Mycobacterium tuberculosis (H37Ra) at the base of the tail. Mice were re-challenged after 21 days by intradermal immunization at the base of the tail with this emulsion. Serum samples were collected at day 30 post injection.

Statistical Analysis

Data are expressed as mean ± s.e.m. unless otherwise indicated in the figure legends. Analysis was performed using Student's t-test, single comparison, or analysis of variance (ANOVA) test for multiple comparisons (one-way or two-way ANOVA followed by Tukey's or Bonferroni's multiple comparisons test, respectively). All experiments were conducted at least two times. P-values smaller than 0.05 were considered significant and are shown as $p<0.05$ (*), $p<0.01$ (**) $p<0.001$ (***), or $p<0.0001$ (****). Graph generation and statistical analyses were performed using the Prism version 8 software (GraphPad, La Jolla, CA) or R.

RESULTS

Btn2a2 Expression Is Up Regulated During Osteoclast Formation

To test our hypothesis of a connection between Btn2a2 expression and osteoclast (OC) differentiation, we analyzed the expression of Btn2a2 in osteoclast progenitor cells (OCP) after addition of RANKL. We observed that expression of Btn2a2 in OCP from wild-type mice is upregulated during the process of osteoclastogenesis, with a peak 4 days after stimulation with RANKL and M-CSF to OCP (**Figure 1A**). No expression of Btn2a2 was detected in OC from Btn2a2$^{-/-}$ mice 2, 4, and 6 days after RANKL addition. At day 2 Btn2a2 expression in wild-type and in mice heterozygous for Btn2a2 (Btn2a2$^{+/-}$) was low and increased at day 4 with an intermediate Btn2a2 expression detected in Btn2a2$^{+/-}$ mice, while at 6 days after RANKL addition expression of Btn2a2 could not be detected (**Figure 1A**). Interestingly we found that the up-regulation of Btn2a2 expression occurs in a dose-dependent manner with a plateau being reached with the addition of 25 ng/ml RANKL (**Figure 1B**), thus proving that Btn2a2 expression is dependent on RANKL stimulation and thereby indicating that it is involved in the process of OC differentiation. Analyzing published data from primary osteoblast during differentiation (32) revealed no expression of Btn2a2 (**Supplementary Figures 2B, C**), indicating that the role of Btn2a2 in bone homeostasis is restricted to effects on osteoclasts.

Loss of Btn2a2 Reduces Expression of Marker Genes Driving OC Formation

To further investigate the role of Btn2a2 in the osteoclast differentiation, we analyzed the expression of markers involved in OC proliferation, differentiation, activation and fusion in OC derived from Btn2a2$^{-/-}$ mice compared to wild-type littermate controls. We observed that lack of Btn2a2 leads to significantly different expression of analyzed markers of OC during osteoclastogenesis (**Figure 2**). 72h and 94h following RANKL stimulation. RANK and OPN expression of Btn2a2$^{-/-}$ OC were significantly lower than expression measured in wild-type OC (**Figures 2A, B**). Cathepsin K expression was significantly decreased in Btn2a2$^{-/-}$ OC after 94h (**Figure 2C**), as well as DC-Stamp and OC-Stamp expression (**Figures 2D, E**). TRAP

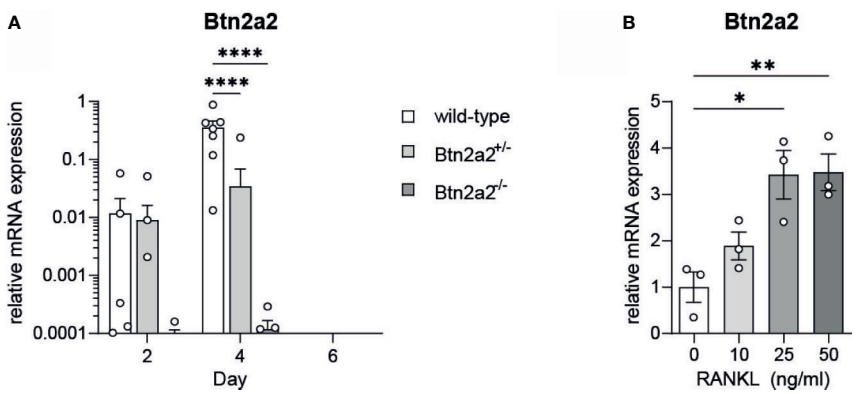

FIGURE 1 | Btn2a2 is regulated during osteoclastogenesis in a RANKL-dependent manner. **(A)** Btn2a2 expression was analyzed by quantitative RT-PCR at days 2, 4 and 6 during osteoclast assay from Btn2a2-/- , Btn2a2+/-, and wild-type littermate controls. Relative expression values normalized to the housekeeping gene GAPDH are shown. **(B)** Quantita tive RT-PCR for determination of relative mRNA levels of Btn2a2 normalized on GAPDH, after 2 hours stimulation of osteoclast precursors with indicated RANKL concentrations. Data are representative of 2 independent experiments, with 3 mice per group. Significance was assessed using one- **(B)** or two-way ANOVA **(A)** and Bonferroni's post-hoc test. Data are shown as means± SEM. *P < 0.05; **P < 0.01. ****P < 0.0001.

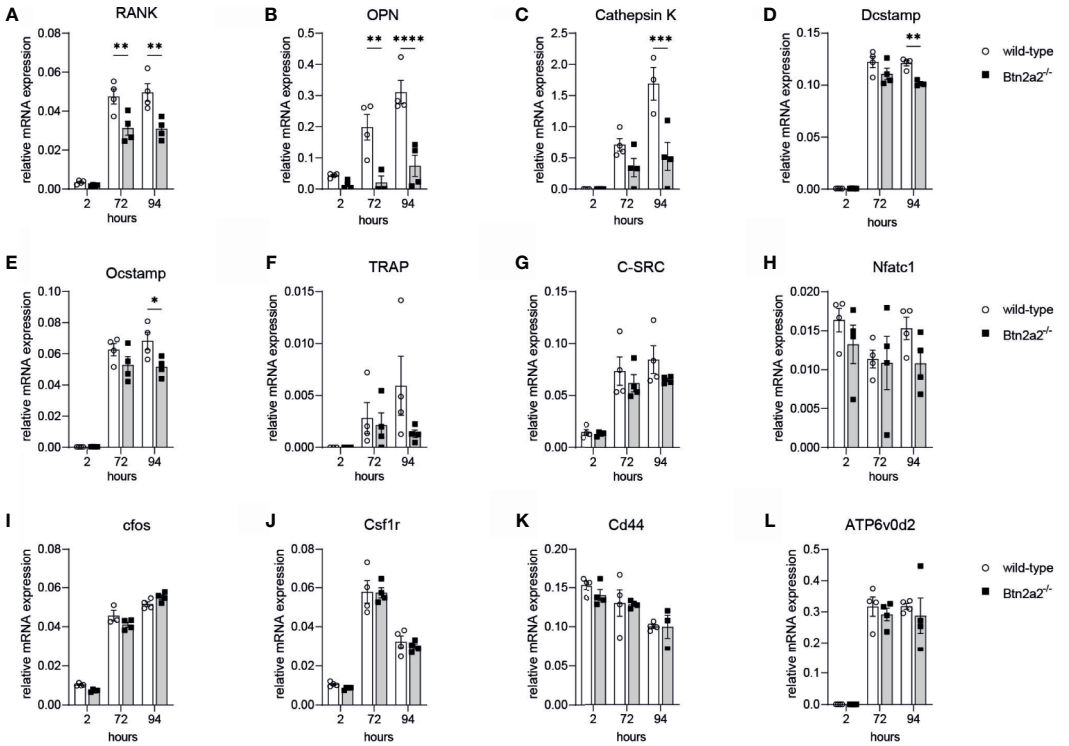

FIGURE 2 | Btn2a2-/- Osteoclasis reveal altered expression of OC-specific transcriptional signature during osteoclastogenesis. **(A–L)** Expression of osteoclast-related genes in wild-type and Btn2a2' osteoclasts after stimulation of osteoclast precursors with RANKL (50 ng/ml)for the indicated time points. Relative expression values normalized to the housekeeping gene GAPDH are shown. Data are representative of two Independent experiments, with 3 mice per group. Significance was assessed using two-way ANOVAand Bonferroni's post-hoc test. Data are shown as means :t SEM. *P < 0.05; **P < 0.01; ***P < 0.001; ****p < 0.0001.

expression was reduced as well though not significantly in Btn2a2$^{-/-}$ OC compared to wild-type OC (**Figure 2F**), while c-Src, NFATc1, cfos, Csf1r, CD44, and ATPv0d2 expression remained unchanged (**Figures 2G–L**). These data further underline the connection between bone homeostasis and Btn2a2 expression in OC.

Loss of Btn2a2 Leads to a Reduced Number of Bone Degrading Osteoclasts

Since we observed a clear difference in expression of differentiation and activation markers of Btn2a2$^{-/-}$ OC compared to wild-type OC, we investigated if these changes in OC marker gene expression is relevant for the differentiation of OC. When analyzing OC differentiation assays we observed that the overall number of OC formed of progenitor cells after addition of M-CSF and RANKL was significantly reduced in Btn2a2$^{-/-}$ mice, with an intermediate number of OC formed from Btn2a2$^{+/-}$ OCP (**Figure 3A**) thereby reflecting the results of decreased expression of OC marker genes relevant for OC formation. Interestingly, while displaying overall less OC in the assays with Btn2a2$^{-/-}$ OCP, we observed significantly higher numbers of OC with more than 20 nuclei in Btn2a2$^{-/-}$ compared to wild-type OC with an intermediate phenotype in Btn2a2$^{+/-}$ OC (**Figures 3B–D**). These data clearly indicate that Btn2a2 favors formation of OC *in vitro* and that loss of Btn2a2 also leads to an abnormal fusion process. In contrast, we did not observe abnormalities in the BM compartment of Btn2a2$^{-/-}$ mice compared to their wild-type counterparts as analyzed by flow cytometry for the frequencies of granulocyte-macrophage progenitors (GMP), common myeloid progenitors (CMP) and megakaryocyte erythrocyte progenitors (MEP) (**Figure 3E**). In addition, no defects in migratory behavior of Btn2a2$^{-/-}$ OC compared to wild-type OC was detected (**Figure 3F**) as well as no difference in *in vitro* resorption capacity (**Figure 3G**) and no differences in resorbed surface per OC was observed (**Figure 3H**).

Loss of Btn2a2 Changes Trabecular Bone Architecture *In Vivo*

Since Btn2a2 is up-regulated in OC after RANKL addition and Btn2a2$^{-/-}$ OC displayed altered expression of differentiation and activation markers that lead to a reduced OC formation and abnormal fusion process, we further investigated if the loss of Btn2a2 has an effect on bone homeostasis *in vivo*. Therefore, we analyzed bones from wild-type and Btn2a2$^{-/-}$ mice by histology and μCT for differences in bone parameters. Histological analysis of bones from W and Btn2a2$^{-/-}$ mice showed no differences both in numbers of OC per bone perimeter and in OC surface per bone surface (**Figures 4A, B**). We also did not observe any differences between Btn2a2$^{-/-}$ and wild-type mice in numbers of osteoblasts (**Supplementary Figure 2A**). However, results obtained from μCT analysis of tibial bones from Btn2a2$^{-/-}$ mice showed a significant

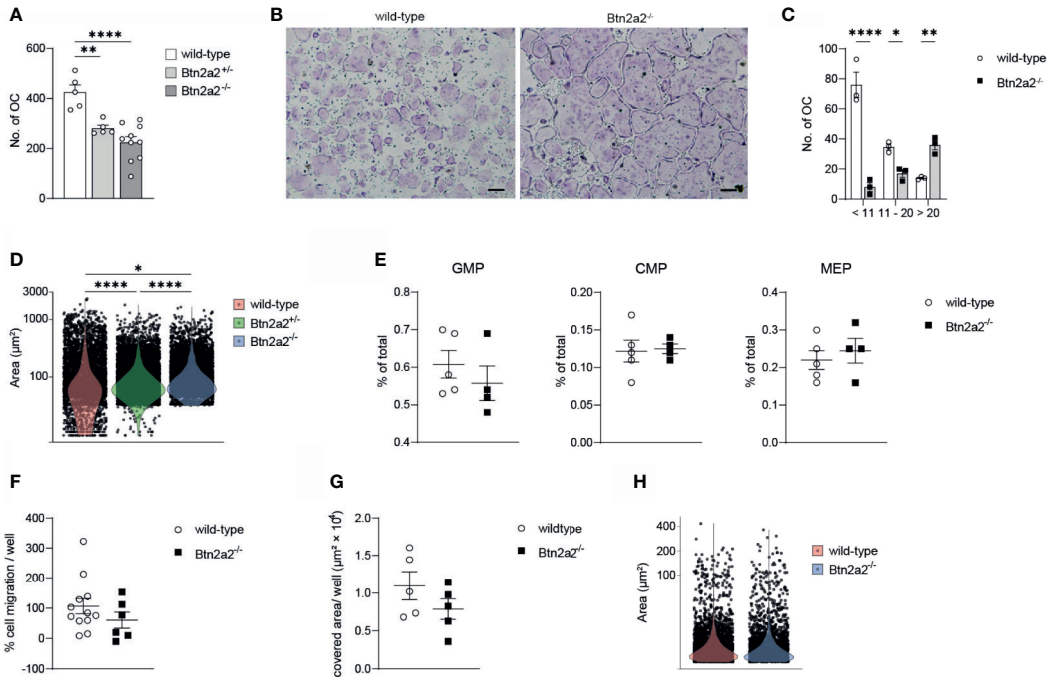

FIGURE 3 | Loss of Btn22 leds to reduced numbers of bone degrading osteoclasts. **(A)** quantification of the number of multinucleated TRAP+ osteoclasts from Wild-type, Btn2a2+/- and Btn2a2-/-mice after osteoclast assay. **(B)** Trap staining of Wild-type and Btn2a2-/- osteoclasts at day 5 of osteoclast assay and **(C)** quantification of the number of multinucleated TRAP+ osteoclasts by their number of nuclei. **(D)** violin plots displaying area of multinucleated TRAP+ osteoclasts at day 5 of osteoclast assay of wild-type Btn2a2+/- and Btn2a2-/- mice with each dot representing one osteoclast. **(E)** Flow cytometric analysis of bone marrow progenitor cells of wild-type and Btn2a2-/- mice. **(F)** OCP migration abilityof wild-type and Btn2a2-/- OCPs was assessed in vitro. Quantification of migrated cells was performed with images captured after 24 hours. Data are representative of two independent experiments, with 3 mice per group. **(G)** Analysis of resorption acitvity of Btn2a2-/- and their wild-type liltermates after 5 days of culture. **(H)** Resorbed area per osteoclast. Data are representative of two independent experiments, with 3-4 mice per group **(B, C, E–G)** or represent two pooled experiments **(A, D, H)**. Significance was assessed using one-way **(A)** or two-way ANOVA **(C)** and Bonferroni's post-hoc test or using two-tailed Students t-test. **(D)** Signifiance was assessed using Krusaii-Wallis test and pairwise comparisons using Wilcoxon rank sum test with Bonferroni's p value adjustments. **(B)** Scale bar indicates 200 µm. Data are shown as means t SEM. *P < 0.05; **P < 0.01; ****P < 0.0001.

increase in trabecular number and a significant decrease in trabecular separation when compared to tibia from wild-type mice, whereas bone volume was not statistically different in Btn2a2$^{-/-}$ mice (**Figures 4C, D**). This indicates that Btn2a2 may subtly influence the remodeling process of bone homeostasis *in vivo*. In addition to analyzing bone parameters, we also measured serum levels of C-terminal telopeptide of type 1 collagen (CTX) and osteoprotegerin (OPG) as markers of bone homeostasis in wild-type and in Btn2a2$^{-/-}$ mice. However, CTX and OPG serum levels were unchanged (**Figure 4E**). Another indication that Btn2a2 could play a role in bone homeostasis comes from measurements of Btn2a2 levels in sera of RA patients as well as from mice with a collagen-induced arthritis (CIA), in which the levels of Btn2a2 were significantly reduced in RA patients and CIA mice compared to normal healthy controls (**Figures 4F, G**), indicating that Btn2a2 is involved in diseases in which bone homeostasis is affected.

DISCUSSION

Osteoclast (OC) differentiation and activation is a multistep process that is critically regulated by RANKL (35, 36). Although RANKL is the main driver of OC differentiation, a number of additional factors have been revealed to be necessary for osteoclastogenesis and a multitude of hormones and cytokines modulate osteoclast formation (37–41). Herein, we show that RANKL induces the expression of the co-stimulatory molecule Btn2a2 in OC. To our knowledge, this is the first observation that Btn2a2 is expressed in OC upon RANKL stimulation and its dose dependent increase in expression indicates that it is involved in the process of OC formation. OC formation includes a series of regulatory steps, including differentiation, activation, migration, as well as their fusion into mature multinucleated OCs that subsequently initiate osteoclastic bone resorption (42, 43). To further investigate the role of Btn2a2 in these processes, we made use of a loss of function model for Btn2a2 and analyzed expression of known, essential marker genes involved in OC formation. We observed that OC deficient for Btn2a2$^{-/-}$ showed decreased expression in RANK, OPN, and cathepsin K, DC-Stamp, and OC-Stamp. RANK is critical for the OC formation and activation, it binds RANKL thereby activating signaling pathways in OC including the members of the TNF receptor activating factor (TRAF) family (44). OPN is one of the most abundant non-collagenous

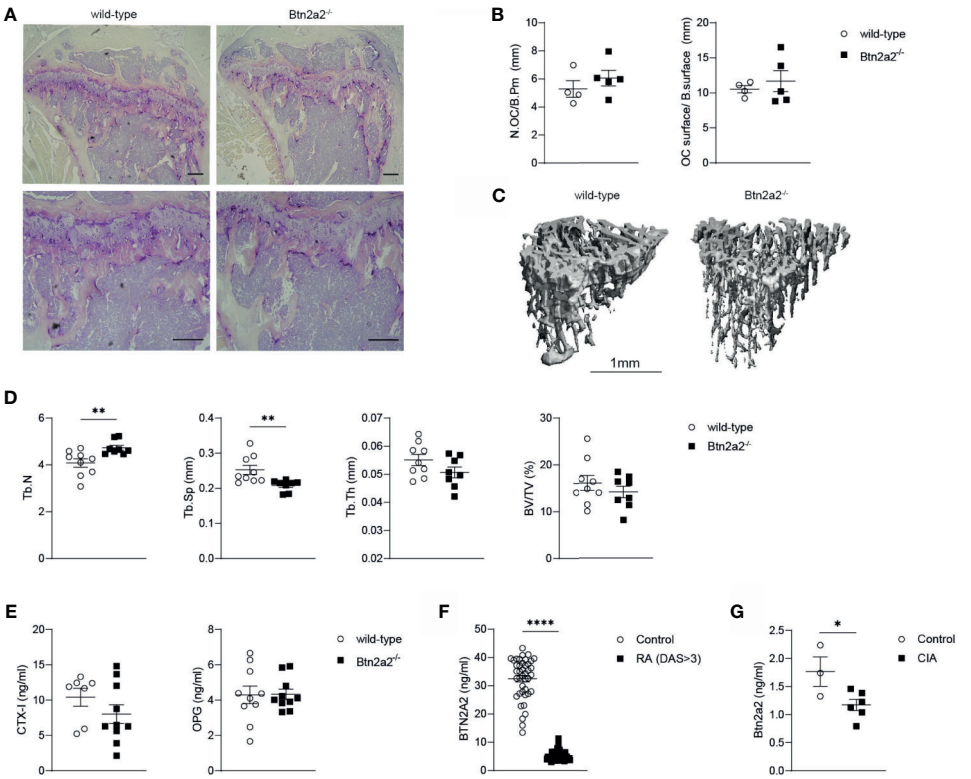

FIGURE 4 | Loss of Btn2a2 changes bone architecture *in vivo*. **(A)** Representative Images of tibiae with TRAP staining of male Btn2a2-/- mice compared with their wild type littermates at 12 weeks of age. Scale bar indicates 200 μm. **(B)** Histomorphometric analysis of the number of osteoclasts per bone perimeter (N.OC/B.Pm) and the osteoclast surface per bone surface (OC.surface/B.surface). **(C)** μCT images of the skeletal phenotype of male Btn2a2-/- mice and their wild-type littermates at 12 weeks of age. Scale bar indicates 1 mm. **(D)** μCT analysis of trabecular bone parameters of tibial bone including bone volume to trabecular volume (BV/TV), trabecular thickness (Tb.Th.), trabecular number (Tb number), and trabecular separation (Tb.Sp.). **(E)** Serum levels of CTX-1 and OPG from Btn2a2-/- mice and wild-type littermates at 12 weeks of age were measured by ELISA. **(F)** BTN2A2 serum levels from RA patients and healthy controls. **(G)** Btn2a2 serum levels from CIA mice compared to healthy controls at day 30 of CIA. Significance was assessed using Student's t-test. Date are shown as means ± SEM. *P < 0.05; **P < 0.01; ****p < 0.0001.

proteins in bone and is an important regulator of inflammation and biomineralization and regulates bone cell adhesion, osteoclast function, and matrix mineralization (45). However, mice lacking OPN show normal development and bone structure but display altered OC formation *in vitro* (46).TRAP is able to degrade skeletal phosphoproteins and is secreted by the OC during bone resorption and secretion correlates with resorptive behavior (47, 48). Cathepsin K is the major mediator of osteoclastic bone resorption (49). Upon differentiation and fusion, OC produce increasing amounts of cathepsin K, and this appears to be regulated by RANKL (50). Down-regulation of these marker genes in Btn2a2$^{-/-}$ progenitor cells suggests a functional defect of OC, further underlining a role of this molecule in the process of OC formation. And indeed, when analyzing OC formation assays, we observed that in those assays in which myeloid progenitors from Btn2a2$^{-/-}$ mice were stimulated with M-CSF and RANKL, significantly less OC were formed compared to assays using wild-type myeloid progenitors. With reduced Cathepsin K expression in Btn2a2$^{-/-}$ OC, we would expect less bone resorption by Btn2a2$^{-/-}$ OC compared to wild-type OC. However, we did not observe difference in resorption capacity between wild-type and Btn2a2$^{-/-}$ OC. This discrepancy could be due to the formation of giant OC in Btn2a2$^{-/-}$, which may compensate the overall lower capacity of resorption. Moreover, although Btn2a2$^{-/-}$ OC seem to be bigger, we observed in total more OC in wild-type compared to Btn2a2$^{-/-}$ mice, which also explains an unchanged BV/TV between wild-type and Btn2a2$^{-/-}$ conditions.

Interestingly, when using Btn2a2$^{-/-}$ monocytes, the number of very large OC (more than 20 nuclei) was significantly increased in comparison to wild-type conditions, pointing to an abnormal fusion process of OC in Btn2a2$^{-/-}$ mice. Since we observed giant OC in Btn2a2$^{-/-}$, we analyzed fusion markers of OC to detect a possible defect in the fusion process. We observed significantly reduced expression of DC-Stamp and OC-Stamp in Btn2a2$^{-/-}$ OC, which seems contradictory to an expected enhanced fusion rate of Btn2a2$^{-/-}$ OC. This may be explained by other proteins that play a role in fusion. Little is known about OC fusion, which is a property of mature osteoclasts and is required for osteoclasts to resorb bone. A number of molecular mediators were reported

to be important for osteoclast fusion (51–55). Nevertheless, the complete sequence of events leading from stimulation of osteoclastogenesis by RANKL to formation of large osteoclasts capable of bone destruction is incompletely understood. In a recent study, it has been shown that OC fission into osteomorphs and can recycle back into OC during RANKL-stimulated bone resorption (56), and since loss of Btn2a2 leads to reduced RANK expression, a decrease in RANK-RANKL signaling could lead to a reduction of recycling and fission events and therefore to the development of bigger OC. More research needs to be done on investigating the role of Btn2a2 in the fusion events of OC and it could be that recycling from osteomorphs is not possible in Btn2a2$^{-/-}$ OC (56, 57). In order to reveal the role of Btn2a2 in the fusion process of OC, further investigations need to be done, by analyzing expression levels of known fusion genes and the process of fission into osteomorphs and fusion back to OC in Btn2a2$^{-/-}$.

In vivo, Btn2a2$^{-/-}$ mice showed differences in trabecular architecture with significantly reduced separation of trabecula and increased trabecula numbers but no differences in bone volume per total volume were observed. The loss of Btn2a2 in the complete knockout mice therefore resulted in an altered bone architecture without a change in total bone mass. From the clear effects in OC from wild-type and Btn2a2$^{-/-}$ mice *in vitro* one would expect that in the Btn2a2$^{-/-}$ mice there is less bone degradation due to impaired OC differentiation, however, the formation of giant OC in Btn2a2$^{-/-}$ cells may counteract this effect *in vivo*, since these giant OC may be able to absorb more bone due to the increased bone surface they can cover.

Moreover, since the work presented here has been conducted in complete Btn2a2$^{-/-}$ mice, other effects of Btn2a2 may have masked the effects on bone homeostasis. Both resorption and formation of bone are tightly coupled processes, and the role of Btn2a2 on other cells needs to be taken into account. A possible role of Bn2a2 on osteoblast function is not known at present. In addition to osteoblasts, T and B lymphocytes are also known to influence the formation and activation of OC.

T cells express RANKL and thereby activated T cells may induce osteoclastogenesis (58), however major T cell cytokines such as IFNg, IL-4 and IL-10 are inhibitory to *in vitro* osteoclastogenesis (23, 59). Regulatory T cells (Treg) have been shown to suppress OC formation and protect from local and systemic bone destruction in arthritis (27, 60, 61). Btn2a2 binds to activated T cells and inhibits activation (13), and Btn2a2 induces Foxp3 expression and a regulatory phenotype in T Lymphocytes (21). As mentioned, loss of Btn2a2 results in a skewed T cell response towards a reduced Treg response (22). Activated T lymphocytes supporting osteoclast formation (58) and reduced Treg numbers in Btn2a2$^{-/-}$ may have an influence on OC differentiation and function *in vivo*. Thus, the effects of T cells on the formation of OC is dependent on a balance between their positive and negative factors. Also other cell types than osteoblasts and T- and B lymphocytes influence OC formation. It has been shown, that ILC2 can suppress OC formation (62, 63) and in our own unpublished work we detected Btn2a2 expression in ILC2 with significant immunomodulatory consequences.

In summary, our data point to a role of Btn2a2 in the differentiation of OC as well as its fusion process highlighting the role of T cell molecules on bone homeostasis.

DATA AVAILABILITY STATEMENT

The datasets presented in this study can be found in online repositories. The names of the repository/repositories and accession number(s) can be found in the article/ **Supplementary Material**.

ETHICS STATEMENT

The studies involving human participants were reviewed and approved by Ethikkommittee der FAU. The patients/participants provided their written informed consent to participate in this study. The animal study was reviewed and approved by Regierung von Unterfranken.

AUTHOR CONTRIBUTIONS

Study design, GeS, MZ, and KS. Study conduct, MF and GrS. Data collection, MF, GrS, FA, MZ, and KS. Data analysis, MF, GrS, and KS. Data interpretation, MF, GrS, MZ, and KS. Drafting manuscript, MF, MZ, and KS. Revising manuscript content, GeS, MZ, and KS. Approving final version of manuscript, MZ and KS. KS takes responsibility for the integrity of the data analysis. All authors contributed to the article and approved the submitted version.

FUNDING

This work was supported by the Deutsche Forschungsgemeinschaft (DFG) DFG-SPP1937 KS and MZ, by the Dr. Rolf Schwiete Stiftung for MF, KS, MZ and by the Else Kröner-Fresenius Stiftung MF and KS. Additional funding was received by the Interdisciplinary Centre for Clinical Research, Erlangen (IZKF) for KS.

ACKNOWLEDGMENTS

We thank all members of our laboratories at the Medical clinic 3 for their support and helpful discussions.

SUPPLEMENTARY MATERIAL

The Supplementary Material for this article can be found online at: https://www.frontiersin.org/articles/10.3389/fendo.2021.685060/full#supplementary-material

REFERENCES

1. WHO Scientific Group on the Burden of Musculoskeletal Conditions at the Start of the New Millennium. The Burden of Musculoskeletal Conditions at the Start of the New Millennium. *World Health Organ Tech Rep Ser* (2003) 919:i–x, 1-218, back cover.
2. Lane JM, Riley EH, Wirganowicz PZ. Osteoporosis: Diagnosis and Treatment. *Instr Course Lect* (1997) 46:445–58.
3. Chavassieux P, Seeman E, Delmas PD. Insights Into Material and Structural Basis of Bone Fragility From Diseases Associated With Fractures: How Determinants of the Biomechanical Properties of Bone are Compromised by Disease. *Endocr Rev* (2007) 28:151–64. doi: 10.1210/er.2006-0029
4. Rodan GA, Martin TJ. Therapeutic Approaches to Bone Diseases. *Science* (2000) 289:1508–14. doi: 10.1126/science.289.5484.1508
5. Han Y, You X, Xing W, Zhang Z, Zou W. Paracrine and Endocrine Actions of Bone-the Functions of Secretory Proteins From Osteoblasts, Osteocytes, and Osteoclasts. *Bone Res* (2018) 6:16. doi: 10.1038/s41413-018-0019-6
6. Boyle WJ, Simonet WS, Lacey DL. Osteoclast Differentiation and Activation. *Nature* (2003) 423:337–42. doi: 10.1038/nature01658
7. Wong BR, Besser D, Kim N, Arron JR, Vologodskaia M, Hanafusa H, et al. TRANCE, a TNF Family Member, Activates Akt/PKB Through a Signaling Complex Involving TRAF6 and C-Src. *Mol Cell* (1999) 4:1041–9. doi: 10.1016/S1097-2765(00)80232-4
8. Zhao Q, Wang X, Liu Y, He A, Jia R. Nfatc1: Functions in Osteoclasts. *Int J Biochem Cell Biol* (2010) 42:576–9. doi: 10.1016/j.biocel.2009.12.018
9. Koga T, Inui M, Inoue K, Kim S, Suematsu A, Kobayashi E, et al. Costimulatory Signals Mediated by the ITAM Motif Cooperate With RANKL for Bone Homeostasis. *Nature* (2004) 428:758–63. doi: 10.1038/nature02444
10. Yi T, Lee HL, Cha JH, Ko SI, Kim HJ, Shin HI, et al. Epidermal Growth Factor Receptor Regulates Osteoclast Differentiation and Survival Through Cross-Talking With RANK Signaling. *J Cell Physiol* (2008) 217:409–22. doi: 10.1002/jcp.21511
11. Afrache H, Gouret P, Ainouche S, Pontarotti P, Olive D. The Butyrophilin (BTN) Gene Family: From Milk Fat to the Regulation of the Immune Response. *Immunogenetics* (2012) 64:781–94. doi: 10.1007/s00251-012-0619-z
12. Arnett HA, Escobar SS, Viney JL. Regulation of Costimulation in the Era of Butyrophilins. *Cytokine* (2009) 46:370–5. doi: 10.1016/j.cyto.2009.03.009
13. Smith IA, Knezevic BR, Ammann JU, Rhodes DA, Aw D, Palmer DB, et al. BTN1A1, the Mammary Gland Butyrophilin, and BTN2A2 are Both Inhibitors of T Cell Activation. *J Immunol* (2010) 184:3514–25. doi: 10.4049/jimmunol.0900416
14. Malcherek G, Mayr L, Roda-Navarro P, Rhodes D, Miller N, Trowsdale J. The B7 Homolog Butyrophilin BTN2A1 Is a Novel Ligand for DC-SIGN. *J Immunol* (2007) 179:3804–11. doi: 10.4049/jimmunol.179.6.3804
15. Jeong J, Rao AU, Xu J, Ogg SL, Hathout Y, Fenselau C, et al. The PRY/SPRY/B30.2 Domain of Butyrophilin 1A1 (BTN1A1) Binds to Xanthine Oxidoreductase: Implications for the Function of BTN1A1 in the Mammary Gland and Other Tissues. *J Biol Chem* (2009) 284:22444–56. doi: 10.1074/jbc.M109.020446
16. Wang H, Henry O, Distefano MD, Wang YC, Raikkonen J, Monkkonen J, et al. Butyrophilin 3A1 Plays an Essential Role in Prenyl Pyrophosphate Stimulation of Human Vgamma2Vdelta2 T Cells. *J Immunol* (2013) 191:1029–42. doi: 10.4049/jimmunol.1300658
17. Sandstrom A, Peigne CM, Leger A, Crooks JE, Konczak F, Gesnel MC, et al. The Intracellular B30.2 Domain of Butyrophilin 3A1 Binds Phosphoantigens to Mediate Activation of Human Vgamma9Vdelta2 T Cells. *Immunity* (2014) 40:490–500. doi: 10.1016/j.immuni.2014.03.003
18. Arnett HA, Viney JL. Immune Modulation by Butyrophilins. *Nat Rev Immunol* (2014) 14:559–69. doi: 10.1038/nri3715
19. Viken MK, Blomhoff A, Olsson M, Akselsen HE, Pociot F, Nerup J, et al. Reproducible Association With Type 1 Diabetes in the Extended Class I Region of the Major Histocompatibility Complex. *Genes Immun* (2009) 10:323–33. doi: 10.1038/gene.2009.13
20. Cubillos-Ruiz JR, Martinez D, Scarlett UK, Rutkowski MR, Nesbeth YC, Camposeco-Jacobs AL, et al. CD277 Is a Negative Co-Stimulatory Molecule Universally Expressed by Ovarian Cancer Microenvironmental Cells. *Oncotarget* (2010) 1:329–38. doi: 10.18632/oncotarget.165
21. Ammann JU, Cooke A, Trowsdale J. Butyrophilin Btn2a2 Inhibits TCR Activation and Phosphatidylinositol 3-Kinase/Akt Pathway Signaling and Induces Foxp3 Expression in T Lymphocytes. *J Immunol* (2013) 190:5030–6. doi: 10.4049/jimmunol.1203325
22. Sarter K, Leimgruber E, Gobet F, Agrawal V, Dunand-Sauthier I, Barras E, et al. Btn2a2, a T Cell Immunomodulatory Molecule Coregulated With MHC Class II Genes. *J Exp Med* (2016) 213:177–87. doi: 10.1084/jem.20150435
23. Takayanagi H, Ogasawara K, Hida S, Chiba T, Murata S, Sato K, et al. T-Cell-Mediated Regulation of Osteoclastogenesis by Signalling Cross-Talk Between RANKL and IFN-Gamma. *Nature* (2000) 408:600–5. doi: 10.1038/35046102
24. Sato K, Suematsu A, Okamoto K, Yamaguchi A, Morishita Y, Kadono Y, et al. Th17 Functions as an Osteoclastogenic Helper T Cell Subset That Links T Cell Activation and Bone Destruction. *J Exp Med* (2006) 203:2673–82. doi: 10.1084/jem.20061775
25. Ciucci T, Ibanez L, Boucoiran A, Birgy-Barelli E, Pene J, Abou-Ezzi G, et al. Bone Marrow Th17 Tnfalpha Cells Induce Osteoclast Differentiation, and Link Bone Destruction to IBD. *Gut* (2015) 64:1072–81. doi: 10.1136/gutjnl-2014-306947
26. Bozec A, Zaiss MM. T Regulatory Cells in Bone Remodelling. *Curr Osteoporos Rep* (2017) 15:121–5. doi: 10.1007/s11914-017-0356-1
27. Zaiss MM, Frey B, Hess A, Zwerina J, Luther J, Nimmerjahn F, et al. Regulatory T Cells Protect From Local and Systemic Bone Destruction in Arthritis. *J Immunol* (2010) 184:7238–46. doi: 10.4049/jimmunol.0903841
28. Hikosaka Y, Nitta T, Ohigashi I, Yano K, Ishimaru N, Hayashi Y, et al. The Cytokine RANKL Produced by Positively Selected Thymocytes Fosters Medullary Thymic Epithelial Cells That Express Autoimmune Regulator. *Immunity* (2008) 29:438–50. doi: 10.1016/j.immuni.2008.06.018
29. Mueller CG, Hess E. Emerging Functions of RANKL in Lymphoid Tissues. *Front Immunol* (2012) 3:261. doi: 10.3389/fimmu.2012.00261
30. Nagashima K, Sawa S, Nitta T, Tsutsumi M, Okamura T, Penninger JM, et al. Identification of Subepithelial Mesenchymal Cells That Induce Iga and Diversify Gut Microbiota. *Nat Immunol* (2017) 18:675–82. doi: 10.1038/ni.3732
31. Steffen U, Andes FT, Schett G. Generation and Analysis of Human and Murine Osteoclasts. *Curr Protoc Immunol* (2019) 125:e74. doi: 10.1002/cpim.74
32. Lee WC, Ji X, Nissim I, Long F. Malic Enzyme Couples Mitochondria With Aerobic Glycolysis in Osteoblasts. *Cell Rep* (2020) 32:108108. doi: 10.1016/j.celrep.2020.108108
33. Patro R, Duggal G, Love MI, Irizarry RA, Kingsford C. Salmon Provides Fast and Bias-Aware Quantification of Transcript Expression. *Nat Methods* (2017) 14:417–9. doi: 10.1038/nmeth.4197
34. Love MI, Huber W, Anders S. Moderated Estimation of Fold Change and Dispersion for RNA-Seq Data With Deseq2. *Genome Biol* (2014) 15:550. doi: 10.1186/s13059-014-0550-8
35. Boyce BF, Xing L. Biology of RANK, RANKL, and Osteoprotegerin. *Arthritis Res Ther* (2007) 9 Suppl 1:S1. doi: 10.1186/ar2165
36. Yasuda H, Shima N, Nakagawa N, Yamaguchi K, Kinosaki M, Mochizuki S, et al. Osteoclast Differentiation Factor Is a Ligand for Osteoprotegerin/Osteoclastogenesis-Inhibitory Factor and is Identical to TRANCE/RANKL. *Proc Natl Acad Sci USA* (1998) 95:3597–602. doi: 10.1073/pnas.95.7.3597
37. Dougall WC, Glaccum M, Charrier K, Rohrbach K, Brasel K, De Smedt T, et al. RANK is Essential for Osteoclast and Lymph Node Development. *Genes Dev* (1999) 13:2412–24. doi: 10.1101/gad.13.18.2412
38. Felix R, Cecchini MG, Hofstetter W, Elford PR, Stutzer A, Fleisch H. Impairment of Macrophage Colony-Stimulating Factor Production and Lack of Resident Bone Marrow Macrophages in the Osteopetrotic Op/Op Mouse. *J Bone Miner Res* (1990) 5:781–9. doi: 10.1002/jbmr.5650050716
39. Grigoriadis AE, Wang ZQ, Cecchini MG, Hofstetter W, Felix R, Fleisch HA, et al. C-Fos: A Key Regulator of Osteoclast-Macrophage Lineage Determination and Bone Remodeling. *Science* (1994) 266:443–8. doi: 10.1126/science.7939685
40. Iotsova V, Caamano J, Loy J, Yang Y, Lewin A, Bravo R. Osteopetrosis in Mice Lacking NF-KappaB1 and NF-KappaB2. *Nat Med* (1997) 3:1285–9. doi: 10.1038/nm1197-1285
41. Tondravi MM, McKercher SR, Anderson K, Erdmann JM, Quiroz M, Maki R, et al. Osteopetrosis in Mice Lacking Haematopoietic Transcription Factor PU.1. *Nature* (1997) 386:81–4. doi: 10.1038/386081a0

42. Oursler MJ. Recent Advances in Understanding the Mechanisms of Osteoclast Precursor Fusion. *J Cell Biochem* (2010) 110:1058–62. doi: 10.1002/jcb.22640
43. Zaidi M. Skeletal Remodeling in Health and Disease. *Nat Med* (2007) 13:791–801. doi: 10.1038/nm1593
44. Wong BR, Josien R, Lee SY, Vologodskaia M, Steinman RM, Choi Y. The TRAF Family of Signal Transducers Mediates NF-Kappab Activation by the TRANCE Receptor. *J Biol Chem* (1998) 273:28355–9. doi: 10.1074/jbc.273.43.28355
45. Giachelli CM, Steitz S. Osteopontin: A Versatile Regulator of Inflammation and Biomineralization. *Matrix Biol* (2000) 19:615–22. doi: 10.1016/S0945-053X(00)00108-6
46. Rittling SR, Matsumoto HN, McKee MD, Nanci A, An XR, Novick KE, et al. Mice Lacking Osteopontin Show Normal Development and Bone Structure But Display Altered Osteoclast Formation in Vitro. *J Bone Miner Res* (1998) 13:1101–11. doi: 10.1359/jbmr.1998.13.7.1101
47. Hayman AR. Tartrate-Resistant Acid Phosphatase (TRAP) and the Osteoclast/Immune Cell Dichotomy. *Autoimmunity* (2008) 41:218–23. doi: 10.1080/08916930701694667
48. Kirstein B, Chambers TJ, Fuller K. Secretion of Tartrate-Resistant Acid Phosphatase by Osteoclasts Correlates With Resorptive Behavior. *J Cell Biochem* (2006) 98:1085–94. doi: 10.1002/jcb.20835
49. Zaidi M, Troen B, Moonga BS, Abe E, Cathepsin K. Osteoclastic Resorption, and Osteoporosis Therapy. *J Bone Miner Res* (2001) 16:1747–9. doi: 10.1359/jbmr.2001.16.10.1747
50. Corisdeo S, Gyda M, Zaidi M, Moonga BS, Troen BR. New Insights Into the Regulation of Cathepsin K Gene Expression by Osteoprotegerin Ligand. *Biochem Biophys Res Commun* (2001) 285:335–9. doi: 10.1006/bbrc.2001.5127
51. Yagi M, Miyamoto T, Sawatani Y, Iwamoto K, Hosogane N, Fujita N, et al. DC-STAMP is Essential for Cell-Cell Fusion in Osteoclasts and Foreign Body Giant Cells. *J Exp Med* (2005) 202:345–51. doi: 10.1084/jem.20050645
52. Ishii M, Iwai K, Koike M, Ohshima S, Kudo-Tanaka E, Ishii T, et al. RANKL-Induced Expression of Tetraspanin CD9 in Lipid Raft Membrane Microdomain is Essential for Cell Fusion During Osteoclastogenesis. *J Bone Miner Res* (2006) 21:965–76. doi: 10.1359/jbmr.060308
53. Lee SH, Rho J, Jeong D, Sul JY, Kim T, Kim N, et al. V-Atpase V0 Subunit D2-Deficient Mice Exhibit Impaired Osteoclast Fusion and Increased Bone Formation. *Nat Med* (2006) 12:1403–9. doi: 10.1038/nm1514
54. Tiedemann K, Le Nihouannen D, Fong JE, Hussein O, Barralet JE, Komarova SV. Regulation of Osteoclast Growth and Fusion by mTOR/Raptor and mTOR/Rictor/Akt. *Front Cell Dev Biol* (2017) 5:54. doi: 10.3389/fcell.2017.00054
55. Bozec A, Bakiri L, Hoebertz A, Eferl R, Schilling AF, Komnenovic V, et al. Osteoclast Size Is Controlled by Fra-2 Through LIF/LIF-Receptor Signalling and Hypoxia. *Nature* (2008) 454:221–5. doi: 10.1038/nature07019
56. McDonald MM, Khoo WH, Ng PY, Xiao Y, Zamerli J, Thatcher P, et al. Osteoclasts Recycle *via* Osteomorphs During RANKL-Stimulated Bone Resorption. *Cell* (2021) 184:1330–47.e13. doi: 10.1016/j.cell.2021.02.002
57. Jacome-Galarza CE, Percin GI, Muller JT, Mass E, Lazarov T, Eitler J, et al. Developmental Origin, Functional Maintenance and Genetic Rescue of Osteoclasts. *Nature* (2019) 568:541–5. doi: 10.1038/s41586-019-1105-7
58. Horwood NJ, Kartsogiannis V, Quinn JM, Romas E, Martin TJ, Gillespie MT. Activated T Lymphocytes Support Osteoclast Formation In Vitro. *Biochem Biophys Res Commun* (1999) 265:144–50. doi: 10.1006/bbrc.1999.1623
59. Kong YY, Feige U, Sarosi I, Bolon B, Tafuri A, Morony S, et al. Activated T Cells Regulate Bone Loss and Joint Destruction in Adjuvant Arthritis Through Osteoprotegerin Ligand. *Nature* (1999) 402:304–9. doi: 10.1038/46303
60. Zaiss MM, Axmann R, Zwerina J, Polzer K, Guckel E, Skapenko A, et al. Treg Cells Suppress Osteoclast Formation: A New Link Between the Immune System and Bone. *Arthritis Rheum* (2007) 56:4104–12. doi: 10.1002/art.23138
61. Zaiss MM, Sarter K, Hess A, Engelke K, Bohm C, Nimmerjahn F, et al. Increased Bone Density and Resistance to Ovariectomy-Induced Bone Loss in Foxp3-Transgenic Mice Based on Impaired Osteoclast Differentiation. *Arthritis Rheum* (2010) 62:2328–38. doi: 10.1002/art.27535
62. Omata Y, Frech M, Lucas S, Primbs T, Knipfer L, Wirtz S, et al. Type 2 Innate Lymphoid Cells Inhibit the Differentiation of Osteoclasts and Protect From Ovariectomy-Induced Bone Loss. *Bone* (2020) 136:115335. doi: 10.1016/j.bone.2020.115335
63. Omata Y, Frech M, Primbs T, Lucas S, Andreev D, Scholtysek C, et al. Group 2 Innate Lymphoid Cells Attenuate Inflammatory Arthritis and Protect From Bone Destruction in Mice. *Cell Rep* (2018) 24:169–80. doi: 10.1016/j.celrep.2018.06.005

Conflict of Interest: The authors declare that the research was conducted in the absence of any commercial or financial relationships that could be construed as a potential conflict of interest.

frontiers in Immunology

REVIEW
published: 05 August 2021
doi: 10.3389/fimmu.2021.687037

Immunoporosis: Role of Innate Immune Cells in Osteoporosis

Yogesh Saxena[†], *Sanjeev Routh*[†] *and Arunika Mukhopadhaya*[*]

Department of Biological Sciences, Indian Institute of Science Education and Research Mohali, Mohali, India

Osteoporosis or porous bone disorder is the result of an imbalance in an otherwise highly balanced physiological process known as 'bone remodeling'. The immune system is intricately involved in bone physiology as well as pathologies. Inflammatory diseases are often correlated with osteoporosis. Inflammatory mediators such as reactive oxygen species (ROS), and pro-inflammatory cytokines and chemokines directly or indirectly act on the bone cells and play a role in the pathogenesis of osteoporosis. Recently, Srivastava et al. (Srivastava RK, Dar HY, Mishra PK. Immunoporosis: Immunology of Osteoporosis-Role of T Cells. Frontiers in immunology. 2018;9:657) have coined the term "immunoporosis" to emphasize the role of immune cells in the pathology of osteoporosis. Accumulated pieces of evidence suggest both innate and adaptive immune cells contribute to osteoporosis. However, innate cells are the major effectors of inflammation. They sense various triggers to inflammation such as pathogen-associated molecular patterns (PAMPs), damage-associated molecular patterns (DAMPs), cellular stress, *etc.*, thus producing pro-inflammatory mediators that play a critical role in the pathogenesis of osteoporosis. In this review, we have discussed the role of the innate immune cells in great detail and divided these cells into different sections in a systemic manner. In the beginning, we talked about cells of the myeloid lineage, including macrophages, monocytes, and dendritic cells. This group of cells explicitly influences the skeletal system by the action of production of pro-inflammatory cytokines and can transdifferentiate into osteoclast. Other cells of the myeloid lineage, such as neutrophils, eosinophils, and mast cells, largely impact osteoporosis *via* the production of pro-inflammatory cytokines. Further, we talked about the cells of the lymphoid lineage, including natural killer cells and innate lymphoid cells, which share innate-like properties and play a role in osteoporosis. In addition to various innate immune cells, we also discussed the impact of classical pro-inflammatory cytokines on osteoporosis. We also highlighted the studies regarding the impact of physiological and metabolic changes in the body, which results in chronic inflammatory conditions such as ageing, ultimately triggering osteoporosis.

Keywords: immunoporosis, inflammation, innate immune cells, proinflammatory cytokines, ROS - reactive oxygen species, osteoporosis

OPEN ACCESS

Edited by:
Rupesh K. Srivastava, All India Institute of Medical Sciences, India

Reviewed by:
Rajeev Aurora, Saint Louis University, United States
Hamid Yousf Dar, Emory University, United States

***Correspondence:**
Arunika Mukhopadhaya
arunika@iisermohali.ac.in

[†]*These authors have contributed equally to this work*

Specialty section:
This article was submitted to Inflammation, a section of the journal Frontiers in Immunology

Received: *28 March 2021*
Accepted: *22 July 2021*
Published: *05 August 2021*

Citation:
Saxena Y, Routh S and Mukhopadhaya A (2021) Immunoporosis: Role of Innate Immune Cells in Osteoporosis. Front. Immunol. 12:687037. doi: 10.3389/fimmu.2021.687037

INTRODUCTION

A typical bone is composed of collagen, matrix proteins, calcium hydroxyapatite crystals, and cellular components. Different cellular components of a bone are osteoblasts (OBs), osteoclasts (OCs), osteocytes (OYs), stromal cells, mesenchymal stem cells (MSCs), hematopoietic stem cells (HSCs), *etc.* Among these, OBs and OCs play a major role in maintenance. OBs are of mesenchymal origin and have bone anabolic activity. They produce type-I collagen, matrix proteins (e.g., osteonectin and osteocalcin) to help calcium deposition in the form of calcium hydroxyapatite crystals. On the other hand, OCs, giant multinucleated cells of HSCs origin, demineralize the bone by releasing substances like hydrochloric acid and proteolytic enzymes, thus keep in check the anabolic activity of OBs (1). The antagonistic activity of OBs and OCs results in continuous formation and resorption of bone, a process called bone remodeling, which is necessary for maintaining calcium levels in the blood. Bone remodeling occurs in several specific spaces in the bone called bone remodeling compartments (BRC) (2). In a healthy bone, the bone homeostasis is regulated by sophisticated coordination among components of BRC's through RANK (receptor activator of nuclear factor-κB), RANKL (ligand for a RANK receptor), and OPG (osteoprotegerin) interactions. OPG is a decoy receptor of RANKL. RANKL secreted by OBs interacts with RANK and triggers differentiation of precursor-osteoclast into bigger multinucleated active OCs. However, to keep bone resorption in check, OBs also secrete OPG, which competitively inhibits RANKL-RANK interaction (1–3). Any imbalance in the homeostasis can lead to bone anomalies such as osteopenia, osteoporosis, osteopetrosis, *etc.* In osteoporosis, there is an increase in the activity of osteoclast, leading to net bone loss (**Figure 1**).

Many different health conditions and medical procedures are correlated with osteoporosis, such as endocrine disorders (e.g., hyperparathyroidism, diabetes, premature menopause and low levels of testosterone and estrogen in men and women respectively, *etc.*), autoimmune disorders (e.g., rheumatoid arthritis or RA, lupus, multiple sclerosis, *etc.*), prostate cancer, thalassemia, liver dysfunction, organ transplant, *etc.* (4). Not only disease conditions, the later phase of life, aging, is also correlated with osteoporosis (1). During aging, epigenetic-metabolic changes in physiology drive chronic inflammation in the body resulting in osteoporosis (5). Hence, a diverse array of factors seems to be involved as the causative agents of osteoporosis. Though initially, it was thought that hormonal imbalance was the leading cause of osteoporosis, later in the 1970s, the role of the immune system first came to light (6, 7). Researchers observed that supernatant from the human PBMCs increased osteoclastic activity in fetal rat bone culture (6). In the past two decades, even more promising reports have emerged indicating firm involvement of immune cells in bone remodeling (8, 9). Age-driven changes in the status of immune cells explain the presence of chronic inflammation resulting in osteoporosis (10). The study of this intricate relationship between the immune system and skeletal system led to the establishment of a new field called "osteoimmunology" (11). Recently, Srivastava et al. have coined the term "immunoporosis" to emphasize the role of immune cells as a cause of osteoporosis (12). Another review by the same group has summarized the role of innate and adaptive immune cells in osteoporosis (13). In this review, we focus on the role of the innate immune cells in osteoporosis in a more detailed manner.

Cells of innate immunity are known to act immediately to various challenges to the body and cause 'inflammation', which has been observed as one of the major triggers of various bone disorders (13–15). According to a recent hypothesis published, inflammatory cell death, 'pyroptosis' of osteoblast, is critical in osteoporosis (16). Various signals that induce inflammation in the body include exogenous signals, such as PAMPs (Pathogen Associated Molecular Patterns) or endogenous signals, DAMPs (Death/Damage Associated Molecular Pattern), which abruptly challenge the immune system and results in acute inflammatory diseases. In addition, metabolic changes, tissue malfunctions or prolonged infections usually result in chronic inflammatory diseases. Therefore, inflammatory mediators produced in such cases play a key role in the co-morbidity of osteoporosis (17–20). 'Focal infection theory' is an old concept that assumes the foci of infection could cause systemic inflammatory diseases (as observed in periodontitis, psoriatic arthritis), resulting in osteoporosis (19, 20).

Innate immune cells are major producers of pro-inflammatory mediators. However, some of them share a common developmental niche with skeletal cells. Various reports suggest that the immune system is highly linked to the skeletal system and actively involved in the manifestation of the disease. In addition to the major producers of pro-inflammatory mediators, macrophages, monocytes, and DCs can act as precursors of osteoclasts (21, 22). Apart from macrophages, monocytes and DCs, other pro-inflammatory innate immune cells of myeloid origin, contribute to osteoporosis are neutrophils, eosinophils and mast cells (23–25). Innate cells of lymphoid lineage, such as NK cells and innate lymphoid cells (ILCs), also contribute to the manifestation of osteoporosis, majorly as producers of pro-inflammatory mediators (26, 27). Among the pro-inflammatory mediators that play a major role in osteoporosis, IL-6, TNF-α, IFN-γ, IL-1β, and ROS are worth mentioning. In this review, we will discuss the role and contribution of different types of innate immune cells and inflammatory mediators in osteoporosis (**Tables 1** and **2**).

CELLS OF THE MYELOID LINEAGE

Macrophages

Macrophages, one of the most potent inflammatory cells also act as the major sentinel cells. They are present in the tissues and can readily sense infection by various pathogens like bacteria, viruses, parasites, *etc.*, and provide a defense to the host system. They have the potential for phagocytosis as well as the induction of inflammatory responses. This ability comes from the presence of a broad range of pattern recognition receptors (PRRs) such as toll-like receptors (TLRs), nod-like receptors (NLRs), *etc.*, as well

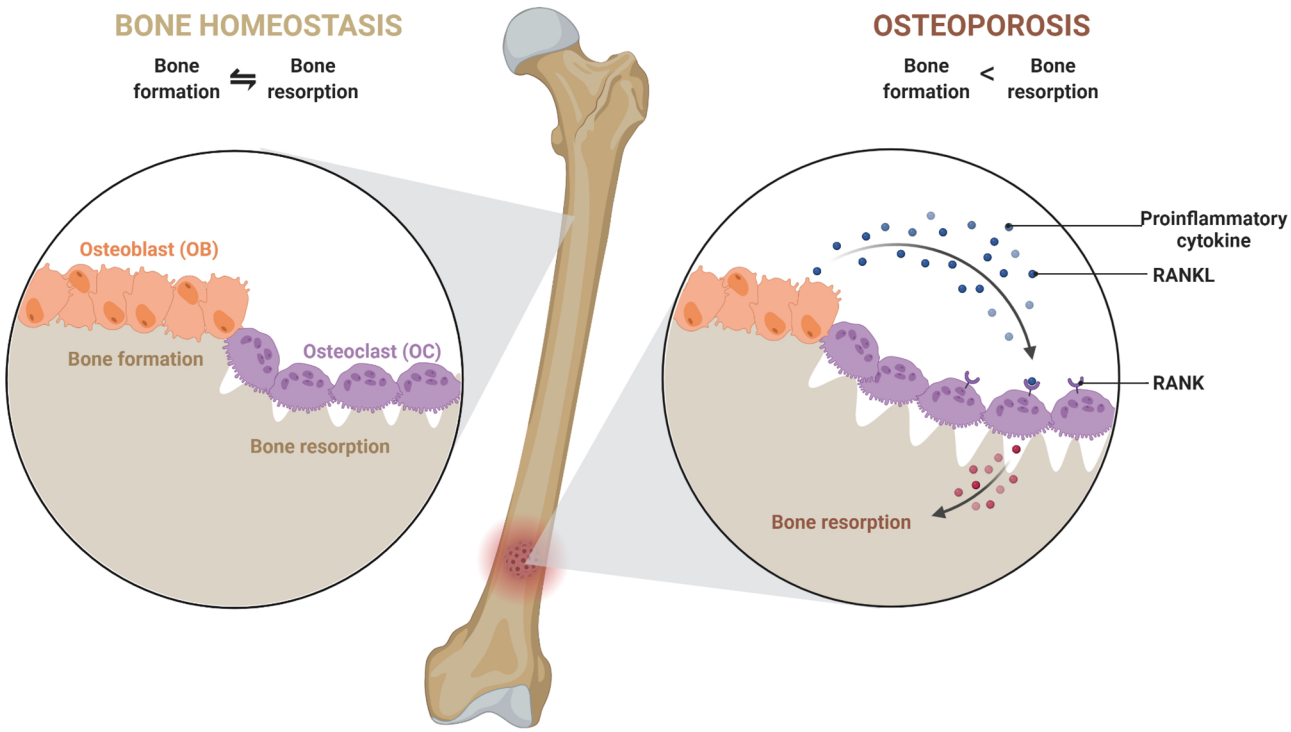

FIGURE 1 | An imbalance in a dynamic equilibrium of bone remodeling leads to osteoporosis. Bone homeostasis is maintained by an equal amount of bone formation, and bone resorption carried out by osteoblast (OB) and osteoclast (OC). Under the influence of various mediators and cellular components, the equilibrium shifts towards greater bone resorption due to exacerbated osteoclast activity. This leads to a decrease in bone mineral density and causes osteoporosis.

as scavenger receptors (SRs) (57). Similar sets of PRRs have been reported to modulate bone metabolism (58–61).

Macrophages are either tissue-resident or differentiated from blood monocytes in response to an inflammatory signal. The tissue-resident macrophages are present in different organs of the body and are known by different names, such as microglia in the brain and kupffer cells in the liver, *etc.* They are adapted uniquely to their location. The bone also possesses different kinds of macrophage populations: bone marrow macrophages (BMMs), OCs, and osteal macrophages or "osteomacs" (62).

TABLE 1 | Function of different innate immune cell types and their role in osteoimmunology.

Cell type	Physiological role	Role in bone biology
Macrophage	Inflammation, phagocytosis, tissue repair	M1 macrophage promotes bone resorption *via* osteoclastogenesis (21, 28); M2 macrophage majorly promotes bone formation by stimulating differentiation of precursor cells into mature OBs (29, 30). However, in the absence of estrogen M2 macrophages can get differentiated in OCs (31). Osteal macrophages help in efficient bone mineralization (32).
Monocyte	Inflammation	Serves as a precursor to OCs, macrophages, and DCs (33). Helps in the recruitment of immune cells to the bone remodeling sites by producing chemokines (34).
Dendritic cell	Inflammation, antigen presentation	Can transdifferentiate to osteoclasts in the inflammatory milieu (35).
Neutrophils	Inflammation, phagocytosis	Promotes bone resorption by increased expression of mRANKL (36).
Eosinophils	Inflammation, allergic response	Found to be increased in number in vitamin D deficiency (37); Source of IL-31 and IL-31 found to be associated in postmenopausal osteoporosis (38)
Mast cell	Allergic response, inflammation	Triggers osteoclastogenesis by producing pro-inflammatory mediators such as, histamine, TNF-α & IL-6 (39, 40).
NK cell	Cellular cytotoxicity, ADCC, inflammation	Promotes osteoclastogenesis by producing RANKL & MCSF (26). Coculture with monocyte in the presence of IL-15 also promotes osteoclast formation (26).
ILCs	Tissue homeostasis, regulation of innate and adaptive immunity	Different subtypes of ILCs produce various factors like RANKL, GMCSF, IL-17 which are involved in multiple bone disorders (27, 41, 42).

TABLE 2 | The role of classical pro-inflammatory cytokines in osteoimmunology.

Pro-inflammatory cytokines	Cellular sources	Role in bone biology
IL-6	OBs, OCs, Stromal cells, OYs, DCs, ILCs Macrophages, *etc.*	RANK-L mediated OCs activation, OCs transmigration (43, 44)
TNF-α	Osteoblast, T cells, B cells, macrophages, monocytes, NK cells, *etc.*	Increases RANK expression on the macrophage (45), increases RANKL production by the stromal cell (45), induces sclerostin in OYs (46), expand OCP pool (47), inhibiting differentiation, proliferation, and activities of osteoblast (48–50), degradation of osterix (48), inhibits differentiation of MSCs (50)
IFN-γ	T cells, NK cells, B cells, ILC1, Neutrophils, Monocytes, Macrophages, MSCs, *etc.*	Fusion of OCs, T cell activation (51)
IL-1β	Osteoblast, T cells, B cells, Macrophages, *etc.*	OCs migration and activation (52–54) Plasminogen cathepsin-B and collagenase secretion (55), Downregulation ALP (56)

Osteal macrophages help in efficient osteoblast mineralization and bone formation (32). Depletion of osteal macrophages shows a decrease in bone mineral density (BMD) (32).

Different tissue microenvironment defines different phenotypes for tissue-resident as well as monocyte-derived macrophages. In addition to inflammation macrophage helps in tissue repair following injury and also maintains tissue homeostasis. To aid these activities (63), they show a great degree of plasticity and hence can undergo a transition between M1 and M2 phenotype depending on the microenvironment (64). M1 is classically activated macrophages (inflammatory phenotype), and M2 is alternatively activated macrophages (reparative phenotype). Macrophage polarization drives bone remodeling activities. Pro-inflammatory cytokines such as, TNF-α and IL-6 can stimulate M1 polarization, whereas anti-inflammatory cytokines such as, IL-4 and IL-13 can stimulate M2 polarization (65), which are generally associated with bone catabolic and anabolic activities, respectively. However, an exciting study by Huang et al. reported that RANKL-induced M1 polarized macrophages display distinct properties compared to LPS and IFN-γ stimulated M1 macrophages (66). In a pathological scenario, it was observed that RANKL-induced M1 macrophages induce bone formation and help in increasing the osteogenic ability of MSC by increasing the expression of osteogenic genes such as *OPN, RUNX2*, *etc.*, while LPS and IFN-γ induced M1 macrophages shows bone destructive activity (66).

Numerous studies suggested a role of M2 macrophages in osteogenesis. Two groups have demonstrated that M2 polarized macrophages can stimulate MSCs, the precursor of OB cells, into mature OBs and increase bone mineralization *in vitro* (29, 30). Further, it has been observed that the co-culture of pre-osteoblastic cells with macrophage increased the osteogenic ability of pro-osteoblastic cells, and this attribute was enhanced by macrophage transition from M1 to M2 type (67). Based on this observation, it was suggested that a transient inflammatory phase is crucial for enhanced bone formation.

M1 macrophage serves as a precursor of osteoclast (28). Researchers had observed that the osteo-inductive mediators, such as bone morphogenetic protein (BMP) 2 and 6, were reduced when macrophages were stimulated by a known M1-phenotype inducer (68). M1 inducer, such as LPS induces a massive production of pro-inflammatory cytokines and triggers osteoclastogenesis in RANKL-dependent or -independent manner leading to bone destruction (**Figure 2A**) (21). Multinucleation of macrophages is driven by RANKL-dependent or -independent signaling pathways that bring about the changes essential for multinucleated osteoclast differentiation and formation (68–70). One of the necessary and key changes observed in macrophage to osteoclast differentiation is the changes in energy metabolism. A report using RAW 264.7 murine macrophage cell line and bone marrow-derived macrophages (BMDMs) suggested that lysine promotes M1 & M2 activation, whereas tyrosine and phenylalanine have opposite effects (71). Another report indicated that differentiated osteoclasts are rich in lysine degrading proteins and show enhanced biosynthesis of tyrosine and phenylalanine (72). These two reports suggested that inhibition of polarization of macrophage enhances osteoclast differentiation. Additionally, there is an increase in mitochondrial biogenesis in RANKL-induced osteoclastogenesis (73). Consequently, the increase in oxidative phosphorylation allows increasing bone resorption by osteoclasts. In another report, it is observed that there is an increase in GLUT1 and other glycolytic enzymes during osteoclast differentiation (73). Both glycolysis and oxidative phosphorylation thus play an important role in osteoclastogenesis. Recent evidence suggested that glucose transporter expression depends on RANKL (74). It explains why macrophage to osteoclast differentiation and bone resorption is associated with an increase in energy metabolism (75).

A study suggested that, M1/M2 macrophage ratio increases in the bone-marrow of ovariectomized (OVX) osteoporotic mice. In the absence of estrogen, M2 macrophages differentiate into osteoclast upon stimulation with RANKL (**Figure 2A**) (31). Thus, estrogen protects M2 macrophages from RANKL stimulation. Therefore, M1/M2 ratio and estrogen are related to the pathogenesis of postmenopausal osteoporosis.

It is well accepted that macrophages play an essential role in the pathogenesis of inflammatory disease rheumatoid arthritis (RA) by producing pro-inflammatory cytokines like TNF-α, IL-1β, IL-6 that can drive osteoclastogenesis and bone destruction. Similar contributions by macrophages were also observed in osteoarthritis (OA) and peri-implant osteolysis (76). The role of macrophages in RA and OA has been elaborately discussed in other reviews (77, 78).

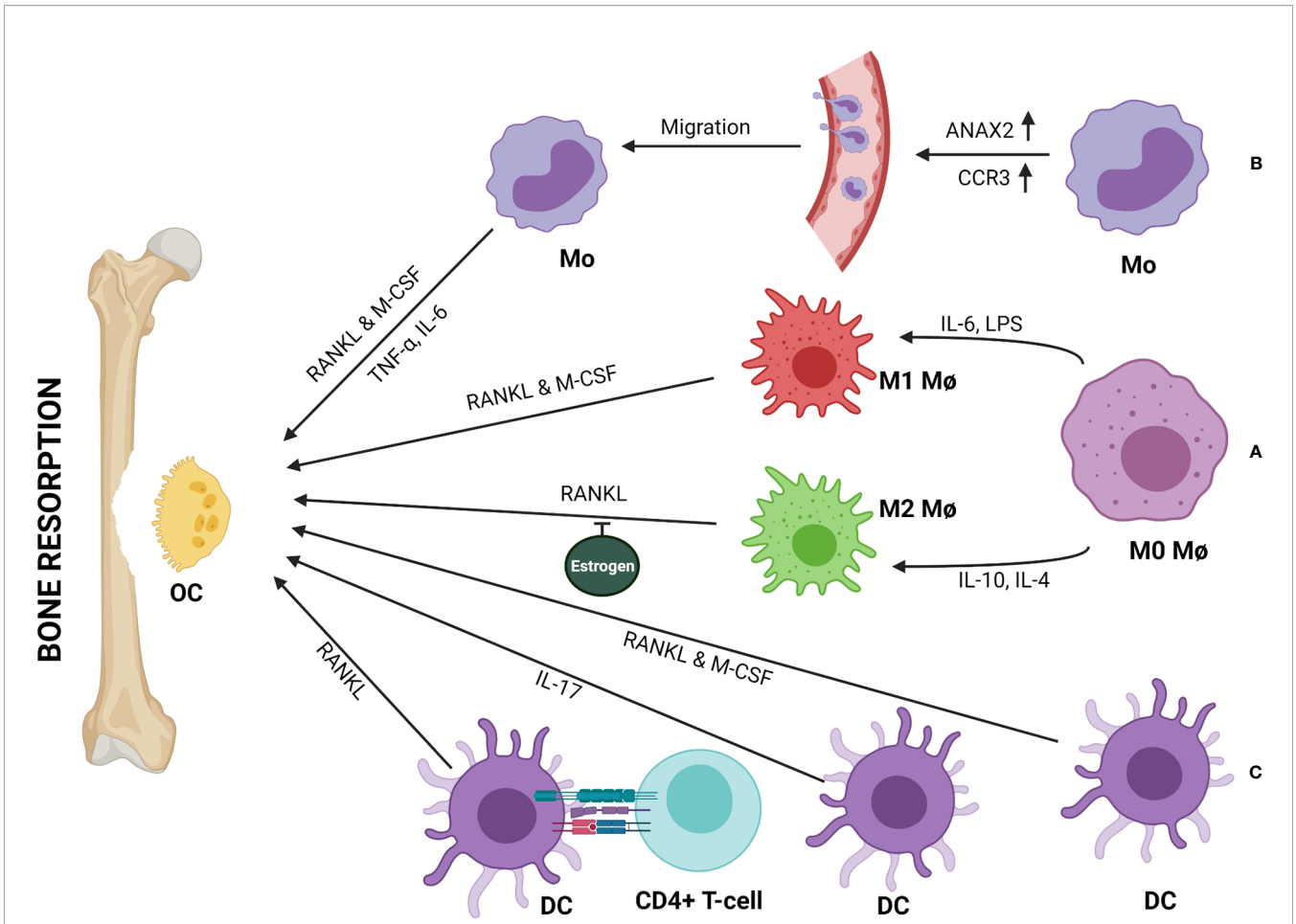

FIGURE 2 | Monocytes (Mo), macrophages (Mφ), and dendritic cells (DCs) can be directly involved in bone resorption by differentiating into osteoclast (OC). **(A)** Both M1 and M2 subtypes of Mφ differentiate into OCs in presence of RANKL & M-CSF or RANKL respectively. Estrogen inhibits RANKL-mediated M2 differentiation to OCs. **(B)** Upregulation of ANAX2 & CCR3 help circulating Mo in trans-endothelial migration and recruitment to the bone remodeling site, where Mo to OC differentiation happens either in the presence of RANKL & M-CSF or TNF-α and IL-6. **(C)** DCs can transdifferentiate into OCs in presence of RANKL & M-CSF or IL-17. Further, immune interaction between CD4+ T-cells and DCs can form OCs in a RANKL/RANK-dependent manner.

Inhibitor studies have helped to elucidate the signaling pathways involved in the RANKL-mediated osteoclastogenesis. Researchers have observed that a Chinese herb, Bergapten inhibits RANKL-induced osteoclastogenesis by suppressing the degradation of IκBα (inhibitor of NF-κB) (79). IκBα keep NF-κB in the cytoplasm by binding to it; degradation of IκB is necessary for translocation of NF-κB to the nucleus and perform its functions. Researchers have also observed that Bergapten attenuates JNK phosphorylation (79). Icariin (ICA) inhibits RANKL-induced osteoclast formation by downregulating signaling mediator TRAF6 (adaptor molecule associated with RANK complex) and further affecting the NF-κB pathway (80). Additionally, it was also observed that ICA inhibits ERK phosphorylation which subsequently leads to a decrease in NFATc expression, which is also a crucial transcription factor for osteoclastogenesis (80). Sappanone A was shown to inhibit RANKL-induced osteoclastogenesis by inhibiting the phosphorylation of AKT and subsequently suppressing the activation of NFATc1 and other osteoclastogenic markers (81). It is interesting to note that RANKL stimulation induces activation of all the three major MAPKs (ERK, JNK, p38); however, only the p38 signaling pathway plays a crucial role in RANKL-mediated differentiation of macrophage to OCs (82). So far no natural inhibitors have been found to inhibit p38 signaling pathway in osteoclastogenesis.

(82, 84)With aging macrophages show an array of dysfunction, including defect in autophagy, morphological changes, and dysregulation of pro-inflammatory cytokine production resulting in age-related altered immune function (10, 83). A study shows significant increase in M1-polarised macrophages in aged mice (84). Aged macrophage shows amplified production of inflammatory mediators (85, 86). Therefore, in macrophage from older people displays an activated phenotype and increased basal level inflammation (86). It is also reported that macrophage polarization dysfunction is related to impaired bone healing in aged mice

and rat populations (86–88). Altogether, macrophage dysregulation contributes to a chronic low-grade inflammation during aging, called Inflammaging, which often correlates with osteoporosis.

Apart from inflammatory responses, recent studies have recognized new regulatory mechanisms of macrophages in osteoporosis. A microarray study on RANKL and CSF1 treated *vs.* non-treated BMMs identified differentially expressed circular RNAs (circRNAs) and found that circRNA_28313 was significantly induced in treated cells. Further, it was observed that knockdown of circRNA_28313 significantly inhibited macrophage differentiation to OCs *in vitro* and OVX-induced bone resorption *in vivo* in mice. Bioinformatic analyses revealed that mir-195a microRNA interacts with 3'UTR of CSF1 in non-treated cells (89). However, circRNA_28313 relieves miR-195a-mediated suppression on CSF1 *via* acting as a competing endogenous RNA (ceRNA), modulating the osteoclast differentiation in BMM cells (89). Another miRNA, miR-128, regulates osteoclastogenesis of BMMs through miR-128/SIRT1/NF-kB signaling axis (90). The overexpression or inhibition of miR-128 can increase or decrease macrophage-derived OCs (90). Further reports suggested that miR-506-3p can selectively inhibit NFATc1 in RANKL-induced activated BMMs in rats and minimize the release of bone resorption enzymes (91). The heterogeneity and plasticity of macrophages make them a critical player in bone homeostasis. A more in-depth study is required to understand the role of macrophages in immunoporosis. Modulation of macrophage phenotype could be a potential therapeutic target in dealing with osteoporosis.

Monocytes

Monocytes constitute 10% of total leukocytes in humans and 2-4% in mice (92). The precursors of monocyte arise from HSC in the bone marrow and finally undergo subsequent differentiation to become a committed monocyte progenitor (cMoP) (92). Similar to macrophages, monocytes also exist as different subsets exhibiting different phenotypes and functions. Different subsets of monocyte show distinct functions during steady-state and inflammation. The inflammatory monocytes show high levels of C-C chemokine receptor 2 (CCR2) and low levels of CXC3 chemokine receptor 1 (CX3CR1), whereas the patrolling monocytes show the reverse expression (93). Their recruitment to the inflammatory site is predominantly CCR2 dependent (94). Traditionally, it is considered that monocyte extravasate from blood vessels to the site of inflammation and differentiates into macrophages or dendritic cells, and contributes to the inflammatory process and repair (95). However, a study demonstrated that CCR2-expressing pro-inflammatory monocyte transitioned into CX3CR1-expressing reparative monocyte (96). However, Jakubzick et al., in their study, reported that monocytes can retain their markers or their identity without differentiating into macrophages and DCs while moving through tissues (97). These studies suggest that the monocyte can participate in the inflammatory process directly apart from acting as precursors only. Accordingly, circulating monocyte plays some crucial role by serving as osteoclast precursor and participating in bone remodeling by producing cytokines (33, 34). Recent reports indicate that erythromyeloid progenitor-derived monocytes (EMP-monocyte) also contribute to this pool of circulating monocytes apart from major contributor HSCs-monocytes (98–100). Interestingly, EMP-monocytes, which reside in the adult spleen postnatally, transmigrate to the bone marrow where they differentiate into functional OCs along with HSCs derived OCs and helps in bone repair in fracture scenarios (98). Similar to macrophages, monocytes also undergo metabolic changes like, increase in glucose uptake, oxidative phosphorylation etc. during differentiating into osteoclast (101). Different environmental cues drive different metabolic changes and as a result, monocyte responds differently. The three phenotypic forms of circulating monocyte in human peripheral blood are Classical ($CD14^{++}$ $CD16^{-}$), intermediate ($CD14^{++}$ $CD16^{+}$), and non-classical ($CD14^{+}CD16^{++}$), which differentiate into osteoclast with different order of resorbing ability, that is, normal, high, and non-absorbing, respectively (75). Reports suggest that non classical human monocyte expresses respiratory chain metabolism whereas classical monocyte depends on carbohydrate metabolism and primed more towards anaerobic energy production (102).

In an infection scenario, intermediate monocytes take the lead to become high bone absorbing osteoclast and may result in bone weakening (74), indicating monocytes could also play a critical role in bone disorders (75). Researchers have made some observations towards it. The Association of monocyte with post-menopausal osteoporosis in Caucasian women was shown by Zhang et al. (29, 102, 103). Network-based proteomics analysis of peripheral blood monocytes (PBM) showed significant downregulation of proteins encoded by four genes, namely, *LOC654188, PPIA, TAGLN2, YWHAB* whereas, upregulation of proteins encoded by three genes, namely *LMNB1, ANXA2P2, ANXA2*, in extremely low- *versus* high-BMD subjects (103). Proteomics analysis of PBM of low-BMD subjects showed upregulation of the ANXA2 protein (104). Cellular studies revealed that ANXA2 is important in monocyte migration across the endothelial barrier. Thus, the elevation of ANXA2 probably stimulates the higher migration rate of monocyte from blood to the bone tissue and then differentiate to OCs and contribute to bone-resorbing activity (**Figure 2B**) (104).

Additionally, a microarray study on circulating monocytes in humans suggested that three genes, *CCR3* (C-C chemokine receptor type 3), *HDC* (histidine decarboxylase, a histamine synthesis enzyme), and *GCR* (glucocorticoid receptor), might contribute to bone metabolism and homeostasis. These three genes are found to be upregulated in subjects with low BMD (105). These genes mediate monocyte chemotaxis, which can lead to monocyte infiltration in bone tissue, histamine production, which induces local inflammation and can mediate OC formation, and glucocorticoid sensitivity which promotes OC formation (105). *In vivo* gene expression profiling in human monocyte suggested upregulation of STAT1 and IFN pathway genes in low BMD groups (106). Based on additional

observations, the researchers proposed that probably in peripheral blood, IFN-mediated by *STAT1* stimulates circulating monocytes to produce cytokines (such as IL-1, TNF, CXCL10, and IL-15) that increase the bone resorption function of osteoclast. Daswani et al. provided further insight into monocyte proteomics, which revealed the involvement of phosphorylated heat-shock protein 27 (HSP27) in low BMD subjects (107). They have observed elevation of total phosphorylated HSP27 (pHSP27) in monocyte of low BMD subjects and validated that pHSP27, not a chemoattractant itself but acts as an actin reorganizer, facilitating migration (107). As Hsp27 inhibits stress-induced apoptosis, and since osteoclast formation involves ROS generation, the anti-apoptotic activity of pHSP27 may foster monocyte survival and hence more precursor for osteoclastogenesis (107). Transcriptome study identified the downregulation of two apoptosis-inducing genes, death-associated protein 6 (DAXX) and polo-like kinase 3 (PLK3), in low BMD subjects (108). This report supported the fact that due to monocyte survival, more precursors are available to augment osteoclastogenesis and hence osteoporosis.

It was observed that the *SBDS* gene, which is responsible for the disease SDS (Shwachman-Diamond Syndrome showing skeletal defects), plays a role in monocyte migration and fusion before osteoclastogenesis (109). Sbds mutant showed a decrease in Rac2 (GTPase required in cytoskeletal remodeling for migration) and RANKL-mediated DC-STAMP (required for fusion of osteoclast precursor) levels. This fusion defect reduces osteoclastogenesis. Reduced osteoclastogenesis expects osteopetrosis phenotype. Surprisingly, SDS patients show an osteoporotic phenotype. The potential explanation for this phenomenon is that since a reduced number of TRAP-positive multinucleated OCs are still present, there is no complete uncoupling of bone remodeling homeostasis, which probably triggers a shift of MSCs towards adipocyte cell lineage instead of osteoblast. Other observations supporting this phenomenon have been reported earlier by the same group (110).

Dendritic Cells

Dendritic cells are majorly antigen-presenting cells (APCs) endowed with abilities to activate the adaptive immune response. They express high levels of MHC class II and co-stimulatory molecules such as CD80 and CD86 which are required for antigen presentation. DCs are distributed throughout the body and survey for external and internal dangers using a broad range of PRRs such as TLRs, CLRs, NLRs, *etc.* Dendritic cells can be divided into three subgroups: plasmacytoid DCs (pDCs) derived from lymphoid progenitors, classical or conventional DCs (cDCs) derived from both lymphoid or myeloid progenitors, and monocyte-derived DCs (moDCs). pDCs function against viral infections by secreting type I IFNs (111). In addition to pDCs, cDCs and moDCs play a role in providing defense against other microbes.

However, the profound effect of DCs on bone metabolism has been widely recognized recently. DCs contribute to inflammation-mediated osteoclastogenesis and take part in inflammatory bone disease. Using an *in vivo* model, Maitra et al. reported the osteolytic potential of DCs (112). They observed that dendritic cells recruit to bone inflammatory sites and participate in bone resorption (112). In addition, DCs can activate T-cells by acting as APCs, and the activated T-cells produce cytokines and soluble factors that drive bone remodeling (113). It was also observed that DCs directly interact with T-cells to form aggregates which play a role in bone pathologies like synovitis and periodontitis (114, 115). In a recent study, the role of DCs in manifesting osteoporosis in OVX mice was reported (116). Estrogen is known to regulate the number of DCs that express IL-7 and IL-15. In the absence of estrogen, the DCs sustains for long and express more IL-7 and IL-15, which, together, induces a subset of memory T-cell to produce IL-17A and TNF-α in an antigen-independent manner. The cytokines so produced drive inflammation-mediated bone loss (116). There are also reports suggesting a more direct role of DCs in osteoclastogenesis. It has been observed that the DCs can potentially trans-differentiate and fuse to form OCs, and this fusion is faster and efficient than monocyte fusion. There is downregulation in the expression of 3997 genes for differentiation from monocytes to OCs, while there is upregulation in the expression of 3821 genes. However, when immature dendritic cells differentiate into OCs, there is downregulation of only 2107 genes and upregulation of 1966 genes suggesting that DCs are more closely related to osteoclast than monocytes (117). The newly formed OCs can summon more DCs by inducing chemotaxis of DCs, and the OC-DC loop continues to increase bone destruction (117).

Studies showed that DCs can trans-differentiate to OCs in the presence of RANKL and macrophage colony-stimulating factor (M-CSF) (**Figure 2C**) (35, 118). Another study suggested that activated DCs (bone-marrow-derived and splenic $CD11c^+$ cells) upon interaction with T helper-cells ($CD4^+$ T cells or Th) can develop into functional OCs ($TRAP^+CT\text{-}R^+cathepsin\text{-}k^+$) in RANKL/RANK-dependent manner (**Figure 2C**) (119). In a report, Th17 cells were shown to play a role in the trans-differentiation of DC to OCs (120). It has been observed in RA patients that inflammatory milieu can recruit Th17 cells, which produce a huge amount of IL-17 to stimulate RANKL production by bone stromal cells and promotes nuclear fusion of immature DCs *via* IL-17R (IL-17 receptor) (**Figure 2C**) (117). T-cells not only augment trans-differentiation of DCs to OCs but also can inhibit it by producing cytokines like IFN-γ. T-cell-derived IFN-γ can inhibit RANKL signaling by blocking TRAF6 to inhibit osteoclast maturation and activation (8). Hence, T-cells could act as a balance switch in mediating DC-OC trans-differentiation. Moreover, in specific conditions, DCs are known to produce TGF-β which is a potent anti-osteoporotic molecule (121–123). This indicates a potential alternative role of DCs in osteoporosis. A more in-depth study is required to understand the full potential of DCs in the induction of immunoporosis.

Neutrophils

Neutrophils are the polymorphonuclear (PMN) phagocytic cells and the first leukocyte to be recruited at the site of inflammation (124). They make up 40-60% of leukocytes in the human blood. Neutrophils contain different granules, which are a source of

several anti-microbial molecules. They continuously monitor for microbial infections and kill the pathogen by various mechanisms that include phagocytosis, production of ROS, and molecules like granzyme-B and perforins (125, 126). In addition, neutrophils also exhibit a unique strategy of immobilizing and killing microorganisms by extruding a meshwork of chromatin fibers covered with granule-derived antimicrobial peptides and enzymes. These are called neutrophils extracellular traps (NET), and the mode of killing is termed as NETosis (127).

Current research has emphasized the diverse role of neutrophils beyond killing pathogens. Neutrophils respond to different signals in the inflammatory milieu by producing cytokines and chemokines, which can regulate inflammation and other pro-inflammatory cells (128, 129). In contradiction to the old belief as short-lived innate effector cells, recent evidence suggested the role of neutrophils in regulating adaptive immune response (130). Thus, neutrophils interact with both innate and adaptive arms of the immune system and differentially respond depending on the context.

Neutrophils are also involved in the pathophysiology of various diseases, including inflammation-mediated bone loss (131). Moreover, neutrophils can produce chemokines and recruit pro-osteoporotic cells such as Th17 (12, 131). A strong correlation was indicated between an increase in RANKL positive neutrophils with inflammatory disease conditions and a decrease in BMD (23). A report demonstrated that neutrophils from the blood of a healthy individual express membrane-associated RANKL (mRANKL) while RANK expression depends on IL-4 and TNF-α stimulation (**Figure 3A**) (132). Interestingly, it was observed that synovial fluid (SF) neutrophils from RA patients express both mRANKL and RANK and also secrete OPG (131, 132). This observation that inflammatory neutrophils impetuously express RANK whereas healthy blood neutrophils express only after stimulation gives an insight into the involvement of neutrophils in bone remodeling. The evidence of inflammatory neutrophils expressing RANK could be related partly to acquiring a dendritic cell phenotype and further activating T-cells in RA condition (133). A study reported that mRANKL of TLR4-activated neutrophils induce osteoclastic bone resorption (**Figure 3A**) (36). The mRANKL of activated neutrophils act on both OCs and their mononuclear precursors, converting them into mature and functional OCs that contribute to bone resorption. Interestingly, they have demonstrated that the membrane fraction of activated neutrophils can augment the osteoclastogenic effect but not the culture supernatant, suggesting the importance of the involvement of mRANKL (22, 36). Another study reported that there is an increase in RANKL positive neutrophil in the blood of chronic obstructive pulmonary disease (COPD) patients compared to smokers and healthy controls, and it is related to low BMD (24).

Neutrophils can augment bone loss; however, some reports suggested that neutrophils play a to reduce bone loss by maintaining a homeostatic condition. The defective neutrophil recruitment in leukocyte adhesion deficiency type I (LAD-I) disorder results in IL-17 driven inflammatory bone loss (134). There is a defect in the expression or function of β2 integrin or related adhesion molecule in LAD-I disorder. Due to this defect, there is an impairment in neutrophil extravasation to the inflammatory site. The absence of neutrophils results in unrestrained production of IL-23 from macrophages, which in turn triggers IL-17 production from T-cells and can drive IL-17-mediated inflammatory bone loss. Another report supported the role of neutrophils in preventing inflammation-mediated bone loss. Gif1 is a molecule in HSC development, and a defect in *Gif1* causes severe neutropenia (135). This condition can induce osteoporosis depending on pathogen load and systemic inflammation (135). Hence, neutrophils can be a very critical player in the regulation and manifestation of osteoporosis.

Eosinophils

Eosinophils are known to be involved in the pathogenesis of various allergic and inflammatory diseases (136). However, recently reported association of Vitamin D (VD) deficiency with an increased number of blood eosinophils indicates potential role of eosinophils in bone biology. Moreover, VD, which is a well-known osteoprotective molecule, decreases production of IgE as well as, release of peroxidase from eosinophil and while increases the production of the osteoprotective cytokine IL-10 (37, 137, 138). Eosinophils play a role in the manifestation of various inflammatory diseases (138), including chronic obstructive pulmonary disease (COPD), eosinophilic esophagitis (EoE), *etc.* (139, 140). Literature indicates a strong correlation between COPD and osteoporosis (141). However, the reason identified for the co-morbidity of osteoporosis is the use of a steroid-based treatment regime. Steroid-based treatments are frequently used to manage symptoms in COPD and EoE. Although, the role of eosinophils with steroid-induced osteoporosis is under scrutiny and not fully understood yet (141, 142).

Eosinophils carry out allergic responses by producing inflammatory mediators such as ROS, cysteinyl leukotrienes, and various cytokines and chemokines (143). Transcription factors such as NF-κB mounts such allergic inflammatory responses. However, such transcription factors can also induce osteoclastogenesis in an inflammatory condition. Interestingly, eosinophils are the source of IL-31 in an inflammatory skin condition called Bullous pemphigoid (BP) (144). IL-31 is a pro-inflammatory cytokine that serves as a biomarker for allergic disease. It is involved in the regulation of cell proliferation and tissue remodeling (145). It is reported to be involved in the regulation of the transcription factors and cytokines that are associated with osteoporosis. It is also observed that there is an increase in serum IL-31 level in post-menopausal women with a decrease in BMD, correlating with age (38). Association of eosinophil with IL-31 suggests that eosinophil may play a role in the manifestation of osteoporosis in an exacerbated allergic and autoimmune inflammatory disease condition. However, more studies are required to understand the contribution of eosinophil towards osteoporosis.

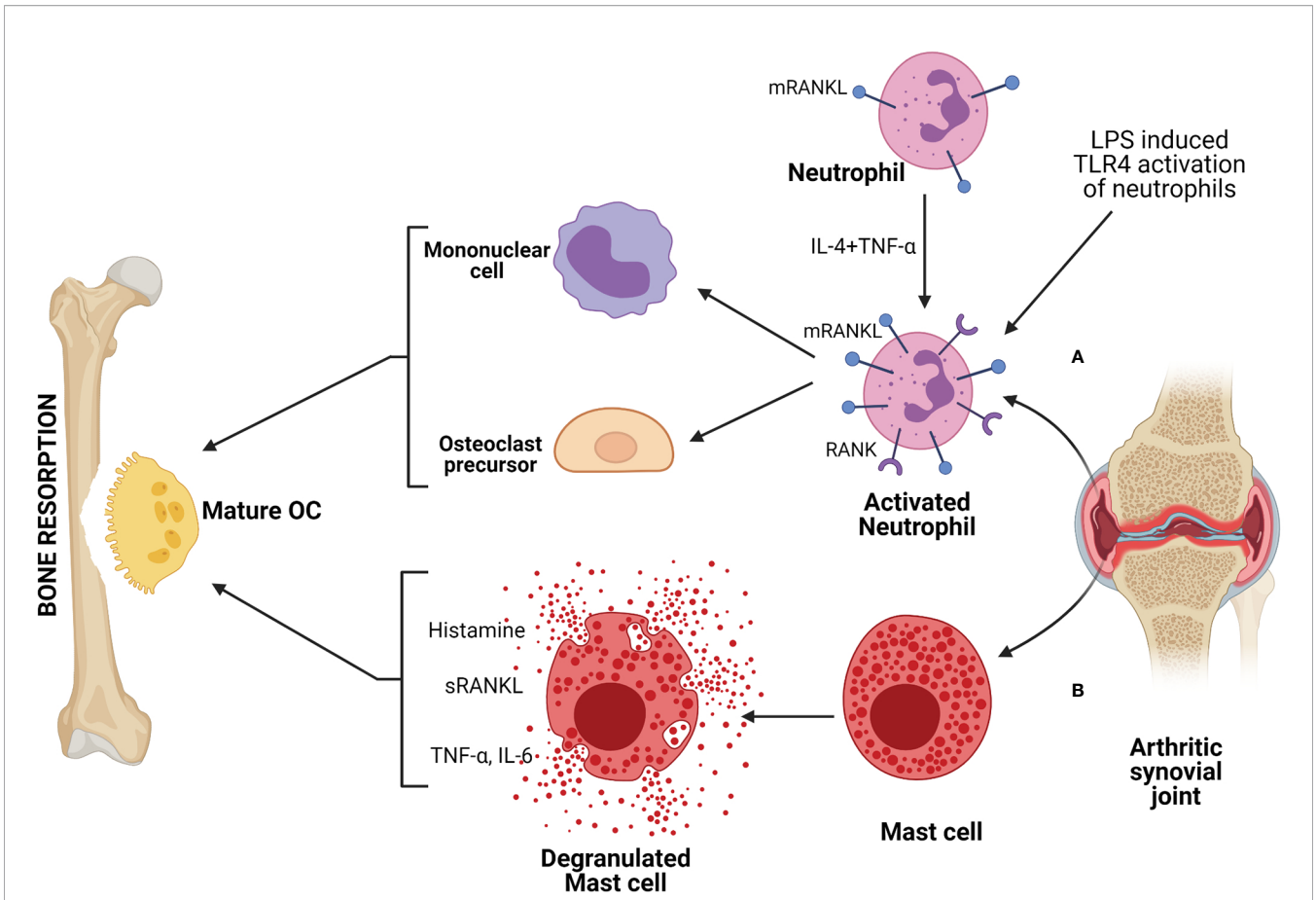

FIGURE 3 | Neutrophils and mast cells are involved in bone resorption by producing factors that can drive osteoclastogenesis. **(A)** Activated neutrophils, either stimulated with TLR agonist or derived from patients with inflammatory disease, such as, from SF (synovial fluid) of RA (rheumatoid arthritis) patient, express higher membrane bound RANKL (mRANKL) and act on OC precursors or mononuclear cells to form mature and functional OCs, resulting in bone resorption. **(B)** Mast cells derived from SF of arthritic patient produces mediators like histamine, TNF-α, IL-6 that drive osteoclastogenesis and further bone resorption.

Mast Cells

Mast cells are the tissue-resident immune cells that originated from pluripotent progenitor cells of bone marrow. Mast cell progenitors migrate into the tissue, where they differentiate and mature (146). Though they are best known for fostering allergic responses, they are also involved in numerous physiological functions and pathophysiology of various diseases (147). Mast cells are the first cells to respond to invading foreign entities as they are present at the tissue boundaries. They can be activated by PAMPs *via* PRRs such as TLRs or complement systems. Mast cells store a wide variety of preformed inflammatory mediators, including histamine, TNF-α, IL-6 as well as proteases in their secretory granules (148). As these inflammatory mediators are known to regulate bone homeostasis and involved in pathogenesis of various bone disorders, mast cells could be a probable candidate associated with bone disorder. Indeed, few reports suggested that there was increase in number of mast cells in the patient with reduced bone density and associated with post-menopausal osteoporosis (149, 150). Experimental evidences suggested that in OVX-induced estrogen depletion there was an increase in numbers of mast cells as well as osteoclasts (151, 152). These observations indicated that mast cells probably promote osteoclast formation in estrogen-deficient conditions. Treatment with calcium and promethazine (a blocker of the histamine H1 receptor) to post-menopausal women helped increase BMD in comparison to calcium alone. The observation that H1 receptor blocking resulted in the termination of osteoclast formation by mast cell supernatant suggested that the histamine, one of the main preformed mediators of mast cell, has a role in the reduction of BMD (153). Other reports indicated that estrogen affects mast cells and the release of its mediators, suggesting estrogen has an inhibitory effect on the osteoclast-inducing potential of mast cells (148). However, there are contradicting reports which indicated that estrogen could induce degranulation of mast cells since estrogen did not stimulate degranulation in ERα (estrogen receptor) knockout mice (154).

Mast cells have been suggested to be involved in the RA disease condition. Similar to other immune cells, mast cells are also abundantly found in inflamed synovial joints of RA patients. Mast cell mediators such as histamine and tryptase were found to be increased in SF (39, 40). Mast cells also contribute to the

inflammatory milieu of SF as activated mast cells can produce mediators like TNF-α, IL-6, etc., which have the ability to induce osteoclastogenesis (**Figure 3B**). Even increased levels of RANKL found in the synovial tissue of RA patients could be contributed by mast cells as activated mast cells secrete RANKL (155). In a mice model of CIA (collagen-induced arthritis), reduction in T-cell numbers (both $CD4^+$ and $CD8^+$) along with reduced IFN-γ and IL-17 were observed upon depletion of mast cells (156). This indicated that mast cells might be involved in regulating T-cell expansion and Th1 and Th17 polarization, which is further involved in T-cell-driven arthritis. Various reports suggested that mast cells also play a role in OA. This could be due to mast cell-driven increased pro-inflammatory responses. An increase in the number of mast cells, as well as histamine or tryptase levels, were observed in SF of OA patients (157–159). It has been observed that in OA, mast cells are activated *via* IgE/FcεRI receptor axis (158). Another report showed that synovial mast cells from OA patients produce TNF-α upon stimulation *via* high-affinity receptor of IgG (160). The link between mast cells and bone was also exemplified by the presence of mast cells during fracture healing. A gradual increase in mast cell numbers was observed in periosteal fracture callus, followed by a decrease during callus remodeling (161). The highest number of mast cells was also found in the vicinity of OCs and bone resorption sites during callus remodeling, indicating that mast cells could be involved in regulating osteoclast activity (162). Further investigation is required to understand the mechanism of action of mast cells in the physiology of bone turnover and bone disorders.

CELLS OF THE LYMPHOID LINEAGE

NK Cells

Natural killer (NK) cells are developed from HSCs in the bone marrow. However, recent evidence suggested that they can also develop and mature in secondary lymphoid tissues (SLTs) and show some adaptive features such as memory generation (163). In the 1970s, NK cells were described as large granular lymphocytes with the ability of "natural cytotoxicity" against various tumor cells. In recent times, it is now appreciated that apart from cytotoxicity against tumor cells, it is also capable of showing cytotoxicity against virus-infected and stressed cells (164, 165). NK cell surveillance system consists of various cell surface activating and inhibitory receptors that help identify and kill target cells (166). Additionally, they can perform antibody-mediated cell cytotoxicity (ADCC), making it a potent effector cell of the humoral response. They also exhibit cytokine-producing effector function. Upon engagement with target cells, they can secrete various pro-inflammatory cytokines and chemokines and, thus, regulate other immune cells' functionality by modulating the local milieu (167). NK cells also play a crucial role in maintaining homeostasis and immunoregulation *via* control of T-cells activity.

Since NK cells are well poised to carry out inflammatory processes and cytotoxicity, they are involved in the manifestation of inflammatory diseases. There are reports which displayed the presence of NK cells in inflamed synovial tissues at an early stage of RA (168, 169). Such NK cells express M-CSF and RANKL, potent activators of osteoclastogenesis (**Figure 4A**). These molecules are further upregulated by IL-15, which is abundantly present in the synovium of RA patients (170). Soderstrom et al. showed that NK cells from SF of RA patients trigger efficient formation OCs from monocyte (**Figure 4A**) (26). They had also demonstrated that OCs formed from monocyte when co-cultured with NK cells were capable of eroding bone in the presence of IL-15 but not in the absence of it (26). In the CIA mice model, many synovial NK cells express RANKL suggesting the role of NK cells in bone erosion, and it was observed that depletion of NK cells prevents bone erosion in CIA.

A study suggested that IL-15 activated NK cells can kill OCs (**Figure 4A**). In the presence of IL-15, it seems that NK cells' action is contradictory to the report mentioned above (171). IL-15 upregulate leucocyte function-associated antigen-1 (LFA-1) and DNAX accessory molecule-1 (DNAM-1) on NK cells. These are ligands of ICAM-1 and CD155 (PVR) receptors, respectively. These receptors are present on OCs, and they are essential for their development, function, and interaction with stromal cells (172). Receptor blocking studies between OCs and NK cells has displayed restoration of bone resorption. Thus, IL-15 activated NK cells kill OC *via* LFA-1 and DNAM-1 (171). Therefore, NK cell-mediated inhibition of osteoclast is contact-dependent, although IL-15-activated NK cells produce soluble factors like IFN-γ that can be anti-osteoclastogenic. Thus, NK cells can control or augment osteoporosis depending on the tissue microenvironment. More in-depth study is required to understand the NK cell-mediated regulation of bone remodeling and osteoporosis.

ILCs

Innate lymphoid-like cells or ILCs are the heterogeneous populations of cells that arise from the lymphoid lineage (173). Although they lack antigen-specific receptors, upon tissue damage or pathogen invasion, they can sense changes in the local milieu by cytokine receptors and modulate subsequent antigen-specific lymphocyte responses. ILCs are mainly tissue-resident cells, especially present at the mucosal surface of the intestine and lungs (174). Based on cytokine signature and transcription factors, ILCs can be divided into four groups: ILC1, ILC2, ILC3, and regulatory ILC (ILCreg). ILC1 functions highly overlap with NK cells as both produce IFN-γ, enhancing the ability of macrophages and DCs to remove intracellular pathogens. ILC2s are the innate counterpart of Th2 cells that produce IL-5 and IL-13 and helps in the expulsion of helminths. Notably, type-2 cytokines produced by ILC2s have tissue repair and anti-inflammatory function post-infection (175, 176). ILC3s are the innate counterpart of Th17 cells as they produce IL-17 and IL-22 in response to IL-1β and IL-23. IL-22 can stimulate the secretion of anti-microbial peptides from intestinal cells and provides a barrier in the intestine, whereas IL-17 induces granulopoiesis (177, 178). IL-17 also drives inflammatory response by recruiting cells to the site of inflammation (179).

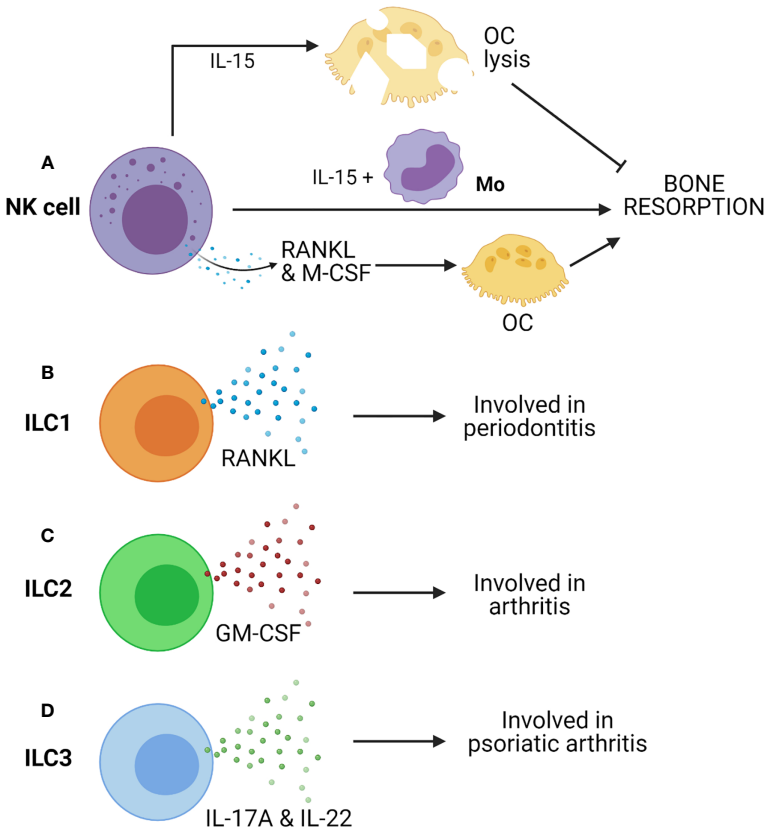

FIGURE 4 | Innate cells from lymphoid lineages, such as Natural killer (NK) cells and Innate lymphoid cells (ILCs) can contribute to bone resorption. **(A)** IL-15 activated NK cells can induce OC lysis and inhibits bone resorption. However, co-culture of NK cells with monocytes (Mo) triggers bone resorption in presence of IL-15. Further, NK cell-mediated production of RANKL & M-CSF can drive osteoclastogenesis. **(B)** ILC1 produces RANKL and is associated with periodontitis. **(C)** ILC2 produces GM-CSF and is associated with arthritis. **(D)** ILC3 produces IL-17A & IL-22 and is associated with psoriatic arthritis.

There are key evidences that suggested the involvement of ILCs in inflammatory bone diseases such as spondylarthritis (SA) (180). It is reported that there is an enrichment in the number of ILC3s in SF of patients with psoriatic arthritis (181). Enrichment of ILC3 is also found in the gut, in the peripheral blood, bone marrow, and SF of patients with ankylosing spondylitis. A recent study has shown that CCR6 positive ILC3s ($ILC3^{CCR6+}$) are enriched in inflamed joints of CIA mice and RA patients and show high IL-17A and IL-22 in arthritic mice (**Figure 4D**) (27). These reports suggested a critical role of ILC3s in the development of all these diseases, probably due to their highly pro-inflammatory nature.

Hirota et al. have reported that GM-CSF-producing ILC2s have a pathogenic role in augmenting arthritis (**Figure 4C**) (41). However, recent studies demonstrated the protective role of ILC2s. They can reduce inflammatory arthritis and prevents bone loss in mice (182). Another study by Omata et al. supported the immune-regulatory role of ILC2s (183). IL-4 and IL-13 secretion from ILC2 trigger STAT6 activation in myeloid cells, resulting in suppression of OC formation, thus preventing OVX-induced bone loss (183). Therefore, ILC2s exert regulatory function on bone homeostasis by impairing osteoclastogenesis. Additionally, ILC2s can have a regulatory effect on bone *via* Treg cells, which are inhibitors of OC formation.

ILC1s are known contributors of IFN-γ and are enriched in many chronic inflammatory diseases. ILC1 is the more predominant ILCs in SF of RA patients (180). ILC1 is the primary subtype of ILCs in gingivitis and periodontitis, and they express RANKL (**Figure 4B**) (42). More descriptive studies on ILC1s expressing RANKL are required to understand their role in bone remodeling.

Recently, a study has recognized a new subset of IL-10 producing ILCs named regulatory ILCs (ILCreg). These are $Lin^{-}CD45^{+}CD127^{+}$ $IL\text{-}10^{+}$ cells and are mostly present in gut tissue (184). In inflammatory conditions, ILCreg can be stimulated in the intestine and acts on other ILCs such as ILC1 and ILC3 to suppress their activation *via* IL-10. Additionally, ILCreg can also produce TGF-β that acts in an autocrine manner for its expansion in inflammatory conditions. Interestingly, IL-10 is a potent anti-inflammatory cytokine that can downregulate the synthesis of pro-inflammatory cytokines such as IL-6, TNF-α, *etc.*, preventing inflammatory-driven osteoclastogenesis and bone resorption (185). Since ILCreg produces IL-10 and suppresses intestinal inflammation, it may also play a role in

suppressing inflammatory bone loss. The role of TGF-β in osteoclastogenesis is very complex and controversial, but TGF-β enhances osteoblast proliferation and survival (186). Thus, TGF-β produced by ILCreg may enhance bone formation. Moreover, detailed studies are required to understand the contribution of ILCreg in the suppression of inflammatory disease conditions such as osteoporosis.

INFLAMMATORY MEDIATORS AND OSTEOPOROSIS

Some of the key pro-inflammatory mediators secreted by innate immune cells are IL-6, TNF-α, IL-1β, ROS, and IFN-γ (1–3, 187, 188).

IL-6 is prominently involved in osteoporosis. An increase in IL-6 in the body induces an increase in osteoclastogenesis *via* the induction of RANKL production from osteoblasts (43). IL-6 upregulates S1PR2 [Sphingosine-1-phosphate (S1P)] receptor on the surface of osteoclast precursor and helps in its transmigration from the bone marrow to the blood and thus play a crucial role in the hallmark systemic bone loss (44). Moreover, two of the inflammatory chemokines CXCL8 and CCL20, enhance osteoblast-induced osteoclastic activity *via* IL-6 production (189).

TNF-α is an important molecule in osteoporotic disorders, especially in post-menopausal osteoporosis (190–193). It acts as pro-osteoporotic either by acting as pro-osteoclastogenic or by impairing osteoblast function. It directly acts on macrophages to increase RANK expression and acts on stromal cells to increase RANKL production (45). TNF-α triggers osteoclastogenesis by synergistically acting with RANKL and M-CSF *via* NF-κB and PI3k/AKT pathway (193). This intensifies the osteoclastic activity by many folds comparing RANKL alone (193). Moreover, another report suggests that TNF-α priming sensitizes M-CSF-induced M2 macrophages to pro-inflammatory M1 macrophage polarization in RelB dependent manner, resulting in expanding osteoclast precursor pool with higher osteoclastic potential (47). TNF-α also induces sclerostin (SOST) expression, which triggers RANKL expression in osteocytes and further enhances osteoclastogenesis (46). Together with IL-6, TNF-α can actively cause osteoclastogenesis independent of RANKL (194).

TNF-α acts as anti-osteogenic by inhibiting differentiation, proliferation, and activities of osteoblast. It upregulates CHIP-ubiquitin ligase protein, which results in the degradation of osterix (pro-osteoblastic transcription factor) (48). TNF-α also inhibits expression of BMP-induced 'special AT-rich sequence binding protein 2' (SATB2), which is another pro-osteoblastic transcription factor, by triggering NF-κB binding to SATB2 promoter (49). Further, TNF-α induces upregulation of purinoreceptor P2Y2 through ERK and JNK signaling pathways and hinder the differentiation of MSCs (48, 50). The Canonical WNT/β-catenin pathway is known to regulate bone homeostasis and development. Both IL-6 and TNF-α hamper the pro-osteoblastic WNT/β-catenin pathway by upregulating its antagonists, Dickkopf-related protein 1 (DKK1) and SOST, which prevent osteoblast differentiation (46, 195).

IFN-γ, a type-II interferon, affects later phases of maturation of osteoclasts. An active osteoclast must fuse to form a functional multinucleated osteoclast. This fusion is aided by a transmembrane protein called DC-STAMP, which is expressed by IFN-γ-induced-transcription factors NFATc1 and c-FOS (51). Moreover, IFN-γ-induced upregulation of MHC-II on APCs helps in T-Cell activation. The activated T-Cells produce more TNF-α and RANKL, which further help in the differentiation and maturation of OCs (51).

IL-1β, another highly pro-inflammatory cytokine, promotes RANKL dependent osteoclast differentiation *via* activation of transcription factors NF-κB and AP-1. IL-1β also increases CCR7, which promotes osteoclast migration and activation (52). IL-1β is a prerequisite for the C5a (complement protein)-induced osteoclast activation (53, 54). IL-1β has also been reported to enhance proteolytic enzymes like plasminogen, collagenases, and cathepsin-B, which break down bone matrix proteins resulting in bone loss (55). In addition, it has also been shown to downregulate osteoblastic activities by inhibiting alkaline phosphatase (ALP), which is required for bone mineralization and collagen synthesis activities *via* modulating STATs and SMAD pathways (56).

Reactive oxygen species or ROS, especially hydrogen peroxide and superoxide ions, has been recently shown critical in osteoclast development. ROS has been shown to increase osteoclastic activities and bone loss (196). It has been reported to induce apoptosis in osteoblasts. ROS-activated FOXOs, a subclass of forkhead proteins involved in cell cycle arrest, hinders the WNT/β-catenin pathway in MSCs, thus impairs osteoblastogenesis (197). Moreover, ROS is critical in maintaining body homeostasis, it would be interesting to understand more about the role of ROS in context of osteoporosis.

CONCLUSION AND FUTURE PERSPECTIVE

Bone is a complex and dynamic tissue. Bone health depends on multiple factors like diet, age, hormonal, and the inflammatory status of the body. In addition to these factors, osteoporosis is also correlated with age-driven complications in the senile population. A considerable impact of aging has been reported on the immune system and associated pathologies (1, 5). Macrophages, which are the major contributor to initiation and resolution of inflammation, sense the age-related metabolic epigenetic changes and with a constitutive change to M1-type play a major role in 'Inflammaging': chronic low-grade inflammation in aged people (10, 83). Thus, our immune system is capable of sensing different stimulus as well as different phases of life and results in pathologies like osteoporosis.

In the past 20 years, the field of osteoimmunology allowed us to appreciate the underlying mechanisms of different bone pathologies by integrating the knowledge from the immune

system and bone biology. Such studies have provided new insights into how both the system functions in a concerted manner to carry out a complex process of bone modeling and remodeling. The advent of the new field of "immunoporosis" emphasizes the role of immune system players in the pathophysiology of osteoporosis. As discussed in the review, several innate immune cells have emerged as key regulators of immunoporosis. These innate immune cells modulate osteoporosis by producing several pro-inflammatory mediators and *via* modulation of cells important for causing osteoporosis largely by affecting the RANK/RANKL/OPG axis. Net bone destructive activity of osteoclasts seemingly is the decisive factor manifesting in bone status. Moreover, the fact that OCs and some major innate immune cells share a common origin as well as developmental niche, allow them to carry various overlapping features such as expression of common array of PRRs, production of various pro-inflammatory cytokines and their receptors, creating an efficient nexus of information between skeletal and immune system. That is how immune system senses the physiological status of the body and controls the skeletal system. Therefore, research towards this can allow us to find more therapeutic molecular targets to tackle osteoporosis. In addition to the innate immune cells discussed above, inflammation-mediated by intestinal epithelial cells, B1 cells, γδ T cells could play an important role in osteoporosis, and further study on these cells could be intriguing.

Additionally, in the past few years, there has been increasing evidence linking gut microbiota with bone health. It is now known that the gut controls several inflammatory diseases by the cross-talk between the innate immune cells and gut-microbiota (198, 199). Further, studying the cross talk between gut microbiota and ILCs and intestinal cells could be important in immunoporosis and of great clinical value.

AUTHOR CONTRIBUTIONS

YS and SR wrote the manuscript, and prepared the figures and table. AM conceived the idea, organized the overall design of the manuscript, and wrote the manuscript. All authors contributed to the article and approved the submitted version.

FUNDING

Funding from Indian Institute of Science Education and Research Mohali.

ACKNOWLEDGMENTS

Figures were prepared with Biorender (Biorender.com).

REFERENCES

1. Clowes JA, Riggs BL, Khosla S. The Role of the Immune System in the Pathophysiology of Osteoporosis. *Immunol Rev* (2005) 208:207–27. doi: 10.1111/j.0105-2896.2005.00334.x
2. Okman-Kilic T. *Estrogen Deficiency and Osteoporosis. Advances in Osteoporosis. Yannis Dionyssiotis*. IntechOpen (2015). doi: 10.5772/59407
3. Walsh MC, Takegahara N, Kim H, Choi Y. Updating Osteoimmunology: Regulation of Bone Cells by Innate and Adaptive Immunity. *Nat Rev Rheumatol* (2018) 14(3):146–56. doi: 10.1038/nrrheum.2017.213
4. Tsukasaki M, Takayanagi H. Osteoimmunology: Evolving Concepts in Bone-Immune Interactions in Health and Disease. *Nat Rev Immunol* (2019) 19(10):626–42. doi: 10.1038/s41577-019-0178-8
5. Ferrucci L, Fabbri E. Inflammageing: Chronic Inflammation in Ageing, Cardiovascular Disease, and Frailty. *Nat Rev Cardiol* (2018) 15(9):505–22. doi: 10.1038/s41569-018-0064-2
6. Horton JE, Raisz LG, Simmons HA, Oppenheim JJ, Mergenhagen SE. Bone Resorbing Activity in Supernatant Fluid From Cultured Human Peripheral Blood Leukocytes. *Science* (1972) 177(4051):793–5. doi: 10.1126/science.177.4051.793
7. Mundy GR, Luben RA, Raisz LG, Oppenheim JJ, Buell DN. Bone-Resorbing Activity in Supernatants From Lymphoid Cell Lines. *New Engl J Med* (1974) 290(16):867–71. doi: 10.1056/NEJM197404182901601
8. Takayanagi H, Ogasawara K, Hida S, Chiba T, Murata S, Sato K, et al. T-Cell-Mediated Regulation of Osteoclastogenesis by Signalling Cross-Talk Between RANKL and IFN-Gamma. *Nature* (2000) 408(6812):600–5. doi: 10.1038/35046102
9. Wong BR, Josien R, Choi Y. TRANCE is a TNF Family Member That Regulates Dendritic Cell and Osteoclast Function. *J Leukocyte Biol* (1999) 65 (6):715–24. doi: 10.1002/jlb.65.6.715
10. Yarbro JR, Emmons RS, Pence BD. Macrophage Immunometabolism and Inflammaging: Roles of Mitochondrial Dysfunction, Cellular Senescence, CD38, and NAD. *Immunometabolism* (2020) 2(3):e200026. doi: 10.20900/immunometab20200026
11. Arron JR, Choi Y. Bone *Versus* Immune System. *Nature* (2000) 408 (6812):535–6. doi: 10.1038/35046196
12. Srivastava RK, Dar HY, Mishra PK. Immunoporosis: Immunology of Osteoporosis-Role of T Cells. *Front Immunol* (2018) 9:657. doi: 10.3389/fimmu.2018.00657
13. Sapra L, Azam Z, Rani L, Saini C, Bhardwaj A, Shokeen N, et al. "Immunoporosis": Immunology of Osteoporosis. *Proc Natl Acad Sci India Section B: Biol Sci* (2021) 1–9. doi: 10.1007/s40011-021-01238-x
14. Hardy R, Cooper MS. Bone Loss in Inflammatory Disorders. *J Endocrinol* (2009) 201(3):309–20. doi: 10.1677/JOE-08-0568
15. Hato T, Dagher PC. How the Innate Immune System Senses Trouble and Causes Trouble. *Clin J Am Soc Nephrology: CJASN* (2015) 10(8):1459–69. doi: 10.2215/CJN.04680514
16. Tao Z, Wang J, Wen K, Yao R, Da W, Zhou S, et al. Pyroptosis in Osteoblasts: A Novel Hypothesis Underlying the Pathogenesis of Osteoporosis. *Front Endocrinol* (2020) 11:548812. doi: 10.3389/fendo.2020.548812
17. Adami G, Saag KG. Osteoporosis Pathophysiology, Epidemiology, and Screening in Rheumatoid Arthritis. *Curr Rheumatol Rep* (2019) 21(7):34. doi: 10.1007/s11926-019-0836-7
18. Cobo G, Lindholm B, Stenvinkel P. *Chronic Inflammation in End-Stage Renal Disease and Dialysis* Vol. 33. Nephrology, dialysis, transplantation: official publication of the European Dialysis and Transplant Association - European Renal Association (2018) p. iii35–40. doi: 10.1093/ndt/gfy175
19. Munoz-Torres M, Aguado P, Dauden E, Carrascosa JM, Rivera R. Osteoporosis and Psoriasis. *Actas dermo-sifiliograficas* (2019) 110(8):642–52. doi: 10.1016/j.ad.2019.02.005
20. Wang CJ, McCauley LK. Osteoporosis and Periodontitis. *Curr Osteoporosis Rep* (2016) 14(6):284–91. doi: 10.1007/s11914-016-0330-3
21. Ponzetti M, Rucci N. Updates on Osteoimmunology: What's New on the Cross-Talk Between Bone and Immune System. *Front Endocrinol* (2019) 10:236. doi: 10.3389/fendo.2019.00236
22. Quinn JM, Neale S, Fujikawa Y, McGee JO, Athanasou NA. Human Osteoclast Formation From Blood Monocytes, Peritoneal Macrophages,

and Bone Marrow Cells. *Calcified Tissue Int* (1998) 62(6):527–31. doi: 10.1007/s002239900473
23. Yu XY, Li XS, Li Y, Liu T, Wang RT. Neutrophil-Lymphocyte Ratio Is Associated With Arterial Stiffness in Postmenopausal Women With Osteoporosis. *Arch GerontoL Geriatrics* (2015) 61(1):76–80. doi: 10.1016/j.archger.2015.03.011
24. Hu X, Sun Y, Xu W, Lin T, Zeng H. Expression of RANKL by Peripheral Neutrophils and its Association With Bone Mineral Density in COPD. *Respirology* (2017) 22(1):126–32. doi: 10.1111/resp.12878
25. Ragipoglu D, Dudeck A, Haffner-Luntzer M, Voss M, Kroner J, Ignatius A, et al. The Role of Mast Cells in Bone Metabolism and Bone Disorders. *Front Immunol* (2020) 11:163. doi: 10.3389/fimmu.2020.00163
26. Soderstrom K, Stein E, Colmenero P, Purath U, Muller-Ladner U, de Matos CT, et al. Natural Killer Cells Trigger Osteoclastogenesis and Bone Destruction in Arthritis. *Proc Natl Acad Sci USA* (2010) 107(29):13028–33. doi: 10.1073/pnas.1000546107
27. Takaki-Kuwahara A, Arinobu Y, Miyawaki K, Yamada H, Tsuzuki H, Irino K, et al. CCR6+ Group 3 Innate Lymphoid Cells Accumulate in Inflamed Joints in Rheumatoid Arthritis and Produce Th17 Cytokines. *Arthritis Res Ther* (2019) 21(1):198. doi: 10.1186/s13075-019-1984-x
28. Lassus J, Salo J, Jiranek WA, Santavirta S, Nevalainen J, Matucci-Cerinic M, et al. Macrophage Activation Results in Bone Resorption. *Clin Orthopaedics Related Res* (1998) 352):7–15. doi: 10.1097/00003086-199807000-00003
29. Gong L, Zhao Y, Zhang Y, Ruan Z. The Macrophage Polarization Regulates MSC Osteoblast Differentiation *In Vitro*. *Ann Clin Lab Sci* (2016) 46(1):65–71.
30. Zhang Y, Bose T, Unger RE, Jansen JA, Kirkpatrick CJ, van den Beucken J. Macrophage Type Modulates Osteogenic Differentiation of Adipose Tissue MSCs. *Cell Tissue Res* (2017) 369(2):273–86. doi: 10.1007/s00441-017-2598-8
31. Dou C, Ding N, Zhao C, Hou T, Kang F, Cao Z, et al. Estrogen Deficiency-Mediated M2 Macrophage Osteoclastogenesis Contributes to M1/M2 Ratio Alteration in Ovariectomized Osteoporotic Mice. *J Bone Mineral Research: Off J Am Soc Bone Mineral Res* (2018) 33(5):899–908. doi: 10.1002/jbmr.3364
32. Chang MK, Raggatt LJ, Alexander KA, Kuliwaba JS, Fazzalari NL, Schroder K, et al. Osteal Tissue Macrophages are Intercalated Throughout Human and Mouse Bone Lining Tissues and Regulate Osteoblast Function *In Vitro* and *In Vivo*. *J Immunol* (2008) 181(2):1232–44. doi: 10.4049/jimmunol.181.2.1232
33. Sprangers S, de Vries TJ, Everts V. Monocyte Heterogeneity: Consequences for Monocyte-Derived Immune Cells. *J Immunol Res* (2016) 2016:1475435. doi: 10.1155/2016/1475435
34. Gebraad A, Kornilov R, Kaur S, Miettinen S, Haimi S, Peltoniemi H, et al. Monocyte-Derived Extracellular Vesicles Stimulate Cytokine Secretion and Gene Expression of Matrix Metalloproteinases by Mesenchymal Stem/Stromal Cells. *FEBS J* (2018) 285(12):2337–59. doi: 10.1111/febs.14485
35. Rivollier A, Mazzorana M, Tebib J, Piperno M, Aitsiselmi T, Rabourdin-Combe C, et al. Immature Dendritic Cell Transdifferentiation Into Osteoclasts: A Novel Pathway Sustained by the Rheumatoid Arthritis Microenvironment. *Blood* (2004) 104(13):4029–37. doi: 10.1182/blood-2004-01-0041
36. Chakravarti A, Raquil MA, Tessier P, Poubelle PE. Surface RANKL of Toll-Like Receptor 4-Stimulated Human Neutrophils Activates Osteoclastic Bone Resorption. *Blood* (2009) 114(8):1633–44. doi: 10.1182/blood-2008-09-178301
37. Sirufo MM, Suppa M, Ginaldi L, De Martinis M. Does Allergy Break Bones? Osteoporosis and Its Connection to Allergy. *Int J Mol Sci* (2020) 21(3):712. doi: 10.3390/ijms21030712
38. Ginaldi L, De Martinis M, Ciccarelli F, Saitta S, Imbesi S, Mannucci C, et al. Increased Levels of Interleukin 31 (IL-31) in Osteoporosis. *BMC Immunol* (2015) 16:60. doi: 10.1186/s12865-015-0125-9
39. Buckley MG, Walters C, Wong WM, Cawley MI, Ren S, Schwartz LB, et al. Mast Cell Activation in Arthritis: Detection of Alpha- and Beta-Tryptase, Histamine and Eosinophil Cationic Protein in Synovial Fluid. *Clin Sci* (1997) 93(4):363–70. doi: 10.1042/cs0930363
40. Malone DG, Irani AM, Schwartz LB, Barrett KE, Metcalfe DD. Mast Cell Numbers and Histamine Levels in Synovial Fluids From Patients With Diverse Arthritides. *Arthritis Rheum* (1986) 29(8):956–63. doi: 10.1002/art.1780290803
41. Hirota K, Hashimoto M, Ito Y, Matsuura M, Ito H, Tanaka M, et al. Autoimmune Th17 Cells Induced Synovial Stromal and Innate Lymphoid Cell Secretion of the Cytokine GM-CSF to Initiate and Augment Autoimmune Arthritis. *Immunity* (2018) 48(6):1220–32.e5. doi: 10.1016/j.immuni.2018.04.009
42. Kindstedt E, Koskinen Holm C, Palmqvist P, Sjostrom M, Lejon K, Lundberg P. Innate Lymphoid Cells are Present in Gingivitis and Periodontitis. *J Periodontol* (2019) 90(2):200–7. doi: 10.1002/JPER.17-0750
43. Wang T, He C. TNF-Alpha and IL-6: The Link Between Immune and Bone System. *Curr Drug Targets* (2020) 21(3):213–27. doi: 10.2174/1389450120666190821161259
44. Tanaka K, Hashizume M, Mihara M, Yoshida H, Suzuki M, Matsumoto Y. Anti-Interleukin-6 Receptor Antibody Prevents Systemic Bone Mass Loss *via* Reducing the Number of Osteoclast Precursors in Bone Marrow in a Collagen-Induced Arthritis Model. *Clin Exp Immunol* (2014) 175(2):172–80. doi: 10.1111/cei.12201
45. Luo G, Li F, Li X, Wang ZG, Zhang B. TNFalpha and RANKL Promote Osteoclastogenesis by Upregulating RANK *via* the NFkappaB Pathway. *Mol Med Rep* (2018) 17(5):6605–11. doi: 10.3892/mmr.2018.8698
46. Ohori F, Kitaura H, Marahleh A, Kishikawa A, Ogawa S, Qi J, et al. Effect of TNF-Alpha-Induced Sclerostin on Osteocytes During Orthodontic Tooth Movement. *J Immunol Res* (2019) 2019:9716758. doi: 10.1155/2019/9716758
47. Zhao Z, Hou X, Yin X, Li Y, Duan R, Boyce BF, et al. TNF Induction of NF-kappaB RelB Enhances RANKL-Induced Osteoclastogenesis by Promoting Inflammatory Macrophage Differentiation But Also Limits It Through Suppression of NFATc1 Expression. *PloS One* (2015) 10(8):e0135728. doi: 10.1371/journal.pone.0135728
48. Xie J, Gu J. Identification of C-Terminal Hsp70-Interacting Protein as a Mediator of Tumour Necrosis Factor Action in Osteoblast Differentiation by Targeting Osterix for Degradation. *J Cell Mol Med* (2015) 19(8):1814–24. doi: 10.1111/jcmm.12553
49. Zuo C, Zhao X, Shi Y, Wu W, Zhang N, Xu J, et al. TNF-Alpha Inhibits SATB2 Expression and Osteoblast Differentiation Through NF-kappaB and MAPK Pathways. *Oncotarget* (2018) 9(4):4833–50. doi: 10.18632/oncotarget.23373
50. Du D, Zhou Z, Zhu L, Hu X, Lu J, Shi C, et al. TNF-Alpha Suppresses Osteogenic Differentiation of MSCs by Accelerating P2Y2 Receptor in Estrogen-Deficiency Induced Osteoporosis. *Bone* (2018) 117:161–70. doi: 10.1016/j.bone.2018.09.012
51. Tang M, Tian L, Luo G, Yu X. Interferon-Gamma-Mediated Osteoimmunology. *Front Immunol* (2018) 9:1508. doi: 10.3389/fimmu.2018.01508
52. Lee J, Park C, Kim HJ, Lee YD, Lee ZH, Song YW, et al. Stimulation of Osteoclast Migration and Bone Resorption by C-C Chemokine Ligands 19 and 21. *Exp Mol Med* (2017) 49(7):e358. doi: 10.1038/emm.2017.100
53. Ignatius A, Schoengraf P, Kreja L, Liedert A, Recknagel S, Kandert S, et al. Complement C3a and C5a Modulate Osteoclast Formation and Inflammatory Response of Osteoblasts in Synergism With IL-1beta. *J Cell Biochem* (2011) 112(9):2594–605. doi: 10.1002/jcb.23186
54. Pobanz JM, Reinhardt RA, Koka S, Sanderson SD. C5a Modulation of Interleukin-1 Beta-Induced Interleukin-6 Production by Human Osteoblast-Like Cells. *J Periodontal Res* (2000) 35(3):137–45. doi: 10.1034/j.1600-0765.2000.035003137.x
55. Panagakos FS, Jandinski JJ, Feder L, Kumar S. Effects of Plasminogen and Interleukin-1 Beta on Bone Resorption *In Vitro*. *Biochimie* (1994) 76 (5):394–7. doi: 10.1016/0300-9084(94)90114-7
56. Ruscitti P, Cipriani P, Carubbi F, Liakouli V, Zazzeroni F, Di Benedetto P, et al. The Role of IL-1beta in the Bone Loss During Rheumatic Diseases. *Mediators Inflamm* (2015) 2015:782382. doi: 10.1155/2015/782382
57. Mukhopadhyay S, Pluddemann A, Gordon S. Macrophage Pattern Recognition Receptors in Immunity, Homeostasis and Self Tolerance. *Adv Exp Med Biol* (2009) 653:1–14. doi: 10.1007/978-1-4419-0901-5_1
58. Alonso-Perez A, Franco-Trepat E, Guillan-Fresco M, Jorge-Mora A, Lopez V, Pino J, et al. Role of Toll-Like Receptor 4 on Osteoblast Metabolism and Function. *Front Physiol* (2018) 9:504. doi: 10.3389/fphys.2018.00504
59. Kassem A, Lindholm C, Lerner UH. Toll-Like Receptor 2 Stimulation of Osteoblasts Mediates Staphylococcus Aureus Induced Bone Resorption and Osteoclastogenesis Through Enhanced RANKL. *PloS One* (2016) 11(6): e0156708. doi: 10.1371/journal.pone.0156708
60. Koduru SV, Sun BH, Walker JM, Zhu M, Simpson C, Dhodapkar M, et al. The Contribution of Cross-Talk Between the Cell-Surface Proteins CD36

and CD47-TSP-1 in Osteoclast Formation and Function. *J Biol Chem* (2018) 293(39):15055–69. doi: 10.1074/jbc.RA117.000633
61. Li X, Wang X, Hu Z, Chen Z, Li H, Liu X, et al. Possible Involvement of the oxLDL/LOX-1 System in the Pathogenesis and Progression of Human Intervertebral Disc Degeneration or Herniation. *Sci Rep* (2017) 7(1):7403. doi: 10.1038/s41598-017-07780-x
62. Michalski MN, McCauley LK. Macrophages and Skeletal Health. *Pharmacol Ther* (2017) 174:43–54. doi: 10.1016/j.pharmthera.2017.02.017
63. Sica A, Mantovani A. Macrophage Plasticity and Polarization: *In Vivo* Veritas. *J Clin Invest* (2012) 122(3):787–95. doi: 10.1172/JCI59643
64. Liu H, Wu X, Gang N, Wang S, Deng W, Zan L, et al. Macrophage Functional Phenotype can be Consecutively and Reversibly Shifted to Adapt to Microenvironmental Changes. *Int J Clin Exp Med* (2015) 8(2):3044–53.
65. Murray PJ. Macrophage Polarization. *Annu Rev Physiol* (2017) 79:541–66. doi: 10.1146/annurev-physiol-022516-034339
66. Huang R, Wang X, Zhou Y, Xiao Y. RANKL-Induced M1 Macrophages are Involved in Bone Formation. *Bone Res* (2017) 5:17019. doi: 10.1038/boneres.2017.19
67. Loi F, Cordova LA, Zhang R, Pajarinen J, Lin TH, Goodman SB, et al. The Effects of Immunomodulation by Macrophage Subsets on Osteogenesis *In Vitro*. *Stem Cell Res Ther* (2016) 7:15. doi: 10.1186/s13287-016-0276-5
68. Champagne CM, Takebe J, Offenbacher S, Cooper LF. Macrophage Cell Lines Produce Osteoinductive Signals That Include Bone Morphogenetic Protein-2. *Bone* (2002) 30(1):26–31. doi: 10.1016/S8756-3282(01)00638-X
69. Takito J, Nakamura M. Heterogeneity and Actin Cytoskeleton in Osteoclast and Macrophage Multinucleation. *Int J Mol Sci* (2020) 21(18):6629. doi: 10.3390/ijms21186629
70. Feng W, Guo J, Li M. RANKL-Independent Modulation of Osteoclastogenesis. *J Oral Biosci* (2019) 61(1):16–21. doi: 10.1016/j.job.2019.01.001
71. Bordbar A, Mo ML, Nakayasu ES, Schrimpe-Rutledge AC, Kim YM, Metz TO, et al. Model-Driven Multi-Omic Data Analysis Elucidates Metabolic Immunomodulators of Macrophage Activation. *Mol Syst Biol* (2012) 8:558. doi: 10.1038/msb.2012.21
72. An E, Narayanan M, Manes NP, Nita-Lazar A. Characterization of Functional Reprogramming During Osteoclast Development Using Quantitative Proteomics and mRNA Profiling. *Mol Cell Proteomics: MCP* (2014) 13(10):2687–704. doi: 10.1074/mcp.M113.034371
73. Park-Min KH. Metabolic Reprogramming in Osteoclasts. *Semin Immunopathol* (2019) 41(5):565–72. doi: 10.1007/s00281-019-00757-0
74. Kim JM, Jeong D, Kang HK, Jung SY, Kang SS, Min BM. Osteoclast Precursors Display Dynamic Metabolic Shifts Toward Accelerated Glucose Metabolism at an Early Stage of RANKL-Stimulated Osteoclast Differentiation. *Cell Physiol Biochem: Int J Exp Cell Physiol Biochem Pharmacol* (2007) 20(6):935–46. doi: 10.1159/000110454
75. Yao Y, Cai X, Ren F, Ye Y, Wang F, Zheng C, et al. The Macrophage-Osteoclast Axis in Osteoimmunity and Osteo-Related Diseases. *Front Immunol* (2021) 12:664871. doi: 10.3389/fimmu.2021.664871
76. Gu Q, Yang H, Shi Q. Macrophages and Bone Inflammation. *J Orthopaedic Transl* (2017) 10:86–93. doi: 10.1016/j.jot.2017.05.002
77. Yang X, Chang Y, Wei W. Emerging Role of Targeting Macrophages in Rheumatoid Arthritis: Focus on Polarization, Metabolism and Apoptosis. *Cell Prolif* (2020) 53(7):e12854. doi: 10.1111/cpr.12854
78. Wu CL, Harasymowicz NS, Klimak MA, Collins KH, Guilak F. The Role of Macrophages in Osteoarthritis and Cartilage Repair. *Osteoarthritis Cartilage* (2020) 28(5):544–54. doi: 10.1016/j.joca.2019.12.007
79. Chen G, Xu Q, Dai M, Liu X. Bergapten Suppresses RANKL-Induced Osteoclastogenesis and Ovariectomy-Induced Osteoporosis *via* Suppression of NF-kappaB and JNK Signaling Pathways. *Biochem Biophys Res Commun* (2019) 509(2):329–34. doi: 10.1016/j.bbrc.2018.12.112
80. Kim B, Lee KY, Park B. Icariin Abrogates Osteoclast Formation Through the Regulation of the RANKL-Mediated TRAF6/NF-Kappab/ERK Signaling Pathway in Raw264.7 Cells. *Phytomedicine: Int J Phytother Phytopharmacol* (2018) 51:181–90. doi: 10.1016/j.phymed.2018.06.020
81. Choo YY, Tran PT, Min BS, Kim O, Nguyen HD, Kwon SH, et al. Sappanone A Inhibits RANKL-Induced Osteoclastogenesis in BMMs and Prevents Inflammation-Mediated Bone Loss. *Int Immunopharmacol* (2017) 52:230–7. doi: 10.1016/j.intimp.2017.09.018
82. Matsumoto M, Sudo T, Saito T, Osada H, Tsujimoto M. Involvement of P38 Mitogen-Activated Protein Kinase Signaling Pathway in Osteoclastogenesis Mediated by Receptor Activator of NF-kappa B Ligand (RANKL). *J Biol Chem* (2000) 275(40):31155–61. doi: 10.1074/jbc.M001229200
83. Stahl EC, Haschak MJ, Popovic B, Brown BN. Macrophages in the Aging Liver and Age-Related Liver Disease. *Front Immunol* (2018) 9:2795. doi: 10.3389/fimmu.2018.02795
84. Kim OH, Kim H, Kang J, Yang D, Kang YH, Lee DH, et al. Impaired Phagocytosis of Apoptotic Cells Causes Accumulation of Bone Marrow-Derived Macrophages in Aged Mice. *BMB Rep* (2017) 50(1):43–8. doi: 10.5483/BMBRep.2017.50.1.167
85. Barrett JP, Costello DA, O'Sullivan J, Cowley TR, Lynch MA. Bone Marrow-Derived Macrophages From Aged Rats are More Responsive to Inflammatory Stimuli. *J Neuroinflamm* (2015) 12:67. doi: 10.1186/s12974-015-0287-7
86. Smallwood HS, Lopez-Ferrer D, Squier TC. Aging Enhances the Production of Reactive Oxygen Species and Bactericidal Activity in Peritoneal Macrophages by Upregulating Classical Activation Pathways. *Biochemistry* (2011) 50(45):9911–22. doi: 10.1021/bi2011866
87. Clark D, Brazina S, Yang F, Hu D, Hsieh CL, Niemi EC, et al. Age-Related Changes to Macrophages Are Detrimental to Fracture Healing in Mice. *Aging Cell* (2020) 19(3):e13112. doi: 10.1111/acel.13112
88. Gibon E, Loi F, Cordova LA, Pajarinen J, Lin T, Lu L, et al. Aging Affects Bone Marrow Macrophage Polarization: Relevance to Bone Healing. *Regenerative Eng Trans Med* (2016) 2(2):98–104. doi: 10.1007/s40883-016-0016-5
89. Chen X, Ouyang Z, Shen Y, Liu B, Zhang Q, Wan L, et al. CircRNA_28313/miR-195a/CSF1 Axis Modulates Osteoclast Differentiation to Affect OVX-Induced Bone Absorption in Mice. *RNA Biol* (2019) 16(9):1249–62. doi: 10.1080/15476286.2019.1624470
90. Shen G, Ren H, Shang Q, Zhang Z, Zhao W, Yu X, et al. miR-128 Plays a Critical Role in Murine Osteoclastogenesis and Estrogen Deficiency-Induced Bone Loss. *Theranostics* (2020) 10(10):4334–48. doi: 10.7150/thno.42982
91. Dinesh P, Kalaiselvan S, Sujitha S, Rasool M. miR-506-3p Alleviates Uncontrolled Osteoclastogenesis *via* Repression of RANKL/NFATc1 Signaling Pathway. *J Cell Physiol* (2020) 235(12):9497–509. doi: 10.1002/jcp.29757
92. Italiani P, Boraschi D. From Monocytes to M1/M2 Macrophages: Phenotypical vs. Functional Differentiation. *Front Immunol* (2014) 5:514. doi: 10.3389/fimmu.2014.00514
93. Auffray C, Fogg D, Garfa M, Elain G, Join-Lambert O, Kayal S, et al. Monitoring of Blood Vessels and Tissues by a Population of Monocytes With Patrolling Behavior. *Science* (2007) 317(5838):666–70. doi: 10.1126/science.1142883
94. Tsou CL, Peters W, Si Y, Slaymaker S, Aslanian AM, Weisberg SP, et al. Critical Roles for CCR2 and MCP-3 in Monocyte Mobilization From Bone Marrow and Recruitment to Inflammatory Sites. *J Clin Invest* (2007) 117(4):902–9. doi: 10.1172/JCI29919
95. Auffray C, Sieweke MH, Geissmann F. Blood Monocytes: Development, Heterogeneity, and Relationship With Dendritic Cells. *Annu Rev Immunol* (2009) 27:669–92. doi: 10.1146/annurev.immunol.021908.132557
96. Kratofil RM, Kubes P, Deniset JF. Monocyte Conversion During Inflammation and Injury. *Arterioscl Thromb Vasc Biol* (2017) 37(1):35–42. doi: 10.1161/ATVBAHA.116.308198
97. Jakubzick C, Gautier EL, Gibbings SL, Sojka DK, Schlitzer A, Johnson TE, et al. Minimal Differentiation of Classical Monocytes as They Survey Steady-State Tissues and Transport Antigen to Lymph Nodes. *Immunity* (2013) 39(3):599–610. doi: 10.1016/j.immuni.2013.08.007
98. Yahara Y, Barrientos T, Tang YJ, Puviindran V, Nadesan P, Zhang H, et al. Erythromyeloid Progenitors Give Rise to a Population of Osteoclasts That Contribute to Bone Homeostasis and Repair. *Nat Cell Biol* (2020) 22(1):49–59. doi: 10.1038/s41556-019-0437-8
99. Yahara Y, Ma X, Gracia L, Alman BA. Monocyte/Macrophage Lineage Cells From Fetal Erythromyeloid Progenitors Orchestrate Bone Remodeling and Repair. *Front Cell Dev Biol* (2021) 9(123):1–16. doi: 10.3389/fcell.2021.622035
100. Jacome-Galarza CE, Percin GI, Muller JT, Mass E, Lazarov T, Eitler J, et al. Developmental Origin, Functional Maintenance and Genetic Rescue of Osteoclasts. *Nature* (2019) 568(7753):541–5. doi: 10.1038/s41586-019-1105-7

101. Da W, Tao L, Zhu Y. The Role of Osteoclast Energy Metabolism in the Occurrence and Development of Osteoporosis. *Front Endocrinol* (2021) 12 (556):1–18. doi: 10.3389/fendo.2021.675385
102. Schmidl C, Renner K, Peter K, Eder R, Lassmann T, Balwierz PJ, et al. Transcription and Enhancer Profiling in Human Monocyte Subsets. *Blood* (2014) 123(17):e90–9. doi: 10.1182/blood-2013-02-484188
103. Zhang L, Liu YZ, Zeng Y, Zhu W, Zhao YC, Zhang JG, et al. Network-Based Proteomic Analysis for Postmenopausal Osteoporosis in Caucasian Females. *Proteomics* (2016) 16(1):12–28. doi: 10.1002/pmic.201500005
104. Deng FY, Lei SF, Zhang Y, Zhang YL, Zheng YP, Zhang LS, et al. Peripheral Blood Monocyte-Expressed ANXA2 Gene is Involved in Pathogenesis of Osteoporosis in Humans. *Mol Cell Proteomics: MCP* (2011) 10(11):M111 011700. doi: 10.1074/mcp.M111.011700
105. Liu YZ, Dvornyk V, Lu Y, Shen H, Lappe JM, Recker RR, et al. A Novel Pathophysiological Mechanism for Osteoporosis Suggested by an *In Vivo* Gene Expression Study of Circulating Monocytes. *J Biol Chem* (2005) 280 (32):29011–6. doi: 10.1074/jbc.M501164200
106. Chen XD, Xiao P, Lei SF, Liu YZ, Guo YF, Deng FY, et al. Gene Expression Profiling in Monocytes and SNP Association Suggest the Importance of the STAT1 Gene for Osteoporosis in Both Chinese and Caucasians. *J Bone Mineral Research: Off J Am Soc Bone Mineral Res* (2010) 25(2):339–55. doi: 10.1359/jbmr.090724
107. Daswani B, Gupta MK, Gavali S, Desai M, Sathe GJ, Patil A, et al. Monocyte Proteomics Reveals Involvement of Phosphorylated HSP27 in the Pathogenesis of Osteoporosis. *Dis Markers* (2015) 2015:196589. doi: 10.1155/2015/196589
108. Liu YZ, Zhou Y, Zhang L, Li J, Tian Q, Zhang JG, et al. Attenuated Monocyte Apoptosis, a New Mechanism for Osteoporosis Suggested by a Transcriptome-Wide Expression Study of Monocytes. *PloS One* (2015) 10 (2):e0116792. doi: 10.1371/journal.pone.0116792
109. Leung R, Cuddy K, Wang Y, Rommens J, Glogauer M. Sbds is Required for Rac2-Mediated Monocyte Migration and Signaling Downstream of RANK During Osteoclastogenesis. *Blood* (2011) 117(6):2044–53. doi: 10.1182/blood-2010-05-282574
110. Leung R, Wang Y, Cuddy K, Sun C, Magalhaes J, Grynpas M, et al. Filamin A Regulates Monocyte Migration Through Rho Small GTPases During Osteoclastogenesis. *J Bone Mineral Res* (2010) 25(5):1077–91. doi: 10.1359/jbmr.091114
111. Swiecki M, Colonna M. The Multifaceted Biology of Plasmacytoid Dendritic Cells. *Nat Rev Immunol* (2015) 15(8):471–85. doi: 10.1038/nri3865
112. Maitra R, Follenzi A, Yaghoobian A, Montagna C, Merlin S, Cannizzo ES, et al. Dendritic Cell-Mediated *In Vivo* Bone Resorption. *J Immunol* (2010) 185(3):1485–91. doi: 10.4049/jimmunol.0903560
113. Gillespie MT. Impact of Cytokines and T Lymphocytes Upon Osteoclast Differentiation and Function. *Arthritis Res Ther* (2007) 9(2):103. doi: 10.1186/ar2141
114. Sarkar S, Fox DA. Dendritic Cells in Rheumatoid Arthritis. *Front Biosci: J Virtual Library* (2005) 10:656–65. doi: 10.2741/1560
115. Teng YT. Protective and Destructive Immunity in the Periodontium: Part 2–T-Cell-Mediated Immunity in the Periodontium. *J Dental Res* (2006) 85 (3):209–19. doi: 10.1177/154405910608500302
116. Cline-Smith A, Axelbaum A, Shashkova E, Chakraborty M, Sanford J, Panesar P, et al. Ovariectomy Activates Chronic Low-Grade Inflammation Mediated by Memory T Cells, Which Promotes Osteoporosis in Mice. *J Bone Mineral Research: Off J Am Soc Bone Mineral Res* (2020) 35(6):1174–87. doi: 10.1002/jbmr.3966
117. Wang B, Dong Y, Tian Z, Chen Y, Dong S. The Role of Dendritic Cells Derived Osteoclasts in Bone Destruction Diseases. *Genes Dis* (2020) 8 (4):401–11. doi: 10.1016/j.gendis.2020.03.009
118. Narisawa M, Kubo S, Okada Y, Yamagata K, Nakayamada S, Sakata K, et al. Human Dendritic Cell-Derived Osteoclasts With High Bone Resorption Capacity and T Cell Stimulation Ability. *Bone* (2021) 142:115616. doi: 10.1016/j.bone.2020.115616
119. Alnaeeli M, Penninger JM, Teng YT. Immune Interactions With CD4+ T Cells Promote the Development of Functional Osteoclasts From Murine CD11c+ Dendritic Cells. *J Immunol* (2006) 177(5):3314–26. doi: 10.4049/jimmunol.177.5.3314
120. Ono T, Takayanagi H. Osteoimmunology in Bone Fracture Healing. *Curr Osteoporosis Rep* (2017) 15(4):367–75. doi: 10.1007/s11914-017-0381-0
121. Jin Y, Wi HJ, Choi M-H, Hong S-T, Bae YM. Regulation of Anti-Inflammatory Cytokines IL-10 and TGF-β in Mouse Dendritic Cells Through Treatment With Clonorchis Sinensis Crude Antigen. *Exp Mol Med* (2014) 46(1):e74–e. doi: 10.1038/emm.2013.144
122. Dumitriu IE, Dunbar DR, Howie SE, Sethi T, Gregory CD. Human Dendritic Cells Produce TGF-β1 Under the Influence of Lung Carcinoma Cells and Prime the Differentiation of CD4+CD25+Foxp3+ Regulatory T Cells. *J Immunol* (2009) 182(5):2795–807. doi: 10.4049/jimmunol.0712671
123. Hughes DE, Dai A, Tiffee JC, Li HH, Mundy GR, Boyce BF. Estrogen Promotes Apoptosis of Murine Osteoclasts Mediated by TGF–β. *Nat Med* (1996) 2(10):1132–6. doi: 10.1038/nm1096-1132
124. Nathan C. Neutrophils and Immunity: Challenges and Opportunities. *Nat Rev Immunol* (2006) 6(3):173–82. doi: 10.1038/nri1785
125. Selders GS, Fetz AE, Radic MZ, Bowlin GL. An Overview of the Role of Neutrophils in Innate Immunity, Inflammation and Host-Biomaterial Integration. *Regenerative Biomaterials* (2017) 4(1):55–68. doi: 10.1093/rb/rbw041
126. Wagner C, Iking-Konert C, Denefleh B, Stegmaier S, Hug F, Hansch GM. Granzyme B and Perforin: Constitutive Expression in Human Polymorphonuclear Neutrophils. *Blood* (2004) 103(3):1099–104. doi: 10.1182/blood-2003-04-1069
127. Kaplan MJ, Radic M. Neutrophil Extracellular Traps: Double-Edged Swords of Innate Immunity. *J Immunol* (2012) 189(6):2689–95. doi: 10.4049/jimmunol.1201719
128. Nauseef WM, Borregaard N. Neutrophils at Work. *Nat Immunol* (2014) 15 (7):602–11. doi: 10.1038/ni.2921
129. Scapini P, Cassatella MA. Social Networking of Human Neutrophils Within the Immune System. *Blood* (2014) 124(5):710–9. doi: 10.1182/blood-2014-03-453217
130. Mantovani A, Cassatella MA, Costantini C, Jaillon S. Neutrophils in the Activation and Regulation of Innate and Adaptive Immunity. *Nat Rev Immunol* (2011) 11(8):519–31. doi: 10.1038/nri3024
131. Hajishengallis G, Moutsopoulos NM, Hajishengallis E, Chavakis T. Immune and Regulatory Functions of Neutrophils in Inflammatory Bone Loss. *Semin Immunol* (2016) 28(2):146–58. doi: 10.1016/j.smim.2016.02.002
132. Poubelle PE, Chakravarti A, Fernandes MJ, Doiron K, Marceau AA. Differential Expression of RANK, RANK-L, and Osteoprotegerin by Synovial Fluid Neutrophils From Patients With Rheumatoid Arthritis and by Healthy Human Blood Neutrophils. *Arthritis Res Ther* (2007) 9(2):R25. doi: 10.1186/ar2137
133. Iking-Konert C, Ostendorf B, Sander O, Jost M, Wagner C, Joosten L, et al. Transdifferentiation of Polymorphonuclear Neutrophils to Dendritic-Like Cells at the Site of Inflammation in Rheumatoid Arthritis: Evidence for Activation by T Cells. *Ann Rheum Dis* (2005) 64(10):1436–42. doi: 10.1136/ard.2004.034132
134. Moutsopoulos NM, Konkel J, Sarmadi M, Eskan MA, Wild T, Dutzan N, et al. Defective Neutrophil Recruitment in Leukocyte Adhesion Deficiency Type I Disease Causes Local IL-17-Driven Inflammatory Bone Loss. *Sci Trans Med* (2014) 6(229):229ra40. doi: 10.1126/scitranslmed.3007696
135. Geissler S, Textor M, Stumpp S, Seitz S, Lekaj A, Brunk S, et al. Loss of Murine Gfi1 Causes Neutropenia and Induces Osteoporosis Depending on the Pathogen Load and Systemic Inflammation. *PloS One* (2018) 13(6): e0198510. doi: 10.1371/journal.pone.0198510
136. Fulkerson PC, Rothenberg ME. Targeting Eosinophils in Allergy, Inflammation and Beyond. *Nat Rev Drug Discov* (2013) 12(2):117–29. doi: 10.1038/nrd3838
137. Arshi S, Ghalehbaghi B, Kamrava S-K, Aminlou M. Vitamin D Serum Levels in Allergic Rhinitis: Any Difference From Normal Population? *Asia Pacif Allergy* (2012) 2(1):45–8. doi: 10.5415/apallergy.2012.2.1.45
138. Azimi A, Ghajarzadeh M, Sahraian MA, Mohammadifar M, Roostaei B, Samani SMV, et al. Effects of Vitamin D Supplements on IL-10 and INFgamma Levels in Patients With Multiple Sclerosis: A Systematic Review and Meta-Analysis. *Maedica* (2019) 14(4):413–7. doi: 10.26574/maedica.2019.14.4.413
139. Rossetti D, Isoldi S, Oliva S. Eosinophilic Esophagitis: Update on Diagnosis and Treatment in Pediatric Patients. *Pediatr Drugs* (2020) 22(4):343–56. doi: 10.1007/s40272-020-00398-z

140. Saha S, Brightling CE. Eosinophilic Airway Inflammation in COPD. *Int J Chronic Obstructive Pulmonary Dis* (2006) 1(1):39–47. doi: 10.2147/copd.2006.1.1.39
141. Loke YK, Cavallazzi R, Singh S. Risk of Fractures With Inhaled Corticosteroids in COPD: Systematic Review and Meta-Analysis of Randomised Controlled Trials and Observational Studies. *Thorax* (2011) 66(8):699–708. doi: 10.1136/thx.2011.160028
142. Otaki F, Daniel W, Geno DM, Tholen C, Alexander JA. Interval Bone Density in Patients With Eosinophilic Esophagitis on Steroids: 368. *Off J Am Coll Gastroenterol | ACG* (2017) 112:S197. doi: 10.14309/00000434-201710001-00368
143. Nagata M, Nakagome K, Soma T. Mechanisms of Eosinophilic Inflammation. *Asia Pacif Allergy* (2020) 10(2):e14. doi: 10.5415/apallergy.2020.10.e14
144. Amber KT, Valdebran M, Kridin K, Grando SA. The Role of Eosinophils in Bullous Pemphigoid: A Developing Model of Eosinophil Pathogenicity in Mucocutaneous Disease. *Front Med* (2018) 5:201. doi: 10.3389/fmed.2018.00201
145. Murdaca G, Greco M, Tonacci A, Negrini S, Borro M, Puppo F, et al. IL-33/IL-31 Axis in Immune-Mediated and Allergic Diseases. *Int J Mol Sci* (2019) 20(23):5856. doi: 10.3390/ijms20235856
146. Krystel-Whittemore M, Dileepan KN, Wood JG. Mast Cell: A Multi-Functional Master Cell. *Front Immunol* (2015) 6:620. doi: 10.3389/fimmu.2015.00620
147. Galli SJ, Tsai M. IgE and Mast Cells in Allergic Disease. *Nat Med* (2012) 18 (5):693–704. doi: 10.1038/nm.2755
148. Kroner J, Kovtun A, Kemmler J, Messmann JJ, Strauss G, Seitz S, et al. Mast Cells Are Critical Regulators of Bone Fracture-Induced Inflammation and Osteoclast Formation and Activity. *J Bone Mineral Research: Off J Am Soc Bone Mineral Res* (2017) 32(12):2431–44. doi: 10.1002/jbmr.3234
149. Fallon MD, Whyte MP, Craig RB Jr, Teitelbaum SL. Mast-Cell Proliferation in Postmenopausal Osteoporosis. *Calcified Tissue Int* (1983) 35(1):29–31. doi: 10.1007/BF02405002
150. McKenna MJ. Histomorphometric Study of Mast Cells in Normal Bone, Osteoporosis and Mastocytosis Using a New Stain. *Calcified Tissue Int* (1994) 55(4):257–9. doi: 10.1007/BF00310402
151. Lesclous P, Guez D, Llorens A, Saffar JL. Time-Course of Mast Cell Accumulation in Rat Bone Marrow After Ovariectomy. *Calcified Tissue Int* (2001) 68(5):297–303. doi: 10.1007/BF02390837
152. Lesclous P, Saffar JL. Mast Cells Accumulate in Rat Bone Marrow After Ovariectomy. *Cells Tissues Organs* (1999) 164(1):23–9. doi: 10.1159/000016639
153. Tyan ML. Effect of Promethazine on Lumbar Vertebral Bone Mass in Postmenopausal Women. *J Internal Med* (1993) 234(2):143–8. doi: 10.1111/j.1365-2796.1993.tb00723.x
154. Zaitsu M, Narita S, Lambert KC, Grady JJ, Estes DM, Curran EM, et al. Estradiol Activates Mast Cells *via* a Non-Genomic Estrogen Receptor-Alpha and Calcium Influx. *Mol Immunol* (2007) 44(8):1977–85. doi: 10.1016/j.molimm.2006.09.030
155. Rivellese F, Nerviani A, Rossi FW, Marone G, Matucci-Cerinic M, de Paulis A, et al. Mast Cells in Rheumatoid Arthritis: Friends or Foes? *Autoimmun Rev* (2017) 16(6):557–63. doi: 10.1016/j.autrev.2017.04.001
156. Feyerabend TB, Weiser A, Tietz A, Stassen M, Harris N, Kopf M, et al. Cre-Mediated Cell Ablation Contests Mast Cell Contribution in Models of Antibody- and T Cell-Mediated Autoimmunity. *Immunity* (2011) 35 (5):832–44. doi: 10.1016/j.immuni.2011.09.015
157. de Lange-Brokaar BJ, Kloppenburg M, Andersen SN, Dorjee AL, Yusuf E, Herb-van Toorn L, et al. Characterization of Synovial Mast Cells in Knee Osteoarthritis: Association With Clinical Parameters. *Osteoarthritis Cartilage* (2016) 24(4):664–71. doi: 10.1016/j.joca.2015.11.011
158. Wang Q, Lepus CM, Raghu H, Reber LL, Tsai MM, Wong HH, et al. IgE-Mediated Mast Cell Activation Promotes Inflammation and Cartilage Destruction in Osteoarthritis. *eLife* (2019) 8:1–23. doi: 10.7554/eLife.39905
159. Nakano S, Mishiro T, Takahara S, Yokoi H, Hamada D, Yukata K, et al. Distinct Expression of Mast Cell Tryptase and Protease Activated Receptor-2 in Synovia of Rheumatoid Arthritis and Osteoarthritis. *Clin Rheumatol* (2007) 26(8):1284–92. doi: 10.1007/s10067-006-0495-8
160. Lee H, Kashiwakura J, Matsuda A, Watanabe Y, Sakamoto-Sasaki T, Matsumoto K, et al. Activation of Human Synovial Mast Cells From Rheumatoid Arthritis or Osteoarthritis Patients in Response to Aggregated IgG Through Fcgamma Receptor I and Fcgamma Receptor II. *Arthritis Rheum* (2013) 65(1):109–19. doi: 10.1002/art.37741
161. Lindholm R, Lindholm S, Liukko P. Fracture Healing and Mast Cells. I. The Periosteal Callus in Rats. *Acta Orthopaedica Scand* (1967) 38(2):115–22. doi: 10.3109/17453676708989624
162. Banovac K, Renfree K, Makowski AL, Latta LL, Altman RD. Fracture Healing and Mast Cells. *J Orthopaedic Trauma* (1995) 9(6):482–90. doi: 10.1097/00005131-199509060-00005
163. Scoville SD, Freud AG, Caligiuri MA. Modeling Human Natural Killer Cell Development in the Era of Innate Lymphoid Cells. *Front Immunol* (2017) 8:360. doi: 10.3389/fimmu.2017.00360
164. Brandstadter JD, Yang Y. Natural Killer Cell Responses to Viral Infection. *J Innate Immun* (2011) 3(3):274–9. doi: 10.1159/000324176
165. Trinchieri G. Biology of Natural Killer Cells. *Adv Immunol* (1989) 47:187–376. doi: 10.1016/S0065-2776(08)60664-1
166. Parham P. MHC Class I Molecules and KIRs in Human History, Health and Survival. *Nat Rev Immunol* (2005) 5(3):201–14. doi: 10.1038/nri1570
167. Fauriat C, Long EO, Ljunggren HG, Bryceson YT. Regulation of Human NK-Cell Cytokine and Chemokine Production by Target Cell Recognition. *Blood* (2010) 115(11):2167–76. doi: 10.1182/blood-2009-08-238469
168. de Matos CT, Berg L, Michaelsson J, Fellander-Tsai L, Karre K, Soderstrom K. Activating and Inhibitory Receptors on Synovial Fluid Natural Killer Cells of Arthritis Patients: Role of CD94/NKG2A in Control of Cytokine Secretion. *Immunology* (2007) 122(2):291–301. doi: 10.1111/j.1365-2567.2007.02638.x
169. Tak PP, Kummer JA, Hack CE, Daha MR, Smeets TJ, Erkelens GW, et al. Granzyme-Positive Cytotoxic Cells are Specifically Increased in Early Rheumatoid Synovial Tissue. *Arthritis Rheum* (1994) 37(12):1735–43. doi: 10.1002/art.1780371205
170. McInnes IB, Leung BP, Sturrock RD, Field M, Liew FY. Interleukin-15 Mediates T Cell-Dependent Regulation of Tumor Necrosis Factor-Alpha Production in Rheumatoid Arthritis. *Nat Med* (1997) 3(2):189–95. doi: 10.1038/nm0297-189
171. Feng S, Madsen SH, Viller NN, Neutzsky-Wulff AV, Geisler C, Karlsson L, et al. Interleukin-15-Activated Natural Killer Cells Kill Autologous Osteoclasts *via* LFA-1, DNAM-1 and TRAIL, and Inhibit Osteoclast-Mediated Bone Erosion *In Vitro*. *Immunology* (2015) 145(3):367–79. doi: 10.1111/imm.12449
172. Kurachi T, Morita I, Murota S. Involvement of Adhesion Molecules LFA-1 and ICAM-1 in Osteoclast Development. *Biochim Biophys Acta* (1993) 1178 (3):259–66. doi: 10.1016/0167-4889(93)90202-Z
173. Colonna M. Innate Lymphoid Cells: Diversity, Plasticity, and Unique Functions in Immunity. *Immunity* (2018) 48(6):1104–17. doi: 10.1016/j.immuni.2018.05.013
174. Mjosberg J, Spits H. Human Innate Lymphoid Cells. *J Allergy Clin Immunol* (2016) 138(5):1265–76. doi: 10.1016/j.jaci.2016.09.009
175. Monticelli LA, Sonnenberg GF, Abt MC, Alenghat T, Ziegler CG, Doering TA, et al. Innate Lymphoid Cells Promote Lung-Tissue Homeostasis After Infection With Influenza Virus. *Nat Immunol* (2011) 12(11):1045–54. doi: 10.1038/ni.2131
176. Turner JE, Morrison PJ, Wilhelm C, Wilson M, Ahlfors H, Renauld JC, et al. IL-9-Mediated Survival of Type 2 Innate Lymphoid Cells Promotes Damage Control in Helminth-Induced Lung Inflammation. *J Exp Med* (2013) 210 (13):2951–65. doi: 10.1084/jem.20130071
177. Stark MA, Huo Y, Burcin TL, Morris MA, Olson TS, Ley K. Phagocytosis of Apoptotic Neutrophils Regulates Granulopoiesis *via* IL-23 and IL-17. *Immunity* (2005) 22(3):285–94. doi: 10.1016/j.immuni.2005.01.011
178. Zheng Y, Valdez PA, Danilenko DM, Hu Y, Sa SM, Gong Q, et al. Interleukin-22 Mediates Early Host Defense Against Attaching and Effacing Bacterial Pathogens. *Nat Med* (2008) 14(3):282–9. doi: 10.1038/nm1720
179. Kuwabara T, Ishikawa F, Kondo M, Kakiuchi T. The Role of IL-17 and Related Cytokines in Inflammatory Autoimmune Diseases. *Mediators Inflamm* (2017) 2017:3908061. doi: 10.1155/2017/3908061

180. Fang W, Zhang Y, Chen Z. Innate Lymphoid Cells in Inflammatory Arthritis. *Arthritis Res Ther* (2020) 22(1):25. doi: 10.1186/s13075-020-2115-4
181. Leijten EF, van Kempen TS, Boes M, Michels-van Amelsfort JM, Hijnen D, Hartgring SA, et al. Brief Report: Enrichment of Activated Group 3 Innate Lymphoid Cells in Psoriatic Arthritis Synovial Fluid. *Arthritis Rheumatol* (2015) 67(10):2673–8. doi: 10.1002/art.39261
182. Omata Y, Frech M, Primbs T, Lucas S, Andreev D, Scholtysek C, et al. Group 2 Innate Lymphoid Cells Attenuate Inflammatory Arthritis and Protect From Bone Destruction in Mice. *Cell Rep* (2018) 24(1):169–80. doi: 10.1016/j.celrep.2018.06.005
183. Omata Y, Frech M, Lucas S, Primbs T, Knipfer L, Wirtz S, et al. Type 2 Innate Lymphoid Cells Inhibit the Differentiation of Osteoclasts and Protect From Ovariectomy-Induced Bone Loss. *Bone* (2020) 136:115335. doi: 10.1016/j.bone.2020.115335
184. Wang S, Xia P, Chen Y, Qu Y, Xiong Z, Ye B, et al. Regulatory Innate Lymphoid Cells Control Innate Intestinal Inflammation. *Cell* (2017) 171 (1):201–16.e18. doi: 10.1016/j.cell.2017.07.027
185. Zhang Q, Chen B, Yan F, Guo J, Zhu X, Ma S, et al. Interleukin-10 Inhibits Bone Resorption: A Potential Therapeutic Strategy in Periodontitis and Other Bone Loss Diseases. *BioMed Res Int* (2014) 2014:284836. doi: 10.1155/2014/284836
186. Kasagi S, Chen W. TGF-Beta1 on Osteoimmunology and the Bone Component Cells. *Cell Biosci* (2013) 3(1):4. doi: 10.1186/2045-3701-3-4
187. Di Munno O, Ferro F. The Effect of Biologic Agents on Bone Homeostasis in Chronic Inflammatory Rheumatic Diseases. *Clin Exp Rheumatol* (2019) 37 (3):502–7.
188. Kaji H. Effects of Myokines on Bone. *BoneKEy Rep* (2016) 5:826. doi: 10.1038/bonekey.2016.48
189. Pathak JL, Bakker AD, Verschueren P, Lems WF, Luyten FP, Klein-Nulend J, et al. CXCL8 and CCL20 Enhance Osteoclastogenesis *via* Modulation of Cytokine Production by Human Primary Osteoblasts. *PloS One* (2015) 10(6): e0131041. doi: 10.1371/journal.pone.0131041
190. Fu SC, Wang P, Qi MX, Peng JP, Lin XQ, Zhang CY, et al. The Associations of TNF-Alpha Gene Polymorphisms With Bone Mineral Density and Risk of Osteoporosis: A Meta-Analysis. *Int J Rheum Dis* (2019) 22(9):1619–29. doi: 10.1111/1756-185X.13647
191. Kotrych D, Dziedziejko V, Safranow K, Sroczynski T, Staniszewska M, Juzyszyn Z, et al. TNF-Alpha and IL10 Gene Polymorphisms in Women With Postmenopausal Osteoporosis. *Eur J Obstet Gynecol Reprod Biol* (2016) 199:92–5. doi: 10.1016/j.ejogrb.2016.01.037
192. Weitzmann MN. Bone and the Immune System. *ToxicoL Pathol* (2017) 45 (7):911–24. doi: 10.1177/0192623317735316
193. Zha L, He L, Liang Y, Qin H, Yu B, Chang L, et al. TNF-Alpha Contributes to Postmenopausal Osteoporosis by Synergistically Promoting RANKL-Induced Osteoclast Formation. *Biomedicine Pharmacother = Biomedecine Pharmacother* (2018) 102:369–74. doi: 10.1016/j.biopha.2018.03.080
194. O'Brien W, Fissel BM, Maeda Y, Yan J, Ge X, Gravallese EM, et al. RANK-Independent Osteoclast Formation and Bone Erosion in Inflammatory Arthritis. *Arthritis Rheumatol* (2016) 68(12):2889–900. doi: 10.1002/art.39837
195. Li S, Yin Y, Yao L, Lin Z, Sun S, Zhang J, et al. TNFalpha Treatment Increases DKK1 Protein Levels in Primary Osteoblasts *via* Upregulation of DKK1 mRNA Levels and Downregulation of Mir3355p. *Mol Med Rep* (2020) 22 (2):1017–25. doi: 10.3892/mmr.2020.11152
196. Callaway DA, Jiang JX. Reactive Oxygen Species and Oxidative Stress in Osteoclastogenesis, Skeletal Aging and Bone Diseases. *J Bone Mineral Metab* (2015) 33(4):359–70. doi: 10.1007/s00774-015-0656-4
197. Manolagas SC. From Estrogen-Centric to Aging and Oxidative Stress: A Revised Perspective of the Pathogenesis of Osteoporosis. *Endocrine Rev* (2010) 31(3):266–300. doi: 10.1210/er.2009-0024
198. Locantore P, Del Gatto V, Gelli S, Paragliola RM, Pontecorvi A. The Interplay Between Immune System and Microbiota in Osteoporosis. *Mediators Inflamm* (2020) 2020:3686749. doi: 10.1155/2020/3686749
199. Pacifici R. Bone Remodeling and the Microbiome. *Cold Spring Harbor Perspect Med* (2018) 8(4):1–20. doi: 10.1101/cshperspect.a031203

Conflict of Interest: The authors declare that the research was conducted in the absence of any commercial or financial relationships that could be construed as a potential conflict of interest.

Publisher's Note: All claims expressed in this article are solely those of the authors and do not necessarily represent those of their affiliated organizations, or those of the publisher, the editors and the reviewers. Any product that may be evaluated in this article, or claim that may be made by its manufacturer, is not guaranteed or endorsed by the publisher.

GLOSSARY

ADCC	Antibody-mediated cell cytotoxicity
APCs	Antigen-presenting cells
BMD	Bone mineral density
BMDMs	Bone marrow-derived macrophages
BMMs	Bone marrow macrophages
BMP	Morphogenetic protein
BRC	Bone Remodelling Compartment
CCR2	C-C chemokine receptor 2
CIA	Collagen-induced arthritis
cMoP	Committed monocyte progenitor
COPD	Chronic obstructive pulmonary disease
CSF1	Colony stimulating factor 1
CX3CR1	CXC3 chemokine receptor 1
DAXX	Death-associated protein 6
DC	Dendritic cells
DNAM-1	DNAX accessory molecule-1
EoE	Eosinophilic esophagitis
GCR	Glucocorticoid receptor
HDC	Histidine decarboxylase
HSCs	Hematopoietic stem cells
HSP27	Heat-shock protein 27
IFN	Interferon
IkBα	Inhibitor of NF-kB
ILCs	Innate lymphoid cells
LAD-I	Leukocyte adhesion deficiency type-I
LFA-1	Leucocyte function-associated antigen-1
MAPKs	Mitogen-activated protein kinase
M-CSF	Macrophage colony stimulating factor
MHC II	Major histocompatibility factor II
MSCs	Mesenchymal stem cells
NET	Neutrophils extracellular traps
NFATc	Nuclear factor of activated T-Cells
NLRs	Nod-like receptors
OA	Osteoarthritis
OBs	Osteoblasts
OCs	Osteoclasts
OPG	Osteoprotegerin
OVX	Ovariectomized
OYs	Osteocytes
PBM	Peripheral blood monocytes
PBMCs	Peripheral blood mononuclear cells
pDCs	Plasmacytoid DCs
PI3K	Phosphoinositide 3-kinase
PLK3	Polo-like kinase 3
PMN	Polymorphonuclear
PRRs	Pattern recognition receptors
RA	Rheumatoid arthritis
RANK	Receptor activator of nuclear factor-κB
RANKL	Receptor activator of nuclear factor-κB ligand
ROS	Reactive oxygen species
SDS	Shwachman-Diamond syndrome showing skeletal defects
SF	Synovial fluid
SRs	Scavenger receptors
STAT1	Signal transducer and activator of transcription
TLRs	Toll-like receptors
TNF	Tumor necrosis factor
RAF	TNF receptor-associated factor
TRAP	Tartrate-resistant acid phosphatase

frontiers in Immunology

ORIGINAL RESEARCH
published: 06 August 2021
doi: 10.3389/fimmu.2021.687065

sCD28, sCD80, sCTLA-4, and sBTLA Are Promising Markers in Diagnostic and Therapeutic Approaches for Aseptic Loosening and Periprosthetic Joint Infection

*Jil M. Jubel[1], Thomas M. Randau[1], Janine Becker-Gotot[2], Sebastian Scheidt[1], Matthias D. Wimmer[1], Hendrik Kohlhof[1], Christof Burger[1], Dieter C. Wirtz[1] and Frank A. Schildberg[1]**

[1] Clinic for Orthopedics and Trauma Surgery, University Hospital Bonn, Bonn, Germany, [2] Institute of Experimental Immunology, University Hospital Bonn, Bonn, Germany

OPEN ACCESS

Edited by:
Katharina Schmidt-Bleek, Charité – Universitätsmedizin Berlin, Germany

Reviewed by:
Gergely Toldi, Semmelweis University, Hungary
Youg R Thaker, Sorrento Therapeutics, United States

***Correspondence:**
Frank A. Schildberg
frank.schildberg@ukbonn.de

Specialty section:
This article was submitted to Inflammation, a section of the journal Frontiers in Immunology

Received: 28 March 2021
Accepted: 26 July 2021
Published: 06 August 2021

Citation:
Jubel JM, Randau TM, Becker-Gotot J, Scheidt S, Wimmer MD, Kohlhof H, Burger C, Wirtz DC and Schildberg FA (2021) sCD28, sCD80, sCTLA-4, and sBTLA Are Promising Markers in Diagnostic and Therapeutic Approaches for Aseptic Loosening and Periprosthetic Joint Infection. Front. Immunol. 12:687065. doi: 10.3389/fimmu.2021.687065

Aseptic prosthetic loosening and periprosthetic joint infections (PJI) are among the most frequent complications after total knee/hip joint arthroplasty (TJA). Current research efforts focus on understanding the involvement of the immune system in these frequent complications. Different immune cell types have already been implicated in aseptic prosthetic loosening and PJI. The aim of this study was to systematically analyze aspirates from knee and hip joints, evaluating the qualitative and quantitative composition of soluble immunoregulatory markers, with a focus on co-inhibitory and co-stimulatory markers. It has been shown that these molecules play important roles in immune regulation in cancer and chronic infectious diseases, but they have not been investigated in the context of joint replacement. For this purpose, aspirates from control joints (i.e., native joints without implanted prostheses), joints with TJA (no signs of infection or aseptic loosening), joints with aseptic implant failure (AIF; i.e., aseptic loosening), and joints with PJI were collected. Fourteen soluble immunoregulatory markers were assessed using bead-based multiplex assays. In this study, it could be shown that the concentrations of the analyzed immunoregulatory molecules vary between control, TJA, AIF, and PJI joints. Comparing TJA patients to CO patients, sCD80 was significantly elevated. The marker sBTLA was significantly elevated in AIF joints compared to TJA joints. In addition, a significant difference for eight markers could be shown when comparing the AIF and CO groups (sCD27, sCTLA-4, sCD137, sCD80, sCD28, sTIM-3, sPD-1, sBTLA). A significant difference was also reached for nine soluble markers when the PJI and CO groups were compared (sLAG-3, sCTLA-4, sCD27, sCD80, sCD28, sTIM-3, sPD-1, IDO, sBTLA). In summary, the analyzed immunoregulatory markers could be useful for diagnostic purposes as well as to develop new therapeutic approaches for AIF and PJI.

Keywords: aseptic loosening, periprosthetic joint infection, immunoregulatory markers, sCD28, sCD80, sCTLA-4, sBTLA, osteoimmunology

INTRODUCTION

In recent years, the continuously aging population and associated age-related morbidity have led to a marked increase in the number of implanted joint endoprostheses (1–3). As a result, an increase in consequent complications has been observed (2). These primarily include aseptic prosthetic loosening (referred to in this study as aseptic implant failure (AIF)) and peri-implant fractures, and also prosthetic joint infections (PJI), which can lead to septic prosthetic loosening (4–6). These typical complications can lead to significant limitations in daily activities due to pain, immobility, and chronic infections (7).

Current research efforts focus on understanding the immune system involvement, both qualitatively and quantitatively, in these frequent complications. Specific cell types of the immune system have been implicated in AIF (aseptic loosening) and PJI. As important mediators of osteolysis, macrophages play a significant role in the former complication (5, 8).

A new field of intensive research is the regulation of the immune system by immunoregulatory molecules, with a particular focus on so-called checkpoint molecules. These checkpoint molecules play an important role in immune regulation in cancer and chronic infectious diseases (9–12). At first, it was assumed that the main cells that are influenced by these molecules are T cells (10, 13–15). It is now known that these immunoregulatory markers also regulate other immune cells, such as macrophages, monocytes, and B cells (16, 17). Checkpoint molecules can be classified into co-stimulatory and co-inhibitory molecules. Co-stimulatory molecules, such as cluster of differentiation 27 (CD27), CD28, and glucocorticoid-induced TNFR-related protein (GITR), enhance the T cell response, while co-inhibitory molecules, such as programmed cell death protein 1 (PD-1) or cytotoxic T-lymphocyte-associated protein 4 (CLTA-4), reduce it (10, 18–20). Recently, soluble forms of checkpoint molecules, such as sPD-1 (soluble PD-1), sPD-L2 (soluble PD-L2), and sCTLA-4 (soluble CTLA-4) were found (21). Their role is not yet understood but first studies have shown that these soluble forms of checkpoint molecules can be involved in positive or negative immune regulation. Furthermore, the development, prognosis, and treatment of cancer (lung, gastric or renal cell cancer) and infectious diseases (hepatitis B) may be affected by changes in the plasma levels of soluble immune markers (22–25).

A recent PubMed query showed that there has not yet been a systematic evaluation of the associations between the concentrations of soluble immunoregulatory molecules and joint implant-associated complications.

Differentiation between aseptic and septic joint inflammation is difficult. Neither clinical nor biochemical markers can distinguish abacterial from bacterial joint inflammation, despite assessment of markers obtained from clinical examinations, blood and joint aspirate analyses, and microbiological and histological tissue analyses (26). For example, a negative bacterial result in a joint aspirate does not reliably exclude a bacterial infection (27, 28). Currently, different scoring systems are used to diagnose a PJI. MSIS criteria, for example, consist of several major and minor parameters. Based on this scoring system, a PJI is diagnosed when one out of two major criteria (two microorganism-positive cultures indicating the same pathogen; sinus tract communicating with the prosthesis) or three out of five minor criteria are fulfilled (CRP >10 mg/L; joint aspirate: leukocytes >3000 cells/µL, neutrophils >85%; single microorganism-positive tissue/aspirate sample; positive histology).

It is crucial to diagnose PJI early, differentiating septic from aseptic implant loosening so that specific therapy can be initiated at an early stage (29). If inflammation is treated inadequately, irreversible joint damage can occur, such as cartilage destruction with subsequent arthrosis and ankylosis (30). These changes can lead to functional loss of the affected joint and thus to permanent disabilities that affect everyday life. If the PJI progresses, the "ultima ratio" is amputation of the affected limb to save the patient's life (31, 32).

The aim of this study was to systematically analyze aspirates from knee and hip joints, evaluating the qualitative and quantitative composition of soluble immunoregulatory markers for evaluating their potential as disease markers. For this purpose, aspirates from control (CO) joints (i.e., native joints without implanted prostheses), joints with total joint arthroplasty (TJA, i.e., fixed prostheses), joints with aseptic implant failure (AIF; i.e., aseptic loosening), and joints with periprosthetic joint infection (PJI) were evaluated and compared. The working hypothesis was that the qualitative and quantitative composition of soluble immunoregulatory molecules exhibits specific variations in aspirates from control, TJA, AIF, and PJI joints. Furthermore, one or more biomarkers may be specific for AIF or PJI. The identification of such biomarkers could lead to a better understanding of the pathomechanisms and new diagnostic and therapeutic approaches.

MATERIAL AND METHODS

Study Population

Consecutive patients (n = 99) treated between 2016 and 2019 at the Clinic for Orthopedics and Trauma Surgery of the University Hospital Bonn, Germany, were recruited. The patients were aged 18–100 years and had undergone synovial fluid aspiration for diagnostic or therapeutic purposes. Patients with sepsis or extra-articular infection were excluded. The included patients were divided into four groups: control (CO) patients with native joints (no prosthesis and no signs of infection); patients with fixed TJA (no signs of infection or aseptic loosening); patients with AIF (i.e., aseptic loosening); and patients with PJI. The ethics committee of the University of Bonn, Germany, approved the study, which was conducted according to the approved guidelines and the Helsinki Declaration.

Classification

The classification developed by the Musculoskeletal Infection Society (MSIS) was used to identify patients with PJI. PJI was diagnosed when one major criterion (out of two major criteria) or three minor criteria (out of five minor criteria) were fulfilled. The major criteria are two microorganism-positive cultures (based on aspirate/tissue samples), indicating the same pathogen and sinus tract communicating with the prosthesis. The minor criteria are CRP >10 mg/L, leukocytes >3000 cells/µL of joint aspirate,

neutrophils >85% in joint aspirate, single microorganism-positive tissue/aspirate sample, and positive histology. The diagnosis of AIF (aseptic loosening) was determined based on the MSIS criteria, clinical examination, and radiological signs.

Data Collection

Data were collected on patient gender, age, BMI, and comorbidities (**Table 1**). In addition, laboratory results such as serum C-reactive protein (CRP), preoperative blood leukocyte counts, joint aspirate cell counts, intraoperative findings, sonication microbiology, and histopathology results were obtained from the medical records. All data were recorded in Microsoft Excel (Microsoft Corporation, Redmond, WA, USA).

Aspirate Sample Collection

Preoperative or intraoperative hip or knee joint aspirates had previously been obtained during diagnostic or therapeutic procedures, and the material not used for clinical diagnostics was utilized in this study. Each synovial fluid sample was centrifuged at 1200 rpm for 10 min (Centrifuge 5810 R; Eppendorf AG, Hamburg, Germany) to remove the cellular components. The resulting supernatant was transferred in 0.5-mL aliquots and stored at -80°C.

Bead-Based Multiplex Assays

Various soluble cytokines were measured using Immuno-Oncology Checkpoint 14-plex ProcartaPlex™ bead-based assays (ThermoFisher, Waltham, MA, USA) according to the manufacturer's instructions. The detected soluble targets were: B- and T-lymphocyte attenuator (BTLA), glucocorticoid-induced TNFR-related protein (GITR), herpesvirus entry mediator (HVEM), indolamin-2,3-dioxygenase (IDO), lymphocyte-activation gene 3 (LAG-3), programmed cell death protein 1 (PD-1), programmed cell death 1 ligand 1 (PD-L1), programmed cell death 1 ligand 2 (PD-L2), T-cell immunoglobulin and mucin-domain containing-3 (TIM-3), cluster of differentiation 28 (CD28), CD80, CD137, CD27, and cytotoxic T-lymphocyte-associated protein 4 (CTLA-4). All samples were immediately thawed before conducting the assay. The wells were prewetted with 10 µL reading buffer and the antibody-labelled magnetic beads were vortexed for 30 s. Next, 12.5 µL of the beads was added to each well. After washing the wells, 12.5 µL of samples (or standards provided with the assay kit) was added to the beads in the wells and incubated in the dark for 120 min at room temperature, with shaking. The beads were then washed twice. Next, 6.25 µL detection antibody mixture was added to each well and incubated in the dark for another 30 min, with shaking. After washing the beads, 12.5 µL streptavidin-phycoerythrin (PE) was added to the wells and the beads were again incubated in the dark for 30 min, with shaking. Following another washing step, the beads were resuspended in 50 µL reading buffer for 5 min, with shaking. Finally, data were acquired using a Flexmap 3D® system (Luminex Corporation, Austin, TX, USA). The raw data were transferred to a Microsoft Excel (Microsoft Corporation, Redmond, WA, USA) table for further analysis.

Statistical Analysis

SPSS version 27 (IBM Corp., Armonk, NY, USA) was used for statistical analysis. The Kolmogorov–Smirnova test was performed to assess normality. The Kruskal-Wallis test was used to evaluate the statistical significance of the differences among the four groups. The Dunn's Test was performed as post-hoc-test. The level of significance was set at $p < 0.05$ (* < 0.05, ** < 0.01, *** < 0.001). Descriptive statistics were calculated using GraphPad Prism 9 (GraphPad Software, La Jolla, CA, USA). All results are presented using boxplots showing the median and interquartile range (IQR).

RESULTS

The qualitative and quantitative composition of soluble immunoregulatory markers, focusing on co-inhibitory and co-stimulatory markers, was evaluated. Aspirates from control joints, joints with fixed TJA (no signs of infection or aseptic loosening), joints with AIF (aseptic loosening), and joints with PJI were compared.

Patient information is presented in **Table 1**. The overall male-to-female ratio was 2:3. The control patients were younger (mean age 48 years) than the patients with TJA (mean age 65 years) and the patients with periprosthetic complications (AIF: mean age 72 years, PJI: mean age 71 years). Furthermore, the control patients had a lower BMI (26 kg/m^2) than the patients in the other three cohorts (TJA: 33 kg/m^2, AIF: 32 kg/m^2, PJI: 33 kg/m^2). Preoperative routine blood analysis showed an increased level of CRP for PJI patients (92 mg/dl), and 44% of the PJI patients had diabetes mellitus.

TABLE 1 | Patient characteristics (n = 99).

Variable	Overall (n = 99)	CO (n = 13)	TJA (n = 23)	AIF (n = 24)	PJI (n = 39)
Age (year)	67 ± 13	48 ± 13	65 ± 10	72 ± 9	71 ± 12
Gender (m:f)	39:60	7:6	10:13	7:17	15:24
Hip	35	2	6	11	16
Knee	64	11	17	13	23
BMI (kg/m^2)	32 ± 8	26 ± 4	33 ± 6	32 ± 6	33 ± 11
Diabetes mellitus	23	1	3	2	17
Rheumatoid arthritis	10	1	3	2	4
CRP (mg/dl)	46 ± 106	2.4 ± 0.7	14 ± 20	8.9 ± 8.9	92 ± 24
Leukocytes (10^9/l)	8.6 ± 3	8.5 ± 0.8	7.6 ± 1.6	8.2 ± 2.9	9 ± 0.6

Data are presented as mean ± standard deviation or as frequency. Patients with a prothesis were in general older than control patients without one. PJI patients had the highest concentration of CRP and leukocytes. CO, control group; TJA, total joint arthroplasty; AIF, aseptic implant failure; PJI, periprosthetic joint infection; BMI, body mass index; CRP, C-reactive protein.

Table 2 shows the mean concentrations of the 14 soluble immunoregulatory markers from hip and knee aspirates (based on bead-based multiplex assays) in each of the four groups. Overall, the control patients tended to have the lowest mean concentrations of immunoregulatory markers. TJA patients tended to have higher mean concentrations than control patients, while AIF patients tended to have higher concentrations than TJA patients. For many markers, the highest mean concentration was found in PJI patients, though sBTLA, sCD80, and sCD27 were higher in AIF patients than PJI patients (**Table 2**).

Figure 1 shows boxplots of the data regarding all 14 immunoregulatory markers, expressed as the median and interquartile range (IQR). In general, the lowest median concentrations of the markers were found in the control patients, whereas the highest were found in either AIF patients (sPD-1, sPD-L1, sPD-L2, sBTLA, sCD80, and sCD137) or PJI patients (sCTLA-4, sTIM-3, sLAG-3, sHVEM, IDO, sCD28, sCD27, and sGITR).

Regarding the results of the Kruskal-Wallis test, TJA patients tended to have higher concentrations than control patients, with significant levels being reached for the co-stimulatory marker sCD80 ($p = 0.015$) (**Figure 1**). In addition, the majority of the concentrations were also significantly higher in AIF patients than in control patients, with sCD28, sCD80, and sBTLA reaching a significance of $p < 0.01$ (**Figure 1**). Moreover, differences in concentrations between the PJI and control groups were significant, with sCTLA-4, IDO, sCD28, and sCD80 reaching a significance of $p < 0.001$ (**Figure 1**).

As shown in **Table 2**, the mean concentrations of all immunoregulatory markers were higher in AIF patients than in TJA patients, except for sCD137 (TJA: 11892.73 pg/ml, AIF: 10649.00 pg/ml). For example, the mean concentration of the co-inhibitory markers PD-1 was 171.75 pg/ml in AIF patients and only 120.61 pg/ml in TJA patients. Regarding the results of the Kruskal-Wallis test concerning the median concentrations, significantly higher levels were found in AIF patients compared to TJA patients for sBTLA ($p = 0.036$) (**Figure 1**).

Additionally, the mean concentrations of all 14 immunoregulatory markers (sCTLA-4, sPD-1, sPD-L1, sPD-L2, sTIM-3, sLAG-3, sBTLA, sHVEM, IDO, sCD28, sCD80, sCD27, sGITR, and sCD137) were higher in PJI patients compared to TJA patients. Kruskal-Wallis tests analyzing the median concentrations showed that sCTLA-4 and IDO reached a significance of $p < 0.001$ (**Figure 1**).

The mean concentrations in PJI patients were generally higher than in AIF patients (**Table 2**). However, AIF patients had higher levels of sBTLA, sCD80, and sCD27 compared to PJI patients. Investigating the median concentrations, no significant differences could be detected (**Figure 1**).

Additionally, we performed supplemental analyses to compare the marker concentrations of hip aspirates in comparison to knee aspirates. No significant trends could be seen, except for sLAG-3 in the PJI group (**Supplementary Table 1**). We also investigated whether diabetes mellitus (DM) had an influence on the investigated markers. In this study, only patients with a DM type II were found. When comparing DM patients with non-DM patients, we could not detect any significant difference (**Supplementary Table 2**). Interesting was the fact that the majority of patients with DM were in the PJI group. Similarly, also no significant difference could be found when comparing patients with and without rheumatoid arthritis (RA) (**Supplementary Table 3**).

In summary, the concentrations of the measured immunoregulatory markers differed between control (native), TJA, AIF, and PJI joints. The lowest levels were generally found in control joints, followed by TJA joints. Higher concentrations were generally found in AIF joints and the highest concentrations were generally found in PJI joints.

DISCUSSION

According to Wengler et al., the number of primary hip arthroplasties in Germany increased by 10.9% to 155,300 per year between 2005 and 2011 (33). During the same period, primary knee arthroplasty procedures increased by 21.6% to 152,500 per year (33).

TABLE 2 | Mean concentrations according to bead-based multiplex assays.

Marker	CO (pg/ml)	TJA (pg/ml)	AIF (pg/ml)	PJI (pg/ml)
sCTLA-4	*59.33 ± 16.92*	222.52 ± 73.29	236.29 ± 33.73	**450.03 ± 58.53**
sPD-1	*32.77 ± 15.32*	120.61 ± 35.10	171.75 ± 28.99	**253.74 ± 59.44**
sPD-L1	*15.31 ± 6.60*	40.83 ± 19.62	92.38 ± 21.37	**289.92 ± 116.94**
sPD-L2	9113.77 ± 2417. 93	*8808.78 ± 1953.44*	15516.71 ± 1977.11	**15966.54 ± 1948.67**
sTIM-3	*6534.31 ± 753.27*	8435.04 ± 931.20	10649.71 ± 743.64	**11032.33 ± 805.93**
sLAG-3	*168.15 ± 67.58*	208.61 ± 49.94	276.38 ± 46.48	**319.69 ± 38.40**
sBTLA	*594.92 ± 199.10*	2220.57 ± 1125.36	**4053.50 ± 818.41**	3716.62 ± 674.90
sHVEM	*13.31 ± 13.31*	140.00 ± 453.79	541.00 ± 2064.83	**896.97 ± 437.64**
IDO	*38.46 ± 16.09*	171.04 ± 83.37	675.17 ± 291.29	**1892.77 ± 519.09**
sCD28	*200.58 ± 167.92*	1956.35 ± 764.85	3300.63 ± 663.01	**4547.46 ± 717.21**
sCD80	*238.23 ± 66.18*	1661.00 ± 450.41	**1911.00 ± 195.57**	1671.92 ± 184.79
sCD27	*5610.23 ± 2444.59*	10570.39 ± 2774.63	**34988.13 ± 8975.34**	32088.36 ± 5436.80
sGITR	59.08 ± 24.95	*55.61 ± 21.63*	70.79 ± 15.44	**175.97 ± 46.54**
sCD137	*1832.83 ± 606.11*	11892.73 ± 3469.32	10649.00 ± 3051.80	**14389.70 ± 8378.15**

Concentrations (pg/ml) of 14 immunoregulatory markers in hip and knee joint aspirates in each of the four groups are expressed as mean ± standard deviation. The highest values in each row are indicated in bold and the lowest values in italic. CO, control group; TJA, total joint arthroplasty; AIF, aseptic implant failure; PJI, periprosthetic joint infection; s, soluble; CTLA-4, cytotoxic T-lymphocyte-associated protein 4; PD-1, programmed cell death protein 1; PD-L1, programmed cell death 1 ligand 1; PD-L2, programmed cell death 1 ligand 2; TIM-3, T-cell immunoglobulin and mucin-domain containing-3; LAG-3, lymphocyte-activation gene 3; BTLA, B- and T-lymphocyte attenuator; HVEM, herpesvirus entry mediator; IDO, indolamin-2,3-dioxygenase; GITR, glucocorticoid-induced TNFR-related protein; CD, cluster of differentiation.

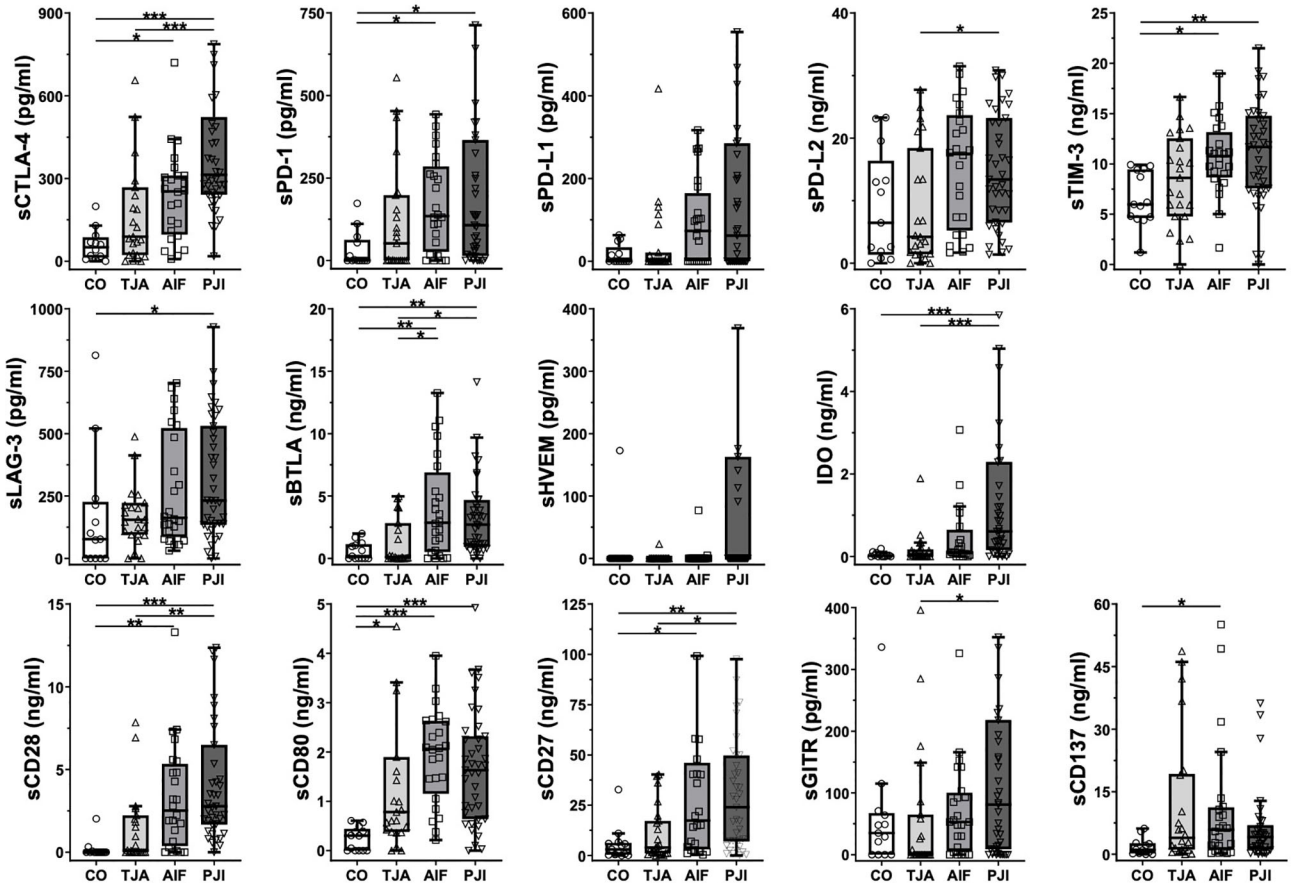

FIGURE 1 | Boxplots of the analyzed immunoregulatory markers. Boxplots show the median and interquartile range for each marker. Concentrations are given in pg/ml or ng/ml. In general, the control (CO) patients tended to have the lowest concentrations, whereas the highest concentrations were measured in AIF (sPD-1, sPD-L1, sPD-L2, sBTLA, sCD80, and sCD137) or PJI (sCTLA-4, sTIM-3, sLAG-3, sHVEM, IDO, sCD28, sCD27, and sGITR) patients. CO, control group; TJA, total joint arthroplasty; AIF, aseptic implant failure; PJI, periprosthetic joint infection; s, soluble; CTLA-4, cytotoxic T-lymphocyte-associated protein 4; PD-1, programmed cell death protein 1; PD-L1, programmed cell death 1 ligand 1; PD-L2, programmed cell death 1 ligand 2; TIM-3, T-cell immunoglobulin and mucin-domain containing-3; LAG-3, lymphocyte-activation gene 3; BTLA, B- and T-lymphocyte attenuator; HVEM, herpesvirus entry mediator; IDO, indolamin-2,3-dioxygenase; GITR, glucocorticoid-induced TNFR-related protein; CD, cluster of differentiation. *$p < 0.05$, **$p < 0.01$, ***$p < 0.001$.

One complication of endoprosthesis is aseptic joint inflammation, which can lead to AIF (aseptic implant failure). Another complication is septic joint inflammation caused by a bacterial infection (PJI), which can lead to septic prosthetic loosening. Wooley et al. reported that aseptic prosthetic loosening occurs in 20–25% of endoprosthetic implants (34), and approximately 1–2% of primary implants become infected, according to Trampuz et al. (2). These complications play significant roles in routine clinical practice, as patients experience severe reductions in quality of life, and the costs of treatment burden the healthcare system (2, 35, 36).

The variations in human immune responses related to joint endoprostheses, AIF, and PJI are not yet fully understood. This study presents an analysis of various soluble immunoregulatory markers (focusing on checkpoint molecules) in joint aspirates obtained during diagnostic or therapeutic procedures.

Checkpoint molecules play an essential role in modulating immune cells (11, 18). They are best known for regulating T cells, though it is now recognized that other immune cells, such as macrophages and monocytes, are also controlled by these molecules (16, 17). T cells are part of the adaptive immune system, i.e., the acquired immune response that acts against specific pathogens. Antigen-presenting cells present previously phagocytosed antigens *via* the major histocompatibility complex (MHC) (37, 38). The MHC binds to the T cell receptor on T cells, which activates them (38–40). Parry et al. found that MHC-dependent antigen presentation alone is not sufficient for T cell activation. A second immunoregulatory signal, a so-called checkpoint molecule, is necessary (41, 42). These molecules either have activating (i.e., co-stimulatory) or inhibiting (i.e., co-inhibitory) effects. Co-stimulatory markers promote T cell activation, proliferation, and differentiation; co-inhibitory markers inhibit T cell functioning and activation (43–45).

In tumors and various chronic infectious diseases, checkpoint molecules play important roles in regulating the immune response (10, 18). For example, in these diseases, PD-1 is

upregulated. This results in the inhibition of immune cell activity so that pathological cells can hide from the immune system (46). This finding has already been applied in tumor therapy. For example, anti-PD-1 antibodies are used to treat melanomas and non-small cell lung cancer (11, 47).

Recently, soluble forms of checkpoint molecules were also found. In contrast to checkpoint molecules on the cell surface, they are less well studied and their role in immune regulation is not well understood. They can be generated *via* expression of the soluble form or by the cleavage of membrane-bound proteins by immune cells or tumor cells (21, 48, 49). There are no robust data for the correlation between the concentration of the soluble markers in synovial fluid or serum with their expression on the surface of immune cells. However, it is assumed that the stronger the surface expression of the markers, the greater the number of soluble markers found in synovial fluid.

In this study, we found that the mean concentrations of soluble immunoregulatory markers were generally lowest in control joints, TJA joints generally had lower concentrations than AIF joints, and PJI joints tended to have the highest concentrations, while sCD27, sBTLA, and sCD80 were the exceptions.

Our study revealed a significant difference for sCD80 comparing the CO and TJA groups, with higher mean concentrations in the TJA group. sCD80 is expressed by monocytes and B cells and is generated by alternative splicing (49). Whereas Kakoulidou et al. found an inhibitory effect on lymphocyte reactions and T cell proliferation, various other studies could describe an enhancement of T cell proliferation and IFN-γ production (21, 49–52). Furthermore, Haile et al. showed that a soluble form of CD80, CD80-Fc, was more effective in preventing the coinhibitory effect of the PD-1/PD-L1 pathway and in restoring T cell activation in comparison to blocking either PD-1 or PD-L1 with antibodies (52). Overlaying this finding with our data, the increased concentration of sCD80 in the TJA group compared to the CO group supports the idea that the prosthesis might activate the local immune system in the joint.

CD80 is expressed by macrophages, which are known to play an important role in aseptic loosening. Particles abraded from the prosthesis activate macrophages and promote osteoclast differentiation (53). This leads to local bone loss, which, in turn, can lead to aseptic loosening of the implant. In our data set, AIF patients showed a higher mean concentration of sCD80 than any other group and reached a statistical significance of < 0.001 when comparing AIF patients with the CO group. These findings suggest a role of macrophages and sCD80 in aseptic loosening. Furthermore, these data also suggest that blocking sCD80 to reduce an activation of the immune system activation could be a possible therapeutic option.

Another interesting soluble checkpoint molecule in our study is sCTLA-4. This marker presented the highest mean concentration in the PJI group and reached a significance < 0.001 when comparing the PJI and CO groups. sCTLA-4 is released by Treg cells, monocytes and immature DCs (48). Higher levels were found during immune activation and in different autoimmune and inflammatory diseases such as lupus, autoimmune thyroiditis, myasthenia gravis, and celiac disease (54–57). Furthermore, in different tumors a high level of sCTLA-4 was associated with a poor prognosis (58, 59). It could be shown that sCTLA-4, similarly to CTLA-4, inhibits T cells. Blocking sCTLA-4 led to elevated levels of cytokines, especially IFN-γ (21, 60). In contrast, other studies found that sCTLA-4 inhibits the inhibitory effect of CTLA-4 on T cells (61, 62). One possible explanation for these contradictory findings might be that the effects of sCTLA-4 depend on the activation status of the involved cells. Whereas sCTLA-4 might inhibit the CD80-CD28 interaction on resting cells, it may inhibit the CD80-CTLA-4 interaction on activated T cells, thereby preventing the inhibition of T cells. In PJI, inhibitory effects on T cells might promote the persistence of the infection. Thus, blocking sCTLA-4 may possibly lead to T cell activation and proliferation and represent a possible therapy.

Based on our data, sCD28 could also be another therapeutic avenue. However, not much is known about this molecule in the current literature. sCD28 is expressed by T cells and increased in autoimmune diseases such as lupus, Sjögren's syndrome, allergic asthma and SLE (63–65). There are, however, as yet no data regarding its mechanism of action.

Our analysis of sBTLA found a significant difference between the AIF with TJA group ($p = 0.036$). Gorgulho et al. could show a positive correlation of sBTLA and BTLA expression on the cell surface (66). Soluble BTLA is increased in sepsis (67, 68). Dong et al. and Bian et al. showed that sBTLA correlated with a poor prognosis in HCC and pancreatic adenocarcinoma (69, 70). Furthermore, it correlated with the risk of death in clear cell renal cell carcinoma patients (22). There are different hypotheses how sBTLA could regulate the immune system. One possibility is that sBTLA could competitively bind HVEM on antigen presenting cells. On the other hand, it's plausible that sBTLA mimics the inhibitory effect of sCTLA-4 (66). Thinking along this line, the elevated sBTLA in our study could regulate the immune system activation in aseptic loosening. Therefore, targeting this molecule might be useful in the therapy of AIF.

Differentiation between aseptic and septic loosening (which are related to AIF and PJI, respectively) is a big problem in everyday clinical practice; currently, neither clinical nor laboratory parameters can be used to clearly differentiate them (26). Various diagnostic tools, such as the MSIS criteria, are currently being used to diagnose PJI (2, 71). However, there is still no proper gold standard for diagnosis. The distinction between aseptic and septic joint inflammation is vital for subsequent treatment. In cases of AIF, the aseptically loosened prostheses can generally be immediately exchanged. PJI must typically be addressed several times (31). For the patient, PJI also means taking antibiotics and experiencing chronic health complaints (31). Comparing the mean concentration of the PJI and AIF group in this study, the PJI group showed higher levels. However, using the Kruskal-Wallis test, no significant difference between the two groups could be shown. Therefore, it could not be found a useful biomarker to differ a PJI from an AIF.

As mentioned earlier, PJI is usually a chronic infection. The role of immunoregulatory markers has already been investigated

multiple times in other chronic diseases (9, 10, 72). In chronic infectious diseases such as HIV or HCV infections, co-inhibitory molecules, e.g., PD-1, show increased concentration (73, 74). Based on previous findings and the current findings, the assumption arises that these co-inhibitory markers play an important role in the immune response during PJI. By inhibiting the immune system, they pave the way for chronic disease. The infection persists within the joint and is not effectively resolved. Targeted blocking of these co-inhibitory markers using antibodies might neutralize the inhibition of the immune system. The infection may then be better addressed by the subsequent increased immune response and thus, satisfactorily treated.

However, one important next step for better diagnostic and therapeutic approaches utilizing the biology of soluble checkpoint inhibitors is not only a better understanding of their expression and mechanism of action but also how reproducible they are across different patient cohorts with differences in age, medication, site of surgery or comorbidities.

To address a potential influence of the site of surgery, we compared the level of checkpoint molecules of hip aspirates in comparison to knee aspirates. No significant trends could be found, except for sLAG-3 in the PJI group. If such an effect can be confirmed in a larger cohort, this would open up a very interesting discussion about differences of the local immunological microenvironment and how this could be used for targeted therapy.

As mentioned before, other comorbidities also need to be investigated in more detail. In this study, 10 patients out of 99 patients presented a RA. Previous publications could show that the levels of soluble immune checkpoints, such as sCD28, sCTLA-4, sCD80, and sPD-1 were higher in RA patients compared to patients without RA (75, 76). In our study, there was no significant difference between patients with and without RA. It is possible that the effect of an implanted protheses, aseptic loosening or PJI on the immune system might influence the expression profile of checkpoint molecules and disguise the influence of the RA. However, the value of this subgroup analysis is very limited due to the few numbers of RA patients. A significantly larger cohort is needed to allow for sufficient statistical power to perform meaningful statistics on the effect of RA. We also investigated whether DM type 2 had an influence on the investigated markers but could not find significant differences. It is noteworthy that most patients with DM type 2 were in the PJI group. This could be explained by the fact that patients with DM type 2 are prone to infections, especially periprosthetic joint infections (77, 78). In addition, DM type 2 is associated with obesity in the context of the metabolic syndrome and patients with a higher BMI have a higher risk for infections (77–79). These subgroup analyses imply that checkpoint molecules are not or only slightly influenced by the site of surgery, RA or DM type 2; however, such analyses have to be repeated in larger (multi-center) studies to clearly verify the comparability of patient groups.

Future studies should continue to investigate the roles of soluble immunoregulatory markers in aseptic and septic joint inflammation. There is hope that this could result in new diagnostic and therapeutic approaches for aseptic and septic joint inflammation. Targeted inhibition of particular markers with antibodies may also influence the chronic course of PJI and result in successful eradication of the infection.

In summary, this study demonstrates that the concentrations of the analyzed immunoregulatory molecules varied between control, TJA, AIF, and PJI joints. Ultimately, this study suggests that immunoregulatory markers, such as sBTLA (AIF vs. TJA) or sCD28 and sCTLA-4 (PJI vs. TJA), could be useful for diagnostic purposes as well as to develop new therapeutic approaches for AIF and PJI.

DATA AVAILABILITY STATEMENT

The original contributions presented in the study are included in the article/**Supplementary Material**. Further inquiries can be directed to the corresponding author.

ETHICS STATEMENT

The studies involving human participants were reviewed and approved by the ethics committee of the University of Bonn, Germany. The patients/participants provided their written informed consent to participate in this study.

AUTHOR CONTRIBUTIONS

All authors listed have made a substantial, direct, and intellectual contribution to the work, and approved it for publication.

FUNDING

This work was supported by a grant from the National Multiple Sclerosis Society (RG 1809-32591 to FS).

ACKNOWLEDGMENTS

We appreciate the technical assistance provided by Ms. Cäcilia Hilgers and Mr. Werner Masson. This work is part of the doctoral thesis of JJ.

SUPPLEMENTARY MATERIAL

The Supplementary Material for this article can be found online at: https://www.frontiersin.org/articles/10.3389/fimmu.2021.687065/full#supplementary-material

REFERENCES

1. Kurtz S, Ong K, Lau E, Mowat F, Halpern M. Projections of Primary and Revision Hip and Knee Arthroplasty in the United States From 2005 to 2030. *J Bone Joint Surg Am* (2007) 89(4):780–5. doi: 10.2106/00004623-200704000-00012
2. Izakovicova P, Borens O, Trampuz A. Periprosthetic Joint Infection: Current Concepts and Outlook. *EFORT Open Rev* (2019) 4(7):482–94. doi: 10.1302/2058-5241.4.180092
3. Maradit Kremers H, Larson DR, Crowson CS, Kremers WK, Washington RE, Steiner CA, et al. Prevalence of Total Hip and Knee Replacement in the United States. *J Bone Joint Surg Am* (2015) 97(17):1386–97. doi: 10.2106/JBJS.N.01141
4. Del Pozo JL, Patel R. Clinical Practice. Infection Associated With Prosthetic Joints. *N Engl J Med* (2009) 361(8):787–94. doi: 10.1056/NEJMcp0905029
5. Landgraeber S, Jager M, Jacobs JJ, Hallab NJ. The Pathology of Orthopedic Implant Failure Is Mediated by Innate Immune System Cytokines. *Mediators Inflammation* (2014) 2014:185150. doi: 10.1155/2014/185150
6. Koh CK, Zeng I, Ravi S, Zhu M, Vince KG, Young SW. Periprosthetic Joint Infection Is the Main Cause of Failure for Modern Knee Arthroplasty: An Analysis of 11,134 Knees. *Clin Orthop Relat Res* (2017) 475(9):2194–201. doi: 10.1007/s11999-017-5396-4
7. Helwig P, Morlock J, Oberst M, Hauschild O, Hubner J, Borde J, et al. Periprosthetic Joint Infection–Effect on Quality of Life. *Int Orthop* (2014) 38 (5):1077–81. doi: 10.1007/s00264-013-2265-y
8. Yang F, Wu W, Cao L, Huang Y, Zhu Z, Tang T, et al. Pathways of Macrophage Apoptosis Within the Interface Membrane in Aseptic Loosening of Prostheses. *Biomaterials* (2011) 32(35):9159–67. doi: 10.1016/j.biomaterials.2011.08.039
9. Jubel JM, Barbati ZR, Burger C, Wirtz DC, Schildberg FA. The Role of PD-1 in Acute and Chronic Infection. *Front Immunol* (2020) 11:487. doi: 10.3389/fimmu.2020.00487
10. Attanasio J, Wherry EJ. Costimulatory and Coinhibitory Receptor Pathways in Infectious Disease. *Immunity* (2016) 44(5):1052–68. doi: 10.1016/j.immuni.2016.04.022
11. Baumeister SH, Freeman GJ, Dranoff G, Sharpe AH. Coinhibitory Pathways in Immunotherapy for Cancer. *Annu Rev Immunol* (2016) 34:539–73. doi: 10.1146/annurev-immunol-032414-112049
12. Leach DR, Krummel MF, Allison JP. Enhancement of Antitumor Immunity by CTLA-4 Blockade. *Science* (1996) 271(5256):1734–6. doi: 10.1126/science.271.5256.1734
13. Wherry EJ, Kurachi M. Molecular and Cellular Insights Into T Cell Exhaustion. *Nat Rev Immunol* (2015) 15(8):486–99. doi: 10.1038/nri3862
14. Patsoukis N, Bardhan K, Chatterjee P, Sari D, Liu B, Bell LN, et al. PD-1 Alters T-Cell Metabolic Reprogramming by Inhibiting Glycolysis and Promoting Lipolysis and Fatty Acid Oxidation. *Nat Commun* (2015) 6:6692. doi: 10.1038/ncomms7692
15. Francisco LM, Salinas VH, Brown KE, Vanguri VK, Freeman GJ, Kuchroo VK, et al. PD-L1 Regulates the Development, Maintenance, and Function of Induced Regulatory T Cells. *J Exp Med* (2009) 206(13):3015–29. doi: 10.1084/jem.20090847
16. Huang X, Venet F, Wang YL, Lepape A, Yuan Z, Chen Y, et al. PD-1 Expression by Macrophages Plays a Pathologic Role in Altering Microbial Clearance and the Innate Inflammatory Response to Sepsis. *PNAS* (2009) 106 (15):6303–8. doi: 10.1073/pnas.0809422106
17. Schildberg FA, Klein SR, Freeman GJ, Sharpe AH. Coinhibitory Pathways in the B7-CD28 Ligand-Receptor Family. *Immunity* (2016) 44(5):955–72. doi: 10.1016/j.immuni.2016.05.002
18. Parry RV, Chemnitz JM, Frauwirth KA, Lanfranco AR, Braunstein I, Kobayashi SV, et al. CTLA-4 and PD-1 Receptors Inhibit T-Cell Activation by Distinct Mechanisms. *Mol Cell Biol* (2005) 25(21):9543–53. doi: 10.1128/MCB.25.21.9543-9553.2005
19. Anderson KM, Czinn SJ, Redline RW, Blanchard TG. Induction of CTLA-4-Mediated Anergy Contributes to Persistent Colonization in the Murine Model of Gastric Helicobacter Pylori Infection. *J Immunol* (2006) 176(9):5306–13. doi: 10.4049/jimmunol.176.9.5306
20. Tang ZS, Hao YH, Zhang EJ, Xu CL, Zhou Y, Zheng X, et al. CD28 Family of Receptors on T Cells in Chronic HBV Infection: Expression Characteristics, Clinical Significance and Correlations With PD-1 Blockade. *Mol Med Rep* (2016) 14(2):1107–16. doi: 10.3892/mmr.2016.5396
21. Gu D, Ao X, Yang Y, Chen Z, Xu X. Soluble Immune Checkpoints in Cancer: Production, Function and Biological Significance. *J Immunother Cancer* (2018) 6(1):132. doi: 10.1186/s40425-018-0449-0
22. Wang Q, Zhang J, Tu H, Liang D, Chang DW, Ye Y, et al. Soluble Immune Checkpoint-Related Proteins as Predictors of Tumor Recurrence, Survival, and T Cell Phenotypes in Clear Cell Renal Cell Carcinoma Patients. *J Immunother Cancer* (2019) 7(1):334. doi: 10.1186/s40425-019-0810-y
23. Chakrabarti R, Kapse B, Mukherjee G. Soluble Immune Checkpoint Molecules: Serum Markers for Cancer Diagnosis and Prognosis. *Cancer Rep (Hoboken)* (2019) 2(4):e1160. doi: 10.1002/cnr2.1160
24. Zhou L, Li X, Huang X, Chen L, Gu L, Huang Y. Soluble Programmed Death-1 Is a Useful Indicator for Inflammatory and Fibrosis Severity in Chronic Hepatitis B. *J Viral Hepat* (2019) 26(7):795–802. doi: 10.1111/jvh.13055
25. Cheng HY, Kang PJ, Chuang YH, Wang YH, Jan MC, Wu CF, et al. Circulating Programmed Death-1 as a Marker for Sustained High Hepatitis B Viral Load and Risk of Hepatocellular Carcinoma. *PloS One* (2014) 9(11): e95870. doi: 10.1371/journal.pone.0095870
26. Gomez-Urena EO, Tande AJ, Osmon DR, Berbari EF. Diagnosis of Prosthetic Joint Infection: Cultures, Biomarker and Criteria. *Infect Dis Clin North Am* (2017) 31(2):219–35. doi: 10.1016/j.idc.2017.01.008
27. Berbari EF, Marculescu C, Sia I, Lahr BD, Hanssen AD, Steckelberg JM, et al. Culture-Negative Prosthetic Joint Infection. *Clin Infect Dis* (2007) 45(9):1113–9. doi: 10.1086/522184
28. Palan J, Nolan C, Sarantos K, Westerman R, King R, Foguet P. Culture-Negative Periprosthetic Joint Infections. *EFORT Open Rev* (2019) 4(10):585–94. doi: 10.1302/2058-5241.4.180067
29. Li C, Renz N, Trampuz A, Ojeda-Thies C. Twenty Common Errors in the Diagnosis and Treatment of Periprosthetic Joint Infection. *Int Orthop* (2020) 44(1):3–14. doi: 10.1007/s00264-019-04426-7
30. van der Kraan PM. The Interaction Between Joint Inflammation and Cartilage Repair. *Tissue Eng Regener Med* (2019) 16(4):327–34. doi: 10.1007/s13770-019-00204-z
31. Gehrke T, Alijanipour P, Parvizi J. The Management of an Infected Total Knee Arthroplasty. *Bone Joint J* (2015) 97-B(10 Suppl A):20–9. doi: 10.1302/0301-620X.97B10.36475
32. Orfanos AV, Michael RJ, Keeney BJ, Moschetti WE. Patient-Reported Outcomes After Above-Knee Amputation for Prosthetic Joint Infection. *Knee* (2020) 27(3):1101–5. doi: 10.1016/j.knee.2019.10.007
33. Wengler A, Nimptsch U, Mansky T. Hip and Knee Replacement in Germany and the USA: Analysis of Individual Inpatient Data From German and US Hospitals for the Years 2005 to 2011. *Dtsch Arztebl Int* (2014) 111(23-24):407–16. doi: 10.3238/arztebl.2014.0407
34. Wooley PH, Schwarz EM. Aseptic Loosening. *Gene Ther* (2004) 11(4):402–7. doi: 10.1038/sj.gt.3302202
35. Kurtz SM, Lau E, Watson H, Schmier JK, Parvizi J. Economic Burden of Periprosthetic Joint Infection in the United States. *J Arthroplasty* (2012) 27(8 Suppl):61–5 e1. doi: 10.1016/j.arth.2012.02.022
36. Akindolire J, Morcos MW, Marsh JD, Howard JL, Lanting BA, Vasarhelyi EM. The Economic Impact of Periprosthetic Infection in Total Hip Arthroplasty. *Can J Surg* (2020) 63(1):E52–E6. doi: 10.1503/cjs.004219
37. Dustin ML. The Cellular Context of T Cell Signaling. *Immunity* (2009) 30 (4):482–92. doi: 10.1016/j.immuni.2009.03.010
38. Irvine DJ, Purbhoo MA, Krogsgaard M, Davis MM. Direct Observation of Ligand Recognition by T Cells. *Nature* (2002) 419(6909):845–9. doi: 10.1038/nature01076
39. Bonilla FA, Oettgen HC. Adaptive Immunity. *J Allergy Clin Immunol* (2010) 125(2 Suppl 2):S33–40. doi: 10.1016/j.jaci.2009.09.017
40. Natarajan K, Li H, Mariuzza RA, Margulies DH. MHC Class I Molecules, Structure and Function. *Rev Immunogenet* (1999) 1(1):32–46.
41. Uede T. The Molecular Mechanism of Costimulatory Signal for T Cell Activation. *Nihon Rinsho* (1995) 53(10):2597–603.
42. Guerder S, Flavell RA. T-Cell Activation. Two for T. *Curr Biol* (1995) 5 (8):866–8. doi: 10.1016/S0960-9822(95)00175-8
43. Chauvin JM, Pagliano O, Fourcade J, Sun Z, Wang H, Sander C, et al. TIGIT and PD-1 Impair Tumor Antigen-Specific CD8(+) T Cells in Melanoma Patients. *J Clin Invest* (2015) 125(5):2046–58. doi: 10.1172/JCI80445

44. Jenkins MK, Taylor PS, Norton SD, Urdahl KB. CD28 Delivers a Costimulatory Signal Involved in Antigen-Specific IL-2 Production by Human T Cells. *J Immunol* (1991) 147(8):2461–6.
45. Yang SY, Denning SM, Mizuno S, Dupont B, Haynes BF. A Novel Activation Pathway for Mature Thymocytes. Costimulation of CD2 (T,p50) and CD28 (T,p44) Induces Autocrine Interleukin 2/Interleukin 2 Receptor-Mediated Cell Proliferation. *J Exp Med* (1988) 168(4):1457–68. doi: 10.1084/jem.168.4.1457
46. Woo SR, Turnis ME, Goldberg MV, Bankoti J, Selby M, Nirschl CJ, et al. Immune Inhibitory Molecules LAG-3 and PD-1 Synergistically Regulate T-Cell Function to Promote Tumoral Immune Escape. *Cancer Res* (2012) 72(4):917–27. doi: 10.1158/0008-5472.CAN-11-1620
47. Hodi FS, O'Day SJ, McDermott DF, Weber RW, Sosman JA, Haanen JB, et al. Improved Survival With Ipilimumab in Patients With Metastatic Melanoma. *N Engl J Med* (2010) 363(8):711–23. doi: 10.1056/NEJMoa1003466
48. Ward FJ, Dahal LN, Wijesekera SK, Abdul-Jawad SK, Kaewarpai T, Xu H, et al. The Soluble Isoform of CTLA-4 as a Regulator of T-Cell Responses. *Eur J Immunol* (2013) 43(5):1274–85. doi: 10.1002/eji.201242529
49. Kakoulidou M, Giscombe R, Zhao X, Lefvert AK, Wang X. Human Soluble CD80 Is Generated by Alternative Splicing, and Recombinant Soluble CD80 Binds to CD28 and CD152 Influencing T-Cell Activation. *Scand J Immunol* (2007) 66(5):529–37. doi: 10.1111/j.1365-3083.2007.02009.x
50. Haile ST, Horn LA, Ostrand-Rosenberg S. A Soluble Form of CD80 Enhances Antitumor Immunity by Neutralizing Programmed Death Ligand-1 and Simultaneously Providing Costimulation. *Cancer Immunol Res* (2014) 2(7):610–5. doi: 10.1158/2326-6066.CIR-13-0204
51. Ostrand-Rosenberg S, Horn LA, Alvarez JA. Novel Strategies for Inhibiting PD-1 Pathway-Mediated Immune Suppression While Simultaneously Delivering Activating Signals to Tumor-Reactive T Cells. *Cancer Immunol Immunother* (2015) 64(10):1287–93. doi: 10.1007/s00262-015-1677-5
52. Haile ST, Dalal SP, Clements V, Tamada K, Ostrand-Rosenberg S. Soluble CD80 Restores T Cell Activation and Overcomes Tumor Cell Programmed Death Ligand 1-Mediated Immune Suppression. *J Immunol* (2013) 191(5):2829–36. doi: 10.4049/jimmunol.1202777
53. Cherian JJ, Jauregui JJ, Banerjee S, Pierce T, Mont MA. What Host Factors Affect Aseptic Loosening After THA and TKA? *Clin Orthop Relat Res* (2015) 473(8):2700–9. doi: 10.1007/s11999-015-4220-2
54. Oaks MK, Hallett KM. Cutting Edge: A Soluble Form of CTLA-4 in Patients With Autoimmune Thyroid Disease. *J Immunol* (2000) 164(10):5015–8. doi: 10.4049/jimmunol.164.10.5015
55. Wang XB, Kakoulidou M, Giscombe R, Qiu Q, Huang D, Pirskanen R, et al. Abnormal Expression of CTLA-4 by T Cells From Patients With Myasthenia Gravis: Effect of an AT-Rich Gene Sequence. *J Neuroimmunol* (2002) 130(1-2):224–32. doi: 10.1016/S0165-5728(02)00228-X
56. Liu MF, Wang CR, Chen PC, Fung LL. Increased Expression of Soluble Cytotoxic T-Lymphocyte-Associated Antigen-4 Molecule in Patients With Systemic Lupus Erythematosus. *Scand J Immunol* (2003) 57(6):568–72. doi: 10.1046/j.1365-3083.2003.01232.x
57. Simone R, Brizzolara R, Chiappori A, Milintenda-Floriani F, Natale C, Greco L, et al. A Functional Soluble Form of CTLA-4 Is Present in the Serum of Celiac Patients and Correlates With Mucosal Injury. *Int Immunol* (2009) 21(9):1037–45. doi: 10.1093/intimm/dxp069
58. Erfani N, Razmkhah M, Ghaderi A. Circulating Soluble CTLA4 (sCTLA4) Is Elevated in Patients With Breast Cancer. *Cancer Invest* (2010) 28(8):828–32. doi: 10.3109/07357901003630934
59. Mansour A, Elkhodary T, Darwish A, Mabed M. Increased Expression of Costimulatory Molecules CD86 and sCTLA-4 in Patients With Acute Lymphoblastic Leukemia. *Leuk Lymphoma* (2014) 55(9):2120–4. doi: 10.3109/10428194.2013.869328
60. Ward FJ, Dahal LN, Khanolkar RC, Shankar SP, Barker RN. Targeting the Alternatively Spliced Soluble Isoform of CTLA-4: Prospects for Immunotherapy? *Immunotherapy* (2014) 6(10):1073–84. doi: 10.2217/imt.14.73
61. Liu Q, Hu P, Deng G, Zhang J, Liang N, Xie J, et al. Soluble Cytotoxic T-Lymphocyte Antigen 4: A Favorable Predictor in Malignant Tumors After Therapy. *Onco Targets Ther* (2017) 10:2147–54. doi: 10.2147/OTT.S128451
62. Saverino D, Brizzolara R, Simone R, Chiappori A, Milintenda-Floriani F, Pesce G, et al. Soluble CTLA-4 in Autoimmune Thyroid Diseases: Relationship With Clinical Status and Possible Role in the Immune Response Dysregulation. *Clin Immunol* (2007) 123(2):190–8. doi: 10.1016/j.clim.2007.01.003
63. Ip WK, Wong CK, Leung TF, Lam CW. Elevation of Plasma Soluble T Cell Costimulatory Molecules CTLA-4, CD28 and CD80 in Children With Allergic Asthma. *Int Arch Allergy Immunol* (2005) 137(1):45–52. doi: 10.1159/000084612
64. Wong CK, Lit LC, Tam LS, Li EK, Lam CW. Aberrant Production of Soluble Costimulatory Molecules CTLA-4, CD28, CD80 and CD86 in Patients With Systemic Lupus Erythematosus. *Rheumatol (Oxford)* (2005) 44(8):989–94. doi: 10.1093/rheumatology/keh663
65. Hebbar M, Jeannin P, Magistrelli G, Hatron PY, Hachulla E, Devulder B, et al. Detection of Circulating Soluble CD28 in Patients With Systemic Lupus Erythematosus, Primary Sjogren's Syndrome and Systemic Sclerosis. *Clin Exp Immunol* (2004) 136(2):388–92. doi: 10.1111/j.1365-2249.2004.02427.x
66. Gorgulho J, Roderburg C, Heymann F, Schulze-Hagen M, Beier F, Vucur M, et al. Serum Levels of Soluble B and T Lymphocyte Attenuator Predict Overall Survival in Patients Undergoing Immune Checkpoint Inhibitor Therapy for Solid Malignancies. *Int J Cancer* (2021) 149(5):1189–98. doi: 10.1002/ijc.33610
67. Monaghan SF, Banerjee D, Chung CS, Lomas-Neira J, Cygan KJ, Rhine CL, et al. Changes in the Process of Alternative RNA Splicing Results in Soluble B and T Lymphocyte Attenuator With Biological and Clinical Implications in Critical Illness. *Mol Med* (2018) 24(1):32. doi: 10.1186/s10020-018-0036-3
68. Lange A, Sunden-Cullberg J, Magnuson A, Hultgren O. Soluble B and T Lymphocyte Attenuator Correlates to Disease Severity in Sepsis and High Levels Are Associated With an Increased Risk of Mortality. *PloS One* (2017) 12(1):e0169176. doi: 10.1371/journal.pone.0169176
69. Dong MP, Enomoto M, Thuy LTT, Hai H, Hieu VN, Hoang DV, et al. Clinical Significance of Circulating Soluble Immune Checkpoint Proteins in Sorafenib-Treated Patients With Advanced Hepatocellular Carcinoma. *Sci Rep* (2020) 10(1):3392. doi: 10.1038/s41598-020-60440-5
70. Bian B, Fanale D, Dusetti N, Roque J, Pastor S, Chretien AS, et al. Prognostic Significance of Circulating PD-1, PD-L1, pan-BTN3As, BTN3A1 and BTLA in Patients With Pancreatic Adenocarcinoma. *Oncoimmunology* (2019) 8(4):e1561120. doi: 10.1080/2162402X.2018.1561120
71. Parvizi J, Tan TL, Goswami K, Higuera C, Della Valle C, Chen AF, et al. The 2018 Definition of Periprosthetic Hip and Knee Infection: An Evidence-Based and Validated Criteria. *J Arthroplasty* (2018) 33(5):1309–14 e2. doi: 10.1016/j.arth.2018.02.078
72. Dong Y, Li X, Zhang L, Zhu Q, Chen C, Bao J, et al. CD4(+) T Cell Exhaustion Revealed by High PD-1 and LAG-3 Expression and the Loss of Helper T Cell Function in Chronic Hepatitis B. *BMC Immunol* (2019) 20(1):27. doi: 10.1186/s12865-019-0309-9
73. Caraballo Cortes K, Osuch S, Perlejewski K, Pawelczyk A, Kazmierczak J, Janiak M, et al. Expression of Programmed Cell Death Protein 1 and T-Cell Immunoglobulin- and Mucin-Domain-Containing Molecule-3 on Peripheral Blood CD4+CD8+ Double Positive T Cells in Patients With Chronic Hepatitis C Virus Infection and in Subjects Who Spontaneously Cleared the Virus. *J Viral Hepat* (2019) 26(8):942–50. doi: 10.1111/jvh.13108
74. Day CL, Kaufmann DE, Kiepiela P, Brown JA, Moodley ES, Reddy S, et al. PD-1 Expression on HIV-Specific T Cells Is Associated With T-Cell Exhaustion and Disease Progression. *Nature* (2006) 443(7109):350–4. doi: 10.1038/nature05115
75. Cao J, Zou L, Luo P, Chen P, Zhang L. Increased Production of Circulating Soluble Co-Stimulatory Molecules CTLA-4, CD28 and CD80 in Patients With Rheumatoid Arthritis. *Int Immunopharmacol* (2012) 14(4):585–92. doi: 10.1016/j.intimp.2012.08.004
76. Wan B, Nie H, Liu A, Feng G, He D, Xu R, et al. Aberrant Regulation of Synovial T Cell Activation by Soluble Costimulatory Molecules in Rheumatoid Arthritis. *J Immunol* (2006) 177(12):8844–50. doi: 10.4049/jimmunol.177.12.8844
77. Blanco JF, Diaz A, Melchor FR, da Casa C, Pescador D. Risk Factors for Periprosthetic Joint Infection After Total Knee Arthroplasty. *Arch Orthop Trauma Surg* (2020) 140(2):239–45. doi: 10.1007/s00402-019-03304-6
78. Kunutsor SK, Whitehouse MR, Blom AW, Beswick AD, Team I. Patient-Related Risk Factors for Periprosthetic Joint Infection After Total Joint Arthroplasty: A Systematic Review and Meta-Analysis. *PloS One* (2016) 11(3):e0150866. doi: 10.1371/journal.pone.0150866

79. Namba RS, Paxton L, Fithian DC, Stone ML. Obesity and Perioperative Morbidity in Total Hip and Total Knee Arthroplasty Patients. *J Arthroplasty* (2005) 20(7 Suppl 3):46–50. doi: 10.1016/j.arth.2005.04.023

Conflict of Interest: The authors declare that the research was conducted in the absence of any commercial or financial relationships that could be construed as a potential conflict of interest.

Publisher's Note: All claims expressed in this article are solely those of the authors and do not necessarily represent those of their affiliated organizations, or those of the publisher, the editors and the reviewers. Any product that may be evaluated in this article, or claim that may be made by its manufacturer, is not guaranteed or endorsed by the publisher.

frontiers in Immunology

ORIGINAL RESEARCH
published: 30 September 2021
doi: 10.3389/fimmu.2021.715267

Chondrogenically Primed Human Mesenchymal Stem Cells Persist and Undergo Early Stages of Endochondral Ossification in an Immunocompetent Xenogeneic Model

Niamh Fahy[1,2†], Virginia Palomares Cabeza[1,3,4†], Andrea Lolli[1], Janneke Witte-Bouma[1], Ana Merino[3], Yanto Ridwan[5,6], Eppo B. Wolvius[1], Martin J. Hoogduijn[3], Eric Farrell[1†] and Pieter A. J. Brama[4†]*

[1] Department of Oral and Maxillofacial Surgery, Erasmus Medical Center, Rotterdam, Netherlands, [2] Department of Orthopaedics and Sports Medicine, Erasmus Medical Center, Rotterdam, Netherlands, [3] Transplantation Institute, Department of Internal Medicine, Erasmus Medical Center, Rotterdam, Netherlands, [4] School of Veterinary Medicine, University College Dublin, Dublin, Ireland, [5] Department of Genetics, Erasmus Medical Center, Rotterdam, Netherlands, [6] Department of Radiology and Nuclear Medicine, Erasmus University Medical Center, Rotterdam, Netherlands

OPEN ACCESS

Edited by:
Katharina Schmidt-Bleek, Charité–Universitätsmedizin Berlin, Germany

Reviewed by:
Christian H. Bucher, Charité–Universitätsmedizin Berlin, Germany
Rokhsareh Rohban, Medical University of Graz, Austria

***Correspondence:**
Eric Farrell
e.farrell@erasmusmc.nl

[†]These authors have contributed equally to this work

Specialty section:
This article was submitted to Inflammation, a section of the journal Frontiers in Immunology

Received: 26 May 2021
Accepted: 10 September 2021
Published: 30 September 2021

Citation:
Fahy N, Palomares Cabeza V, Lolli A, Witte-Bouma J, Merino A, Ridwan Y, Wolvius EB, Hoogduijn MJ, Farrell E and Brama PAJ (2021) Chondrogenically Primed Human Mesenchymal Stem Cells Persist and Undergo Early Stages of Endochondral Ossification in an Immunocompetent Xenogeneic Model. Front. Immunol. 12:715267. doi: 10.3389/fimmu.2021.715267

Tissue engineering approaches using progenitor cells such as mesenchymal stromal cells (MSCs) represent a promising strategy to regenerate bone. Previous work has demonstrated the potential of chondrogenically primed human MSCs to recapitulate the process of endochondral ossification and form mature bone *in vivo*, using immunodeficient xenogeneic models. To further the translation of such MSC-based approaches, additional investigation is required to understand the impact of interactions between human MSC constructs and host immune cells upon the success of MSC-mediated bone formation. Although human MSCs are considered hypoimmunogenic, the potential of chondrogenically primed human MSCs to induce immunogenic responses *in vivo*, as well as the efficacy of MSC-mediated ectopic bone formation in the presence of fully competent immune system, requires further elucidation. Therefore, the aim of this study was to investigate the capacity of chondrogenically primed human MSC constructs to persist and undergo the process of endochondral ossification in an immune competent xenogeneic model. Chondrogenically differentiated human MSC pellets were subcutaneously implanted to wild-type BALB/c mice and retrieved at 2 and 12 weeks post-implantation. The percentages of $CD4^+$ and $CD8^+$ T cells, B cells, and classical/non-classical monocyte subsets were not altered in the peripheral blood of mice that received chondrogenic MSC constructs compared to sham-operated controls at 2 weeks post-surgery. However, MSC-implanted mice had significantly higher levels of serum total IgG compared to sham-operated mice at this timepoint. Flow cytometric analysis of retrieved MSC constructs identified the presence of T cells and macrophages at 2 and 12 weeks post-implantation, with low levels of immune cell infiltration to implanted MSC constructs

detected by CD45 and CD3 immunohistochemical staining. Despite the presence of immune cells in the tissue, MSC constructs persisted *in vivo* and were not degraded/resorbed. Furthermore, constructs became mineralised, with longitudinal micro-computed tomography imaging revealing an increase in mineralised tissue volume from 4 weeks post-implantation until the experimental endpoint at 12 weeks. These findings indicate that chondrogenically differentiated human MSC pellets can persist and undergo early stages of endochondral ossification following subcutaneous implantation in an immunocompetent xenogeneic model. This scaffold-free model may be further extrapolated to provide mechanistic insight to osteoimmunological processes regulating bone regeneration and homeostasis.

Keywords: mesenchymal stem cells, endochondral ossification, xenogeneic, immunocompetence, adaptive immunity, innate immunity, graft rejection, osteoimmunology

INTRODUCTION

Tissue engineering approaches using progenitor cells, such as mesenchymal stromal cells (MSCs), represent a promising strategy to generate bone graft substitutes for the repair of bone defects (1, 2). Previous work has highlighted the potential of chondrogenically primed human MSCs to recapitulate the natural process of endochondral ossification and form mature bone *in vivo*, following subcutaneous implantation in immunodeficient animal models after 8 to 12 weeks (3–8). Implantation of chondrogenic MSC constructs in immunodeficient animals is known to lead to the maturation of hypertrophic cartilage, followed by blood vessel invasion, remodelling of the cartilaginous template, and eventual conversion to bone (3, 4, 9). In these studies, chondrogenically primed MSC constructs were found to form a bone ossicle containing a bone marrow cavity with evidence of vascularisation, indicating full integration with the host (4). Upon translation of an MSC-based approach for large bone defect repair to the patient, potential interactions between MSC constructs and immune cells of the host may be key in determining the success of MSC-mediated bone formation (10). Therefore, new models of bone formation, such as humanised or immune-competent mouse models, that are more relevant to the clinical situation with regard to osteoimmunology are required. Human MSCs are considered to be hypoimmunogenic (11), with chondrogenically primed human MSCs previously shown to not induce immunogenic responses *in vitro* (12, 13). However, the potential of chondrogenically primed human MSCs to induce immunogenic responses *in vivo*, as well as the efficacy of MSC-mediated ectopic bone formation in the presence of fully competent immune system, requires further elucidation.

MSCs are considered to have low immunogenic properties due to their low expression of Major Histocompatibility Complex (MHC) class I, and a lack of MHC class II and other costimulatory molecules required for recognition by immune cells of the host (11, 14). Additionally, MSCs have been shown to have an immunomodulatory capacity towards cells of both the innate (15, 16) and adaptive immune system (17–19). Undifferentiated human MSCs have been previously shown to suppress immune responses in xenogeneic models utilising immunocompetent mice (20). However, current reports on the potential of chondrogenically differentiated MSCs to modulate host immune responses are conflicting. Some authors claim that chondrogenically primed human MSCs retain their immunosuppressive properties and can modulate allogeneic T cell proliferation (11, 12), dendritic cell (DC) maturation (13), and natural killer (NK)-mediated cytotoxicity (21) *in vitro*. On the other hand, others have reported immunogenic reactions when co-culturing chondrogenically differentiated MSCs with allogeneic peripheral blood mononuclear cells (PBMCs) (22). In addition, Chen et al. showed an increase in DC maturation and T cell proliferation when co-culturing chondrogenically primed rat-derived MSCs with human PBMCs *in vitro* (23). In light of these findings, the potential of chondrogenically differentiated human MSCs to persist and form bone *in vivo* in the presence of the host immune system in a xenogeneic model remains unclear.

Given the central role played by the immune system during the natural process of bone homeostasis (24) and fracture healing (25, 26), additional investigation of the potential interaction between chondrogenically primed human MSCs and the immune system of an immune competent host may further our current understanding of these mechanisms (27). Also, increasing interest in the potential ability to use allogeneic cells in various regenerative medicine approaches further necessitates the development of new models of bone formation encompassing a functional immune system. Hence, the aim of this study was to determine to what extent chondrogenically primed human MSC constructs elicit host immune responses, persist, and recapitulate the process of endochondral ossification following subcutaneous implantation in an immune competent xenogeneic model.

MATERIALS AND METHODS

Isolation and Expansion of Human MSCs

Human MSCs were isolated from surplus iliac crest bone chip material harvested from paediatric patients undergoing alveolar bone graft surgery (Donor 1: female, <18 years old; donor 2: female, 10 years old; donor 3: male, 10 years old). All human samples were obtained with the approval of the Erasmus University Medical Center Medical Research Ethics Committee

(MEC-2014-16). Written consent was not required in accordance with institutional guidelines for the use of waste surgical material, and an opt-out option was available. Iliac crest bone chips were washed with expansion medium composed of Minimum Essential Medium (MEM)-α (containing nucleosides) supplemented with heat inactivated 10% v/v foetal bovine serum (FBS), 1.5 μg/ml fungizone, 50 μg/ml gentamicin (all Thermo Fisher Scientific, Waltham, MA, USA), 25 μg/ml L-ascorbic acid 2-phosphate (Sigma-Aldrich, St. Louis, MO, USA), and 1 ng/ml fibroblast growth factor-2 (Instruchemie, Delfzijl, Netherlands), and the resulting cell suspension was seeded in T75 flasks. Cells were washed twice with phosphate buffered saline (Thermo Fisher Scientific) supplemented with 2% v/v heat inactivated FBS 24 h following seeding to remove non-adherent cells. MSCs were cultured at 37°C and 5% carbon dioxide under humidified conditions, with expansion medium refreshed every 3–4 days. MSCs were subcultured upon reaching 80–90% confluency using 0.25% w/v trypsin-EDTA (Thermo Fisher Scientific) and reseeded at a cell density of 2,300 cells/cm^2. MSCs were used at passage 3 for chondrogenic pellet cultures.

Chondrogenic Differentiation of MSCs

For chondrogenic differentiation, 2×10^5 MSCs were suspended in 500 μl of chondrogenic differentiation medium composed of high glucose Dulbecco's Modified Eagle Medium supplemented with 1.5 μg/ml fungizone, 50 μg/ml gentamicin, 1 mM sodium pyruvate (All Thermo Fisher Scientific), 1% v/v Insulin-Transferrin-Selenous acid (ITS^{TM}+ Premix, Corning, Bedford, MA, USA), 40 μg/ml proline (Sigma-Aldrich), 25 μg/ml L-ascorbic acid 2-phosphate, 100 nM Dexamethasone (Sigma-Aldrich), and 10 ng/ml transforming growth factor-β3 (R&D systems, Minneapolis, MN, USA). The cell suspension was added to 15 ml conical polypropylene tubes (VWR, Radnor, PA, USA) and centrifuged at 300 g for 8 min to facilitate pellet formation. Chondrogenic MSC pellets were cultured at 37°C and 5% carbon dioxide in a humidified atmosphere, and culture medium was refreshed every 3–4 days for 21 days. Chondrogenic differentiation of MSCs *in vitro* following 21 days of culture was confirmed histologically by thionine staining (**Supplementary Figure S1**).

Subcutaneous Implantation Model

Animal experiments were conducted with the approval of the Animal Ethical Committee of the Erasmus University Medical Center (Licence number AVD101002015114, work protocol number 15-114-101). Male BALB/c mice (BALB/cAnNCr, 8–9 weeks old, 24.6 ± 2.2g; Charles River Laboratories, Wilmington, MA, USA) were housed in groups of three under a standard 12 h light-dark cycle with water and standard chow *ad libitum*. Mice were anaesthetised with 3% isoflurane, 0.8 L/min O_2 (Pharmachemie BV, Haarlem, Netherlands), and 0.05 mg/kg buprenorphine (Temgesic, RB Pharmaceuticals Limited, Slought, UK) was injected subcutaneously 30 min prior to the procedure as analgesic. Four incisions were made dorsally, bilateral at the level of shoulders and hips, and four subcutaneous pockets were created. Three MSC pellets were implanted per subcutaneous pocket, with pellets of one MSC donor implanted per mouse. At 2 and 12 weeks post-implantation, peripheral blood was harvested for flow cytometric analysis by cardiac puncture of mice under general anaesthesia at each experimental time point. Mice were euthanised by cervical dislocation, and MSC constructs were retrieved for histological and flow cytometric analysis. As a reference point to compare early endochondral ossification in immunodeficient mice, tissue sections resulting from a separate study were included in the present study for histological evaluation of MSC-mediated endochondral ossification after 4 weeks *in vivo*. In this separate study (conducted with the approval of the Animal Ethical Committee of the Erasmus University Medical Center, licence number AVD101002015114 and work protocol, number 18-6166-01), male BALB/c nude mice (CAnN.Cg-Foxn1nu/Crl, 8 weeks old; Charles River Laboratories) were subcutaneously implanted with human MSC pellets from one donor as already described. Mice were euthanised by cervical dislocation, and MSC constructs were retrieved for histological analysis at 4 weeks post-implantation.

Flow Cytometric Analysis (Peripheral Blood and Pellet Digest)

One hundred μl of whole blood was centrifuged at 400 g for 5 min, following which the serum was removed and replaced with an equal volume of PBS. Diluted blood was subsequently stained for CD19 and CD138 to identify B cells, CD3, CD4 and CD8 for T cells, and CD11b, CD115, Ly6G, Ly6C, and CD62L for monocyte subsets (**Table 1**). Staining with a Via-probe^{TM} (T cells, B cells; BD Biosciences, San Jose, CA, USA) or LIVE/DEAD^{TM} Fixable Dead Cell Stain (Macrophages; Thermo Fisher Scientific) was included for dead cell exclusion. Blood was stained for 10 min and subsequently lysed for 10 mins with 3 ml of FACS Lysis Solution (BD Biosciences) in the dark and washed twice with FACSFlow buffer (BD Biosciences). Samples were resuspended in FACSFlow buffer and stored at 4°C prior to analysis. For analysis of immune cell subsets within MSC constructs, retrieved pellets were subjected to enzymatic digestion. MSC pellets were incubated with 3 mg/ml collagenase A (Sigma-Aldrich) and 1.5 mg DNase I (Sigma-

TABLE 1 | Panel of antibodies used to detect T and B cell responses by flow cytometry.

Antibody	Clone	Fluorochrome	Company
CD19	6D5	APC-Cy7	BioLegend, San Diego, CA, USA
CD138	281-2	APC	BD Biosciences, San Jose, CA, USA
CD3	17A2	FITC	Thermo Fisher Scientific, Waltham, MA, USA
CD4	RPA-T4	V450	BD Biosciences, San Jose, CA, USA
CD8a	53-6.7	PE-Cy7	BD Biosciences, San Jose, CA, USA

Aldrich) in RPMI-1640 media (Thermo Fisher Scientific) containing 5% FBS, at 37°C for 90 min. Following incubation, the resulting cell suspension was filtered through a 100 μm cell strainer and pelleted by centrifugation at 400 g for 5 min. Cells were washed and resuspended in FACSFlow buffer and stained for the expression of CD3, CD4, and CD8 for the identification of T cells, and F4/80, CD11b, CD86, CD206, CD163 for macrophages (**Table 2**). Staining with Via-probe™ (T cells; BD Biosciences) or LIVE/DEAD™ Fixable Dead Cell Stain (Macrophages; Thermo Fisher Scientific) was performed to facilitate the exclusion of dead cells. Cells were incubated in the dark at 4°C for 30 min, washed with FACSFLow buffer, and fixed with 2% paraformaldehyde (Sigma-Aldrich) in PBS. Finally, samples were washed twice with FACSFlow buffer and stored at 4°C prior to analysis. All samples were analysed using a BD FACS Canto II cytometer (BD, Franklin Lakes, NJ, USA), and data were analysed using FlowJo software version 10.0.7 (FlowJo LLC, Ashland, OR, USA). The gating strategies applied for flow cytometric analysis are presented in **Supplementary Figures S2** and **S3**.

Histological Analysis

In vitro chondrogenically differentiated MSC pellets were fixed for 2 h in 4% formaldehyde (BoomLab, Meppel, Netherlands). A fixation period of 2 h was previously determined to be adequate for the fixation of MSC pellets that were chondrogenically primed *in vitro* for 21 days (17, 28). Due to the potential of chondrogenically primed MSC pellets to form mineralised tissue following subcutaneous implantation *in vivo* (28), MSC pellets that were retrieved from mice at 2 and 12 weeks post-implantation were fixed for 24 h in 4% formaldehyde to ensure adequate fixation, and subsequently decalcified for 10 days in 10% w/v ethylenediaminetetraacetic acid (Sigma-Aldrich) in deionised water. Following embedding in paraffin, sections of 6 μm thickness were cut from all samples. Sections from *in vitro* chondrogenically differentiated MSC pellets were deparaffinised and stained with thionine as described previously (29). Sections of MSC pellets retrieved from mice were deparaffinised, and staining with haematoxylin and eosin (H&E) was performed as previously described (28).

For human specific Glyceraldehyde 3-phosphate dehydrogenase (GAPDH) staining, antigen retrieval was achieved by heat-induced epitope retrieval (HIER) in citrate buffer (10 mM tri-sodium citrate dihydrate, 0.05% Tween 20; pH 6.0; Sigma-Aldrich) for 25 min at 95°C. Slides were then rinsed with Tris-buffered saline (TBS; 50 mM Tris-HCl pH 7.5, 150 mM NaCl; Sigma-Aldrich)/0.025% v/v Triton X-100 (Sigma-Aldrich), and sections pre-incubated with 10% v/v normal goat serum (NGS; Southern Biotech, Birmingham, USA) in TBS/1% w/v bovine serum albumin (BSA; Sigma-Aldrich) + 1% w/v Elk milk powder (Campina, Amersfoort, Netherlands) for 60 min. Following the blocking of non-specific binding sites, sections were incubated with a primary antibody against human GAPDH (Rabbit monoclonal; Abcam, Cambridge UK, ab128915; 0.2 μg/ml) or rabbit IgG (Dako, Glostrup, Denmark, X0903) in TBS/1% w/v BSA for 1 h at room temperature. Next, sections were incubated with a biotinylated anti-rabbit Ig link (Biogenex, Fremont, CA, USA, HK-326-UR; 2% v/v) followed by a streptavidin-alkaline phosphatase label (Biogenex, HK-321-UK; 2% v/v), and staining was visualised by Neu Fuchsin substrate (Chroma, Köngen, Germany). Slides were mounted with VectaMount (Vector Laboratories, Burlingame, CA, USA).

For CD3 staining, antigen retrieval was performed by HIER in Tris-EDTA buffer (10 mM Tris Base, 1 mM EDTA Solution, 0.05% Tween 20; pH 9.0; Sigma-Andrich) at 95°C for 20 min. Sections were rinsed with phosphate buffered saline (PBS; Sigma-Aldrich) and pre-incubated with 10% v/v NGS in PBS/1% w/v BSA/1% w/v Elk milk powder for 60 min. Next, sections were incubated with a primary antibody against CD3 (Rabbit monoclonal, Abcam, ab16669; 1:100) or rabbit IgG in PBS/1% w/v BSA for 1 h. Sections were incubated with a biotinylated anti-rabbit Ig link (2% v/v) followed by a streptavidin-alkaline phosphatase label (2% v/v), and staining was visualised by Neu Fuchsin substrate. Slides were mounted with VectaMount.

For CD45 staining, antigen retrieval was achieved by HIER in citrate buffer for 25 min at 95°C. Following rinsing with PBS, sections were pre-incubated with 5% v/v rabbit serum (Jackson ImmunoResearch laboratories, PA, USA) and 5% v/v mouse serum (Jackson ImmunoResearch laboratories) in PBS/1% w/v BSA/1% w/v Elk milk powder for 30 min. Sections were then incubated with a primary antibody against CD45 (Rat monoclonal; Biolegend, San Diego, CA, USA, 103101; 1 μg/ml) or rat IgG2a (eBioscience, San Diego, CA, USA, 14432182) in PBS/1% w/v BSA/1% w/v Elk milk powder for 1 h. Endogenous peroxidase was blocked with 1% v/v H_2O_2 (Sigma-Aldrich) in PBS, and sections were incubated with a biotinylated rabbit anti-rat IgG antibody (Vector Laboratories, BA-4000; 6 μg/ml) in PBS/1% w/v BSA with 5% v/v Mouse/5% v/v human serum (CLB, Netherlands) for 30 min. Next, sections were incubated with a streptavidin-peroxidase label (Biogenex, HK-320-UK; 2% v/v) and staining visualised using a DAB substrate solution

TABLE 2 | Panel of antibodies used to detect monocyte and macrophage responses by flow cytometry.

Antibody	Clone	Fluorochrome	Company
Monocyte analysis panel			
Anti-mouse/human CD11b	M1/70	PerCP-Cy5.5	BioLegend, San Diego, CA, USA
Anti-mouse CD115	AFS98	PE	BioLegend, San Diego, CA, USA
Anti-mouse Ly6C	HK1.4	FITC	BioLegend, San Diego, CA, USA
Anti-mouse CD62L	MEL-14	APC	BioLegend, San Diego, CA, USA
Anti-mouse Ly6G	1A8	PE-Cy7	BioLegend, San Diego, CA, USA
Macrophage analysis panel			
Anti-mouse F4/80	BM8	FITC	BioLegend, San Diego, CA, USA
Anti-mouse/human CD11b	M1/70	PerCP-Cy5.5	BioLegend, San Diego, CA, USA

(0.05% DAB, 0.015% v/v H_2O_2, 0.01M PBS, pH 7.2; Sigma-Aldrich). Finally, sections were dehydrated and slides mounted with Depex (Merck, Darmstadt, Germany).

Micro-Computed Tomography Imaging

Micro-Computed Tomography (μCT) scanning was performed every 2 weeks starting from week 4 post-implantation up to week 12, at the Applied Molecular Imaging Erasmus MC facility using the Quantum-GX2 (Perkin-Elmer, Groningen, Netherlands). Scanning was performed using a 30 mm field of view for 4 min (90 kV/160 uA), voxel size of 72 μm, and X ray filter Cu 0,06 mm + Al 0,5 mm. An automated reconstruction utilising the Quantum-GX2 software was performed after imaging. Scans were quantified using two phantoms with a known mineral density (0.25 and 0.75 g/cm3), under the same scan conditions. Bone mineralisation was assessed using the software Analyze 11.0 (AnalyzeDirect, Overland Park, KS, USA).

Total IgG ELISA Analysis

Levels of IgG in the sera of MSC-implanted and sham-operated mice were quantified utilising a commercially available mouse total IgG ELISA kit (Thermo Fisher Scientific) according to manufacturer's instructions.

Statistical Analyses

Analyses were performed using IBM SPSS version 24 (IBM, Armonk, NY, USA). For the comparison of sham-operated and MSC-implanted mice at 2 weeks post-implantation, normality testing was performed using a Shapiro-Wilk test and data analysed using an independent T test. Analysis of repeated measures data was performed using a linear mixed model with Bonferroni post-correction. Values are plotted as the mean +/− the standard deviation (SD), and a p value <0.05 was considered to be statistically significant. N=6 MSC-implanted mice per experimental time point, with four subcutaneous pockets per mouse and N=3 human MSC donors. N=3 mice per sham-operated group.

RESULTS

Chondrogenically Differentiated Human MSC Pellets Do Not Induce Systemic Monocyte and T Cell–Mediated Immune Responses Following Subcutaneous Implantation in Immune Competent Mice

In order to determine the potential of chondrogenically differentiated MSCs to initiate systemic innate or adaptive immune responses which may lead to acute rejection of implanted constructs, peripheral blood levels of monocyte subsets, T cells, and B cells were analysed following MSC pellet implantation. The distribution of classical, intermediate, and non-classical monocyte subsets in the blood of MSC-implanted mice did not significantly differ compared to sham-operated control mice at 2 weeks post-implantation (**Figure 1A**). Furthermore, the percentage of circulating $CD3^+$ T cells (**Figure 1B**), as well as the ratio of $CD4^+$ to $CD8^+$ T (**Figure 1C**) cells in the peripheral blood of MSC-implanted mice, did not significantly differ compared to sham-operated control mice at this time point. Levels of $CD19^+CD138^+$ B cells present in the peripheral blood were also not altered in response to the subcutaneous implantation of chondrogenically differentiated MSC pellets at 2 weeks post-implantation (**Figure 1D**). The proportion of T cell subsets and B cells present in the peripheral blood of mice at 12 weeks post-implantation was in line with levels observed in the blood of MSC-implanted and sham-operated mice at 2 weeks post-implantation (**Figures 1B–D**). However, serum concentrations of total IgG were significantly higher in MSC-implanted mice compared to control animals at 2 weeks (**Figure 1E**; p=0.001). Interestingly, serum levels of total IgG of mice at 12 weeks post-implantation were lower than concentrations detected in the serum of MSC-implanted mice at 2 weeks (363.60 ± 80.67 μg/ml *vs* 451.27 ± 64.03 μg/ml at week 2), although still higher than levels detected in sham-operated control mice (206.29 ± 48.21 μg/ml; **Figure 1D**).

Chondrogenically Differentiated MSC Constructs Persist With Cells of the Innate and Adaptive Immune System Present at 2 Weeks Post-Subcutaneous Implantation

Chondrogenically differentiated human MSC constructs were found to persist at 2 weeks post-implantation, with the presence of human cells within the construct detected by human-specific GAPDH immunohistochemical staining (**Figure 2A**). Furthermore, the majority of cells within the core of retrieved MSC pellets were human $GAPDH^+$. Expression of CD45 was detected within adjacent tissue surrounding MSC constructs as well as the border of MSC pellets, with no staining observed within the cartilaginous matrix of retrieved pellets. Similarly, expression of CD3 as determined by immunohistochemistry was primarily localised to the periphery of MSC constructs and surrounding tissue, with a similar pattern of staining localisation observed in constructs of all three MSC donors. No immune cell infiltrate indicative of rejection was observed. Flow cytometric analysis of MSC constructs that were retrieved with a surrounding layer of subcutaneous tissue attached to pellets confirmed the presence of CD3+ T cells and additionally identified the presence of $CD4^+$ and $CD8^+$ T cell subsets, as well as $F4/80^+$ macrophages within tissue digests (**Figure 2B**).

No Signs of Pellet Rection Are Observed in MSC Pellets at 12 Weeks Post-Implantation

Chondrogenically differentiated human MSC constructs had the capacity to survive in an immune-competent xenogeneic host following 12 weeks of subcutaneous implantation and were not associated with dense immune cell infiltration (**Figure 3**). Human $GAPDH^+$ cells were observed in all samples, highlighting the persistence of human cells at 12 weeks post-implantation (**Figure 3**). The presence of $CD45^+$ cells within the constructs,

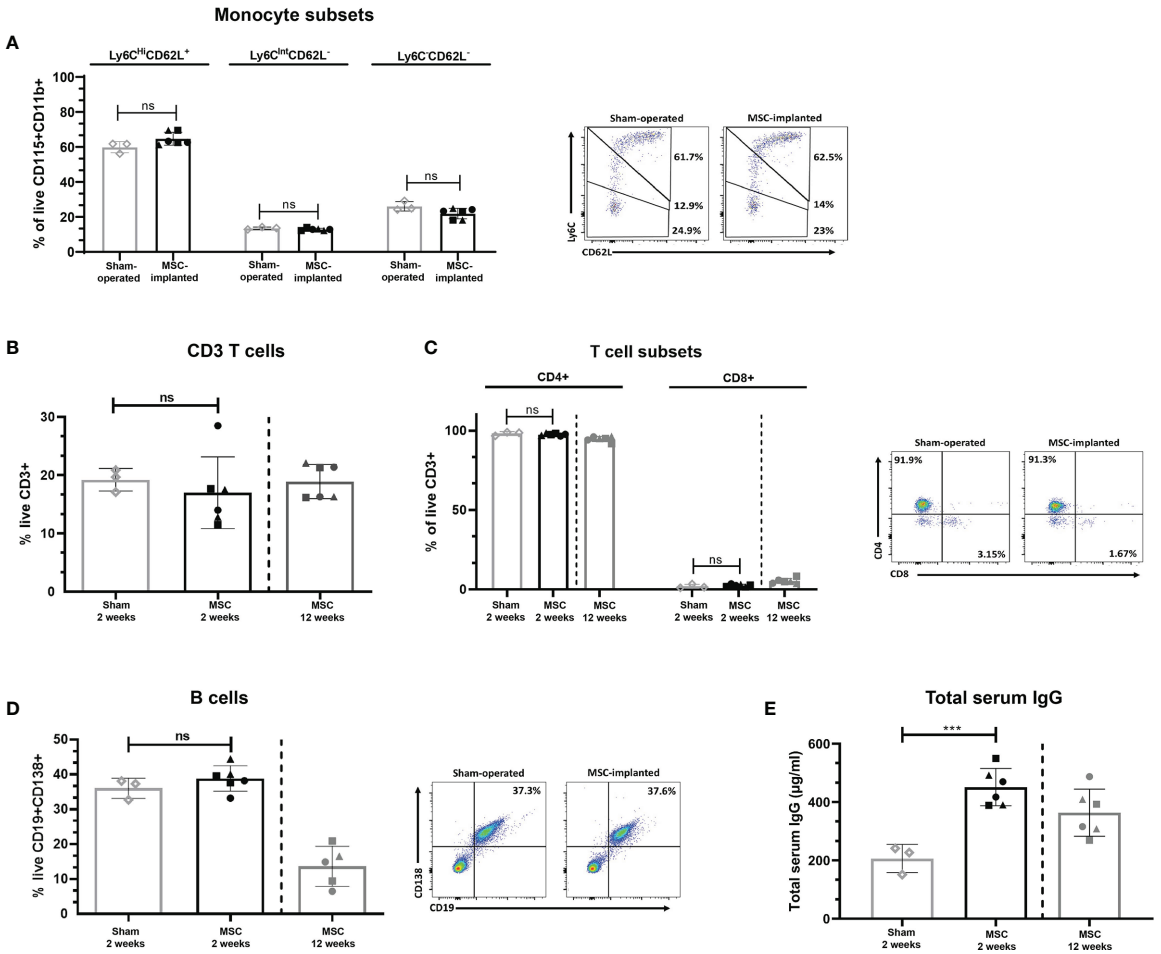

FIGURE 1 | Subcutaneous implantation of chondrogenically differentiated human MSC pellets does not alter the percentage of innate or adaptive immune cell subsets systemically. Proportion of monocyte subsets present in peripheral blood of implanted mice compared to sham-operated controls at 2 weeks, as determined by flow cytometry **(A)**. $CD3^+$ **(B)** and $CD4^+/CD8^+$ T cells **(C)**, and B cells **(D)** present in the peripheral blood of sham-operated control and MSC-implanted mice at 2 and 12 weeks, as determined by flow cytometry. **(E)** Total serum IgG levels of human MSC-implanted mice compared to sham-operated controls at 2 weeks post-implantation, and levels detected at 12 weeks post-MSC implantation. Data represent mean ± standard deviation, n=3 sham-operated mice and n=6 for MSC-implanted mice. N=5 MSC-implanted mice for B cell analysis at 12 weeks post-implantation, due to loss of blood sample during handling. ***p = 0.001, ns, not significant, data analysed using an independent T test. Filled symbols of MSC-implanted groups represent different MSC donors.

as detected by immunohistochemical staining, was mainly localised to the periphery of pellets, with some expression detected within the matrix. Additionally, a low number of CD3+ cells was observed throughout the constructs by immunohistochemistry, with CD3 expression primarily detected at the MSC pellet margin and surrounding subcutaneous tissue. In accordance with histological analysis, a low percentage of $CD3^+$ T cells (**Figure 3B**; 3.32% of total cells ± 1.18%) were detected within digested constructs by flow cytometry, with lower levels of CD3+ T cells observed in comparison with digested constructs analysed at 2 weeks post-implantation (**Figure 2B**; 10.48 ± 2.84%). Furthermore, $CD11b^+F4/80^+$ macrophages were also detected by flow cytometry within tissue digests at 12 weeks (**Figure 3B**; 9.78 ± 6.74%), at levels comparable with constructs retrieved at 2 weeks post-implantation (**Figure 2B**; 6.91 ± 3.48%).

Chondrogenically Primed MSCs Generate Mineralised Constructs That Persist After 12 Weeks in an Immune Competent Animal Model

Upon retrieval of the constructs after 12 weeks of implantation, haematoxylin and eosin staining revealed a chondrogenic structure with abundant extracellular matrix (**Figure 4A**). This staining further revealed some differences across donors in their levels of chondrogenesis, with an altered appearance of the cartilage extracellular matrix observed in some of the samples, indicating active remodelling, consistent with ongoing endochondral ossification. For comparison, **Supplementary Figure S4** demonstrates the degree of bone formation in an immune compromised mouse after only 4 weeks *in vivo*. Furthermore, calcified cartilage was observed in all samples.

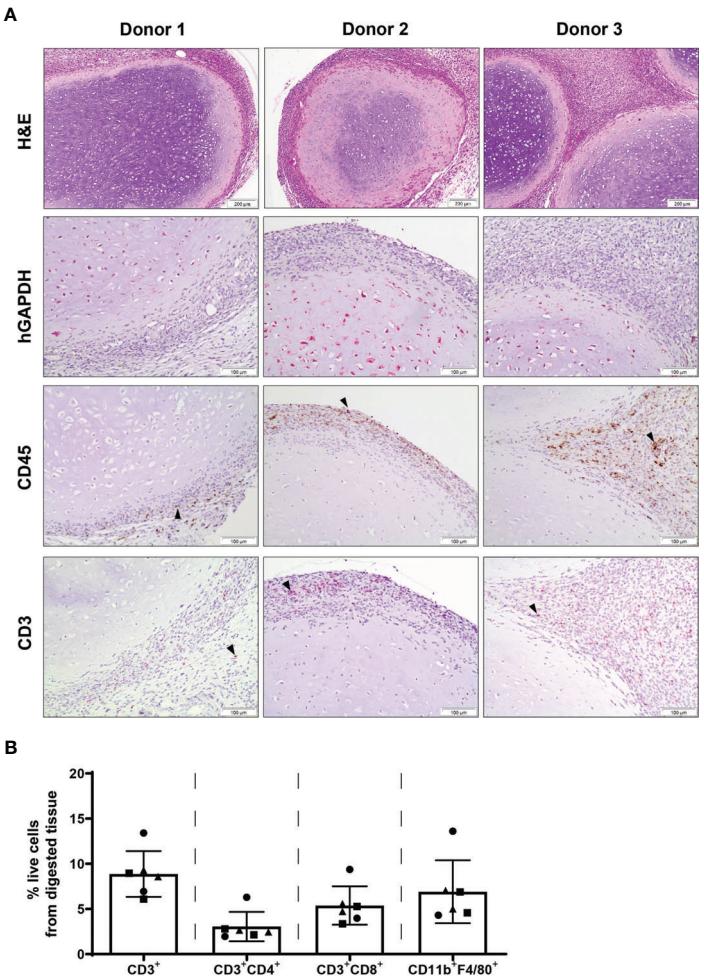

FIGURE 2 | Chondrogenically differentiated MSC pellets persist with cells of the innate and adaptive immune system present at 2 weeks post-subcutaneous implantation. **(A)** H&E, human specific GAPDH, CD45 and CD3 immunohistochemical staining of human MSC constructs retrieved at 2 weeks post-implantation. Images are representative of three individual mice and three human MSC donors; black arrowheads indicate positive staining. **(B)** Detection of T cells ($CD3^+$, $CD4^+$, $CD8^+$) and macrophages ($CD11b^+F4/80^+$) within digested MSC constructs retrieved at 2 weeks post-implantation. Data represent mean ± standard deviation, n=6 mice and n=3 human MSC donors (two constructs per donor).

Mineralisation of constructs was observed by μCT scans from 4 weeks post-implantation in all donors (**Figure 4B**), increasing in volume in all donors every 2 weeks up to week 12 (**Figure 4C**, **Supplementary Figure S5**).

DISCUSSION

The use of human MSCs for bone regeneration has been previously studied in immune deficient mouse models. In order to further determine the underlying mechanisms governing the process of MSC-mediated ectopic bone formation, as well as other mechanisms in bone-related diseases and development, new models of bone formation in a functioning immune system are required. In this context, we sought to determine the potential of human chondrogenically differentiated MSCs to persist and recapitulate endochondral bone formation in the presence of a xenogeneic immune system. Our findings indicate that the proportion of monocyte subsets, $CD4^+$ and $CD8^+$ T cells, and $CD19^+CD138^+$ B cells are not altered systemically following 2 weeks of implantation of human MSC-derived chondrogenic constructs, and highlight prolonged persistence of MSC-derived pellets until 12 weeks following implantation. These pellets are mineralised at 4 weeks, and progress along the endochondral ossification pathway, albeit at a slower rate than is usual in immunocompromised animals (3, 7), having not formed the marrow cavity by 12 weeks. These findings highlight the potential of immunocompetent xenogeneic models as a tool to assay human MSC-mediated tissue formation and examine the role of host immune responses during this process.

Previously it has been shown that systemic infusion of undifferentiated human MSCs to immune competent mice can suppress innate and adaptive immune responses in inflammatory

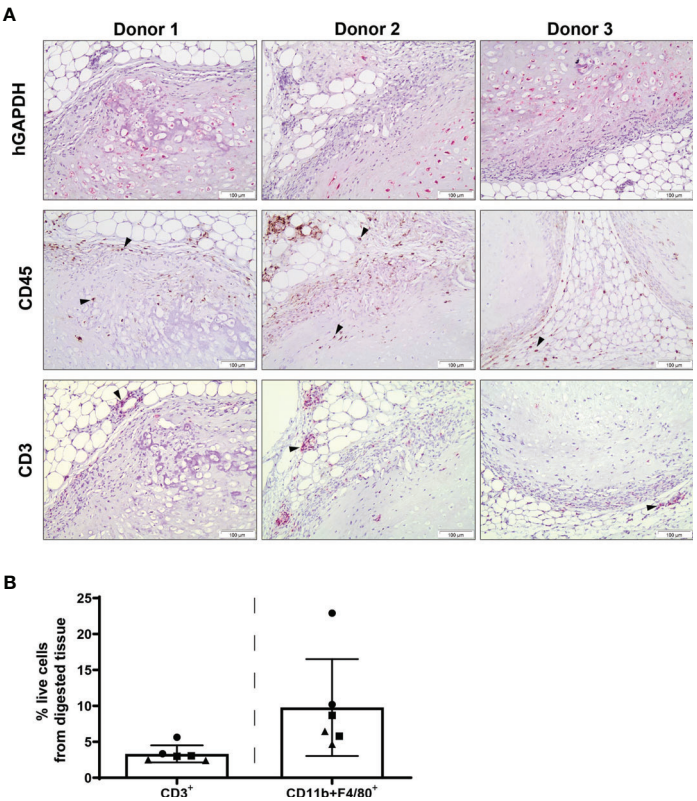

FIGURE 3 | Innate and adaptive immune cell subsets are present at the site of human MSC constructs following 12 weeks of subcutaneous implantation. **(A)** Human specific GAPDH, CD45 and CD3 immunohistochemical staining of MSC constructs retrieved at 12 weeks post-implantation. Images are representative of three individual mice and three human MSC donors; black arrowheads indicate positive staining. **(B)** Detection of T cells ($CD3^+$) and macrophages ($CD11b^+F4/80^+$) within digested MSC constructs retrieved at 12 weeks post-implantation. Data represent mean ± standard deviation, n=6 mice and n=3 human MSC donors (two constructs per donor).

disease models (30–32). Such studies have demonstrated the potential of xenogeneic models as a useful tool to investigate the immune suppressive activity of human MSCs (20). Although MSCs are considered hypoimmunogenic, they have been reported to have the potential to generate immune responses following *in vivo* implantation in animal models (33, 34). Additionally, it has been proposed that host rejection of MSCs may be determined by the balance between their immunosuppressive and immunogenic activity (35). Reports to date on the potential of differentiated human MSCs to evade host immune responses and survive in an immunocompetent xenogeneic model have not fully determined the suitability of this model system to examine MSC-mediated tissue formation. The findings of our study highlight prolonged persistence and low immune cell infiltration of chondrogenically differentiated human MSC pellets in immune competent mice, which are in line with previous findings demonstrating the capacity of human MSCs to retain their immunosuppressive activity following chondrogenic priming (11–13). Interestingly, the dense extracellular matrix of intact cartilage has been previously postulated to play a role in providing protection against the recognition of chondrocytes by the host immune system following allogeneic transplantation (36–38). However, in contrast to our results with chondrogenically primed human MSCs, the xenotransplantation of cartilage explants has been reported to result in chronic rejection and destruction of implanted grafts (39, 40). Additional investigation at later time points is required to determine potential immune responses towards human MSC constructs following further tissue remodelling and vascularisation. Niemeyer et al. have previously reported decreased survival of osteogenically differentiated MSCs seeded on mineralised collagen scaffolds, following 8 weeks of subcutaneous implantation in immunocompetent xenogeneic hosts (41). Furthermore, higher levels of macrophage and T cell infiltration of osteogenic-MSC seeded biomaterial scaffolds were also observed in this study in comparison to implanted scaffolds containing undifferentiated MSCs (41). In contrast to our findings, Longoni et al. have observed local innate and adaptive immune cell responses following the implantation of chondrogenically differentiated human MSCs embedded in a collagen carrier to the site of a critical-sized femoral defect in immunocompetent rats (42). However, in a similar manner to the present study, mineralised tissue volumes were observed by 12 weeks post-human MSC implantation which were comparable to the size of implanted constructs, although no full bridging of the defect was observed in

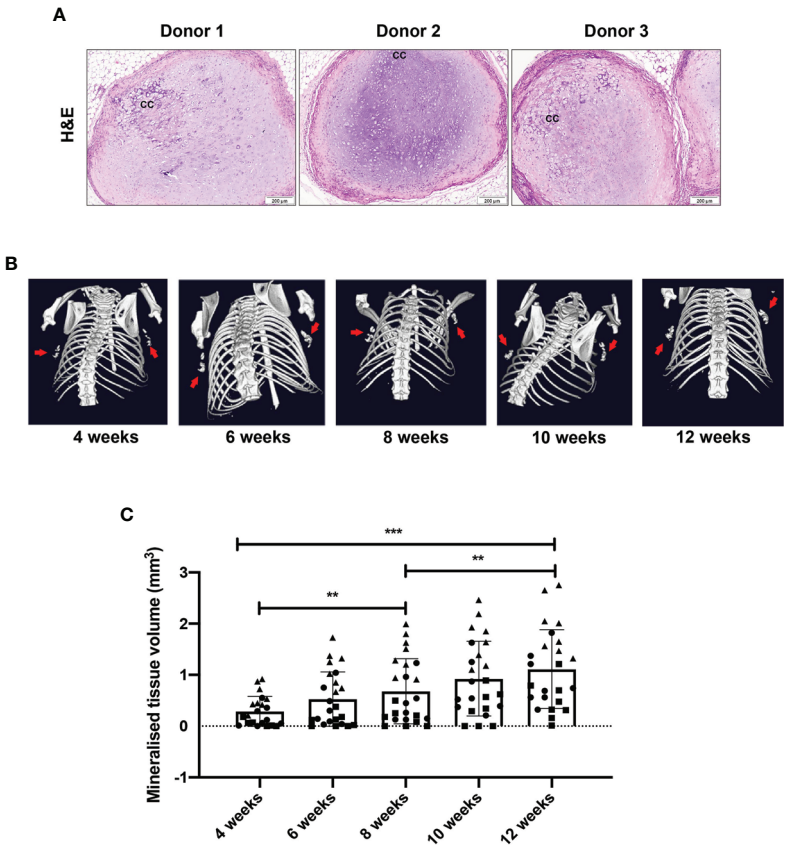

FIGURE 4 | Chondrogenically differentiated human MSC constructs persist and become mineralised at 12 weeks post-implantation. **(A)** Representative images of H&E staining of three individual mice and three MSC donors. **(B)** Representative images by μCT showing mineralised tissue volume and **(C)** quantification. Data represent mean ± standard deviation, with n=6 mice and n=3 human MSC donors (eight constructs per donor). Each datapoint represents one MSC construct, with four MSC constructs implanted per mouse and symbols representing different MSC donors. CC= calcified cartilage. $^{**}p < 0.01$, $^{***}p \leq 0.001$.

this model (42). Further investigation is required to determine whether these observed differences in immunogenic responses of chondrogenically differentiated human MSCs may be attributable to the ectopic *versus* orthotopic implantation sites, as well as the use of a biomaterial.

In addition to their potential to modulate cell-mediated immune processes (14, 16, 43), MSCs may also alter humoral immune responses following implantation in the host. Allogeneic undifferentiated MSCs have been reported to induce the formation of allo-antibodies in various immune competent animal models (44–46), highlighting the capacity of MSCs to stimulate an active humoral response. In the present study, although we did not observe expansion of circulating $CD19^{+}CD138^{+}$ B cells at 2 weeks post-implantation of chondrogenically differentiated human MSC constructs, the concentration of total IgG in the sera of MSC implanted mice was increased compared to sham-operated control animals. Interestingly, Longoni and colleagues have detected the production of anti-human antibodies following implantation of chondrogenically primed human MSCs in a rat femur defect model (42). Although we found human MSC constructs to persist and remain intact following 12 weeks of subcutaneous implantation, further investigation is required to fully confirm a lack of long-term systemic effects and antibody-mediated destruction of subcutaneously implanted human MSC constructs in immune competent mice. Furthermore, we did not evaluate local humoral immune responses at the site of implanted MSC constructs, which is a limitation of our study. Future studies performing an in-depth analysis of humoral immune responses locally at the site of implanted human MSC constructs, as well as systemically, are required to further develop the present findings. Additionally, the long-term presence of implanted chondrogenically primed MSC constructs and the potential of the dense extracellular matrix to protect such constructs against immune rejection requires further investigation. Interestingly, a low percentage of circulating CD8+ T cells were detected in the peripheral blood of both sham-operated and MSC-implanted mice at both experimental time points in our study. BALB/c mice have been previously reported to have a higher predominance of circulating CD4+ *versus* CD8+ T cells compared to other mouse strains (47, 48), and T cell subsets distribution may fluctuate with ageing (49). However, whether such factors may have contributed to the low levels of circulating CD8+ T cells observed in our study also requires additional investigation.

Previous work investigating ectopic endochondral bone formation by chondrogenically primed human MSCs has implemented the use of immunodeficient athymic mouse models and demonstrated the formation of a bone ossicle containing a bone marrow cavity by 8 weeks following subcutaneous implantation (3). In the presence of a fully functional host immune system, we have observed the initiation and progression of mineralisation by chondrogenically differentiated MSC pellets during the 12-week period following subcutaneous implantation, recapitulating early phases during the process of endochondral ossification. This progression of cartilage calcification and mineralisation, which we have observed, is known to precede bone and marrow cavity formation during MSC-mediated endochondral bone formation in immunodeficient animals (3, 28). However, in the present study the progression of this process appears to be slower compared with immune compromised mice, given that previous studies have observed the progression of chondrogenically primed MSCs towards a hypertrophic phenotype and onset of mineralisation at 4 weeks post-implantation in immunodeficient animals (50). In a separate unpublished dataset, we have also observed a comparable degree of cartilage matrix remodelling at 4 weeks post-implantation of chondrogenically differentiated human MSC pellets in immunodeficient BALB/c nude mice (**Supplementary Figure S4**), which is known to progress to form bone and bone marrow at 12 weeks post-implantation (3, 28). This data further corroborate our present findings suggesting delayed but ongoing MSC-mediated endochondral ossification in an immunocompetent xenogeneic model. However, we cannot rule out that the bone formation process is proceeding at a normal rate in the presence of a complete immune system and it is simply accelerated in immune compromised animals. Future experiments should take a later time point as the endpoint (16+ weeks) to confirm that complete endochondral ossification occurs in these animals. Interestingly, athymic mice have been previously reported to have elevated natural killer cell and macrophage activity levels compared to their wild-type counterparts (51, 52). Furthermore, *recombination activating gene 1* knockout mice, which lack an adaptive immune system, have been reported to have accelerated endochondral ossification and remodelling during fracture healing compared to wild-type mice (53). In addition, El Khassawna and colleagues have identified a critical role of T and B cells in the regulation of mineralisation, matrix formation, and subsequent quality of bone formed during fracture healing (54), highlighting the importance of experimental models encompassing a complete immune system to examine bone formation processes. Whether the differences in immune system composition between immunocompetent and immunodeficient mouse models may potentially play a role in determining the rate of extracellular matrix remodelling and progression of MSC-mediated endochondral bone formation requires further elucidation. Additionally, further investigation is required to determine the impact of a potential foreign body reaction following the subcutaneous implantation of human chondrogenically primed MSC pellets, which may also influence MSC-mediated endochondral bone formation (55).

In conclusion, the findings of the present study indicate that chondrogenically differentiated human MSC pellets can persist, eliciting only a minor immune response and undergo the early stages of endochondral ossification following subcutaneous implantation in an immunocompetent xenogeneic model. However, the nature of the differences in the speed of the endochondral ossification process in an immune competent scenario, compared with immunodeficient mouse models, needs to be further investigated. This scaffold-free model may be further extrapolated to provide mechanistic insight into the underlying mechanisms by which the immune system might influence the process of MSC-mediated endochondral ossification.

DATA AVAILABILITY STATEMENT

The raw data supporting the conclusions of this article will be made available by the authors, without undue reservation.

ETHICS STATEMENT

The studies involving human participants were reviewed and approved by the Erasmus University Medical Center Medical Research Ethical Committee (MEC-2014-16). Written consent was not required in accordance with institutional guidelines for the use of waste surgical material, and an opt-out option was available. Written informed consent from the participants' legal guardian/next of kin was not required to participate in this study in accordance with the national legislation and the institutional requirements. The animal study was reviewed and approved by the Animal Ethical Committee of the Erasmus University Medical Center (Licence number AVD101002015114, work protocol number 15-114-101).

AUTHOR CONTRIBUTIONS

NF: conception and design, collection of data, data analysis and interpretation, and manuscript writing. VC: conception and design, collection of data, data analysis and interpretation, and manuscript writing. AL: design, collection of data, and final approval of manuscript. JW-B: collection of data and final approval of manuscript. AM: design, collection of data, and final approval of manuscript. YR: collection of data. EW: conception and final approval of manuscript. MH: conception and design, data interpretation, and final approval of manuscript. PB: conception, data analysis and interpretation, and final approval of manuscript. EF: conception and design, data analysis and interpretation, and manuscript writing. All authors contributed to the article and approved the submitted version.

FUNDING

This research was partly supported by the AO Foundation, Switzerland (AOCMF-15-27F). AL is supported by the

European Union Horizon 2020 Research and Innovation Program under grant agreement 801159.

ACKNOWLEDGMENTS

The authors thank Nicole Kops for her assistance with immunohistochemical staining and imaging. This work was supported through the use of imaging equipment provided by the Applied Molecular Imaging Erasmus MC facility.

SUPPLEMENTARY MATERIAL

The Supplementary Material for this article can be found online at: https://www.frontiersin.org/articles/10.3389/fimmu.2021.715267/full#supplementary-material

Supplementary Figure S1 | Chondrogenic differentiation of human MSC donors *in vitro*. Thionine staining indicates GAG deposition following 21 days of culture in the presence of TGF- β3 (10 ng/ml).

Supplementary Figure S2 | Flow cytometric gating strategy for T and B cell analysis. Representative plots showing the gating strategy applied to detect T and B cells in peripheral blood **(A)**, and T cells in digested MSC constructs retrieved following subcutaneous implantation **(B)**.

Supplementary Figure S3 | Flow cytometric gating strategy for monocyte and macrophage analysis. Representative plots showing the gating strategy applied to detect peripheral blood monocyte subsets **(A)**, and macrophages in digested MSC-constructs retrieved following subcutaneous implantation **(B)**.

Supplementary Figure S4 | Cartilage matrix remodelling at 4 weeks post-implantation of chondrogenically primed human MSCs pellets in immunodeficient mice. Representative image of H&E staining of human MSC pellets retrieved at 4 weeks following subcutaneous implantation in an immunodeficient BALB/c nude mouse. Scale bar = 250 μm.

Supplementary Figure S5 | Representative image by μCT at 12 weeks following MSC implantation showing mineralised tissue volume at all four MSC implantation sites.

REFERENCES

1. Amini AR, Laurencin CT, Nukavarapu SP. Bone Tissue Engineering: Recent Advances and Challenges. *Crit Rev BioMed Eng* (2012) 40(5):363–408. doi: 10.1615/CritRevBiomedEng.v40.i5.10
2. Zhang Y, Xing Y, Jia L, Ji Y, Zhao B, Wen Y, et al. An *In Vitro* Comparative Study of Multisource Derived Human Mesenchymal Stem Cells for Bone Tissue Engineering. *Stem Cells Dev* (2018) 27(23):1634–45. doi: 10.1089/scd.2018.0119
3. Farrell E, Both SK, Odorfer KI, Koevoet W, Kops N, O'Brien FJ, et al. *In-Vivo* Generation of Bone via Endochondral Ossification by *In-Vitro* Chondrogenic Priming of Adult Human and Rat Mesenchymal Stem Cells. *BMC Musculoskelet Disord* (2011) 12:31. doi: 10.1186/1471-2474-12-31
4. Scotti C, Piccinini E, Takizawa H, Todorov A, Bourgine P, Papadimitropoulos A, et al. Engineering of a Functional Bone Organ Through Endochondral Ossification. *Proc Natl Acad Sci USA* (2013) 110(10):3997–4002. doi: 10.1073/pnas.1220108110
5. Pelttari K, Winter A, Steck E, Goetzke K, Hennig T, Ochs BG, et al. Premature Induction of Hypertrophy During *In Vitro* Chondrogenesis of Human Mesenchymal Stem Cells Correlates With Calcification and Vascular Invasion After Ectopic Transplantation in SCID Mice. *Arthritis Rheum* (2006) 54(10):3254–66. doi: 10.1002/art.22136
6. Thompson EM, Matsiko A, Kelly DJ, Gleeson JP, O'Brien FJ. An Endochondral Ossification-Based Approach to Bone Repair: Chondrogenically Primed Mesenchymal Stem Cell-Laden Scaffolds Support Greater Repair of Critical-Sized Cranial Defects Than Osteogenically Stimulated Constructs *In Vivo*. *Tissue Eng Pt A* (2016) 22(5-6):556–67. doi: 10.1089/ten.tea.2015.0457
7. Gawlitta D, Farrell E, Malda J, Creemers LB, Alblas J, Dhert WJA. Modulating Endochondral Ossification of Multipotent Stromal Cells for Bone Regeneration. *Tissue Eng Part B-Re* (2010) 16(4):385–95. doi: 10.1089/ten.teb.2009.0712
8. Huang JI, Durbhakula MM, Angele P, Johnstone B, Yoo JU. Lunate Arthroplasty With Autologous Mesenchymal Stem Cells in a Rabbit Model. *J Bone Joint Surg Am* (2006) 88a(4):744–52. doi: 10.2106/JBJS.E.00669
9. Farrell E, van der Jagt OP, Koevoet W, Kops N, van Manen CJ, Hellingman CA, et al. Chondrogenic Priming of Human Bone Marrow Stromal Cells: A Better Route to Bone Repair? *Tissue Eng Part C-Me* (2009) 15(2):285–95. doi: 10.1089/ten.tec.2008.0297
10. Longoni A, Knezevic L, Schepers K, Weinans H, Rosenberg A, Gawlitta D. The Impact of Immune Response on Endochondral Bone Regeneration. *NPJ Regener Med* (2018) 3:22. doi: 10.1038/s41536-018-0060-5
11. Le Blanc K, Tammik C, Rosendahl K, Zetterberg E, Ringden O. HLA Expression and Immunologic Properties of Differentiated and Undifferentiated Mesenchymal Stem Cells. *Exp Hematol* (2003) 31(10):890–6. doi: 10.1016/S0301-472X(03)00110-3
12. Kiernan CH, Hoogduijn MJ, Franquesa M, Wolvius EB, Brama PAJ, Farrell E. Allogeneic Chondrogenically Differentiated Human Mesenchymal Stromal Cells Do Not Induce Immunogenic Responses From T Lymphocytes *In Vitro*. *Cytotherapy* (2016) 18(8):957–69. doi: 10.1016/j.jcyt.2016.05.002
13. Kiernan CH, KleinJan A, Peeters M, Wolvius EB, Farrell E, Brama PAJ. Allogeneic Chondrogenically Differentiated Human Bone Marrow Stromal Cells Do Not Induce Dendritic Cell Maturation. *J Tissue Eng Regener Med* (2018) 12(6):1530–40. doi: 10.1002/term.2682
14. Tse WT, Pendleton JD, Beyer WM, Egalka MC, Guinan EC. Suppression of Allogeneic T-Cell Proliferation by Human Marrow Stromal Cells: Implications in Transplantation. *Transplantation* (2003) 75(3):389–97. doi: 10.1097/01.TP.0000045055.63901.A9
15. Zhao ZG, Xu W, Sun L, You Y, Li F, Li QB, et al. Immunomodulatory Function of Regulatory Dendritic Cells Induced by Mesenchymal Stem Cells. *Immunol Invest* (2012) 41(2):183–98. doi: 10.3109/08820139.2011.607877
16. Spaggiari GM, Capobianco A, Abdelrazik H, Becchetti F, Mingari MC, Moretta L. Mesenchymal Stem Cells Inhibit Natural Killer-Cell Proliferation, Cytotoxicity, and Cytokine Production: Role of Indoleamine 2,3-Dioxygenase and Prostaglandin E2. *Blood* (2008) 111(3):1327–33. doi: 10.1182/blood-2007-02-074997
17. Knuth CA, Kiernan CH, Palomares Cabeza V, Lehmann J, Witte-Bouma J, Ten Berge D, et al. Isolating Pediatric Mesenchymal Stem Cells With Enhanced Expansion and Differentiation Capabilities. *Tissue Eng Part C Methods* (2018) 24(6):313–21. doi: 10.1089/ten.tec.2018.0031
18. Palomares Cabeza V, Hoogduijn MJ, Kraaijeveld R, Franquesa M, Witte-Bouma J, Wolvius EB, et al. Pediatric Mesenchymal Stem Cells Exhibit Immunomodulatory Properties Toward Allogeneic T and B Cells Under Inflammatory Conditions. *Front Bioeng Biotechnol* (2019) 7:142. doi: 10.3389/fbioe.2019.00142
19. Luk F, Carreras-Planella L, Korevaar SS, de Witte SFH, Borras FE, Betjes MGH, et al. Inflammatory Conditions Dictate the Effect of Mesenchymal Stem or Stromal Cells on B Cell Function. *Front Immunol* (2017) 8:1042. doi: 10.3389/fimmu.2017.01042
20. Prockop DJ, Oh JY, Lee RH. Data Against a Common Assumption: Xenogeneic Mouse Models Can Be Used to Assay Suppression of Immunity by Human MSCs. *Mol Ther* (2017) 25(8):1748–56. doi: 10.1016/j.ymthe.2017.06.004
21. Du WJ, Reppel L, Leger L, Schenowitz C, Huselstein C, Bensoussan D, et al. Mesenchymal Stem Cells Derived From Human Bone Marrow and Adipose Tissue Maintain Their Immunosuppressive Properties After Chondrogenic Differentiation: Role of HLA-G. *Stem Cells Dev* (2016) 25(19):1454–69. doi: 10.1089/scd.2016.0022
22. Ryan AE, Lohan P, O'Flynn L, Treacy O, Chen X, Coleman C, et al. Chondrogenic Differentiation Increases Antidonor Immune Response to

Allogeneic Mesenchymal Stem Cell Transplantation. *Mol Ther* (2014) 22 (3):655–67. doi: 10.1038/mt.2013.261
23. Chen X, McClurg A, Zhou GQ, McCaigue M, Armstrong MA, Li G. Chondrogenic Differentiation Alters the Immunosuppressive Property of Bone Marrow-Derived Mesenchymal Stem Cells, and the Effect Is Partially Due to the Upregulated Expression of B7 Molecules. *Stem Cells* (2007) 25 (2):364–70. doi: 10.1634/stemcells.2006-0268
24. Walsh MC, Kim N, Kadono Y, Rho J, Lee SY, Lorenzo J, et al. Osteoimmunology: Interplay Between the Immune System and Bone Metabolism. *Annu Rev Immunol* (2006) 24:33–63. doi: 10.1146/annurev.immunol.24.021605.090646
25. Schlundt C, Reinke S, Geissler S, Bucher CH, Giannini C, Mardian S, et al. Individual Effector/Regulator T Cell Ratios Impact Bone Regeneration. *Front Immunol* (2019) 10. doi: 10.3389/fimmu.2019.01954
26. Schlundt C, El Khassawna T, Serra A, Dienelt A, Wendler S, Schell H, et al. Macrophages in Bone Fracture Healing: Their Essential Role in Endochondral Ossification. *Bone* (2018) 106:78–89. doi: 10.1016/j.bone.2015.10.019
27. Kovach TK, Dighe AS, Lobo PI, Cui QJ. Interactions Between MSCs and Immune Cells: Implications for Bone Healing. *J Immunol Res* (2015) 2015 (752510):17. doi: 10.1155/2015/752510
28. Knuth CA, Witte-Bouma J, Ridwan Y, Wolvius EB, Farrell E. Mesenchymal Stem Cell-Mediated Endochondral Ossification Utilising Micropellets and Brief Chondrogenic Priming. *Eur Cell Mater* (2017) 34:142–61. doi: 10.22203/eCM.v034a10
29. Kiernan CH, Asmawidjaja PS, Fahy N, Witte-Bouma J, Wolvius EB, Brama PAJ, et al. Allogeneic Chondrogenic Mesenchymal Stromal Cells Alter Helper T Cell Subsets in CD4+ Memory T Cells. *Tissue Eng Part A* (2020) 26(9-10):490–502. doi: 10.1089/ten.tea.2019.0177
30. Cruz FF, Borg ZD, Goodwin M, Sokocevic D, Wagner D, McKenna DH, et al. Freshly Thawed and Continuously Cultured Human Bone Marrow-Derived Mesenchymal Stromal Cells Comparably Ameliorate Allergic Airways Inflammation in Immunocompetent Mice. *Stem Cells Transl Med* (2015) 4 (6):615–24. doi: 10.5966/sctm.2014-0268
31. Choi H, Lee RH, Bazhanov N, Oh JY, Prockop DJ. Anti-Inflammatory Protein TSG-6 Secreted by Activated MSCs Attenuates Zymosan-Induced Mouse Peritonitis by Decreasing TLR2/NF-kappaB Signaling in Resident Macrophages. *Blood* (2011) 118(2):330–8. doi: 10.1182/blood-2010-12-327353
32. Krasnodembskaya A, Samarani G, Song Y, Zhuo H, Su X, Lee JW, et al. Human Mesenchymal Stem Cells Reduce Mortality and Bacteremia in Gram-Negative Sepsis in Mice in Part by Enhancing the Phagocytic Activity of Blood Monocytes. *Am J Physiol Lung Cell Mol Physiol* (2012) 302(10):L1003–13. doi: 10.1152/ajplung.00180.2011
33. Francois M, Romieu-Mourez R, Stock-Martineau S, Boivin MN, Bramson JL, Galipeau J. Mesenchymal Stromal Cells Cross-Present Soluble Exogenous Antigens as Part of Their Antigen-Presenting Cell Properties. *Blood* (2009) 114(13):2632–8. doi: 10.1182/blood-2009-02-207795
34. Eliopoulos N, Stagg J, Lejeune L, Pommey S, Galipeau J. Allogeneic Marrow Stromal Cells Are Immune Rejected by MHC Class I- and Class II-Mismatched Recipient Mice. *Blood* (2005) 106(13):4057–65. doi: 10.1182/blood-2005-03-1004
35. Ankrum JA, Ong JF, Karp JM. Mesenchymal Stem Cells: Immune Evasive, Not Immune Privileged. *Nat Biotechnol* (2014) 32(3):252–60. doi: 10.1038/nbt.2816
36. Cui P, Liu P, Li S, Ma R. De-Epithelialized Heterotopic Tracheal Allografts Without Immunosuppressants in Dogs: Long-Term Results for Cartilage Viability and Structural Integrity. *Ann Otol Rhinol Laryngol* (2021) 130 (5):441–9. doi: 10.1177/0003489420957357
37. Revell CM, Athanasiou KA. Success Rates and Immunologic Responses of Autogenic, Allogenic, and Xenogenic Treatments to Repair Articular Cartilage Defects. *Tissue Eng Part B Rev* (2009) 15(1):1–15. doi: 10.1089/ten.teb.2008.0189
38. Bolano L, Kopta JA. The Immunology of Bone and Cartilage Transplantation. *Orthopedics* (1991) 14(9):987–96. doi: 10.3928/0147-7447-19910901-10
39. Stone KR, Walgenbach AW, Abrams JT, Nelson J, Gillett N, Galili U. Porcine and Bovine Cartilage Transplants in Cynomolgus Monkey: I. A Model for Chronic Xenograft Rejection. *Transplantation* (1997) 63(5):640–5. doi: 10.1097/00007890-199703150-00005
40. Arzi B, DuRaine GD, Lee CA, Huey DJ, Borjesson DL, Murphy BG, et al. Cartilage Immunoprivilege Depends on Donor Source and Lesion Location. *Acta Biomater* (2015) 23:72–81. doi: 10.1016/j.actbio.2015.05.025
41. Niemeyer P, Vohrer J, Schmal H, Kasten P, Fellenberg J, Suedkamp NP, et al. Survival of Human Mesenchymal Stromal Cells From Bone Marrow and Adipose Tissue After Xenogenic Transplantation in Immunocompetent Mice. *Cytotherapy* (2008) 10(8):784–95. doi: 10.1080/14653240802419302
42. Longoni A, Pennings I, Cuenca Lopera M, van Rijen MHP, Peperzak V, Rosenberg A, et al. Endochondral Bone Regeneration by Non-Autologous Mesenchymal Stem Cells. *Front Bioeng Biotechnol* (2020) 8:651. doi: 10.3389/fbioe.2020.00651
43. Nemeth K, Leelahavanichkul A, Yuen PS, Mayer B, Parmelee A, Doi K, et al. Bone Marrow Stromal Cells Attenuate Sepsis via Prostaglandin E(2)-Dependent Reprogramming of Host Macrophages to Increase Their Interleukin-10 Production. *Nat Med* (2009) 15(1):42–9. doi: 10.1038/nm.1905
44. Schu S, Nosov M, O'Flynn L, Shaw G, Treacy O, Barry F, et al. Immunogenicity of Allogeneic Mesenchymal Stem Cells. *J Cell Mol Med* (2012) 16(9):2094–103. doi: 10.1111/j.1582-4934.2011.01509.x
45. Isakova IA, Dufour J, Lanclos C, Bruhn J, Phinney DG. Cell-Dose-Dependent Increases in Circulating Levels of Immune Effector Cells in Rhesus Macaques Following Intracranial Injection of Allogeneic MSCs. *Exp Hematol* (2010) 38 (10):957–67.e1. doi: 10.1016/j.exphem.2010.06.011
46. Poncelet AJ, Vercruysse J, Saliez A, Gianello P. Although Pig Allogeneic Mesenchymal Stem Cells Are Not Immunogenic *In Vitro*, Intracardiac Injection Elicits an Immune Response *In Vivo*. *Transplantation* (2007) 83 (6):783–90. doi: 10.1097/01.tp.0000258649.23081.a3
47. Chen J, Harrison DE. Quantitative Trait Loci Regulating Relative Lymphocyte Proportions in Mouse Peripheral Blood. *Blood* (2002) 99(2):561–6. doi: 10.1182/blood.V99.2.561
48. Chen JC, Flurkey K, Harrison DE. A Reduced Peripheral Blood CD4(+) Lymphocyte Proportion Is a Consistent Ageing Phenotype. *Mech Ageing Dev* (2002) 123(2-3):145–53. doi: 10.1016/S0047-6374(01)00347-5
49. Pinchuk LM, Filipov NM. Differential Effects of Age on Circulating and Splenic Leukocyte Populations in C57BL/6 and BALB/c Male Mice. *Immun Ageing* (2008) 5:1. doi: 10.1186/1742-4933-5-1
50. Scotti C, Tonnarelli B, Papadimitropoulos A, Scherberich A, Schaeren S, Schauerte A, et al. Recapitulation of Endochondral Bone Formation Using Human Adult Mesenchymal Stem Cells as a Paradigm for Developmental Engineering. *Proc Natl Acad Sci USA* (2010) 107(16):7251–6. doi: 10.1073/pnas.1000302107
51. Sharp AK, Colston MJ. The Regulation of Macrophage Activity in Congenitally Athymic Mice. *Eur J Immunol* (1984) 14(1):102–5. doi: 10.1002/eji.1830140119
52. Budzynski W, Radzikowski C. Cytotoxic Cells in Immunodeficient Athymic Mice. *Immunopharmacol Immunotoxicol* (1994) 16(3):319–46. doi: 10.3109/08923979409007097
53. Toben D, Schroeder I, El Khassawna T, Mehta M, Hoffmann JE, Frisch JT, et al. Fracture Healing Is Accelerated in the Absence of the Adaptive Immune System. *J Bone Mineral Res* (2011) 26(1):113–24. doi: 10.1002/jbmr.185
54. El Khassawna T, Serra A, Bucher CH, Petersen A, Schlundt C, Konnecke I, et al. T Lymphocytes Influence the Mineralization Process of Bone. *Front Immunol* (2017) 8:562. doi: 10.3389/fimmu.2017.00562
55. Miron RJ, Bosshardt DD. Multinucleated Giant Cells: Good Guys or Bad Guys? *Tissue Eng Part B Rev* (2018) 24(1):53–65. doi: 10.1089/ten.teb.2017.0242

Conflict of Interest: The authors declare that the research was conducted in the absence of any commercial or financial relationships that could be construed as a potential conflict of interest.

Publisher's Note: All claims expressed in this article are solely those of the authors and do not necessarily represent those of their affiliated organizations, or those of the publisher, the editors and the reviewers. Any product that may be evaluated in this article, or claim that may be made by its manufacturer, is not guaranteed or endorsed by the publisher.

frontiers in Endocrinology

ORIGINAL RESEARCH
published: 08 November 2021
doi: 10.3389/fendo.2021.666140

Single-Cell RNA Sequencing Reveals B Cells Are Important Regulators in Fracture Healing

Hao Zhang[1†], Renkai Wang[1,2†], Guangchao Wang[1†], Bo Zhang[3], Chao Wang[3], Di Li[1], Chen Ding[1], Qiang Wei[1], Zhenyu Fan[1], Hao Tang[1] and Fang Ji[1,4*]*

[1] Department of Orthopedics, Changhai Hospital, Secondary Military Medical University, Shanghai, China, [2] Guangdong Key Lab of Orthopedic Technology and Implant Materials, Key Laboratory of Trauma and Tissue Repair of Tropical Area of People's Liberation Army (PLA), Hospital of Orthopedics, General Hospital of Southern Theater Command of People's Liberation Army, Guangzhou, China, [3] Department of Bioinformatics, Novel Bioinformatics Ltd., Co. Shanghai, China, [4] Department of Orthopedics, The Ninth People's Hospital, Shanghai Jiaotong University, Shanghai, China

OPEN ACCESS

Edited by:
Rupesh K. Srivastava, All India Institute of Medical Sciences, India

Reviewed by:
Bhupendra Verma, All India Institute of Medical Sciences, India
Subhashis Pal, Emory University, United States

***Correspondence:**
Hao Tang
tanghao1978@163.com
Fang Ji
doctorjif@126.com

[†]These authors have contributed equally to this work

Specialty section:
This article was submitted to Bone Research, a section of the journal Frontiers in Endocrinology

Received: *03 March 2021*
Accepted: *25 May 2021*
Published: *08 November 2021*

Citation:
Zhang H, Wang R, Wang G, Zhang B, Wang C, Li D, Ding C, Wei Q, Fan Z, Tang H and Ji F (2021) Single-Cell RNA Sequencing Reveals B Cells Are Important Regulators in Fracture Healing. Front. Endocrinol. 12:666140. doi: 10.3389/fendo.2021.666140

The bone marrow microenvironment is composed primarily of immune and stromal cells that play important roles in fracture healing. Although immune cells have been identified in mouse bone marrow, variations in their numbers and type during the fracture healing process remain poorly defined. In this study, single-cell RNA sequencing was used to identify immune cells in fracture tissues, including neutrophils, monocytes, T cells, B cells, and plasma cells. The number of B cells decreased significantly in the early stage of fracture healing. Furthermore, B cells in mice fracture models decreased significantly during the epiphyseal phase and then gradually returned to normal during the epiphyseal transformation phase of fracture healing. The B-cell pattern was opposite to that of bone formation and resorption activities. Notably, B-cell–derived exosomes inhibited bone homeostasis in fracture healing. In humans, a decrease in the number of B cells during the epiphyseal phase stimulated fracture healing. Then, as the numbers of osteoblasts increased during the callus reconstruction stage, the number of B cells gradually recovered, which reduced additional bone regeneration. Thus, B cells are key regulators of fracture healing and inhibit excessive bone regeneration by producing multiple osteoblast inhibitors.

Keywords: scRNA-seq, fracture healing, B cells, exosome, bone marrow

INTRODUCTION

Bone fractures are the most common bone traumatic diseases worldwide (1). Severe multiple fractures caused by car accident or fall injury are usually accompanied by delayed healing and even nonunion (2). Fracture healing is directly regulated by the function and number of osteoblasts and osteoclasts (3, 4). However, numerous risk factors affect bone repair, including age, infection, malnutrition, distribution of blood vessels, activation of immune response, and inappropriate fracture fixation (5, 6). In the initial inflammatory stage, necrotic tissues are removed, and specific immune cells create a suitable bone marrow microenvironment for fracture healing.

Notably, the immune system is suppressed by fracture, and an increase in T regulatory cells inhibits active adaptive immune responses (7). Furthermore, mesenchymal stem cells maintain a hypoimmunogenic state, revealing that immune cells can inhibit fracture healing (8). However, the effects of immune cells on fracture healing have yet to be fully determined.

Several cytokines or other factors are essential for B cell development, including the receptor activators of NF-κB ligand (RANKL), OPG, IL-7, and CXCL-12, which are secreted by bone marrow stromal cells or osteoblasts (9, 10). Furthermore, B cells themselves can secret RANKL, suggesting that B cells can affect the differentiation of osteoclasts (11). In fact, mice lacking RANKL in B lymphocytes are partially protected from bone loss associated with ovariectomy. However, in mice with conditional knockout of RANKL in T lymphocytes, there is no effect on such bone loss (11). Moreover, B cells can inhibit bone formation in rheumatoid arthritis by suppressing osteoblast differentiation (12), which reveals that B cells have an important role in osteoimmunology. However, owing to the complexity of the bone marrow microenvironment in fracture healing, the effect of B cells on fracture healing remains unclear.

Single-cell RNA sequencing (scRNA-seq) has recently revolutionized study of the bone marrow microenvironment (13). With this approach, individual single cells can be clustered by transcriptome analysis rather than by surface markers. Furthermore, numerous cell types can be characterized between control and case samples, which helps to comprehensively understand the heterogeneity of diseases, including cancers, inflammation, and infection, among others (14, 15). During fracture healing, multiple cell types are involved in the bone marrow microenvironment, including immune cells, endothelial cells, hematopoietic stem cells, bone marrow stromal cells, osteoblasts, and osteoclasts (16). Therefore, to understand the mechanism for delayed fracture healing and bone nonunion, the developmental pseudotime trajectory needs to be constructed and cell–cell interactions determined.

In this study, the focus was on the roles of B cells in fracture healing. The scRNA-seq revealed fewer B cells in a patient with old fracture tissues than in one with fresh fracture tissues. Therefore, a mice fracture model was generated, and scRNA-seq showed that B cells decreased during the epiphyseal phase and increased during the callus reconstruction stage. Exosomes derived from B cells (BC-Exos) affected bone homeostasis *in vitro* by promoting osteoclastic bone resorption and inhibiting osteoblastic bone formation. Furthermore, osteogenic activity was inhibited *in vivo* in mice injected with BC-Exos. Thus, these results reveal that B cells and BC-Exos have important regulatory roles in fracture healing.

MATERIALS AND METHODS

Preparation of Human Fracture Tissues

Following surgical resection, samples from human fracture tissues were collected from two patients with femur fractures in Shanghai Changhai Hospital, Second Military Medical University. The approval for this clinical study was provided by the Committees of Clinical Ethics of Shanghai Changhai Hospital, Second Military Medical University. Informed consent was obtained from the patients.

Mice

All animal experiments were undertaken in accordance with the National Institute of Health Guide for the Care and Use of Laboratory Animals and with the approval of the Scientific Investigation Board of Second Military Medical University (Shanghai, China). C57BL/6 mice (6 to 8 weeks old) were obtained from Shanghai SLAC Laboratory Animal Co., Ltd. All mice were housed at the animal center of the Second Military Medical University.

For construction of mice fracture models, briefly, after anesthesia and surgical site sterilization, we first cut the skin, fascia, and muscle tissues to expose the femur and patella. Then, we construct transverse femoral fractures by pendulum saw. A Kirschner wire with a diameter of 0.5 mm was then inserted into the bone marrow space to stabilize the fracture. Then, we placed muscle over the osteotomy site and stitched with absorbable sutures prior to closing the skin with wound clips.

For delivery of B Cell Exosomes *in vivo*, 100μl exosomes in 0.1 ml saline buffer was locally injected into tail vein once every 3 days for 2 weeks.

Isolation of Bone Tissues

To obtain bone and bone marrow cells for scRNA-seq, bone fracture tissues (including bone and bone marrow) were dissected from patients, transported to the research facility, and then placed in DMEM (4.5 g/L, Gibco, USA). The bone fracture tissues were cut into small fragments and digested with 0.2 mg/ml collagenase II (Invitrogen) for 2 h at 37°C. After digestion, the cells were filtered through a 70-μm strainer (Corning) into a collection tube. Erythrocytes were lysed in ACK-lysis buffer (Sigma) for 5 min. Following centrifugation at 1,000 rpm at 4°C for 8 min, the supernatant was decanted and discarded. For further experiments, cells were resuspended in PBS (Gibco) and filtered through a 70-μm strainer on ice.

Cell Culture

BaF cells were cultured in RPMI-1640 (Hyclone, USA), containing 10% FBS (Thermo, USA), 10 ng/ml IL-3 (PeproTech, USA), and 1% penicillin–streptomycin (Thermo) at 37°C in a 5% CO_2 humidified incubator.

To induce osteoblast differentiation, BMSC cells were seeded in a 12-well plate with osteogenic differentiation complete medium (including osteogenic differentiation basal medium, 175 ml; osteogenic differentiation fetal bovine serum, 20 ml; penicillin-streptomycin, 2 ml; glutamine, 2 ml; ascorbate, 400 μl; β-glycerophosphate, 2 ml; and dexamethasone, 20 μl) (Cyagen), which was changed every 3 days. At day 21, the cells were stained with Alizarin red (pH 5.5) to analyze osteogenic differentiation.

For osteoclast differentiation, mouse bone marrow monocytes isolated from femurs and tibias were seeded at 1×10^6 cells per well in a 24-well plate. The cells were cultured in DMEM (4.5 g/L, Gibco) supplemented with 10% FBS (Thermo), 50 ng/ml M-CSF

(PeproTech, USA), and 1% penicillin–streptomycin (Thermo) for 3 days at 37°C in a 5% CO_2 humidified incubator. Nonadherent cells were discarded, and the adherent cells were cultured in DMEM (4.5 g/L, Gibco) supplemented with 10% FBS (Thermo), 50 ng/ml M-CSF (PeproTech), 100 ng/ml soluble RANKL (PeproTech), and 1% penicillin–streptomycin (Thermo) for 5 days. The medium was changed every 3 days. At day 8, the cells were stained with TRAP using a commercial kit according to the manufacturer's instructions (Sigma) (17).

Isolation of B Cell Exosomes

The exosomes of B cells were extracted as previously described (18). Briefly, BaF cells were cultured in complete medium containing EV-free FBS (BI) for 24 h. Then, the supernatant containing BC-Exos was centrifuged at 2,000 rpm for 30 min to eliminate dead cells and cellular debris. The supernatant containing the cell-free culture media was transferred to a new tube, and 0.5 volumes of the Total Exosome were added.

The culture media and an isolation reagent (Thermo) were mixed by vortexing or by pipetting up and down until a homogenous solution was obtained. The solution was incubated at 2°C to 8°C overnight. After incubation, the samples were centrifuged at 10,000×*g* for 1 h at 2°C to 8°C. The supernatant was aspirated and discarded, and exosomes were contained in the pellet at the bottom of the tube. The pellet was resuspended in 1× PBS. Protein content of BC-Exos was determined by using a BCA Protein Assay Kit (Thermo Fisher Scientific, USA).

Characterization of B Cell Exosomes

The morphology of BC-Exos was observed with a transmission electron microscope (Hitachi, Japan). The size distribution of BC-Exos was determined using a Nanosizer™ (Malvern Instruments) (18). The expression of surface markers (CD9, CD63) on BC-Exos was identified with Western blot (WB).

Immunofluorescence Staining

Fresh bone tissues dissected from mice fracture models were fixed in 4% paraformaldehyde overnight. Tissues were decalcified with 0.5 M EDTA with constant shaking, and then, bone tissues were embedded in OCT (Sakura). Bone sections, 6 μm, were stained with antibodies B220 (1:100, Abcam) and osteocalcin (1:100, Abcam). Then, secondary antibodies conjugated with fluorescence (1:100, Jackson) were used, and nuclei were counterstained with DAPI. Bone tissues were observed under a confocal microscope.

Reverse-Transcription Quantitative PCR

Total RNA from cultured cells was prepared using TRIzol reagent (Thermo) and then reverse-transcribed into cDNA with a cDNA reverse-transcription kit (Applied Biosystems, USA). Reverse-transcription quantitative PCR (RT-qPCR) was performed with an ABI Prism 7900 HT Sequence detection system (Applied Biosystems). The primer sequences used in the RT-qPCR were as follow: Alp: forward, 5′-CCA ACT CTT TTG TGC CAG AGA-3′; reverse, 5′-GGC TAC ATT GGT GTT GAG CTT TT-3′; BGLAP: forward, 5′-CTG ACC TCA CAG ATG CCA AGC-3′; reverse, 5′-TGG TCT GAT AGC TCG TCA CAA G-3′; Ctsk: forward, 5′-CTC GGC GTT TAA TTT GGG AGA-3′; reverse, 5′-TCG AGA GGG AGG TAT TCT GAG T-3′; and TRAF-6: forward, 5′-AAG GTG GTG GCG TTA TAC TGC-3′; reverse, 5′-CTG GCA CAG CGG ATG TGA G-3′ (4).

μCT Analysis

Femur samples were dissected from mice and analyzed through micro-CT machine (Quantum GX, PE). We performed micro-CT scans under the same conditions: voltage 120 kV, current 60 mA, spatial resolution 10 mm, scanning 1000 continuous sections. Then the data was collected and analyzed automatically to analyze the number of trabecular bones (Tb.N), trabecular bone thickness (Tb.Th), trabecular bone space (Tb.Sp), bone volume fraction (BV/TV), and other indicators.

Single-Cell RNA Sequencing Experiment

The transcriptomic information of single cells was captured by using the BD Rhapsody system. Single-cell capture was achieved by random distribution of a single-cell suspension across >200,000 microwells through a limited dilution approach (13), Which fracture tissues were dissected and cut into small pieces. Then, they were digested by 3 mg/ml protease (thermo, usa) for 60 minutes and 2 mg/ml collagenase P (thermo, USA) for 2 to 3 h. Beads with oligonucleotide bar codes were added to saturation so that a bead was paired with a cell in a microwell. Cell-lysis buffer was added to hybridize poly-adenylated RNA molecules to the beads. Beads were collected into a single tube for reverse transcription. After cDNA synthesis, each cDNA molecule was tagged on the 5′ end (that is, the 3′ end of a mRNA transcript) with a unique molecular identifier (UMI) and cell label indicating its cell of origin. Whole transcriptome libraries were prepared using the BD Rhapsody single-cell whole-transcriptome amplification workflow. In brief, second-strand cDNA was synthesized, followed by ligation of the WTA adaptor for universal amplification. Eighteen cycles of PCR amplified the adaptor-ligated cDNA products. Sequencing libraries were prepared using random priming PCR of the whole-transcriptome amplification products to enrich the 3′ end of the transcripts linked with the cell label and UMI. Sequencing libraries were quantified using a High Sensitivity DNA chip (Agilent) on a Bioanalyzer 2200 in a Qubit High Sensitivity DNA assay (Thermo Fisher Scientific). The library for each sample was sequenced by HiSeq Xten (Illumina) in a 150-bp paired-end run.

Cell Normalization

The Seurat (v 3.0) [https://satijalab.org/seurat/] package was applied according to the cell raw counts calculated by UMI-Tools for cell normalization and cell filtering considering the MT percentage (20% MT expression) and minimum (200) and maximum (5,000) gene numbers. Seurat regression was based on the MT and UMI counts for batch effector removal to achieve scaled data. PCA and t-SNE analysis were used to reduce the dimensions of the highly variable genes (13).

Cell Clusters and Subclusters

Clusters were identified by a graph-based and k-mean-based clustering approach implemented by the FindCluster function in Seurat [https://satijalab.org/seurat/]. The Wilcox *t*-test was used in the FindAllMarkers function in Seurat to discover the marker genes of each cluster.

Cell Communication

To enable a systematic analysis of cell–cell communication molecules, cell communication analysis was based on the CellPhoneDB (19), a public repository of ligands, receptors, and their interactions. The membrane, secreted, and peripheral proteins of a cluster at different time points were annotated. Significant mean and cell communication significance ($p < 0.05$) were calculated based on the interaction and the normalized cell matrix achieved by Seurat normalization.

Pseudotime Analysis

In the Seurat package including clustering and cell marker identification, Monocle2 (20) was used for pseudotime analysis. The state of cell processing was analyzed, and single cells were placed in a cluster along a trajectory according to a biological process, such as cell differentiation, by taking advantage of an individual cell's asynchronous progression in those processes.

Single-Cell RNA Statistical Analysis

To obtain clean data, fastp with default parameters was used to filter the adaptor sequences and remove the low-quality reads. UMI-Tools was used in the Single Cell Transcriptome Analysis to identify the cell bar code white list. To obtain the UMI counts of each sample, UMI-based clean data were mapped to the mouse genome (Ensemble v 92) using STAR (21) mapping with customized parameters from the UMI-Tools standard pipeline (22). To minimize the sample batch, down-sample analysis was applied among samples sequenced according to the mean reads per cell of each sample to finally achieve a cell expression table with sample bar codes. Cells that contained over 200 expressed genes and mitochondria UMI rate below 20% passed the cell quality filtering. Mitochondria genes were removed from the expression table but were used for cell expression regression in order to avoid the effects of the cell status on the clustering and marker analyses of each cluster.

The Seurat package (v 2.3.4, https://satijalab.org/seurat/) was used for cell normalization and regression based on the expression table according to the UMI counts of each sample and percent of mitochondria rate to obtain the scaled data. PCA was conducted based on the scaled data with all highly variable genes, and the top eight principals were used for t-SNE construction. A graph-based cluster method was used to acquire the unsupervised cell cluster results on the basis of the top eight principals. The marker genes were calculated by the FindAllMarkers function with the Wilcox rank-sum test algorithm under the following criteria: logFC > 0.25; $p < 0.05$; min. pct. > 0.1. To identify the cell type detailed, osteoblast and osteoclast cells were selected for re-tSNE analysis, graph-based clustering, and marker analysis.

Statistical Analyses

Data are presented as the mean ± standard deviation (SD). Two-tailed Student's *t*-test was used to compare means between two groups, and one-way ANOVA was used to compare means between multiple groups. GraphPad Prism Software was used for statistical analyses, with significance at $^{*}p < 0.05$ and $^{**}p < 0.01$.

Data Availability

Single-cell RNA-seq data are available at GEO (Gene Expression Omnibus) under accession numbers GSE142786 and GSE132884.

RESULTS

Single-Cell Profiling of Human Fracture Tissue Cells

To isolate human fracture tissue cells at different stages following fracture, fresh fracture tissues (control, less than 5 days) and old fracture tissues (case, more than 30 days) were obtained from two patients that had hip replacement surgery (**Figure 1A**). In total, 9,976 individual cells associated with fracture were sequenced, of which 9,339 were retained after rigorous filtration for subsequent analysis.

To investigate the cell populations that played key roles in fracture healing, 13 cell clusters were identified with *t*-distributed stochastic neighbor embedding (t-SNE) (**Figures 1B, C**), including six neutrophil clusters (expressing CSF3R, ELANE, FCGR3B, MKI67, MPO, MS4A3, and OLR1), two early erythrocyte clusters (expressing GYPA, HBA1, and HBB), two T cell clusters (expressing CD3D, CD3E, CD3G, CD4, CD8, and NKG7), one B cell cluster (expressing CD22, CD79A, and MS4A1), one plasma cell cluster (expressing CD79A, IGHG1, and IGKC), and one monocyte cluster (expressing CD1C, HLA-DRA, ITGAM, and S100A9). Representative markers for neutrophils, early erythrocytes, T cells, B cells, plasma cells, and monocytes were identified (**Figure 1D**).

To investigate differences in the cell populations between fresh and old fracture patients, the cell clusters of the two groups were compared in t-SNE (**Figure 1E**). There were many differences in the amount of B cells. The B cells in the bone marrow microenvironment can affect the differentiation of osteoblasts and osteoclasts (23, 24). Moreover, scRNA-seq showed little or no difference in the numbers of the other immune cells (**Figures S1, S2**), including monocytes, neutrophils, and T cells. Therefore, the focus was on the roles of B cells in fracture healing.

B Cells in Human Fracture Tissues

To investigate the roles of B cells in fracture healing, five populations of B cells in human fracture tissues were defined: pDC cells (expressing CLEC4C), pro-B cells (expressing HLA-DRA and CD74), mature B cells (expressing CD23 and CD24), and plasma cells (including P1 and P2, expressing J-chain). Then, the relationships between B cells and fracture healing were analyzed to identify distinctive cluster markers (**Figures 2A, B**). Furthermore, the ratios among different cells

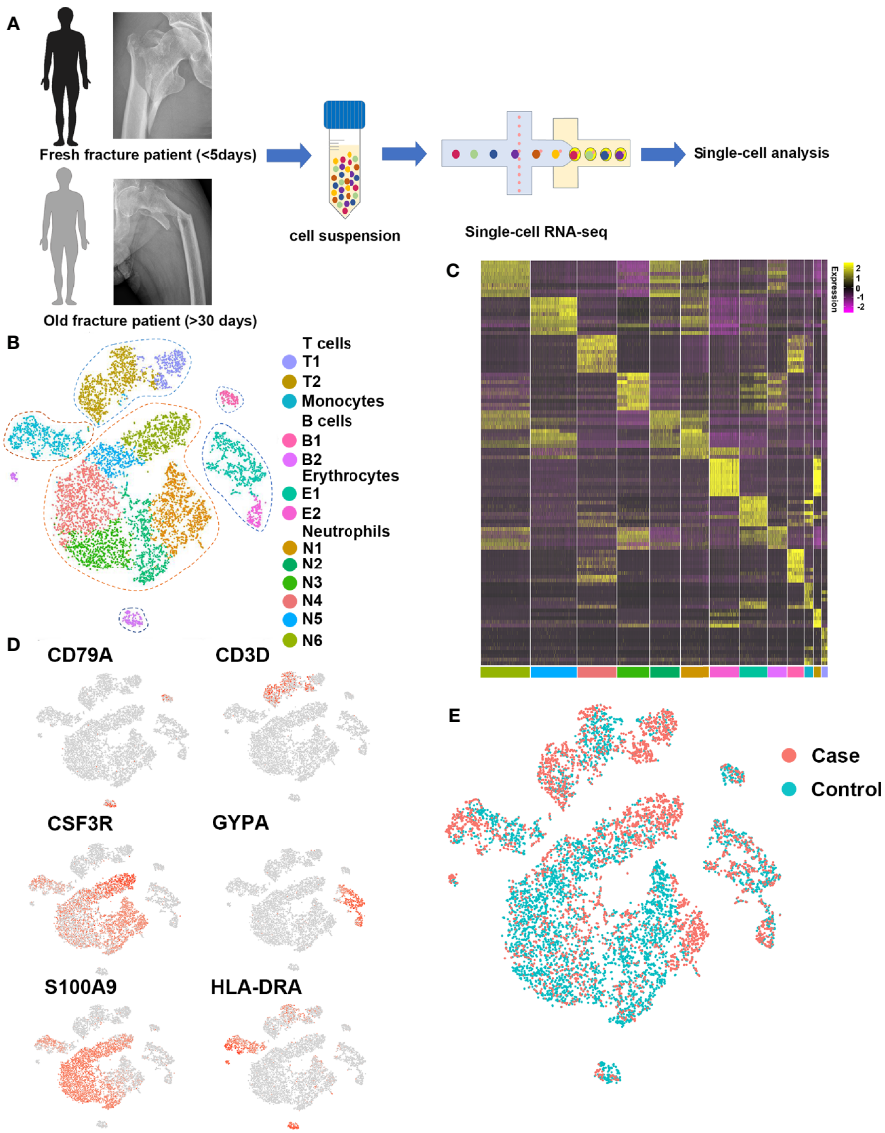

FIGURE 1 | Single-cell profiling of human fracture tissue cells. **(A)** Schematic of the experimental strategy. **(B)** t-SNE visualization of human fracture tissue cells. **(C)** Heat map of the scaled expression of differentially expressed genes for each cluster in human fracture tissue cells. **(D)** Dot plots showing the expression of markers for each cell cluster in human fracture tissue cells. **(E)** t-SNE visualization for old fracture patient (case, red) and fresh fracture patient (control, green).

were calculated, and the numbers and proportions of B cells in the case group were less than those in the control group (**Figure 2C, Table 1**). However, the pseudotime trajectory axis indicated that the B cell constitution in each period in the case group was comparable with that in the control group (**Figure 2D**), suggesting that all B cell subsets decreased in the stages of hematoma and osteophyte formation. Collectively, the results indicated that B cells decreased significantly in the old fracture, which might affect fracture healing.

B Cells in Mice Fracture Models

To further investigate the role of B cells in fracture healing *in vivo*, mice fracture models were generated, and cells within 0.5 mm of the fracture were isolated at different stages (control group and on days 3, 7, and 14) (**Figure 3**). The B cells cluster was reclustered into six subclusters (**Figure 4A**), including T2B and T1B cells, immature B cells (B1 and B2), and B1b cells (B1b1 and B1b2), and the differentially expressed genes (DEGs) in the six subclusters were identified (**Figure 4B**). Consistent with the results in patients, the pseudotime trajectory axis indicated that the fewest B cells occurred in the callus formation stage, compared with those in the other stage of fracture healing and the normal bone marrow microenvironment (**Figure 4C**, **Tables 2**, **3**). By contrast, the callus healing stage had the most B cells. Furthermore, the bone formation and bone resorption activities in the mice fracture models were the most active in the osteophyte formation stage (day 7), compared with those

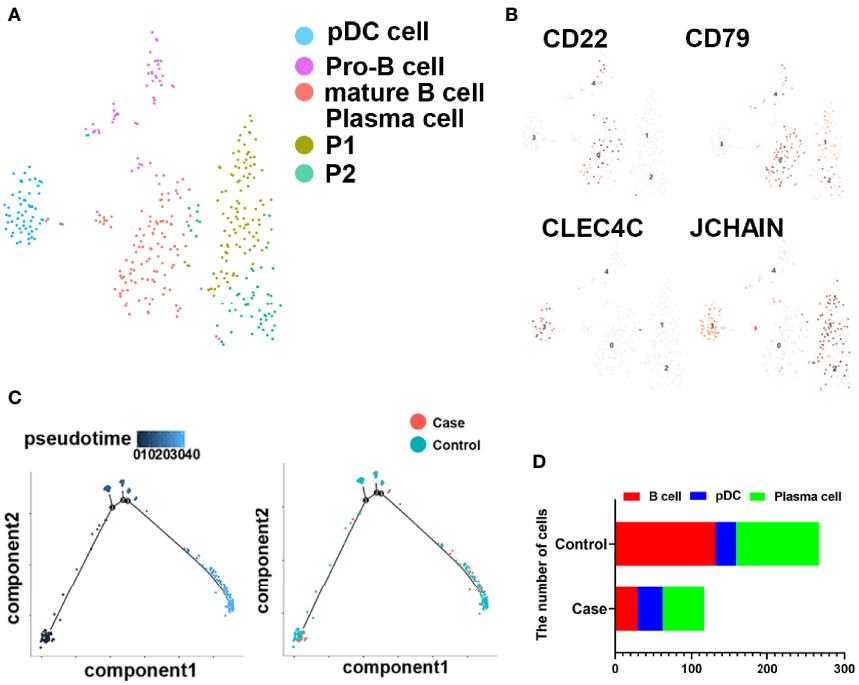

FIGURE 2 | B cells in human fracture tissue. **(A)** t-SNE visualization of B cell subpopulations in human fracture tissues. **(B)** Dot plots showing the expression of markers for each cell cluster in the B cell cluster. **(C)** Monocle2 pseudotime trajectory of the differentiation of B cells in human fracture tissues. **(D)** Composition and proportion of cells in case and control groups.

TABLE 1 | The number of immune cells in the case group and the control group.

Sample	CellType	Percentage	Number
Case	B_Cell	1.93%	74
Case	Early_Erythroblast	11.99%	460
Case	Granulocyte_Progenitor	12.43%	477
Case	Granulocytes	19.36%	743
Case	MDSC	13.34%	512
Case	Monocyte	9.17%	352
Case	NK_Cell	8.76%	336
Case	Plasma_Cell	1.33%	51
Case	Proliferating_Granulocyte_Progenitor	5.71%	219
Case	T_Cell	15.98%	613
Control	B_Cell	2.85%	157
Control	Early_Erythroblast	9.94%	547
Control	Granulocyte_Progenitor	14.36%	790
Control	Granulocytes	12.09%	665
Control	MDSC	30.30%	1667
Control	Monocyte	7.27%	400
Control	NK_Cell	1.96%	108
Control	Plasma_Cell	2.00%	110
Control	Proliferating_Granulocyte_Progenitor	10.71%	589
Control	T_Cell	8.52%	469

processes in the other stage of fracture healing. However, in the osteophyte healing stage (day 14), bone formation and resorption activities decreased (**Figure 4D**). These results indicated that the decrease in B cells promoted osteoblast and osteoclast differentiation during callus formation, whereas the increase during callus healing inhibited osteoblast and osteoclast differentiation.

Moreover, DEGs related to osteogenesis were highly expressed during callus formation (**Figure 4E**). Gene Ontology analysis demonstrated that the set of DEGs in the osteophyte healing stage was involved in bone development and ossification (**Figure 4F**). Cell phone communication also showed that B cells regulated the differentiation of osteoblasts, osteoclasts (**Figure 4G**, **Figure S4**). Immunofluorescence further verified the changes in the numbers and percentages of B cells during fracture healing (**Figure 4H**) and showed the fewest B cells occurred on day 7. Thus, the scRNA-seq revealed that B cells might play an important role in fracture healing.

B Cell Exosomes Inhibited Osteoblast Differentiation and Promoted Osteoclast Formation *In Vitro*

To investigate the role of B cells in skeletal biology, whether B cells could affect osteoblasts or osteoclasts was determined. BMSCs or BMMs were co-cultured with BaF cells in a transwell system, and osteoclastic differentiation increased and osteogenic differentiation decreased when co-cultured with B cells (**Figure 5A**). Then, the exosomes derived from BaF cells (BC-Exos) were extracted and characterized. The BC-Exos had a cup-like morphology ranging from 70 to 150 nm (**Figures S3A, S3B**) and expressed CD63 and CD9 with Western blot analysis (**Figure S3C**).

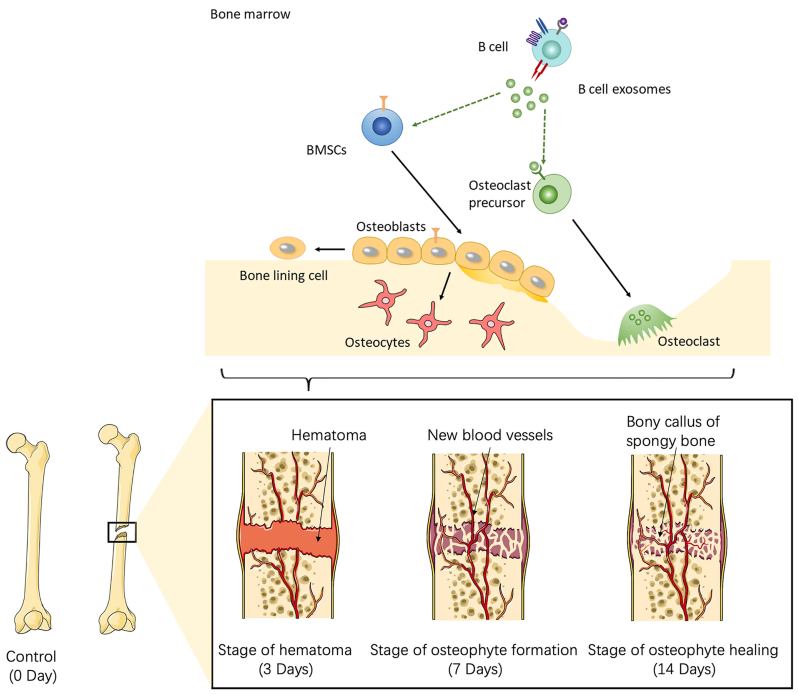

FIGURE 3 | Schematic of the working hypothesis. B cells are consumed to the lowest level *via* inflammation during the hematoma stage, which promotes the recruitment of mesenchymal stem cells (MSCs) into osteogenic differentiation and angiogenesis. During the osteophyte formation stage, osteoblasts promote the maturation of B cells, which then inhibit the differentiation of osteoblasts and the abnormal proliferation of osteophytes. B cells can also promote the differentiation of osteoclasts and allow the body to enter the osteophyte healing stage. During osteophyte healing, osteoblasts and vascular endothelial cells decrease because of cytokines secreted by B cells, which then gradually return to normal levels. To summarize, B cells are a key regulator of fracture healing and inhibit excessive bone regeneration by producing multiple osteoblast inhibitors.

To confirm the role of BC-Exos in bone homeostasis *in vitro*, mouse bone marrow monocytes were treated with BC-Exos or an equal volume of PBS. Osteoclastic differentiation increased as the concentration of BC-Exos increased (**Figures 5B, C**). Furthermore, Osteoclast differentiation marker genes Ctsk and DC-STAMP mRNA expression levels were upregulated by BC-Exos, compared with their negative controls at day 7 (**Figure 5D**). Moreover, pre-osteoblast MC3T3-E1 cells were also treated with BC-Exos or an equal volume of PBS *in vitro*. Osteoblast maturation marker genes BGLAP and Alp mRNA expression levels were downregulated by BC-Exos at day 21 (**Figure 5E**). Consistent with the results of BGLAP and Alp expression, mineral deposition in BC-Exos-treated cells decreased, compared with that in the negative control in pre-osteoblast MC3T3-E1 cells (**Figure 5F**). Thus, these data suggested that BC-Exos inhibited osteoblast differentiation and promoted osteoclast formation *in vitro*.

B Cell Exosomes Inhibited Bone Formation *In Vivo*

To determine the role of BC-Exos *in vivo*, BC-Exos or an equal volume of PBS was injected into the tail vein of 8-week-old male mice twice per week for eight weeks. Microcomputed tomography (μ-CT) showed significantly lower trabecular bone volume, trabecular number, and trabecular thickness and higher trabecular separation in mice injected with BC-Exos than in their controls (**Figures 6A, B**).

DISCUSSION

In this study, immune cells in the bone marrow microenvironment were investigated at single-cell resolution in different stages of fracture healing. There were fewer B cells in old fracture tissues than in fresh fracture tissues. In addition, the callus formation stage had the fewest B cells, in contrast to the callus healing stage with the most. These results suggest that B cells have an important role in fracture healing. The B cell exosomes were characterized. Furthermore, B cell exosomes inhibited osteoblast differentiation and promoted osteoclast formation *in vitro*, and when injected in mice, osteogenic activity decreased significantly. In conclusion, B cell exosomes could regulate osteoblast and osteoclast differentiation and this might be used as a nano-medicine to treat diseases such as fractures or osteoporosis.

B cells are involved in the pathogenesis of rheumatic diseases, including rheumatoid arthritis, Vasculitis (25), and multiple sclerosis (26, 27), which are related to anti-neutrophil

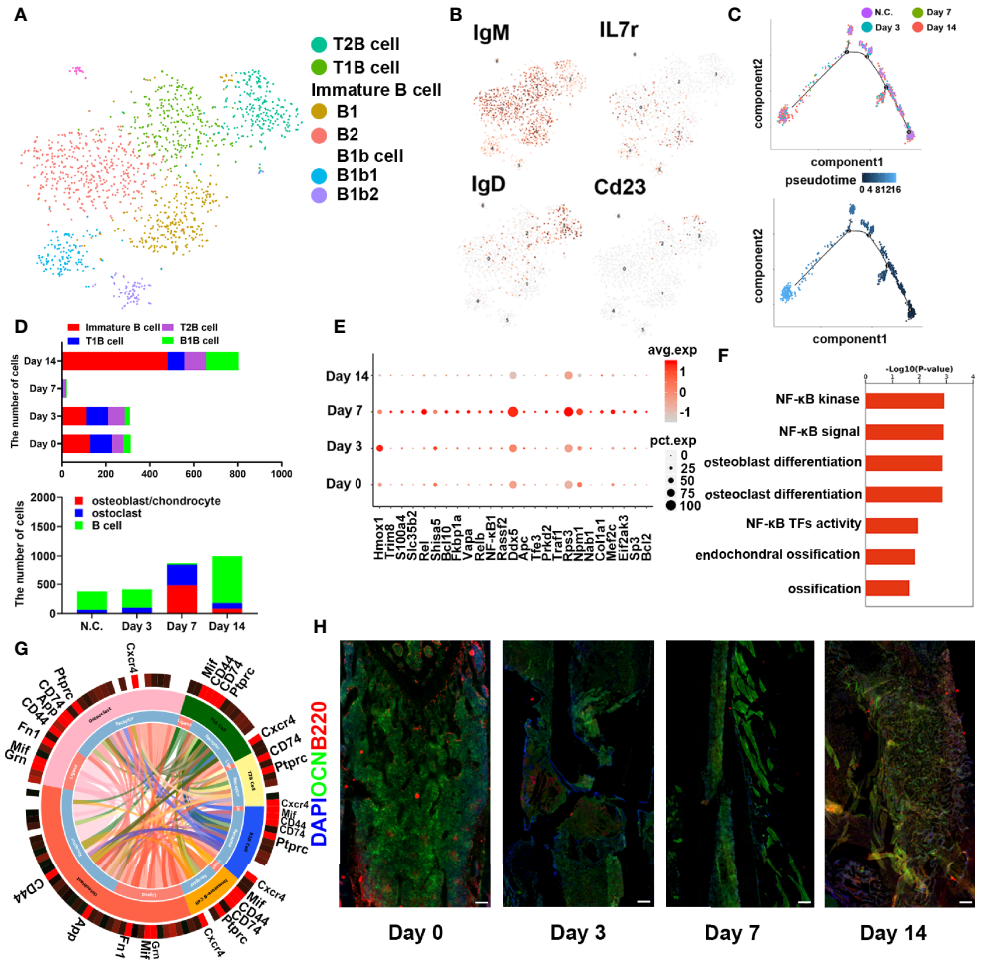

FIGURE 4 | B cells in fracture models in mice. **(A)** t-SNE visualization of B cell subpopulations in mice fracture models. **(B)** Dot plots showing the expression of markers for each cell cluster in the B cell cluster. **(C)** Monocle2 pseudotime trajectory of the differentiation of B cells in mice fracture models. **(D)** Composition and proportion of B cells in the different periods in mice fracture models (control, day 0; hematoma stage, day 3; osteophyte formation stage, day 7; osteophyte healing stage, day 14). **(E)** Heat map of the scaled expression of differentially expressed genes related to fracture healing in the different periods in mice fracture models. **(F)** GO enrichment analysis of differentially expressed genes in the different periods in mice fracture models. **(G)** Cell phone communications between B cells and osteoblasts and osteoclasts. **(H)** Representative immunostaining images of B220 in B cells (red) and osteocalcin in osteoblasts (OCN, green). Scale bar: 100 μm.

cytoplasmic antibodies through B cell intrinsic, antibody-mediated (28), and T cell-dependent mechanisms (29). Furthermore, dysregulated B cell expression of RANKL and OPG correlates with loss of bone mineral density in HIV infection (30). However, the relations between B cells and fracture-related disease remain unclear. In this study, B cells

TABLE 2 | The number of B cells in the case group and the control group.

Sample	CellType	Percentage	Number
Case	B Cell	30.40%	38
Case	pDC	26.40%	33
Case	Plasma Cell	43.20%	54
Control	B Cell	49.06%	131
Control	pDC	10.11%	27
Control	Plasma Cell	40.82%	109

TABLE 3 | The number of B cells in the control, Day 3, Day 7, Day 14 groups.

Sample	Celltype	Percentage	Number
0Day	B1B Cell	10.86%	34
0Day	Immature B Cell	40.58%	127
0Day	T1B Cell	32.27%	101
0Day	T2B Cell	16.29%	51
3Day	B1B Cell	7.44%	23
3Day	Immature B Cell	35.92%	111
3Day	T1B Cell	32.36%	100
3Day	T2B Cell	24.27%	75
7Day	B1B Cell	9.09%	2
7Day	Immature B Cell	4.55%	1
7Day	T1B Cell	18.18%	4
7Day	T2B Cell	68.18%	15
14Day	B1B Cell	18.28%	147
14Day	Immature B Cell	59.83%	481
14Day	T1B Cell	9.45%	76
14Day	T2B Cell	12.44%	100

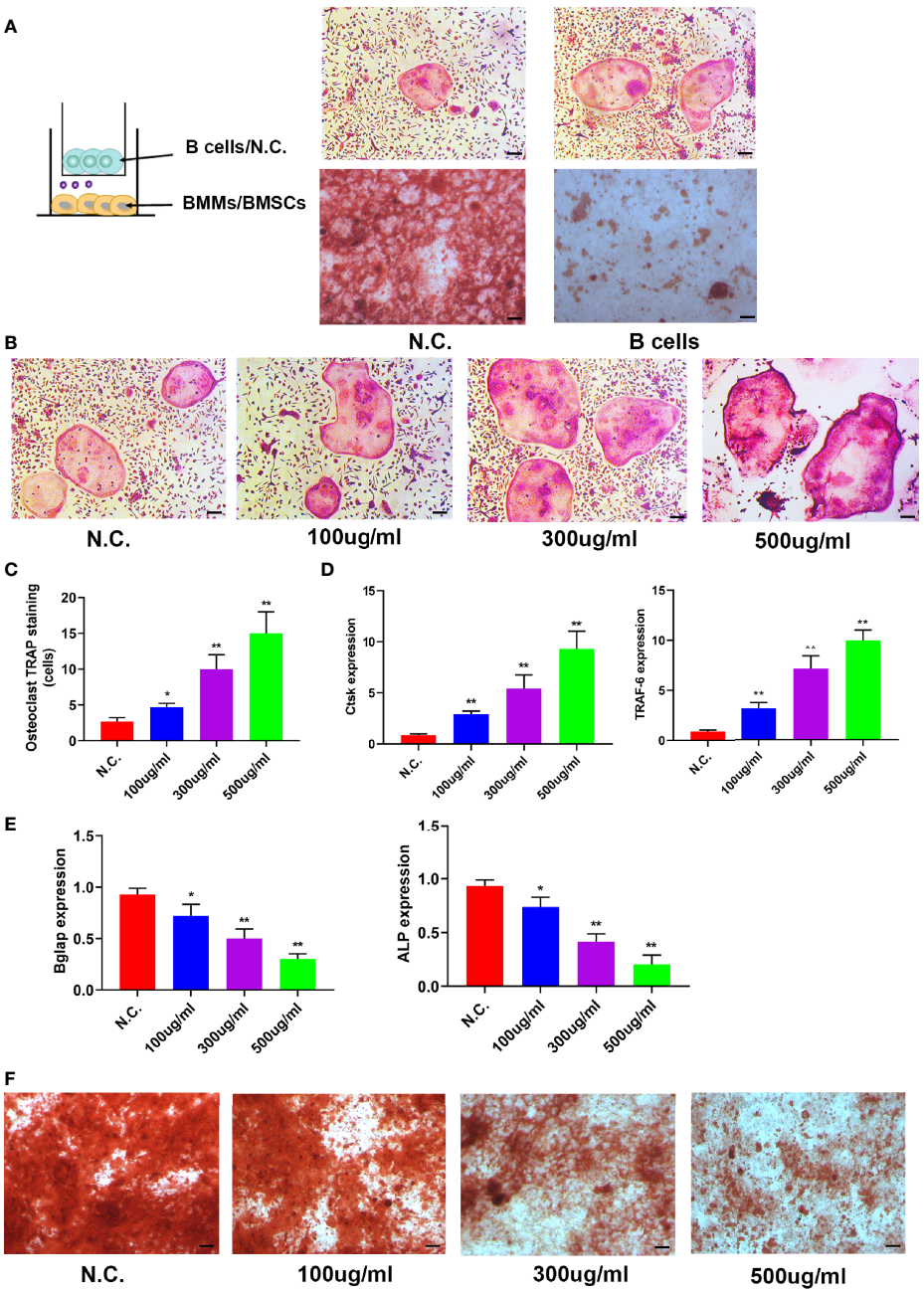

FIGURE 5 | B cell exosomes (BC-Exos) inhibit osteoblast differentiation and promote osteoclast formation *in vitro*. **(A)** Representative images of TRAP-stained osteoclasts (top) and Alizarin red S-stained osteoblasts (bottom). Scale bar: 100 μm. **(B)** Representative images of TRAP-stained osteoclasts treated with different concentrations of BC-Exos. Scale bar: 100 μm. **(C)** Quantitative analysis of the cells of TRAP-stained osteoclasts in **(B)** (*$p < 0.05$, **$p < 0.01$). **(D)** Reverse-transcription qPCR (RT-qPCR) of the relative levels of Ctsk (left) and TRAF-6 (right) mRNA expression in osteoclasts in **(B)**. **(E)** RT-qPCR of the relative levels of Bglap (left) and ALP (right) mRNA expression in BMSCs at day 21. Data are reported as the mean ± SD of three independent experiments. **(F)** Representative images of Alizarin red S staining in osteoblasts at day 21. Scale bar: 100 μm.

were confirmed as regulators of fracture healing. In the early stage of callus formation, differentiation of osteoblasts and osteoclasts increased with a decrease in the number of B cells. During the callus healing stage, excessive osteoblast differentiation was inhibited with increasing numbers of B cells, which implied that that changes in the number of B cells in the bone marrow microenvironment might cause bone loss. Furthermore, Btk has been reported to regulate osteoclast differentiation by RANK and ITAM signals, which congenital defect can cause an arrest in B cell development and

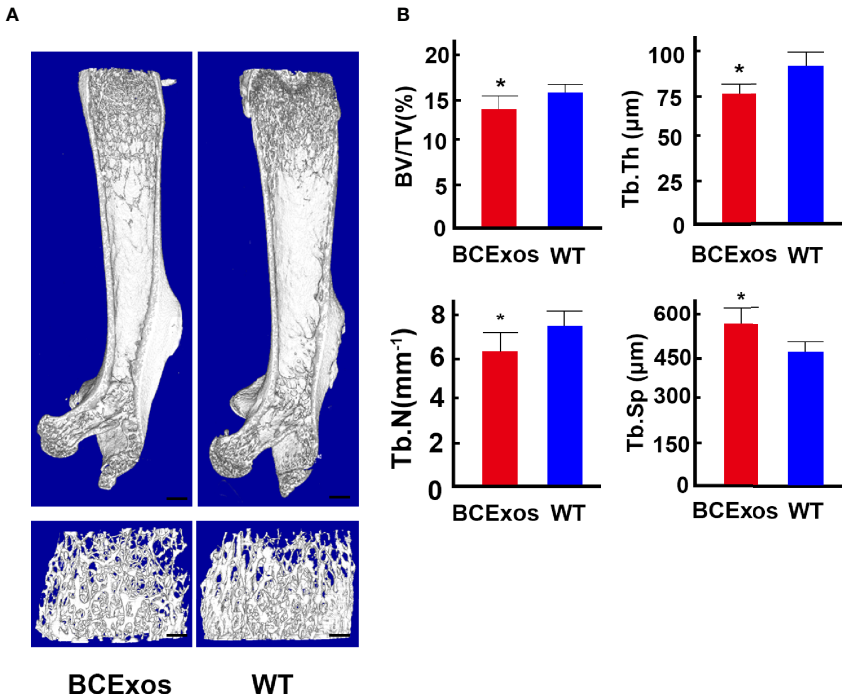

FIGURE 6 | B cell exosomes (BC-Exos) inhibit bone formation *in vivo*. **(A)** Representative microcomputed tomography images in femora from BC-Exos mice and their controls (n = 7 per group). Scale bar: 100 μm. **(B)** Quantitative microcomputed tomography analysis of trabecular bone microarchitecture in femora of BC-Exos mice and their controls. BV/TV, trabecular bone volume per tissue volume; Tb. Th, trabecular thickness; Tb. Sp, trabecular separation; Tb. N, trabecular number (n = 7 per group). *$p < 0.05$.

immunodeficiency (31).This indicated that it might lead to insufficient RANK signal which in turn leads to a decrease in the differentiation of osteoclasts or osteoblasts. In our study, we found that B cell exosomes could regulate osteoblast and osteoclast differentiation, which can be used as a nanomedicine to treat fractures or osteoporosis. Therefore, this work should stimulate future works to investigate the correlation between bone formation and B cell development, which could lead to potential new therapeutic targets.

Single-cell RNA sequencing has recently revolutionized study of the bone marrow microenvironment and its related diseases (32, 33). The heterogeneity of pathogenic T-helper 17 cells was determined by combining scRNA-seq and mouse experimental autoimmune encephalomyelitis models (34). In addition, scRNA-seq was used to analyze tumor-infiltrating T cells and revealed exhaustion programs in human metastatic melanoma (35). However, research that combines scRNA-seq with exosomes remains rare. In this study, MC3T3-E1 cells or BMMs were treated with BC-Exos based on scRNA-seq results. The BC-Exos inhibited osteoblast differentiation and promoted osteoclast formation *in vitro*, and thus, these results expanded the application of single-cell technology. Furthermore, the interactions between different cells in the bone marrow microenvironment were identified *via* cell phone bioinformatics analysis, which helped to understand the importance of those interactions. These results also provide a basis to increase understanding for the safe use of exosomes in the targeted delivery of biological nanomaterials.

DATA AVAILABILITY STATEMENT

The data presented in the study are deposited in the GEO dataset repository, accession number (GSE142786 and GSE132884).

ETHICS STATEMENT

The animal study was reviewed and approved by Scientific Investigation Board of Second Military Medical University.

AUTHOR CONTRIBUTIONS

RW and HZ contributed to the conception and design of this study, the performance of experiments, interpretation, data analysis, and manuscript writing. BZ and ZF performed data analysis and interpretation. HT and FJ contributed to the design of this study, acquiring financial support, data analysis, interpretation, manuscript writing, and the final approval of the manuscript. All authors contributed to the article and approved the submitted version.

FUNDING

The National Natural Science Foundation of China supported this study (nos. 81572637, 81702666, 81272942, 81202122, and 30973019).

ACKNOWLEDGMENTS

We thank Yujie Liu for the support of bioinformatics analysis. The National Natural Science Foundation of China supported this study (nos. 81572637, 81702666, 81272942, 81202122, and 30973019).

SUPPLEMENTARY MATERIAL

The Supplementary Material for this article can be found online at: https://www.frontiersin.org/articles/10.3389/fendo.2021.666140/full#supplementary-material

REFERENCES

1. Einhorn TA, Gerstenfeld LC. Fracture Healing: Mechanisms and Interventions. *Nat Rev Rheumatol* (2015) 11:45–54. doi: 10.1038/nrrheum.2014.164
2. Wang R, Zhang H, Cui H, Fan Z, Xu K, Liu P, et al. Clinical Effects and Risk Factors of Far Cortical Locking System in the Treatment of Lower Limb Fractures. *Injury* (2019) 50:432–7. doi: 10.1016/j.injury.2018.09.013
3. Xu R, Yallowitz A, Qin A, Wu Z, Shin DY, Kim JM, et al. Targeting Skeletal Endothelium to Ameliorate Bone Loss. *Nat Med* (2018) 24:823–33. doi: 10.1038/s41591-018-0020-z
4. Wang R, Zhang H, Ding W, Fan Z, Ji B, Ding C, et al. miR-143 Promotes Angiogenesis and Osteoblast Differentiation by Targeting HDAC7. *Cell Death Dis* (2020) 11:179. doi: 10.1038/s41419-020-2377-4
5. Gaston MS, Simpson AH. Inhibition of Fracture Healing. *J Bone Joint Surg Br* (2007) 89:1553–60. doi: 10.1302/0301-620X.89B12.19671
6. Clark D, Nakamura M, Miclau T, Marcucio R. Effects of Aging on Fracture Healing. *Curr Osteoporos Rep* (2017) 15:601–8. doi: 10.1007/s11914-017-0413-9
7. Al-Sebaei MO, Daukss DM, Belkina AC, Kakar S, Wigner NA, Cusher D, et al. Role of Fas and Treg Cells in Fracture Healing as Characterized in the Fas-Deficient (Lpr) Mouse Model of Lupus. *J Bone Miner Res* (2014) 29:1478–91. doi: 10.1002/jbmr.2169
8. Bragdon B, Lam S, Aly S, Femia A, Clark A, Hussein A, et al. Earliest Phases of Chondrogenesis Are Dependent Upon Angiogenesis During Ectopic Bone Formation in Mice. *Bone* (2017) 101:49–61. doi: 10.1016/j.bone.2017.04.002
9. Zhu J, Garrett R, Jung Y, Zhang Y, Kim N, Wang J, et al. Osteoblasts Support B-lymphocyte Commitment and Differentiation From Hematopoietic Stem Cells. *Blood* (2007) 109:3706–12. doi: 10.1182/blood-2006-08-041384
10. Ponzetti M, Rucci N. Updates on Osteoimmunology: What's New on the Cross-Talk Between Bone and Immune System. *Front Endocrinol (Lausanne)* (2019) 10:236. doi: 10.3389/fendo.2019.00236
11. Onal M, Xiong J, Chen X, Thostenson JD, Almeida M, Manolagas SC, et al. Receptor Activator of Nuclear Factor Kappab Ligand (RANKL) Protein Expression by B Lymphocytes Contributes to Ovariectomy-Induced Bone Loss. *J Biol Chem* (2012) 287:29851–60. doi: 10.1074/jbc.M112.377945
12. Sun W, Meednu N, Rosenberg A, Rangel-Moreno J, Wang V, Glanzman J, et al. B Cells Inhibit Bone Formation in Rheumatoid Arthritis by Suppressing Osteoblast Differentiation. *Nat Commun* (2018) 3;9(1):5127. doi: 10.1038/s41467-018-07626-8
13. Chen H, Ye F, Guo G. Revolutionizing Immunology With Single-Cell RNA Sequencing. *Cell Mol Immunol* (2019) 16:242–9. doi: 10.1038/s41423-019-0214-4
14. Sun H, Wen X, Li H, Wu P, Gu M, Zhao X, et al. Single-Cell RNA-seq Analysis Identifies Meniscus Progenitors and Reveals the Progression of Meniscus Degeneration. *Ann Rheum Dis* (2020) 79:408–17. doi: 10.1136/annrheumdis-2019-215926
15. Savas P, Virassamy B, Ye C, Salim A, Mintoff CP, Caramia F, et al. Single-Cell Profiling of Breast Cancer T Cells Reveals a Tissue-Resident Memory Subset Associated With Improved Prognosis. *Nat Med* (2018) 24:986–93. doi: 10.1038/s41591-018-0078-7
16. Greenblatt MB, Ono N, Ayturk UM, Debnath S, Lalani S. The Unmixing Problem: A Guide to Applying Single-Cell RNA Sequencing to Bone. *J Bone Miner Res* (2019) 34:1207–19. doi: 10.1002/jbmr.3802
17. Wang L, You X, Lotinun S, Zhang L, Wu N, Zou W. Mechanical Sensing Protein PIEZO1 Regulates Bone Homeostasis *Via* Osteoblast-Osteoclast Crosstalk. *Nat Commun* (2020) 11:282. doi: 10.1038/s41467-019-14146-6
18. Hu Y, Zhang Y, Ni CY, Chen CY, Rao SS, Yin H, et al. Human Umbilical Cord Mesenchymal Stromal Cells-Derived Extracellular Vesicles Exert Potent Bone Protective Effects by CLEC11A-Mediated Regulation of Bone Metabolism. *Theranostics* (2020) 10:2293–308. doi: 10.7150/thno.39238
19. Vento-Tormo R, Efremova M, Botting RA, Turco MY, Vento-Tormo M, Meyer KB, et al. Single-Cell Reconstruction of the Early Maternal-Fetal Interface in Humans. *Nature* (2018) 563:347–53. doi: 10.1038/s41586-018-0698-6
20. Trapnell C, Cacchiarelli D, Grimsby J, Pokharel P, Li S, Morse M, et al. The Dynamics and Regulators of Cell Fate Decisions Are Revealed by Pseudotemporal Ordering of Single Cells. *Nat Biotechnol* (2014) 32:381–6. doi: 10.1038/nbt.2859
21. Dobin A, Davis CA, Schlesinger F, Drenkow J, Zaleski C, Jha S, et al. STAR: Ultrafast Universal RNA-seq Aligner. *Bioinformatics* (2013) 29:15–21. doi: 10.1093/bioinformatics/bts635
22. Smith T, Heger A, Sudbery I. UMI-Tools: Modeling Sequencing Errors in Unique Molecular Identifiers to Improve Quantification Accuracy. *Genome Res* (2017) 27:491–9. doi: 10.1101/gr.209601.116
23. Loi F, Cordova LA, Pajarinen J, Lin TH, Yao Z, Goodman SB. Inflammation, Fracture and Bone Repair. *Bone* (2016) 86:119–30. doi: 10.1016/j.bone.2016.02.020
24. Wang C, Inzana JA, Mirando AJ, Ren Y, Liu Z, Shen J, et al. NOTCH Signaling in Skeletal Progenitors Is Critical for Fracture Repair. *J Clin Invest* (2016) 126:1471–81. doi: 10.1172/JCI80672
25. Lu DR, McDavid AN, Kongpachith S, Lingampalli N, Glanville J, Ju CH, et al. And Innate Immune Pathways Differentially Drive Autoreactive B Cell Responses in Rheumatoid Arthritis. *Arthritis Rheumatol* (2018) 70:1732–44. doi: 10.1002/art.40578
26. Jones RB, Furuta S, Tervaert JW, Hauser T, Luqmani R, Morgan MD, et al. Rituximab Versus Cyclophosphamide in ANCA-associated Renal Vasculitis: 2-Year Results of a Randomised Trial. *Ann Rheum Dis* (2015) 74:1178–82. doi: 10.1136/annrheumdis-2014-206404
27. Stone JH, Merkel PA, Spiera R, Seo P, Langford CA, Hoffman GS, et al. Rituximab Versus Cyclophosphamide for ANCA-Associated Vasculitis. *N Engl J Med* (2010) 363:221–32. doi: 10.1056/NEJMoa0909905
28. Yuseff MI, Pierobon P, Reversat A, Lennon-Dumenil AM. How B Cells Capture, Process and Present Antigens: A Crucial Role for Cell Polarity. *Nat Rev Immunol* (2013) 13:475–86. doi: 10.1038/nri3469
29. Rubin SJS, Bloom MS, Robinson WH. B Cell Checkpoints in Autoimmune Rheumatic Diseases. *Nat Rev Rheumatol* (2019) 15:303–15. doi: 10.1038/s41584-019-0211-0
30. Titanji K, Vunnava A, Sheth AN, Delille C, Lennox JL, Sanford SE, et al. Dysregulated B Cell Expression of RANKL and OPG Correlates With Loss of Bone Mineral Density in HIV Infection. *PloS Pathog* (2014) 10:e1004497. doi: 10.1371/journal.ppat.1004497
31. Shinohara M, Koga T, Okamoto K, Sakaguchi S, Arai K, Yasuda H, et al. Tyrosine Kinases Btk and Tec Regulate Osteoclast Differentiation by Linking RANK and ITAM Signals. *Cell* (2008) 132:794–806. doi: 10.1016/j.cell.2007.12.037

32. Baryawno N, Przybylski D, Kowalczyk MS, Kfoury Y, Severe N, Gustafsson K, et al. A Cellular Taxonomy of the Bone Marrow Stroma in Homeostasis and Leukemia. *Cell* (2019) 177:1915–32.e16. doi: 10.1016/j.cell.2019.04.040
33. Oetjen KA, Lindblad KE, Goswami M, Gui G, Dagur PK, Lai C, et al. Human Bone Marrow Assessment by Single-Cell RNA Sequencing, Mass Cytometry, and Flow Cytometry. *JCI Insight* (2018) 163(6):1400–12. doi: 10.1172/jci.insight.124928
34. Gaublomme JT, Yosef N, Lee Y, Gertner RS, Yang LV, Wu C, et al. Single-Cell Genomics Unveils Critical Regulators of Th17 Cell Pathogenicity. *Cell* (2015) 163:1400–12. doi: 10.1016/j.cell.2015.11.009
35. Tirosh I, Izar B, Prakadan SM, Wadsworth MH2nd, Treacy D, Trombetta JJ, et al. Dissecting the Multicellular Ecosystem of Metastatic Melanoma by Single-Cell RNA-Seq. *Science* (2016) 352:189–96. doi: 10.1126/science.aad0501

Conflict of Interest: BZ and CW were employed by the company Novel Bioinformatics Ltd., Co. Shanghai, China.

The remaining authors declare that the research was conducted in the absence of any commercial or financial relationships that could be construed as a potential conflict of interest.

Publisher's Note: All claims expressed in this article are solely those of the authors and do not necessarily represent those of their affiliated organizations, or those of the publisher, the editors and the reviewers. Any product that may be evaluated in this article, or claim that may be made by its manufacturer, is not guaranteed or endorsed by the publisher.

Advantages of publishing in Frontiers

OPEN ACCESS
Articles are free to read for greatest visibility and readership

FAST PUBLICATION
Around 90 days from submission to decision

HIGH QUALITY PEER-REVIEW
Rigorous, collaborative, and constructive peer-review

TRANSPARENT PEER-REVIEW
Editors and reviewers acknowledged by name on published articles

Frontiers
Avenue du Tribunal-Fédéral 34
1005 Lausanne | Switzerland

Visit us: www.frontiersin.org
Contact us: frontiersin.org/about/contact

REPRODUCIBILITY OF RESEARCH
Support open data and methods to enhance research reproducibility

DIGITAL PUBLISHING
Articles designed for optimal readership across devices

FOLLOW US
@frontiersin

IMPACT METRICS
Advanced article metrics track visibility across digital media

EXTENSIVE PROMOTION
Marketing and promotion of impactful research

LOOP RESEARCH NETWORK
Our network increases your article's readership